

LUND UNIVERSITY

Probabilistic and AI-based Methods for Moisture-safe and Sustainable Building Envelope Design

Bayat Pour, Mohsen

2025

Document Version:
Publisher's PDF, also known as Version of record

Link to publication

Citation for published version (APA):
Bayat Pour, M. (2025). *Probabilistic and AI-based Methods for Moisture-safe and Sustainable Building Envelope Design*. Department of Building and Environmental Technology, Lund University.

Total number of authors:
1

Creative Commons License:
CC BY

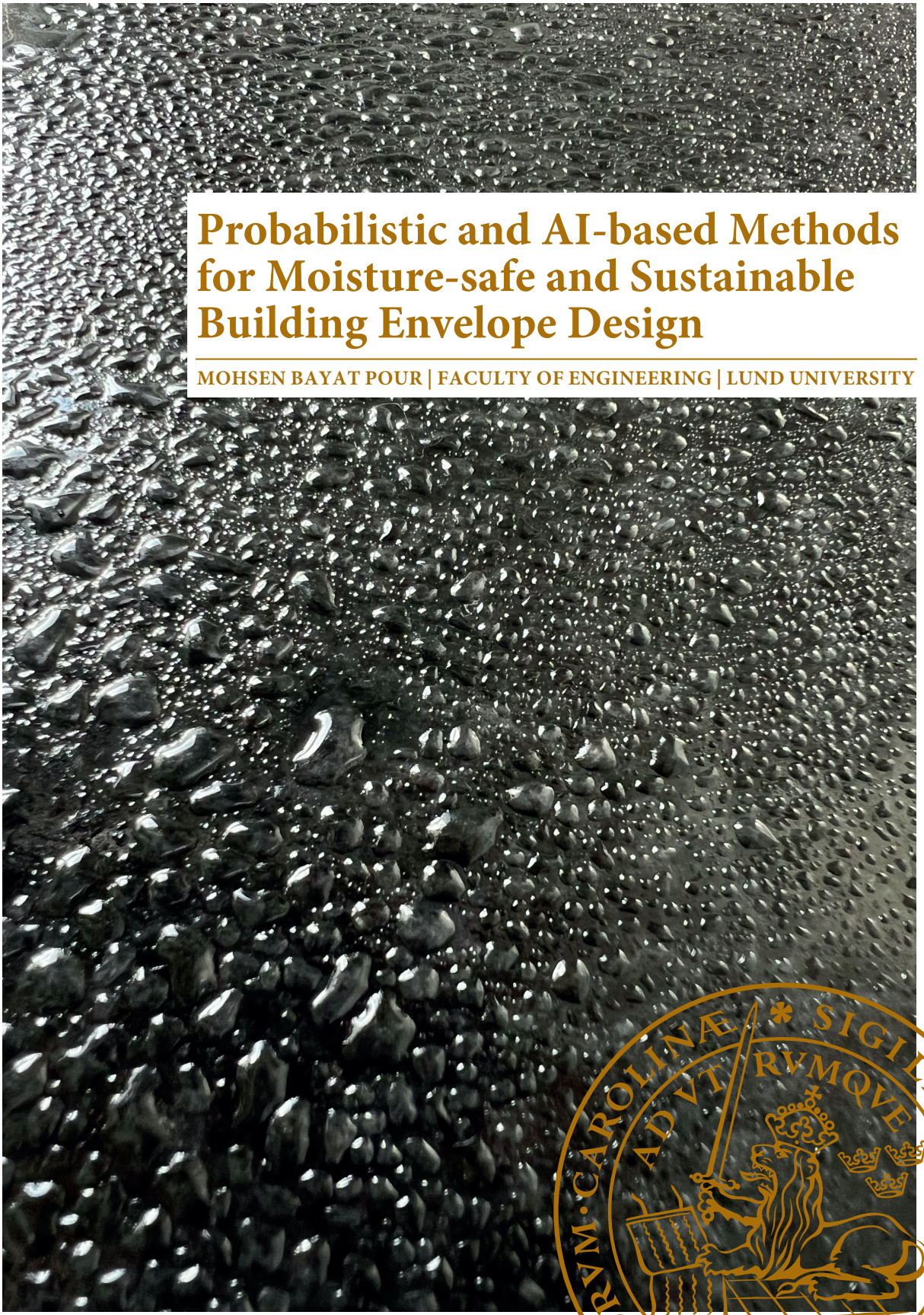
General rights
Unless other specific re-use rights are stated the following general rights apply:
Copyright and moral rights for the publications made accessible in the public portal are retained by the authors and/or other copyright owners and it is a condition of accessing publications that users recognise and abide by the legal requirements associated with these rights.
• Users may download and print one copy of any publication from the public portal for the purpose of private study or research.
• You may not further distribute the material or use it for any profit-making activity or commercial gain
• You may freely distribute the URL identifying the publication in the public portal

Read more about Creative commons licenses: https://creativecommons.org/licenses/

Take down policy
If you believe that this document breaches copyright please contact us providing details, and we will remove access to the work immediately and investigate your claim.

LUND UNIVERSITY

PO Box 117
221 00 Lund
+46 46-222 00 00



Probabilistic and AI-based Methods for Moisture-safe and Sustainable Building Envelope Design

MOHSEN BAYAT POUR | FACULTY OF ENGINEERING | LUND UNIVERSITY

Probabilistic and AI-based Methods for Moisture-safe and Sustainable Building Envelope Design

Mohsen Bayat Pour | Faculty of Engineering | Lund University

Probabilistic and AI-based Methods for Moisture-safe and Sustainable Building Envelope Design

By Mohsen Bayat Pour



LUND
UNIVERSITY

DOCTORAL DISSERTATION

Doctoral dissertation for the degree of Doctor of Philosophy (PhD) at the Faculty of Engineering, Department of Building & Environmental Technology, at Lund University to be publicly defended on the 20th of May 2025, at 10:00 in the lecture hall V:A, V-Huset, Klas Anshelms väg 14, Lund

Faculty opponent
Professor Angela Sasic Kalagasidis
Chalmers University of Technology

Organization	Document name
LUND UNIVERSITY Department of Building and Environmental Technology Division of Structural Engineering Box 118, SE–221 00 LUND, Sweden	**DOCTORAL DISSERTATION** Date of disputation **2025-05-20**
Author(s) **Mohsen Bayat Pour**	Sponsoring organization **FORMAS**

Title and subtitle

Probabilistic and AI-based Methods for Moisture-safe and Sustainable Building Envelope Design

Abstract

The increasing demand for energy-efficient and sustainable construction necessitates the need for building envelope designs that effectively balance moisture safety with sustainability. Improper moisture management in building envelopes can lead to severe consequences, including construction damage, decreased energy performance, and health risks associated with microbial growth. For instance, water infiltration in multi-family wood-frame buildings between 1993 and 2000 caused an estimated one billion Canadian dollars in damage. Similarly, in Belgium, water-tightness issues accounted for nearly half of all documented building damage cases between 2010 and 2015, with water penetration being the most prevalent issue. In Sweden, over 30% of single-family homes have been affected by mould and other moisture-related problems, with microbial growth impacting 60–80% of single-family houses with cold attics in the Gothenburg region.

This thesis begins with a comprehensive state-of-the-art literature review of probabilistic hygrothermal analyses for building envelopes, through which critical research gaps are identified. In response to these gaps, the thesis introduces a set of probabilistic methodologies that integrate machine learning algorithms and decision analysis frameworks to optimise the design of moisture-safe and sustainable building envelopes. Three novel methodologies are proposed: Mould Reliability Analysis (MRA), Mould Sensitivity Analysis (MSA), and Inutility Decision Analysis (IDA). MRA leverages a probabilistic approach to address uncertainties in hygrothermal performance, employing a machine learning metamodel (based on random forests algorithm) to predict mould indices efficiently. MSA combines linear and non-linear sensitivity analyses to identify important variables affecting moisture-related damage. IDA expands traditional decision-making frameworks by incorporating sustainability metrics, such as life cycle costing (LCC) and life cycle assessment (LCA), alongside hygrothermal performance.

The results from case studies demonstrate the effectiveness of these methodologies. Probabilistic analyses exposed the limitations of deterministic approaches, which often underestimate moisture-related risks. The integration of machine learning significantly reduced computational time, enabling the evaluation of millions of scenarios with high precision. Sensitivity analyses pinpointed influential variables and highlighted variations in their importance under different conditions. IDA findings revealed that designs with no probability of mould growth might not always be optimal if their initial environmental and economic impacts are high. In certain cases, designs with manageable mould growth risks, lower initial costs, and environmental impacts were found to be more advantageous over the building's lifespan.

This research demonstrates the potential of integrating AI-based probabilistic moisture safety design with sustainability to develop robustness and environmentally responsible building envelopes. The proposed methodologies provide practitioners with advanced framework to address uncertainties, enhance design robustness, and incorporate multi-criteria decision-making into construction projects. Future research opportunities include expanding the framework to encompass energy performance and health consequences, further enhancing its utility and impact in the construction industry.

Keywords: **probabilistic analysis, metamodeling, AI-based models, hygrothermal analysis, sustainability, building envelope, decision analysis**

Classification system and/or index terms (if any)

ISRN LUTVDG/TVBK-1060/25-SE (153)		Language **English**
ISSN and key title 0349-4969		**ISBN** 978-91-8104-467-6 (print) **ISBN** 978-91-8104-468-3 (electronic)
Recipient's notes	**Number of pages: 153**	Price
	Security classification	

I, the undersigned, being the copyright owner of the abstract of the above-mentioned dissertation, hereby grant to all reference sources permission to publish and disseminate the abstract of the above-mentioned dissertation.

Signature  Date 2025-04-16

Probabilistic and AI-based Methods for Moisture-safe and Sustainable Building Envelope Design

By Mohsen Bayat Pour



LUND
UNIVERSITY

Cover photo by Mina Dabirinezhad
© Mohsen Bayat Pour 2025

Paper I © Elsevier
Paper II © Elsevier
Paper III © Elsevier
Paper IV © Author
Paper V © Elsevier
Paper VI © Author

Faculty of Engineering
Department of Building & Environmental Technology
Division of Structural Engineering

Report TVBK-1060
ISBN 978-91-8104-467-6 (print)
ISBN 978-91-8104-468-3 (electronic)
ISSN 0349-4969
ISRN LUTVDG/TVBK-1060/25-SE (153)

Printed in Sweden, V-huset, Lund University
Lund 2025

Table of Contents

Acknowledgements ..... **i**

Popular science summary ..... **v**

Sammanfattning ..... **vii**

Nomenclature ..... **ix**

Abbreviations ix

Latin letters xi

Greek letters xiii

Publications ..... **xv**

Appended papers xv

Author's contribution to appended papers xvi

Other related publications xvii

1 Introduction **1**

1.1 Background 1

1.2 Objectives and research questions 3

1.3 Research methodology 4

1.4 Limitations 6

1.5 Outline of the thesis 6

2 Hygrothermal analysis theory for the building envelope **9**

2.1 Background 9

2.2 Numerical hygrothermal analysis 11

2.2.1 Moisture (mass) balance equation 11

2.2.2 Energy balance equation 16

2.2.3 Air (gas) balance equation 18

2.2.4 Boundary conditions 19

2.3 Durability and damage models 23

2.3.1 Durability 23

2.3.2 Mould growth 23

2.3.3 Decay 26

2.3.4 Moisture creep 26

2.3.5 Weathering of wood 27

3 Probabilistic hygrothermal assessment (PHA) **29**

3.1 Literature review 29

3.1.1 Background 29

3.1.2 Main findings....31
3.1.3 Identified gaps....32
3.2 Probabilistic analysis (PA)....33
3.2.1 Probabilistic analysis vs deterministic analysis....33
3.2.2 Application of probabilistic analysis in hygrothermal analysis..34
3.3 Hygrothermal uncertainty propagation....35
3.3.1 Sampling technique....36
3.3.2 Probabilistic hygrothermal and mould growth analyses....38
3.3.3 Results and discussion....40
3.4 AI-based metamodeling....45
3.4.1 Metamodeling....45
3.4.2 Random forests (RF) machine learning algorithm....47
3.4.3 Metamodeling sampling....49
3.4.4 Results and discussion....51
3.5 Hygrothermal sensitivity analysis (HSA)....54
3.5.1 Sensitivity analysis (SA)....54
3.5.2 Mould sensitivity analysis (MSA) method....55
3.5.3 Results and discussion....58
4 Sustainability in building envelope design....61
4.1 Background....61
4.2 Inutility decision analysis (IDA) framework....63
4.3 Retrofitting/maintenance/remediation scenarios coupled with circularity concept....65
4.4 Economic impacts assessment....68
4.4.1 Method....68
4.4.2 Results and discussion....70
4.5 Environmental impacts analysis....71
4.5.1 Method....71
4.5.2 Results and discussion....73
4.6 Decision analysis....76
4.6.1 Method....76
4.6.2 Results and discussion....79
5 Conclusions....83
6 Future research potential....89
6.1 Bridging building physics and medical sciences....89
6.2 Incorporating energy performance analysis into the IDA method....90
6.3 Connecting building physics with structural engineering....91
6.4 Region-based hygrothermal analysis tools development....91

6.5 Incorporating user behaviour in PHA 92
7 Summary of the appended papers 95
References 99

Acknowledgements

First and foremost, I would like to express my deepest gratitude to my parents, Kavous and Zhila. Your unwavering love, sacrifices, and dedication have been the cornerstone of my life. You have devoted yourselves wholeheartedly to ensuring that I had a high-quality life, even when it meant setting aside your own needs and desires. You created a nurturing and supportive environment that allowed me to dream big and achieve even bigger. My mom, an experienced and skilled teacher, has been an invaluable inspiration during my teaching tasks at Lund University, where I drew heavily on her wisdom and pedagogical expertise. Similarly, I have learned so much from my dad's exceptional leadership and strength, which he developed through his role as a leader and head in his career. The values, determination, and strength you instilled in me have been my guiding light throughout this journey. This PhD is as much yours as mine, for without your belief in me, this achievement would have been impossible.

To my beloved wife, Mina, words cannot capture the depth of my gratitude for you. Living with a PhD student is no easy task, as my time and energy were often consumed by my research, yet you carried the weight of our life on your shoulders with grace and determination. Being a dentistry student, working simultaneously, and being the wife of a PhD student—all simultaneously—is an almost unimaginable challenge, yet you managed it all so neatly and seamlessly, proving yourself to be a real-life leader. Your strength, resilience, and ability to balance these demanding roles demonstrate how powerful and extraordinary you truly are. Mina's kind and loving heart, coupled with her strong personality, has been the greatest source of support I could ever ask for. This PhD could not have been completed without your unwavering support, patience, and understanding. You are my rock, greatest cheerleader, and most significant source of love. You are not just my partner; you are my hero. Chanel, our sweet cat, you have been a surprising yet essential part of this journey. Your loving eyes and comforting presence in my most stressful moments have been an emotional balm, offering a sense of relief and calm when I needed it most. You are, without a doubt, the best therapist anyone could ask for.

Hosi, my beloved brother, and his wife, Setare, you both have been pillars of strength and inspiration in my life. Hosi, words cannot fully express my gratitude for everything you have done for me. I will never forget your unbelievable support when I came to Sweden—your encouragement, guidance, and unwavering belief in

me were the stepping stones that led me to this moment. You have been more than a brother; you have been my best friend, greatest guide, and pillar of strength, from your immense knowledge in AI and computer science, which you generously shared to help me solve countless technical challenges during my PhD, to your kind and compassionate heart that has always been there to uplift me in tough times, you embody everything I aspire to be. Your emotional understanding and wisdom are unmatched, and I feel truly blessed to have you in my life. Hosi, I want you to know that I always owe you and carry that gratitude in my heart daily. I am so lucky to have a brother like you—a constant source of love, inspiration, and unwavering support. You are, and always will be, the best of everything in my life. Setare, your boundless energy and positive attitude never fail to uplift everyone around you, including me. Your encouragement and cheerful spirit have been a constant source of motivation, reminding me to keep pushing forward.

I would like to express my heartfelt gratitude to my supervisor, Dr. Eva Frühwald Hansson, for her exceptional guidance and unwavering support throughout my PhD journey. Eva, your generosity, intelligence, and caring nature have profoundly impacted me personally and professionally. You have been a source of constant encouragement, and your insightful feedback and constructive advice have been instrumental in shaping my academic growth. Working with you has been a privilege, and I deeply admire your ability to lead with empathy and expertise. Thank you for inspiring me to aim higher and always believing in me.

I am also deeply grateful to my co-supervisor, Dr. Jonas Niklewski, for his invaluable contributions and steady support throughout this journey. Jonas, your patience and willingness to listen have meant the world to me, particularly during challenging moments. Our meaningful discussions and your insightful suggestions have helped me refine my work and gain clarity during pivotal moments in this project. I will always appreciate your calm demeanour, thoughtful guidance, and readiness to offer advice or lend an ear when I need it most. Your presence has been a significant source of support and comfort.

I extend my heartfelt thanks to my co-supervisor, Dr. Amir Naghibi, who joined me during the second half of my PhD journey. Amir, your expertise in AI and metamodeling brought a new dimension to my research, significantly enriching its quality and depth. Your kindness, openness, and willingness to answer my questions—no matter how small—have been deeply appreciated. Thank you for enhancing my understanding of advanced methodologies and being a wonderful mentor. Your support and enthusiasm for my work have been genuinely motivating.

I would like to extend my sincere gratitude to Dr. Akram Abdul Hamid for his invaluable support and collaboration throughout my PhD journey. As a co-author of some of my publications, your expertise and dedication have been instrumental in shaping the quality of my PhD project. I am thankful for your feedback on Chapter 2 of this thesis, which significantly enriched the section on building physics

fundamentals. Your guidance has dramatically enhanced my understanding of building physics and deepened my knowledge of numerical simulations. Thank you for your unwavering support and for being such an integral part of my academic growth.

I would like to dedicate a heartfelt acknowledgement to my two close friends and colleagues during my PhD journey, Mohammad and Amro, whose support and companionship have meant the world to me. Mohammad, your unwavering encouragement, insightful advice, and genuine kindness have been a source of strength for me throughout these years. From our long discussions on research challenges to navigating the complexities of academic life, you have been more than a colleague—you are a true friend. Your positive outlook and resilience have inspired me during tough times, and I will always cherish the countless moments we shared, both in research and beyond. Amro, your enthusiasm and collaborative spirit have made the journey much lighter and more enjoyable. Together, we faced the trials and triumphs of the PhD process, learning and growing alongside each other. I am truly grateful for the friendship and support you both have provided, and I feel incredibly fortunate to have had you by my side during this transformative phase of my life.

I would like to thank my colleagues at the Division of Structural Engineering for creating such a welcoming and inspiring environment throughout my PhD journey. Sven, Miklos, Annika, Ivar, Anders, Sebastian, Martin, Elena, Christoffer, Oskar, Paulina, Simone, Leandro, and Maria, your positive attitudes and friendly demeanours have made working in this division a delightful experience. Whether sharing ideas, engaging in stimulating discussions or enjoying lighter moments together, I truly value our time as a team. Your kindness, collaboration, and encouragement have made this journey memorable and fulfilling. Thank you for being such wonderful colleagues and for enriching my time at Lund University with your presence.

I would like to extend my heartfelt thanks to all my dear friends and colleagues, including Hossein, Mohammad, Elham, Amirhosein, Kourosh, Vahid, Kavan, Marziyeh, Alireza, Behshid, Hassan, and Shokoufeh. Your kindness and unwavering support throughout my PhD journey have been truly invaluable. The warm moments we shared in the Fika room and the spirited football matches we enjoyed brought joy and balance to my academic life. I sincerely appreciate your encouragement and the light-hearted moments that made the challenges of this journey so much easier to bear. Thank you for being such a vital part of my experience and making these years memorable.

Popular science summary

Global warming is one of the most pressing challenges facing humanity today. It has increased Earth's temperature, resulting in catastrophic consequences such as more frequent wildfires, rising sea levels, and severe climatic events. A key contributor to global warming is the emission of carbon dioxide (CO_2), a greenhouse gas released through human activities such as burning fossil fuels. To combat global warming, it is essential to reduce CO_2 emissions and adopt sustainable practices across all sectors. The building sector plays a significant role in global CO_2 emissions, accounting for approximately 30% of worldwide emissions. Buildings consume large amounts of energy, particularly for heating, cooling, and lighting, which often rely on fossil fuel-derived energy sources. Energy-efficient building strategies have become a priority in construction to reduce energy consumption and its associated CO_2 emissions. These strategies include adding insulation layers to walls and roofs and constructing highly airtight building envelopes to prevent heat loss.

While these measures improve energy efficiency, they can also create unintended moisture-related problems, such as increased risk of condensation. Increasing the indoor temperature and relative humidity simultaneously could lead to microbial growth, such as mould. Moisture-related problems not only compromise the durability of the building but can also impact the health of its occupants. One way to minimise the risk of moisture-related problems is to design more reliably and robustly, including the design parameters' uncertainties. This PhD thesis focuses on addressing this challenge and ensuring moisture safety in building envelope designs. The research introduces a methodology incorporating advanced tools and analyses to optimise building designs while accounting for sustainability and moisture safety.

One of the core methods developed in this thesis is mould reliability analysis (MRA). This method uses probabilistic modelling to account for building design uncertainties, such as material properties variations. Instead of relying on a single "ideal" scenario using a deterministic approach, probabilistic analysis evaluates thousands or even millions of possible scenarios to assess the probability of moisture-related problems like mould growth. By employing machine learning, a subset of artificial intelligence (AI), and specifically utilising the random forests algorithm, this research significantly reduces the computational time required to predict mould risks across these scenarios.

Another method introduced is mould sensitivity analysis (MSA). This analysis identifies which design parameter has the most significant impact on mould growth. For example, it examines how changes in material properties influence the risk of mould. Understanding these relationships helps designers focus on the most critical variables during construction, making designs more efficient against moisture-related issues.

The third method is inutility decision analysis (IDA), which takes the research a step further by integrating sustainability into the moisture-safe design process. This method combines moisture safety assessments with environmental and economic evaluations. Using life cycle costing (LCC) and life cycle assessment (LCA), IDA evaluates different building designs' long-term financial and environmental impacts. For instance, while one design may have lower initial costs and environmental impacts, it may be costly and increase CO_2 emissions over the building's lifespan due to higher moisture-induced maintenance and renovation needs.

The findings of this research highlight several key insights. First, traditional building design approaches, which often assume ideal conditions, tend to underestimate the risks associated with moisture-related issues. In contrast, the probabilistic methods developed in this thesis offer a more comprehensive risk assessment by providing performance metrics rather than a binary "works" or "does not work" outcome. This makes them particularly suitable for design analysis and for ranking different design alternatives based on their moisture safety performance. Second, integrating machine learning with probabilistic analysis enables the evaluation of millions of scenarios within a fraction of the time, significantly improving both the speed and robustness of decision-making processes. Third, incorporating economic and environmental considerations into moisture safety design ensures that sustainability metrics are systematically accounted for throughout the design process. These advancements have important implications for the construction industry, equipping architects, engineers, and building professionals with the potential to develop more advanced tools for designing sustainable and moisture-resilient buildings. By addressing uncertainties and integrating sustainability considerations, this research contributes to the development of more durable, resource-efficient, and environmentally responsible construction practices. Looking ahead, the methodologies introduced in this thesis can be expanded to incorporate energy performance assessments and health-related consequences of moisture problems, further broadening their applicability. Ultimately, this research provides a foundation for achieving a more sustainable and circular built environment.

Sammanfattning

Den ökande efterfrågan på energieffektiva och hållbara byggnader understryker behovet av byggnadsdelar som balanserar fuktsäkerhet med hållbarhet. Otillräcklig hantering av fukt i byggnadskomponenter kan få allvarliga konsekvenser, inklusive skador på konstruktionen, minskad energiprestanda och hälsorisker kopplade till mikrobiell tillväxt. Till exempel orsakade vatteninträngning i flerbostadshus med trästommar i Kanada mellan 1993 och 2000 skador till ett uppskattat värde av en miljard kanadensiska dollar. På samma sätt stod problem med täthet för nästan hälften av alla dokumenterade byggnadsskador i Belgien mellan 2010 och 2015, där vatteninträngning genom byggnadshöljet var den vanligaste orsaken. I Sverige har över 30 % av enfamiljshusen påverkats av mögel och andra fuktrelaterade problem, med mikrobiell tillväxt på träelementen i den kalla vinden som drabbat 60–80 % av alla hus med ventilerade vindsutrymmen i Göteborgsregionen.

Avhandlingen inleds med en omfattande litteraturstudie av probabilistiska hygrotermiska analyser för klimatskärm, där viktiga forskningsluckor identifieras. Utifrån dessa luckor föreslås en probabilistisk metodik som integrerar maskininlärningsalgoritmer och beslutsanalysramverk för att optimera fuktsäkra och hållbara byggnadsdesign. Metodiken introducerar tre nya tillvägagångssätt: Mould Reliability Analysis (MRA), Mould Sensitivity Analysis (MSA) och Inutility Decision Analysis (IDA). MRA använder probabilistiska metoder för att hantera osäkerheter i hygrotermiska prestanda, med hjälp av en maskininlärningsmetamodell (baserad på algoritmen random forests) för att effektivt förutsäga mögelindex. MSA kombinerar linjära och icke-linjära känslighetsanalyser för att identifiera viktiga variabler som påverkar fuktrelaterade skador. IDA utökar traditionella beslutsramverk genom att inkludera hållbarhetsmått, såsom livscykelkostnad (LCC) och livscykelanalys (LCA), tillsammans med hygrotermisk prestanda för att underlätta optimala designbeslut.

Resultaten från fallstudier visar metodernas effektivitet. Probabilistiska analyser avslöjar begränsningarna hos deterministiska metoder, som ofta underskattar risken för fuktrelaterade problem. Integreringen av maskininlärning minskar avsevärt beräkningstiden och möjliggör utvärdering av miljontals scenarier med hög precision. Känslighetsanalyser identifierar inflytelserika variabler och visar variationer i deras betydelse under olika förhållanden. IDA-resultaten visar att design med hanterbara mögelrisker, tillsammans med lägre initiala kostnader och

miljöpåverkan, i vissa fall kan vara mer fördelaktiga över byggnadens livslängd jämfört med alternativ utan mögelrisk men med högre initial påverkan.

Denna forskning betonar vikten av att integrera probabilistisk fuktsäker design med hållbarhet för att utveckla robusta och miljömässigt ansvarsfulla byggnadsdelar. Den föreslagna metoden förser praktiker med avancerade ramverk för att hantera osäkerheter, förbättra designens robusthet och integrera flerkriterieanalys i byggprojekt. Framtida forskningsmöjligheter inkluderar en utökning ramverket för att omfatta energiprestanda och hälsokonsekvenser, vilket ytterligare förstärker dess tillämpning och påverkan inom byggindustrin.

Nomenclature

Abbreviations

1D	One-dimensional
2D	Two-dimensional
3D	Three-dimensional
AI	Artificial Intelligence
ASHRAE	American Society of Heating, Refrigeration and Air-Conditioning Engineers
BBR	Swedish Building Regulations
BRS	Basic Random Sampling
CE	Circular Economy
CO_2	Carbon Dioxide
cov	Covariance
CL	Cellulose
CLT	Cross-Laminated Timber
CNN	Convolutional Neural Networks
CPIF	Consumer Price Index with Fixed Interest
CS	Case Study
DL	Deep Learning
EC	Economic impacts of mould growth
ENV	Environmental impacts of mould growth
EPD	Environmental Product Declaration
EPS	Expanded Polystyrene
ES	Experimental Study

ETICS	External Thermal Insulation Composite System
GAM	Generalised Additive Models
GHG	Greenhouse Gas
GWP	Global Warming Potential
HAM	Heat, Air, and Moisture
HSA	Hygrothermal Sensitivity Analysis
HUP	Hygrothermal Uncertainty Propagation
IEA	International Energy Agency
IDA	Inutility Decision Analysis
IPCC	Intergovernmental Panel on Climate Change
LCA	Life Cycle Assessment
LCC	Life Cycle Costing
LCIA	Life Cycle Impact Assessment
LHS	Latin Hypercube Sampling
LSTM	Long Short-Term Memory
MA	Metamodel Analysis
MAE	Mean Absolute Error
ML	Machine Learning
MLP	Multilayer Perceptron
MMI	Maximum Mould Index
MRA	Mould Reliability Analysis
MSA	Mould Sensitivity Analysis
MW	Mineral Wool
NN	Neural Networks
OSB	Oriented Strand Board
OF	Objective Function
PA	Probabilistic Analysis
PCR	Product Category Rules
PHA	Probabilistic Hygrothermal Assessment

PLS	Partial Least Squares	
PPE	Personal Protective Equipment	
RCC	Rank Correlation Coefficient	
RF	Random Forests	
RH	Relative Humidity	%
RMSE	Root Mean Square Error	
RNN	Recurrent Neural Networks	
SA	Sensitivity Analysis	
SLS	Serviceability Limit State	
SPR	Single-Point Rate	
SVM	Support Vector Machines	
VTT	Technical Research Centre of Finland	
WDR	Wind-Driven Rain	
WF	Wood Fibre	
WF_C	Weighting Factor	
WHO	World Health Organization	

Latin letters

A_0	Today's costs	€
C_R	Terrain roughness coefficient	-
c_p	Specific heat capacity	J/(kg.K)
C_{TP}	Topography coefficient	-
D	Hourly mean wind direction from north	°
D_l	Liquid water diffusivity	m^2/s
$D_{v,air}$	Vapour diffusivity in still air	m^2/s
$D_{v,mat}$	Vapour diffusion coefficient in porous material	m^2/s
d_i	Design alternative	
$E[\overline{U}]$	Expected value of the inutilities	

G	Gothenburg	
g_k	Gravitational acceleration	m/s^2
g_m	Limit state function	
g_r	Growth rate	%
h	Specific enthalpy	J/kg
$h_{evap.}$	Latent heat of evaporation	J/kg
$I_{M,ls}$	Mould Limit State	-
$I_{M,PEI}$	Mould Performance Evaluation Indicator	-
I_{WDR}	WDR intensity	mm/h
i_r	Interest rate	%
$j^{Q}_{k,cond}$	Conductive heat flux	J/(m^2.s)
$j^{m_a}_{k,adv}$	Advective flux of dry air	kg/(m^2.s)
$j^{m_g}_{k,adv}$	Advective flux of gas phase	kg/(m^2.s)
$j^{m_l}_{k,adv}$	Advective flux of liquid water	kg/(m^2.s)
$j^{m_v}_{k,adv}$	Advective flux of water vapour	kg/(m^2.s)
$j^{m_v}_{k,diff}$	Diffusive flux of water vapour	kg/(m^2.s)
K_g	Permeability of the gas phase	s
K_l	Liquid water conductivity	s
N_T	Total number of scenarios	
O	Obstruction factor	-
P	Present value	€
P_a	Ambient air pressure	Pa
P_c	Capillary pressure	Pa
P_g	Gas partial pressure	Pa
P_l	Total liquid pressure	Pa
$P(H)$	Probability of the health consequence	%
$P(M_{Ij})$	Probability of mould index j	%

R	Rensjön	
R^2	Coefficient of determination	-
R_h	Rainfall through the horizontal plane	mm/h
R_v	Constant of water vapour	J/(kg·K)
$R(M_{Ij})$	Reliability of mould index j	%
r	radius	m
S_d-value	Diffusion equivalent air layer thickness	m
T	Temperature	˚C, K
T_a	Ambient air temperature	˚C, K
$T_{ref.}$	Reference temperature	˚C, K
t	Duration (time)	s
t_p	Prediction time per scenario	s
t_s	Simulation time per scenario	s
$\overline{U}$	Inutility	
W	Wall factor	-
w_s	Reference wind speed	m/s
x_k	Spatial coordinate in the k direction	
y_i	Original data	
$\bar{y}_i$	Mean of the original data	
$\hat{y}_i$	Predicted data	

Greek letters

α	Water contact angle to the surface	°
γ	Surface tension	N/m
ε_i	Convergence value	-
θ	Wall orientation relative to the north	°
θ_l	Moisture content	m^3/m^3
λ	Thermal conductivity	W/(m.K)

μ	Water vapour diffusion resistance factor	-
ρ	Spearman's correlation coefficient	-
ρ_g	Gas mass density	kg/m^3
ρ_l	Liquid water density	kg/m^3
ρ^m	Mass density	kg/m^3
ρ_g^m	Mass (water vapour/dry air) concentration in the gas phase	kg/kg
ρ^u	Internal energy density	J/m^3
σ	Standard deviation	
σ^m	Mass (moisture/dry air) source or sink	kg/(m^3.s)
σ^u	Energy source or sink	J/(m^3.s)

Publications

Appended papers

I. *A literature review of probabilistic hygrothermal assessment for building envelopes*
M. Bayat Pour, J. Niklewski, A. Naghibi, & E. Frühwald Hansson, (2024)
Building and Environment journal, vol. 261, p. 111756.
doi: https://doi.org/10.1016/j.buildenv.2024.111756

II. *Robust probabilistic modelling of mould growth in building envelopes using random forests machine learning algorithm*
M. Bayat Pour, J. Niklewski, A. Naghibi, & E. Frühwald Hansson, (2023)
Building and Environment journal, vol. 243, p. 110703.
doi: https://doi.org/10.1016/j.buildenv.2023.110703

III. *Impact of extruded mortar joints on the hygrothermal performance of brick veneer walls: A probabilistic study*
M. Bayat Pour & S. Kahangi Shahreza, (2024)
Journal of Building Engineering, vol. 94, p. 109936.
doi: https://doi.org/10.1016/j.jobe.2024.109936

IV. *Influence of extruded mortar joints on mould growth in timber frame wall with brick veneer: Probabilistic and machine learning modelling*
M. Bayat Pour, S. Kahangi Shahreza, & A. Abdul Hamid, (2025)
Journal of Building Physics.
(Manuscript submitted based on special issue invitation)

V. *Towards a sustainable decision analysis approach for moisture-safe building envelope design*
M. Bayat Pour & A. Abdul Hamid, (2024)
Journal of Building Engineering, vol. 97, p. 110955.
doi: https://doi.org/10.1016/j.jobe.2024.110955

VI. *Probabilistic analysis of various hygroscopic insulations: Impacts on mould growth and energy efficiency in timber frame walls*
M. Bayat Pour, O. Ranefjärd, & J. Niklewski, (2025)
Proceedings of the 6th Central European Symposium on Building Physics (6th CESBP 2025), September 11-13, 2025, Budapest, Hungary.

Author's contribution to appended papers

I. The author independently conducted all steps of the comprehensive literature review, including identifying and gathering relevant literature, performing statistical analyses, and creating visualisations, figures, and tables. The author was responsible for conceptualising the study and drafting the original manuscript. Revisions were made based on feedback received from the co-authors.

II. The author developed the methodologies introduced in the paper and created the advanced simulation setup, enabling automated batch simulations and constructing an AI-based prediction model. The author carried out all simulations, calculations, modelling, and visualisation. The conceptualisation was conducted in collaboration with the second and third authors. Additionally, the author prepared the original manuscript draft, which was reviewed by the co-authors.

III. The author created the probabilistic model for this paper, including Python coding to automate the simulations. The study's conceptualisation was carried out collaboratively with the second author. The author prepared the original draft of the manuscript, which was subsequently revised based on feedback from the second author.

IV. The author created the probabilistic model for the study and developed the coding necessary to automate the simulations as well as the AI-based metamodel. The conceptualisation was conducted in collaboration with the second author. The author wrote the original manuscript and revised it following the input provided by the co-authors.

V. The author developed the innovative decision analysis methodology introduced in this paper. The author performed all study aspects, including conceptualisation, visualisations, simulations, and metamodeling integrated with environmental and economic analyses. The author and the second author jointly defined the renovation scenarios. The author wrote the original draft of the paper, which the second author then reviewed.

VI. The author, in collaboration with the co-authors, conceptualised the framework for this study. The author carried out all probabilistic analyses and numerical simulations. The original manuscript was written by the author and revised according to comments and suggestions provided by the co-authors.

Other related publications

Scientific contributions not included in the present thesis:

Journal papers

A. *Towards rational decision-making on repointing to mitigate moisture damage in building envelopes: A probabilistic study*
S. Kahangi Shahreza, **M. Bayat Pour** & A. Abdul Hamid, (2024)
Developments in the Built Environment. 19, 100510.
doi: https://doi.org/10.1016/j.dibe.2024.100510
B. *A multi-criteria decision analysis for building envelope design: Bridging moisture safety and health risks*
M. Bayat Pour, (2025)
Submitted to Journal of Building Engineering, Elsevier (Under review)
C. *From experimental studies to predictive machine learning modelling: Polypropylene fibre reinforced concrete*
M. Bayat Pour, (2025)
Submitted to Results in Materials, Elsevier (Under review)

Conference papers

A. *Mould reliability analysis combined with mould health risks for decision support*
M. Bayat Pour, J. Niklewski, E. Frühwald Hansson, & S. Thöns.
AIP Conference Proceedings of the 5th Central European Symposium on Building Physics (5th CESBP 2022), September 5-7, 2022, Bratislava, Slovakia.
B. *Effect of extruded mortar joints on mould growth in timber frame wall with brick veneer: Probabilistic and machine learning modelling*
M. Bayat Pour, S. Kahangi Shahreza, & A. Abdul Hamid.
Proceedings of the 9th International Building Physics Conference (9th IBPC 2024), July 25-27, 2024, Toronto, Canada.
C. *Strategies for enhanced energy efficiency and moisture management in brick–AAC cavity walls*
S. Kahangi Shahreza, **M. Bayat Pour,** A. Abdul Hamid, & M. Molnár.
Proceedings of the 18th International Brick and Block Masonry Conference (18th IB^{2}MaC 2024), July 21-24, 2024, Birmingham, England.
D. *Evaluation of solidification/stabilization technology performance by combining economic and environmental impacts assessment for a port in Sweden*
E. Tamadonyazdian, M. Gholampoor, K. Farsäter, & **M. Bayat Pour**.

19th Nordic Geotechnical Meeting, September 18-20, 2024, Gothenburg, Sweden.

1 Introduction

1.1 Background

Moisture-safe building design is a cornerstone of construction projects, as moisture-related problems significantly impact building durability [1], economy [2], environmental performance [3], and human health [4]. Excess moisture can lead to material degradation [5], mould growth [6], and frost damage [7], which affects the buildings' serviceability and lifespan. These challenges highlight the importance of moisture-safe designs to ensure long-term building performance while safeguarding environmental and human well-being.

According to the World Health Organization (WHO) guidelines [8], indoor dampness and mould are major contributors to serious health issues, including respiratory diseases such as asthma, coughing, and wheezing, as well as cancer and skin disorders. The guidelines stress the importance of preventing dampness and mould to safeguard human health. Numerous studies have further linked exposure to damp environments with a range of health problems, including neurological problems [9], liver issues [10], skin disorders [11, 12], and respiratory symptoms [11-16]. A tragic example of the severe consequences of mould exposure occurred in December 2020, when Awaab Ishak, a two-year-old child, died due to a severe respiratory condition caused by prolonged exposure to mould in his home. An inquest led by a coroner concluded that the mould problem had not been adequately treated and prevented [17, 18]. Wang [19] evaluated the relationship between home environmental factors and respiratory conditions, such as asthma and rhinitis, among adults in Sweden and China, identifying dampness and mould as the primary risk factors. Similarly, Urlaub et al. [20] highlighted that unhealthy living environments, characterised by dampness and mould, lead to illnesses and associated costs, including medication expenses, employee sick leave, and hospital admissions. Over 80 million people in Europe live in homes affected by dampness [20, 21], suggesting a substantial opportunity for cost savings in healthcare.

The detrimental effects of moisture-related problems are also significant regarding building damage and the associated costs. Kayll [2] highlighted the substantial costs of rebuilding building envelopes due to water infiltration. For instance, water infiltration issues in multi-family wood-frame buildings between 1993 and 2000 caused approximately one billion Canadian dollars in damage. In Belgium, watertightness issues accounted for nearly 50% of all documented building damage

cases between 2010 and 2015, with water penetration through the building envelope being the most prevalent damage cause [22]. Rain-penetrating building envelopes accounted for 64% of housing repairs costs reported in France from 2018 to 2020 [23]. Sweden has faced comparable challenges, particularly with a particular type of external thermal insulation composite wall system (ETICS) installed in approximately 17,000 to 27,000 buildings constructed before 2007 [24]. These wall systems were highly susceptible to moisture, with around 55% of the buildings affected by mould-related damage in at least one exterior wall [24, 25]. The estimated cost of repairing these damaged walls was approximately 2.5 to 2.9 billion euros [24]. These examples illustrate the critical need for moisture-safe building designs to mitigate economic losses and enhance the durability of structures.

More than 30% of single-family homes in Sweden have been estimated to have mould and other moisture-related problems [26]. In the Gothenburg region, 60–80% of single-family houses with cold attics have been impacted by microbial growth, further emphasising the severity of the problem [27, 28]. In order to reduce moisture-induced damages and their associated health risks, Swedish building regulations (BBR) [29] necessitate moisture-safe building designs. Effectively addressing these issues necessitates accurate predictions and the development of robust mitigation strategies. The effective method for this aim is hygrothermal analysis, which models the interaction of heat, air, and moisture in building assemblies. Originating in the 1930s [30], hygrothermal analysis has undergone substantial advancements in accuracy, reliability, and computational robustness over the past few decades [31-39]. These developments have positioned hygrothermal analysis as an essential method for ensuring moisture-safe and durable building designs.

In the field of building physics, the deterministic approach has traditionally been the dominant approach for analysing building performance [40]. This method treats input parameters—such as material properties, outdoor and indoor climates, and geometric configurations—as fixed, discrete values. While deterministic models are simple and computationally efficient, they fail to account for the inherent uncertainties associated with real-world scenarios, such as variations in material properties or fluctuations in environmental conditions. As a result, deterministic approaches often produce a single or limited set of outcomes, which may inadequately capture the variability and risks present in building performance [41].

By contrast, probabilistic modelling considers input parameters stochastic variables, representing their inherent uncertainties through probability distributions [42]. This approach generates a range of potential outcomes, offering a more comprehensive understanding of design performance [43]. Probabilistic methods also allow quantifying failure probabilities, providing critical insights for risk assessment and informed decision-making [44]. For instance, when evaluating the risk of moisture-related problems in external walls, probabilistic modelling can account for variations in material characteristics, outdoor and indoor climates, boundary

conditions, and geometric factors—parameters that significantly influence the analysis outcomes. This capability makes probabilistic approaches vital for developing a robust moisture-safe design under diverse and uncertain conditions.

Probabilistic methods, particularly those employing Monte Carlo simulations, often require thousands of iterations to capture the variability and uncertainties in building performance [45]. While straightforward, probabilistic methods can be computationally intensive, posing significant challenges in fields such as hygrothermal analysis, where simulations are inherently transient and highly complex [46]. To address these computational challenges, researchers have increasingly turned to metamodels to develop predictive models for hygrothermal performance assessment of buildings while significantly reducing computational effort [47-50]. Despite their potential to significantly enhance computational efficiency, metamodels have inherent limitations. Their accuracy and reliability heavily depend on the training dataset's quality and diversity. Poorly trained metamodels may yield misleading results, introducing errors that could compromise design decisions and risk assessments. Therefore, achieving a balance between efficiency and accuracy is essential when integrating metamodels into hygrothermal performance analysis for buildings.

1.2 Objectives and research questions

The primary aim of this thesis is to develop a probabilistic methodology to support decision-making for designing sustainable and moisture-safe building envelopes. A key focus of the study is using bio-based materials to address pressing sustainability concerns, including environmental impacts and resource efficiency. The research seeks to enhance the understanding and assessment of moisture safety performance in building envelopes and contribute to advancing hygrothermal analysis techniques. While particular emphasis is placed on wall assemblies incorporating bio-based materials, the methodologies presented are also intended to be broadly applicable to other construction materials. This research aims to aid in identifying critical factors influencing moisture safety, thereby supporting the development of a comprehensive framework for sustainable and moisture-safe building envelope design. The ultimate goal is to bridge the gap between probabilistic hygrothermal analysis and practical decision-making frameworks, ensuring that sustainable construction practices are scientifically grounded and practically feasible. To achieve these objectives, the thesis addresses the following specific research questions:

Q1- What are the latest progress in probabilistic hygrothermal assessment (PHA)? What are the gaps? What potential methods and uncertain variables should be considered during PHA?

Q2- How can the robustness and effectiveness of PHA be improved using novel methods such as artificial intelligence (AI) algorithms?

Q3- How can PHA be utilised to investigate the influence of workmanship uncertainties on moisture-related issues?

Q4- How can PHA be applied to examine the impact of wind-driven rain (WDR) loads and varying water penetration criteria on the hygrothermal performance of external walls?

Q5- How can the outputs of PHA be integrated into a decision analysis framework to support sustainability assessments in practical applications?

Q6- How do various hygroscopic insulations influence the risk of mould growth when applying the PHA methodology under Swedish climatic conditions?

By addressing these questions, the research aims to provide actionable insights for the development of moisture-safe, durable, and sustainable building envelope design, contributing to the field of building physics and advancing sustainable construction practices.

1.3 Research methodology

This PhD project was initiated with a comprehensive literature review of studies on PHA. A state-of-the-art review was conducted to map the latest advancements and identify existing research gaps. Figure 1 illustrates the research methodology workflow and corresponding appended papers coupled with the research questions outlined in Section 1.2. This initial step also involved a conceptual review of uncertainty propagation and sensitivity analysis (SA) methods, providing the foundation to address the first research question (Q1).

The subsequent stages of the research utilised advanced numerical analyses to explore and address the remaining research questions. A probabilistic hygrothermal simulation framework was developed using computational tools, with Delphin 6.1—a widely used software for hygrothermal simulation—automated through Python scripting. This automation enabled the execution of hundreds of thousands of simulations, significantly enhancing computational efficiency. The advanced PHA methodology was subsequently integrated with mould growth risk assessment. Given the high acceptance and broad applicability of the Finnish mould growth model, it has been chosen as the primary mould damage assessment tool for this PhD research. The implementation of this mould model is achieved using Python-based programming. Following this, novel metamodeling techniques were explored. Drawing on insights from the literature review, various machine learning (ML) algorithms and statistical methods were tested, with the random forests (RF) ML

algorithm ultimately selected due to its superior performance. This stage specifically addressed Q2 by improving the robustness and time efficiency of the simulation process.

The developed AI-based probabilistic hygrothermal analysis method was then applied to examine uncertainties related to workmanship, including the effects of water penetration criteria and variations in WDR loads. During this phase, the methodology was further refined to enhance sampling efficiency and overcome extrapolation challenges, thereby addressing Q3 and Q4.

Incorporating sustainability aspects, the finalised methodology integrated economic and environmental impact assessments into a decision analysis framework. This integration facilitated practical applications of the research, providing a comprehensive tool for sustainability assessments and addressing Q5.

To address Q6, various insulation materials with different hygroscopic properties—including bio-based and fossil-based options—were investigated to evaluate their hygrothermal responses. This analysis aimed to identify optimal solutions for minimising moisture-related risks while ensuring robust and sustainable building envelope designs under Swedish climatic conditions.

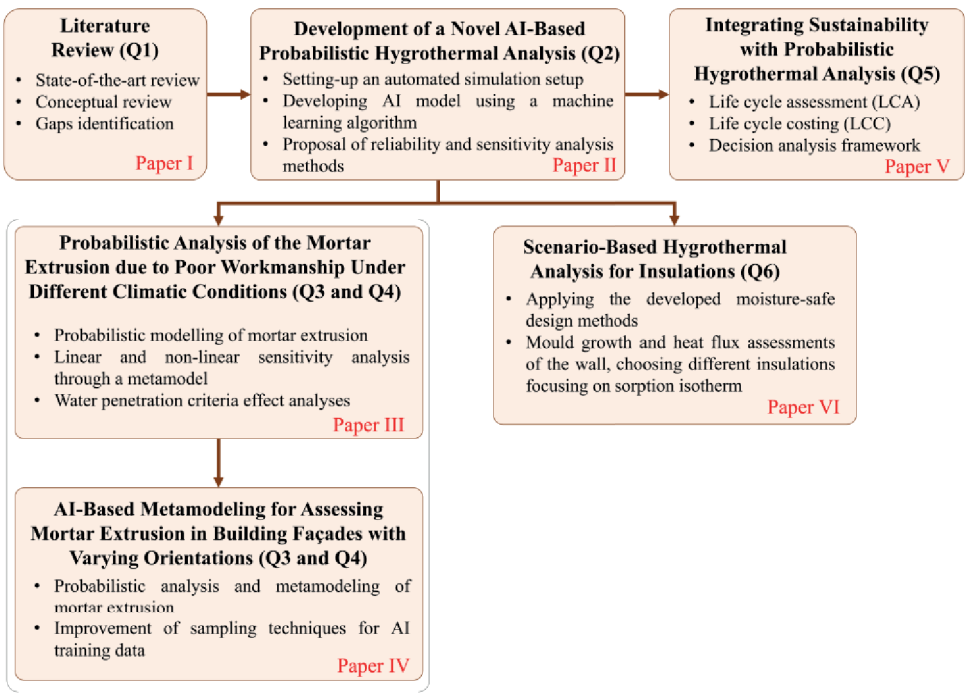


Figure 1: Research methodology workflow and corresponding appended papers.

1.4 Limitations

A general limitation of this thesis lies in excluding specific building usage scenarios that could significantly influence the indoor climate. This limitation is particularly relevant for case studies addressing indoor surface moisture issues, such as those discussed in *Paper II*. Furthermore, the research primarily focuses on Swedish climate conditions and includes case studies with specific assumptions. Consequently, while the numerical results may not be directly generalisable to other climatic regions or building types, the methodologies and approaches developed in this thesis remain broadly applicable across diverse building usages and geographic locations.

In *Papers II and V*, the primary objective was to introduce methodological frameworks rather than to conduct exhaustive hygrothermal performance analyses. Certain variables were excluded to simplify the modelling processes. For instance, uncertainties related to indoor and outdoor climatic conditions were not accounted for. Paper II omitted the WDR penetration through façades from the hygrothermal model. Incorporating these factors would enhance the accuracy of simulations, particularly for assessing moisture performance in internal wall layers, such as timber studs. Although probabilistic modelling addressed some moisture safety uncertainties in Paper V, other limitations persist, such as the reliance on 1D modelling, which overlooks multidimensional moisture transport phenomena (the same for *Papers II and VI*). Additionally, the life cycle assessment (LCA) and life cycle costing (LCC) analyses did not account for uncertainties associated with environmental product declarations (EPDs), inflation rates, and interest rates.

Papers III and IV also include assumptions that, while necessary for the scope of the analyses, introduce limitations. For instance, the extruded mortar layer was modelled as consistently absorbing and retaining rainwater penetration. However, real-world scenarios are more complex, often involving mechanisms such as dripping droplets and rainwater runoff within air gaps. These dynamics, which could alter moisture accumulation and distribution, were not fully captured in the current model. Moreover, the study employed a uniform distribution model to represent moisture sources, assuming even moisture penetration across the extruded mortar layer. This simplification may not accurately reflect the reality of moisture ingress, which might occur as concentrated or point sources, potentially leading to variations in moisture performance based on specific building envelope configurations.

1.5 Outline of the thesis

This section is an outline of the seven chapters that structure the thesis. The appended papers on which this thesis is based are provided at the end. While the

chapters synthesise the main findings from these papers, readers are encouraged to refer to the original publications for a more comprehensive understanding of the methodologies and results.

Chapter 2: Hygrothermal Analysis Fundamentals

This chapter presents the fundamental theory for hygrothermal analysis used in this study. The governing equations for energy and moisture mass balance, as implemented in this thesis, are detailed. Additionally, this chapter explains how Delphin performs hygrothermal analysis, detailing the scientific formulations and principles underlying its computational processes. The chapter also discusses damage models relevant to hygrothermal analysis, focusing on mould growth assessment.

Chapter 3: Probabilistic Hygrothermal Analysis

This chapter covers the fundamentals of PHA. It begins with an overview of uncertainty propagation techniques, followed by a detailed explanation of the methods applied in this research. Key findings related to uncertainty propagation and their implications for reliability analysis are discussed. The chapter also presents the hygrothermal sensitivity analysis (HSA) methods developed during this study, highlighting linear and non-linear correlations. Furthermore, it introduces an AI-based metamodel built using machine learning algorithms and its application to reliability analysis and the associated findings.

Chapter 4: Integration of Sustainability and Probabilistic Hygrothermal Analysis

This chapter integrates sustainability considerations into AI-based probabilistic hygrothermal analysis. Environmental impacts are assessed using the LCA methodology, while economic impacts are evaluated through LCC. The chapter details how LCA and LCC outputs are combined with hygrothermal analysis results to form a decision analysis framework. Integrating these approaches aims to provide a holistic view of moisture-safe building design's environmental and economic implications.

Chapter 5: Conclusions and Summary of Findings and Implications

This chapter summarises the main findings of the research and discusses their broader implications. It evaluates how the research successfully addressed the aims and research questions outlined in Chapter 1. Additionally, it reflects on the applicability of the developed methods and their potential impact on advancing moisture-safe and sustainable building design.

Chapter 6: Future Research Directions

This chapter identifies potential areas for future research in the field of PHA and moisture safety design. Suggestions include exploring advanced modelling techniques, considering medical disciplines coupled with hygrothermal analysis,

and integrating energy performance and structural analysis into the developed methods to enhance prediction accuracy and robustness.

Chapter 7: Summary of Appended Papers

The final chapter summarises the appended papers and their key findings. It highlights the individual contributions of each paper to the overall research objectives. This chapter serves as a clear overview of the body of work conducted throughout this PhD project, emphasising how each study aligns with and contributes to the thesis as a whole.

2 Hygrothermal analysis theory for the building envelope

The core focus of this thesis is hygrothermal analysis, making it essential to understand the fundamental concepts underlying the associated calculations and simulations. This chapter begins with a brief overview of the history of hygrothermal analysis, followed by a detailed explanation of the fundamental theories employed in the analyses conducted in this thesis. Additionally, the chapter explains the damage models used as post-processors for hygrothermal analysis outputs, with particular emphasis on mould growth models.

2.1 Background

Hygrothermal modelling plays a crucial role in evaluating the energy, moisture, and air balances of building envelopes. The hygrothermal performance of a building component is influenced by the transfer of heat, air, and moisture (HAM) between the indoor and outdoor environments and through the building envelope. According to Hens [30], the origins of hygrothermal analysis date back to the mid-1930s, initially focusing on condensation [51]. This interest emerged when insulating cavities in timber-framed envelopes became common practice, leading to early reports of paint peeling on exterior sheathing. This phenomenon provoked concerns that insulation might attract moisture to exterior layers, fostering the perception that it should not be used [30].

Despite these initial doubts, experts in the field proposed solutions to mitigate condensation-related issues. Teesdale [52] introduced placing a vapour barrier on the insulation's warm side and ensuring proper attic ventilation. By plotting the temperature curve across a wall section and comparing it with the dew point indoors, one could predict condensation risk if the dew point intersected the temperature curve within the insulation layer (Figure 2, middle). Roger [53] supported this solution, noting that condensation occurs only when the partial water vapour pressure exceeds the water vapour saturation pressure, as illustrated in Figure 2, right side.

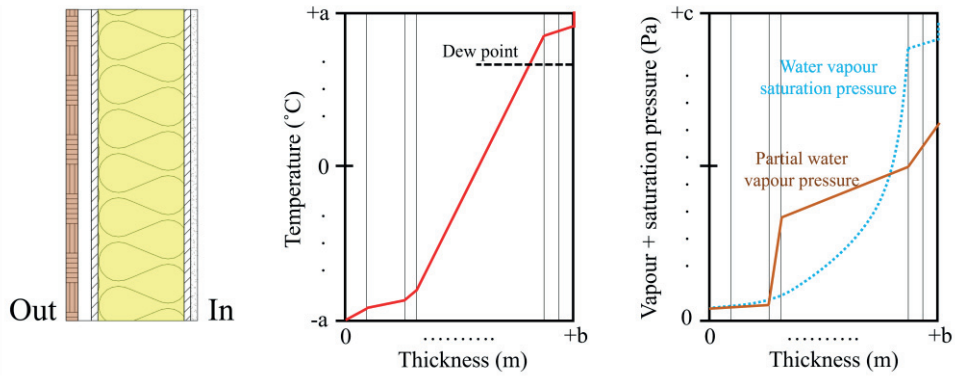


Figure 2: *Left:* Timber frame wall, *Middle:* dew point vs temperature, *Right:* partial water vapour pressure vs water vapour saturation pressure. Intersections mean interstitial condensation.

A significant milestone was achieved by Glaser in the 1950s [54], who introduced a method combining vapour diffusion and heat conduction under steady-state conditions [30]. This approach, often referred to as the "dew point method" [55], provided a framework for manual analysis of surface condensation in building materials [6]. However, its reliability was limited by the absence of moisture transportation mechanisms, such as capillary liquid transport and moisture-dependent hygrothermal functions in porous building materials [6].

Subsequent advancements addressed these limitations by incorporating models for air transport [56, 57], indoor climate classifications [58, 59], reference-year outdoor climate data [30], WDR effects [60-63], capillary suction (liquid transport) [64], and convection flow effects on heat and moisture transport [65]. These enhancements significantly improved the accuracy of hygrothermal analysis by integrating essential physical phenomena [30]. By the 1990s, however, most national building codes and standards offered limited guidance on HAM performance. To address this, 14 countries collaborated from 1991 to 1996 under Annex 24, a project dedicated to studying the physics of HAM transport in highly insulated envelopes and assessing its impact on durability [66, 67].

The rapid growth in computational power since the 1990s has facilitated the development of advanced hygrothermal simulation tools. The recent advanced ones employ finite element methods to solve partial differential equations governing heat, moisture, and air transport. They enable transient, multidimensional simulations of composite building assemblies [31, 68]. A comprehensive review of the hygrothermal simulation tools can be found in [69, 70]. The outputs of these tools serve as inputs for a wide range of moisture-related damage models, which are used as post-processors to assess potential durability issues.

2.2 Numerical hygrothermal analysis

A comprehensive state-of-the-art literature review conducted at the outset of this PhD project [71] revealed statistics regarding hygrothermal simulation tools employed in PHA. The tools identified for this purpose include Delphin [72], WUFI [73], HAM-Tools [74], NEV3 [75], HAMFEM [76], HAMBASE [77], 1D-HAM [78], EnergyPlus [79], hygIRC [80], COMSOL [81], and IDA ICE [82]. Delphin [72] and WUFI [73] are the most frequently utilised, likely due to their accessibility and user-friendly interfaces. Both tools have been validated in numerous studies [83, 84]. Delphin, however, offers a significant advantage over WUFI in its capacity for batch calculations. This functionality is particularly beneficial in PHA studies, where thousands of simulations are often required. Delphin substantially reduces computational time and enhances workflow efficiency by enabling simulation automation. Consequently, Delphin was selected as the primary hygrothermal simulation tool for this thesis. The following subsections present the governing equations used in hygrothermal simulations conducted with Delphin, providing a detailed understanding of the theoretical framework supporting the analyses performed in this research.

2.2.1 Moisture (mass) balance equation

The balance equation is fundamentally based on the principle that the rate of change in a conserved quantity over time must equal the sum of all incoming and outgoing fluxes, along with any source or sink production rates [85]. In the case of moisture, below 0 °C, the pores of a moist material can contain air, liquid water, vapour, ice, and, in some cases, dissolved salts and other substances. To simplify the analysis, salts and other substances are assumed to be absent. Above 0 °C, ice is no longer present, but air, liquid water, and water vapour remain. In the absence of ice formation, moisture primarily exists in the liquid water and water vapour phases. Consequently, the moisture mass balance equation represents a merged two-phase system. This equation accounts for changes in moisture content by incorporating two primary transport mechanisms: advection, driven by fluid flow, and diffusion, driven by concentration gradients and microscopic molecular movements. Mathematically, this relationship is expressed in Eq. (1):

$$\frac{\partial \rho^{m_{l+v}}}{\partial t} = -\frac{\partial}{\partial x_k}\left[j_{k,diff}^{m_v} + j_{k,adv}^{m_v} + j_{k,adv}^{m_l}\right] + \sigma^{m_{l+v}} \quad (1)$$

Where:

- $\rho^{m_{l+v}}$: Total moisture density [kg/m^3], where l and v denote liquid and vapour phases, respectively,

- t: Time in differential equations, which represents changes in the conserved quantity over time,
- x_k: Spatial coordinate in the k direction, representing changes in the conserved quantity over space,
- $j_{k,diff}^{m_v}$: Diffusive flux of water vapour [kg/(m^2.s)],
- $j_{k,adv}^{m_v}$: Advective flux of water vapour [kg/(m^2.s)],
- $j_{k,adv}^{m_l}$: Advective flux of liquid water [kg/(m^2.s)],
- $\sigma^{m_{l+v}}$: Source or sink term representing moisture production or removal within the system [kg/(m^3.s)].

The differentiation between vapour and liquid phases and their respective flux mechanisms ensures the model captures a wide range of moisture transport phenomena, offering accurate insights into moisture accumulation, transportation, and removal within building envelopes.

2.2.1.1 Diffusive flux of water vapour

The diffusive flux of water vapour, $j_{k,diff}^{m_v}$, represents the movement of water vapour driven by concentration gradients, a process referred to as diffusion. Water vapour naturally migrates from regions of higher concentration to regions of lower concentration. Under isobaric conditions, this process is governed by Fick's law [86], which describes diffusion as proportional to the gradient of vapour pressure, P_v. For free air, the diffusive flux of water vapour can be expressed by Eq. (2) [86]:

$$j_{k,diff}^{m_v} = -\frac{D_{v,air}}{R_v.T_a}.\frac{\partial P_v}{\partial x_k} \quad (2)$$

Where:

- T_a: Ambient air temperature [K],
- R_v: Constant of water vapour [J/(kg·K)],
- $D_{v,air}$: Vapour diffusivity in still air [m^2/s].

Schirmer [86] provides an empirical expression for vapour diffusivity in still air as a function of ambient air temperature, T_a, and ambient air pressure, P_a, given by Eq. (3):

$$D_{v,air} = \frac{2.26173}{P_a}.\left(\frac{T_a}{273.15}\right)^{1.81} \quad (3)$$

At 1 atmosphere (1 bar, 101,300 Pa) of moist air, this relationship is as Eq. (4):

$$D_{v,air} = 8.69 \times 10^{-10} {T_a}^{1.81} \quad (4)$$

In porous materials, water vapour diffusion is significantly hindered due to the tortuosity and reduced porosity of the material. This resistance is characterised by the vapour diffusion resistance factor, μ, which quantifies the material's resistance to vapour diffusion relative to still air. In essence, μ indicates how many times slower vapour diffuses through a material compared to air. Thus, the vapour diffusion coefficient in porous material, $D_{v,mat}$, is calculated using Eq. (5):

$$D_{v,mat} = \frac{D_{v,air}}{\mu} \quad (5)$$

By substituting Eq. (5) into Eq. (2), the diffusive flux of water vapour within a porous material can be calculated based on Eq. (6):

$$j_{k,diff}^{m_v} = -\frac{D_{v,air}}{\mu.R_v.T_a} \cdot \frac{\partial P_v}{\partial x_k} \quad (6)$$

2.2.1.2 Advective flux of water vapour

The advective flux of water vapour, $j_{k,adv}^{m_v}$, describes the transport of water vapour due to air movement. This mechanism is critical for understanding moisture transport in scenarios where air infiltration or ventilation plays a significant role, particularly in building envelopes with high air infiltration or in cases involving significant air pressure differences across components. This flux is calculated by the advective flux of the gas phase and the concentration of water vapour mass in the gas phase, as expressed in Eq. (7) [85]:

$$j_{k,adv}^{m_v} = \rho_g^{m_v} . j_{k,adv}^{m_g} \quad (7)$$

Where:

- $\rho_g^{m_v}$: Water vapour mass concentration in the gas phase [kg/kg], representing the mass fraction of water vapour in the gas phase,
- $j_{k,adv}^{m_g}$: Advective flux of gas phase [kg/(m^2.s)], which quantifies the rate at which air moves through a given area (further detailed in Section 2.2.3.2).

2.2.1.3 Advective flux of liquid water

The advective flux of liquid water, $j_{k,adv}^{m_l}$, represents the movement of liquid water within a porous material driven by bulk motion, similar to the principles described by Darcy's law [87]. This flux quantifies the rate at which liquid water is transported, primarily influenced by pressure gradients. Under the assumption of isobaric conditions in the gas phase and no positive liquid water pressure, the

advective flux can be expressed as a product of liquid water conductivity and the primary driving forces: the capillary pressure gradient, $\frac{\partial P_c}{\partial x_k}$, and gravitational force, $\rho_l . g_k$. The relationship is given by Eq. (8) [85]:

$$j_{k,adv}^{m_l} = K_l(\theta_l).\left[\frac{\partial P_c}{\partial x_k} + \rho_l . g_k\right] \quad (8)$$

Where:

- $K_l(\theta_l)$: Liquid water conductivity [s], strongly dependent on the pore structure and moisture content level, θ_l [m^3/m^3]), and the temperature,
- ρ_l: Liquid water density [kg/m^3],
- g_k: Gravitational acceleration [m/s^2],
- P_c: Capillary pressure [Pa].

If extra liquid pressure is present, then it should be added to the capillary pressure and the total liquid pressure, P_l, instead of capillary pressure, P_c, should be used.

The advective flux of liquid water, $j_{k,adv}^{m_v}$, can be also described by moisture content as the motive potential and liquid water diffusivity, $D_l(\theta_l)$, as shown in Eq. (9) [85]:

$$j_{k,adv}^{m_l} = -\rho_l . D_l(\theta_l).\left[\frac{\partial \theta_l}{\partial x_k}\right] \quad (9)$$

Where:

- $D_l(\theta_l)$: Liquid water diffusivity [m^2/s], which depends on the material's pore structure and moisture content level (θ_l [m^3/m^3]),
- ρ_l: Liquid water density [kg/m^3].

Determining liquid water diffusivity, $D_l(\theta_l)$, typically requires a moisture content profile, which can be obtained through water absorption or drying tests. However, these methods can be time-consuming and complex due to the transient nature of moisture content profiles [88]. Advancements in non-destructive techniques have enabled more efficient measurement of moisture content profiles, which are essential for estimating liquid water diffusivity [88]. Despite these technological improvements, the experimental determination of liquid water diffusivity remains challenging. To address this, researchers have proposed simplified approaches to approximate $D_l(\theta_l)$, reducing the need for extensive laboratory testing while maintaining reasonable accuracy [85].

Capillary pressure (P_c)

In pores containing both air and water, capillary action arises from the interactions between water molecules (cohesion), the reduced cohesion at the air interface, and the adhesion between water molecules and the pore walls. This interplay is influenced by the surface tension of water, γ [N/m], which decreases with increasing temperature. When water contacts air, the pores affect the capillary behaviour through the contact angle, α. For hydrophilic materials, such as most stone and wood-based materials, adhesion to the pore wall exceeds the attraction to air. This results in a contact angle between 0° and 90°, causing the meniscus to creep up along the pore wall (Figure 3, left) [86]. Conversely, in hydrophobic materials, such as certain synthetic materials or water-repellent surfaces, wall adhesion is weaker than air attraction, producing a contact angle between 90° and 180° and pushing the meniscus away from the pore wall (Figure 3, right) [86]. Capillary pressure can be described by the Young-Laplace equation, which relates the capillary pressure to the surface tension of water, γ [N/m], the contact angle, α, and the capillary radius r [m], given in Eq. (10):

$$P_c = \frac{2\gamma.\cos\alpha}{r} \tag{10}$$

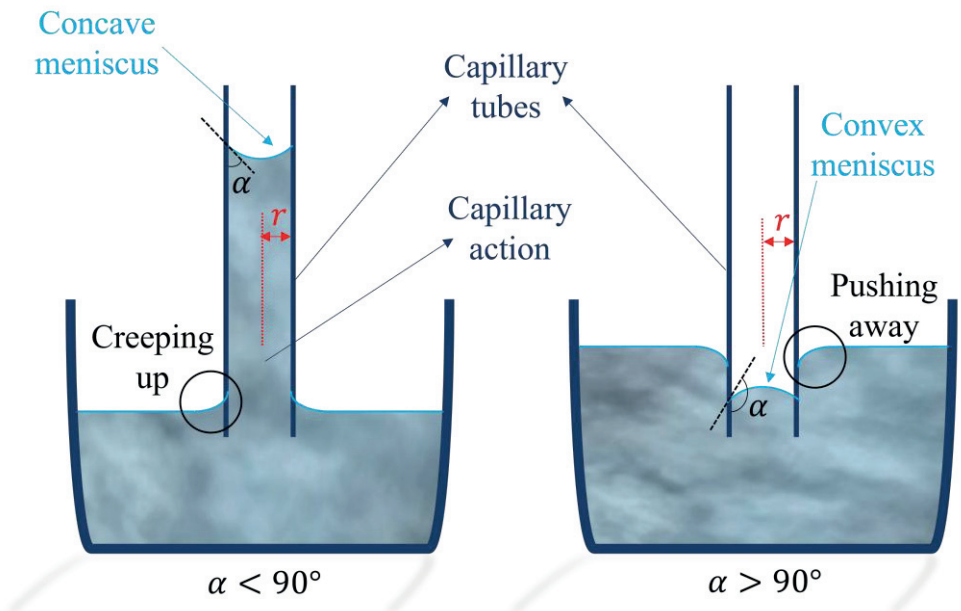


Figure 3: Capillary phenomena in cylindrical capillaries (schematic drawing). *Left:* Water creeps up the pore wall, giving a contact angle of 0° to 90°. *Right:* Water is pushed away from the pore wall, giving a contact angle of 90° to 180°.

2.2.2 Energy balance equation

The energy balance equation describes energy transfer within a material element, accounting for multiple heat and mass transfer mechanisms. These include conductive heat flux, energy transported by advective fluxes of liquid water and gas (including dry air and water vapour), and vapour diffusion flux. Additionally, external energy sources or sinks are incorporated. The general energy balance equation governing heat transfer in hygrothermal analysis is expressed in Eq. (11) [85]:

$$\frac{\partial \rho^u}{\partial t} = -\frac{\partial}{\partial x_k}\left[j^Q_{k,cond} + (h_v - h_a).j^{m_v}_{k,diff} + h_l.j^{m_l}_{k,adv} + h_g.j^{m_g}_{k,adv}\right] + \sigma^u \quad (11)$$

Where:

- ρ^u: Internal energy density [J/m^3], representing the total energy stored within the material per unit volume,
- $j^Q_{k,cond}$: Conductive (diffusive) heat flux [J/(m^2.s)],
- $j^{m_g}_{k,adv}$: Advective flux of gas phase [kg/(m^2.s)] (explained in detail in section 2.2.3.2),
- h_v, h_l, h_a, and h_g: Specific enthalpies of water vapour, liquid water, dry air, and gas phase, respectively [J/kg],
- σ^u: Source or sink of energy [J/(m^3.s)], representing external energy inputs (e.g., condensation heating) or losses (e.g., evaporation cooling).

2.2.2.1 Conductive heat flux

The conductive heat flux, $j^Q_{k,cond}$ (or q_x) represents heat transfer through a material due to its thermal conductivity. This process is described by Fourier's law of heat conduction, introduced by the French physicist Fourier in 1822 [86]. The law states that conductive heat flux is directly proportional to the temperature gradient within the material. The mathematical expression for this relationship is provided in Eq. (12):

$$q_x = -\lambda \frac{\partial T}{\partial x} \quad (12)$$

Where:

- λ is the thermal conductivity [W/(m.K)], a measure of the material's ability to conduct heat.
- T is temperature [K].

This equation is a vector relation, indicating that the conductive heat flux varies proportionally to the temperature gradient. The negative sign reflects the thermodynamic principle that heat naturally flows from regions of higher temperature to lower temperature regions unless acted upon by external forces. Thermal conductivity, λ, varies depending on the material type and its moisture content. In hygrothermal analyses, the impact of moisture on thermal conductivity is critical, as the presence of moisture can significantly alter heat transfer rates within porous building materials.

2.2.2.2 Energy flux due to mass flow

Section 2.2.2.1 focused on conservation laws in systems without mass flow. This section expands the scope to porous media where air, liquid water, and water vapour are in motion, contributing to energy transfer through enthalpy flows. Enthalpy is a thermodynamic measure that captures the total energy within a system, encompassing both its internal energy and the energy exchanged with its surroundings through work. The specific enthalpy, defined as the energy per unit mass, provides a practical framework for modelling energy fluxes associated with different phases in porous materials. For hygrothermal processes, the energy flux resulting from mass flow is calculated by incorporating the specific enthalpy of each phase. Eq. (13-15) for the specific enthalpies of water vapour, h_v, liquid water, h_l, and dry air, h_a, are given as follows [86]:

$$h_v = c_{p,v}\left(T - T_{ref.}\right) + h_{evap.} \tag{13}$$

$$h_l = c_{p,l}\left(T - T_{ref.}\right) \tag{14}$$

$$h_a = c_{p,a}\left(T - T_{ref.}\right) \tag{15}$$

Where:

- $c_{p,v}$, $c_{p,l}$, and $c_{p,a}$: Specific heat capacities of water vapour, liquid water, and dry air, respectively [J/(kg.K)],
- T: Current temperature of the system [K],
- $T_{ref.}$: Reference temperature [K],
- $h_{evap.}$: Latent heat of evaporation at 0°C, equal to 2,500,000 J/kg [86] (energy required to transition water from its liquid phase to vapour).

2.2.3 Air (gas) balance equation

The air mass balance equation describes the relationship between the rate of change in the mass density of dry air and the combined effects of advective flux, the diffusive flux of water vapour, and sources or sinks of dry air. This relationship is mathematically described in Eq. (16) [86]. The inclusion of vapour diffusion in the air mass balance equation is essential because it impacts the spatial distribution of dry air via a process known as counter-diffusion. When water vapour migrates into a region, it displaces dry air, which moves in the opposite direction to maintain mass conservation. As a result, the magnitude of the diffusive flux for dry air equals that of water vapour but acts reversely.

$$\frac{\partial \rho^{m_a}}{\partial t} = -\frac{\partial}{\partial x_k}\left[j_{k,adv}^{m_a} - j_{k,diff}^{m_v}\right] + \sigma^{m_a} \tag{16}$$

Where:

- ρ^{m_a}: Mass density of dry air [kg/m^3],
- $j_{k,adv}^{m_a}$: Advective flux of dry air [kg/(m^2.s)],
- σ^{m_a}: Source or sink of dry air [kg/(m^3.s)].

2.2.3.1 Advective flux of dry air

The advective flux of dry air, $j_{k,adv}^{m_a}$, quantifies the dry air transport caused by the gas phase's bulk motion. This flux is calculated as the product of the dry air mass concentration within the gas phase and the advective flux of the gas phase itself. The relationship is described mathematically in Eq. (17):

$$j_{k,adv}^{m_a} = \rho_g^{m_a} . j_{k,adv}^{m_g} \tag{17}$$

Where:

- $\rho_g^{m_a}$: The dry air mass concentration in the gas phase [kg/kg], representing the proportion of dry air in the gas phase,
- $j_{k,adv}^{m_g}$: The advective flux of gas phase [kg/(m^2.s)].

2.2.3.2 Advective flux of gas phase

The advective flux of the gas phase, $j_{k,adv}^{m_g}$, is determined by the gradient of gas pressure, $\frac{\partial P_g}{\partial x}$, and the permeability of the gas phase, K_g [s], referred to as the gas advective coefficient. Additionally, the buoyancy and gravitational effects on the gas phase are accounted for by the term, $\rho_g . g_k$, which incorporates the mass density

of the gas and gravitational acceleration. The relationship between these parameters is described in Eq. (18):

$$j_{k,adv}^{m_g} = -K_g \cdot \left[\frac{\partial P_g}{\partial x} + \rho_g \cdot g_k\right] \quad (18)$$

Where:

- P_g: Gas partial pressure [Pa],
- ρ_g: Gas mass density [kg/m^3],
- g_k: Gravitational acceleration [m/s^2].

2.2.4 Boundary conditions

2.2.4.1 Surface heat transfer coefficient

Heat transfer at the internal and external surfaces of building elements, such as walls and roofs, is a crucial process influenced by both convective and radiative exchanges with the surrounding environment. In Delphin, the convective heat exchange coefficient quantifies the energy transfer rate between the building element's surface and the ambient air, typically driven by air movement. According to ISO 15026 [89], the recommended convective heat exchange coefficient for typical building assemblies is 12 W/(m^2·K), while assemblies exposed to higher wind conditions may require a coefficient of 20 W/(m^2·K) as suggested by [90]. In addition to convection, the radiation heat exchange coefficient accounts for thermal radiation exchanges between the surface of the building element and surrounding surfaces, such as the sky or nearby surfaces, primarily due to long-wave radiation. In Delphin, this term is generally neglected if long-wave radiation exchange is accounted for separately in the model. For interior surfaces, Delphin defaults to a value of 8 W/(m^2·K) for the heat transfer coefficient (convective + radiative) [72]. Together, these coefficients determine the overall heat exchange rate, which directly influences the thermal energy balance of the building element. This ensures the modelling of the surface's response to external temperature changes and varying environmental conditions.

2.2.4.2 Surface vapour diffusion exchange coefficient

The vapour diffusion mass transfer coefficient at the internal and external surfaces of building envelope components is driven by vapour concentration differences between the surrounding air and the building material. This coefficient quantifies the rate at which water vapour is exchanged between the surface of the wall and the surrounding air. According to ISO 15026 [89], the typical outdoor surface vapour diffusion coefficient value is 7.5×10^{-8} s/m. Additionally, the S_d-value, representing

the vapour diffusion resistance of surface coatings or paints, can be specified. An S_d-value of 0 m indicates no resistance, allowing unhindered vapour exchange through the surface. For typical paints or coatings, the S_d-value is usually set to 5 m [72]. Delphin's default value for interior surfaces' vapour diffusion coefficient is 2.5×10^{-8} s/m, which reflects typical indoor conditions [72].

2.2.4.3 Wind-driven rain (WDR)

WDR, the combined effect of wind and rain, is recognised as a significant moisture source that can damage building façades, impacting both hygrothermal performance and durability [91-96]. When studying the effects of WDR on buildings, key factors such as rain intensity, wind speed, and the characteristics of the building itself are considered. WDR occurs when wind forces raindrops to strike external surfaces, leading to moisture penetration. The BS 8104 standard [97], initially developed after extensive measurements of WDR across various UK buildings and locations, was the foundation for more generalised models. The ISO model [98], based on BS 8104, was established to provide a broader framework for quantifying the rate at which WDR impacts building façades. Delphin uses the ISO standard (DIN EN ISO 15927-3) [98] due to its comprehensive approach, which incorporates various microclimate parameters influencing WDR deposition. These factors include terrain characteristics, topography, obstacles, and the WDR distribution on building's wall, as described by Eq. (19):

$$I_{WDR} = \left(\frac{2}{9}\sum w_s \,.\, R_h{}^{\frac{8}{9}}.\cos(D-\theta)\right).C_R.C_{TP}.O.W \tag{19}$$

Where:

- I_{WDR}: WDR intensity [mm/h],
- w_s: Reference wind speed (unobstructed streamwise wind speed at 10 m height) [m/s],
- R_h: Rainfall rate on the horizontal plane [mm/h],
- D: Hourly mean wind direction from north [°],
- θ: Wall orientation relative to the north [°],
- C_R: Roughness coefficient, accounting for terrain variations,
- C_{TP}: Topography coefficient, adjusting for wind speed increase over hills,
- O: Obstruction factor, representing the effect of obstacles in the path of wind,
- W: Wall factor, WDR distribution on the wall surface.

The roughness coefficient, C_R, is used to adjust the wind speed based on site-specific characteristics such as terrain and elevation. The coefficient depends on whether the site is above or below a defined minimum height. It classifies the area into four categories, ranging from rough open sea to urban areas with dense building coverage [98]:

I) Rough open sea; lake shore with at least 5 km open water upwind and smooth flat country without obstacles,

II) Farmland with boundary hedges, occasional small farm structures, houses or trees,

III) Suburban or industrial areas and permanent forests,

IV) Urban areas in which at least 15 % of the surface is covered with buildings of average height exceeding 15 m.

The topography coefficient, C_{TP}, addresses the increase in wind speed due to isolated hills, which can affect wind velocity as it moves over these features. This coefficient is particularly relevant for locations that are above the half height of the hill or within 1.5 times the height of a cliff from the ground.

The obstruction factor, O, reflects the presence of physical barriers, such as nearby buildings or trees, that reduce the intensity of WDR. This factor is determined by the horizontal distance from the wall to the nearest obstacle of comparable height. Potential changes, like the falling of trees in the development of a housing estate, should be considered while assessing the obstacles. The obstruction factor fluctuates between 0.2 and 1.0 based on the distance to the closest barrier. If the wind is funnelled toward the wall due to the specific surrounding layout and urban design, the obstruction factor is set to 1, even in the presence of obstacles.

The wall factor, W, adjusts the WDR model based on the characteristics of the wall, such as its height, overhangs, and roof shape. In most cases, the wall factor rises with increasing wall height and ranges from 0.2 to 0.5. The ISO Standard assumes the same wall factor across the wall's width, even though numerous WDR measurements show that the WDR intensity rises from the centre of the façade to the sides [99].

It is important to note that the ISO model [98] is not applicable in specific scenarios, such as mountainous regions with steep cliffs, areas experiencing frequent convective storms, or regions where snow constitutes a significant portion of precipitation. Additionally, the model has limitations [100]:

- The wall factor provides limited spatial variation information across the façade,
- The model primarily focuses on low-rise buildings, as it was initially developed with masonry wall configurations in mind.

Despite these limitations, the ISO model remains a valuable tool for assessing the impact of WDR on building façades and informing strategies to mitigate moisture-related issues in building design.

2.2.4.4 Solar radiations

Solar radiation is critical in hygrothermal analysis, influencing thermal and moisture dynamics within building envelopes. It is typically categorised into three types: direct, diffuse, and global radiation, with global radiation being the sum of direct and diffuse components. These elements are essential for accurately simulating energy exchanges between a building's surfaces and the surrounding environment.

Shortwave Radiation

Shortwave radiation, with wavelengths ranging from 0.1 μm to 4 μm, represents the energy received from the sun that directly impacts heat flow density on building surfaces. This interaction depends on the surface's inclination and orientation. Once solar radiation reaches a surface, it can be absorbed, reflected, or transmitted, with the outcome determined by the material properties of the surface. In Delphin, shortwave radiation is modelled by incorporating direct and diffuse solar radiation data imported from climate files. The solar absorption coefficient, a dimensionless value, is derived from the material's surface colour and texture as specified in Delphin's database [72]. The concept of albedo—a measure of surface reflectivity—is also considered. Albedo quantifies the fraction of incoming solar energy reflected by a surface, with values ranging from 0 (complete absorption) to 1 (complete reflection). For instance, an albedo of 0.3 indicates that 30% of solar radiation is reflected. The albedo of a building's surroundings, including the atmosphere, ocean, and land, significantly affects how much solar energy is absorbed or reflected, impacting the heat flow around the building envelope.

Longwave Radiation

Longwave radiation, in the wavelength range of 4 μm to 100 μm, involves electromagnetic and thermal radiation emitted by surfaces, the atmosphere, and clouds [101]. It governs the thermal radiation exchange between the building surface and its surroundings, particularly at night when surface temperatures decrease. Delphin assigns a longwave emissivity coefficient to model this exchange, which depends on the material's surface characteristics, such as colour and texture. Emissivity measures a material's ability to emit thermal radiation relative to a perfect black body with an emissivity of 1 (100%). Real-world materials typically have emissivity values between 0 and 1. A higher emissivity indicates that a surface emits more thermal radiation, influencing how heat scatters to the cooler night sky. This parameter plays a significant role in determining the surface temperature of building elements.

2.3 Durability and damage models

2.3.1 Durability

Durability, as defined by Isaksson et al. [1], refers to the ability of a structure to maintain its required performance throughout its intended service life while accounting for the effects of degradation processes. Among the various factors influencing durability, moisture-related damages are particularly significant. These damages include mould growth, decay, moisture-induced creep, and the weathering of wood, which can result in health problems, weaken building materials' structural integrity, and aesthetic issues. Some of these moisture-related damages have been mathematically modelled and are applied as post-processors to the outputs of hygrothermal simulations. Within the scope of this research, the primary emphasis is placed on mould growth, as it represents a critical area of investigation in this project. However, while not the primary focus, other types of moisture-induced damages are also discussed briefly in the subsequent subsections to provide a more comprehensive understanding of their impacts.

2.3.2 Mould growth

Mould growth on building materials and within building envelopes poses significant challenges due to its adverse health effects and aesthetic concerns. Key factors influencing mould growth include relative humidity levels, temperature, substrate type, and exposure duration. Secondary factors such as the presence of mould spores, pH, light, oxygen availability, and surface roughness also contribute but are less critical [102]. The complexity of mould growth increases further under fluctuating environmental conditions, which involve dynamic cycles of favourable and unfavourable periods alongside processes such as absorption, desorption, and condensation [103-105]. Material-specific characteristics, including sapwood or heartwood content, surface quality, finishing systems, wood treatments, and drying schedules, also significantly impact mould growth.

A review by Bayat Pour et al. [71] revealed that approximately half of PHAs incorporated mould growth models as post-processors to hygrothermal analysis outputs. About 30% of studies excluded moisture-related damage models, while the remaining 20% employed other types of damage models. These findings show the importance of mould growth as a critical degradation mechanism, which aligns with the findings from Labat and Woloszyn [106], who identified it as one of the most significant degradation mechanisms.

Efforts to mathematically represent mould growth have resulted in various mould assessment models widely applied in building engineering. These models assess mould growth over time to identify its occurrence and intensity under specific

conditions. A systematic review by Gradeci et al. [103] compared several mould models, including the mould germination graph [6], Finnish mould growth model [107], mould resistance design (MRD) [108], and m-model [109, 110]. The review also highlights the following key observations:

- Although many models incorporate similar governing factors, differences exist in their scope, limitations, and the weight assigned to each parameter,
- Several models employ comparable frameworks for mould prediction but differ in how they account for interdependencies and factor contributions to the final results,
- While all models share the common goal of predicting mould activity, they vary significantly in their methods of representation and evaluation,
- The outcomes of mould growth assessment using these models reveal both areas of agreement and divergence among several studies.

The Finnish mould growth model [107] has been identified as the most widely adopted approach in PHA, as highlighted by the state-of-the-art review conducted by Bayat Pour et al. [71]. This model was applied in 88% of the studies that incorporated mould growth as a post-processor for damage evaluation. In contrast, alternative mould models were used far less frequently in the reviewed publications. The widespread adoption of the Finnish mould growth model may be because it can be applied to a wide range of building materials. Incorporating sensitivity and decline classes effectively accounts for variations in surface types and coatings [107].

The Finnish mould growth model [107], derived from the VTT model [111, 112], serves as a robust framework for assessing mould development. The VTT model, an empirical approach created by Hukka and Viitanen [111, 112], employs differential equations to quantify mould growth dynamics. Its initial formulation was based on laboratory experiments conducted on pine and spruce sapwood [113], where the concept of critical RH, dependent on temperature, was introduced to define the threshold for mould germination. The model also incorporates the effects of unfavourable conditions that inhibit mould growth, representing these dynamics through a decrement in the mould growth index. To expand its applicability, the authors later introduced an improved version of the VTT model [112], which updated the coefficients to accommodate a broader range of building materials. Additionally, four sensitivity classes were established to cover the variability in material properties, as outlined in Table 1.

Table 1: Mould sensitivity classes according to the Finnish mould growth model [111, 112]

Sensitivity class		Description	Construction materials
Very sensitive	1	Untreated wood, which contains high amounts of nutrients.	Roughly sawn and dimensioned plank (pine, spruce and hardwood), planed pine, birch plywood, untreated porous wood fibre board, cardboard-surfaced gypsum board.
sensitive	2	Planed timber, materials and films with paper coating wood-based boards.	Planed spruce, paper-based bituminized/treated products and films, wood-based glued boards, pine or spruce plywood, bituminized/treated porous fibre board.
medium resistant	3	Cement or plastic-based materials, mineral wool.	Mineral wools, plastic-based materials, autoclaved aerated concrete, expanded-clay lightweight concrete, carbonated old concrete, cement-based products, bricks, cement bonded fibreboard, fibreglass-surfaced gypsum board.
resistant	4	Glass and metals, alkaline new concrete, products containing mould-preventive additives.	-

The duration of exposure to unfavourable conditions determines the decline in mould growth. If the exposure lasts less than six hours or exceeds 24 hours, a decrement in mould growth is accounted for. However, no decline occurs when the exposure duration falls within the 6-to-24-hour range [111]. It is important to note that the development of this mould decline model relied on a limited set of experimental data. Conditions such as temperatures below 0°C and extended unfavourable periods exceeding 14 days were excluded from the dataset [102]. Furthermore, the experiments verifying this model were conducted using daily or longer time intervals, with no data available at an hourly resolution [102]. Ojanen et al. [111] emphasised that incorporating hourly temporal resolution is crucial for capturing the dynamic variations in environmental conditions that significantly influence mould growth risk.

The risk of mould growth is quantified using the mould index, which ranges from 0 to 6, as detailed in Table 2. This index can serve as a design criterion, depending on the specific application of the study. According to [102], a mould index of 1 is commonly regarded as the maximum acceptable value, marking the onset of spore germination. This threshold aligns with the WHO guidelines [8], which stress the importance of preventing dampness and mould due to their adverse health effects. Preventing mould growth involves controlling environmental factors before spore germination begins, as outlined in [6]. Once germination occurs, mould hyphae and mycelia develop, allowing the mould to grow, spread, and access nutrients, even under conditions with limited surface moisture. As such, the mould germination point, corresponding to a mould index of 1 in the Finnish mould growth model [107], is considered the critical failure threshold for mitigating health risks. On the other hand, the American Society of Heating, Refrigerating, and Air-Conditioning

Engineers (ASHRAE) [114] suggests a mould index of 3 as an acceptable threshold for wall assemblies.

Table 2: Mould index classification according to Finnish mould growth model [111, 112]

Mould index	Mould growth	Description	
0	No growth.	Clean surface (Spores not activated).	
1	Growth is seen with a microscope.	Germination point (growth is beginning in some places).	Microscopic level
2	Clear growth is seen with a microscope.	Mould growth covers less than 10% of the area studied (microscope). Several mould colonies have formed.	
3	Growth is seen with the naked eye, Clear growth is seen with a microscope.	Mould growth covers less than 10% of the area studied (naked eye), Mould growth covers less than 50% of the area studied (microscope), New spores are starting to form.	Visually detectable
4	Clear growth is seen with the naked eye, Rich growth is seen with a microscope.	Mould growth covers more than 10% of the area studied (naked eye), Mould growth covers more than 50% of the area studied (microscope).	
5	Rich growth is seen with the naked eye.	Mould growth covers more than 50% of the area studied (naked eye).	
6	Very rich growth.	Mould growth covers almost 100% of the area studied, dense mould growth.	

2.3.3 Decay

Wooden materials are vulnerable to degradation caused by both biotic and abiotic factors, which can lead to significant deterioration over time [115]. Among these, rot decay is a form of microbiological damage that alters wood's physical and mechanical properties. This type of decay weakens the material by reducing its stiffness, strength, and overall resistance capabilities. Once rot decay begins, the façade's integrity is susceptible, potentially resulting in functional failures or even complete structural collapse. Such outcomes can lead to substantial financial costs and other safety consequences [116]. The degree of decay can be quantified using the model proposed in [115]. This model employs a dose-response function to calculate the cumulative decay over a period of n-days, based on the total dose received during that time frame. The assessment uses the decay rating system outlined in EN-252 [117], which provides a standardised framework for evaluating the extent of wood decay.

2.3.4 Moisture creep

When considering moisture-related challenges in timber buildings, mould growth and decay are often the most immediate concerns. However, the moisture content

of wood also significantly impacts its creep behaviour, which is critical for assessing the serviceability limit state (SLS). Creep refers to the gradual increase in deformation that occurs when a material is subjected to a long-term, sustained load. Various factors, including the type of wood, the duration and magnitude of the applied load, and the moisture content within the wood, influence the extent of creep. Higher moisture content accelerates the creep process. According to [118], experimental studies reveal that wood with elevated moisture levels experiences more pronounced creep deformations than wood with lower moisture content. Furthermore, fluctuations in moisture levels, particularly when combined with applied loads, can significantly amplify these deformations. Higher temperatures exacerbate this effect, leading to increased creep, an essential consideration in designing multi-storey timber buildings that bear substantial dead loads. Numerous mathematical models have been developed to describe creep behaviour. For example, the standard EN 1995-1-1 [119] introduces the coefficient, k_{def}, which accounts for the influence of moisture on deformation. This coefficient modifies the mean modulus of elasticity for SLS calculations based on the duration of load exposure and the anticipated moisture conditions.

2.3.5 Weathering of wood

Weathering refers to the gradual deterioration of materials caused by prolonged exposure to environmental conditions. While the degradation mechanisms vary depending on the material, they generally result from a combination of natural factors, including moisture, sunlight, temperature fluctuations, chemical interactions, windblown-induced abrasion, and biological agents [120]. In the case of wood, understanding the chemical processes involved in weathering requires a knowledge of its macroscopic properties, such as specific gravity, earlywood/latewood, and its texture. Weathering-induced chemical changes often include the formation of free radicals and hydroperoxides, degradation to a specific depth (leading to visible colour changes), and the effects of acids. These chemical alterations compromise the aesthetic appearance of the wood over time. Various chemical treatments are available to mitigate the effects of weathering, including the application of chromic acid, chemically bonded stabilisers, water-repellent preservatives, paints, stains, and other chemical modifications. These interventions can significantly slow down the degradation process. For a detailed review of the mechanisms and mitigation strategies associated with wood weathering, readers are referred to Williams [120].

3 Probabilistic hygrothermal assessment (PHA)

This chapter begins with a literature review of existing studies on PHA, highlighting key findings and identifying research gaps to guide future work in this field. Following this, three critical methodological toolsets essential for conducting PHA are introduced: uncertainty propagation, sensitivity analysis, and metamodeling techniques. These toolsets have been recognised as foundational components for PHA, as emphasised in Annex 55, Subset 2 of the International Energy Agency (IEA) report [121]. The subsequent sections of this chapter present the contributions of this thesis to advancing the state of the art in PHA. Each section explores the additional developments in these methodological toolsets, provides insights into their practical application, and discusses the results, demonstrating their significance for achieving reliable and robust hygrothermal analyses.

3.1 Literature review

Recently, Bayat Pour et al. [71] conducted a comprehensive state-of-the-art literature review focusing on PHA. This review, which directly addresses the first research question of this thesis (Q1), was based on an analysis of 143 relevant publications. The study provided statistical insights into several critical aspects of PHA, including the methods used for uncertainty propagation and SA, the geographical distribution of studies, the climatic conditions considered, and sustainability perspectives. It also examined the groups of uncertain parameters, the types of metamodels employed, the hygrothermal analysis tools used, and the dimensionality of the models (e.g., one-dimensional or multi-dimensional). Furthermore, it explored the application of PHA across different building usage types and its integration with moisture-related damage models.

3.1.1 Background

Figure 4 illustrates the annual distribution of PHA studies, with the most recent search conducted in October 2023. The statistics shown in this figure are derived

from multiple literature sources: [3, 5-7, 24, 28, 37-40, 44-47, 50, 75, 85, 106, 122-246].

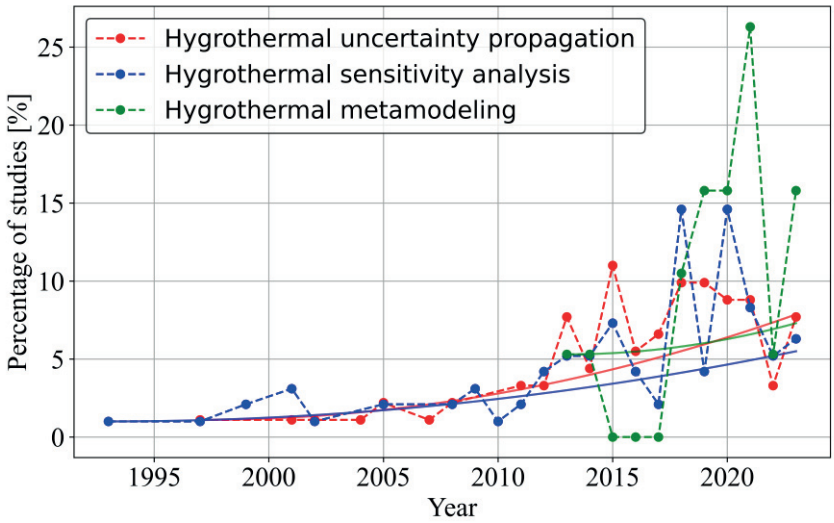


Figure 4: Annual distribution of probabilistic hygrothermal assessment (PHA) studies. Literature until the 1st of October 2023 was considered (a total of 143 publications [3, 5-7, 24, 28, 37-40, 44-47, 50, 75, 85, 106, 122-246] as the basis for the statistics).

The literature review by Bayat Pour et al. [71] identifies the origins of HSA research in 1993 when Hokoi and Kumaran [227] conducted an SA of the drying process in wet glass fibre insulation. A marked increase in the number of studies occurred between 2013 and 2023, as seen in Figure 4. Before 2013, only 22 studies were found to be relevant to this field. However, the number of publications grew substantially between 2013 and 2023, with 74 studies published during this period, highlighting a growing research interest in HSA. These publications focused on improving HSA methodologies by incorporating techniques capable of handling non-linear analysis and accounting for interactions among input variables.

Similarly, hygrothermal uncertainty propagation (HUP) research began in 1997, when Geving [167] introduced a systematic approach to hygrothermal analysis using Monte Carlo simulation. As with HSA, there was a noticeable increase in HUP-related publications from 2013 to 2023. While only 13 studies before 2013 were identified as relevant, 68 publications were released during the subsequent decade, reflecting sustained interest in the field (see Figure 4). Advances during this period focused on refining HUP methodologies by implementing sampling techniques to improve sample efficiency and minimise computational costs. Research activity in this area peaked in 2015, accounting for 11% of all studies.

Metamodeling in PHA emerged in 2013 with the introduction of the response surface methodology by Ramos et al. [166], followed by additional studies in 2014 [143] (see Figure 4). Between 2018 and 2023, the range of used metamodeling techniques expanded significantly. These advancements included methods such as neural networks [137, 162, 174], RF [172], partial least squares [47, 189], Kriging [50, 164], generalised additive models [127], and polynomial regression methods [5].

3.1.2 Main findings

The literature review by Bayat Pour et al. [71] offered overarching conclusions regarding PHA studies, which are summarised below:

A) Among the various uncertainty propagation methods, Monte Carlo simulations have been the most frequently used due to their ability to account for a wide range of potential scenarios in PHA. However, achieving greater accuracy and robustness in the results necessitates improvements in sampling efficiency and a convergence study.

B) SA in hygrothermal studies is inherently challenging due to the interactions among input variables and its transient nature, which introduces non-linearity. Addressing these complexities requires advanced methods capable of handling non-linear and interactive analyses. While no single method is without limitations, a conservative approach involves employing multiple SA techniques to capture transient conditions appropriately. In practice, methods with low computational demands are often prioritised to facilitate application.

C) Research on PHA has been predominantly concentrated in northern and western Europe and North America. Regions in Asia and Oceania have produced fewer studies, likely due to their predominantly dry climates, while no research output from Africa was found. Despite this, areas within these regions with similar climatic conditions to northern and western Europe could benefit from additional investigation.

D) Most PHA studies have focused on buildings in continental (category D) and temperate (category C) climates, with limited exploration of other climatic zones.

E) Approximately 95.1% of PHA studies did not explicitly address sustainability dimensions, including environmental, economic, or social aspects.

F) In PHA studies, material properties have been identified as the most commonly used uncertain input variables, while hygrothermal or material functions are less frequently considered. More than half of the studies

excluded indoor and outdoor ambient conditions as stochastic variables. Additionally, the review indicated that most studies did not factor in specific building usage scenarios, likely due to a lack of research on including indoor climates as stochastic variables in PHA.

G) A detailed understanding of the strengths and limitations of various metamodeling techniques is crucial for conducting reliable and robust hygrothermal analyses. To ensure the accuracy of results, particular attention must be given to mitigating risks such as overfitting.

3.1.3 Identified gaps

The statistical insights and conclusions drawn from the literature review conducted by Bayat Pour et al. [71] revealed research gaps in the field of PHA, as outlined below:

A) There is a pressing need to develop metamodels using robust and efficient algorithms. These metamodels should prioritise interpretability, the ability to handle non-linear relationships, and computational efficiency to enhance their practicality in PHA.

B) Advancements in SA methodologies are crucial. A conservative approach that combines multiple SA methods is necessary to address transient conditions effectively while minimising computational costs.

C) Enhancing the accuracy of PHA requires treating hygrothermal functions as uncertain input variables. Given their significant potential to impact hygrothermal performance more than individual material properties, their inclusion is vital.

D) Approximately 90% of existing PHA studies have been limited to one-dimensional (1D) modelling. To capture more complex interactions and details, further research is needed to expand the scope to two-dimensional (2D) and three-dimensional (3D) modelling.

E) Integrating sustainability dimensions, such as environmental, economic, and social factors, into PHA is essential to improve decision-making processes for sustainable moisture-safe building designs and retrofitting strategies.

F) Tropical climates, which are particularly susceptible to moisture-related issues, require greater attention in PHA case studies.

G) Occupant behaviour significantly influences indoor humidity levels through activities, adjustments to heating or cooling set points, and the operation of shading devices. These variations in internal loads can affect hygrothermal performance. Therefore, incorporating building usage scenarios into

hygrothermal analyses is necessary for more accurate and reliable outcomes.

H) A promising avenue for future research involves developing PHA frameworks that incorporate limit states for quantitative decision-making. Such approaches could mitigate the health impacts of dampness and mould by bridging hygrothermal analysis with medical science perspectives. The inutility decision analysis (IDA) method offers significant potential in this context and would require interdisciplinary collaboration across fields like construction, design, and medicine.

I) The evolution of region-based metamodels presents an opportunity to create user-friendly solutions for hygrothermal analysis, which can be particularly beneficial for practitioners without expertise in specialised simulation tools.

The research questions in this thesis were derived from the findings of this literature review [71]. Specifically, gaps A through E informed the formulation of research questions Q2 to Q6, while the remaining gaps (F to I) are proposed for exploration in future studies.

3.2 Probabilistic analysis (PA)

3.2.1 Probabilistic analysis vs deterministic analysis

The deterministic approach assumes that input parameters and conditions are precisely defined, yielding a single, fixed outcome. This method is commonly applied in conventional building design [41], where specific values for variables such as material properties and environmental loads are used without accounting for inherent uncertainties. However, in certain building-related fields, such as structural design, safety factors are introduced to account for potential uncertainties. In contrast to deterministic approach, the probabilistic approach acknowledges variability and uncertainty in input parameters by treating them as random variables characterised by probability distributions. By incorporating these uncertainties, the probabilistic method generates a spectrum of possible outcomes, often represented as probability distributions. This approach enables more robust and informed decision-making, particularly in complex engineering systems where variations in material properties, environmental conditions, and performance requirements can substantially influence long-term safety and sustainability.

Figure 5 schematically illustrates the differences between deterministic and probabilistic analyses. In deterministic analysis, a single outcome (green arrow) is derived from fixed input data. As shown on the left side of Figure 5, if the red dashed line represents the acceptable threshold, the deterministic result may indicate that

the design falls within the acceptable range. However, such outcomes can be significantly influenced by the uncertainties of parameters within the simulation model, potentially introducing bias or inaccuracies.

In contrast, the right side of Figure 5 illustrates two hypothetical probabilistic outcomes (solid and dashed black curves). This example highlights how deterministic analyses may fail to capture critical scenarios that could lead to failures. The solid curve suggests that the actual risk far exceeds the threshold, indicating a high probability of failure. On the other hand, the dashed curve indicates a low probability of failure, which might be considered acceptable. Without conducting a probabilistic analysis (PA), one would lack insight into whether the design aligns with the solid curve, the dashed curve, or any other distribution. This limitation depicts the value of probabilistic approaches for evaluating uncertainties and potential risks in building design.

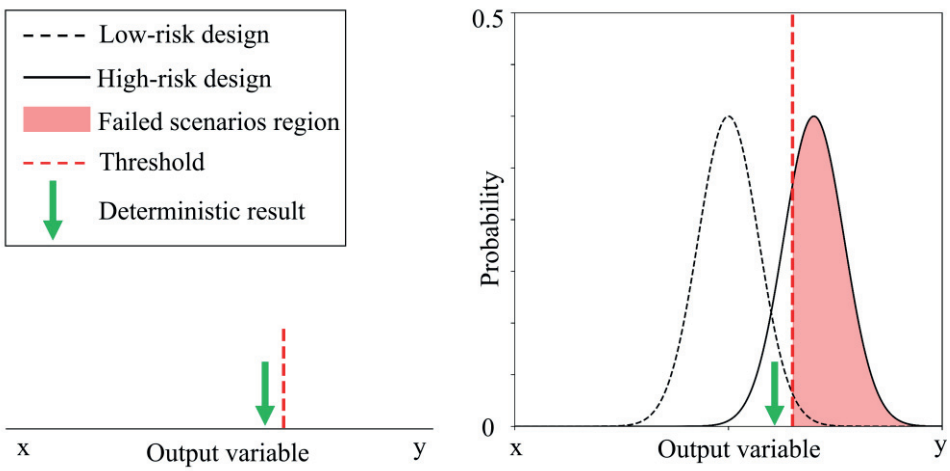


Figure 5: Visualisation of deterministic (left) and probabilistic (right) analyses. The red dashed line indicates the performance threshold, with values to the left considered acceptable. For clarity, probability values exceeding 0.5 on the y-axis have been omitted from the visualisation.

3.2.2 Application of probabilistic analysis in hygrothermal analysis

In hygrothermal analysis, as in other engineering fields, numerical tools have become an integral part of daily engineering practice. These tools are predominantly used in a deterministic manner, assuming fixed values for material properties and/or climatic boundary conditions—typically mean values or conservative estimates. However, in reality, such precise data is rarely available during the design phase. Therefore, designers must account for uncertainties in the input variables to ensure a reliable design.

Figure 6 illustrates the benefits of adopting a probabilistic approach in hygrothermal analysis. This example involves optimising the design of a building envelope by considering both energy performance and hygrothermal behaviour. Specifically, two parameters— thermal transmittance (U-value) and maximum mould index— are evaluated, each required to meet specified thresholds (e.g., a maximum mould index below three and a thermal transmittance below 0.15 W/(m²·K)). To achieve an acceptable design, the design point must fall within the green region in the figure.

In the deterministic approach (Figure 6a), the design may be deemed acceptable as it satisfies the thresholds for both criteria. However, the probabilistic approach (Figure 6b) evaluates a broader range of scenarios by accounting for uncertainties in the design parameters. This creates a "cloud" of potential outcomes around the deterministic point, indicating that some scenarios could violate the thresholds for one or both criteria. In response to these findings, the designer can refine the design to ensure that the entire cloud of scenarios lies within the safe region (Figure 6c). This process demonstrates how PA provides a more robust and reliable framework for optimising building envelope designs, enabling better management of uncertainties and risks.

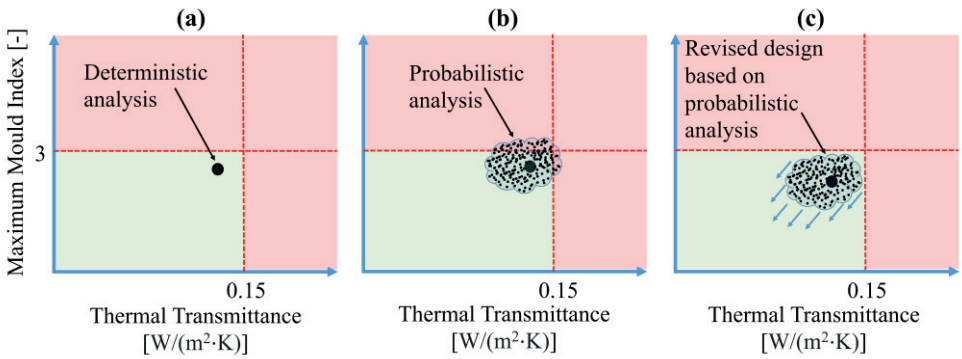


Figure 6: Probabilistic analysis (PA) application in hygrothermal analysis.

3.3 Hygrothermal uncertainty propagation

Uncertainty in building applications can originate from various sources and is generally categorised into aleatoric (stochastic) and epistemic (subjective) uncertainties [247]. Aleatoric uncertainty reflects the inherent randomness within a system and represents an irreducible form of variability. In contrast, epistemic uncertainty arises from a lack of knowledge about the accurate values of certain parameters and can be reduced by improving models or acquiring additional data. These two types of uncertainty are often linked in practical applications [247].

Uncertainty is present at every stage of a building's lifecycle. Numerous parameters remain unknown during the early design phase due to limited detailed knowledge. As the project progresses and more information becomes available, many of these parameters are fixed, reducing the epistemic uncertainty. However, stochastic uncertainties persist, as they are inherent to the system and cannot be eliminated.

In the context of reliable, energy-efficient building design, analysing these uncertainties is referred to as forward uncertainty propagation [121]. While several probabilistic approaches exist for uncertainty propagation, building physics primarily utilises simulation-based methods (e.g., Monte Carlo simulations), scenario-based methods (e.g., future climate or occupant scenarios), and approximation techniques (e.g., first- and second-order reliability methods).

According to the literature review by Bayat Pour et al. [71], over 85% of PHA studies employed the Monte Carlo method for uncertainty propagation. Monte Carlo methods comprise a broad class of computational algorithms based on repeated random sampling to generate numerical results. This approach propagates uncertainty by drawing numerous samples from input probability distributions and performing simulations for each sample, yielding a comprehensive understanding of potential outcomes, a methodology also employed in this thesis.

3.3.1 Sampling technique

Sampling plays a significant role in Monte Carlo simulations, as it involves generating representative sets of input parameters from joint probability distributions or specified ranges. These sampled inputs are then used to assess the variability and uncertainty in model outputs. The range and distribution of input parameters are crucial in determining the accuracy and reliability of PHA. Properly defining these parameters, often based on a combination of experimental data and expert judgment [43], ensures meaningful and robust results. The choice of statistical distribution for each parameter depends on the corresponding assumptions and the data's nature. The spread and overall trend of the data are influenced by specific shapes and properties of several distributions, including normal, uniform, and lognormal [42].

The Basic Random Sampling (BRS) method is the simplest technique for Monte Carlo simulations [121]. In BRS, samples are selected randomly without any stratification or prefiltering, offering a straightforward yet unstructured approach. However, when computational resources are limited, BRS poses challenges, as reducing the number of samples may fail to capture the full variability of input parameters. Accurate results often require a large number of samples, making the process computationally expensive and time-consuming [153, 248]. Therefore, given the computational complexity of transient hygrothermal models, selecting an appropriate sampling technique is critical.

According to Bayat Pour et al. [71], Latin Hypercube Sampling (LHS) and BRS are the most commonly used techniques in PHAs, accounting for 37.4% and 34% of studies, respectively. Due to the challenges posed by BRS in capturing complex hygrothermal phenomena with fewer samples, LHS was chosen as the sampling technique for this thesis. Compared to BRS, LHS achieves comparable accuracy with significantly fewer samples, reducing computational demands [249, 250]. Several studies [85, 251-253] have consistently shown that LHS produces more robust and uniform results, even for computationally expensive models. Its ability to reduce bias and computational costs makes LHS a preferred choice in complex probabilistic analyses [6, 7, 85, 249-255].

Latin Hypercube Sampling (LHS) technique

LHS, introduced by McKay et al. in 1979, provides a systematic and efficient sampling method for PA [251]. It stratifies each input variable's probability distribution into *n* non-overlapping intervals, each with an equal probability. The number of samples is equal to the number of intervals [254, 256] (see Figure 7, red dashed lines). Within each interval, a single random value is selected, ensuring that the entire range of the input distribution is represented in the sample (see Figure 7, green dots). To prevent correlations between variables, the values within one variable's intervals are randomly permuted and paired with the sampled values of other variables. This creates a sample matrix where each row represents a unique combination of parameter values, uniformly covering the input space. LHS ensures that values with higher probabilities are sampled more frequently, aligning with the realistic probability distribution of the input variables. For instance, as shown in Figure 7, when a normal distribution is assumed for a variable, values closer to the mean are selected more often than extreme values, reflecting the higher probability of occurrence near the mean. This structured and balanced sampling approach enables LHS to achieve more accurate and efficient results compared to simple random sampling methods.

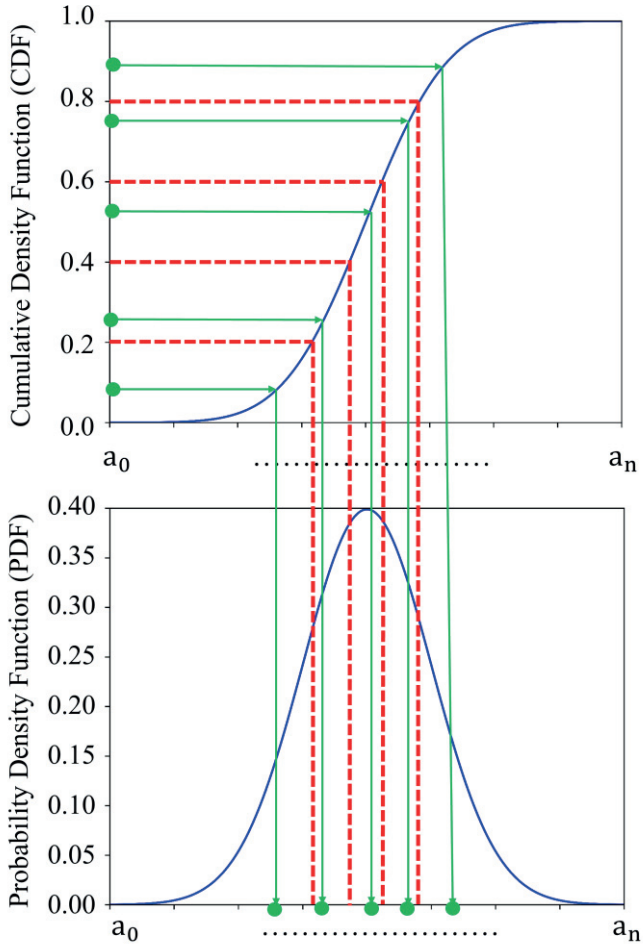


Figure 7: Latin hypercube sampling (LHS).

3.3.2 Probabilistic hygrothermal and mould growth analyses

Figure 8 illustrates the procedure for conducting probabilistic hygrothermal and mould growth analyses, which is a subset of the mould reliability analysis (MRA) methodology developed by Bayat Pour et al. [172]. The process begins with sampling using the LHS technique, followed by hygrothermal simulations for the generated scenarios. Relevant outputs are then extracted, including parameters used directly, such as heat flux for assessing thermal performance, and variables required for further analysis, such as T and RH. The post-processing stage applies moisture-related damage models, such as mould growth, rot decay, or frost damage. This study specifically focuses on mould growth assessment.

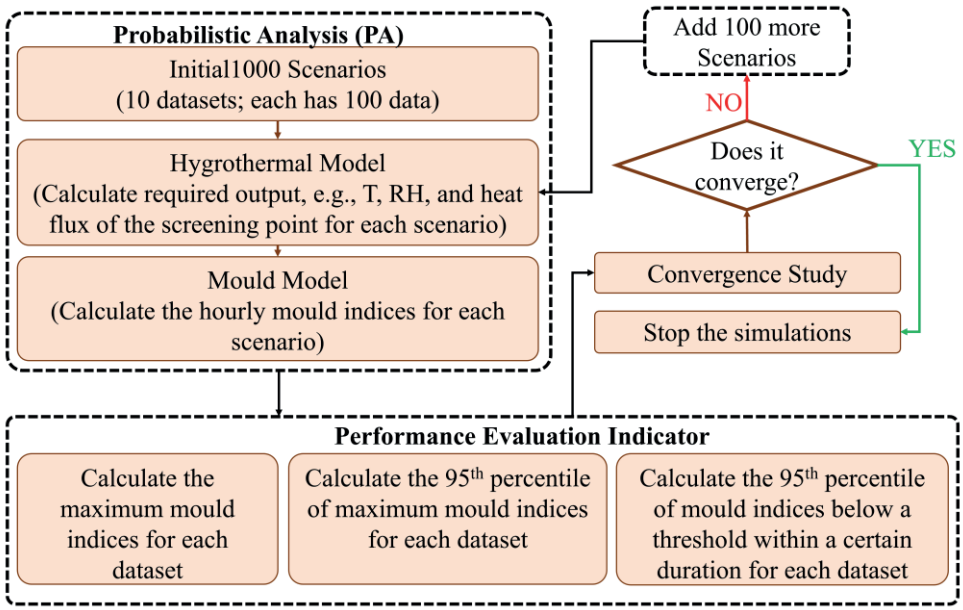


Figure 8: Probabilistic hygrothermal and mould growth analyses procedure.

As depicted in Figure 8, the output of the mould model can be analysed in multiple ways depending on the study's objectives. The performance evaluation indicator varies based on the study's requirements. For instance:

- In Paper II, maximum mould indices were calculated as the evaluation metric for training a metamodel.
- In Papers III, only the PA component was utilised, and the 95th percentile of maximum mould indices was considered to exclude extreme outliers.
- Paper IV, an extension of Paper III, employed maximum mould indices for metamodel training and subsequently calculated the 95th percentile of predicted maximum mould indices. This facilitated the evaluation of mortar extrusion effects using a simplified 2D model integrated with a 1D model.
- Paper V calculated the 95th percentile of mould indices below a threshold (mould index 3) within 10 years. This performance indicator was used to train a metamodel that incorporated more uncertainties using big data. The indicator identified scenarios where mould indices remained below 3 in 95% of instances over 10 years, defining them as acceptable.

A convergence study is critical for determining PA's required number of simulations (i.e., scenarios or sample size). Bayat Pour et al. [172] adapted an equation from [257] for convergence analysis in PHA studies. This approach

systematically increases the number of simulations while monitoring a target variable, which may be one of the performance evaluation indicators shown in Figure 8. The convergence criterion involves tracking changes in the target variable across the preceding 10 iterations. Each iteration consists of 100 unique scenarios, with 100 new scenarios added incrementally to form subsequent iterations. According to [172], the simulation process continues until the convergence value drops below a predefined threshold of 0.001. The convergence value (ε_i) is calculated using Eq. (20):

$$\varepsilon_i = \frac{\left|\sum_{i-9}^{i-5} OF_i - \sum_{i-4}^{i} OF_i\right|}{\sum_{i-4}^{i} OF_i} \tag{20}$$

Where:

- i is the current iteration number (>10),
- OF_i represents the objective function (e.g., target variables) for the i^{th} iteration,

Among the publications of this PhD project, Papers III and VI performed convergence analysis in direct connection with the PA component. In other publications, convergence was linked to metamodel outputs to monitor the results of the numerical analysis setup.

3.3.3 Results and discussion

3.3.3.1 Probabilistic hygrothermal analysis vs deterministic hygrothermal analysis

Figure 9 illustrates the advantages of probabilistic hygrothermal analysis over deterministic analysis, using a case study presented in Paper II [172]. The figure highlights the capability of PA (represented by grey bands) in calculating mould indices by comparing its results to those obtained through deterministic analysis (depicted by red lines). The gap between the deterministic output and the maximum value within the range of mould indices calculated by PA was analysed to evaluate the uncertainties in deterministic hygrothermal analysis results. The comparison reveals 26.3% uncertainties for the considered case study. This finding demonstrates that PA captures the uncertainties and risks that deterministic methods fail to account for. For example, PA indicates a risk of failure (i.e., the probability of a mould index exceeding one), while deterministic analysis suggests that the case study is safe (i.e., mould index less than one). This discrepancy demonstrates the limitations of deterministic approaches in addressing uncertainties, potentially leading to misleading conclusions and suboptimal design decisions.

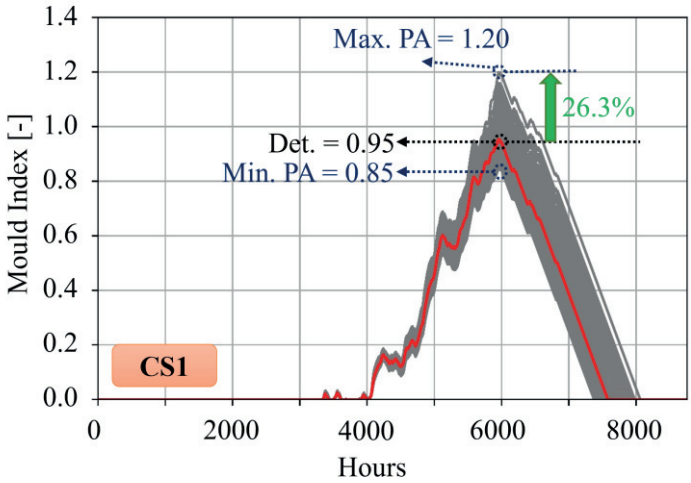


Figure 9: Temporal variation of mould index for a case study (CS1) in Paper II [172], shown for the deterministic case (red line) and the probabilistic analysis (grey region). Abbreviations: Det.: deterministic hygrothermal analysis result, Max. PA and Min. PA: maximum and minimum values of the maximum mould indices according to the probabilistic hygrothermal analysis.

3.3.3.2 Probabilistic hygrothermal modelling of mortar extrusion

The PA methodology developed in this thesis was applied to model the effects of mortar extrusion due to workmanship uncertainties, as discussed in Paper III [258]. Mortar extrusion, illustrated in Figure 10, is a phenomenon that can occur during bricklaying when mortar from the joints spills into the air cavity layer. This extrusion (depicted as grey areas in Figure 10) can disrupt the cavity's ventilation function and facilitating moisture movement from the brick layer to other wall components. The extruded mortar can be limited to the cavity space in front of the joint, but in severe cases, it can bridge the gap between the brick and the weather-resistant barrier. This connection eliminates the air gap around the extrusion, compromising the cavity's ability to manage moisture.

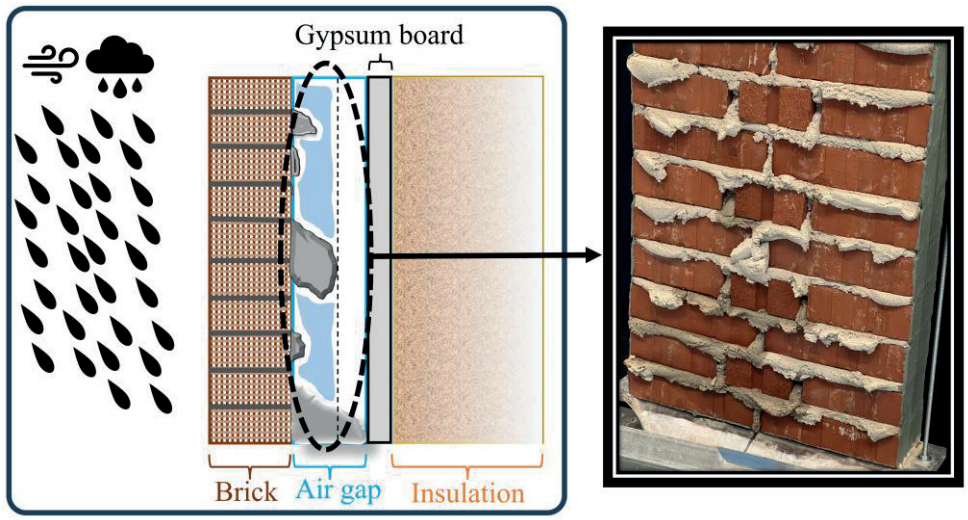


Figure 10: Mortar extrusion phenomenon for clay brick cladding (the dimensions are not scaled).

To incorporate this phenomenon into hygrothermal modelling, Papers III and IV accounted for the influence of extruded mortar on moisture transport. While 2D simulations offer greater accuracy in capturing this issue, they are computationally expensive, particularly when paired with probabilistic approaches. A custom material was introduced to approximate the extrusion layer in a 1D model to address this challenge. The 1D model was verified using 2D simulations before being applied for probabilistic modelling. The 1D mortar extrusion model can predict more than 90% of variations in the 2D models' mould indices, according to the high coefficient of determination (R^2) between the 1D and 2D models (over 90% in the majority of cases). In addition, using a 1D model instead of a 2D model results in relatively small mean absolute error (MAE) values. Given the significant time savings of using a 1D model—roughly 5 minutes per simulation as opposed to 760 minutes per simulation for a 2D model—these inaccuracies are still within an acceptable range. The MAE and R^2 are calculated using Eq. (22) and (23).

Additionally, in Paper III [258], a comparison was made between two water penetration criteria to evaluate how using different WDR-induced water penetration criteria affects the mould growth assessment within a probabilistic framework. The first criterion, based on the ASHRAE standard 160–2021 [114], considers that 1% of the rainwater reaching the exterior surface penetrates through the wall. The second criterion, derived from an experimental study (ES) [259], considers the moisture content of the brick as an indicator for applying WDR-induced water penetration. According to this ES criterion, water penetration only occurs when the masonry wall is nearly saturated. Before reaching saturation, the wall can absorb and retain WDR-induced water, preventing penetration. This criterion utilises the

portion of WDR that penetrates the wall as a moisture source in the hygrothermal analysis, referred to as the fraction of normal rain. In this study, the moisture source's position and size were adjusted based on the depth of the extruded mortar, with the moisture distributed throughout the depth of the extrusion.

Table 3 summarises the 95th percentile of maximum mould indices for a case study presented in Paper III [258]. The analysis considered two climatic conditions in Sweden: Gothenburg (G), characterised by high WDR exposure, and Rensjön (R), representing a region with low WDR exposure [260]. These conditions were used to investigate the effects of different water penetration criteria based on different climatic conditions. Under Gothenburg's climatic conditions, using the ES criterion resulted in a relatively small reduction—approximately 6%—in the 95th percentile of maximum mould indices compared to the ASHRAE criterion. However, under the low WDR exposure conditions of Rensjön, the ES criterion led to a more significant reduction of approximately 22%. This highlights the greater impact of the ES criterion in climates with lower WDR loads, where it accounts for the water content of masonry walls.

Table 3: Mould growth calculations. G: Gothenburg, R: Rensjön, ES: case studies based on experimental study data, ASHRAE: case studies based on ASHRAE 160–2021 standard.

Case study	95th percentile of the maximum mould indices	Required number of simulations to achieve convergence
ASHRAE_G	5.89	1400
ES_G	5.57	1200
ASHRAE_R	1.25	1600
ES_R	0.98	3000

As shown in Table 3, the differences between the ASHRAE and ES criteria under Gothenburg's climatic conditions were relatively minor. This is attributed to the higher WDR loads in Gothenburg, which led to elevated brick water content frequently surpassing the saturation threshold specified by the ES criterion. Consequently, moisture sources associated with WDR were more consistently incorporated into the hygrothermal simulations, resulting in comparable outcomes for both criteria under high WDR conditions. In contrast, Rensjön experiences significantly lower WDR loads, allowing the masonry to absorb rainwater without consistently exceeding the saturation threshold set by the ES criterion. Unlike the Gothenburg case, the brick's water content in Rensjön rarely surpassed this threshold and only did so for brief periods. This minimal probability of water penetration illustrates the importance of accounting for brick masonry's water content and absorption capacity, as captured by the ES criterion, in regions with lower WDR exposure. Thus, the ES criterion proves more beneficial for accurately modelling moisture behaviour in scenarios characterised by low WDR loads, where the traditional ASHRAE criterion may overestimate moisture sources. Conversely, in climates with frequent and intense WDR, such as Gothenburg, the outcomes of

the ASHRAE and ES criteria align closely, making either approach suitable under such conditions.

3.3.3.3 Probabilistic analysis for hygroscopic insulations' hygrothermal performances

The PA component of the MRA methodology was utilised in Paper VI [261] to evaluate the hygrothermal performance of wall assemblies incorporating different hygroscopic insulation materials. Four types of insulation—cellulose (CL), wood fibre (WF), expanded polystyrene (EPS), and mineral wool (MW)—were analysed under the climatic conditions of Stockholm. The PA focused on mould growth on the wooden stud and heat flow through the insulation layer, while accounting for uncertainty in material properties and boundary conditions.

Figure 11 compares mould growth conditions and total heat flux across the wall assembly. Among the insulation types, CL demonstrated the best performance, with no risk of mould growth throughout the year. Initially, this outcome was attributed to its enhanced moisture storage (that is defined based on its sorption isotherm). However, this conclusion could not be generalised, as wood fibre—with an even more pronounced moisture storage—exhibited the highest potential for mould growth among the cases studied. Several factors may explain this difference between WF and CL. While both materials exhibit high moisture storage, CL has a higher water absorption coefficient (approximately 100 times more), indicating a faster liquid water transport process. The restricted liquid water transport in WF slows down the drying process of accumulated moisture at the interstitial surfaces between wall layers, thereby increasing the risk of mould growth. In contrast, the mould indices for EPS and MW remained below 1, indicating a minimal risk of mould growth. These findings highlight the significant role of interactions between material properties and boundary conditions, as evidenced by WF's poor performance.

The results further reveal that CL insulation, despite its superior mould growth performance, exhibited the highest heat flux, showing higher heat loss. This behaviour is correlated with its thermal conductivity, which can increase up to 0.7 W/(m·K) depending on moisture content. However, EPS has a lower heat flux because of its lower thermal conductivity and relative stability under different moisture levels. Furthermore, additional factors, such as the enthalpy flow caused by liquid advection and vapour diffusion, impact the overall heat flux. These procedures can result in differences in heat flux between various insulation materials, highlighting the complex nature of hygrothermal interactions. Therefore, for well-informed choices about insulating material selection, an in-depth evaluation of hygrothermal performance—including thermal conductivity and moisture transport mechanisms—is suggested by this study. These results show that moisture safety, durability, and thermal performance should be balanced to optimise the design.

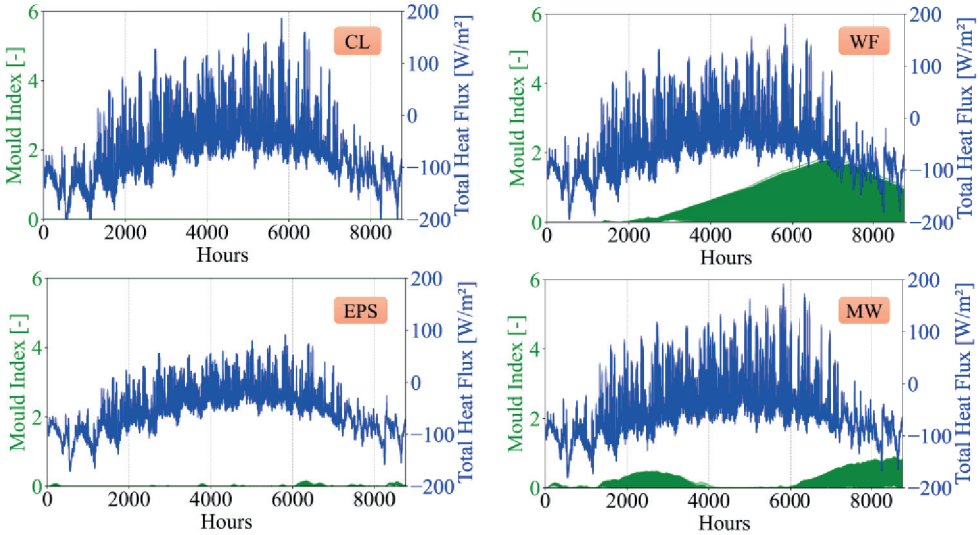


Figure 11: Mould index [-] and total heat flux [W/m^2]. CL: cellulose, WF: wood fibre, EPS: expanded polystyrene, and MW: mineral wool.

3.4 AI-based metamodeling

3.4.1 Metamodeling

The Monte Carlo-based probabilistic methodology often requires running thousands of simulations, making the process computationally expensive and time-consuming. To mitigate these challenges, metamodels have been developed as simplified representations that approximate a building's hygrothermal performance, enabling faster predictions.

Figure 12 depicts how metamodels can significantly aid designers by accommodating millions of scenarios, enhancing building design robustness. Figure 12(a) represents the "cloud" of scenarios previously introduced in Figure 6. This cloud can expand further (Figure 12(b)) when additional scenarios are incorporated into the analysis. However, the computational burden associated with running extensive probabilistic analyses may discourage designers from pursuing such an exhaustive approach. This is where metamodels provide a crucial advantage. By training metamodels, designers can predict outcomes without conducting full-scale simulations, substantially reducing computational time and resources. As a result, they can identify additional failure scenarios through extrapolation and refine their designs to move the broader cloud of outcomes into the safe region (the green region in Figure 12(c)). This capability allows for a more robust and efficient design

process, ensuring that critical safety and performance thresholds are met while optimising computational efficiency.

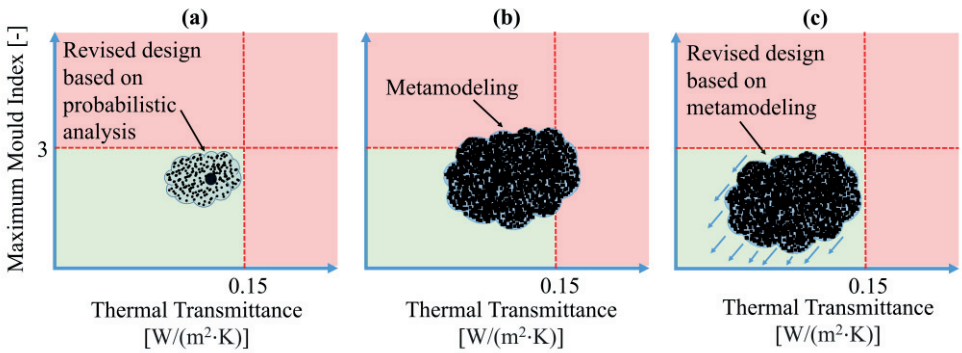


Figure 12: Metamodeling application in connection with probabilistic hygrothermal analysis.

Metamodeling is a pivotal toolset introduced in Annex 55, Subset 2 of the IEA report [121]. According to the literature review conducted by Bayat Pour et al. [71], from 2018 to 2023, the use of metamodels significantly expanded, incorporating a variety of advanced techniques.

Tijskens et al. [45, 46, 137, 161,162, 188] applied neural networks as surrogates for numerical models to reduce computational demands. Their research focused on utilising various machine learning algorithms to predict response time series rather than single response values. They evaluated the effectiveness and training time of common neural network architectures, including multilayer perceptron (MLP), recurrent neural networks (RNN), and convolutional neural networks (CNN). Their findings revealed that CNNs were the most accurate and efficient in predicting transient and non-linear hygrothermal time series for the selected case studies.

Aggarwal et al. [47, 189] employed partial least squares (PLS) regression to develop metamodels using hourly historical climate data for cities across various Canadian climate zones for hygrothermal simulations. The study demonstrated that the metamodels accurately predicted the hygrothermal performance of brick-clad wood-frame wall assemblies under historical and future climatic conditions.

Marincioni et al. [127] developed metamodels using generalised additive models (GAM) to assess the moisture risk in internally insulated wall assemblies. Their analysis showed that the metamodel predictions closely aligned with simulation results in most cases, with some exceptions where the predicted values underestimated the actual outcomes.

3.4.2 Random forests (RF) machine learning algorithm

The AI Galaxy in Figure 13 illustrates the hierarchical structure of AI and its key subfields, encompassing machine learning (ML), neural networks (NN), and deep learning (DL) [262]. At the outermost layer, AI encompasses broad capabilities such as expert systems, automated reasoning, and problem-solving strategies. Within this domain, ML forms a subset that includes various statistical and algorithmic approaches, such as decision trees, support vector machines (SVM), and ensemble methods like random forests. Further within, neural networks represent a specialized subset of ML, comprising models like radial basis function networks, self-organising maps, and RNN. At the core of this hierarchy lies deep learning, a subfield of neural networks that employs advanced architectures such as CNN, long short-term memory (LSTM) networks, and transformer models. The figure metaphorically represents AI as a galaxy, highlighting the relationships between these methodologies and their interconnected role in advancing intelligent systems across diverse applications. The literature review by Bayat Pour et al. [71] explored various metamodeling techniques used in hygrothermal analyses. To the best of the author's knowledge, the RF machine learning algorithm has not yet been applied in any PHA studies. However, it has been identified as a promising method with the potential to enhance the robustness and reliability of such analyses.

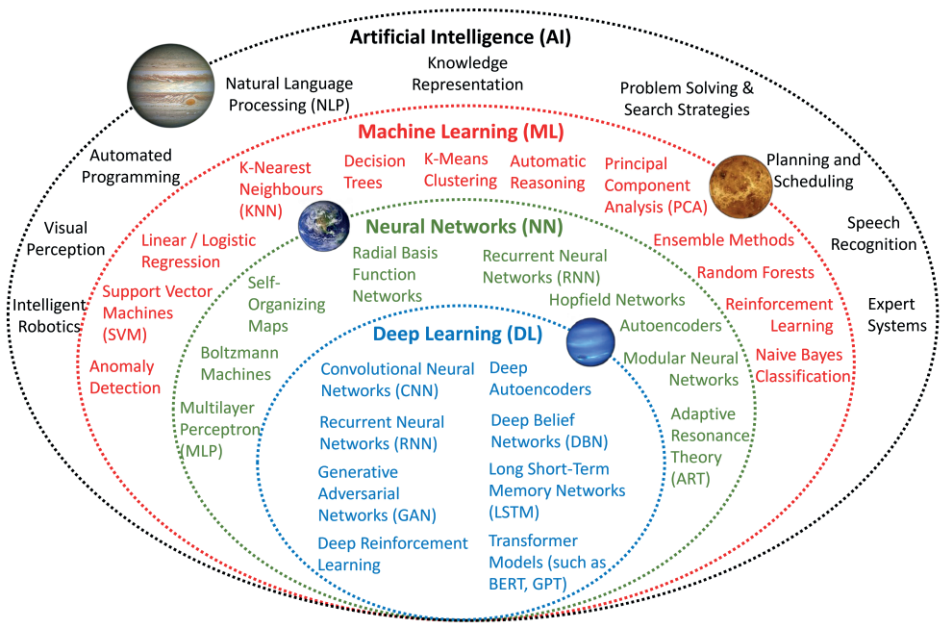


Figure 13: AI galaxy, adopted from [262] edited and designed by Mohsen Bayat Pour.

The RF algorithm, introduced by Breiman [263], is a powerful method for solving regression and classification problems through model aggregation. It builds upon the concept of bagging [264], one of its earlier iterations, and incorporates random feature selection [265]. The algorithm generates numerous decision trees using bootstrapped datasets derived from the original dataset. A random subset of input variables is selected at each node of these decision trees, increasing diversity among the trees and enabling RF to handle datasets with high-dimensional predictors [266]. Key parameters in the RF model include the number of trees and the number of predictors used to determine splits at each node. Each tree in the ensemble uses a different bootstrap sample of the original dataset, further enhancing variability among the regression trees [267]. This ability to randomly vary input variables and re-sample data allows RF to achieve greater diversity and accuracy.

RF offers some advantages that make it a powerful machine learning algorithm for various applications. One of its key strengths is interpretability, as it provides more transparency compared to complex models like neural networks [263, 268]. While the presence of multiple decision trees can reduce efficiency in interpretation, RF still allows for visualisation and analysis of individual trees, offering insights into the decision-making process. Additionally, its feature importance indices help identify the most influential variables, further enhancing interpretability. RF is also highly effective in handling non-linear relationships, making it well-suited for modelling complex interactions between input factors and outcomes [269]. Another advantage is its robustness against overfitting, as the ensemble learning mechanism balances model complexity and stability, improving generalisation performance [263]. This property is particularly valuable in hygrothermal analysis, where variable interactions evolve dynamically. Moreover, RF provides an intrinsic measure of feature importance, enabling non-linear sensitivity analysis SA and aiding in efficient variable selection [270]. Its computational efficiency is another strength, as RF can process large datasets with high-dimensional feature spaces efficiently. The algorithm supports parallelisation during training, making it computationally faster than many alternative metamodeling techniques [271]. However, RF also has some limitations, particularly its sensitivity to hyperparameters. The model's performance depends on parameters such as the number of trees, maximum depth, and minimum samples per leaf, and improper tuning can lead to suboptimal results. Optimising these hyperparameters often requires extensive experimentation and computational effort.

In this PhD project, the optimal number of input variables for the metamodel is determined through a two-step process. First, the R^2 was calculated between each input variable and the output (one of the performance evaluation indicators) to assess their correlations. Then, a parametric study is conducted to identify the optimal number of input variables that would yield the highest metamodel accuracy. Similarly, the optimal number of trees in the RF model is determined by gradually

increasing the number of trees and monitoring accuracy improvements until further increases no longer enhanced performance.

To train and test the metamodel, the dataset is randomly split into training (70%) and testing (30%) subsets. The RF model is trained using the training dataset, and its accuracy is evaluated using the hold-out test dataset. Three performance metrics— root mean square error (RMSE), MAE, and R^2—are used to assess the model's predictive capability. These accuracy metrics are computed using Eq. (21–23).

$$RMSE = \sqrt{\frac{1}{n}\sum_{i=1}^{n}\left(y_i - \hat{y}_i\right)^2} \tag{21}$$

$$MAE = \frac{1}{n}\sum_{i=1}^{n}\left|y_i - \hat{y}_i\right| \tag{22}$$

$$R^2 = 1 - \frac{\sum_{i=1}^{n}\left(y_i - \hat{y}_i\right)^2}{\sum_{i=1}^{n}(y_i - \bar{y}_i)^2} \tag{23}$$

Here, y_i represents the observed data (original data from test dataset), $\hat{y}_i$ denotes the predicted data, $\bar{y}_i$ is the mean of the observed data, and n is the total number of data points. Eq. (21-23) provide quantitative metrics for assessing the model's predictive capability, particularly for estimating the maximum mould index. RMSE and MAE measure the average deviation between predicted and observed values, with lower values indicating higher accuracy. The R^2 value, on the other hand, represents the proportion of variation in the observed data that can be explained by the input variables in the model. A lower RMSE and MAE, combined with a higher R^2, determine better model performance in predicting.

3.4.3 Metamodeling sampling

Figure 14 illustrates the process of the MRA methodology, which consists of two main components: probabilistic analysis (PA) and metamodel analysis (MA). A key challenge arises when both components use the same predefined probability distributions for input variables sampling, particularly regarding the handling of extreme values. For instance, in the PA component, if 1,000 samples are generated using the LHS method, each probability distribution is divided into 1,000 equal intervals, with one sample selected from each. However, in the MA component, where a much larger dataset (e.g., 10 million samples) is generated using the same distribution, the extreme values (tails) are divided into significantly more intervals. This results in a higher proportion of extreme values in the MA component compared to the PA component. Since the RF metamodel is trained on the PA distributions, it encounters difficulties when faced with these extreme values in the

MA component, leading to outliers that require extrapolation—a task for which RF is not well-suited.

To address this limitation, a tailored sampling strategy was adopted, as shown within the dotted-line box in the PA component of Figure 14. This strategy involves comparing the ranges of the primary samples (used for hygrothermal simulations) with those of the secondary samples (used for metamodel predictions). The range of the primary samples is then adjusted by including values below the minimum and above the maximum of the secondary sample range. Additionally, the PA component applies a uniform distribution to each input variable. This decision was made to avoid clustering samples near the mean, which could occur if a normal distribution is used. By adopting a uniform distribution, equal weights are assigned to all segments of the input variable distributions, ensuring that the training dataset for the RF metamodel is diverse and representative of the entire input range. This approach prevents overfitting around the mean and enhances the metamodel's performance across various scenarios, including extreme conditions [272].

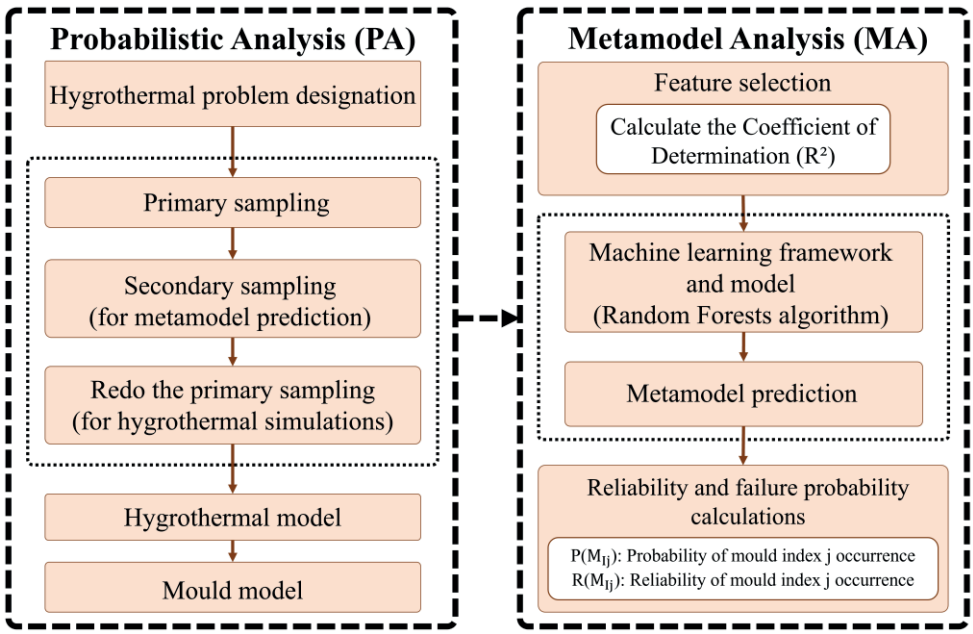


Figure 14: Mould reliability analysis (MRA) method, from [172].

Failure probability and reliability are calculated in the last stage of the MRA methodology. The failure probability is determined analogously to structural reliability assessments, where failure is defined as the condition when applied load effects exceed the system's resistance (capacity). In this context, the limit state function, g_m, incorporates two key parameters:

- Mould Limit State, $I_{M,ls}$: Analogous to the capacity in structural reliability analysis, this parameter represents the predefined threshold for acceptable mould growth.
- Mould Performance Evaluation Indicator, $I_{M,PEI}$: Corresponding to the load effect in structural reliability, this parameter is a function of T, RH, and time (t).

The limit state function is defined by Eq. (24):

$$g_m = I_{M,ls} - I_{M,PEI}(T, RH, t) \tag{24}$$

A violation of the limit state occurs when $g_m < 0$, indicating that the mould performance evaluation indicator (see Figure 8), $I_{M,PEI}$, exceeds the predefined mould limit state, $I_{M,ls}$, for a given scenario. The probability of failure, specifically the occurrence of mould index *j*, $P(M_{Ij})$, is calculated using Eq. (25):

$$P(M_{Ij}) = \frac{N(g_m<0)}{N_T} \tag{25}$$

where:

- $N(g_m < 0)$: Number of scenarios that violate the limit state function (failed scenarios),
- N_T: Total number of scenarios.

The reliability associated with the occurrence of mould index *j*, $R(M_{Ij})$, is complementary to the probability of failure and is expressed by Eq. (26):

$$R(M_{Ij}) = 1 - P(M_{Ij}) \tag{26}$$

This framework enables the quantitative assessment of mould growth risks by integrating probabilistic hygrothermal analysis with reliability evaluation.

3.4.4 Results and discussion

3.4.4.1 Time comparison between probabilistic hygrothermal analysis and metamodeling

Table 4 provides a comparative analysis of the simulation time (t_s) required for calculating the maximum mould index using the PA approach versus the prediction time (t_p) achieved with the RF algorithm in the MA. Three case studies from Paper II [172] were examined, showing significant speedups of 3.1×10^5, 7.3×10^5, and 2.7×10^5 for CS1, CS2, and CS3, respectively. Notably, the training time for

developing the metamodel was remarkably negligible, requiring less than one second for all cases evaluated. The findings highlight that integrating MA with PA can dramatically reduce the time needed to analyse a large number of scenarios for any given case study. This time reduction enables considering more scenarios, thereby addressing more uncertainties. Consequently, the MRA method facilitates a comprehensive evaluation of the robustness of hygrothermal analyses.

Table 4: Metamodel time comparison for three case studies (CS1, CS2, and CS3). RMSE: root mean square error, MAE: mean absolute error, R^2: coefficient of determination between the predicted and observed data, t_p: Prediction time per scenario, t_s: Simulation time per scenario.

Case studies	R^2	MAE	RMSE	Time comparison (Second/Scenario)		Metamodel training time (Second)
				t_p	t_s	
CS1	0.855	0.011	1×10^{-6}	10×10^{-6}	3.15	0.48
CS2	0.958	0.007	1×10^{-6}	5.5×10^{-6}	4.04	0.23
CS3	0.942	0.007	1×10^{-6}	19×10^{-6}	5.16	0.55

A computational computer with an "Intel(R) Core (TM) i9-9820X CPU @ 3.31GHz" processor and "64 GB" of RAM is used for all simulations and predictions in this thesis.

According to Table 4, the RF metamodel achieves varying but high levels of predictive accuracy across the three case studies (CS) with R^2 between 0.855 and 0.958. Additionally, the MAE and RMSE metrics for all three cases show minimal errors close to zero, illustrating the metamodel's acceptability.

Several factors contribute to variations in R^2 during metamodel development. A key factor is the variability in the training data, which significantly influences the performance of machine learning models. Greater variability can complicate the identification of patterns, leading to reduced predictive accuracy and a lower R^2. The differences in wall construction and hygrothermal behaviours among CS1, CS2, and CS3 account for variations in the metamodel's performance across these cases. Furthermore, the relevance and selection of input features play a critical role. For instance, the features selected for CS1 may not have been as informative as those used for CS2 and CS3, contributing to its lower R^2. Nevertheless, the R^2 value for CS1 remains acceptable within the study's scope.

Hyperparameter tuning is essential to optimise the RF model's performance. This study's optimisation involved adjusting parameters such as the number of trees, identifying the most impactful features, and estimating the model's generalisation performance using out-of-bag samples. Other hyperparameter values were considered based on values from [273].

3.4.4.2 Metamodeling vs probabilistic hygrothermal analysis

In Paper IV [274], the PA method was integrated with a machine learning-based metamodel to evaluate the influence of extruded mortar joints on mould growth across four different orientations of a building envelope. The results for the east-facing orientation, analysed under the ASHRAE water penetration criterion, are illustrated in Figure 15. The figure highlights the added capability of MA in identifying scenarios with higher risks that may have been overlooked by PA alone. In the PA simulations, the grey lines represent the range of scenarios, showing a maximum mould index of 4.76. However, the performance evaluation indicator used in this study, the 95th percentile of maximum mould indices, was calculated as 4.16 based solely on PA results (blue lines).

By incorporating MA with PA, predictions were extended to a significantly larger dataset of scenarios (10^7), allowing for a more comprehensive evaluation. The 95th percentile of maximum mould indices predicted by the metamodel reached 4.85. This value is 17% higher than the corresponding result derived from PA alone, demonstrating the ability of the MA to uncover potential risks that might otherwise remain undetected.

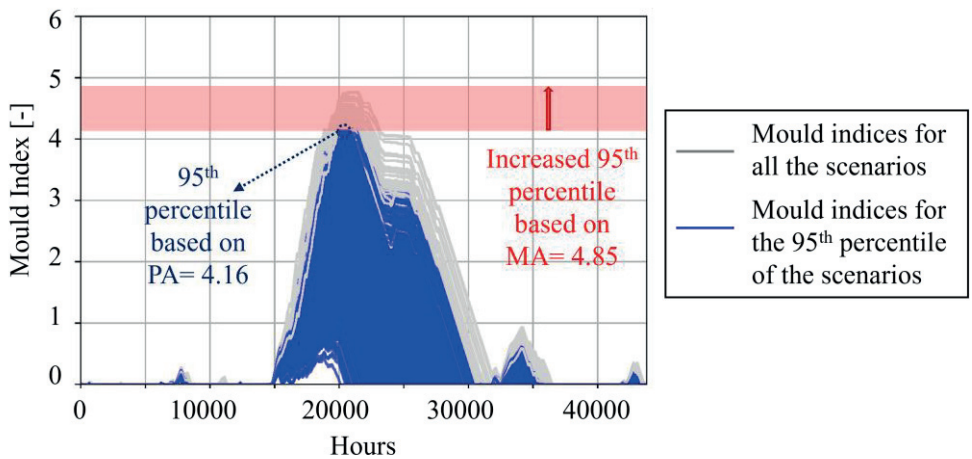


Figure 15: Metamodeling analysis (MA) vs probabilistic analysis (PA) based on a case study in paper IV [274]. Blue lines: mould indices for the 95th percentile of the scenarios based on PA, grey lines: mould indices for all the scenarios based on PA, red band: 95th percentile of the maximum mould indices based on MA.

3.5 Hygrothermal sensitivity analysis (HSA)

3.5.1 Sensitivity analysis (SA)

SA examines how variations in input parameters influence the results of interest, providing insights into the relative significance of each parameter in affecting the output. This process is crucial for understanding how uncertainties in input variables propagate through a model with stochastic inputs. It addresses essential aspects, such as:

- Identifying Sensitive Parameters: Recognising the parameters that impact the outcome most enables designers to prioritise these variables, improving design efficiency. It also allows for a reduction in computational effort by omitting non-sensitive parameters.
- Evaluating Model Reliability: Determining whether the numerical model reliably captures real-world behaviours, as it may exhibit sensitivities that are not observed in practice, thereby revealing potential uncertainties within the model [275].

Bayat Pour et al. [71] reviewed various SA methods commonly applied in hygrothermal studies. They can be broadly classified into local, global, and screening methods [276]. While local and global analyses yield quantitative metrics that quantify the contribution of each input variable to variations in model output, screening methods produce qualitative insights by ranking parameters based on their relative influence [248]. Various methodological approaches support these SA methods, including One-At-A-Time, correlation-, regression-, variance-, density-, and segmentation-based. This diversity enables researchers to align the SA with the specific demands and objectives of hygrothermal modelling.

- Local SA examines the sensitivity of model outputs concerning individual input parameters around specific reference values, often focusing on a narrow range or single point such as the mean value. This approach is particularly useful for evaluating sensitivity near a defined baseline.
- Global SA, on the other hand, considers the entire range or distribution of input parameters, offering a broader perspective on how input variability impacts model outcomes [277].
- Screening methods are designed to handle complex models with numerous input variables efficiently. These methods identify the most impactful parameters while disregarding those with minimal influence. Unlike local and global methods, screening does not rely on input distributions but instead evaluates inputs at predefined discrete levels [248].

The same review [71] identified a total of 21 distinct SA methods applied in HSA studies. Among these, approximately 70% of the studies utilised global SA to evaluate the influence of input uncertainties on the outcomes. The review also highlighted the limitations associated with SA methods, primarily stemming from the transient and non-linear nature of hygrothermal modelling. Furthermore, interactions among input variables were found to significantly affect results, demonstrating the need for methods that account for non-linearity and variable interactions. Adopting a conservative strategy that combines multiple SA methods within the HSA studies is recommended to address these challenges. This approach ensures a more comprehensive assessment of transient conditions while mitigating the limitations of individual methods. Additionally, computational efficiency is critical for practical applications, particularly in large-scale projects. Thus, selecting methods that are computationally less intensive is essential. For example, Annex 55: Subtask 2 [121] emphasises the combined use of Spearman's rank correlation coefficients and scatterplots as an effective strategy for building performance evaluations. This approach provides reliable insights while significantly reducing computational effort compared to resource-intensive methods.

3.5.2 Mould sensitivity analysis (MSA) method

The mould sensitivity analysis (MSA) method introduced in this thesis utilises output data from MRA, specifically the maximum mould index. This is combined with input data obtained from samples generated either for hygrothermal simulations within the PA component or for hygrothermal predictions in the MA component of the MRA methodology. The input parameters can include material properties as well as outdoor and indoor boundary conditions. As depicted in Figure 16, the MSA method incorporates two distinct approaches within its framework:

- Feature importance analysis, which identifies the relative significance of various input parameters in influencing the model output.
- Correlation analysis, which examines the relationships and dependencies between input variables and the maximum mould index, providing insights into their degree of influence and potential interactions.

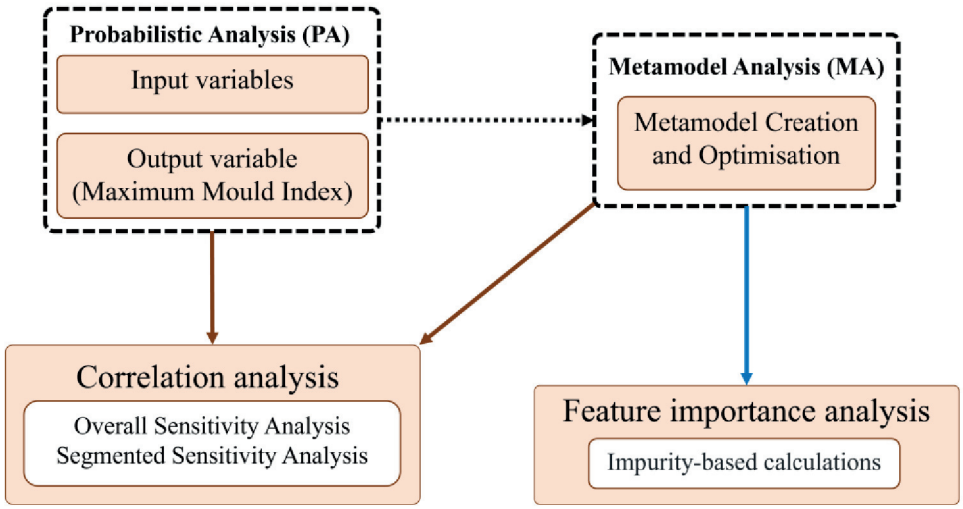


Figure 16: Mould sensitivity analysis (MSA) procedure. Brown arrows: linear sensitivity analysis using Spearman's correlation analysis, blue arrow: linear and non-linear sensitivity analyses using feature importance analysis.

3.5.2.1 Spearman correlation coefficient

The correlation analysis in this study is conducted using two distinct SA modes. The first, overall SA, involves calculating the Spearman's correlation coefficient, $\rho_{X_{ri},Y_{rj}}$, for variable pairs based on the entire input and output distributions [85]. The calculation follows Eq. (27):

$$\rho_{X_{ri},Y_{rj}} = \frac{cov(X_{ri},Y_{rj})}{\sigma_{X_{ri}}.\sigma_{Y_{rj}}} \tag{27}$$

where:

- $cov(X_{ri},Y_{rj})$: the covariance of two ranked variables,
- $\sigma_{X_{ri}}$: the standard deviation of ranked input variables,
- $\sigma_{Y_{rj}}$: the standard deviation of ranked output variables.

Spearman's correlation coefficient, the Rank Correlation Coefficient (RCC), measures the monotonic relationship between two variables and ranges from -1 to +1 [275]. Its interpretation is as follows [278]:

- 0.00: No relationship,
- 0.00 – 0.09: Negligible relationship,

- 0.10 – 0.39: Weak relationship,
- 0.40 – 0.69: Moderate relationship,
- 0.70 – 0.89: Strong relationship,
- 0.90 – 1.00: Very strong relationship.

The sign of this coefficient indicates the direction of the relationship. A positive sign signifies a direct correlation, where both variables increase or decrease together. Conversely, a negative sign implies an inverse relationship, where an increase in one variable corresponds to a decrease in the other and vice versa.

The MSA incorporates a segmented SA to enhance the analysis, concentrating on scenarios where mould indices approach the failure threshold. The corresponding input data for these critical scenarios are extracted and organised into a segmented dataset for focused examination. Spearman's correlation coefficient is then recalculated for this subset, offering a targeted understanding of the relationship between critical input variables and mould indices near the failure threshold. This approach reveals the factors most strongly influencing mould growth at critical thresholds, enabling more precise identification of risk factors.

3.5.2.2 Feature importance analysis

This study employs the RF algorithm to perform feature importance analysis, leveraging its capability to capture both linear and non-linear relationships between inputs and outputs. RF, an ensemble learning method, constructs multiple decision trees, each comprising internal nodes or branches. A feature (input variable) is selected at each internal node to partition the dataset into two subsets based on their corresponding responses. The selection of features for these splits is guided by criteria such as Gini impurity for classification tasks and variance reduction (via sum of squared residual calculations) for regression tasks. The degree to which each feature contributes to reducing impurity during a split is quantified. The feature that achieves the highest reduction in impurity—minimising Gini impurity or the Sum of Squared Residuals—is selected as the splitting criterion for a given node. Feature importance is then determined by calculating the average reduction in impurity contributed by each feature. This aggregated metric serves as a measure of the feature's significance in the ML model. Thus, features with higher importance scores are considered more influential in predicting the output variable within the RF model [273]. This methodology provides a robust framework for identifying critical parameters in complex datasets, aiding in developing reliable and efficient predictive models.

3.5.3 Results and discussion

3.5.3.1 Segmented vs overall sensitivity analyses

In Paper II [172], the developed MSA method evaluated three illustrative case studies for mould growth assessment on their interior surfaces. This approach was employed to demonstrate its application in hygrothermal analysis. The correlation analysis, a component of the MSA, was conducted in two modes: segmented SA and overall SA. The segmented SA targeted scenarios with mould indices exceeding 0.95 encompassing not only failed scenarios but also those approaching failure.

Figure 17 highlights the distinctions between segmented and overall SAs. For instance, the solar absorption coefficient consistently correlated negatively with the maximum mould index in both analysis modes, as indicated by the negative Spearman correlation coefficients. This trend arises from the observation that higher solar absorption coefficients enhance the material's drying potential, thereby mitigating mould growth risks. However, the sensitivity magnitude differed between the two modes. While overall SA considered all scenarios and revealed a stronger relationship between solar absorption and mould growth, segmented SA — focusing on critical scenarios near the failure threshold—demonstrated a notably diminished sensitivity. This reduced sensitivity in the segmented mode demonstrates the importance of tailored analyses for specific risk scenarios, offering a more in-depth understanding of the factors influencing mould growth under failure-prone conditions.

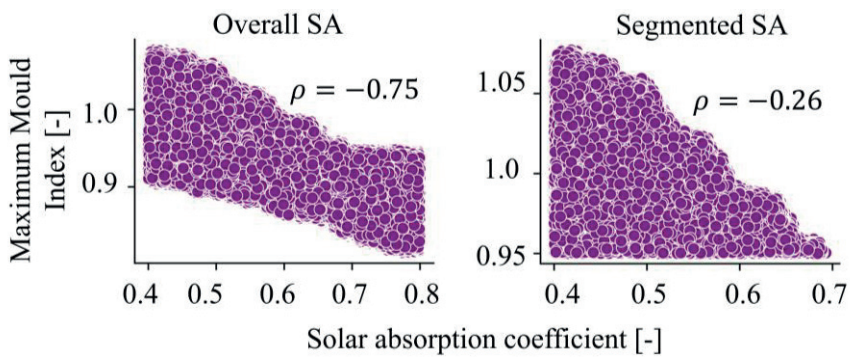


Figure 17: Overall vs segmented sensitivity analysis according to MSA method.

The segmented SA narrows its analysis to data near the mould index threshold, focusing specifically on failure or near-failure conditions. This narrowed scope inherently reduces the variability in both dependent variables (e.g., mould index) and independent variables (e.g., solar absorption coefficient). Consequently, the monotonic relationships between variables become less pronounced, often resulting in lower Spearman correlation coefficients. Despite this reduction in apparent

correlation strength, the segmented SA isolates high-risk scenarios, enabling a more precise identification of variables critical under failure-prone conditions. This targeted approach is particularly valuable for understanding factors directly influencing mould growth near the threshold rather than general trends across all scenarios. For instance, in Paper II [172], one case study revealed that the thermal conductivity of wood fibre insulation exhibited a moderate sensitivity to the maximum mould index in the segmented SA mode, while its sensitivity was deemed negligible in the overall SA mode. Relying solely on the overall Spearman correlation coefficient would have overlooked the significance of this variable. Segmented SA provides designers and engineers with localised insights by focusing on scenarios near the failure threshold, allowing them to prioritise interventions for conditions most likely to lead to failure.

3.5.3.2 Feature importance analysis and Spearman correlation coefficient

Feature importance analysis offers valuable insights, especially for detecting non-linear correlations, and serves as a verification tool for the previously performed SA. This analysis enhances the scope of identified influential parameters by identifying additional important variables (identified by red ellipses in Figure 18), even if their degree of importance is comparatively lower. For instance, using the feature importance analysis in Paper II [172], the solar absorption coefficient was identified as the most significant variable, demonstrating a clear distinction in its importance relative to other input parameters in a case study. This finding was consistent with segmented and overall SA results, which revealed a negative correlation between the solar absorption coefficient and the maximum mould index. In addition to the solar absorption coefficient, other input variables, such as the indoor surface heat transfer coefficient, outdoor convection heat exchange coefficient, and the thermal conductivity of wood fibre insulation, were identified as sensitive parameters by both Spearman correlation coefficient and feature importance analysis.

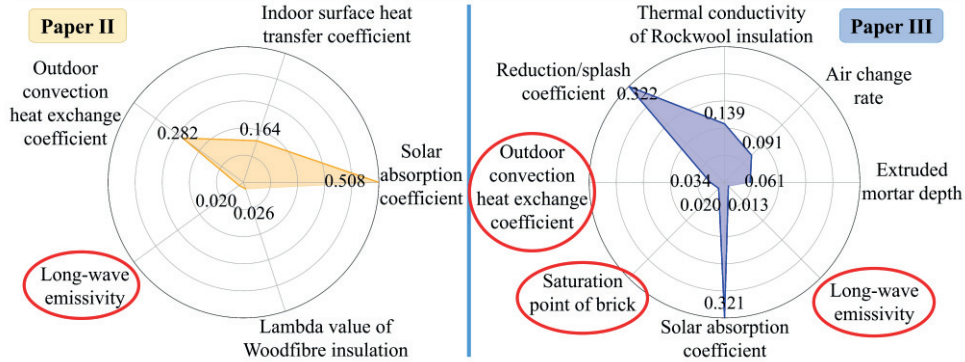


Figure 18: Feature importance analysis. The values highlighted in the red ellipse represent additional sensitive variables identified through feature importance analysis, which were overlooked by the Spearman correlation coefficient method.

The analysis presented in Figure 18 (indicated by the red ellipse) highlights additional sensitive input variables through feature importance analysis that were not identified via correlation analysis. For example, in Paper II [172], the long-wave emissivity was important in predicting the maximum mould index through the non-linear sensitivity approach of feature importance analysis, but it was overlooked in linear correlation analysis. This distinction arises because feature importance analysis captures non-linear effects, whereas correlation analysis primarily focuses on linear relationships. In Paper III [258], the investigation of extruded mortar joints further demonstrated the utility of feature importance analysis in identifying influential variables. Alongside the extruded mortar depth, other sensitive parameters influencing mould growth were identified, such as air change rate, the thermal conductivity of Rockwool insulation, reduction/splash coefficient, outdoor convection heat exchange coefficient, saturation point of brick, solar absorption coefficient, and long-wave emissivity. Additionally, feature importance analysis revealed more distinct differences in the significance levels of these variables. For instance, under low WDR load climatic conditions, the importance of extruded mortar depth was substantially lower compared to other parameters, as illustrated in Figure 18 on the right side. This result suggests that in regions with minimal WDR loads, extruded mortar has a negligible impact on moisture transport. This is because the absence of WDR-related moisture sources leaves the extruded mortar dry, reducing its influence on hygrothermal behaviour and mould growth.

The findings demonstrate that combining Spearman correlation analysis (both overall and segmented) with feature importance analysis provides a more comprehensive, robust, and reliable understanding of the factors influencing mould growth. This dual approach enhances confidence in identifying sensitive parameters for hygrothermal performance and mould growth assessments.

4 Sustainability in building envelope design

This chapter begins by mentioning the importance of sustainability in building design and its role within PHA studies. As outlined in Annex 55, Subset 2 of the IEA report [121], economic optimisation was identified as a pivotal toolset for advancing PHA, particularly in enhancing decision-making processes for building envelope design and retrofitting strategies. This toolset, along with its relevance and application, is discussed in the subsection on economic impact analysis. Subsequently, this chapter explores additional toolsets and methodologies that can complement or extend current practices, highlighting their potential as developments in the PHA field. These sections detail novel approaches for integrating sustainability considerations into building performance assessments, reflecting the evolving needs for environmentally, economically, and socially responsible design solutions. Through detailed exploration and practical application insights, this chapter aims to contribute to the advancement of PHA methodologies. It shows the necessity of incorporating sustainability perspectives to achieve comprehensive, robust, and reliable hygrothermal analyses, offering a pathway for informed decision-making in sustainable building envelope design.

4.1 Background

Sustainability has emerged as a critical approach for addressing the pressing environmental, economic, and social challenges of the 21st century. It focuses on fulfilling current needs while safeguarding the resources necessary for future generations, fostering a balance between development and environmental preservation. The growing global demand for resources has accelerated the depletion of natural reserves, reduced biodiversity, and intensified climate change [279, 280]. These factors increasingly threaten ecosystems, economic stability, and human well-being. The Intergovernmental Panel on Climate Change (IPCC) report identifies greenhouse gas (GHG) emissions as a primary driver of climate change and global warming [281]. Embracing sustainable practices becomes essential in mitigating these impacts by enhancing resilience, reducing ecological footprints, and promoting fair resource allocation. Sustainability now stands as a necessity

rather than a choice, crucial for counteracting the detrimental effects of unchecked industrialisation, deforestation, and pollution. By embedding sustainable principles into policies, industries, and everyday activities, societies can foster environmental health and ensure a more stable and equitable future.

Sustainable building design plays a key role in creating environmentally responsible and resource-efficient buildings. The building sector contributes to approximately 30% of global GHG emissions [282]. By implementing energy-efficient strategies, it is possible to reduce energy-related GHG emissions by more than 40% [283]. Green building principles are designed to minimise environmental impacts throughout a building's lifecycle [284], guiding architects and engineers to reduce ecological footprints while maintaining occupant comfort and functional performance. Innovations such as passive solar design, high-performance insulation, and energy-efficient lighting systems significantly reduce operational energy demands. Additionally, green roofs, rainwater harvesting systems, and waste recycling initiatives support resource conservation [285]. Adopting materials with low embodied energy, such as recycled steel and sustainably sourced timber, further contributes to sustainability goals.

Adopting bio-based materials, particularly wooden elements, offers a promising solution to mitigate the environmental impact of the built environment and combat climate change [116] by reducing the built-in energy. Wooden components can be utilised as both structural elements—such as cross-laminated timber (CLT) and timber studs [286]—and as insulation materials [287]. Improving a building's energy performance by adding insulation to the building envelope is a widely adopted and highly effective strategy for reducing operational energy demands [122]. Despite these advantages, highly insulated walls present moisture-related challenges, including condensation, rot decay, and microbial growth [122, 287, 288]. While wood demonstrates remarkable durability under dry conditions, maintaining consistently dry conditions throughout a building's lifespan, particularly for multi-storey structures, poses significant challenges [289]. These buildings face high wind pressure and increased exposure to WDR. Moreover, the extended on-site construction periods typical for multi-storey projects heighten the vulnerability of wooden elements to moisture [116].

When selecting an optimal building envelope for a construction project, evaluating sustainability alongside hygrothermal performance is imperative. A design may fulfil moisture safety requirements but fail to align with environmental or economic objectives, undermining long-term sustainability goals. Therefore, decision analysis approaches must comprehensively assess trade-offs between hygrothermal performance, environmental impact, and cost considerations. A recent literature review by Bayat Pour et al. [71] highlighted a significant gap in current research, revealing that 95% of PHA studies did not consider sustainability considerations. This demonstrated the need for advancing methodologies integrating

environmental, economic, and societal perspectives to guide practitioners toward more balanced and responsible design choices.

An exemplary initiative highlighting the integration of PHA with LCA and LCC is the RIBuild project (robust internal thermal insulation of historic buildings) [290]. This project established a probabilistic methodology for evaluating the environmental impacts and global costs of internal insulation solutions for historic structures [39]. Similarly, the TallFacade project [116] explored the application of LCA and LCC, leveraging PHA outputs to design robust and economically feasible solutions for tall timber facades. Despite these advancements, critical research gaps persist in designing sustainable building envelopes. The first notable gap involves developing a holistic decision analysis framework that integrates hygrothermal assessments with LCA and LCC. Previous projects performed these analyses independently, but effective decision-making demands a multi-criteria approach where results from various parameters are cohesively evaluated. A second gap lies in incorporating metamodels within decision analysis frameworks to enhance and expedite PHA. This approach would enable considering a wider range of scenarios, yielding more comprehensive and robust insights. Current studies have faced limitations in managing extensive scenario datasets efficiently. Lastly, prior investigations have focused on narrow case studies, such as historical walls with internal insulation or timber-frame facades in high-rise buildings. Expanding the scope to encompass diverse building types and materials is essential for developing broadly applicable, sustainable design strategies.

4.2 Inutility decision analysis (IDA) framework

A central objective of this PhD thesis is to integrate sustainability measures with PHA to enable a more informed and comprehensive decision analysis process. The innovative contributions in this area aim to address the research gaps outlined in Section 4.1, thereby advancing the sustainable building envelope design field. A novel decision analysis method termed IDA is introduced in this thesis, synthesising sustainability considerations—including environmental and economic impacts—with PHA. This innovative framework addresses key gaps in sustainable building envelope design by integrating multi-criteria decision-making elements. The methodology identifies the optimal solution by selecting case studies with the lowest inutilities, thereby minimising drawbacks. Figure 19 outlines eight steps for implementing the IDA framework, with detailed coverage of steps one to five coupled with step eight in this thesis, as presented in Paper V. Steps six and seven are reserved for future studies to extend the decision analysis capabilities. Each step addresses critical factors such as economic consequences, environmental impacts, health implications, and energy consumption stemming from moisture-related

challenges—all treated as inutilities. Below is a summary of each step in the proposed IDA framework:

1) Case Studies Definition: Defines various building envelope case studies and outlines the motivations for their selection.
2) Probabilistic Hygrothermal Analysis: Incorporates input variables for relevant damage models, such as mould growth, rot decay, frost, and algae. The failure probability of these models is calculated in this step.
3) Definition of Retrofitting/Maintenance/Remediation Scenarios: Specifies retrofitting, maintenance, or remediation scenarios due to moisture-induced damages over the building's lifecycle.
4) Life Cycle Costing (LCC): Assesses the economic impacts of selecting each building envelope alternative. This includes initial and running costs associated with retrofitting, maintenance, or remediation scenarios.
5) Life Cycle Assessment (LCA): Evaluates environmental impacts for each case study, considering the initial selection of building materials and the retrofitting or remediation processes.
6) Health Consequence Analysis (Future Research): Connects outputs from hygrothermal analyses to potential health issues related to moisture problems.
7) Energy Performance Analysis (Future Research): Assesses energy performance using whole-building analyses or single indicators like thermal transmittance for assemblies.
8) Decision Analysis: Integrates outputs from previous steps to identify the most optimal building envelope exhibiting the lowest inutility index.

The following subsections will explore each step in detail, while health consequences and energy performance analyses will be addressed in the future research potential section.

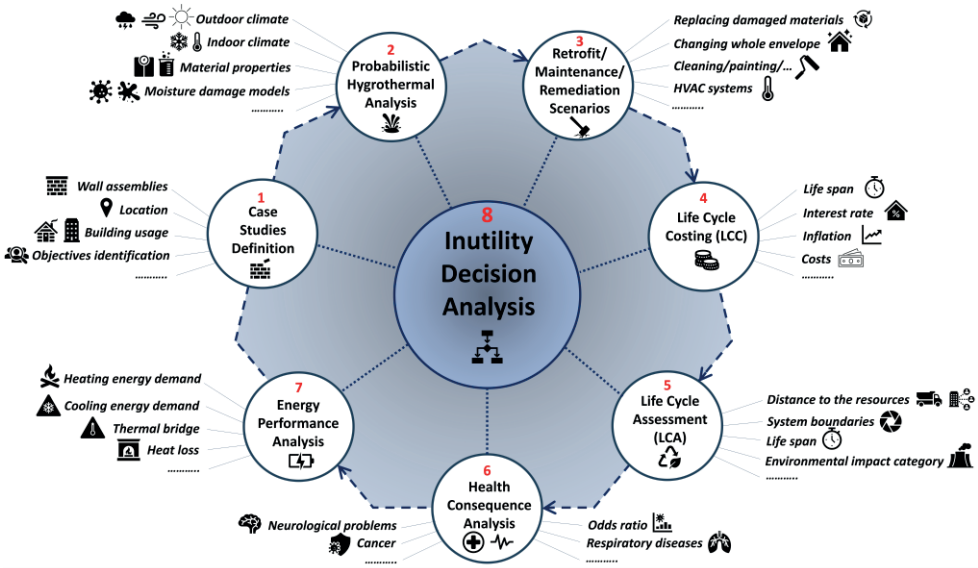


Figure 19: Inutility decision analysis (IDA) procedure.

4.3 Retrofitting/maintenance/remediation scenarios coupled with circularity concept

Construction projects may focus on either new constructions or renovating existing buildings. The framework outlined in Figure 19 is adaptable for both contexts and tailored to project-specific requirements. The third step, i.e., the "Retrofitting, Maintenance, and Remediation Scenarios Definition", evaluates potential scenarios and actions based on the severity of moisture-related issues to guide effective remediation strategies. The necessary interventions vary depending on the extent of moisture damage. When mould growth is detected on material surfaces, remediation steps should adhere to established guidelines [291, 292], which may involve the following:

A) Identifying and Mitigating Moisture Sources: Repairing leaks in building envelopes, fixing plumbing issues, and enhancing ventilation systems to address sources of moisture penetration are critical first steps.

B) Containing Affected Areas: Sealing off doorways, vents, and other openings using plastic sheeting and duct tape prevents the spread of mould spores throughout the building.

C) Ensuring Personal Protective Equipment (PPE): Staff involved in remediation must use gloves, goggles, and respirator masks to minimise exposure to mould spores and toxins.

D) Cleaning Non-Porous Surfaces: Surfaces can be scrubbed with detergent solutions or specialised mould cleaners, followed by thorough rinsing and drying to remove mould traces.

E) Removing Mould from Porous Materials: Affected materials such as gypsum boards, insulation, or wooden sheets should be removed and properly discarded. In cases of shallow mould growth, minor repairs may suffice.

F) Disinfecting Surrounding Areas: Disinfectants can remove residual mould spores and prevent regrowth.

G) Ensuring Adequate Ventilation: Maintaining airflow during and after remediation promotes effective drying. Fans and open windows are recommended to support this process.

H) Preventing Recurrence: Post-remediation measures should enhance ventilation systems, maintain optimal humidity levels, and implement regular inspections to identify early signs of moisture source or mould growth.

These steps illustrate an approach to managing moisture-related challenges, ensuring improved durability and sustainability of building envelopes while promoting a healthier indoor environment. Selecting appropriate retrofitting, maintenance, or remediation strategies requires comprehensive evaluation involving technical insights from experts and practitioners and the preferences of building owners and other stakeholders. This collaborative approach ensures that the proposed actions align with technical feasibility and stakeholder priorities, facilitating informed decision-making. These interventions must also be evaluated against the sustainability criteria outlined in the IDA framework to comprehensively address environmental, economic, health, and energy considerations.

Integrating the Circular Economy (CE) concept into retrofitting and remediation strategies is critical to this decision-making process. CE promotes resource efficiency by minimising waste, retaining long-term value, reducing dependence on primary resources, and fostering material reuse through closed or open loops of products and components [293]. Key attributes of CE principles include:

- Waste Minimisation: Reducing construction and demolition waste through resource recovery,
- Material Reuse: Salvaging and repurposing materials like timber, steel, and insulation products,

- Value Retention: Prolonging the lifespan of building components to optimise resource use,
- Environmental Protection: Minimising carbon emissions and resource extraction while ensuring biodiversity conservation.

CE practices in building projects offer substantial potential for fostering sustainable development, contributing to environmental preservation, and mitigating resource depletion [294]. CE strategies support a shift toward greener, more resilient building practices and promote long-term socioeconomic benefits.

The "10 R Strategies for CE"

The framework introduced by Potting et al. [295] presents a hierarchical approach to achieving circularity structured around resource optimisation and sustainability. Figure 20 illustrates these strategies, organised into three primary categories—Smarter Product Use and Manufacture, Extending Product Lifespan, and Useful Application of Materials—where each strategy is designed to minimise resource consumption, reduce waste, and retain value within the economy. At the top of the hierarchy are short-loop strategies, such as Refuse (R_0), Rethink (R_1), and Reduce (R_2), which focus on eliminating unnecessary consumption, optimising product usage and improving efficiency. Medium-loop strategies, including Reuse (R_3), Repair (R_4), Refurbish (R_5), Remanufacture (R_6), and Repurpose (R_7), emphasise prolonging the lifecycle of products and their components. Finally, long-loop strategies, such as Recycle (R_8) and Recover (R_9), address the end-of-life phase by reclaiming materials or energy from waste. Figure 20 highlights the linear economy's reliance on landfills and incineration, contrasting it with circular practices that reduce environmental impacts. Circular strategies, particularly those higher on the hierarchy, promote environmental care, resource conservation, and economic resilience by circulating materials for as long as possible.

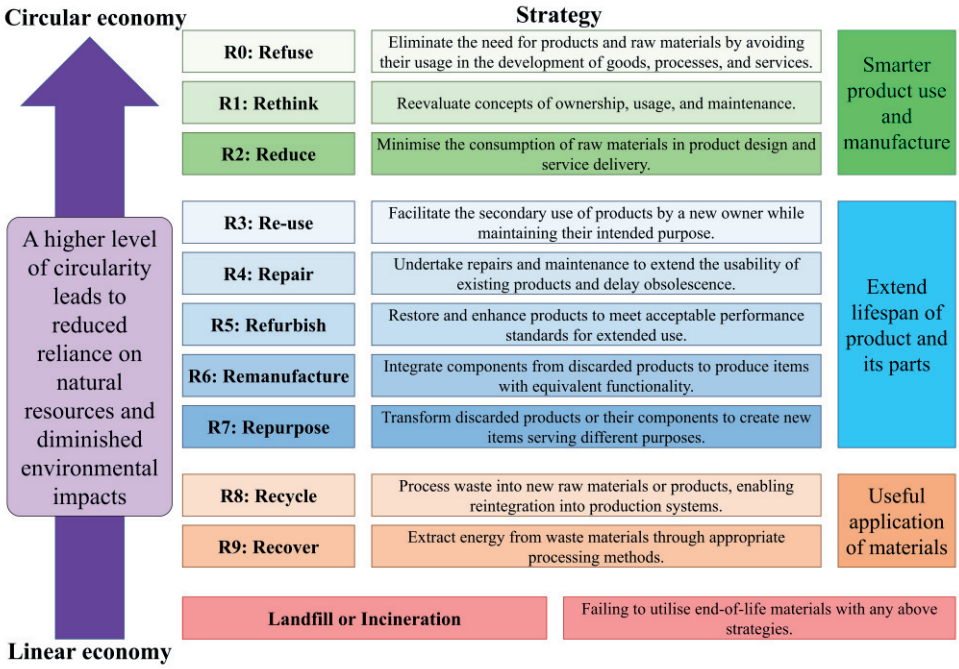


Figure 20: Circularty strategies within the production chain, in order of priority, adopted from [295] edited and designed by Mohsen Bayat Pour.

4.4 Economic impacts assessment

4.4.1 Method

The economic evaluation of building envelope selection in this PhD thesis uses the LCC methodology outlined in ISO 15686-5 [296]. The study utilises net present value calculation procedures [297] to estimate the present value of a case study by integrating both initial costs and running costs.

- *Initial Costs:* These costs include expenses associated with material procurement, labour, and installation [297-300].
- *Running Costs:* These are expenses arising from retrofitting, maintenance, or remediation scenarios, as described in Section 4.3. Running costs also encompass the procurement of new materials, labour, and installation costs for repair and replacements, along with demolition, dismantling, and construction waste management for old or damaged materials [297-300].

Material prices for a case study can be determined by averaging quotations obtained from various construction suppliers. Labour, installation, and associated costs are evaluated based on the specific requirements of the construction process. For example, in the light-frame timber wall case studies presented in Paper V [301], the following assumptions are made:

- *Installation Costs:* These include accessories, supplementary and ancillary materials, and equipment such as mortar for bricklaying, screws and netting for gypsum boards, scaffolding, fencing, signage, protective foils, drying machines, and lifters.
- *Waste Management Costs:* These involve expenses for waste containers, disposal, and the transportation of waste materials.

In this PhD thesis, labour and installation costs were estimated at 3% of material prices for simplification purposes, following assumptions from [287]. Similarly, an additional 3% of material prices was considered for demolition, dismantling, and construction waste management associated with damaged and old materials. The Swedish construction market was chosen for this analysis, and the calculations were conducted in euros. Prices for the materials were identified by contacting four Swedish construction suppliers [302-305], and the average of these prices was utilised in the LCC calculations. However, for real-world projects, it is recommended to extract this data from specialised databases, such as those mentioned in [306].

To illustrate the application of the proposed decision analysis method, three case studies were analysed (as detailed in Paper V [301]). It is important to note that the primary objective of this research is to demonstrate the utility and application of the proposed decision analysis framework rather than calculating the exact values. This framework facilitates evaluating and integrating diverse design perspectives, including moisture safety, environmental considerations, and economic impact analyses. Efforts were made to incorporate the most realistic examples within the study's scope to ensure the practical relevance of the findings.

To convert the future costs associated with the running costs of building envelope assemblies over their lifespan into their present value (P), Eq. (28) is utilised. This equation incorporates parameters such as today's costs (A_0), growth rate (g_r), interest rate (i_r), and the building lifespan (N) [299]:

$$P = A_0(1 + i_r)^{1-N}(1 + g_r)^{N-1} \tag{28}$$

The interest rate used in the calculations is based on the daily average interest rate established by the Swedish Central Bank (Riksbank) over the past 29 years (1994–2023) [307]. This yielded an average interest rate of 2.27%. It is important to note that interest rate predictions reflect expectations regarding future monetary policy and are influenced by economic developments within Sweden and globally. As

such, these predictions carry inherent uncertainty, especially for longer-term projections. The Swedish Central Bank often presents alternative scenarios in its monetary policy reports to account for potential variations in future interest rates [308].

The growth rate is assessed using a price index, which measures the evolution of price levels over 12 months. Sweden's consumer price index with fixed interest (CPIF) is the standard metric for this purpose [309]. Historical CPIF data obtained from the Swedish Central Bank's official website indicate an average growth rate of 2.68% over the past 35 years (1988–2023). These values are used in the economic analyses to reflect realistic market conditions.

4.4.2 Results and discussion

The analysis in Figure 21 combines insights from two complementary perspectives:

- Economic Impacts Across Life Cycle Stages (depicted in the pie chart) – This visualisation highlights the proportionate financial contributions of various life cycle stages (e.g., material procurement, installation, maintenance, retrofitting, remediation, and waste management) to the total economic impact of the building envelope assemblies.
- Average Material Costs per Square Metre (illustrated in the bar chart) – This representation breaks down the material costs per square metre used for the analysed case studies, offering a comparative view of the financial burden associated with each assembly type.

The pie chart in Figure 21 reveals the proportional contributions of initial construction costs (orange) and long-term retrofitting/maintenance/remediation expenses (blue) for the three case studies (CS1, CS2, and CS3), focusing on mould-related issues. CS1 consisted of a non-ventilated timber frame wall. CS2 featured a ventilated timber frame wall with an external plaster layer. CS3 included a ventilated timber frame wall with a brick veneer. Among the cases, CS3's initial costs are the highest, primarily due to the incorporation of high-cost materials, such as brick. Notably, CS3's retrofitting/maintenance/remediation costs are significantly lower than its initial costs. This reduction reflects the brick's minimal need for remediation, effectively minimising mould-related maintenance requirements over time.

The bar chart in Figure 21 complements the pie chart by breaking down average material costs per square metre, framing their contributions to initial expenses. Brick is the most expensive material, with a price of 132.2 €/m², far exceeding that of other materials. However, this higher cost corresponds to the brick's exceptional durability and resistance to environmental degradation, as noted in [258]. These

attributes reduce the need for frequent repairs or replacements, leading to lower proportional running costs for CS3 than for CS1 and CS2.

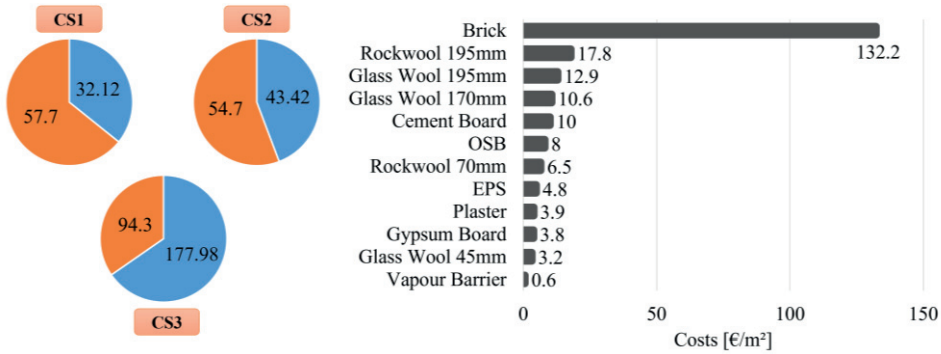


Figure 21: Pie chart: Potential economic impacts [€/m^2] of each case study for different building life cycle stages during the lifespan of the building (blue: initial costs, orange: running costs). Bar chart: Average used materials prices [€/m^2].

4.5 Environmental impacts analysis

4.5.1 Method

Life cycle assessment (LCA) assesses a product's possible environmental impacts over the course of its lifecycle following EN ISO 14040 [310]. The methodology adheres to international standards for LCA, including EN ISO 14040 [310], the European standards for the environmental performance assessment of buildings (EN ISO 15978) [311], and the environmental product declaration (EPD) core rules for construction products (EN 15804) [312].

The LCA conducted in this PhD thesis focuses on analysing the environmental impact of various moisture-related damage scenarios, as outlined in Section 4.3. The system boundary follows the modular lifecycle framework defined in EN 15978 [311], illustrated in Figure 22. This modular system evaluates cradle-to-grave impacts across four main life cycle stages:

- Product Stage (Modules A1–A3): Includes raw material extraction, transportation, and product manufacturing.
- Construction Stage (Modules A4–A5): Covers the transportation of products to the construction site and the construction/installation process.
- Use Stage (Modules B1–B7): Encompasses use, maintenance, repair, replacement, refurbishment, and operational energy and water use.

- End-of-Life Stage (Modules C1–C4): Includes deconstruction/demolition, waste transportation, waste processing, and disposal.

These modules collectively enable a comprehensive assessment of the environmental impacts of the initial building design and the defined retrofitting, maintenance, and remediation scenarios, ensuring alignment with industry standards and sustainability goals.

System boundaries (X=modules included in this study) according to EN 15978																			
A1-A3 Product stage			A4-A5 Construction Process stage		B1-B7 Use stage							C1-C4 End-of-life				D1-D4 Benefits and loads beyond the system boundary			
A1	A2	A3	A4	A5	B1	B2	B3	B4	B5	B6	B7	C1	C2	C3	C4	D1	D2	D3	D4
Raw material supply	Transport	Manufacturing	Transport	Construction installation process	Use	Maintenance	Repair	Replacement	Refurbishment	Operational energy use	Operational water use	Deconstruction	Transport	Waste processing	Disposal	Reuse	Recovery	Recycling	Exported energy/potential
X	X	X	X	X	X	X	X	X	X	X	X	X	X	X	X				

Figure 22: System boundaries with respect to life cycle stages covered in this thesis [311].

This study's life cycle environmental impact was assessed primarily through Global Warming Potential (GWP). EPDs were extracted for life cycle modules A1–A3, A5, B1–B7, C1, and C3–C4. The optional Module D, which accounts for the potential positive impacts of processing or reusing materials post-end-of-life, was excluded. The EPD data were compiled from four databases: epddanmark [313], EPD International [314], epd-norway [315], and ibu-epd [316]. The average of the relevant EPD data was used. These databases align with the construction Product Category Rules (PCR) defined in EN 15804 [312], ensuring consistency and reliability.

Throughout the building's expected 50-year lifespan, 1 m^2 of external wall assemblies serve as the functional unit for this evaluation. The transportation modules (A4 and C2) were calculated using OpenLCA version 2.1.1 [317], a software tool for life cycle impact assessment (LCIA). The LCIA results were derived using the CML baseline method developed by the University of Leiden in 2001, a widely recognised framework for environmental impact categories in LCA studies [318].

Transportation Modules:

- *Module A4:* Accounts for transporting materials and products from manufacturing to construction sites, including intermediate storage and distribution. It is computed based on:
  A) Average transport distance (assumed as 200 km [3] from production to the building site in Gothenburg, Sweden).
  B) Material weights (calculated using the average material densities).
  C) Emission factors from the means of transportation. The selected transportation provider was "Lorry transport, Euro 0, 1, 2, 3, 4 mix, 22 t total weight, 17.3 t max payload – RER", in accordance with [287].
- *Module C2:* Represents transport from the building site to waste processing locations, including recycling, incineration, and landfill facilities. The assumed transport distance was 50 km [3], calculated using the same methodology as Module A4.

By utilising up-to-date, standardised EPD data and reliable software tools, the study ensures robust environmental impact calculations, offering meaningful insights into the life cycle performance of external wall assemblies.

4.5.2 Results and discussion

The potential environmental impacts [kg CO_2 eq./m²] are depicted by a pie chart in Figure 23 for each case study across various building life cycle stages over the building's lifespan. It provides a breakdown of initial CO_2 emissions (indicated by blue colour) and life span environmental impacts related to mould growth scenarios for each case study (indicated by orange colour).

Key Observations:

- *CS3 Environmental Impact:* The environmental impacts associated with mould growth for CS3 were approximately 23% lower than its initial environmental impacts. This reduction stems from the durability of bricks, which did not require replacement under retrofitting/maintenance/remediation scenarios. However, CS3 required retrofitting/maintenance/remediation for five layers in the event of mould growth, leading to higher environmental impacts in damage scenarios compared to CS1 and CS2.
- *Comparison Between CS1 and CS2:* CS2 exhibited higher environmental impacts during replacement actions than CS1. This is attributed to the two layers of gypsum board and a vapour barrier in CS2, which needed replacement to access the main insulation layer. Conversely, CS1 utilised a

combination of a single layer of gypsum board and oriented strand board (OSB), resulting in lower environmental impacts for its retrofitting/maintenance/remediation scenarios.

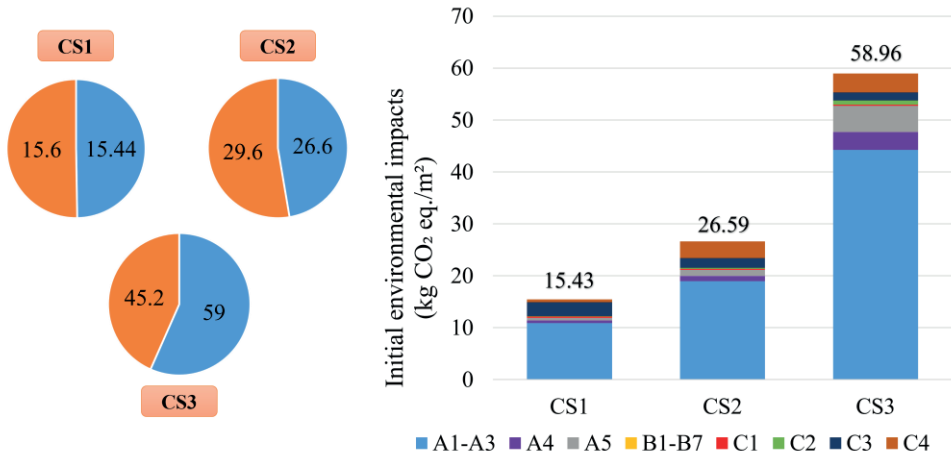


Figure 23: Pie chart: Potential environmental impacts [kg CO_2 eq./m²] of each case study for different building life cycle stages during the lifespan of the building (blue: initial design, orange: over the life span of the building). Bar chart: Initial environmental impacts [kg CO_2 eq./m²] of each case study based on different building life cycle stages and modules.

The materials used in the case studies presented in Figure 23 encompass a range of construction components, including brick, plaster, EPS insulation, glass wool insulation, Rockwool insulation, OSB, cement board, gypsum board, and vapour barriers. The thickness of insulation layers varies across the cases, as detailed in Paper V [301], reflecting different design configurations. Notably, the study revealed no significant impacts during the use stage (B1-B7), as the materials examined had lifespans exceeding the building's expected lifespan and did not involve the consumption of energy or water during their use phase. Consequently, no maintenance or repair was required during this period, aligning with the criteria outlined in EN ISO 15978 [311]. Transportation impacts, calculated under modules A4 and C2, highlighted that bricks generated the highest CO_2 emissions, due to their substantial weight per square metre. These emissions illustrate the importance of considering material mass in evaluating environmental impacts during transportation.

Bricks also demonstrated notably higher CO_2 emissions during the product stage (A1-A3) and the construction installation process (A5). These emissions result from the combined effects of raw material extraction, manufacturing processes, and on-site construction activities. Bricks are predominantly made from clay, which often requires energy-intensive mining operations involving heavy machinery [319].

Furthermore, firing clay in kilns at elevated temperatures, a critical step in brick production consumes significant energy, often derived from fossil fuels such as natural gas or coal [319]. Additionally, the overall construction process contributes to emissions through activities like on-site material handling, water usage, and waste management, further amplifying the environmental footprint [311]. The variations in CO_2 emissions observed among materials stem from differences in raw materials, production methods, and energy requirements. Although bricks exhibit higher initial CO_2 emissions, their durability and extended lifespan reduce maintenance and retrofitting needs over time, making them an environmentally advantageous choice for long-term applications.

The modules deconstruction (C1), waste treatment for reuse, recovery, and recycling (C3), as well as disposal (C4), are influenced by several parameters. A notable example is the gypsum board, which consists of gypsum plaster layered between sheets of paper. While gypsum is a non-toxic, naturally occurring mineral [320], incorporating paper and additional manufacturing substances can make disposal more challenging. Efficient recycling and safe disposal typically involve extra processing steps, which may require considerable labour and energy. These challenges are further exacerbated if the gypsum board becomes contaminated with other materials during construction or demolition activities. Despite their lighter weight compared to traditional materials like brick, gypsum boards and OSB can still contribute substantially to the overall waste volume on construction sites, particularly in large-scale developments. The management of this waste often generates emissions, especially when transportation to specialised disposal or recycling facilities is necessary. Moreover, certain additives or coatings applied to gypsum boards may necessitate specific handling protocols due to concerns related to health and environmental safety [321]. OSB, produced by bonding wood strands with adhesives [322], presents additional waste processing and disposal challenges. The adhesives and other components can complicate recycling and may result in increased emissions during waste management operations. Combined, these factors demonstrate the complexity and environmental burden associated with handling construction waste, particularly from materials such as gypsum boards and OSB.

It is essential to note that LCA evaluates potential environmental impacts but does not provide exact or definitive predictions of environmental outcomes. This limitation arises from several factors, such as the inherent uncertainties in modelling environmental impacts and the forward-looking nature of some potential consequences [310].

4.6 Decision analysis

4.6.1 Method

The final stage entails performing a decision analysis by combining the results of PHA with evaluations of economic, environmental, health, and energy performance. This approach utilises methodologies based on the IDA framework developed by Bayat Pour et al. [323]. Figure 24 presents a flowchart outlining the steps of the IDA process, which identifies the optimal alternative by minimising inutilities and drawbacks. While the number of case studies can be unlimited, this study includes three case studies, previously described in Section 4.4.2, to demonstrate the application of the IDA method. Economic and environmental impacts, health-related issues, and building energy consumption are treated as inutilities due to their adverse consequences. It is important to note that health issues and energy performance, highlighted in grey in Figure 24, are proposed for inclusion in future studies to enhance the scope and capabilities of the decision analysis.

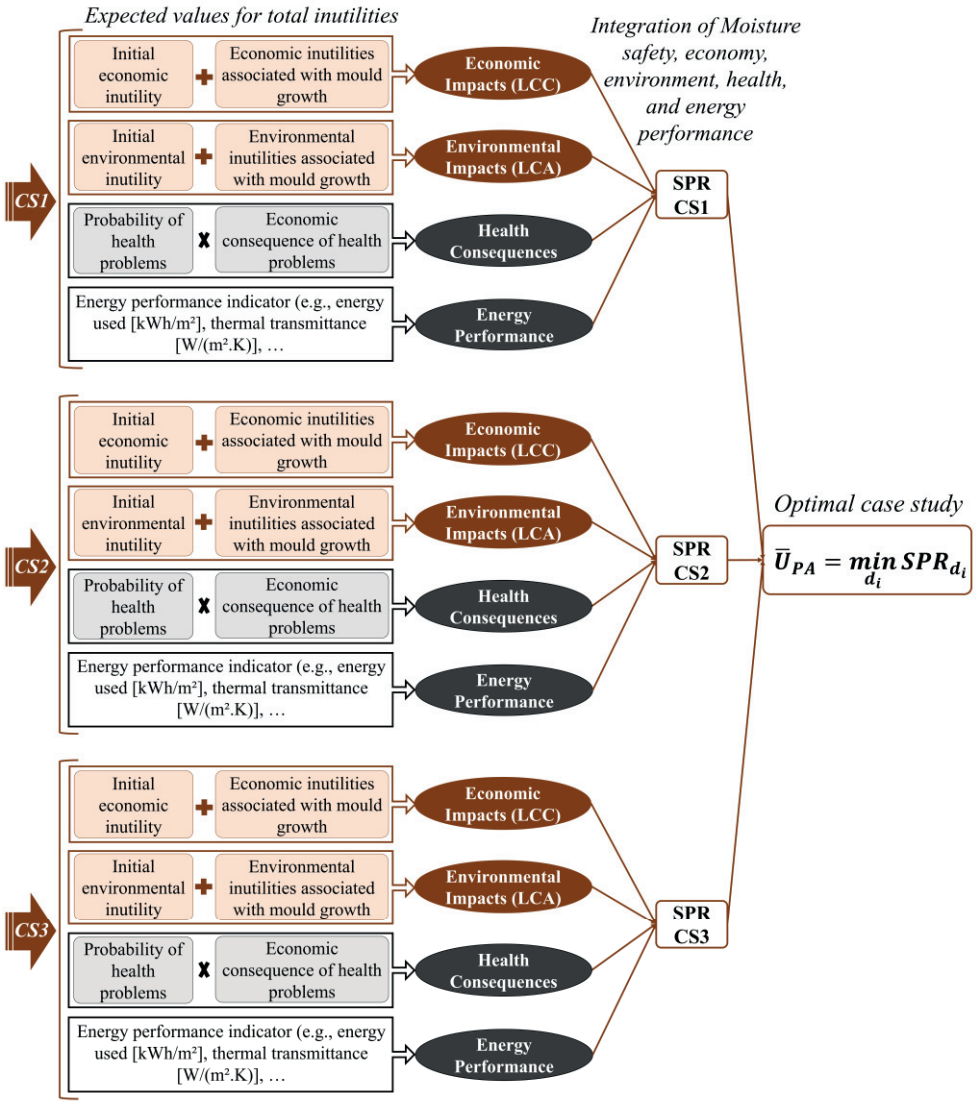


Figure 24: Inutility decision analysis (IDA) flowchart. SPR: Single-point rate. Health consequences and energy performance are not included yet.

The inutilities associated with mould growth are quantified using a risk-based approach, where the risk is calculated as the product of the probability of failure and the corresponding consequences. This methodology is integral to implementing the IDA process. Eq. (29) and (30) are employed to determine the expected values of economic and environmental inutilities. These values are obtained by combining the

initial inutilities with those arising from mould growth, providing a comprehensive assessment of the associated impacts.

$$E\left[\overline{U}\left(EC_{I_j|d_i}\right)\right] = \overline{U_{EC}}\left(Initial_{d_i}\right) + P\left(I_j|d_i\right) \cdot EC \quad (29)$$

$$E\left[\overline{U}\left(ENV_{I_j|d_i}\right)\right] = \overline{U_{ENV}}\left(Initial_{d_i}\right) + P\left(I_j|d_i\right) \cdot ENV \quad (30)$$

Where:

- $E\left[\overline{U}\left(EC_{I_j|d_i}\right)\right]$: Expected value of economic inutilities,
- $E\left[\overline{U}\left(ENV_{I_j|d_i}\right)\right]$: Expected value of environmental inutilities,
- $\overline{U_{EC}}\left(Initial_{d_i}\right)$: Initial economic inutilities (initial costs),
- $\overline{U_{ENV}}\left(Initial_{d_i}\right)$: Initial environmental inutilities,
- $P\left(I_j|d_i\right)$: Probability of failure owing to mould growth,
- EC: Economic impacts of mould growth,
- ENV: Environmental impacts of mould growth,
- d_i: design alternative,
- j: mould index threshold.

The expected inutility of health-related consequences ($E\left[\overline{U}\left(H_{I_j|d_i}\right)\right]$) is determined using Eq. (31). This calculation involves multiplying the probability of the health consequence ($P(H)$) by its monetized inutility value ($\overline{U}(H)$). The inutility value should account for the monetized costs associated with health treatment, lost working days, reduced working hours, and non-work-related activities such as childcare, housework, or studying. These values can be sourced from relevant medical literature [324-326].

$$E\left[\overline{U}\left(H_{I_j|d_i}\right)\right] = P(H) \cdot \overline{U}(H) \quad (31)$$

The expected value of the inutility for energy use, $\mathrm{E}\left[\overline{\mathrm{U}}\left(\mathrm{ENE}_{\mathrm{I_j|d_i}}\right)\right]$, can be calculated by evaluating the energy performance of the building for each case study. This evaluation may involve employing a whole-building simulation approach, as demonstrated in [287], or a simplified energy performance indicator, such as the thermal transmittance.

The results for energy performance, moisture-related health consequences, LCA, and LCC are integrated using the Single Point Rate (SPR) method, as defined in Eq. (32) [287]. This study treats SPR as an inutility index, with values normalised to a range between 0 and 1, providing a unified performance measure across the evaluated dimensions.

$$SPR_{d_i} = \frac{E\left[\bar{U}\left(EC_{I_j|d_i}\right)\right]}{\max_{d_i} E\left[\bar{U}\left(EC_{I_j|d_i}\right)\right]} \times WF_{C_{EC}} + \frac{E\left[\bar{U}\left(ENV_{I_j|d_i}\right)\right]}{\max_{d_i} E\left[\bar{U}\left(ENV_{I_j|d_i}\right)\right]} \times WF_{C_{ENV}} + \frac{E\left[\bar{U}\left(H_{I_j|d_i}\right)\right]}{\max_{d_i} E\left[\bar{U}\left(H_{I_j|d_i}\right)\right]} \times WF_{C_H} + \frac{E\left[\bar{U}\left(ENE_{I_j|d_i}\right)\right]}{\max_{d_i} E\left[\bar{U}\left(ENE_{I_j|d_i}\right)\right]} \times WF_{C_{ENE}} \quad (32)$$

Where:

- $WF_{C_{EC}}$: Weighting factor for economic consequences,
- $WF_{C_{ENV}}$: Weighting factor for environmental consequences,
- WF_{C_H}: Weighting factor for health problems consequences,
- $WF_{C_{ENE}}$: Weighting factor for energy performance.

The case study with the lowest inutility index (SPR value), as defined in Eq. (33), is identified as the most optimal option and designated as the predicted action. A lower inutility index signifies a more favourable case study, reflecting reduced risks associated with mould growth as well as minimised economic and environmental impacts, health problems, and energy used.

$$\bar{U}_{PA} = \min_{d_i} SPR_{d_i} \quad (33)$$

Where:

- $\bar{U}_{PA}$: Inutility index of the predicted action.

4.6.2 Results and discussion

Figure 25 illustrates the outcomes of the decision analysis conducted for three external wall assembly case studies (introduced in section 4.4.2). Among these, CS2 emerged as the most optimal configuration, with the lowest inutility index (SPR value) of 0.293, when both economic and environmental impacts were considered. However, as detailed in Paper V [301], CS2 exhibited a slight probability of mould failure, measured at 2.27%, over the building's 50-year lifespan. This failure probability led to environmental and economic impacts of 0.672 kg CO_2 eq./m² and 1.242 €/m², respectively, attributable to the associated maintenance or repair actions

necessitated by mould growth. A comparative analysis of CS2 and CS3 demonstrates the trade-offs in selecting wall assemblies. While CS3 demonstrated no probability of mould failure throughout its lifespan—eliminating any economic or environmental consequences associated with mould growth—its higher initial economic and environmental impacts rendered it a less favourable wall assembly. Specifically, CS3 incurred significantly greater costs and emissions, primarily due to using high-impact materials such as bricks. This analysis highlights an important insight: in specific scenarios, selecting a wall assembly with a manageable risk of mould failure, coupled with minor repair and replacement needs, may offer greater overall advantages compared to choosing an assembly with no failure risk but significantly higher initial costs and environmental negative consequences.

In contrast, CS1 stood out for its minimal initial economic and environmental impacts compared to the other two case studies. However, its inadequate hygrothermal performance led to a considerably higher probability of mould failure, estimated at 32.67%, as detailed in Paper V [301]. Over the building's 50-year lifespan, this elevated failure probability resulted in significantly increased economic and environmental costs, effectively negating the benefits of its lower initial impacts. This outcome highlights the trap of focusing solely on low initial costs and environmental footprints without addressing long-term performance. Poor hygrothermal performance throughout the building's lifecycle can necessitate frequent maintenance and repairs, thereby amplifying overall economic and environmental burdens. Therefore, selecting a solution with lower initial impacts does not always align with optimal decision-making.

The preceding discussion highlighted the effectiveness of the proposed decision analysis method in integrating multiple dimensions of building envelope design to identify the most optimal alternative. Nonetheless, the reliability of this method could be enhanced by incorporating additional parameters, such as the building's energy performance and the health implications of mould growth, as outlined in Steps 6 and 7 of Figure 19 or denoted by the grey boxes in Figure 24. For example, if greater weight were assigned to the health consequences associated with mould growth relative to economic and environmental factors, CS3 might emerge as the preferred alternative over CS1. This shift would reflect the substantial health risks posed to occupants due to the high probability of mould growth in CS1, outweighing its lower initial economic and environmental impacts. Accounting for these health considerations, CS3 could be recognised as a more sustainable and occupant-friendly choice despite its higher initial costs and environmental footprint.

Emphasising the role of clients and property owners in decision-making processes regarding moisture-related risks is crucial. While CS2 emerges as the most favourable external wall assembly in terms of economic and environmental balance, its slight probability of mould growth can present a potential risk that requires careful consideration. It is necessary to ensure that clients and house owners are well-informed about such risks and their possible long-term implications on the

building's durability, performance, and occupant health. Effective communication that transparently outlines these risks, along with a comprehensive explanation of the associated costs and benefits, would empower clients to make decisions that align with their priorities and risk tolerance. Moreover, the perception of construction risks within the market is likely to develop as environmental concerns gain greater prominence. In this context, opting for a solution with manageable risks, such as CS2, may align with current environmental objectives and emerging market trends. This illustrates the importance of a holistic evaluation approach that balances initial economic and environmental impacts with long-term performance and risk mitigation, fostering sustainable and moisture-safe decisions.

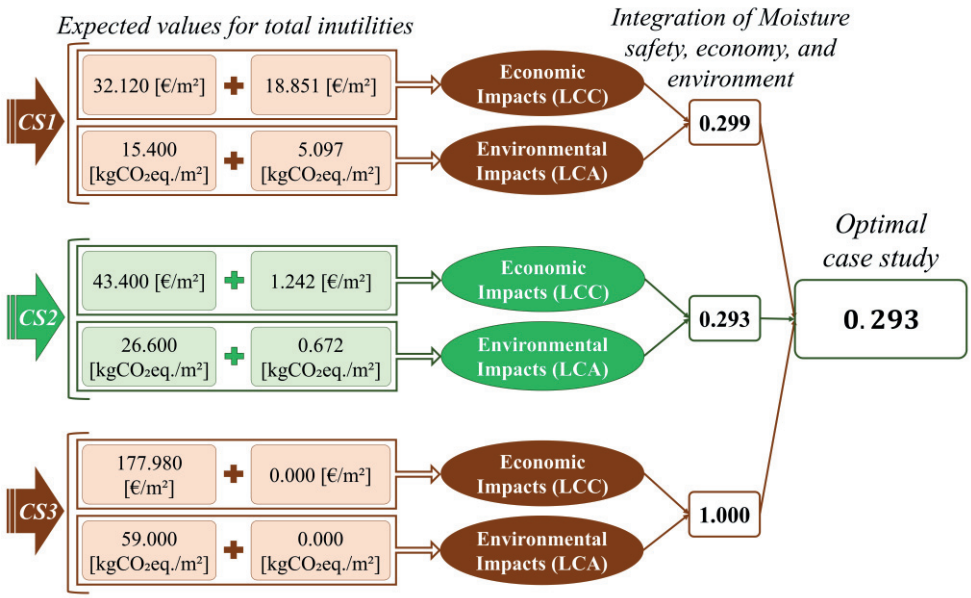


Figure 25: Finding the optimal case study using the inutility decision analysis (IDA) method.

Figure 26 illustrates the impact of varying weighting factors (WF_C) for economic and environmental considerations in a parametric study conducted in this thesis. The results demonstrate that choosing WF_C significantly influences identifying the most optimal case study. The initial assumptions allocated 20% weight to the LCA (environmental impacts) and 80% to the LCC (economic impacts), under which CS2 emerged as the most favourable option, balancing hygrothermal performance with economic and environmental impacts.

However, the parametric study revealed a shift in the optimal case study when the WF_C for the LCC decreased below 75%, with the LCA WF_C correspondingly exceeding 25% (as indicated by the red arrow in Figure 26). Under these conditions,

CS1 became the preferred choice. This finding demonstrates the sensitivity of decision-making outcomes to the relative prioritisation of economic versus environmental factors. Determining an appropriate weighting scheme is inherently challenging due to the subjective nature of prioritising economic and environmental impacts. Involving experts from both domains is critical to establishing a balanced and justified weighting system. Such an approach ensures that the decision analysis is credible, widely accepted, and incorporates diverse perspectives, thereby leading to more comprehensive and sustainable outcomes. This highlights the importance of a transparent and participatory process in establishing WF_C to guide decision-making in building envelope design.

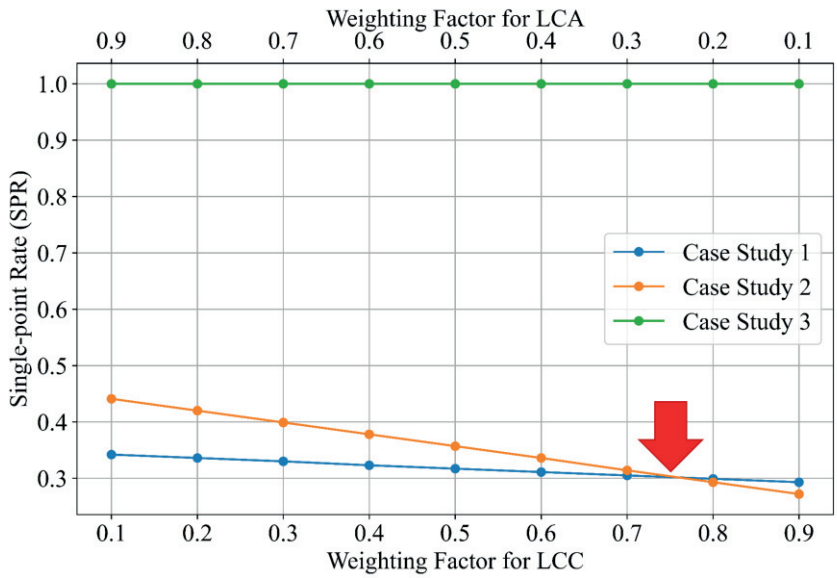


Figure 26: Parametric study on the effect of weighting factors on single-point rate (SPR).

5 Conclusions

This thesis aimed to develop a probabilistic methodology to support decision-making for designing sustainable and moisture-safe building envelopes. By integrating probabilistic hygrothermal assessment (PHA), artificial intelligence (AI)-based models, and decision analysis frameworks, this research provided new insights into building physics and sustainability. Three innovative methods were introduced: mould reliability analysis (MRA) for reliability assessments and metamodeling, mould sensitivity analysis (MSA) for understanding input-output relationships, and inutility decision analysis (IDA) for holistic decision-making. Below, the key contributions of this work are structured around the six research questions.

Research questions:

Q1- What are the latest progress in PHA? What are the gaps? What potential methods and uncertain variables should be considered during PHA?

Q2- How can the robustness and effectiveness of PHA be improved using novel methods such as AI algorithms?

Q3- How can PHA be utilised to investigate the influence of workmanship uncertainties on moisture-related issues?

Q4- How can PHA be applied to examine the impact of wind-driven rain (WDR) loads and varying water penetration criteria on the hygrothermal performance of external walls?

Q5- How can the outputs of PHA be integrated into a decision analysis framework to support sustainability assessments in practical applications?

Q6- How do hygroscopic bio-based insulations influence the risk of mould growth when applying the PHA methodology under Swedish climatic conditions?

Drawn conclusions:

1) ***Latest advancements in probabilistic hygrothermal assessment and identified research gaps***

   A comprehensive state-of-the-art review of PHA methods revealed several key findings and research gaps. Monte Carlo simulations emerged as the

most widely used uncertainty propagation technique due to their ability to evaluate a broad range of scenarios. However, ensuring reliable and accurate results necessitates the incorporation of sampling efficiency and convergence studies. Sensitivity analysis (SA) in hygrothermal modelling is particularly challenging due to the non-linearity and complex interactions among input variables, requiring multiple SA methods to effectively address transient conditions. Practical applications demand low-computation-time SA methods to improve efficiency without compromising accuracy. Despite the advancements in PHA, a critical gap was identified in sustainability integration—approximately 95.1% of studies did not explicitly incorporate environmental, economic, or social dimensions into moisture safety assessments. This shows the necessity of a comprehensive decision analysis framework to bridge moisture safety design with sustainability measures. Regarding stochastic input variables, material properties were found to be the most frequently analysed, whereas hygrothermal functions and indoor climate conditions, remained underexplored. Delphin was identified as the most frequently used hygrothermal simulation tool due to its user-friendly interface and batch simulation capabilities, which streamline probabilistic analysis workflows. In terms of degradation mechanisms, four moisture-induced damage processes were identified—mould growth, frost damage, fungal decay, and algae growth—with mould growth being the focal point of nearly half of all PHA studies.

2) Advancing probabilistic hygrothermal analysis using AI-based methods

The integration of probabilistic analysis (PA) with AI-based metamodeling significantly enhanced the robustness and efficiency of hygrothermal risk assessments. Robustness was improved by incorporating a wider range of uncertainties in the design, while efficiency was achieved by addressing computational challenges to evaluate a large number of scenarios and consequently calculate their mould indices. The results demonstrated that the developed MRA method dramatically reduced computational time while maintaining acceptable accuracy. The output can be utilised for SA, guiding users in making further design adaptations. The random forests (RF) machine learning algorithm proved particularly effective for this task, as it enabled the extraction of feature importance metrics directly from the model. This approach identified influential input variables that correlation-based methods failed to capture, providing deeper insights into the key factors affecting moisture safety. Additionally, the introduced segmented SA technique proved valuable in detecting critical variables near the failure threshold, allowing for targeted adjustments that enhance design performance and mitigate moisture-related risks.

3) ***Evaluating the impact of workmanship uncertainties on moisture-related risks***

This research applied the developed PHA method to assess the influence of workmanship-related uncertainties on moisture performance, focusing on the impact of mortar extrusion. To improve computational efficiency while maintaining accuracy, a 1D mortar extrusion model was developed and validated against a more computationally demanding 2D model. The 1D approach achieved over 90% accuracy in predicting mould indices while offering substantial computational savings, making it a practical alternative for large-scale probabilistic assessments. The results from MRA and MSA demonstrated a strong positive correlation between extruded mortar depth and mould growth. These findings highlight the importance of incorporating workmanship uncertainties into hygrothermal risk assessments and demonstrate how probabilistic modelling can inform design improvements to mitigate the risks associated with construction defects.

4) ***Assessing WDR loads and water penetration criteria in mould growth under mortar extrusion***

This research applied PHA to evaluate the impact of WDR loads and different water penetration criteria on external wall hygrothermal performance. The results confirmed that mortar extrusion has a strong positive correlation with mould growth, particularly in regions with high WDR exposure. However, its influence diminishes in low WDR load areas due to the lack of sufficient moisture sources. A comparison of water penetration criteria revealed that under high WDR loads, the ES (experimental study) criterion resulted in a 6% reduction in the 95^{th} percentile of maximum mould indices compared to the ASHRAE criterion, suggesting comparable performance between the two. In contrast, under low WDR loads, the ES criterion led to reductions of 22% and 15% in the 95^{th} percentile of mould indices across two case studies, indicating that the ASHRAE criterion tends to overestimate mould risks under milder WDR loads. These findings highlight the necessity of selecting appropriate water penetration criteria when assessing moisture risks, as well as the importance of integrating probabilistic approaches to better capture the combined effects of climatic conditions and workmanship-related uncertainties.

5) ***Integrating sustainability considerations into moisture-safe building design***

This research introduced the IDA method to integrate sustainability considerations into moisture-safe building envelope design. The findings demonstrated that a case study with no probability of mould growth might not necessarily be the optimal choice when economic and environmental

impacts are considered, highlighting the trade-offs involved in decision-making. In some cases, selecting a wall assembly with a minor, manageable risk of mould growth proved to be more advantageous than one with zero risk but significantly higher initial costs and environmental burdens. However, low initial costs and environmental impacts alone do not always indicate the best-performing assembly, as the long-term consequences of mould growth—such as increased maintenance, energy use, and material replacement—can lead to higher inutility indices. These results illustrate the importance of a holistic decision-making framework that balances moisture safety, economic impacts, and environmental consequences, rather than prioritising a single performance criterion. By integrating IDA into probabilistic hygrothermal analysis, this research provides a novel approach for evaluating building envelope designs in a way that accounts for both immediate and long-term trade-offs, contributing to more moisture-safe and resource-efficient construction practices.

6) ***Investigating the role of hygroscopic bio-based insulation materials in moisture performance***

This research examined the influence of different hygroscopic bio-based insulation materials on mould growth under Stockholm's climatic conditions. The findings demonstrated that, in a certain case, hygroscopic bio-based materials can help mitigate mould growth risks. However, in another case, its use increased mould growth potential, particularly when the material had limited liquid water transport capacity. This demonstrated the need for a comprehensive evaluation of hygrothermal performance, considering both heat and moisture transport mechanisms to optimise design. Another identified risk was an increase in heat flux due to the use of hygroscopic insulation, which could impact overall energy performance. These results highlight the importance of a balanced approach when selecting insulation materials, ensuring that moisture safety considerations are carefully integrated alongside thermal performance and durability assessments.

Probabilistic methods combined with AI-based metamodels enable the efficient evaluation of millions of scenarios, effectively identifying moisture-related risks while significantly reducing computational time and costs. Integrating environmental and economic assessments into decision-making offers a holistic approach, ensuring optimal solutions that balance initial costs, long-term performance, and sustainability. To enhance practical applications, the methodologies developed in this thesis can be further developed into a user-friendly tool, assisting practitioners in selecting materials and designs that minimise the risks of mould growth and other moisture-related issues. By adopting these methodologies, stakeholders can better align with sustainability goals by incorporating life cycle costing (LCC) and life cycle assessment (LCA) into the

early design phases. Effective collaboration among designers, clients, and experts is crucial for tailoring these tools to specific projects, fostering sustainable and moisture-safe construction practices.

6 Future research potential

The methodologies and findings of this thesis contribute to the ongoing efforts in sustainable and moisture-safe building envelope design. While meaningful progress has been made, there remain some opportunities for further investigation to enhance the understanding and application of PHA. Expanding the scope of PHA to incorporate additional measures could improve the comprehensiveness and reliability of building envelope performance evaluations. This chapter discusses potential research directions that may help address existing gaps and further develop knowledge in this field. The proposed ideas, outlined in the following subsections, aim to encourage innovative approaches and methodologies that align with evolving industry needs and sustainability goals.

6.1 Bridging building physics and medical sciences

Indoor dampness and mould are recognised as significant health hazards, as outlined in WHO guidelines [8] and other medical literature [10-16] as explained in section 1.1 of this thesis. The IDA framework proposed by Bayat Pour et al. [323] represents an advancement in integrating building physics with medical sciences. It offers a comprehensive approach that incorporates occupant health and future healthcare costs. Optimising building envelope designs through the IDA framework can identify health risks and associated societal costs. This shows the importance of a multidisciplinary approach that leverages expertise from construction, design, medicine, and related fields. Advancing this methodology demands a collaboration to improve building standards, inform policies, and influence users' behaviours. Such efforts will drive holistic, health-centred building practices, ultimately benefiting individuals, governments, and insurers.

6.2 Incorporating energy performance analysis into the IDA method

Energy performance analysis is critical to sustainable building envelope design, directly impacting operational energy use, greenhouse gas emissions, and long-term economic and environmental outcomes. Future research should focus on embedding energy performance analysis as an additional step in the IDA method to enhance its robustness and applicability in real-world scenarios. Energy performance analysis typically involves assessing parameters such as energy consumption for heating and cooling and the building envelope's thermal transmittance. The integration of energy performance analysis into the IDA method would address several critical aspects:

- Operational Energy Consumption: Evaluating energy use enables the identification of building envelopes that minimise operational energy demands, align with climate goals and reduce lifecycle energy costs.
- Resilience to Climate Variability: Future climatic conditions, including temperature fluctuations and extreme weather events, may significantly influence a building's energy performance. By including energy performance analysis in IDA, researchers can simulate scenarios under varying climate models, providing a robust basis for selecting designs resilient to future conditions.
- Integration of Moisture and Thermal Analysis: Moisture and thermal performance are intrinsically linked, with moisture levels significantly influencing the thermal conductivity of insulation materials. For instance, the thermal conductivity of cellulose insulation at saturation is more than ten times greater than in its dry state [116]. While many insulation materials exhibit minimal changes in thermal conductivity below 80% RH, bio-based insulation materials are particularly sensitive. For mineral wool, a notable increase in thermal conductivity is observed only at RH levels exceeding 95%. Excessive RH affects insulation performance and increases energy consumption and heating costs. High humidity levels reduce the building envelope's insulation efficiency, and because humid indoor air absorbs heat, heating systems must work harder to maintain comfortable temperatures.

In future iterations of the IDA framework, incorporating energy performance analysis could involve coupling hygrothermal simulation tools (e.g., Delphin) with energy modelling software (e.g., IDA ICE). This integration would allow for simultaneous evaluation of moisture safety and energy performance, streamlining the decision-making process. Furthermore, leveraging ML models within the IDA

framework could enable rapid predictions of energy performance based on probabilistic inputs, facilitating the inclusion of more scenarios for robust results.

6.3 Connecting building physics with structural engineering

Hygro-thermo-mechanical analysis is essential for evaluating the hygrothermal performance of construction assemblies, such as walls and roofs, while complementing structural assessments considering other static or dynamic loads [327]. The hygrothermal model can then be extended to incorporate mechanical effects through the total stress/strain additive decomposition principle. The study conducted by Ramirez et al. [327] demonstrated the complexity of the hygro-thermo-mechanical response of brick masonry walls. Integrating PHA with structural design and analysis allows for considering potential structural failures resulting from hygrothermal-related issues.

In the study by Lal et al. [328], the non-linear bending response of a hygro-thermo-mechanically loaded laminated composite spherical shell panel was investigated, taking into account slight random variations in system variables. Moisture effects, as highlighted in [329-331], generate residual hygral stresses and interfacial degradation. Utilising PHA as a pre-processor to structural analysis for composite materials can enhance the robustness of the design of structural components like plates, shell panels, and beams made from laminated composites. This integrated approach ensures a comprehensive understanding of the potential effects of hygrothermal conditions on the durability and structural integrity of construction elements.

6.4 Region-based hygrothermal analysis tools development

The application of AI in hygrothermal analysis offers significant potential for improving efficiency, accuracy, and predictive capabilities. One promising direction, as done in this thesis, involved integrating metamodels into hygrothermal analysis to streamline computations and reduce computational costs. Moving forward, there is a unique opportunity to develop region-based metamodels tailored to distinct locations. These models could potentially replace conventional hygrothermal analysis tools by leveraging regional data and characteristics, thus making the process more accessible and efficient.

Such region-based metamodels could categorise countries based on geographic locations, climatic conditions, commonly used building materials, and lifestyle factors, which significantly influence indoor climate. This approach would enable location-specific analyses, ensuring results are tailored to the unique requirements of each region. AI-based metamodels also offer a user-friendly solution, particularly for practitioners or homeowners who lack expertise in hygrothermal simulation tools. These tools could reduce reliance on specialised consultancy services by empowering non-specialists to perform essential analyses independently.

To ensure these tools are accessible and practical, developing clear and concise guidelines for interpreting their outputs is essential. Such guidelines would give users the necessary knowledge to make informed decisions based on the results. A relevant example is the study by Tijskens et al. [174], which provided general guidelines for hygrothermal analyses across various European climates and wall compositions. Building on such initiatives, region-based metamodels could bridge the gap between technical complexity and practical application, fostering widespread adoption and improved building performance.

6.5 Incorporating user behaviour in PHA

User behaviour significantly influences indoor humidity levels and, consequently, the hygrothermal performance of building envelopes. Activities such as cooking, bathing, drying clothes, and adjusting heating or cooling set points [155] and shading devices can create significant variations in internal moisture loads. Current hygrothermal models often overlook these behavioural factors, leading to potential inaccuracies in performance predictions.

Bui et al. [159] proposed a methodology for evaluating the impact of various occupancy scenarios on the hygrothermal performance of indoor spaces. Their findings indicated that seasonal variations significantly influence the indoor heat and moisture balance under different occupancy conditions. Similarly, the Generation of Indoor Heat and Moisture (GIHM) tool [332], developed by Oak Ridge National Laboratory, provides a comprehensive framework for capturing the probabilistic nature of hourly indoor heat and moisture generation in residential buildings. The GIHM tool incorporates variables such as user behaviour, building usage, appliance operation, and climate zones, making it a valuable resource for PHA processes.

In another relevant study, Buechler et al. [333] probabilistically calculated indoor climate data and analysed the effects of location and building usage on indoor conditions across various regions in the United States. The results illustrated the importance of incorporating location-specific and usage-based factors into PHA to enhance their accuracy and robustness. As highlighted in their study, indoor climate

data play a pivotal role in evaluating building performance. This includes assessing indoor health and comfort, air quality, HVAC efficiency, and mould growth risks.

The integration of tools such as GIHM and regionally tailored indoor climate data into hygrothermal analyses offers an opportunity for more comprehensive and user-oriented evaluations, addressing critical variables often overlooked in traditional modelling approaches. Future research should focus on developing advanced PHA methodologies that incorporate dynamic user behaviour scenarios. Additionally, integrating AI-based tools to predict and simulate user behaviour using historical data and real-time monitoring could enhance the accuracy of hygrothermal analyses. The inclusion of user behaviour would also allow researchers to explore the interplay between human actions and building systems.

7 Summary of the appended papers

Paper I

This paper presents a comprehensive literature review of the evolution of probabilistic hygrothermal assessment (PHA) of building envelopes. The state-of-the-art review employs a systematic methodology encompassing scoping and systematic searches, quality assessment, and study analysis. Based on 143 selected publications, the study provides detailed statistical insights into key aspects, including hygrothermal analysis tools, climatic conditions, uncertainty propagation and sensitivity analysis (SA) methods, model dimensions, moisture-related damage models, uncertain parameter groups, building usage, geographical distributions, sustainability perspectives, and employed metamodels. The findings reveal significant gaps in current research: Over 95% of PHA studies did not explicitly integrate sustainability perspectives—environmental, economic, and societal—into their analyses. Moreover, incorporating hygrothermal functions as uncertain input variables is highlighted as essential, given their considerable impact on hygrothermal performance compared to single input variables such as material properties. Approximately 90% of studies are confined to 1D modelling; thus, expanding research to 2D and 3D modelling is recommended to include more design details. Additionally, tropical climates, prone to moisture-related issues, are underrepresented in existing case studies. The paper also explains the limitations of several SA methods in addressing transient conditions and variable interactions, advocating for advanced methods capable of non-linear and interactive analyses with low computational expenses. Furthermore, omitting ambient conditions and building usage as stochastic variables in many studies limits the comprehensiveness of current analyses. The review highlights the importance of understanding the strengths and weaknesses of metamodeling methods to ensure robust and reliable hygrothermal assessments. The paper concludes by identifying critical research gaps and providing actionable recommendations for advancing the field of PHA.

Paper II

This study introduces two novel methods for conducting robust mould reliability and sensitivity analyses. Probabilistic hygrothermal modelling is conducted by sampling inputs based on their stochastic properties, with the resulting mould indices integrated into a metamodel constructed using the random forests algorithm. The metamodel facilitates the prediction of maximum mould indices by re-sampling

from input variable distributions, enabling the determination of the probability of exceeding a specified mould limit state. The sensitivity analysis (SA) method further explores linear and non-linear relationships between input variables and mould growth outcomes. To illustrate the application of these methods, three external wall assemblies are analysed. The mould reliability analysis method quantifies the influence of uncertainties in hygrothermal variables on the maximum mould index, providing insights into the robustness of mould assessments. Additionally, the SA identifies critical parameters affecting mould growth, aiding designers in making informed decisions. By integrating a metamodel with probabilistic analysis, the computational effort required to evaluate a large number of scenarios is significantly reduced. This study shows the potential of the proposed methods to enhance the efficiency and reliability of mould risk assessments in the design of moisture-safe building envelopes.

Paper III

This paper investigates the impact of mortar extrusion, resulting from suboptimal workmanship during bricklaying, on the hygrothermal performance of timber frame walls with brick masonry cladding. Mortar extrusion can bridge the clay brick masonry veneer and adjacent layers, such as insulation or weather-resistant barriers, facilitating water penetration caused by wind-driven rain (WDR). Despite its significance, no consensus exists on incorporating WDR-induced water penetration into moisture safety designs. This research uses two distinct water penetration criteria (ASHRAE and ES) to examine the influence of extruded mortar joints on the hygrothermal performance of wall assemblies. Specifically, it evaluates the impact of extruded mortar joints in clay brick masonry claddings on timber frame walls, focusing on their vulnerability to mould growth. A probabilistic approach was applied to assess mould growth risk, followed by linear and non-linear sensitivity analyses to identify the most influential parameters under two different climatic conditions in Sweden. The results revealed a congruence between the ASHRAE and ES criteria in regions with high WDR loads. However, under low WDR loads, the ASHRAE criterion predicted higher maximum mould indices than the ES criterion. Furthermore, linear and non-linear mould sensitivity analyses showed a positive correlation between the depth of extruded mortar and maximum mould indices. This correlation's strength varied depending on WDR loads and the selected water penetration criteria, highlighting the importance of considering these factors in moisture-safe building designs.

Paper IV

As an extension of paper III, this paper investigates the impact of extruded mortar joints caused by improper bricklaying techniques on the hygrothermal performance of different wall orientations. In this study, an AI-based metamodel was integrated with the probabilistic approach, expanding upon the methodology presented in Paper III. Additionally, the sampling technique previously used in Paper II was

further refined to address the extrapolation challenges inherent to the random forests algorithm, enhancing its predictive robustness. The study evaluated four façade orientations for a case study in Gothenburg to account for the directional influence of wind-driven rain (WDR). The mentioned method was employed to predict the maximum mould index (MMI) and analyse the effects of two water penetration criteria—ASHRAE and ES—on extruded mortar joints. The results revealed that the ASHRAE and ES criteria produced similar MMIs for orientations exposed to significant WDR loads (e.g., south). However, for orientations with lower WDR loads (e.g., north), the ASHRAE criterion predicted a higher MMI than the ES criterion. Linear and non-linear SA demonstrated a positive correlation between extruded mortar depth and MMI. However, the strength of this correlation varied depending on WDR loads and the chosen water penetration criteria. Additionally, other influential variables on the MMI were identified, including air change rate (negative correlation), solar absorption coefficient (negative correlation), WDR reduction/splash coefficient (positive correlation), and the thermal conductivity of Rockwool insulation (positive correlation). These findings provide insights into the effects of extruded mortar joints on moisture safety and highlight the effect of considering the water penetration criterion in the results.

Paper V

Energy-efficient building designs can reduce greenhouse gas emissions and energy use by more than 40%. However, these improvements may also increase the risk of condensation. Therefore, a comprehensive decision analysis approach is essential for selecting optimal building envelope assemblies that account for their hygrothermal, economic, and environmental impacts. This study presents an innovative decision analysis method based on the concept of IDA, where the building envelope with the lowest inutility is deemed the optimal choice. First, a machine learning metamodel coupled with probabilistic hygrothermal analysis was used to evaluate various building envelope assemblies. Then, considering the moisture-related damages, each assembly's economic and environmental effects were calculated. The combination of these outputs produced inutility indices for the case studies, which facilitated the identification of the most optimal alternative. According to the findings, depending on size of initial and running costs associated with different case studies, and the chosen weighting factors, different cases will be seen as optimal. As an example, a case with some minor risk might have lower inutility as another case without risk, due to different choice of material. Achieving a balance between costs, environmental aspects, occupant health, and building longevity is essential.

Paper VI

External wall assemblies with high insulation thickness are widely used to improve building energy efficiency. However, evidence suggests these assemblies can contribute to moisture-related problems, such as mould growth. Recent research

indicates that insulation materials with highly hygroscopic properties, which offer greater moisture buffering value, might help reduce relative humidity and, in turn, decrease the probability of mould growth. This study examines the impact of such insulation materials on mould growth and heat flux through a series of probabilistic hygrothermal simulations. Four types of insulation—EPS, mineral wool, wood fibre, and cellulose—are assessed under the climatic conditions of Stockholm. The analysis incorporates material properties and boundary conditions uncertainties, focusing on critical parameters such as mould growth and heat flux within the insulation layers, particularly on wooden studs. Findings from the study suggest that using hygroscopic insulation material may or may not mitigate the risk of mould growth. The results emphasise that the interaction between material properties and boundary conditions, along with other hygrothermal functions such as liquid water transport potential, plays a crucial role in determining moisture performance. In some cases, a higher hygroscopic property in the insulation layers is linked to an increase in heat flux, which in turn reduces the energy efficiency of the wall assembly. More hygroscopic materials have a greater capacity to absorb and retain moisture, leading to higher moisture content within the material. This increased moisture content can enhance heat transfer, thereby elevating the overall heat flux and potentially compromising the thermal performance of the wall. These results highlight the need for a balanced approach in the design of insulated wall assemblies, considering moisture safety, durability, and thermal performance.

References

[1] T. Isaksson, S. Thelandersson, A. Ekstrand-Tobin, and P. Johansson, 'Critical conditions for onset of mould growth under varying climate conditions', *Building and Environment*, vol. 45, no. 7, pp. 1712–1721, Jul. 2010, doi: 10.1016/j.buildenv.2010.01.023.

[2] D. G. Kayll, 'The Role of the Building Envelope Professional in the Aftermath of Vancouver's Leaky Condominium Crisis', *Buildings VIII/Wall Design and Building Science*, pp. 2–7, 2001.

[3] S. M. Fufa, C. Skaar, K. Gradeci, and N. Labonnote, 'Assessment of greenhouse gas emissions of ventilated timber wall constructions based on parametric LCA', *Journal of Cleaner Production*, vol. 197, pp. 34–46, Oct. 2018, doi: 10.1016/j.jclepro.2018.06.006.

[4] W. J. Fisk, Q. Lei-Gomez, and M. J. Mendell, 'Meta-analyses of the associations of respiratory health effects with dampness and mold in homes', *Indoor Air*, vol. 17, no. 4, pp. 284–296, Aug. 2007, doi: 10.1111/j.1600-0668.2007.00475.x.

[5] L. Wang, H. Ge, and L. Wang, 'Metamodel Development for Predicting Hygrothermal Performance of Wood-Frame Wall under Rain Leakage', in *XV International Conference on Durability of Building Materials and Components. eBook of Proceedings*, CIMNE, 2020. doi: 10.23967/dbmc.2020.095.

[6] H. J. Moon, 'Assessing Mold Risks in Buildings under Uncertainty', Doctoral thesis, Georgia Institute of Technology, Atlanta, GA, USA, 2005.

[7] K. Calle and N. Van Den Bossche, 'Probabilistic assessment of the impact of material properties on the risk of frost damage in masonry constructions', in *4th Central European Symposium on Building Physics (CESBP 2019)*, Prague, Czech Republic: MATEC Web of Conferences, 2019, p. 6. doi: 10.1051/matecconf/201928202084.

[8] E. Heseltine, J. Rosen, and World Health Organization, Eds., *WHO guidelines for indoor air quality: dampness and mould*. Copenhagen: WHO, 2009.

[9] E. Anyanwu, A. W. Campbell, J. Jones, J. E. Ehiri, and A. I. Akpan, 'The Neurological Significance of Abnormal Natural Killer Cell Activity in Chronic Toxigenic Mold Exposures', *The Scientific World JOURNAL*, vol. 3, pp. 1128–1137, 2003, doi: 10.1100/tsw.2003.98.

[10] J. D. Thrasher and S. Crawley, 'The biocontaminants and complexity of damp indoor spaces: more than what meets the eyes', *Toxicol Ind Health*, vol. 25, no. 9–10, pp. 583–615, Oct. 2009, doi: 10.1177/0748233709348386.

[11] R. Rylander and R. Etzel, 'Introduction and summary: workshop on children's health and indoor mold exposure.', *Environ Health Perspect*, vol. 107, no. suppl 3, pp. 465–468, Jun. 1999, doi: 10.1289/ehp.99107s3465.
[12] A. Delanoë, N. Heutte, S. Gente, V. Séguin, and D. Garon, 'Relationships between Exposure to Bioaerosols, Moldy Surface and Symptoms in French Mold-Damaged Homes', *Atmosphere*, vol. 11, no. 3, p. 223, Feb. 2020, doi: 10.3390/atmos11030223.
[13] J. D. Thacher *et al.*, 'Mold and dampness exposure and allergic outcomes from birth to adolescence: data from the BAMSE cohort', *Allergy*, vol. 72, no. 6, pp. 967–974, Jun. 2017, doi: 10.1111/all.13102.
[14] J. K. Peat, J. Dickerson, and J. Li, 'Effects of damp and mould in the home on respiratory health: a review of the literature', *Allergy*, vol. 53, no. 2, pp. 120–128, Feb. 1998, doi: 10.1111/j.1398-9995.1998.tb03859.x.
[15] D. Norbäck, Z. Hashim, F. Ali, and J. H. Hashim, 'Asthma symptoms and respiratory infections in Malaysian students-associations with ethnicity and chemical exposure at home and school', *Environmental Research*, vol. 197, p. 111061, Jun. 2021, doi: 10.1016/j.envres.2021.111061.
[16] S. Li *et al.*, 'Household mold exposure in association with childhood asthma and allergic rhinitis in a northwestern city and a southern city of China', *J Thorac Dis*, vol. 14, no. 5, pp. 1725–1737, May 2022, doi: 10.21037/jtd-21-1380.
[17] M. Brown and R. Booth, 'Death of two-year-old from mould in flat a "defining moment", says coroner', *The Guardian*, Nov. 15, 2022. Accessed: Dec. 03, 2024. [Online]. Available: https://www.theguardian.com/uk-news/2022/nov/15/death-of-two-year-old-awaab-ishak-chronic-mould-in-flat-a-defining-moment-says-coroner
[18] Y. Dong *et al.*, 'Environmental sustainable decision making– The need and obstacles for integration of LCA into decision analysis', *Environmental Science & Policy*, vol. 87, pp. 33–44, Sep. 2018, doi: 10.1016/j.envsci.2018.05.018.
[19] J. Wang, 'Asthma and Rhinitis among Adults in Sweden and China, Risk Factors in the Home Environment', Doctoral thesis, Uppsala University, Sweden, 2018. doi: 10.33063/diva-427327.
[20] S. Urlaub, G. Grün, and P. Foldbjerg, 'Mould and dampness in European homes and their impact on health', Fraunhofer-Institut für Bauphysik IBP, Stuttgart, Germany, EER-058/2016/950, Nov. 2016. doi: 10.13140/RG.2.2.18770.76488.
[21] G. Grün and S. Urlaub, 'Towards an identification of European indoor environments' impact on health and performance - homes and schools', Fraunhofer-Institut für Bauphysik IBP, Stuttgart, Germany, Dec. 2014.
[22] J. Vos, A. Blommaert, and N. Bossche, 'Statistical Analysis on Belgian Building Defects', in *XV International Conference on Durability of Building Materials and Components. eBook of Proceedings*, CIMNE, 2020. doi: 10.23967/dbmc.2020.130.
[23] Observatoire de la Qualité de la Construction, Edition 2021.Observatoire de la Qualité de la Construction, Edition 2021.

[24] S. Pallin, 'Risk Assessment of Hygrothermal Performance - Building Envelope Retrofit', Doctoral thesis, Chalmers University of Technology, Gothenburg, Sweden, 2013.
[25] Anders Jansson, Putsade regelväggar, Erfarenheter från undersökningar som SP har utfört, (Eng. ETICS 2011 - Experiences from field studies made by SP) SP Rapport 2011:61. Borås: SP, Technical Research Institute of Sweden.
[26] P. Johansson, 'Determination of the Critical Moisture Level for Mould Growth on Building Materials', Doctoral thesis, Lund University, Faculty of Engineering, Lund, Sweden, 2014. Accessed: Oct. 26, 2021. [Online]. Available: https://portal.research.lu.se/ws/files/3846997/4419062.pdf
[27] C. Ahrnens, E. Borglund, Fukt på kallvindar - en kartläggning av småhus i Västra Götalands län. Master Thesis, Chalmers University of Technology. 2007.
[28] C.-E. Hagentoft and A. S. Kalagasidis, 'Moisture safe cold attics - Assessment based on risk analyses of performance and cost', in *Proceedings of 10th Nordic Symposium on Building Physics*, Lund, Sweden, 2014, p. 10.
[29] 'Boverket´s mandatory provisions and general recommendations, BBR, BFS 2011:6 with amendments up to BFS 2018:4', 2011, p. 154.
[30] H. L. S. C. Hens, 'Combined heat, air, moisture modelling: A look back, how, of help?', *Building and Environment*, vol. 91, pp. 138–151, Sep. 2015, doi: 10.1016/j.buildenv.2015.03.009.
[31] C. Rode, P. N. Hansen, and K. Hansen, 'Combined heat and moisture transfer in building constructions', Technical University of Denmark, LFV-214, Sep. 1990.
[32] H. Janssen, B. Blocken, and J. Carmeliet, 'Conservative modelling of the moisture and heat transfer in building components under atmospheric excitation', *International Journal of Heat and Mass Transfer*, vol. 50, no. 5–6, pp. 1128–1140, Mar. 2007, doi: 10.1016/j.ijheatmasstransfer.2006.06.048.
[33] P. W. M. H. Steskens, H. Janssen, and C. Rode, 'Influence of the Convective Surface Transfer Coefficients on the Heat, Air, and Moisture (HAM) Building Performance', *Indoor and Built Environment*, vol. 18, no. 3, pp. 245–256, Jun. 2009, doi: 10.1177/1420326X09105682.
[34] L. Van Gelder, P. Das, H. Janssen, and S. Roels, 'Comparative study of metamodelling techniques in building energy simulation: Guidelines for practitioners', *Simulation Modelling Practice and Theory*, vol. 49, pp. 245–257, Dec. 2014, doi: 10.1016/j.simpat.2014.10.004.
[35] A. A. Hamid, P. Wallentén, and D. Johansson, 'Moisture Supply Set Point for Avoidance of Moisture Damage in Swedish Multifamily Houses', *Energy Procedia*, vol. 78, pp. 901–906, Nov. 2015, doi: 10.1016/j.egypro.2015.11.016.
[36] A. Holm and H. M. Künzel, 'Two-dimensional transient heat and moisture simulations of rising damp with WUFI2d', in *Research in Building Physics*, 1st ed., J. Carmeliet, H. Hens, and G. Vermeir, Eds., CRC Press, 2020, pp. 363–367. doi: 10.1201/9781003078852-52.
[37] E. Vereecken, L. Van Gelder, H. Janssen, and S. Roels, 'Interior insulation for wall retrofitting – A probabilistic analysis of energy savings and hygrothermal

risks', *Energy and Buildings*, vol. 89, pp. 231–244, Feb. 2015, doi: 10.1016/j.enbuild.2014.12.031.
[38] A. Sasic Kalagasidis and C. Rode, 'Annex 55, Reliability of Energy Efficient Building Retrofitting - Probability Assessment of Performance and Cost (RAP-RETRO), Framework for probabilistic assessment of the building envelope', Chalmers University of Technology, Gothenburg, Sweden, ISSN 1652-9162, 2015:5, 2015.
[39] E. J. de Place Hansen, E. B. Møller, and M. Ørsager, 'Guidelines for internal Insulation of historic Buildings', in *12th Nordic Symposium on Building Physics (NSB 2020)*, J. Kurnitski and T. Kalamees, Eds., Tallinn, Estonia: E3S Web of Conferences, Jun. 2020, p. 01004. doi: 10.1051/e3sconf/202017201004.
[40] L. V. Gelder, H. Janssen, and S. Roels, 'Retrofitting cavity walls – probabilistic study of energy savings and moisture risks', in *5th International Building Physics Conference*, Kyoto, Japan, May 2012, p. 7.
[41] K. Gradeci, 'A probabilistic-based methodology for evaluation of timber façade constructions', Doctoral thesis, Norwegian university of science and technology (NTNU), Trondheim, Norway, 2018.
[42] M. H. Faber, *Statistics and Probability Theory*, vol. 18. in Topics in Safety, Risk, Reliability and Quality, vol. 18. Dordrecht: Springer Netherlands, 2012. doi: 10.1007/978-94-007-4056-3.
[43] W. Feller, *An Introduction to Probability Theory and Its Applications*, 2 vols. in Wiley Series in Probability and Statistics. Wiley, 1970.
[44] K. Gradeci, N. Labonnote, B. Time, and J. Köhler, 'A probabilistic-based methodology for predicting mould growth in façade constructions', *Building and Environment*, vol. 128, pp. 33–45, Jan. 2018, doi: 10.1016/j.buildenv.2017.11.021.
[45] A. Tijskens, S. Roels, and H. Janssen, 'Hygrothermal assessment of timber frame walls using a convolutional neural network', *Building and Environment*, vol. 193, p. 107652, Apr. 2021, doi: 10.1016/j.buildenv.2021.107652.
[46] A. Tijskens, S. Roels, and H. Janssen, 'Neural networks for metamodelling the hygrothermal behaviour of building components', *Building and Environment*, vol. 162, p. 106282, Sep. 2019, doi: 10.1016/j.buildenv.2019.106282.
[47] C. Aggarwal, H. Ge, and M. Defo, 'Assessing mould growth risk of wood-frame walls using partial least squares (PLS) regression considering climate model uncertainties', *Building and Environment*, vol. 238, p. 110374, Jun. 2023, doi: 10.1016/j.buildenv.2023.110374.
[48] N. Bansal, M. Defo, and M. A. Lacasse, 'Application of Support Vector Regression to the Prediction of the Long-Term Impacts of Climate Change on the Moisture Performance of Wood Frame and Massive Timber Walls', *Buildings*, vol. 11, no. 5, p. 188, Apr. 2021, doi: 10.3390/buildings11050188.
[49] R. Z. Freire, G. H. dos Santos, and L. dos S. Coelho, 'Hygrothermal Dynamic and Mould Growth Risk Predictions for Concrete Tiles by Using Least Squares Support Vector Machines', *Energies*, vol. 10, no. 8, p. 1093, Jul. 2017, doi: 10.3390/en10081093.

[50] K. Calle and N. Van Den Bossche, 'Sensitivity of the hygrothermal behaviour of homogeneous masonry constructions: from Sobol indices to decision trees', in *12th Nordic Symposium on Building Physics (NSB 2020)*, J. Kurnitski and T. Kalamees, Eds., Tallinn, Estonia: E3S Web Conf., Jun. 2020, p. 07001. doi: 10.1051/e3sconf/202017207001.
[51] H. S. L. C. Hens, Ed., *Research in building physics: proceedings of the 2nd International Conference on Building Physics, Leuven, 14-18 September 2003, Antwerpen, Belgium*. Lisse [Netherlands] ; Exton, PA: A.A. Balkema Publishers, 2003.
[52] L. V. Teesdale, 'Condensation in walls and attics', *U. S. Department of Agriculture, Forest Service*, p. 12, Dec. 1937.
[53] T. S. Rogers, 'Preventing Condensation in Insulated Structures.', *ARCHT. REC.*, vol. 83, pp. 109–19, 1938.
[54] R. and A.-C. Engineers. American Society of Heating, *2001 ASHRAE handbook : fundamentals*. Atlanta, GA.: ASHRAE, 2001.
[55] ASHRAE. Handbook of fundamentals. Atlanta: American Society of Heating, Refrigerating and Air Conditioning Engineers; 1993.
[56] H. Hens, A. Janssens, Heat and Moisture Response of Vented and Compact Cathedral Ceilings: A Test House Evaluation, in ASHRAE Transactions, Atlanta, USA, 1999, vol. 105.
[57] J. Kronvall, 'Air flows in building components', Doctoral thesis, Byggnadsfysik LTH, Lunds Tekniska Högskola, Lund, Sweden, 1980.
[58] A. Janssens and H. Hens, 'DEVELOPMENT OF INDOOR CLIMATE CLASSES TO ASSESS HUMIDITY IN DWELLINGS', p. 7.
[59] ISO 13788:2012 - Hygrothermal performance of building components and building elements - Internal surface temperature to avoid critical surface humidity and interstitial condensation - Calculation methods.
[60] J. F. Straube, 'Moisture Control and Enclosure Wall Systems', p. 336.
[61] B. Blocken and J. Carmeliet, 'A review of wind-driven rain research in building science', *Journal of Wind Engineering and Industrial Aerodynamics*, vol. 92, no. 13, pp. 1079–1130, Nov. 2004, doi: 10.1016/j.jweia.2004.06.003.
[62] J. Straube and E. F. P. Burnett, 'Rain Control and Design Strategies', *Journal of Thermal Envelope and Building Science*, vol. 23, no. 1, pp. 41–56, Jul. 1999, doi: 10.1177/109719639902300105.
[63] B. Blocken and J. Carmeliet, 'Driving Rain on Building Envelopes- I. Numerical Estimation and Full-Scale Experimental Verification', *Journal of Thermal Envelope and Building Science*, p. 25, Jul. 2000, doi: 10.1106/UJ12-PFHK-VQFP-8GAL.
[64] B. H. Vos, 'Internal Condensation in Structures', p. 16.
[65] J. Grunewald, Diffusiver und konvektiver Stoff- und Energietransport in kapillarporösen Baustoffen, Doctoral thesis, Fakultät Bauingenieurwesen, Technischen Universität Dresden, 1997.
[66] H. Hens, 'Annex_24_Heat, Air and Moisture Transfer in Highly Insulated Building Envelopes (Hamtie)', Laboratory of Building Physics, Department of Civil Engineering, Leuven, Belgium, 1996.

[67] M. K. Kumaran, ‘Heat, air and moisture transfer in insulated envelope parts: task 3 material properties’, Laboratorium Bouwfysica, Leuven, Belgium, 1996.
[68] A. Karagiozis, ‘Advanced Hygrothermal Models and Design Models’, in *eSim-The Canadian conference on building energy simulation*, Ottawa, Canada, Jun. 2001, p. 8.
[69] J. M. P. Q. Delgado, E. Barreira, N. M. M. Ramos, and V. P. de Freitas, *Hygrothermal Numerical Simulation Tools Applied to Building Physics*. in SpringerBriefs in Applied Sciences and Technology. Berlin, Heidelberg: Springer Berlin Heidelberg, 2013. doi: 10.1007/978-3-642-35003-0.
[70] J. M. P. Q. Delgado, N. M. M. Ramos, E. Barreira, and V. P. de Freitas, ‘A critical review of hygrothermal models used in porous building materials’, *J Por Media*, vol. 13, no. 3, Art. no. 3, 2010, doi: 10.1615/JPorMedia.v13.i3.30.
[71] M. Bayat Pour, J. Niklewski, A. Naghibi, and E. Frühwald Hansson, ‘A Literature Review of Probabilistic Hygrothermal Assessment for Building Envelopes’, *Building and Environment*, vol. 261, p. 111756, Jun. 2024, doi: 10.1016/j.buildenv.2024.111756.
[72] ‘DELPHIN’. Accessed: May 26, 2021. [Online]. Available: https://bauklimatik-dresden.de/delphin/index.php?aLa=en
[73] ‘WUFI (en)’. Accessed: May 26, 2021. [Online]. Available: https://wufi.de/en/
[74] A. S. Kalagasidis, ‘HAM-Tools - An Integrated Simulation Tool for Heat, Air and Moisture Transfer Analyses in Building Physics’, Chalmers University of Technology, 2004. Accessed: May 26, 2021. [Online]. Available: https://research.chalmers.se/en/publication/485
[75] Z. Sadovský, O. Koronthályová, P. Matiašovský, and K. Mikulová, ‘Probabilistic modelling of mould growth in buildings’, *Journal of Building Physics*, vol. 37, no. 4, pp. 348–366, Apr. 2014, doi: 10.1177/1744259113496370.
[76] H. Janssen, B. Blocken, and J. Carmeliet, ‘Conservative modelling of the moisture and heat transfer in building components under atmospheric excitation’, *International Journal of Heat and Mass Transfer*, vol. 50, no. 5–6, pp. 1128–1140, Mar. 2007, doi: 10.1016/j.ijheatmasstransfer.2006.06.048.
[77] M. de Wit, *HAMBASE: Heat, Air and Moisture model for Building And Systems Evaluation*. Eindhoven: Technische Universiteit Eindhoven, Faculteit Bouwkunde, 2006.
[78] C.-E. Hagentoft, ‘Simplified analysis of combined heat, moisture and air transport for one-dimensional cases’, Lund University, Sweden, Tl-S-92/04, 1992.
[79] ‘EnergyPlus | EnergyPlus’. Accessed: May 26, 2021. [Online]. Available: https://energyplus.net/
[80] W. Maref, S. M. Cornick, K. Abdulghani, and D. van Reenen, ‘An Advanced hygrothermal design tool “hygIRC 1-D”’, in *eSim 2004 Conference*, Vancouver, Canada, Jun. 2004, p. 6.
[81] COMSOL AB, *Heat Transfer Module Users Guide With Comsol.* COMSOL, 2018.

[82] ‘Building Performance - Simulation Software | EQUA’. Accessed: May 26, 2021. [Online]. Available: https://www.equa.se/en/
[83] M. Defo, M. Lacasse, and A. Laouadi, ‘A comparison of hygrothermal simulation results derived from four simulation tools’, *Journal of Building Physics*, p. 174425912098876, Feb. 2021, doi: 10.1177/1744259120988760.
[84] B. Hejazi, N. Rodrigues Marques Sakiyama, J. Frick, and H. Garrecht, ‘Hygrothermal Simulations Comparative Study: Assessment of Different Materials Using WUFI and DELPHIN Software’, presented at the Building Simulation 2019, Rome, Italy, May 2021, pp. 4674–4681. doi: 10.26868/25222708.2019.211033.
[85] J. Zhao, ‘Development of a Novel Statistical Method and Procedure for Material Characterization and a Probabilistic Approach to Assessing the Hygrothermal Performance of Building Enclosure Assemblies’, Dissertation, College of Engineering and Computer Science, Syracuse University, Syracuse, NY, USA, 2012.
[86] H. Hens, *Building Physics Heat, Air and Moisture*, 3rd ed. Leuven, Belgium: Ernst & Sohn, 2017.
[87] A. Atangana, ‘Principle of Groundwater Flow’, in *Fractional Operators with Constant and Variable Order with Application to Geo-Hydrology*, Elsevier, 2018, pp. 15–47. doi: 10.1016/B978-0-12-809670-3.00002-3.
[88] S. Roels *et al.*, ‘A Comparison of Different Techniques to Quantify Moisture Content Profiles in Porous Building Materials’, *Journal of Thermal Envelope and Building Science*, vol. 27, no. 4, pp. 261–276, Apr. 2004, doi: 10.1177/1097196304042117.
[89] EN 15026:2007 - Hygrothermal performance of building components and building elements - Assessment of moisture transfer by numerical simulation.
[90] ISO 6946:2017 - Building components and building elements – Thermal resistance and thermal transmittance – Calculation methods.
[91] T. Ritchie and J. Davison, ‘Factors Affecting Bond Strength and Resistance to Moisture Penetration of Brick Masonry’, *Symposium on Masonry Testing*, pp. 16–30, Jan. 1963, doi: 10.1520/STP39541S.
[92] T. Ritchie and W. G. Plewes, ‘A review of literature on rain penetration of unit masonry’, *Technical Paper (National Research Council of Canada. Division of Building Research)*, vol. 47, p. 76, 1957, doi: 10.4224/40001176.
[93] N. Van Den Bossche, N. A. Lacasse, and A. Janssens, ‘Watertightness of masonry walls: an overview’, in *12th International Conference on the Durability of Building Materials and Components (12DBMC)*, Apr. 2011, pp. 1–8.
[94] K. Calle, C. Coupillie, A. Janssens, and N. Van Den Bossche, ‘Implementation of rainwater infiltration measurements in hygrothermal modelling of non-insulated brick cavity walls’, *Journal of Building Physics*, vol. 43, no. 6, pp. 477–502, May 2020, doi: 10.1177/1744259119883909.
[95] S. Kahangi Shahreza, M. Bayat Pour, and A. Abdul Hamid, ‘Towards rational decision-making on repointing to mitigate moisture damage in building

envelopes: A probabilistic study', *Developments in the Built Environment*, vol. 19, p. 100510, Oct. 2024, doi: 10.1016/j.dibe.2024.100510.
[96] S. Kahangi Shahreza, M. Bayat Pour, A. Abdul Hamid, and M. Molnár, 'Strategies for Enhanced Energy Efficiency and Moisture Management in Brick–AAC Cavity Walls', in *18th International Brick and Block Masonry Conference*, in Lecture Notes in Civil Engineering, vol. 613. Switzerland: Springer Nature Switzerland, 2025, pp. 804–819. doi: 10.1007/978-3-031-73314-7_62.
[97] B. S. Institution, *Code of Practice for Assessing Exposure of Walls to Wind-driven Rain*, British Standards Institution, UK., 1992.
[98] ISO 15927-3:2009 - Hygrothermal performance of buildings – Calculation and presentation of climatic data – Part 3: Calculation of a driving rain index for vertical surfaces from hourly wind and rain data.
[99] B. Blocken and J. Carmeliet, 'Overview of three state-of-the-art wind-driven rain assessment models and comparison based on model theory', *Building and Environment*, vol. 45, no. 3, pp. 691–703, Mar. 2010, doi: 10.1016/j.buildenv.2009.08.007.
[100] B. Blocken and J. Carmeliet, 'A review of wind-driven rain research in building science', *Journal of Wind Engineering and Industrial Aerodynamics*, vol. 92, no. 13, pp. 1079–1130, Nov. 2004, doi: 10.1016/j.jweia.2004.06.003.
[101] Intergovernmental Panel On Climate Change (Ipcc), *Climate Change 2021 – The Physical Science Basis*, 1st ed. Cambridge University Press, 2023. doi: 10.1017/9781009157896.
[102] E. Vereecken and S. Roels, 'Review of mould prediction models and their influence on mould risk evaluation', *Building and Environment*, vol. 51, pp. 296–310, May 2012, doi: 10.1016/j.buildenv.2011.11.003.
[103] K. Gradeci, N. Labonnote, B. Time, and J. Köhler, 'Mould growth criteria and design avoidance approaches in wood-based materials – A systematic review', *Construction and Building Materials*, vol. 150, pp. 77–88, Sep. 2017, doi: 10.1016/j.conbuildmat.2017.05.204.
[104] H. L. S. C. Hens, 'Fungal Defacement in Buildings: A Performance Related Approach', *HVAC&R Res.*, vol. 5, no. 3, pp. 265–280, Jul. 1999, doi: 10.1080/10789669.1999.10391237.
[105] P. Johansson and T. Svensson, 'Predicting mould growth on building materials- the PJ-model', in *12th Nordic Symposium on Building Physics (NSB)*, Tallinn, Estonia, 2020, p. 6. doi: 10.1051/e3sconf/202017220001.
[106] M. Labat and M. Woloszyn, 'Moisture balance assessment at room scale for four cases based on numerical simulations of heat–air–moisture transfers for a realistic occupancy scenario', *Journal of Building Performance Simulation*, vol. 9, no. 5, pp. 487–509, Sep. 2016, doi: 10.1080/19401493.2015.1107136.
[107] 'Finnish mould growth model | Building Physics | Tampere Universities', Building Physics. Accessed: Jun. 30, 2022. [Online]. Available: https://research.tuni.fi/buildingphysics/finnish-mould-growth-model/

[108] S. Thelandersson and T. Isaksson, 'Mould resistance design (MRD) model for evaluation of risk for microbial growth under varying climate conditions', *Building and Environment*, vol. 65, pp. 18–25, Jul. 2013, doi: 10.1016/j.buildenv.2013.03.016.
[109] Å. Togerö, C. Svensson Tengberg, B. Bengtsson. The m-model: a method to assess the risk for mould growth in wood structures with fluctuating hygrothermal conditions., NSB 2011 - 9th Nordic Symposium on Building Physics, Tampere, Finland, 2011.
[110] L. Wadsö, B. Bengtsson, and P. Johansson, 'The m-model for prediction of mould growth', 2022, *Lund, Sweden*.
[111] T. Ojanen, H. Viitanen, and R. Peuhkuri, 'Modelling of mould growth in building envelopes', in *IEA ECBCS Annex 41 Closing Seminar : Nordic Building Physics Conference*, Copenhagen, Denmark, 2007, p. 18.
[112] H. Viitanen and T. Ojanen, 'Improved Model to Predict Mold Growth in Building Materials', in *10th Thermal Performance of the Exterior Envelopes of Whole Buildings Conference*, Clearwater Beach, United States, Dec. 2007, p. 8.
[113] H. A. Viitanen, 'Modelling the Time Factor in the Development of Mould Fungi - the Effect of Critical Humidity and Temperature Conditions on Pine and Spruce Sapwood', *hfsg*, vol. 51, no. 1, pp. 6–14, 1997, doi: 10.1515/hfsg.1997.51.1.6.
[114] *ASHRAE, Standard 160-2021, Criteria for Moisture-Control Design Analysis in Buildings*, 160–2021, USA., 2021.
[115] C. Brischke and L. Meyer-Veltrup, 'Modelling timber decay caused by brown rot fungi', *Mater Struct*, vol. 49, no. 8, pp. 3281–3291, Aug. 2016, doi: 10.1617/s11527-015-0719-y.
[116] A. Tietze, A. Ott, S, Boulet, K. Gradeci, N. Labonnote, S. Grynning, J. Noreen, A. Pousette. Tall Timber Facades – Identification of Cost-effective and Resilient Envelopes for Wood Constructions Scientific Project Report; Technical University Munich; Munich; 31.07.2017.
[117] EN 252:2014 - Field test method for determining the relative protective effectiveness of a wood preservative in ground contact.
[118] E. Borgström and R. Karlsson, Design of timber structures, Structural aspects of timber construction, SW: Swedish Forest Industries Federation, 2:2016.
[119] DIN EN 1995-1-1:2010. Eurocode 5: Design of timber structures – Common rules and rules for buildings.
[120] S. R. Williams, Weathering of wood. Handbook of wood chemistry and wood composites. Boca Raton : CRC Press, 2005: pages 139-185.
[121] H. Janssen, S. Roels, L. Van Gelder, and P. Das, 'Annex 55, Reliability of Energy Efficient Building Retrofitting - Probability Assessment of Performance and Cost (RAP-RETRO), Probabilistic Tools', Chalmers University of Technology, Gothenburg, Sweden, ISSN 1652-9162, 2015:4, 2015.

[122] L. Wang and H. Ge, ‘Stochastic modelling of hygrothermal performance of highly insulated wood framed walls’, *Building and Environment*, vol. 146, pp. 12–28, Dec. 2018, doi: 10.1016/j.buildenv.2018.09.032.
[123] S. Panico, M. Larcher, V. Marincioni, A. Troi, C. Baglivo, and P. M. Congedo, ‘Identifying key parameters through a sensitivity analysis for realistic hygrothermal simulations at wall level supported by monitored data’, *Building and Environment*, vol. 229, p. 109969, Feb. 2023, doi: 10.1016/j.buildenv.2022.109969.
[124] K. Gradeci, N. Labonnote, B. Time, and J. Köhler, ‘A proposed probabilistic-based design methodology for predicting mould occurrence in timber façades’, in *World Conference on Timber Engineering (WCTE)*, Vienna, Austria, Aug. 2016, p. 9.
[125] H. J. Moon and G. Augenbroe, ‘Empowerment of decision-makers in mould remediation’, *Building Research & Information*, vol. 36, no. 5, Art. no. 5, Oct. 2008, doi: 10.1080/09613210801996203.
[126] K. Gradeci and U. Berardi, ‘Application of probabilistic approaches to the performance evaluation of building envelopes to withstand mould growth’, *Journal of Building Physics*, vol. 43, no. 3, Art. no. 3, Nov. 2019, doi: 10.1177/1744259119861784.
[127] V. Marincioni, G. Marra, and H. Altamirano-Medina, ‘Development of predictive models for the probabilistic moisture risk assessment of internal wall insulation’, *Building and Environment*, vol. 137, pp. 257–267, Jun. 2018, doi: 10.1016/j.buildenv.2018.04.001.
[128] J. Zhao, J. “Jensen” Zhang, J. Grunewald, and S. Feng, ‘A probabilistic-based method to evaluate hygrothermal performance of an internally insulated brick wall’, *Build. Simul.*, vol. 14, no. 2, pp. 283–299, Apr. 2021, doi: 10.1007/s12273-020-0702-6.
[129] A. H. Holm and H. M. Kuenzel, ‘Practical application of an uncertainty approach for hygrothermal building simulations—drying of an AAC flat roof’, *Building and Environment*, p. 7, 2002, doi: 10.1016/S0360-1323(02)00047-1.
[130] M. Salonvaara, A. Karagiozis, and A. Holm, ‘Stochastic Building Envelope Modeling— The Influence of Material Properties’, in *Building VIII*, 1995, p. 8.
[131] J. Goffart, M. Rabouille, and N. Mendes, ‘Uncertainty and sensitivity analysis applied to hygrothermal simulation of a brick building in a hot and humid climate’, *Journal of Building Performance Simulation*, vol. 10, no. 1, Art. no. 1, Jan. 2017, doi: 10.1080/19401493.2015.1112430.
[132] Z. Sadovský and O. Koronthályová, ‘Exploration of probabilistic mould growth assessment’, *Applied Mathematical Modelling*, vol. 42, pp. 566–575, Feb. 2017, doi: 10.1016/j.apm.2016.10.049.
[133] C.-E. Hagentoft, ‘Reliability of energy efficient building retrofitting - probability assessment of performance and cost (Annex 55, RAP-RETRO)’,

Energy and Buildings, vol. 155, pp. 166–171, Nov. 2017, doi: 10.1016/j.enbuild.2017.09.007.
[134] K. Pietrzyk, 'A systemic approach to moisture problems in buildings for mould safety modelling', *Building and Environment*, vol. 86, pp. 50–60, Apr. 2015, doi: 10.1016/j.buildenv.2014.12.013.
[135] H. J. Moon and G. Augenbroe, 'A Mixed Simulation Approach to Analyze Mold Growth Under Uncertainty', in *Ninth International IBPSA Conference*, Montreal, Canada: Building Simulation, Aug. 2005, p. 9.
[136] H. J. Moon and G. Augenbroe, 'Application of probabilistic simulation and bayesian decision theory in the selection of mold remediation actions', in *10th International IBPSA Conference*, Beijing, China: Building Simulation, 2007, p. 8.
[137] A. Tijskens, H. Janssen, and S. Roels, 'Using convolutional neural networks for hygrothermal predictions to extrapolate to other external climates', in *12th Nordic Symposium on Building Physics (NSB 2020)*, J. Kurnitski and T. Kalamees, Eds., Tallinn, Estonia: E3S Web of Conferences, Jun. 2020, p. 04001. doi: 10.1051/e3sconf/202017204001.
[138] P. Boudreaux, S. Pallin, G. Accawi, A. Desjarlais, R. Jackson, and D. Senecal, 'A rule-based expert system applied to moisture durability of building envelopes', *Journal of Building Physics*, vol. 42, no. 3, Art. no. 3, Nov. 2018, doi: 10.1177/1744259117750370.
[139] A. Tijskens, H. Janssen, and S. Roels, 'A simplified dynamic zone model for a probabilistic assessment of hygrothermal risks in building components', in *11th Nordic Symposium on Building Physics*, Trondheim, Norway: Energy Procedia, Oct. 2017, pp. 717–722. doi: 10.1016/j.egypro.2017.10.012.
[140] S. Ott, A. Tietze, and S. Winter, 'Introduction of a semi-probabilistic moisture safety model for tall timber-based building shell – a risk based durability approach', in *Life-Cycle of Engineering Systems*, Delft, Netherlands: CRC Press, Nov. 2016, pp. 262–262. doi: 10.1201/9781315375175-205.
[141] J. Zhao, R. Plagge, N. M. M. Ramos, M. Lurdes Simões, and J. Grunewald, 'Concept for development of stochastic databases for building performance simulation – A material database pilot project', *Building and Environment*, vol. 84, pp. 189–203, Jan. 2015, doi: 10.1016/j.buildenv.2014.10.030.
[142] H. Sulaiman and F. Olsina, 'Comfort reliability evaluation of building designs by stochastic hygrothermal simulation', *Renewable and Sustainable Energy Reviews*, vol. 40, pp. 171–184, Dec. 2014, doi: 10.1016/j.rser.2014.07.162.
[143] N. M. M. Ramos, E. Barreira, M. L. Simões, and J. M. P. Q. Delgado, 'Probabilistic Risk Assessment Methodology of Exterior Surfaces Defacement Caused by Algae Growth', *J. Constr. Eng. Manage.*, vol. 140, no. 12, Art. no. 12, Dec. 2014, doi: 10.1061/(ASCE)CO.1943-7862.0000909.
[144] S. Pallin, M. Kehrer, and W. A. Miller, 'A Hygrothermal Risk Analysis Applied to Residential Unvented Attics', in *Thermal Performance of*

the Exterior Envelopes of Whole Buildings XII International Conference, Clearwater, Florida, United States of America, Dec. 2013, p. 17.

[145] B. Boucham, A. Chateauneuf, and E. A. A. Bedia, 'An Uncertainty Method for Moisture Concentration Assessment in Composite Material Plates T300/5208 under Hygrothermal Conditions Effects', *Turkish Journal of Engineering and Environmental Sciences*, vol. 32, no. 5, p. 12, Jan. 2008.

[146] K. Kurkinen, K. Pietrzyk, E.-L. Wentzel, and C.-E. Hagentoft, 'Probabilistic Analysis of Indoor Surface Hygrothermal Conditions Accounting for Thermal and Hygric Memory of the Building Component', in *9th International Conference Thermal Performance of Exterior Envelopes of Whole Buildings*, Clearwater, USA, 2004, p. 9.

[147] A. Brás, A. Valença, and P. Faria, 'Performance-based methods for masonry building rehabilitation using innovative leaching and hygrothermal risk analyses', *Sustainable Cities and Society*, vol. 28, pp. 321–331, Jan. 2017, doi: 10.1016/j.scs.2016.09.010.

[148] K. Gradeci, U. Berardi, B. Time, and J. Köhler, 'Evaluating highly insulated walls to withstand biodeterioration: A probabilistic-based methodology', *Energy and Buildings*, vol. 177, pp. 112–124, Oct. 2018, doi: 10.1016/j.enbuild.2018.07.059.

[149] K. Gradeci, N. Labonnote, B. Time, and J. Köhler, 'A probabilistic-based approach for predicting mould growth in timber building envelopes: Comparison of three mould models', in *11th Nordic Symposium on Building Physics*, Trondheim, Norway: Energy Procedia, Jun. 2017, pp. 393–398. doi: 10.1016/j.egypro.2017.09.641.

[150] E. Arumägi, M. Pihlak, and T. Kalamees, 'Reliability of Interior Thermal Insulation as a Retrofit Measure in Historic Wooden Apartment Buildings in Cold Climate', in *6th International Building Physics Conference*, Torino, Italy: Energy Procedia, Jun. 2015, pp. 871–876. doi: 10.1016/j.egypro.2015.11.010.

[151] T. Hou, D. Nuyens, S. Roels, and H. Janssen, 'Quasi-Monte Carlo based uncertainty analysis: Sampling efficiency and error estimation in engineering applications', *Reliability Engineering & System Safety*, vol. 191, p. 106549, Nov. 2019, doi: 10.1016/j.ress.2019.106549.

[152] F. Haldi, 'Predicting the Risk of Moisture Induced Damages on the Building Envelope Using Stochastic Models of Building Occupants' Behaviour', in *6th International Building Physics Conference*, Torino, Italy: Energy Procedia, Jun. 2015, pp. 1377–1382. doi: 10.1016/j.egypro.2015.11.157.

[153] H. Janssen, 'Monte-Carlo based uncertainty analysis: Sampling efficiency and sampling convergence', *Reliability Engineering & System Safety*, vol. 109, pp. 123–132, Jan. 2013, doi: 10.1016/j.ress.2012.08.003.

[154] L. Wang and H. Ge, 'Effect of rain leakage on hygrothermal performance of highly insulated wood-framed walls: a stochastic approach', *Can. J. Civ. Eng.*, vol. 46, no. 11, Art. no. 11, Nov. 2019, doi: 10.1139/cjce-2019-0223.

[155] S. Ilomets, T. Kalamees, and J. Vinha, ‘Indoor hygrothermal loads for the deterministic and stochastic design of the building envelope for dwellings in cold climates’, *Journal of Building Physics*, vol. 41, no. 6, Art. no. 6, May 2018, doi: 10.1177/1744259117718442.
[156] L. Wang and H. Ge, ‘Hygrothermal performance of cross-laminated timber wall assemblies: A stochastic approach’, *Building and Environment*, vol. 97, pp. 11–25, Feb. 2016, doi: 10.1016/j.buildenv.2015.11.034.
[157] T. Defraeye, B. Blocken, and J. Carmeliet, ‘Influence of uncertainty in heat–moisture transport properties on convective drying of porous materials by numerical modelling’, *Chemical Engineering Research and Design*, vol. 91, no. 1, Art. no. 1, Jan. 2013, doi: 10.1016/j.cherd.2012.06.011.
[158] J. Zhao, R. Plagge, A. Nicolai, J. Grunewald, and J. S. Zhang, ‘Stochastic study of hygrothermal performance of a wall assembly - The influence of material properties and boundary coefficients’, *HVAC&R Research*, vol. 17, no. 4, Art. no. 4, 2011, doi: 10.1080/10789669.2011.585421.
[159] R. Bui, M. Labat, and S. Lorente, ‘Impact of the occupancy scenario on the hygrothermal performance of a room’, *Building and Environment*, vol. 160, p. 106178, Aug. 2019, doi: 10.1016/j.buildenv.2019.106178.
[160] E. Arumägi, T. Kalamees, and U. Kallavus, ‘Indoor climate conditions and hygrothermal loads in historic wooden apartment buildings in cold climates’, *Proc. Estonian Acad. Sci.*, vol. 64, no. 2, Art. no. 2, 2015, doi: 10.3176/proc.2015.2.03.
[161] A. Tijskens, H. Janssen, and S. Roels, ‘The impact of a reduced training subspace on the prediction accuracy of neural networks for hygrothermal predictions’, *Journal of Building Performance Simulation*, vol. 14, no. 1, Art. no. 1, Jan. 2021, doi: 10.1080/19401493.2020.1832148.
[162] A. Tijskens, H. Janssen, and S. Roels, ‘Optimising Convolutional Neural Networks to Predict the Hygrothermal Performance of Building Components’, *Energies*, vol. 12, no. 20, Art. no. 20, Oct. 2019, doi: 10.3390/en12203966.
[163] A. Tijskens, S. Roels, and H. Janssen, ‘Predicting the hygrothermal behaviour of building components using neural networks’, in *4th Central European Symposium on Building Physics (CESBP 2019)*, Prague, Czech Republic: MATEC Web of Conferences, Sep. 2019, p. 6. doi: 10.1051/matecconf/201928202036.
[164] K. Calle and N. Van Den Bossche, ‘Sensitivity analysis of the hygrothermal behaviour of homogeneous masonry constructions: Interior insulation, rainwater infiltration and hydrophobic treatment’, *Journal of Building Physics*, vol. 44, no. 6, Art. no. 6, May 2021, doi: 10.1177/17442591211009937.
[165] R. Bui, J. Goffart, F. McGregor, M. Woloszyn, A. Fabbri, and A.-C. Grillet, ‘Uncertainty and sensitivity analysis applied to a rammed earth wall: evaluation of the discrepancies between experimental and numerical data’, in *12th Nordic Symposium on Building Physics (NSB 2020)*, Tallinn, Estonia: E3S Web of Conferences, Jun. 2020, p. 7. doi: 10.1051/e3sconf/202017217004.

[166] N. Ramos, E. Barreira, M. L. Simões, J. Delgado, Probabilistic risk assessment applied to biological growth on external surfaces with ETICS, in: 13th Conference of the International Building Performance Simulation Association, Chambéry, France, August, 2013: p. 6.
[167] Å. Togerö, C. Svensson Tengberg, B. Bengtsson. The m-model: a method to assess the risk for mould growth in wood structures with fluctuating hygrothermal conditions., NSB 2011 - 9th Nordic Symposium on Building Physics, Tampere, Finland, 2011.
[168] C. E. Hagentoft and A. S. Kalagasidis, 'Hygrothermal Conditions and Mould Growth Potential in Cold Attics: Impact of Weather, Building System and Construction Design Characteristics', in *Hygrothermal Behavior, Building Pathology and Durability*, vol. 1, in Building Pathology and Rehabilitation, vol. 1. , Berlin, Heidelberg: Springer Berlin Heidelberg, 2013, pp. 61–91. doi: 10.1007/978-3-642-31158-1_4.
[169] C.-E. Hagentoft, 'Probabilistic Analysis of Hygrothermal Conditions and Mould Growth Potential in Cold Attics. Impact of Weather, Building System and Construction Design Characteristics', in *12th International Conference on Durability of Building Materials and Components*, Porto, Portugal, Apr. 2011, p. 8.
[170] V. Kukk, J. Kers, T. Kalamees, L. Wang, and H. Ge, 'Impact of built-in moisture on the design of hygrothermally safe cross-laminated timber external walls: A stochastic approach', *Building and Environment*, vol. 226, p. 109736, Dec. 2022, doi: 10.1016/j.buildenv.2022.109736.
[171] R. M. S. F. Almeida and E. Barreira, 'Monte Carlo Simulation to Evaluate Mould Growth in Walls: The Effect of Insulation, Orientation, and Finishing Coating', *Advances in Civil Engineering*, vol. 2018, pp. 1–12, Aug. 2018, doi: 10.1155/2018/8532167.
[172] M. Bayat Pour, J. Niklewski, A. Naghibi, and E. Frühwald Hansson, 'Robust probabilistic modelling of mould growth in building envelopes using random forests machine learning algorithm', *Building and Environment*, vol. 243, p. 110703, Sep. 2023, doi: 10.1016/j.buildenv.2023.110703.
[173] L. Wang, M. Defo, Z. Xiao, H. Ge, and M. A. Lacasse, 'Stochastic Simulation of Mould Growth Performance of Wood-Frame Building Envelopes under Climate Change: Risk Assessment and Error Estimation', *Buildings*, vol. 11, no. 8, p. 333, Jul. 2021, doi: 10.3390/buildings11080333.
[174] A. Tijskens, H. Janssen, and S. Roels, 'Probabilistic hygrothermal assessment of various timber frame wall compositions', *Building and Environment*, vol. 243, p. 110619, Sep. 2023, doi: 10.1016/j.buildenv.2023.110619.
[175] D. Chung and J. Wen, 'Building Envelope Moisture Transport in the Context of Assembly Aging and Uncertainty', *Technology|Architecture + Design*, vol. 3, no. 2, pp. 221–233, Jul. 2019, doi: 10.1080/24751448.2019.1640540.
[176] N. Grint, V. Marincioni, and C. A. Elwell, 'Sensitivity and Uncertainty analyses on a DELPHIN model: the impact of material properties

on moisture in a solid brick wall', in *12th Nordic Building Physics Conference NSB*, J. Kurnitski and T. Kalamees, Eds., Tallinn, Estonia, Sep. 2020, p. 04006. doi: 10.1051/e3sconf/202017204006.
[177] A. Tijskens, S. Roels, and H. Janssen, 'A convolutional neural network for the hygrothermal assessment of timber frame walls', presented at the 2021 Building Simulation Conference, Bruges, Belgium, Sep. 2021. doi: 10.26868/25222708.2021.30605.
[178] D. Chung, J. Wen, and L. C. J. Lo, 'Examining the impact of stochastic multi-year weather and air infiltration on hygrothermal moisture risks', *Journal of Building Physics*, vol. 47, no. 1, pp. 4–35, Jul. 2023, doi: 10.1177/17442591231163459.
[179] V. Kukk, J. Kers, T. Kalamees, L. Wang, and H. Ge, 'Hygrothermal Criteria for Design of Cross-Laminated Timber External Walls', in *Proceedings of the 5th International Conference on Building Energy and Environment*, in Environmental Science and Engineering. Singapore: Springer Nature Singapore, 2023, pp. 811–815. doi: 10.1007/978-981-19-9822-5_87.
[180] M. Gutland, S. Bucking, and M. Santana Quintero, 'Hygrothermal modelling of historic rubble masonry walls: Accounting for geometric and compositional variability', *Journal of Building Engineering*, vol. 48, p. 103929, May 2022, doi: 10.1016/j.jobe.2021.103929.
[181] S. Sahyoun, L. Wang, H. Ge, M. Defo, and M. Lacasse, 'Durability of Internally Insulated Historical Solid Masonry Under Future Climates: A Stochastic Approach', in *XV International Conference on Durability of Building Materials and Components. eBook of Proceedings*, CIMNE, 2020. doi: 10.23967/dbmc.2020.044.
[182] V. Kukk, J. Kers, and T. Kalamees, 'The use of an internal airtight membrane in CLT external wall in terms of hygrothermal performance', in *Journal of Physics: Conference Series*, Nov. 2021, p. 3. doi: 10.1088/1742-6596/2069/1/012208.
[183] L. Wang, M. Defo, A. Gaur, and M. A. Lacasse, 'Development of moisture reference years for assessing long-term mould growth risk of wood-frame building envelopes', in *8th International Building Physics Conference (IBPC 2021)*, Copenhagen, Denmark, Nov. 2021, p. 012015. doi: 10.1088/1742-6596/2069/1/012015.
[184] J. Woods and J. Winkler, 'Effective moisture penetration depth model for residential buildings: Sensitivity analysis and guidance on model inputs', *Energy and Buildings*, vol. 165, pp. 216–232, Apr. 2018, doi: 10.1016/j.enbuild.2018.01.040.
[185] S. Ott, A. Tietze, and S. Winter, 'Wind driven rain and moisture safety of tall timber houses – Evaluation of simulation methods', *Wood Material Science & Engineering*, vol. 10, no. 3, pp. 300–311, Jul. 2015, doi: 10.1080/17480272.2015.1068371.
[186] V. M. Nik, S. O. Mundt-Petersen, A. S. Kalagasidis, and P. De Wilde, 'Future moisture loads for building facades in Sweden: Climate change

and wind-driven rain', *Building and Environment*, vol. 93, pp. 362–375, Nov. 2015, doi: 10.1016/j.buildenv.2015.07.012.
[187] D. Chung, J. Wen, and L. J. Lo, 'Development and verification of the open source platform, HAM-Tools, for hygrothermal performance simulation of buildings using a stochastic approach', *Build. Simul.*, vol. 13, no. 3, Art. no. 3, Jun. 2020, doi: 10.1007/s12273-019-0594-5.
[188] A. Tijskens, S. Roels, and H. Janssen, 'Neural networks to predict the hygrothermal response of building components in a probabilistic framework', in *Healthy, Intelligent and Resilient Buildings and Urban Environments*, International Association of Building Physics (IABP), 2018, pp. 1169–1174. doi: 10.14305/ibpc.2018.ms-6.04.
[189] C. Aggarwal, H. Ge, M. Defo, and M. A. Lacasse, 'Hygrothermal performance assessment of wood frame walls under historical and future climates using partial least squares regression', *Building and Environment*, vol. 223, p. 109501, Sep. 2022, doi: 10.1016/j.buildenv.2022.109501.
[190] I. Lee, P. Roppel, and P. Eng, 'Guiding Design Teams by Hygrothermal, Energy, and Thermal Comfort Analysis while Managing Uncertainty', in *Buildings XIII Conference*, Florida, USA: ASHRAE, Dec. 2016, p. 19.
[191] D. Xia *et al.*, 'Impact of coupled heat and moisture transfer on indoor comfort and energy demand for residential buildings in hot-humid regions', *Energy and Buildings*, vol. 288, p. 113029, Jun. 2023, doi: 10.1016/j.enbuild.2023.113029.
[192] V. M. Nik, A. Sasic Kalagasidis, and E. Kjellström, 'Assessment of hygrothermal performance and mould growth risk in ventilated attics in respect to possible climate changes in Sweden', *Building and Environment*, vol. 55, pp. 96–109, Sep. 2012, doi: 10.1016/j.buildenv.2012.01.024.
[193] V. Nik, 'Mould Growth inside an Attic concerning Four Different Future Climate Scenarios', in *NSB2011 9th Nordic Symposium on Building Physics*, Finland, Jun. 2011.
[194] S. M. Cornick, W. Alan Dalgliesh, and W. Maref, 'Sensitivity of hygrothermal analysis to uncertainty in rain data', *Journal of ASTM International*, vol. 6, no. 4, p. 19, 2009, doi: 10.1520/JAI102032.
[195] X. Lü, T. Lu, C. Kibert, K. Vahtikari, M. Hughes, and Y. Zhao, 'A dynamic modelling approach for simulating climate change impact on energy and hygrothermal performances of wood buildings', *Build. Simul.*, vol. 11, no. 3, Art. no. 3, Jun. 2018, doi: 10.1007/s12273-017-0421-9.
[196] T. Alioua, B. Agoudjil, A. Boudenne, and K. Benzarti, 'Sensitivity analysis of transient heat and moisture transfer in a bio-based date palm concrete wall', *Building and Environment*, vol. 202, p. 108019, Sep. 2021, doi: 10.1016/j.buildenv.2021.108019.
[197] I. Othmen, P. Poullain, and N. Leklou, 'Sensitivity analysis of the transient heat and moisture transfer in a single layer wall', *European Journal of Environmental and Civil Engineering*, vol. 24, no. 13, Art. no. 13, Nov. 2020, doi: 10.1080/19648189.2018.1500947.

[198] X. Liu, Y. Liu, X. Guo, N. Luo, and G. Chen, 'Effect of Uncertainty in the Hygrothermal Properties on Hygrothermal Modeling', in *Proceedings of the 11th International Symposium on Heating, Ventilation and Air Conditioning (ISHVAC 2019)*, in Environmental Science and Engineering. Singapore: Springer Singapore, 2020, pp. 461–470. doi: 10.1007/978-981-13-9528-4_47.

[199] A. H. Holm, H. M. Kuenzel, and J. Radon, 'Uncertainty Approaches for Hygrothermal Building Simulations— Drying of AAC in Hot and Humid Climates', in *Buildings VIII*, 2001, p. 6.

[200] A. Holm and H. M. Kuenzel, 'Uncertainty Approaches for Hygrothermal Building Simulations - Drying of an AAC Flat Roof in Different Climates', in *Seventh International IBPSA*, Rio de Janeiro, Brazil: Building Simulation, Aug. 2001, p. 8.

[201] C. Aggarwal, L. Wang, M. Defo, H. Ge, M. Junginger, and M. A. Lacasse, 'Sensitivity analysis of hygrothermal performance of wood framed wall assembly under different climatic conditions: the impact of cladding properties', in *8th International Building Physics Conference (IBPC 2021), Journal of Physics*, Copenhagen, Denmark, 2021, p. 9. doi: 10.1088/1742-6596/2069/1/012010.

[202] L. Havinga and H. Schellen, 'Applying internal insulation in post-war prefab housing: Understanding and mitigating the hygrothermal risks', *Building and Environment*, vol. 144, pp. 631–647, Oct. 2018, doi: 10.1016/j.buildenv.2018.08.035.

[203] V. Kukk, L. Kaljula, J. Kers, and T. Kalamees, 'Designing highly insulated cross-laminated timber external walls in terms of hygrothermal performance: Field measurements and simulations', *Building and Environment*, vol. 212, p. 108805, Mar. 2022, doi: 10.1016/j.buildenv.2022.108805.

[204] M. Gutland, S. Bucking, and M. Santana Quintero, 'Two-dimensional hygrothermal modelling of masonry walls accounting for imperfections at the masonry joint', in *12th Nordic Symposium on Building Physics (NSB)*, Tallinn, Estonia, 2020, p. 7. doi: 10.1051/e3sconf/202017208003.

[205] M. Gutland, S. Bucking, and M. Quintero, 'Detailed Modelling of the Masonry Unit-Mortar Interface Using Hygrothermal Simulation', in *XV International Conference on Durability of Building Materials and Components. eBook of Proceedings*, CIMNE, 2020. doi: 10.23967/dbmc.2020.223.

[206] J. Kočí, V. Kočí, and J. Maděra, 'Uncertainty in moisture transport modelling and its effect on ice formation in porous building materials', presented at the THERMOPHYSICS 2018: 23rd International Meeting of Thermophysics 2018, Smolenice, Slovakia, 2018, p. 6. doi: 10.1063/1.5047614.

[207] M. Bianchi Janetti, L. P. M. Colombo, F. Ochs, and W. Feist, 'Effect of evaporation cooling on drying capillary active building materials', *Energy and Buildings*, vol. 166, pp. 550–560, May 2018, doi: 10.1016/j.enbuild.2017.12.048.

[208] J. Kwiatkowski, M. Woloszyn, and J.-J. Roux, 'Modelling of hysteresis influence on mass transfer in building materials', *Building and*

Environment, vol. 44, no. 3, pp. 633–642, Mar. 2009, doi: 10.1016/j.buildenv.2008.05.006.
[209] S. Panico, M. Larcher, D. Herrera Avellanosa, C. Baglivo, A. Troi, and P. Maria Congedo, 'Hygrothermal simulation challenges: Assessing boundary condition choices in retrofitting historic European buildings', *Energy and Buildings*, vol. 297, p. 113464, Oct. 2023, doi: 10.1016/j.enbuild.2023.113464.
[210] I. Costa-Carrapiço, B. Croxford, R. Raslan, and J. Neila González, 'Hygrothermal calibration and validation of vernacular dwellings: A genetic algorithm-based optimisation methodology', *Journal of Building Engineering*, vol. 55, p. 104717, Sep. 2022, doi: 10.1016/j.jobe.2022.104717.
[211] J. Tchiotsop, S. Bonnet, T. S. Kiessé, N. Issaadi, and P. Poullain, 'Local and global sensitivity analysis of a coupled heat and moisture transfers model: effect of the variability of cob material properties', *Heat Mass Transfer*, Sep. 2023, doi: 10.1007/s00231-023-03409-0.
[212] M. Tonini De Araújo, H. A. De Souza, and A. P. Gomes, 'Computer simulation of moisture transfer in walls: impacts on the thermal performance of buildings', *Architectural Engineering and Design Management*, vol. 18, no. 4, pp. 453–472, Jul. 2022, doi: 10.1080/17452007.2021.1916426.
[213] C. D'Erme *et al.*, 'Preliminary study of the mechanical and hygrothermal performance of concrete reinforced with fibrillated cellulose', presented at the The 1st International Conference on Innovations for Computing, Engineering and Materials, 2021, Ho Chi Minh City, Vietnam, 2021, p. 020012. doi: 10.1063/5.0068522.
[214] A. Brambilla and E. Gasparri, 'Hygrothermal behaviour of emerging timber-based envelope technologies in Australia: A preliminary investigation on condensation and mould growth risk', *Journal of Cleaner Production*, vol. 276, p. 124129, Dec. 2020, doi: 10.1016/j.jclepro.2020.124129.
[215] C. Boardman and S. Glass, 'Improving the Accuracy of a Hygrothermal Model for Wood-Frame Walls: A Cold-Climate Study', *Buildings*, vol. 10, no. 12, p. 236, Dec. 2020, doi: 10.3390/buildings10120236.
[216] H. Lee, A. Ozaki, M. Lee, and T. Yamamoto, 'Humidity control effect of vapor-permeable walls employing hygroscopic insulation material', *Indoor Air*, vol. 30, no. 2, pp. 346–360, Mar. 2020, doi: 10.1111/ina.12622.
[217] B. Reich, H. Ge, and J. Wang, 'Effect of Vapor Diffusion Port on Drying of Wood-Frame Walls', in *XV International Conference on Durability of Building Materials and Components. eBook of Proceedings*, CIMNE, 2020. doi: 10.23967/dbmc.2020.160.
[218] J. Berger, S. Gasparin, D. Dutykh, and N. Mendes, 'On the Solution of Coupled Heat and Moisture Transport in Porous Material', *Transp Porous Med*, vol. 121, no. 3, pp. 665–702, Feb. 2018, doi: 10.1007/s11242-017-0980-3.
[219] G. Xing-guo, L. Hongtao, Z. Jingxin, L. Xiang-wei, and C. Guo-jie, 'Sensitivity Analysis applied to Hygrothermal Simulation of a Brick Building in Hot and Humid Climate', in *10th International Symposium on Heating,*

Ventilation and Air Conditioning, ISHVAC, Jinan, China, Oct. 2017, pp. 665–671. doi: 10.1016/j.proeng.2017.09.838.

[220] K. Abahri, R. Bennacer, and R. Belarbi, 'Sensitivity analyses of convective and diffusive driving potentials on combined heat air and mass transfer in hygroscopic materials', *Numerical Heat Transfer, Part A: Applications*, vol. 69, no. 10, pp. 1079–1091, May 2016, doi: 10.1080/10407782.2015.1109389.

[221] A. Ronzino and V. Corrado, 'Measuring the Hygroscopic Properties of Porous Media in Transient Regime. From the Material Level to the Whole Building HAM Simulation of a Coated Room', in *6th International Building Physics Conference, IBPC*, Torino, Italy, Nov. 2015, pp. 1501–1506. doi: 10.1016/j.egypro.2015.11.177.

[222] J. Prata, A. Tadeu, and N. Simões, 'Influence of material properties and boundary conditions on the dynamic thermal behaviour of a building corner', presented at the ECO-ARCHITECTURE 2014, Siena, Italy, Sep. 2014, pp. 333–345. doi: 10.2495/ARC140291.

[223] A. Evrard, C. Flory-Celini, M. Claeys-Bruno, and A. De Herde, 'Influence of liquid absorption coefficient on hygrothermal behaviour of an existing brick wall with Lime–Hemp plaster', *Building and Environment*, vol. 79, pp. 90–100, Sep. 2014, doi: 10.1016/j.buildenv.2014.04.031.

[224] E. Stephan, A. Caucheteux, R. Cantin, S. Tasca-Guernouti, and P. Michel, 'Sensitivity Analysis Of An Energyplus Simulation Model Of The Ambient Humidity In An Old Building', presented at the 2017 Building Simulation Conference, Aug. 2013. doi: 10.26868/25222708.2013.2161.

[225] A. Dung Tran Le, C. Maalouf, O. Douzane, T. Hoang Mai, T. Langlet, and M. Lachi, 'Parametric Study of Hygrothermal Behaviour of A Room Made Of Hemp Concrete', presented at the 2017 Building Simulation Conference, Aug. 2013. doi: 10.26868/25222708.2013.1004.

[226] T. Oreszczyn and S. E. C. Pretlove, 'Condensation Targeter II: Modelling surface relative humidity to predict mould growth in dwellings', *Building Services Engineering Research and Technology*, vol. 20, no. 3, pp. 143–153, Aug. 1999, doi: 10.1177/014362449902000307.

[227] S. Hokoi and M. K. Kumaran, 'Experimental and Analytical Investigations of Simultaneous Heat and Moisture Transport through Glass Fiber Insulation', *Journal of Thermal Insulation and Building Envelopes*, vol. 16, no. 3, pp. 263–292, Jan. 1993, doi: 10.1177/109719639301600307.

[228] M. Benkhaled, S.-E. Ouldboukhitine, A. Bakkour, and S. Amziane, 'Sensitivity analysis of the parameters for assessing a hygrothermal transfer model HAM in bio-based hemp concrete material', *International Communications in Heat and Mass Transfer*, vol. 132, p. 105884, Mar. 2022, doi: 10.1016/j.icheatmasstransfer.2022.105884.

[229] I. Vandemeulebroucke, S. Caluwaerts, and N. Van Den Bossche, 'Factorial Study on the Impact of Climate Change on Freeze-Thaw Damage, Mould Growth and Wood Decay in Solid Masonry Walls in Brussels', *Buildings*, vol. 11, no. 3, p. 134, Mar. 2021, doi: 10.3390/buildings11030134.

[230] O. May Tzuc *et al.*, 'Modeling of hygrothermal behavior for green facade's concrete wall exposed to nordic climate using artificial intelligence and global sensitivity analysis', *Journal of Building Engineering*, vol. 33, p. 101625, Jan. 2021, doi: 10.1016/j.jobe.2020.101625.

[231] I. Vandemeulebroucke, S. Caluwaerts, and N. Bossche, 'Freeze-Thaw Risk in Solid Masonry: Are 'Hygrothermal Response Based' Analyses Mandatory when Studying the Sensitivity of Building Envelopes to Climate Change?', in *XV International Conference on Durability of Building Materials and Components. eBook of Proceedings*, CIMNE, 2020. doi: 10.23967/dbmc.2020.070.

[232] J. Kočí, V. Kočí, J. M. D. Silva, Z. Hlaváčová, and J. Maděra, 'Hygrothermal model for description of ice-forming process in porous building materials: Sensitivity analysis of input material parameters', presented at the INTERNATIONAL CONFERENCE OF COMPUTATIONAL METHODS IN SCIENCES AND ENGINEERING 2018 (ICCMSE 2018), Thessaloniki, Greece, 2018, p. 040012. doi: 10.1063/1.5079098.

[233] G. B. A. Coelho, H. E. Silva, and F. M. A. Henriques, 'Calibrated hygrothermal simulation models for historical buildings', *Building and Environment*, vol. 142, pp. 439–450, Sep. 2018, doi: 10.1016/j.buildenv.2018.06.034.

[234] M. Bart, S. Moissette, Y. Ait Oumeziane, and C. Lanos, 'Transient hygrothermal modelling of coated hemp-concrete walls', *European Journal of Environmental and Civil Engineering*, vol. 18, no. 8, pp. 927–944, Sep. 2014, doi: 10.1080/19648189.2014.911122.

[235] I. Othmen, 'Sensitivity analysis of the Künzel model: application to the study of the hygrothermal transfer in a tuffeau wall', presented at the HEAT TRANSFER 2014, Ph. Poullain, A. Caucheteux, and N. Leklou, Eds., A Coruña, Spain, Jul. 2014, pp. 417–428. doi: 10.2495/HT140361.

[236] E. Barreira and V. P. De Freitas, 'External Thermal Insulation Composite Systems: Critical Parameters for Surface Hygrothermal Behaviour', *Advances in Materials Science and Engineering*, vol. 2014, pp. 1–16, 2014, doi: 10.1155/2014/650752.

[237] V. Kočí, J. Maděra, and R. Černý, 'Exterior thermal insulation systems for AAC building envelopes: Computational analysis aimed at increasing service life', *Energy and Buildings*, vol. 47, pp. 84–90, Apr. 2012, doi: 10.1016/j.enbuild.2011.11.030.

[238] P. Cabrera, H. Samuelson, and M. Kurth, 'Simulating Mould Risks under Future Climate Conditions', presented at the Building Simulation 2019, Rome, Italy, pp. 1530–1538. doi: 10.26868/25222708.2019.211130.

[239] J. Selih and R. Zarnic, 'Influence of environmental conditions upon behaviour of historical buildings', in 6th International Conference on Structural Studies, Repairs and Maintenance of Historical Buildings (STREMAH 99), CESBP 2022, Dresden Germany, Jun. 1999, p. 10.

[240] B. Vanderschelden and N. V. D. Bossche, 'Fit for purpose brick clustering for hygrothermal material properties: Sensitivity to climate

conditions', in *5th Central European Symposium on Building Physics, CESBP 2022*, Bratislava, Slovakia, Nov. 2023, p. 020065. doi: 10.1063/5.0173303.
[241] A. D. Tran Le, C. Maalouf, K. C. Mendonça, T. H. Mai, and E. Wurtz, 'Study of moisture transfer in a double-layered wall with imperfect thermal and hydraulic contact resistances', *Journal of Building Performance Simulation*, vol. 2, no. 4, pp. 251–266, Dec. 2009, doi: 10.1080/19401490903082459.
[242] K. Zhang and R. Richman, 'Parametric analysis of moisture sorption isotherms for wood sheathing using hygrothermal modelling', *Journal of Building Engineering*, vol. 28, p. 101047, Mar. 2020, doi: 10.1016/j.jobe.2019.101047.
[243] J. Winkler, J. Munk, and J. Woods, 'Effect of occupant behavior and air-conditioner controls on humidity in typical and high-efficiency homes', *Energy and Buildings*, vol. 165, pp. 364–378, Apr. 2018, doi: 10.1016/j.enbuild.2018.01.032.
[244] V. Nik and A. S. Kalagasidis, 'Influence of the uncertainties in future climate scenarios on the hygrothermal simulation of an attic', in *International Conference on Building Envelope Systems and Technologies, ICBEST 2010*, Vancouver, Canada, June 27-30.
[245] H. Sulaiman, F. Olsina, S. Velez, Probabilistic assessment of discomfort risk in buildings, in: 13th conference of international building performance simulation association, Chambéry, France, 2013: p. 9.
[246] M. Gutland, S. Bucking, and M. Santana Quintero, 'A methodology for hygrothermal modelling of imperfect masonry interfaces', *Journal of Building Physics*, vol. 44, no. 6, Art. no. 6, May 2021, doi: 10.1177/1744259121989388.
[247] J. C. Helton, 'Uncertainty and sensitivity analysis techniques for use in performance assessment for radioactive waste disposal', *Reliability Engineering & System Safety*, vol. 42, no. 2–3, Art. no. 2–3, Jan. 1993, doi: 10.1016/0951-8320(93)90097-I.
[248] L. Rivalin, P. Stabat, D. Marchio, M. Caciolo, and F. Hopquin, 'A comparison of methods for uncertainty and sensitivity analysis applied to the energy performance of new commercial buildings', *Energy and Buildings*, vol. 166, pp. 489–504, May 2018, doi: 10.1016/j.enbuild.2018.02.021.
[249] S. Marino, I. B. Hogue, C. J. Ray, and D. E. Kirschner, 'A methodology for performing global uncertainty and sensitivity analysis in systems biology', *Journal of Theoretical Biology*, vol. 254, no. 1, Art. no. 1, Sep. 2008, doi: 10.1016/j.jtbi.2008.04.011.
[250] M. D. McKay, R. J. Beckman, and W. J. Conover, 'Comparison of Three Methods for Selecting Values of Input Variables in the Analysis of Output from a Computer Code', *Technometrics*, vol. 21, no. 2, pp. 239–245, May 1979, doi: 10.1080/00401706.1979.10489755.
[251] I. A. Macdonald, 'Comparison of sampling techniques on the performance of Monte Carlo based sensitivity analysis', in *11th International IBPSA*, Glasgow, Scotland, 2009, p. 9.

[252] R. I. Cukier, C. M. Fortuin, K. E. Shuler, A. G. Petschek, and J. H. Schaibly, ‘Study of the sensitivity of coupled reaction systems to uncertainties in rate coefficients. I Theory’, *The Journal of Chemical Physics*, vol. 59, no. 8, Art. no. 8, Oct. 1973, doi: 10.1063/1.1680571.
[253] J.e. Helton, F.J. Davis, Sampling-Based Methods for Uncertainty and Sensitivity Analysis, Sandia National Laboratories Albuquerque, New Mexico, July, 2000.
[254] G. D. Wyss and K. H. Jorgensen, ‘A user`s guide to LHS: Sandia`s Latin Hypercube Sampling Software’, SAND--98-0210, 573301, Feb. 1998. doi: 10.2172/573301.
[255] J. C. Helton and F. J. Davis, ‘Latin hypercube sampling and the propagation of uncertainty in analyses of complex systems’, *Reliability Engineering & System Safety*, vol. 81, no. 1, Art. no. 1, Jul. 2003, doi: 10.1016/S0951-8320(03)00058-9.
[256] L. P. Swiler and G. D. Wyss, ‘A user’s guide to Sandia’s latin hypercube sampling software : LHS UNIX library/standalone version.’, SAND2004-2439, 919175, Jul. 2004. doi: 10.2172/919175.
[257] O. M. Querin, M. Victoria, C. Alonso, R. Ansola, and P. Martí, ‘Discrete Method of Structural Optimization’, in *Topology Design Methods for Structural Optimization*, Elsevier, 2017, pp. 27–46. doi: 10.1016/B978-0-08-100916-1.00003-9.
[258] M. Bayat Pour and S. Kahangi Shahreza, ‘Impact of extruded mortar joints on the hygrothermal performance of brick veneer walls: a probabilistic study’, *Journal of Building Engineering*, vol. 94, p. 109936, Jun. 2024, doi: 10.1016/j.jobe.2024.109936.
[259] S. Kahangi Shahreza, J. Niklewski, and M. Molnár, ‘Novel water penetration criterion for clay brick masonry claddings’, *Construction and Building Materials*, vol. 353, p. 129109, Oct. 2022, doi: 10.1016/j.conbuildmat.2022.129109.
[260] ‘Swedish Meteorological and Hydrological Institute (SMHI)’. Accessed: May 30, 2023. [Online]. Available: https://www.smhi.se/data
[261] M. Bayat Pour, O. Ranefjärd, and J. Niklewski, ‘Probabilistic Analysis of Various Hygroscopic Insulations: Impacts on Mould Growth and Energy Efficiency in Timber Frame Walls’, in *6th Central European Symposium on Building Physics*, Budapest, Hungary: Springer, Sep. 2025, p. 8.
[262] F. Alfarra, H. K. Ozcan, P. Cihan, A. Ongen, S. Y. Guvenc, and M. N. Ciner, ‘Artificial intelligence methods for modeling gasification of waste biomass: a review’, *Environ Monit Assess*, vol. 196, no. 3, p. 309, Mar. 2024, doi: 10.1007/s10661-024-12443-2.
[263] L. Breiman, “Random Forests”, Machine Learning, 45(1), 5-32, 2001.
[264] L. Breiman, ‘Bagging predictors’, *Mach Learn*, vol. 24, no. 2, pp. 123–140, Aug. 1996, doi: 10.1007/BF00058655.

[265] Tin Kam Ho, 'The random subspace method for constructing decision forests', *IEEE Trans. Pattern Anal. Machine Intell.*, vol. 20, no. 8, pp. 832–844, Aug. 1998, doi: 10.1109/34.709601.
[266] S. A. Naghibi, H. R. Pourghasemi, and B. Dixon, 'GIS-based groundwater potential mapping using boosted regression tree, classification and regression tree, and random forest machine learning models in Iran', *Environ Monit Assess*, vol. 188, no. 1, p. 44, Jan. 2016, doi: 10.1007/s10661-015-5049-6.
[267] P. Vorpahl, H. Elsenbeer, M. Märker, and B. Schröder, 'How can statistical models help to determine driving factors of landslides?', *Ecological Modelling*, vol. 239, pp. 27–39, Jul. 2012, doi: 10.1016/j.ecolmodel.2011.12.007.
[268] M. Banerjee, Y. Ding, and A.-M. Noone, 'Identifying representative trees from ensembles', *Statist. Med.*, vol. 31, no. 15, pp. 1601–1616, Jul. 2012, doi: 10.1002/sim.4492.
[269] W. Aertsen, V. Kint, J. van Orshoven, K. Özkan, and B. Muys, 'Comparison and ranking of different modelling techniques for prediction of site index in Mediterranean mountain forests', *Ecological Modelling*, vol. 221, no. 8, pp. 1119–1130, Apr. 2010, doi: 10.1016/j.ecolmodel.2010.01.007.
[270] C. Strobl, A.-L. Boulesteix, A. Zeileis, and T. Hothorn, 'Bias in random forest variable importance measures: Illustrations, sources and a solution', *BMC Bioinformatics*, vol. 8, no. 1, p. 25, Dec. 2007, doi: 10.1186/1471-2105-8-25.
[271] A. Liaw and M. Wiener, 'Classification and Regression by randomForest', vol. 2, p. 5, Dec. 2002.
[272] M. Bayat Pour, S. Kahangi Shahreza, and A. Abdul Hamid, 'Effect of Extruded Mortar Joints on Mould Growth in Timber Frame Wall with Brick Veneer: Probabilistic and Machine Learning Modelling', in *9th International Building Physics Conference (IBPC 2024)*, Totonto, Canada: Springer Nature, 2025, pp. 17–22. doi: 10.1007/978-981-97-8305-2_2.
[273] 'sklearn.ensemble.RandomForestRegressor', scikit-learn. Accessed: Mar. 05, 2023. [Online]. Available: https://scikit-learn/stable/modules/generated/sklearn.ensemble.RandomForestRegressor.html
[274] M. Bayat Pour, S. Kahangi Shahreza, and A. Abdul Hamid, 'Influence of extruded mortar joints on mould growth in timber frame wall with brick veneer: Probabilistic and Machine Learning Modelling', Journal of Building Physics, 2025 (Manuscript submitted based on special issue invitation).
[275] D. M. Hamby, 'A review of techniques for parameter sensitivity analysis of environmental models', *Environ Monit Assess*, vol. 32, no. 2, Art. no. 2, Sep. 1994, doi: 10.1007/BF00547132.
[276] A. Saltelli, Ed., *Sensitivity analysis in practice: a guide to assessing scientific models*. Hoboken, NJ: Wiley, 2004.

[277] D. M. Hamby, ‘A Comparison of Sensitivity Analysis Techniques’, *Health Physics*, vol. 68, no. 2, pp. 195–204, Feb. 1995, doi: 10.1097/00004032-199502000-00005.
[278] P. Schober, C. Boer, and L. A. Schwarte, ‘Correlation Coefficients: Appropriate Use and Interpretation’, *Anesthesia & Analgesia*, vol. 126, no. 5, pp. 1763–1768, May 2018, doi: 10.1213/ANE.0000000000002864.
[279] G. H. Brundtland, Our Common Future: Report of the World Commission on Environment and Development. Oxford University Press, 1987.
[280] E. Tamadonyazdian, M. Gholampoor, K. Farsäter, and M. Bayat Pour, ‘Evaluation of Solidification/Stabilization Technology Performance by Combining Economic and Environmental Impacts Assessment for a Port in Sweden’, presented at the 19th Nordic Geotechnical Meeting, Gothenburg, Sweden, Sep. 2024, p. 12.
[281] IPCC, Climate change widespread, rapid, and intensifying. Intergovernmental Panel on Climate Change, Switzerland, 2021.
[282] ‘Transition to sustainable buildings: strategies and opportunities to 2050’, IEA Publ, Paris, Jul. 2013. [Online]. Available: https://www.iea.org/reports/transition-to-sustainable-buildings
[283] I. Hamilton *et al.*, ‘Energy Efficiency 2020’, International Energy Agency (IEA), Japan, 2020.
[284] D. J. Kibert, Sustainable Construction: Green Building Design and Delivery. John Wiley & Sons, 2016.
[285] B. Reza, R. Sadiq, and K. Hewage, ‘Sustainability assessment of flooring systems in the city of Tehran: An AHP-based life cycle analysis’, *Construction and Building Materials*, vol. 25, no. 4, pp. 2053–2066, Apr. 2011, doi: 10.1016/j.conbuildmat.2010.11.041.
[286] P. Santos, J. R. Correia, L. Godinho, A. M. P. G. Dias, and A. Dias, ‘Life cycle analysis of cross-insulated timber panels’, *Structures*, vol. 31, pp. 1311–1324, Jun. 2021, doi: 10.1016/j.istruc.2020.12.008.
[287] M. Bayat Pour and M. L. Elsayed, ‘Assessment of the environmental impacts, energy performance and economic aspects of various construction materials’, Master thesis, Lund University, Faculty of Engineering, Lund, Sweden, 2020.
[288] H. Viitanen, Factors affecting the development of mould and brown rot decay in wooden material and wooden structures, Doctoral thesis, Department of Forest Products, Swedish University of Agricultural Sciences, Uppsala, Sweden, 1996.
[289] N. Lolli, S. M. Fufa, and M. Inman, ‘A Parametric Tool for the Assessment of Operational Energy Use, Embodied Energy and Embodied Material Emissions in Building’, *Energy Procedia*, vol. 111, pp. 21–30, Mar. 2017, doi: 10.1016/j.egypro.2017.03.004.
[290] ‘RIBuild’, RIBuild. Accessed: Dec. 03, 2023. [Online]. Available: https://www.ribuild.eu

[291] Mold Remediation in Schools and Commercial Buildings, Indoor Environments Division (IED) of the U.S. Environmental Protection Agency (EPA), 2008.
[292] E. Bloom, P. Fjällström, B. Sahlberg, and A.-B. Antonsson, 'God praxis för säker mögelsanering', IVL Svenska Miljöinstitutet, Stockholm, Sweden, B 2234, Jan. 2015.
[293] P. Morseletto, 'Targets for a circular economy', *Resources, Conservation and Recycling*, vol. 153, p. 104553, Feb. 2020, doi: 10.1016/j.resconrec.2019.104553.
[294] A. Murray, K. Skene, and K. Haynes, 'The Circular Economy: An Interdisciplinary Exploration of the Concept and Application in a Global Context', *J Bus Ethics*, vol. 140, no. 3, pp. 369–380, Feb. 2017, doi: 10.1007/s10551-015-2693-2.
[295] J. Potting, M. Hekkert, E. Worrell, and A. Hanemaaijer, 'Circular economy measuring innovation in the product chain', *PBL Netherlands Environmental Assessment Agency*, no. 2544, p. 46, Jan. 2017.
[296] EN ISO 15686-5:2008 - Buildings and constructed assets – Service-life planning – Part 5 Life-cycle costing..
[297] R. A. Chadderton, *Purposeful Engineering Economics*. Cham: Springer International Publishing, 2015. doi: 10.1007/978-3-319-18848-5.
[298] B. S. Dhillon, *Life cycle costing for engineers*. Boca Raton, FL: Taylor & Francis, 2010.
[299] C. S. Park, *Contemporary engineering economics*, 4th ed. Upper Saddle River, N.J: Prentice Hall, 2007.
[300] C. S. Park, *Fundamentals of engineering economics*. Upper Saddle River, NJ: Pearson/Prentice Hall, 2004.
[301] M. Bayat Pour and A. Abdul Hamid, 'Towards a sustainable decision analysis approach for moisture-safe building envelope design', *Journal of Building Engineering*, vol. 97, p. 110955, Nov. 2024, doi: 10.1016/j.jobe.2024.110955.
[302] 'HORNBACH', HORNBACH. Accessed: May 07, 2024. [Online]. Available: https://www.hornbach.se/
[303] 'BAUHAUS'. Accessed: May 07, 2024. [Online]. Available: https://www.bauhaus.se/
[304] 'Byggmax', Byggmax. Accessed: May 07, 2024. [Online]. Available: https://www.byggmax.se
[305] 'Beijer Byggmaterial', Beijer Byggmaterial. Accessed: May 07, 2024. [Online]. Available: https://www.beijerbygg.se/privat
[306] 'Kalkylprogram för bygg, el och vvs – Wikells | Wikells'. Accessed: Jun. 19, 2024. [Online]. Available: https://wikells.se/
[307] 'Policy rate, deposit and lending rate'. Accessed: Mar. 07, 2024. [Online]. Available: https://www.riksbank.se/sv/statistik/rantor-och-valutakurser/styrranta-in--och-utlaningsranta/

[308] ‘What is the forecast for the policy rate?’ Accessed: Mar. 07, 2024. [Online]. Available: https://www.riksbank.se/sv/penningpolitik/vad-ar-penningpolitik/vad-ar-prognosen-for-styrrantan/
[309] ‘Underlying inflation according to CPIF, 12-month change, percent’, Statistikmyndigheten SCB. Accessed: Mar. 07, 2024. [Online]. Available: https://www.scb.se/hitta-statistik/statistik-efter-amne/priser-och-konsumtion/konsumentprisindex/konsumentprisindex-kpi/pong/tabell-och-diagram/konsumentprisindex-med-fast-ranta-kpif-och-kpif-xe/kpif-12-manadersforandring/
[310] EN ISO 14040:2006 - Environmental management – Life cycle assessment – Principles and framework.
[311] EN ISO 15978:2011 - Sustainability of construction works – Assessment of environmental performance of buildings – Calculation method.
[312] EN ISO 15804:2012+A1:2013 - Sustainability of construction works – Environmental product declarations – Core rules for the product category of construction products.
[313] E. P. D. Danmark, ‘epddanmark’, EPD Databasen. Accessed: May 08, 2024. [Online]. Available: https://www.epddanmark.dk/epd-databasen/
[314] ‘EPD International’. Accessed: May 08, 2024. [Online]. Available: https://www.environdec.com/library
[315] ‘EPD Norge’, EPD Norge. Accessed: May 08, 2024. [Online]. Available: https://www.epd-norge.no/epder/
[316] A. Kietzmann, ‘ibu-epd, Institut Bauen und Umwelt e.V.’, Institut Bauen und Umwelt e.V. Accessed: May 08, 2024. [Online]. Available: https://ibu-epd.com/en/published-epds/
[317] ‘openLCA Nexus: The source for LCA data sets’. Accessed: Jun. 23, 2024. [Online]. Available: https://nexus.openlca.org/
[318] A. P. Acero, C. Rodríguez, A. Ciroth; LCIA methods, Impact assessment methods in Life Cycle Assessment and their impact categories, GreenDelta, 3: 2015.
[319] A. Abbas *et al.*, ‘Assessment of long-term energy and environmental impacts of the cleaner technologies for brick production’, *Energy Reports*, vol. 7, pp. 7157–7169, Nov. 2021, doi: 10.1016/j.egyr.2021.10.072.
[320] N. Lushnikova and L. Dvorkin, ‘Sustainability of gypsum products as a construction material’, in *Sustainability of Construction Materials*, Elsevier, 2016, pp. 643–681. doi: 10.1016/B978-0-08-100370-1.00025-1.
[321] S. Shahbazi, N. Singer, M. Majeed, M. Kavgic, and R. Foruzanmehr, ‘Cementitious Insulated Drywall Panels Reinforced with Kraft-Paper Honeycomb Structures’, *Buildings*, vol. 12, no. 8, p. 1261, Aug. 2022, doi: 10.3390/buildings12081261.
[322] H. Abobakr, M. Raji, H. Essabir, M. O. Bensalah, R. Bouhfid, and A. E. K. Qaiss, ‘Enhancing oriented strand board performance using wheat straw for eco-friendly construction’, *Construction and Building Materials*, vol. 417, p. 135135, Feb. 2024, doi: 10.1016/j.conbuildmat.2024.135135.

[323] M. Bayat Pour, J. Niklewski, E. Frühwald Hansson, and S. Thöns, ‘Mould reliability analysis combined with mould health risks for decision support’, in *AIP Conference Proceedings*, Bratislava, Slovakia, Nov. 2023, p. 020006. doi: 10.1063/5.0172276.
[324] D. Mudarri and W. J. Fisk, ‘Public health and economic impact of dampness and mold’, *Indoor Air*, vol. 17, no. 3, pp. 226–235, Jun. 2007, doi: 10.1111/j.1600-0668.2007.00474.x.
[325] U. Haverinen-Shaughnessy, ‘Prevalence of dampness and mold in European housing stock’, *J Expo Sci Environ Epidemiol*, vol. 22, no. 5, pp. 461–467, Sep. 2012, doi: 10.1038/jes.2012.21.
[326] S. Accordini *et al.*, ‘The Cost of Persistent Asthma in Europe: An International Population-Based Study in Adults’, *Int Arch Allergy Immunol*, vol. 160, no. 1, pp. 93–101, 2013, doi: 10.1159/000338998.
[327] R. Ramirez, B. Ghiassi, P. Pineda, and P. B. Lourenço, ‘Hygro-Thermo-Mechanical Analysis of Brick Masonry Walls Subjected to Environmental Actions’, *Applied Sciences*, vol. 13, no. 7, p. 4514, Apr. 2023, doi: 10.3390/app13074514.
[328] A. Lal, B. N. Singh, and S. Anand, ‘Nonlinear bending response of laminated composite spherical shell panel with system randomness subjected to hygro-thermo-mechanical loading’, *International Journal of Mechanical Sciences*, vol. 53, no. 10, Art. no. 10, Oct. 2011, doi: 10.1016/j.ijmecsci.2011.07.008.
[329] S. Roy, W. Xu, S. Patel, and S. Case, ‘Modeling of moisture diffusion in the presence of bi-axial damage in polymer matrix composite laminates’, *International Journal of Solids and Structures*, 2001.
[330] Z. Sereir, E. A. Adda-Bedia, and A. Tounsi, ‘Effect of temperature on the hygrothermal behaviour of unidirectional laminated plates with asymmetrical environmental conditions’, *Composite Structures*, vol. 72, no. 3, pp. 383–392, Mar. 2006, doi: 10.1016/j.compstruct.2005.01.008.
[331] M. A. Khiat, Z. Sereir, and A. Chateauneuf, ‘Uncertainties of unidirectional composite strength under tensile loading and variation of environmental condition’, *Theoretical and Applied Fracture Mechanics*, vol. 56, no. 3, Art. no. 3, Dec. 2011, doi: 10.1016/j.tafmec.2011.11.005.
[332] S. Pallin, P. Boudreaux, S. J. Jo, M. Perez, and A. Albaugh, ‘Simulations of Indoor Moisture Generation in U.S. Homes’, in *Advances in Hygrothermal Performance of Building Envelopes: Materials, Systems and Simulations*, Pennsylvania, USA: ASTM International, Sep. 2017, pp. 261–290. doi: 10.1520/STP159920160111.
[333] E. Buechler, S. Pallin, P. Boudreaux, and M. Stockdale, ‘Probabilistic modeling of the indoor climates of residential buildings using EnergyPlus’, *Journal of Building Physics*, vol. 41, no. 3, pp. 225–246, Nov. 2017, doi: 10.1177/1744259117701893.

Paper I

Building and Environment 261 (2024) 111756



Contents lists available at ScienceDirect

Building and Environment

journal homepage: www.elsevier.com/locate/buildenv





A literature review of probabilistic hygrothermal assessment for building envelopes

Mohsen Bayat Pour [a,*], Jonas Niklewski [a], Amir Naghibi [b], Eva Frühwald Hansson [a]

[a] Division of Structural Engineering, Department of Building and Environmental Technology, Lund University, John Ericssons väg 1, SE-223 63, Lund, Sweden
[b] Department of Water Resources Engineering & Center for Advanced Middle Eastern Studies, Lund University, Lund, Sweden

ARTICLE INFO

Keywords:
Probabilistic hygrothermal assessment
Moisture damage
Building envelopes
Uncertainty analysis
Sensitivity analysis

ABSTRACT

This study presents a state-of-the-art review of the evolution of probabilistic hygrothermal assessments of building envelopes. First, relevant literature was identified by employing a systematic methodology, including scoping and systematic searches, quality assessment, and study analysis. The analysis, based on 143 selected publications, provides statistical insights into uncertainty propagation and sensitivity analysis methods, geographical distributions, climatic conditions, sustainability perspectives, uncertain parameter groups, employed metamodels, hygrothermal analysis tools, model dimensions, building usage, and moisture-related damage models. The results illustrate that the majority of probabilistic hygrothermal assessment studies, exceeding 95 %, are not explicitly incorporating sustainability perspectives, including environmental, economic, and societal. Also, to enhance the accuracy in this field, it is important to integrate hygrothermal functions as uncertain input variables, given their potential to significantly impact hygrothermal performance compared to single material properties. While 90 % of studies are confined to 1D modelling, extending research to 2D and 3D is advised to capture more complicated details. Moreover, case studies in tropical climates, where moisture-related issues can be prevalent, are noticeably lacking. Sensitivity analysis faces limitations due to its transient nature and variable interactions, necessitating identification of methods capable of non-linear and interactive analyses with low computational costs. Furthermore, several studies neglect ambient conditions and building usage considerations as stochastic variables, highlighting the need for comprehensive analyses. Lastly, understanding the merits and limitations of metamodeling methods is crucial for achieving reliable and robust hygrothermal analyses. The paper concludes by outlining the identified gaps and offering recommendations for future research in this field.

1. Introduction

1.1. Background

Among the several existing methods for improving the energy performance of buildings and reducing their operational energy demands, the addition of insulation to building envelopes is a commonly used and effective method [1]. However, while highly insulated walls effectively conserve energy, they pose an increased risk of condensation and other moisture-related issues such as microbial growth and rot decay [1–3]. Microbial growth could be detrimental to human health as it could cause respiratory diseases, skin disorders, and cancer [4,5]. In Sweden, almost 30 % of single-family houses are affected by mould or moisture-related problems [6]. In the Gothenburg region of Sweden, 60–80 % of single-family houses have been affected by microbial growth [7,8]. According to Swedish building regulations (BBR) [9], it is mandatory to design moisture-safe buildings to ensure that moisture does not cause damage or give rise to human health problems. To overcome moisture-related problems in buildings, it is crucial to predict these problems in advance and develop mitigation strategies.

Hygrothermal analysis is an effective tool for predicting moisture-related problems in buildings. It aims to model a combination of heat, air, and moisture for building assemblies to determine various parameters such as temperature, relative humidity, and moisture content under diverse boundary and climatic conditions. The origins of hygrothermal analysis can be traced back to the 1930s, when the use of

* Corresponding author. John Ericssons väg 1, SE-223 63, Lund, Sweden
E-mail addresses: mohsen.bayat_pour@kstr.lth.se (M. Bayat Pour), jonas.niklewski@kstr.lth.se (J. Niklewski), amir.naghibi@tvrl.lth.se (A. Naghibi), eva.fruhwald_hansson@kstr.lth.se (E. Frühwald Hansson).

https://doi.org/10.1016/j.buildenv.2024.111756
Received 24 March 2024; Received in revised form 7 June 2024; Accepted 15 June 2024
Available online 15 June 2024
0360-1323/© 2024 The Authors. Published by Elsevier Ltd. This is an open access article under the CC BY license (http://creativecommons.org/licenses/by/4.0/).

insulated timber-framed walls first emerged [10]. Over the last few decades, numerous researchers have attempted to advance hygrothermal analysis to enhance its robustness and reliability. According to Panico et al. [11], designing energy-efficient measures, evaluating living comfort, and preventing building damage depend on the reliability of hygrothermal simulations of building components. Duong Hung Anh and Pasztory [12] demonstrated that moisture content was one of the most critical parameters affecting the thermal conductivity of materials and that it could be identified through a reliable hygrothermal analysis. A powerful method for increasing the robustness and reliability of hygrothermal analysis is a probabilistic approach that addresses design uncertainties [13].

Probabilistic approaches treat inputs as stochastic variables that encompass associated uncertainties, thereby generating a distribution of potential outcomes and enabling a more comprehensive assessment of design performance. The probability of failure can be determined using probabilistic methods, revealing valuable insights into decision-making processes. In contrast, deterministic approaches treat inputs such as material properties, climatic conditions, and geometry as discrete variables. However, these approaches may fail to account for uncertainties. Over the past two decades, the probabilistic approach has advanced significantly in the field of hygrothermal analysis, owing to the contributions of numerous researchers.

Annex 55 [14], a report from the International Energy Agency (IEA), aims to establish a foundation for integrating probabilistic approaches into the design and analysis of hygrothermal performance of buildings. This foundation comprises four subtasks. Subtask 2 [14] assesses the advantages and disadvantages of probabilistic methods for both qualitative and quantitative assessments, considering their applicability in the context of building performance design and analysis. According to Annex 55: Subtask 2 [14], five sets of tools are essential for a probabilistic analysis. These tools include *qualitative exploration*, *uncertainty propagation*, *sensitivity analysis*, *metamodeling methods*, and *economic optimisation*. This literature review focuses on hygrothermal analysis research utilising a probabilistic analysis approach, and comprehensively covers these five sets of tools in distinct sections.

1.2. Objectives of the study

According to Ref. [15], the purpose of a "state-of-the-art review" is to update readers on the latest research on a specific technical subject such as engineering. Further, the term "conceptual review" aims to integrate areas of conceptual knowledge that can contribute to a better comprehension of those areas. Hence, this literature review had three main objectives.

1) Perform a state-of-the-art review of probabilistic hygrothermal assessment studies to map the latest progress.
2) Carry out a conceptual review of uncertainty propagation and sensitivity analysis methods used in the probabilistic hygrothermal assessment field and discuss their specifications.
3) Map out the statistics regarding hygrothermal uncertainty propagation (HUP), hygrothermal sensitivity analysis (HSA), and hygrothermal metamodeling studies and discuss gaps and future research opportunities.

2. Methodology

2.1. State-of-the-art review of the hygrothermal uncertainty propagation (HUP) and hygrothermal sensitivity analysis (HSA) studies

As outlined in Ref. [16], a successful literature review should use a systematic approach encompassing key steps, such as conducting a scoping search, executing a systematic search, undertaking quality assessment, and synthesising and analysing the studies explored. The scope of this literature review was identified based on the objectives explained in Section 1.2.

To conduct a systematic search for state-of-the-art reviews of HUP and HSA studies, three electronic databases were selected: Scopus [17], Web of Science [18], and ScienceDirect [19]. The search was limited to article titles, abstracts, and keywords. English articles including journal papers, conference papers, book chapters, and reports, were considered. Table 1 presents the keyword combination operators used during the initial phase of the search. To encompass a broader spectrum of references within the ScienceDirect database, certain words were written in truncated form—such as using "uncertaint*" to encompass "uncertainty" and "uncertainties", or "criteri*" to encompass "criterion" and "criteria". However, in the Scopus database, truncation was unnecessary as it automatically accounts for various wording styles (e.g., "uncertainty/uncertainties" or "mould/mold"). Conversely, when using the Web of Science, different wording styles required separate searches. Additionally, keywords were excluded to prevent the inclusion of irrelevant literature. The most recent search was conducted in October 2023.

For the quality assessment of studies explored, four exclusion criteria were used. Fig. 1 shows the exclusion steps and the corresponding number of hits following each exclusion. Most exclusions occurred during the initial step because of duplication. The second exclusion step involved assessing the abstracts to identify and remove irrelevant articles. The third exclusion step aimed to identify unavailable full texts, predominantly conference papers and non-open access articles. The fourth step involved the removal of irrelevant articles based on their main text. Cross-referencing and author searching were utilised during literature screening based on the full content to identify additional relevant literature. Finally, 143 articles were selected.

2.2. Conceptual review of the used hygrothermal uncertainty propagation and sensitivity analysis methods

Uncertainty analysis involves quantifying and examining the uncertainties associated with the input variables in a model. The analysis explores the range of potential outcomes by considering the variability of the input parameters. Further, various sources of uncertainty are also considered, including measurement errors, data variability, assumptions, and model uncertainty. In general, two main categories of uncertainties impact the analysis: "epistemic uncertainties", which can be minimised through improved user knowledge and realistic considerations, and "aleatoric uncertainties", which are inherent and irreducible variations in the variables [13].

Sensitivity analysis evaluates how changes in the input variables influence the outcomes of interest, aiding in understanding the relative importance of different inputs (with regard to variability in the outcome, considering a model with stochastic inputs). The analysis reveals the effect of input uncertainties on the output and addresses crucial questions such as:

1) *Sensitive Parameters:* Identifying the sensitive parameters enables designers to focus on those parameters, streamline the design efficiency, and reduce the computation time by excluding non-sensitive parameters.
2) *Model Reliability:* Assessing whether the performance of the numerical model is sufficiently reliable, as the model may exhibit sensitivity to a parameter that is not the case in reality, uncovering potential model uncertainties [20].

According to Ref. [20], terms like "sensitive", "important", "most influential", "major contributor", "effective", or "correlated" are often used interchangeably when describing the degree to which an input parameter affects the model output. However, there is a distinction between important and sensitive parameters. A sensitive parameter may lead to variability in model output, whereas an important parameter is a sensitive parameter with uncertainty. Therefore, studies can identify important parameters by performing a sensitivity analysis based on

Table 1
Potential keywords to search in the systematic review. AND, OR, NOT represent the Boolean operations. The asterisk (*) indicates the truncated form of the keywords.

What?		For/In?		Where?		How?		Exclude
Probabilistic	AND	Moisture	AND	Wall	AND	Simulation/s	NOT	Pipe
OR		OR		OR		OR		OR
Stochastic		Hygrothermal		Façade		Analysis		Reservoir
OR		OR		OR		OR		OR
Uncertainty		Hygro-thermal		Building		Assessment		Soil
OR		OR		OR		OR		OR
Metamodel		Mould/s		House		Investigat*		Food
OR		OR		OR		OR		OR
Meta-model		Mold/s		Cladding		Criteri*		pollution
OR		OR		OR		OR		OR
Sensitivity		Fung*		Envelop*		Predict*		casting
OR		OR				OR		OR
Parametric		Rot				Calculation		hydrology
		OR				OR		
		Algae				Model*		
		OR				OR		
		Freeze-thaw				Risk		
		OR				OR		
		Frost				Consequence/s		

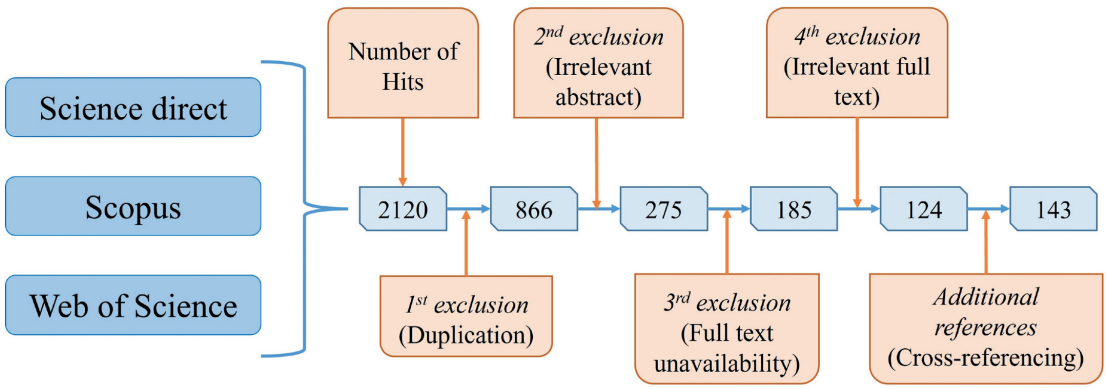


Fig. 1. Number of hits and exclusion criteria for the state-of-the-art review.

predetermined uncertain values of each input variable (e.g. probability distribution and/or range of values).

This study discusses the uncertainty propagation and sensitivity analysis methods employed in HUP and HSA in building envelopes. To provide a conceptual review, these methods were investigated by cross-referencing various types of literature, such as journal papers, conference papers, reports, books, and websites.

2.3. Statistical analysis, gaps and future research opportunities

Various statistical aspects of the probabilistic hygrothermal assessment studies were reported and discussed to synthesise and analyse the outcomes of state-of-the-art reviews. These aspects include the following:

1. Uncertainty propagation methods in HUP studies.
2. Sensitivity analysis methods in HSA studies.
3. *Yearly distributions of explored HUP and HSA studies:* Examine and report the temporal distribution of studies related to HUP and HSA.
4. *Geographical distribution:* Categorised references based on geographical aim(s) using macro geographical regions according to the United Nations Statistics Division definition [21].
5. *Climatic conditions:* Climatic conditions were defined based on the updated Köppen-Geiger climate classification method [22], considering tropical, dry, temperate, cold (continental), and polar climates.
6. *Sustainability:* Analysed sustainability from three perspectives: environment, economy, and society.
7. *Uncertain parameters groups:* Different parameter groups are classified as:
   - Material properties including density, specific heat capacity, water absorption coefficient, porosity, thermal conductivity, and water vapour diffusion resistance factor.
   - Outdoor climate including the temperature, relative humidity, wind speed, wind pressure, rain, diffuse short-wave radiation, direct short-wave radiation, long-wave counterradiation, air pressure, and orientation.
   - Indoor climate including the indoor temperature and relative humidity, ventilation rate, occupants' behaviour, indoor airflow, and indoor moisture production rate.
   - Surface/boundary conditions including the outdoor convection heat exchange coefficient, solar absorption coefficient, long-wave emissivity, reduction/splash coefficient of the WDR, indoor surface heat transfer coefficient, air infiltration, rain deposition factor, indoor surface vapour diffusion coefficient, and air change rate (ACR) in the air gap.

- Hygrothermal functions including thermal transport, thermal storage, vapour transport, liquid transport, and moisture storage.
- Modelling including mesh sizes, layers' thickness, users, and tools.

8. Utilised Metamodels.
9. *Hygrothermal simulation tools and model dimensions used:* Investigated the tools used and model dimensions (1D, 2D, and 3D) in both the HUP and HSA studies.
10. *Investigated building usages:* It includes residential, office, educational, etc.
11. *Investigated moisture-related damage models:* These include mould growth, algae growth, frost damage, and fungal decay.

These statistics provide a comprehensive understanding of the landscape in the probabilistic hygrothermal assessment studies of building envelopes. The identified gaps and research ideas are proposed as future perspectives.

3. Results and discussions

3.1. Hygrothermal uncertainty propagation (HUP)

A state-of-the-art review was conducted to map the various aspects of HUP studies. This section focuses on the applied uncertainty propagation methods and provides insights into the annual distributions of the explored HUP studies. The literature included in this section, having passed through all the exclusion steps, comprises references [1,8,11,23–110].

In the context of reliable energy-efficient building design, this analysis is called forward uncertainty propagation [14]. Although several probabilistic approaches are available for evaluating the uncertainty propagation, building physics predominantly relies on simulation-based methods (such as Monte Carlo simulations), scenario-based methods (such as future climate or occupant scenarios), and approximation methods (such as first- and second-order reliability methods).

3.1.1. Uncertainty propagation methods

Monte Carlo methods are a broad class of computational algorithms that rely on repeated random sampling to obtain numerical results. This technique propagates uncertainty by drawing multiple samples from the input distribution range and conducting simulations based on these samples. For instance, when analysing the hygrothermal performance of a building, random samples of thermal conductivity and moisture content of the used materials are generated to simulate their effects on overall performance. The Monte Carlo simulation involved four main steps. First, it requires defining the problem and identifying the relevant variables. In the second step, the inputs are sampled from the joint probability distributions or a range of values. The third step involves running simulations using selected random samples within the model. Finally, the system uncertainty is derived from the distribution of outputs. Regarding the sampling process in the second step, the most straightforward technique for Monte Carlo simulations is the basic random sampling (BRS) method [14]. In the BRS, samples were chosen without prefiltering, providing a random selection. However, BRS may pose challenges when the computational capacity is limited. Simply reducing the number of samples could result in full variability of variables not being adequately represented. Achieving more accurate results requires a larger number of samples, which leads to a time-consuming and computationally expensive simulation process [62,111]. HUP studies that employed the BRS method are [8,23,24,34,35,38,46,48–51,54,56,59,61,64,67–70,81,83–85,95,99,100,104,107,108].

In addition to sampling techniques, the range and distribution of input parameters are crucial in determining the uncertainty of outputs in Monte Carlo simulations. Properly defining these parameters is essential for ensuring the accuracy and reliability of probabilistic hygrothermal assessments. When selecting the range of input parameters, it is important to consider both experimental data and expert judgment [112]. The choice of statistical distribution for a given parameter depends on the nature of the data and underlying assumptions. Different distributions, such as normal, uniform, and lognormal, have distinct shapes and properties that influence the spread and central tendency of the modelled data [113].

Sampling techniques are employed to generate representative sets of input parameters, which are then used to evaluate variability and uncertainty in model outputs. The selection of an appropriate sampling technique is crucial in HUP studies because hygrothermal models are inherently computationally expensive, particularly due to their transient nature. This underscores the importance of the sampling technique, as it directly affects the accuracy and efficiency of simulation outcomes. An effective sampling method ensures that the entire variables' space is adequately explored, thereby providing reliable estimates of the system's performance under varying conditions. According to the statistics derived from the state-of-the-art review depicted in Fig. 2, various sampling techniques have been employed to enhance the efficiency of the HUP. It indicates that MC_LHS (Monte Carlo method coupled with Latin Hypercube Sampling technique) and MC_BRS (Monte Carlo method coupled with basic random sampling) emerged as the most widely applied techniques in this field, constituting 37.4 % and 34 % of the statistical distribution, respectively.

Latin Hypercube Sampling (LHS), developed by McKay et al., in 1979, offers a strategic approach to sampling in probabilistic analyses [114]. LHS involves dividing the input space into n non-overlapping intervals with equal probabilities, where the number of samples equals the number of intervals [115,116]. All input variables were sampled, and scenarios were created based on the permutation of the samples from each interval. Compared with BRS, LHS requires fewer samples to achieve equivalent accuracy [117,118]. Macdonald [114] emphasised that LHS provides a more robust output than BRS under similar conditions. Multiple studies [32,119,120] have highlighted LHS as a reliable and efficient sampling technique capable of delivering robust results even with a limited number of samples. This has contributed to the widespread adoption of LHS, particularly for complex models, because it significantly reduces computational expenses [118,121]. LHS is the preferred sampling technique among researchers because it tends to yield more unbiased, uniform, and robust samples [29,32,77,114,115,117–121]. The HUP studies that used LHS method are [1,11,26–33,36,37,40,41,43,52,57,58,62,63,65,77–79,82,86,87,90,96–98,101,102,106].

Some studies have investigated the sampling efficiency and convergence of Monte Carlo simulations to minimise computational expenses. For instance, in the case of LHS, further optimisations were presented in Refs. [122–125], primarily focusing on achieving a better space-filling character. Previous research on sampling efficiency [62] suggested that space-filling sampling is preferred because of its faster convergence compared with random sampling or standard LHS. An advanced technique introduced to enhance the efficiency of LHS is the multilayered sampling scheme [126], employing a maximin sampling scheme. This distance-based space-filling method maximises the minimal distance between the LHS points. A multilayered sampling scheme allows the sorting of parameters based on their conceptual meaning and assigning these parameter categories to different layers. Consequently, all design options are subject to the same uncertainties, enabling a direct comparison of multiple future scenarios [126]. A multilayered sampling scheme was utilised in two HUP studies [42,92], resulting in approximately 2.2 % of the utilised uncertainty propagation methods in the HUP field.

The Monte Carlo method with BRS is a widely used because of its ease of application. However, Quasi-Monte Carlo (QMC) sampling has emerged as a promising alternative to address the time-consuming drawbacks associated with BRS [127,128]. As shown in Fig. 2,

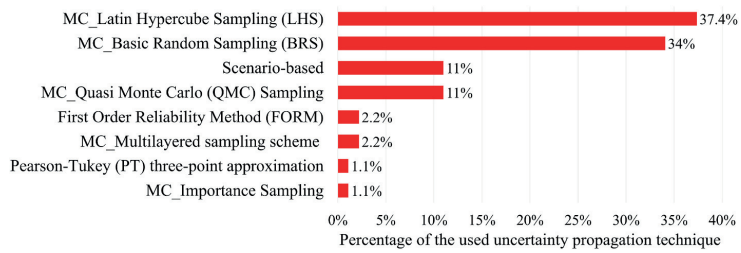


Fig. 2. Statistics of utilised uncertainty propagation methods in hygrothermal uncertainty propagation research publications (total of 91 publications [1,8,11, 23–110] as the basis for the statistics). MC: Monte Carlo method.

approximately 11 % of HUP studies utilised QMC as the sampling technique in the Monte Carlo simulation process. This approach involves dividing the range of values based on equally distributed sequences to ensure a more uniform integration of samples. The fundamental concept of QMC is the use of low-discrepancy sequences, also known as quasi-random sequences, rather than random sequences [111]. HUP studies that used the QMS method are [44,45,47,60,72–76,91].

Importance sampling was only used in Ref. [53] and constituted approximately 1.1 % of the uncertainty propagation methods used in the HUP field. This sampling technique involves dividing the input space into non-overlapping subregions (strata) based on the importance of each parameter region. A single value is then randomly drawn from each stratum [120]. The term "importance sampling" originates from the fact that strata are partly defined based on the significance of the data contained in each dataset for the outcome of the analysis. Importance sampling is frequently employed to ensure the inclusion of datasets with high consequences but low probabilities in an analysis [120]. Importance sampling method require a certain level of detailed knowledge regarding optimal efficiency. This knowledge is often primarily based on the most probable failure or design point [129].

Some studies of state-of-the-art review did not employ specific sampling techniques; rather, they defined a predetermined number of scenarios to propagate uncertainties. Consequently, these studies have been categorised separately as "scenario-based" within the scope of this literature review. Possible scenarios can be defined either subjectively or randomly. For example, scenarios may include variations in outdoor climate data to study their impact on a moisture-related damage. Nik et al. [110] examined the probability of mould growth using hygrothermal analysis across four different future climate scenarios. They employed regional climate model (RCM) simulations downscaled from four different global climate models (GCMs), to calculate daily mould doses. Further studies by Nik et al. delved into fundamental uncertainty factors related to scenarios involving future climatic conditions, including GCMs, RCMs, and emission scenarios, which can be found in Refs. [25,109]. Labata and Woloszyn [94] explored occupancy scenarios by investigating the moisture interactions between the indoor air and materials, ventilation systems, and indoor moisture sources. Lee et al. [103] analysed various retrofit scenarios using different insulation and brick samples to assess the risk of freeze-thaw damage. Other studies using scenario-based uncertainty propagation include [71,80,88,89, 105].

Three studies used approximation methods (also called point-based methods) to conduct HUP. Among them, two studies [39,55] employed the First-Order Reliability Method (FORM). FORM was previously found to have an application in reliability analysis within ventilation design by Pietrzyk and Hagentoft [130]. A third study [93] employed the Pearson-Tukey (PT) three-point approximation technique to propagate simulated outcomes. Pearson and Tukey (PT) [131] developed discrete approximation techniques that calculate the mean value of distributions based on three key percentile points. Approximation techniques such as FORM offer the advantage of reduced calculation time compared to other simulation methods. For example, FORM can be used to estimate the probability of mould growth in a building envelope by approximating the effect of uncertainties in temperature and relative humidity. However, it is essential to note that the accuracy of the approximations may not always be guaranteed, particularly for complex numerical models [111]. This limitation is applicable to other approximation techniques such as PT, which may oversimplify complex distributions and assumptions, potentially affecting the accuracy of the results.

Fig. 2 shows that the majority of HUP studies (85.7 %) employed the MC method in probabilistic hygrothermal analysis. Using the MC method has several advantages. For example, MC methods are straightforward to implement and can handle complex and non-linear models with ease [132]. They also provide a detailed understanding of output variability by exploring the entire input parameter space and can accommodate a wide range of input distributions [133]. However, as previously mentioned, the MC method often requires a large number of runs to achieve accurate results, making it time-consuming, especially for models with high-dimensional input spaces. This necessitates extensive computational resources, which can limit the practical application of MC methods for large-scale problems. To address this shortcoming, metamodels, also known as surrogate models, are used to simplify the representation of complex numerical models. Metamodels are constructed using a limited set of simulations and are designed to predict the behaviour of the detailed model with significantly reduced computational cost [134]. They can be updated and refined as more data become available, improving their accuracy over time [135]. However, metamodels have some shortcomings. For instance, constructing an accurate metamodel can be time-consuming [134]. The prediction quality depends on the chosen metamodel type and the amount of training data; poorly constructed metamodels can lead to inaccurate predictions [135]. Detailed statistics and explanations about the probabilistic hygrothermal studies that used metamodels are provided in section 3.3.5.

In general, a convergence study is crucial for determining the number of simulations (scenarios) required for probabilistic analysis, independent of the type of sampling technique used. Bayat Pour et al. [90] adapted an equation from Ref. [136] to facilitate convergence analysis in the HUP. This entails tracking the target variable (e.g. the maximum mould index) while methodically increasing the number of runs. Monitoring the change in the target variable over the ten previous rounds was part of the convergence criterion. Every iteration has unique scenarios and new iterations are created by gradually adding new scenarios to earlier iterations. According to Ref. [90], the simulation process was continued until the convergence value was lower than the predefined threshold of 0.001. Eq. (1) is used to calculate the convergence value.

$$\varepsilon_i = \frac{\left|\sum_{i-9}^{i-5} OF_i - \sum_{i-4}^{i} OF_i\right|}{\sum_{i-4}^{i} OF_i} \quad (1)$$

where i is the current iteration number (>10), OF_i is the ith iteration of the objective function, and ε_i is the convergence value of the OF_i.

Among the identified studies, Pietrzyk [39], Kurkinen et al. [55], Gradeci et al. [26,27], and Bayat Pour et al. [90,137] expanded the HUP to hygrothermal reliability analysis using the demand–capacity model, which is well-known as a load–resistance model [138] in the field of structural design.

3.1.2. Yearly distribution of hygrothermal uncertainty propagation studies

Fig. 3 illustrates the annual number of articles published in HUP. The beginning of HUP research was marked by the first publication in 1997 by Geving [23], who introduced a systematic method for hygrothermal analysis based on a Monte Carlo simulation. Notably, a substantial increase in the number of references is observed from 2013 to 2023. Only 13 references published prior to 2013 were considered relevant to this study, whereas between 2013 and 2023, there were 68 publications, indicating that research interest has remained high in recent years. Publications during the latter period primarily focused on advancing HUP by incorporating the various sampling techniques mentioned earlier, with the aim of enhancing sample efficiency and reducing computational time. The number of studies in this field peaked in the year 2015, contributing to 11 % of all studies.

3.2. Hygrothermal sensitivity analysis (HSA)

Another objective of this state-of-the-art review was to explore various aspects of HSA studies. This section is dedicated to the investigation into the sensitivity analysis methods applied in the HSA along with their corresponding yearly distributions. The literature included in this section, having passed through all the exclusion steps, encompasses 96 references [1,11,23–36,40,43,45,53,54,57,59–61,64,65,67,68,76–78,82,83,86,87,90,91,95,99,103,107–110,139–189].

The literature review identified several methods (or *techniques* in some studies [20]) for performing a sensitivity analysis. These methods can be categorised into three main types: local, global, and screening [190]. Local and global sensitivity analyses yield quantitative results that provide the weight of each input variable to the outputs. In contrast, screening methods offer qualitative results by highlighting parameters with significant or negligible effects relative to each other [111]. Furthermore, these methods employ various approaches, including One-At-A-Time (OAT), correlation-, regression-, variance-, density-, and segmentation-based approaches. The diversity of these approaches allows researchers to fit the sensitivity analyses to the specific requirements of hygrothermal analysis.

Local sensitivity analysis (LSA) focuses on the sensitivity relative to the point estimates of parameters, typically around a specific point or within a particular range of values. In the context of hygrothermal analysis, the mean value is used as a specific point. Global sensitivity analysis (GSA) explores sensitivity concerning the entire parameter distribution [191]. For example, in the context of evaluating the hygrothermal performance of a building, LSA can determine the effect of a slight change in thermal conductivity of insulation material on the overall moisture transportation rate. However, GSA investigates the influence of the change in the entire range of thermal conductivity of insulation material. Screening methods cover the entire input space to qualitatively identify the most influential inputs, typically using a limited number of simulations [111]. In situations where a complex model involves many input parameters, screening methods are designed to quickly analyse the model, thereby eliminating non-influential inputs. An example of a screening technique in a building hygrothermal performance model is to rank the importance of various input parameters, such as specific heat capacity, porosity, and the water absorption coefficient of each material, on the temperature and relative humidity of a target point within a wall assembly. Screening methods do not require the use of inputs as distributions; rather, they operate at discrete levels [111].

The most straightforward sensitivity analysis approach is One-At-Time (OAT) [20,192]. This approach involves measuring sensitivity by altering one variable at a time and observing its effects on the output while keeping the other variables constant. The correlation-based approach investigates the association between independent (input) and dependent (output) variables, whereas the regression-based approach illustrates their numerical relationships [20]. The variance-based approach assesses the impact of input variables on the variance of the output variable [14]. The density-based approach considers the entire probability density function (PDF) of the model output instead of considering only its variance. This approach is particularly useful when variance alone is not a sufficient proxy for uncertainty, such as in cases where the output distribution is highly skewed or multi-modal [193]. Segmentation-based sensitivity analysis techniques [14] involve dividing a set of inputs or outputs into different segments and then evaluating whether the corresponding output or input segments originate from the same population.

Statistics obtained from a state-of-the-art review revealed 21 sensitivity analysis methods used in HSA studies. Fig. 4 illustrates that differential sensitivity analysis (DSA), scenario-based analysis, and the

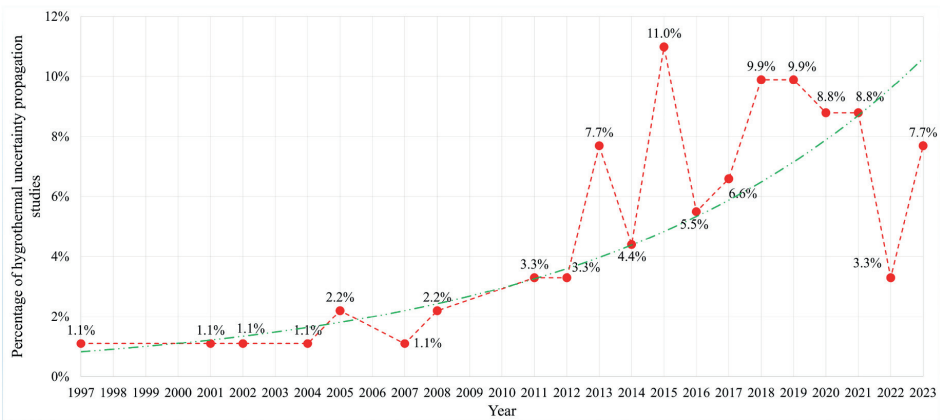


Fig. 3. Yearly distribution of hygrothermal uncertainty propagation studies. Literature until the October 1, 2023 was considered (a total of 91 publications [1,8,11,23–110] as the basis for the statistics).

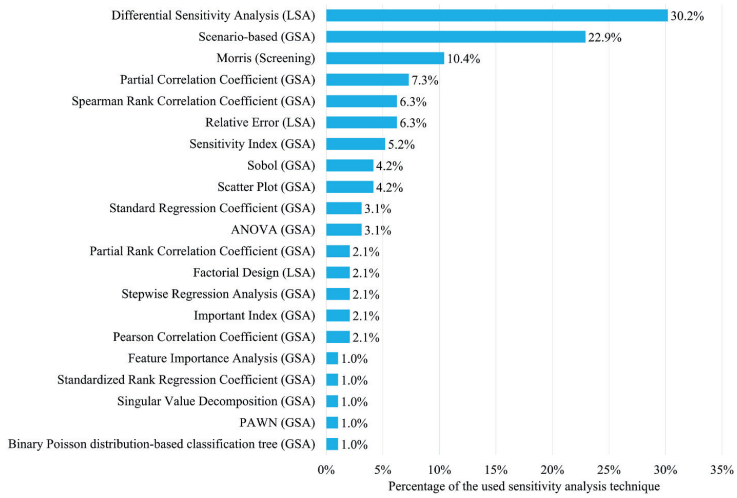


Fig. 4. Statistics of different sensitivity analysis methods used in hygrothermal sensitivity analysis research publications (a total of 96 publications [1,11, 23–36, 40, 43, 45, 53, 54, 57, 59–61, 64, 65, 67, 68, 76–78, 82, 83, 86, 87, 90, 91, 95, 99, 103, 107–110, 139–189] as the basis for the statistics). LSA: local sensitivity analysis, GSA: global sensitivity analysis.

Morris method are the most frequently applied methods, comprising 30.2, 22.9, and 10.4 % of the statistics, respectively. The summation of the percentages in Fig. 4 is higher than 100 % because some studies used more than one sensitivity analysis method. The following sub-sections provide detailed discussions of the methods employed, shedding light on their contributions and applications in HSA studies.

3.2.1. Local sensitivity analysis (LSA) methods

Local Sensitivity Analysis (LSA) involves investigating a specific part of the input space for each variable. Three of the 21 sensitivity analysis methods identified were dedicated to LSA.

Approximately one-third of HSA studies [27,34,35,54,59,67,95,103, 108,139,143–145,147,148,151–153,161,163,165,166,170,172,179, 181,182,184,186] employed DSA as the LSA method. DSA is often considered the backbone of various other sensitivity analysis approaches [20], and in some literature, it is referred to as the "direct method" [20]. The fundamental concept of DSA involves designating one primary value (M) as the best estimate of the variable and then determining the various values altered within the range of ($M \pm \Delta M$). This process is applied to all variables to identify the dominant parameters, following the OAT approach. The popularity of the DSA may be attributed to its simplicity; however, it should be noted that it does not consider interactions between variables.

Relative error is a metric used to calculate the magnitude of the error between an actual value and an approximation/measurement relative to the size of the actual value. This provides a quantitative measure of the accuracy of an approximation/measurement. A smaller relative error indicates a closer approximation or a measurement that is closer to the actual value, whereas a larger relative error indicates a greater deviation. In HSA studies, relative error is employed to compare the outputs of simulations carried out with varying input parameters ($\Delta = \pm 5$ % or ± 10 %) with a reference simulation [180]. The relative error is typically presented as a value between 0 and 1, or it can also be expressed as a percentage. Approximately 6.3 % of HSA studies [91,142,146,169,177, 180] used this sensitivity analysis method.

Two HSA studies [65,174] employed factorial design by selecting a specified number of samples for each parameter and running the model for all combinations of these samples. The results obtained through this process were then used to estimate parameter sensitivity. Notably, when dealing with a large number of parameters, an extensive number of simulations are required owing to the large number of combinations. To address this computational challenge, some studies have opted for a fractional factorial design that allows the same information to be obtained using fewer trials [20].

3.2.2. Global sensitivity analysis (GSA) methods

Approximately 70 % of the HSA studies (67 out of 96) employed GSA methods to determine the impact of input uncertainties on the output. Of the 21 sensitivity analysis methods identified, 17 were dedicated to GSA (Fig. 4).

Scenario-based methods assess the response of a model to various hypothetical scenarios or sets of input parameters. They can be used as GSA because the scenarios are crafted to encompass a representative sampling of the input parameter space. In this study, approximately one-fifth of all HSA studies explored [25,61,87,109,110,149,150,154,159, 160,162,164,167,168,171,176,178,183,185,187–189] employed the scenario-based method. A potential drawback of this method is its reliance on a limited number of scenarios, which may result in the oversight of certain potential conditions/events.

The Pearson correlation coefficient, also known as the correlation coefficient or Pearson's *r*, is a measure used to represent linear correlation by calculating the correlation coefficient of the input and output variables [194]. Typically, the correlation coefficient is computed by dividing the covariance of the two parameters by the product of their standard deviations, as applied in two HSA studies [57,64]. Pearson's *r* determines the strength and direction of the linear correlation of variables using the correlation coefficient [32]. The magnitude of Pearson's *r* ranges from -1 to $+1$, where zero signifies no linear correlation between the intended variables. Values closer to ± 1 indicate a stronger linear correlation between the variables, with positive and negative values signifying direct and inverse linear correlation, respectively [20]. A significant drawback of using the correlation coefficient is its reliance on the assumption of a linear input/output relationship, making it less suitable for hygrothermal analysis where non-linear relationships are common.

To mitigate the impact of non-linear data in the sensitivity analysis, rank transformation was introduced by Iman and Canover in 1979 [195]. This technique applies ranks instead of the actual values of the

variables to linearise non-linear correlations; however, it requires monotonic data [20]. The degree of monotonicity in the variables is measured using Spearman's ρ rank correlation coefficient (RCC), resulting in a value between +1 and −1 [32]. Six studies [23,24,32,57,76,90] incorporated RCC into HSA.

The partial correlation coefficient (PCC) technique is a correlation-based approach that was used in seven HSA studies [1,32,33,57,68,86,99]. In this approach, the influences of other variables are excluded, and the data must be linear and monotonic. In cases where the model is non-linear but monotonic, calculating the corresponding ranks can be beneficial for the purpose of linearising the model [120]. The aforesaid correlation coefficient, referred to as "partial rank correlation coefficient (PRCC)", was applied in two HSA studies, including [57,65].

The calculation of the standardized regression coefficient (SRC) is another sensitivity analysis technique that follows regression-based and OAT approaches [32]. To eliminate the influence of the units, standardisation is applied to the variable values to create more comparable conditions [32]. The higher the SRC value, the higher the importance of the variable. Similar to Pearson's *r*, the sign of the SRC indicates whether outputs tend to vary directly or inversely with the inputs [196]. The reliability of the SRC relies on the linearity of the model. This method was adopted in three HSA studies [32,33,57]. If the ranking technique is applied to the SRC method, the regression coefficient is referred to as the "standardized rank regression coefficient (SRRC)" [32], which was used in one HSA study [57]. The values of both SRRC and PRCC range between ±1, illustrating the degree of monotonicity and the influence of the input variables on the output variables.

Stepwise regression analysis (SRA) is an improved version of the SRC; it operates based on a step-by-step sequence of variables. The sequence is constructed according to the importance of the variables, such that the most important parameter is included in the first model. Subsequently, the next model incorporates the next most important variable, continuing until the last predefined important variable is included [32]. This method was utilised in two HSA studies, including [32,77].

A scatter plot is a graphical sensitivity analysis method and has been utilised in four HSA studies [32,76,82,173]. Using a scatter plot, the input values can be represented visually against the output values [197].

The sensitivity index (SI) is calculated by dividing the output range of the value by the maximum value of the output results. The output range of the values is obtained by running the model based on the minimum and maximum values of the input variables [20]. This method was employed in five HSA studies [24,83,107,141,157]. The importance index (II) [191], which is the variance ratio of the input and output values, was used in two HSA studies, including [53,83]. However, neither the SI nor II methods identify parameter interactions and may be considered inefficient for complex numerical models [20,191].

ANOVA (ANalysis Of VAriance) is a variance-based approach that was employed in three HSA studies, including [32,36,78]. ANOVA quantifies the proportion of the total variance attributable to each factor, aiding in identifying the most influential parameters and understanding their impact on the model's behaviour [198]. It is essential to assume that the model is independent and that the variances of all the variables are equal for ANOVA to be effectively carried out [199].

Global sensitivity indices, introduced by Sobol [200,201] were utilised to identify the dominant variables. However, a notable disadvantage is its high computational cost, particularly for complex models [202]. This method quantifies the contributions of individual and joint variations in the input variables to the total variance in the model output, explaining their relative importance. HSA studies that have employed this method include [43,45,60,76].

Feature importance analysis is based on a trained random forests (RF) algorithm [203] and was used in one HSA study [90]. This method considers both linear and non-linear connections between the inputs and outputs. RF, an ensemble machine learning method consisting of multiple decision trees, employs specific features at the internal nodes to split the data into distinct sets with related responses. The criteria for feature selection involve Gini impurities and variance reduction in the classification and regression tasks, respectively. Quantification of the impact of each feature on impurity reduction enables the identification of the most influential features. The feature importance is determined by computing the average impurity reduction across all trees. A higher feature importance value signifies increased feature relevance in the machine learning model. This method demonstrates a remarkable speed depending on the amount of data [90].

Pianosi and Wagener [193] presented an innovative sensitivity analysis method named PAWN. The fundamental concept involves characterising the output distributions through cumulative distribution functions (CDFs) rather than probability density functions (PDFs), following the density-based approach. The authors asserted that this method was computationally efficient and did not require tuning of the parameters. The sensitivity indices can be computed across the entire output variation range or within specific sub-ranges. This flexibility is particularly advantageous in applications that primarily focus on a specific region of the output distribution, such as the tail. One HSA study used this method [175].

Singular value decomposition (SVD) [204] is a linear algebraic technique primarily applied to analyse linear relationships. Additionally, it is not inherently designed to identify the interactions between inputs or variables in a non-linear context. In an HSA study [140], this method was employed to identify the most influential input variables in a hygrothermal dynamic model.

The binary Poisson distribution-based classification tree, utilised in the study referenced as [76], is a segmentation-based technique. It operates as a top-down method and relies on the variance within the generated binary subsets. This method is advantageous because it avoids the assumptions of linearity or monotony during the sensitivity analysis.

3.2.3. Screening methods

Screening methods can be valuable when applied before uncertainty propagation and quantitative sensitivity analysis, aiding in excluding non-dominant parameters through initial filtering [111]. Moreover, these methods can function independently as sensitivity analysis techniques. The Morris method is the only screening method identified in this study and featured in 10 HSA publications [11,26,28–31,40,155,156,158].

The Morris method, also known as the factorial sampling method or elementary effect (EE) method, is a well-known screening method involving *r* simulations based on the OAT approach. Its most important characteristic is cost-effectiveness, which is particularly suitable for large and complex models with multiple variables. The Morris method can be applied, irrespective of the linearity and monotonicity status of the model [205]. Morris introduced two key indicators, namely mean (μ) and standard deviation (σ), to assess the sensitivity of each variable. Elevated mean and standard deviation values signify greater importance of the variables. Furthermore, a higher standard deviation indicates a greater dependence of the target variables on other variables [29].

The risk of Type II errors endangers the accuracy of the Morris method of sensitivity analysis when both positive and negative values exist in the sets of EE samples. This risk is particularly pronounced when calculating the mean value because positive values may nullify the effects of negative values, especially in models with non-monotonic values or variable interactions. Morris suggested considering both the mean and standard deviation of sets of EE samples to overcome Type II errors. This dual consideration is crucial because removing positive and negative values affects the mean value, whereas the standard deviation reflects a large value even when such removals occur [206]. To address this challenge, Campolongo et al. [207] introduced a new indicator, μ*, which calculates the mean by considering the absolute values of sets of EE samples. Using the absolute mean value, μ*, effectively resolved the Type II errors associated with the Morris method. Furthermore, Saltelli et al. [206] recommend calculating all three indicators—σ, μ, and μ*—,

to extract the maximum sensitivity of the variables and choose the worst case.

3.2.4. Yearly distribution of hygrothermal sensitivity analysis studies

Fig. 5 illustrates the annual number of published articles in the HSA over time. The inception of HSA research dates back to 1993, when Hokoi and Kumaran [172] conducted a sensitivity analysis of the drying process of wet glass fibre insulation. Similar to the HUP studies, a notable increase in the number of references was evident between 2013 and 2023. Before 2013, only 22 studies were deemed relevant. However, from 2013 to 2023, there is a noticeable increase, with 74 publications underscoring heightened research interest in recent years. Publications from 2013 to 2023 predominantly aimed to improve the HSA by employing methods capable of non-linear analysis and accounting for interactions among input variables.

To conclude Section 3.2, it is important to recognise the limitations of sensitivity analysis methods in HSA studies. The inherently transient nature of hygrothermal analysis introduces non-linearity, and potential interactions between the input variables can influence the results. Given these challenges, selecting a method that can accommodate both non-linear and interactive analyses is essential. However, as discussed above, each method has its own set of limitations. To address this complexity, a conservative solution involves employing multiple sensitivity analysis methods in an HSA study to ensure the proper consideration of transient conditions. In addition, because computational costs are a significant factor in real projects, prioritising methods with low time requirements is crucial. For instance, the ultimate recommendation in Annex 55: Subtask 2 [14] for building performance assessment involves the combined use of Spearman's coefficients and scatterplots. This approach yielded reliable results with considerably fewer runs than the other methods. Several HSA studies have applied multiple sensitivity analysis methods [24,32,33,57,65,76,83,90].

3.3. Statistics related to the state-of-the-art review of the hygrothermal uncertainty propagation (HUP) and hygrothermal sensitivity analysis (HSA) studies

This section explores other aspects of HUP and HSA studies, including geographical distribution, climatic conditions, sustainability considerations, uncertain parameter groups, metamodels, hygrothermal simulation tools, hygrothermal model dimensions, building usage, and moisture-related damage models. A total of 143 studies were included in this statistical analysis, with 91 studies utilised for the HUP and 96 for the HSA statistics. Notably, 44 studies were incorporated in both the HUP and HSA statistical analyses, as they employed both uncertainty propagation and sensitivity analyses simultaneously. The statistics presented in these sections are derived from the following literature sources: [1,8,11,23–110,139–189,208].

3.3.1. Geographical distributions and climatic conditions

Geographical distributions of the HUP and HSA studies, that is the locations of the case studies, are shown in Fig. 6 (left). Northern Europe contributed the most to HUP studies (35.2 %). For HSA studies, Western Europe emerged as the leading contributor (25 %). Generally, three key regions, Northern Europe, Northern America, and Western Europe, dominated research efforts in both the HUP and HSA. By contrast, Asian countries and Oceania have comparatively lower research outputs. Additionally, there is a lack of relevant research related to Africa. One plausible explanation for the limited development of probabilistic approaches in these regions could be their predominantly dry climate, where outdoor relative humidity may not be a significant concern. However, some regions in Asia, Oceania, and Africa have climatic conditions similar to those in northern and western Europe, suggesting the potential need for increased research on HUP and HSA in these areas.

As shown in Fig. 6 (right), most of the research in both the HUP and HSA fields was conducted under continental (D category) and temperate (C category) climatic conditions. This emphasis can be attributed to the concentration of Northern European countries and certain parts of North America, particularly Canada, which fall within continental climatic conditions. Similarly, Western European countries, notably Belgium, which is situated in temperate climatic conditions, also contributed significantly to research under these conditions. The limited contribution of tropical (category A) climatic conditions to the HUP and HSA studies highlights the need for increased attention in this area. A tropical climate has a unique set of challenges characterised by consistently favourable temperature and relative humidity, which increases the risk of microbial growth. Conversely, dry (category B) climatic conditions, commonly experienced in regions such as some parts of Oceania and Africa, are characterised by lower relative humidity and higher temperature. These climatic conditions have attracted less attention in probabilistic hygrothermal assessment research, possibly because of the perceived lower risk of moisture-related problems, including microbial growth.

In Fig. 6, it is observed that the total percentage exceeds 100 % for HUP studies, owing to certain studies utilising multiple geographical locations and climatic conditions. Conversely, in the case of HSA studies, the total percentage was less than 100 % because certain studies did not specify any geographical location or climatic conditions, conducting their analyses based solely on hypothetical values for climatic input variables without geographical specifications.



Fig. 5. Yearly distribution of hygrothermal sensitivity analysis studies. Literature until the October 1, 2023 was considered (a total of 96 publications [1,11, 23–36, 40, 43, 45, 53, 54, 57, 59–61, 64, 65, 67, 68, 76–78, 82, 83, 86, 87, 90, 91, 95, 99, 103, 107–110, 139–189] as the basis for the statistics).

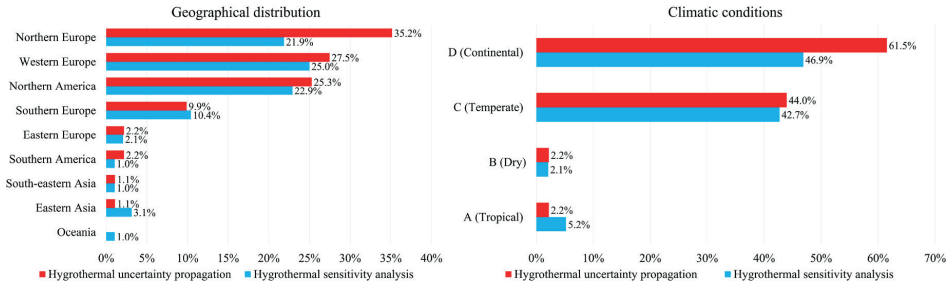


Fig. 6. Geographical distribution (left) and climatic conditions (right) for case studies in hygrothermal uncertainty propagation (HUP) research publications (total of 91 publications) and hygrothermal sensitivity analysis (HSA) research publications (total of 96 publications).

3.3.2. Investigated building usages

Building usage is a critical factor in hygrothermal analysis because of variations in occupant behaviours and schedules. According to Ref. [209], field measurements indicate that occupants' activities can increase the likelihood of condensation. The statistical data presented in Fig. 7 reveal that more than half of HUP (50.5 %) and HSA studies (56.3 %) did not account for specific building usage in their analysis. Residential buildings were considered more frequently in probabilistic hygrothermal assessments than other building usages, such as historical/cultural, office, educational, and worship buildings. Occupant behaviour and intensity play significant roles in manipulating heating/cooling systems and influencing moisture production rates [64]. These details can potentially impact indoor boundary conditions, thereby affecting the hygrothermal performance and the risk of moisture-related issues, such as mould growth. Bui et al. [69] introduced a methodology for estimating the influence of occupancy scenarios on the hygrothermal performance of a room. They discovered that different occupancy scenarios significantly affected the indoor heat and moisture balance, primarily due to seasonal effects.

The Generation of Indoor Heat and Moisture (GIHM) tool [210], developed by Oak Ridge National Laboratory, captures the probabilistic nature of hourly indoor moisture and heat generation in residential buildings. This tool considers factors such as the building usage, occupant behaviour, climate zone, and appliance usage. The output of the GIHM tool can be valuable input for probabilistic hygrothermal assessment processes [210]. In a study by Buechler et al. [211], indoor climate data were calculated probabilistically, and the effects of location and building usage on indoor climate were analysed across the United States. The results of this study can be utilised as input for a probabilistic hygrothermal assessment to enhance the robustness of such analyses. As highlighted in Ref. [211], indoor climate data are generally essential for analysing building performance, including evaluating indoor health and comfort, environmental air quality, HVAC system performance, moisture durability, and mould growth.

3.3.3. Sustainability perspectives

Sustainability has three main perspectives: environmental, economic, and social. As shown in Fig. 8, a notable portion of the probabilistic hygrothermal analysis research publications (95.1 %) did not explicitly address any sustainability perspectives. Among those that did, the environmental perspective was covered in 2.1 % of the studies [45,48,97], whereas the economic perspective was considered in 4.2 % [8,28,29,41,45,48]. Incorporating social perspective of sustainability into hygrothermal calculations is inherently complex and potentially explains the absence of studies in this category. A comprehensive approach should involve integrating environmental impact calculations, such as life cycle assessment (LCA), and economic analyses, including life cycle costing (LCC), with a probabilistic hygrothermal assessment. This integration allows for a more holistic methodology, as demonstrated in Refs. [45,48].

An exemplary project that exemplifies the integration of probabilistic hygrothermal assessment with LCA and LCC was RIBuild (Robust Internal Thermal Insulation of Historic Buildings) [212]. RIBuild comprises eight work packages (WP), with five WPs contributing inputs to WP6, where the website, guidelines, and web tool were developed. The input encompassed data on the historic building stock, historic building materials, internal insulation systems, and experiences from the case studies (WP1-WP3). An efficient strategy for probabilistic hygrothermal assessment (WP4) was introduced, and a probabilistic methodology for assessing the environmental impacts and global costs of internal insulation solutions for historical buildings (WP5) was developed [45].

Another example for integrating LCA and LCC with probabilistic hygrothermal assessment is the TallFacade project [213]. The primary aim of this project was to streamline the development of robust and

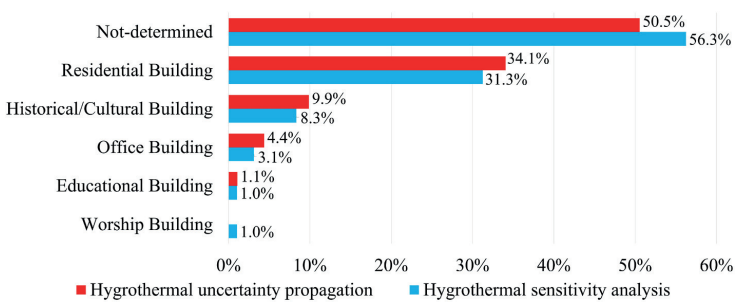


Fig. 7. Building usages for the case studies in hygrothermal uncertainty propagation (HUP) research publications (total of 91 publications) and hygrothermal sensitivity analysis (HSA) research publications (total of 96 publications).

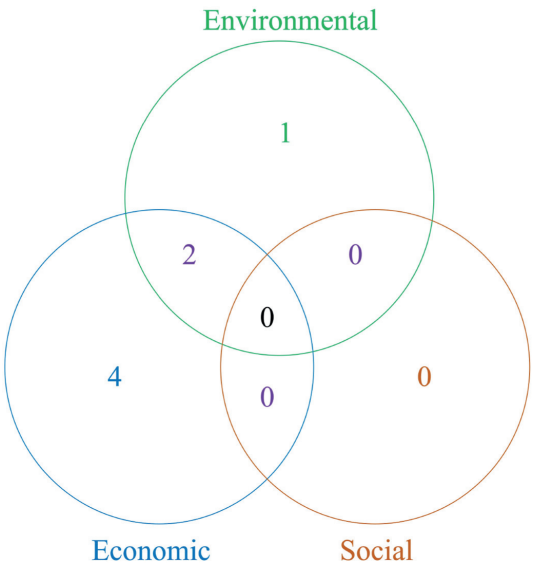


Fig. 8. Number of publications that covered sustainability perspectives in probabilistic hygrothermal assessment research publications (total of 143 publications as the basis for the statistics).

economically viable design solutions for tall timber facades. Utilising the risk-based RiFaTool, which considers the exposure and vulnerability of facade systems, will facilitate the consistent implementation of moisture-resistant design practices.

3.3.4. Uncertain parameter groups

The first toolset, introduced in Ref. [14], is a qualitative exploration that serves a dual purpose: factor identification and flowchart formation. Fig. 9 presents the statistics related to the uncertain parameter groups considered in the HUP and HSA studies. This information aligns with *factor identification*, which aims to systematically map all relevant parameters that can impact the outcome of the analysis. *Flowchart formation* seeks to establish the relationships between the identified parameters and results.

In both the HUP and HSA studies, as illustrated in Fig. 9, the material properties emerged as the most frequently considered uncertain input variables, constituting 64.8 % and 69.8 %, respectively. Conversely, hygrothermal functions (also referred to as material functions in some studies) represented the smallest proportion of uncertain variables in both HUP and HSA studies, accounting for 9.9 % and 12.5 %, respectively. The observed trend illustrates the need to increase the accuracy of probabilistic hygrothermal assessments by incorporating a greater number of hygrothermal functions, as they can have a greater influence on hygrothermal performance than single material properties. In Fig. 9, it should be noted that the total percentage was greater than 100 % for both HUP and HSA studies. This arises from the studies that have incorporated multiple groups of uncertain parameters into their analyses.

Fig. 9 also presents the proportions of other uncertain parameter groups, namely outdoor and indoor climates, surface/boundary conditions, and modelling. The consideration of each of these parameter groups is crucial for avoiding potential inaccuracies in the results. For instance, Thybring et al. [214] investigated different sorption isotherm models and compared their predictions with independently measured values. This study revealed that the physical quantities predicted by parabolic sorption isotherm models are not valid for water in wooden materials. Various uncertainties related to the outdoor climate data, have been explored, including the type of climate data (e.g. typical meteorological years [154] and single-year climate data [98]) and the factors influencing uncertainties in future climate data [109]. Vandemeulebroucke et al. [215] introduced a decision framework for selecting moisture reference years for hygrothermal simulations. Integrating such decision frameworks with a probabilistic hygrothermal assessment can contribute to a more robust analysis, particularly when addressing uncertainties related to outdoor climate data.

3.3.5. Utilised Metamodels

Fig. 10 illustrates the metamodels employed in the HUP and HSA studies as part of the fourth toolset in Annex 55, Subtask 2 [14]. Metamodeling in probabilistic hygrothermal assessment began with the introduction of the response surface methodology (RSM) in 2013 by Ramos et al. [79], followed by subsequent studies the following year [52]. Between 2018 and 2023, the variety of metamodels expanded by incorporating different techniques, as shown in the pie chart in Fig. 10. Neural networks (NN) have emerged as an intensively utilised metamodeling method and featured in 11 studies [42,44,72–75,80,92,96,101,175]. An NN is a machine learning concept inspired by the structure and function of the human brain. They are a class of algorithms designed to recognise patterns and interpret complex data through a process that mimics the way the human brain operates. NNs have gained widespread popularity because of their ability to handle complex data such as images, text, and audio, and perform tasks such as image recognition, natural language processing, and voice recognition. More details about different types of NNs could be found in Ref. [216]. Additionally, other metamodeling methods used in probabilistic hygrothermal assessment include the random forests (RF) [90], partial least squares (PLS) [88,89], Kriging (kr) [43,76], generalised additive models (GAM) [31], and polynomial regression (PR) methods [101].

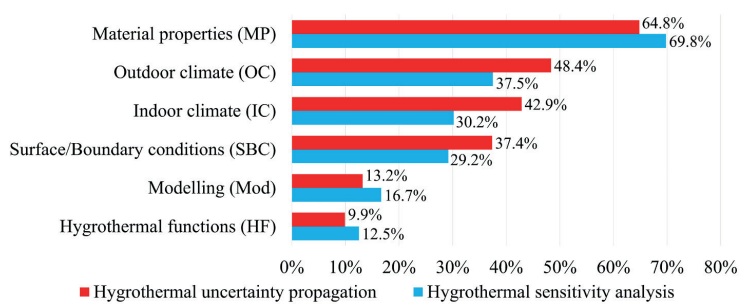


Fig. 9. Uncertain parameters for case studies in hygrothermal uncertainty propagation (HUP) research publications (total of 91 publications) and hygrothermal sensitivity analysis (HSA) research publications (total of 96 publications).

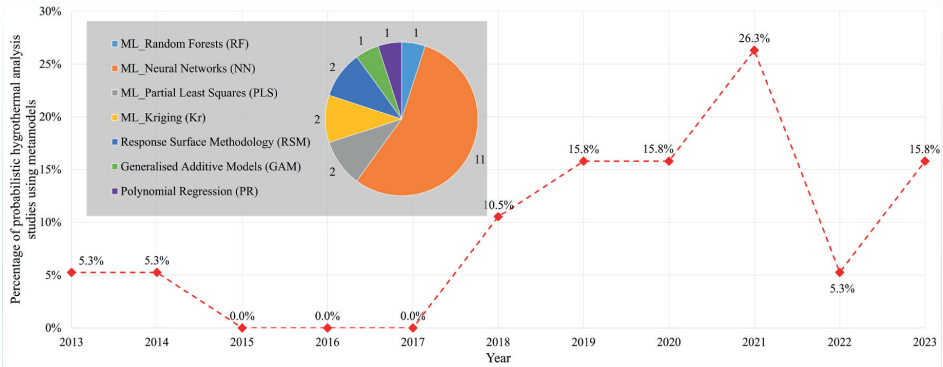


Fig. 10. Utilised metamodels in probabilistic hygrothermal analysis research publications (total of 20 publications as the basis for the statistics). ML: Machine learning.

Metamodels are crucial for addressing the time-consuming nature of probabilistic hygrothermal assessment. Aggarwal et al. [88] used a regression model based on PLS to estimate the hygrothermal performance of a wall without the need for simulations, effectively reducing the computation time. They asserted that this metamodel is user-friendly, particularly for practitioners lacking expertise in hygrothermal simulation tools.

In addition to the application of metamodels in probabilistic hygrothermal analysis, their applicability was extended to accelerate the time-consuming processes of 2D/3D deterministic hygrothermal and mould growth analyses. For instance, support vector machine (SVM) was employed by Freire et al. [217] to demonstrate a substantial reduction in computational time from 120 h to 30 s for a 2D simulation. Vapnik introduced the SVM concept in 1979 [218,219]. Originally developed for binary object classification, the method was subsequently adapted for numerical value prediction (also known as support vector regression, or SVR). Bansal et al. [220] predicted long-term hygrothermal responses using a 31-year climate data series across three Canadian cities. After training the model with the data from the first five years of each series, they utilised SVM to predict hygrothermal responses, demonstrating the potential of metamodels in handling extensive and time-consuming analyses.

It is crucial to evaluate the accuracy of a metamodel using validation data that are not used in the training process. Notably, the accuracy of the metamodel is as significant as the calculation time, with potential savings in time and cost compared to the Monte Carlo analysis of the original model. Optimising the metamodel algorithm involves calculating the sensitivity indices for the training samples and excluding less significant model parameters to streamline the process, particularly in polynomial regression [14].

In metamodeling, the risk of overfitting arises when the training data fit perfectly; however, the model struggles with unseen data, particularly in larger training sets. To address this issue, validation sets comprising additional input/output combinations are introduced, which helps assess the predictions of the metamodel against the output of the original model [14]. Overfitting can be mitigated by reducing model complexity during training or through pruning. The pruning process aims to enhance the generalisation capability of a model by reducing the number of coefficients, particularly in complex models [14].

A comprehensive understanding of the advantages and disadvantages of each metamodeling method is crucial to ensure reliable and robust hygrothermal analysis. Several studies [203,221–227] provided detailed insights into the various metamodels highlighted in Fig. 10. For example, in addition to the advantages of the RF machine learning algorithm [203], such as interpretability, the ability to handle non-linear relationships, metamodel robustness, feature importance analysis, and computation efficiency, it is essential to recognise its inherent limitations in performing extrapolation. The RF algorithm may encounter challenges when predicting outcomes for extreme scenarios that fall outside the range of the trained dataset. By carefully choosing the training data, this disadvantage can be mitigated, and the model can still be used to make predictions for a wide variety of cases while maintaining a reasonable training time. Tijskens et al. [73] similarly addressed this issue in the context of NN, emphasising the importance of wise selection of training data to enhance the reliability of predictions, especially for scenarios beyond the trained dataset ranges.

3.3.6. *Utilised hygrothermal simulation tools*

Fig. 11 provides statistics regarding the hygrothermal simulation tools employed in the HUP and HSA studies based on a state-of-the-art review. Delphin [228] and WUFI [229] emerged as the most frequently used tools, potentially because of their widespread availability and user-friendliness. Delphin has an advantage over WUFI owing to its capability of batch calculations. This feature is particularly valuable in the context of HUP and HSA studies, because it enables the automation of numerous simulations and significantly reduces the overall time required. Both Delphin and WUFI have been verified in various studies [230,231].

Fig. 11 shows that 15.4 % of the HUP and 21.9 % of the HSA studies utilised non-commercial software, encompassing finite-element Heat, Air, and Mass (HAM) models and codes written using MATLAB or Python. These custom codes often incorporate different heat and mass transfer models such as the HAMT, EMPD, or Kunzel model [232]. The use of other hygrothermal simulation tools, including HAM-Tools [233], NEV3 [84], HAMFEM [234], HAMBASE [235], 1D-HAM [236], EnergyPlus [237], hygIRC [238], COMSOL [239], and IDA ICE [240], is rare in probabilistic hygrothermal assessments. Only one study [175] applied measurement techniques for HSA, specifically to estimate the hygrothermal parameters and ambient temperature. In Fig. 11, it can be observed that the total percentage is more than 100 % for HUP studies. This is the results of studies using more than one hygrothermal simulation tool or utilising 1D and 2D simulations, simultaneously in their analyses. A comprehensive review of the advantages and disadvantages of hygrothermal simulation tools can be found in Refs. [241,242]. Gutland et al. [208] emphasised that, although software such as COMSOL or hydrogeological modelling can be employed for hygrothermal modelling, they may lack a specific setup for hygrothermal calculations that can be found in commercial tools such as Delphin and WUFI.

The pie charts in Fig. 11 reveal that most of the HUP (95.6 %) and HSA (88.5 %) studies were conducted in 1D simulations. The primary

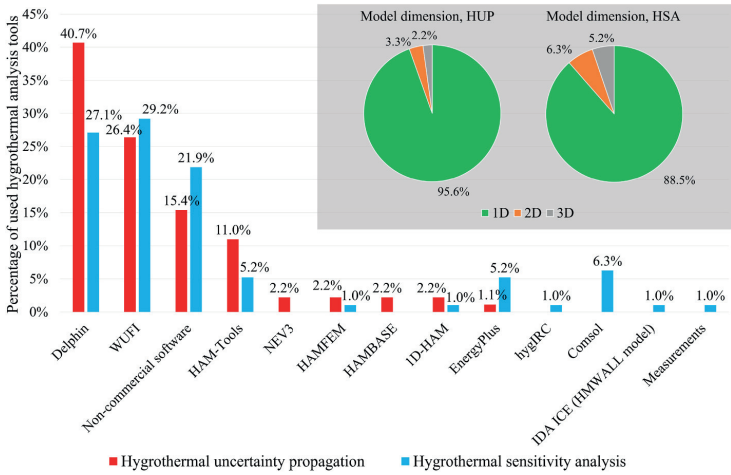


Fig. 11. Statistics of the employed hygrothermal analysis tools and model dimensions in hygrothermal uncertainty propagation (HUP) research publications (total of 91 publications) and hygrothermal sensitivity analysis (HSA) research publications (total of 96 publications).

rationale behind the prevalent use of 1D models is the reduced computational time compared with that of 2D and 3D models. However, a study based on the RIBuild project [45] suggested that further research is required to extend this to 2D and 3D. This expansion was proposed to improve web tools and capture more complex details of hygrothermal modelling. Including more details in 2D or 3D modelling allows designers to investigate specific areas having thermal bridge potential, such as balconies. Decreased surface temperatures, especially those close to thermal bridge zones, may lead to mould growth, as highlighted in Ref. [243]. Additionally, building corners or intersections of construction elements (e.g. roofs and external walls) can be overlooked in 1D models, potentially affecting the accuracy of hygrothermal analyses. Prata et al. [167] conducted a sensitivity analysis of 2D thermal numerical modelling to investigate the impact of building corners.

3.3.7. Investigated moisture-related damage models

As defined by Isaksson et al. [244], durability refers to the capacity of a structure to deliver the required performance during the intended service period, considering the influence of degradation mechanisms. Moisture-related damage can significantly impact durability. According to this state-of-the-art review, four main degradation mechanisms were identified in conjunction with a probabilistic hygrothermal assessment. Mould growth emerged as the most frequently utilised damage model, accounting for 47.6 % of the cases. Other damage models included frost damage (11.9 %), decay fungi (8.4 %), and algae growth (1.4 %). The remaining probabilistic hygrothermal analysis studies (30.7 %) did not apply any damage models as post processors in their studies. Considering these degradation mechanisms within the context of a probabilistic hygrothermal assessment aid in assessing and mitigating potential durability issues in structures.

Labat and Woloszyn [94] emphasised that mould growth was the most likely degradation mechanism, which aligns with the findings of the analysis conducted in this study that approximately half of the probabilistic hygrothermal analysis studies employed mould models as damage models. Notably, the Finnish mould growth model [245] emerged as the most widely accepted model, having been utilised in 88 % of the studies that employed mould growth as the damage model. Conversely, other mould models were used less frequently in the publications identified in this study. For a more comprehensive understanding of mould growth models, a systematic review by Gradeci et al. [246] provides in-depth information.

3.4. Future research projects opportunities

In addition to the statistical analyses presented in this literature review, the authors propose research topics that could advance the field and present new challenges by leveraging probabilistic hygrothermal analysis in future research projects.

3.4.1. Connecting building physics with medical sciences

According to WHO guideline [4], scientific evidence suggests that indoor dampness and mould can contribute to significant health problems, including respiratory diseases (e.g. asthma, cough, and wheezing), skin disorders, and even cancer. Considering this guideline, it is recommended that dampness and mould occurrence should be prevented.

Wang [247] conducted an evaluation of the associations between home environmental factors and asthma, rhinitis, and respiratory symptoms among adults in Sweden and China. The main risk factors identified were dampness and mould. In Sweden, window pane condensation in winter has also been identified as a risk factor for asthma symptoms. Urlaub et al. [248] investigated the impact of mould and dampness on healthy living environments, emphasising that unhealthy homes may contribute to illnesses and result in direct/indirect health costs, such as medication, hospital admission, and employees' sick leave. Over 80 million people in Europe live in homes with at least some degree of dampness [248,249]. This means that there is a potential for significant cost savings in healthcare if the relationship between the presence of mould or dampness and the prevalence of certain diseases, particularly respiratory diseases, is clearly understood in more details in terms of magnitude. Various studies have investigated the influence of dampness and mould on health problems, including asthma, rhinitis, respiratory symptoms [250–255], skin disorders [252,253], neurological problems [256], and liver issues [257].

The inutility decision analysis (IDA) method, introduced by Bayat Pour et al. [137], bridges building envelope design and medical science perspective, specifically focusing on the health consequences of mould. This method extends beyond considerations such as structural safety, energy efficiency, environmental impact, and economic aspects by incorporating occupant health and associated future costs into the decision analysis. By utilising and improving the IDA method, designers can optimise building envelopes to mitigate health problems and reduce the corresponding costs for individuals, society, governments, and insurance companies. Integrating these methods into the building design

process underscores the importance of multidisciplinary research approaches. Advancing the IDA method requires collaboration across diverse fields by combining expertise, knowledge, and methods from construction, design, medicine, and other relevant disciplines. A comprehensive and holistic research program is essential to enhance current understanding and improve building design and maintenance practices, ultimately informing policy and shaping human behaviour.

3.4.2. Development of AI-based hygrothermal analysis tools

Artificial intelligence (AI) can be employed in hygrothermal analysis to enhance the efficiency, accuracy, and prediction capabilities. Integrating metamodels with hygrothermal analyses is crucial for streamlining computations and managing computational costs. Looking ahead, there is an opportunity for creating metamodels specific to different locations, thereby replacing the need for hygrothermal analysis tools. This would involve categorising countries based on factors such as geographical location, climate data, commonly used building materials, and lifestyle (to accurately consider the indoor climate). An exemplary initiative in this direction is the study by Tijskens et al. [92], who presented general guidelines for various European climates and wall compositions.

One of the most promising AI techniques in this field is the application of Neural Networks (NN) that have been used in some hygrothermal analysis studies including [42,44,72–75,80,96,101,175]. These studies demonstrated that NN can model complex hygrothermal behaviours with an acceptable degree of accuracy. However, there remains considerable potential for further refinement and development. Wang et al. [258] created a novel clustering framework using combined machine learning methods for better extraction of the characteristics of hygrothermal transfer on the time series data. In conclusion, the development of AI-based hygrothermal analysis tools, particularly through the refinement of different machine/deep learning techniques, promises more accurate predictions for practical applications in building design.

4. Conclusion

A state-of-the-art review of probabilistic hygrothermal assessment studies at different stages was conducted to map the progress and current gaps in this field. This review identified the following points:

General Conclusion:

1. Among the various uncertainty propagation methods, a Monte Carlo simulation, simulation-based approach, has been widely employed because of their capability to encompass numerous potential scenarios in probabilistic hygrothermal assessments. However, enhancing the accuracy and robustness of the results requires integration of sampling efficiency and a convergence study.
2. Sensitivity analysis in hygrothermal analysis studies has limitations owing to its transient nature (leading to non-linearity) and potential interactions among input variables. Addressing these challenges requires methods capable of performing non-linear and interactive analyses; however, every method has limitations. A conservative approach involves the use of multiple sensitivity analysis methods in the hygrothermal sensitivity analysis to properly consider transient conditions. Prioritising methods with low computational time is crucial for real projects.
3. Research on probabilistic hygrothermal assessment is concentrated in northern and western Europe, and North America. The countries in Asia and Oceania had lower outputs, possibly because of their predominantly dry climates. There is a lack of explored relevant research related to Africa. However, certain regions of these locations with climates similar to those of northern and western Europe may require further research.
4. Most probabilistic hygrothermal assessment studies were conducted under continental (category D) and temperate (category C) climatic conditions.
5. Most probabilistic hygrothermal assessment studies (approximately 95.1 %) did not explicitly address sustainability perspectives, including environmental, economic, and social.
6. In probabilistic hygrothermal assessment studies, material properties have emerged as the predominant uncertain input variables, whereas hygrothermal functions (material functions) constitute a comparatively small proportion of the uncertain variables. More than half of the studies omitted ambient conditions, encompassing both indoor and outdoor climates, as stochastic variables. Furthermore, the statistical analysis indicated that a significant portion of the studies did not integrate specific considerations regarding building usage into their analyses. This may be attributed to the lack of research addressing the inclusion of the indoor climate as a stochastic variable.
7. A thorough understanding of the merits and limitations associated with each metamodeling method is important for achieving reliable and robust hygrothermal analyses. Additionally, mitigating potential risks such as overfitting is crucial.
8. Delphin and WUFI are the most frequently used tools in probabilistic hygrothermal assessment studies, potentially because of their extensive availability and user-friendly interfaces. Delphin distinguishes itself with its capability for performing batch calculations, which sets it apart from other hygrothermal simulation tools. This feature is valuable for probabilistic hygrothermal assessment because it enables the automation of numerous simulations, thereby substantially reducing the time required.
9. Four primary degradation mechanisms were identified in association with probabilistic hygrothermal assessment. Approximately half of the studies focused on mould growth analysis, whereas others utilised damage models for frost damage, fungal decay, and algae growth.

Gaps and Future Studies Recommendations:

1. Case studies under tropical climatic conditions requires more attention because this climate is highly prone to moisture-related problems.
2. To enhance the robustness of decision analysis for moisture-safe building design and retrofitting strategies, probabilistic hygrothermal assessment studies must incorporate sustainability perspectives, including environmental, economic, and social.
3. Enhancing the accuracy of probabilistic hygrothermal assessment requires incorporating hygrothermal functions as uncertain input variables. This is essential because of their potential to have a more pronounced influence on hygrothermal performance than single material properties.
4. Most probabilistic hygrothermal assessment studies (approximately 90 %) have been conducted in 1D. However, further research is suggested to extend this to 2D and 3D to capture more complex details in hygrothermal modelling.
5. Occupants play a crucial role in influencing humidity levels within a building, primarily through their activities, changing heating/cooling set points, and controlling shading devices. Fluctuations in internal loads resulting from occupant behaviour can substantially affect indoor humidity, thereby influencing hygrothermal performance. Consequently, building usage considerations should be incorporated into hygrothermal performance analyses to ensure more accurate and robust outcomes.
6. A potential future path could focus on the development of probabilistic hygrothermal analysis with limit states for quantitative decision support. This can be used to mitigate the health consequences related to dampness and mould in buildings by bridging the gap between hygrothermal analysis and medical science perspectives.

The inutility decision analysis (IDA) method is a promising approach in this regard. This approach requires collaborative efforts across diverse fields integrating expertise, knowledge, and methods from construction, design, medicine, and other relevant disciplines.

7. The evolution of AI-based metamodels for hygrothermal analysis offers a user-friendly solution that is particularly beneficial for practitioners lacking expertise in hygrothermal simulation tools.

CRediT authorship contribution statement

Mohsen Bayat Pour: Writing – review & editing, Writing – original draft, Visualization, Validation, Software, Methodology, Investigation, Formal analysis, Data curation, Conceptualization. **Jonas Niklewski:** Writing – review & editing, Visualization, Supervision, Conceptualization. **Amir Naghibi:** Writing – review & editing, Supervision. **Eva Frühwald Hansson:** Writing – review & editing, Supervision, Project administration, Funding acquisition, Conceptualization.

Declaration of competing interest

The authors declare that they have no known competing financial interests or personal relationships that could have appeared to influence the work reported in this paper.

Data availability

Data will be made available on request.

Acknowledgement

The authors gratefully acknowledge the financial support from FORMAS (the Swedish Research Council for Sustainable Development), grant number 2019–00673. The second author received funding from FORMAS, grant number 2021-02053.

References

[1] L. Wang, H. Ge, Stochastic modelling of hygrothermal performance of highly insulated wood framed walls, Build. Environ. 146 (Dec. 2018) 12–28, https://doi.org/10.1016/j.buildenv.2018.09.032.
[2] M. Bayat Pour, M.L. Elsayed, Assessment of the Environmental Impacts, Energy Performance and Economic Aspects of Various Construction Materials, Master thesis, Lund University, Faculty of Engineering, Lund, Sweden, 2020.
[3] H. Viitanen, Factors Affecting the Development of Mould and Brown Rot Decay in Wooden Material and Wooden Structures, Doctoral Thesis, Department of Forest Products, Swedish University of Agricultural Sciences, Uppsala, Sweden, 1996.
[4] E. Heseltine, J. Rosen, World Health Organization (Eds.), WHO Guidelines for Indoor Air Quality: Dampness and Mould, WHO, Copenhagen, 2009.
[5] H.A. Burge, An update on pollen and fungal spore aerobiology, J. Allergy Clin. Immunol. 110 (4) (Oct. 2002) 544–552, https://doi.org/10.1067/mai.2002.128674.
[6] P. Johansson, Determination of the Critical Moisture Level for Mould Growth on Building Materials, Lund University, Faculty of Engineering, Lund, Sweden, 2014. Doctoral thesis.
[7] C. Ahrnens, E. Borglund, Fukt på kallvindar - en kartläggning av småhus i Västra Götalands län, Chalmers University of Technology, Master Thesis, 2007.
[8] C.-E. Hagentoft, A.S. Kalagasidis, Moisture safe cold attics - assessment based on risk analyses of performance and cost, in: Proceedings of 10th Nordic Symposium on Building Physics, Lund, Sweden, 2014, p. 10.
[9] Boverket's Mandatory Provisions and General Recommendations, BBR, BFS 2011: 6 with Amendments up to BFS 2018:4, 2011, p. 154.
[10] H.L.S.C. Hens, Combined heat, air, moisture modelling: a look back, how, of help? Build. Environ. 91 (Sep. 2015) 138–151, https://doi.org/10.1016/j.buildenv.2015.03.009.
[11] S. Panico, M. Larcher, V. Marincioni, A. Troi, C. Baglivo, P.M. Congedo, Identifying key parameters through a sensitivity analysis for realistic hygrothermal simulations at wall level supported by monitored data, Build. Environ. 229 (Feb. 2023) 109969, https://doi.org/10.1016/j.buildenv.2022.109969.
[12] L.D. Hung Anh, Z. Pásztory, An overview of factors influencing thermal conductivity of building insulation materials, J. Build. Eng. 44 (Dec. 2021) 102604, https://doi.org/10.1016/j.jobe.2021.102604.
[13] K. Gradeci, A Probabilistic-Based Methodology for Evaluation of Timber Façade Constructions', Doctoral Thesis, Norwegian university of science and technology (NTNU), Trondheim, Norway, 2018.
[14] H. Janssen, S. Roels, L. Van Gelder, P. Das, Annex 55, Reliability of Energy Efficient Building Retrofitting - Probability Assessment of Performance and Cost (RAP-RETRO), Probabilistic Tools, Chalmers University of Technology, Gothenburg, Sweden, 2015. ISSN 1652-9162, 2015:4.
[15] M. Petticrew, H. Roberts, Systematic Reviews in the Social Sciences: A Practical Guide, first ed., Wiley, 2006.
[16] A. Booth, A. Sutton, D. Papaioannou, Systematic Approaches to a Successful Literature Review, second ed., SAGE, Los Angeles London New Delhi Singapore Washington DC Melbourne, 2016.
[17] Scopus - Document search | signed in. https://www.scopus.com/search/form.uri?display=basic#basic. (Accessed 9 January 2024).
[18] Document search - web of science core collection. https://www.webofscience.com/wos/woscc/basic-search. (Accessed 9 January 2024).
[19] ScienceDirect.com | Science, health and medical journals, full text articles and books. https://www.sciencedirect.com/. (Accessed 9 January 2024).
[20] D.M. Hamby, A review of techniques for parameter sensitivity analysis of environmental models, Environ. Monit. Assess. 32 (2) (Sep. 1994) 135–154, https://doi.org/10.1007/BF00547132.
[21] Unsd — methodology. https://unstats.un.org/unsd/methodology/m49/. (Accessed 10 January 2024).
[22] M.C. Peel, B.L. Finlayson, T.A. McMahon, Updated world map of the Köppen-Geiger climate classification, Hydrol. Earth Syst. Sci. (2007) 12.
[23] S. Geving, A systematic method for hygrothermal analysis of building constructions using computer models, in: Fifth International IBPSA Conference, 1997. Prague, Check Republic.
[24] A. Sasic Kalagasidis, C. Rode, Annex 55, Reliability of Energy Efficient Building Retrofitting - Probability Assessment of Performance and Cost (RAP-RETRO), Framework for Probabilistic Assessment of the Building Envelope, Chalmers University of Technology, Gothenburg, Sweden, 2015. ISSN 1652-9162, 2015:5.
[25] V.M. Nik, S.O. Mundt-Petersen, A.S. Kalagasidis, P. De Wilde, Future moisture loads for building facades in Sweden: climate change and wind-driven rain, Build. Environ. 93 (Nov. 2015) 362–375, https://doi.org/10.1016/j.buildenv.2015.07.012.
[26] K. Gradeci, N. Labonnote, B. Time, J. Köhler, A proposed probabilistic-based design methodology for predicting mould occurrence in timber façades, in: *World Conference On Timber Engineering (WCTE)*, Vienna, Austria, 2016, p. 9.
[27] K. Gradeci, N. Labonnote, B. Time, J. Köhler, A probabilistic-based methodology for predicting mould growth in façade constructions, Build. Environ. 128 (Jan. 2018) 33–45, https://doi.org/10.1016/j.buildenv.2017.11.021.
[28] H.J. Moon, G. Augenbroe, Empowerment of decision-makers in mould remediation, Build. Res. Inf. 36 (5) (Oct. 2008) 486–498, https://doi.org/10.1080/09613210801996203.
[29] H.J. Moon, Assessing Mold Risks in Buildings under Uncertainty', Doctoral Thesis, Georgia Institute of Technology, Atlanta, GA, USA, 2005.
[30] K. Gradeci, U. Berardi, Application of probabilistic approaches to the performance evaluation of building envelopes to withstand mould growth, J. Build. Phys. 43 (3) (Nov. 2019) 187–207, https://doi.org/10.1177/1744259119861784.
[31] V. Marincioni, G. Marra, H. Altamirano-Medina, Development of predictive models for the probabilistic moisture risk assessment of internal wall insulation, Build. Environ. 137 (Jun. 2018) 257–267, https://doi.org/10.1016/j.buildenv.2018.04.001.
[32] J. Zhao, Development of a novel statistical method and procedure for material characterization and a probabilistic approach to assessing the hygrothermal performance of building enclosure assemblies. College of Engineering and Computer Science, Syracuse University, Syracuse, NY, USA, 2012. Dissertation.
[33] J. Zhao, J. Jensen, Zhang, J. Grunewald, S. Feng, A probabilistic-based method to evaluate hygrothermal performance of an internally insulated brick wall, Build. Simulat. 14 (2) (Apr. 2021) 283–299, https://doi.org/10.1007/s12273-020-0702-6.
[34] A.H. Holm, H.M. Kuenzel, Practical application of an uncertainty approach for hygrothermal building simulations—drying of an AAC flat roof, Build. Environ. (2002) 7, https://doi.org/10.1016/S0360-1323(02)00047-1.
[35] M. Salonvaara, A. Karagiozis, A. Holm, Stochastic building envelope modeling—the influence of material properties, in: Building VIII, 1995, p. 8.
[36] J. Goffart, M. Rabouille, N. Mendes, Uncertainty and sensitivity analysis applied to hygrothermal simulation of a brick building in a hot and humid climate, Journal of Building Performance Simulation 10 (1) (Jan. 2017) 37–57, https://doi.org/10.1080/19401493.2015.1112430.
[37] Z. Sadovský, O. Koronthályová, Exploration of probabilistic mould growth assessment, Appl. Math. Model. 42 (Feb. 2017) 566–575, https://doi.org/10.1016/j.apm.2016.10.049.
[38] C.-E. Hagentoft, Reliability of energy efficient building retrofitting - probability assessment of performance and cost (Annex 55, RAP-RETRO), Energy Build. 155 (Nov. 2017) 166–171, https://doi.org/10.1016/j.enbuild.2017.09.007.
[39] K. Pietrzyk, A systemic approach to moisture problems in buildings for mould safety modelling, Build. Environ. 86 (Apr. 2015) 50–60, https://doi.org/10.1016/j.buildenv.2014.12.013.
[40] H.J. Moon, G. Augenbroe, A mixed simulation approach to analyze mold growth under uncertainty, in: Ninth International IBPSA Conference, Montreal, Canada, 2005, p. 9.
[41] H.J. Moon, G. Augenbroe, Application of probabilistic simulation and bayesian decision theory in the selection of mold remediation actions, in: 10th International IBPSA Conference, Beijing, China, 2007, p. 8.

[42] A. Tijskens, S. Roels, H. Janssen, Hygrothermal assessment of timber frame walls using a convolutional neural network, Build. Environ. 193 (Apr. 2021) 107652, https://doi.org/10.1016/j.buildenv.2021.107652.

[43] K. Calle, N. Van Den Bossche, Sensitivity of the hygrothermal behaviour of homogeneous masonry constructions: from Sobol indices to decision trees, in: 12th Nordic Symposium on Building Physics (NSB 2020), 172, Tallinn, Estonia, 2020 07001, https://doi.org/10.1051/e3sconf/202017207001.

[44] A. Tijskens, H. Janssen, S. Roels, Using convolutional neural networks for hygrothermal predictions to extrapolate to other external climates, in: 12th Nordic Symposium on Building Physics (NSB 2020), 172, Tallinn, Estonia, 2020 04001, https://doi.org/10.1051/e3sconf/202017204001.

[45] E.J. de Place Hansen, E.B. Møller, M. Ørsager, Guidelines for internal insulation of historic buildings, in: 12th Nordic Symposium on Building Physics (NSB 2020), 172, Tallinn, Estonia, 2020 01004, https://doi.org/10.1051/e3sconf/202017201004.

[46] P. Boudreaux, S. Pallin, G. Accawi, A. Desjarlais, R. Jackson, D. Senecal, A rule-based expert system applied to moisture durability of building envelopes, J. Build. Phys. 42 (3) (Nov. 2018) 416–437, https://doi.org/10.1177/1744259117750370.

[47] A. Tijskens, H. Janssen, S. Roels, A simplified dynamic zone model for a probabilistic assessment of hygrothermal risks in building components, in: 11th Nordic Symposium on Building Physics, Trondheim, Norway 132, 2017, pp. 717–722, https://doi.org/10.1016/j.egypro.2017.10.012.

[48] S. Ott, A. Tietze, S. Winter, Introduction of a semi-probabilistic moisture safety model for tall timber-based building shell – a risk based durability approach, in: Life-Cycle of Engineering Systems, Delft, Netherlands, 2016, p. 262, https://doi.org/10.1201/9781315375175-205, 262.

[49] E. Vereecken, L. Van Gelder, H. Janssen, S. Roels, Interior insulation for wall retrofitting – a probabilistic analysis of energy savings and hygrothermal risks, Energy Build. 89 (Feb. 2015) 231–244, https://doi.org/10.1016/j.enbuild.2014.12.031.

[50] J. Zhao, R. Plagge, N.M.M. Ramos, M. Lurdes Simões, J. Grunewald, Concept for development of stochastic databases for building performance simulation – a material database pilot project, Build. Environ. 84 (Jan. 2015) 189–203, https://doi.org/10.1016/j.buildenv.2014.10.030.

[51] H. Sulaiman, F. Olsina, Comfort reliability evaluation of building designs by stochastic hygrothermal simulation, Renew. Sustain. Energy Rev. 40 (Dec. 2014) 171–184, https://doi.org/10.1016/j.rser.2014.07.162.

[52] N.M.M. Ramos, E. Barreira, M.L. Simões, J.M.P.Q. Delgado, Probabilistic risk assessment methodology of exterior surfaces defacement caused by algae growth, J. Construct. Eng. Manag. 140 (12) (Dec. 2014) 05014012, https://doi.org/10.1061/(ASCE)CO.1943-7862.0000909.

[53] S. Pallin, M. Kehrer, W.A. Miller, A hygrothermal risk analysis applied to residential unvented attics, in: Thermal Performance of the Exterior Envelopes of Whole Buildings XII International Conference, Clearwater, Florida, United States of America, 2013, p. 17.

[54] B. Boucham, A. Chateauneuf, E.A.A. Bedia, An uncertainty method for moisture concentration assessment in composite material plates t300/5208 under hygrothermal conditions effects, Turk. J. Eng. Environ. Sci. 32 (5) (Jan. 2008) 12.

[55] K. Kurkinen, K. Pietrzyk, E.-L. Wentzel, C.-E. Hagentoft, Probabilistic analysis of indoor surface hygrothermal conditions accounting for thermal and hygric memory of the building component, in: 9th International Conference Thermal Performance of Exterior Envelopes of Whole Buildings, Clearwater, USA 9, 2004, p. 9.

[56] A. Brás, A. Valença, P. Faria, Performance-based methods for masonry building rehabilitation using innovative leaching and hygrothermal risk analyses, Sustain. Cities Soc. 28 (Jan. 2017) 321–331, https://doi.org/10.1016/j.scs.2016.09.010.

[57] K. Gradeci, U. Berardi, B. Time, J. Köhler, Evaluating highly insulated walls to withstand biodeterioration: a probabilistic-based methodology, Energy Build. 177 (Oct. 2018) 112–124, https://doi.org/10.1016/j.enbuild.2018.07.059.

[58] K. Gradeci, N. Labonnote, B. Time, J. Köhler, A probabilistic-based approach for predicting mould growth in timber building envelopes: comparison of three mould models, in: 11th Nordic Symposium on Building Physics, Trondheim, Norway 132, 2017, pp. 393–398, https://doi.org/10.1016/j.egypro.2017.09.641.

[59] E. Arumägi, M. Pihlak, T. Kalamees, Reliability of interior thermal insulation as a retrofit measure in historic wooden apartment buildings in cold climate, in: 6th International Building Physics Conference, Torino, Italy, 78, 2015, pp. 871–876, https://doi.org/10.1016/j.egypro.2015.11.010.

[60] T. Hou, D. Nuyens, S. Roels, H. Janssen, Quasi-Monte Carlo based uncertainty analysis: sampling efficiency and error estimation in engineering applications, Reliab. Eng. Syst. Saf. 191 (Nov. 2019) 106549, https://doi.org/10.1016/j.ress.2019.106549.

[61] F. Haldi, Predicting the risk of moisture induced damages on the building envelope using stochastic models of building occupants' behaviour, in: 6th International Building Physics Conference, Torino, Italy 78, 2015, pp. 1377–1382, https://doi.org/10.1016/j.egypro.2015.11.157.

[62] H. Janssen, Monte-Carlo based uncertainty analysis: sampling efficiency and sampling convergence, Reliab. Eng. Syst. Saf. 109 (Jan. 2013) 123–132, https://doi.org/10.1016/j.ress.2012.08.003.

[63] L. Wang, H. Ge, Effect of rain leakage on hygrothermal performance of highly insulated wood-framed walls: a stochastic approach, Can. J. Civ. Eng. 46 (11) (Nov. 2019) 979–989, https://doi.org/10.1139/cjce-2019-0223.

[64] S. Ilomets, T. Kalamees, J. Vinha, Indoor hygrothermal loads for the deterministic and stochastic design of the building envelope for dwellings in cold climates, J. Build. Phys. 41 (6) (May 2018) 547–577, https://doi.org/10.1177/1744259117718442.

[65] L. Wang, H. Ge, Hygrothermal performance of cross-laminated timber wall assemblies: a stochastic approach, Build. Environ. 97 (Feb. 2016) 11–25, https://doi.org/10.1016/j.buildenv.2015.11.034.

[66] H. Sulaiman, F. Olsina, S. Velez, Probabilistic assessment of discomfort risk in buildings, in: 13th Conference of International Building Performance Simulation Association, Chambéry, France, 2013, p. 9.

[67] T. Defraeye, B. Blocken, J. Carmeliet, Influence of uncertainty in heat–moisture transport properties on convective drying of porous materials by numerical modelling, Chem. Eng. Res. Des. 91 (1) (Jan. 2013) 36–42, https://doi.org/10.1016/j.cherd.2012.06.011.

[68] J. Zhao, R. Plagge, A. Nicolai, J. Grunewald, J.S. Zhang, Stochastic study of hygrothermal performance of a wall assembly - the influence of material properties and boundary coefficients, HVAC R Res. 17 (4) (2011) 13, https://doi.org/10.1080/10789669.2011.585421.

[69] R. Bui, M. Labat, S. Lorente, Impact of the occupancy scenario on the hygrothermal performance of a room, Build. Environ. 160 (Aug. 2019) 106178, https://doi.org/10.1016/j.buildenv.2019.106178.

[70] E. Arumägi, T. Kalamees, U. Kallavus, Indoor climate conditions and hygrothermal loads in historic wooden apartment buildings in cold climates, Proc. Est. Acad. Sci. 64 (2) (2015) 146, https://doi.org/10.3176/proc.2015.2.03.

[71] D. Chung, J. Wen, L.J. Lo, Development and verification of the open source platform, HAM-Tools, for hygrothermal performance simulation of buildings using a stochastic approach, Build. Simulat. 13 (3) (Jun. 2020) 497–514, https://doi.org/10.1007/s12273-019-0594-5.

[72] A. Tijskens, S. Roels, H. Janssen, Neural networks for metamodelling the hygrothermal behaviour of building components, Build. Environ. 162 (Sep. 2019) 106282, https://doi.org/10.1016/j.buildenv.2019.106282.

[73] A. Tijskens, H. Janssen, S. Roels, The impact of a reduced training subspace on the prediction accuracy of neural networks for hygrothermal predictions, Journal of Building Performance Simulation 14 (1) (Jan. 2021) 20–37, https://doi.org/10.1080/19401493.2020.1832148.

[74] A. Tijskens, H. Janssen, S. Roels, Optimising convolutional neural networks to predict the hygrothermal performance of building components, Energies 12 (20) (Oct. 2019) 3966, https://doi.org/10.3390/en12203966.

[75] A. Tijskens, S. Roels, H. Janssen, Predicting the hygrothermal behaviour of building components using neural networks, in: 4th Central European Symposium on Building Physics (CESBP 2019), Prague, Czech Republic 282, 2019, p. 6, https://doi.org/10.1051/matecconf/201928202036.

[76] K. Calle, N. Van Den Bossche, Sensitivity analysis of the hygrothermal behaviour of homogeneous masonry constructions: interior insulation, rainwater infiltration and hydrophobic treatment, J. Build. Phys. 44 (6) (May 2021) 510–538, https://doi.org/10.1177/17442591211009937.

[77] K. Calle, N. Van Den Bossche, Probabilistic assessment of the impact of material properties on the risk of frost damage in masonry constructions, in: 4th Central European Symposium on Building Physics (CESBP 2019), Prague, Czech Republic 282, 2019, p. 6, https://doi.org/10.1051/matecconf/201928202084.

[78] R. Bui, J. Goffart, F. McGregor, M. Woloszyn, A. Fabbri, A.-C. Grillet, Uncertainty and sensitivity analysis applied to a rammed earth wall: evaluation of the discrepancies between experimental and numerical data, in: 12th Nordic Symposium on Building Physics (NSB 2020), 172, Tallinn, Estonia, 2020, p. 7, https://doi.org/10.1051/e3sconf/202017217004.

[79] N. Ramos, E. Barreira, M.L. Simões, J. Delgado, Probabilistic risk assessment applied to biological growth on external surfaces with ETICS, in: 13th Conference of the International Building Performance Simulation Association, Chambéry, France, August, 2013, p. 6.

[80] A. Tijskens, S. Roels, H. Janssen, Neural networks to predict the hygrothermal response of building components in a probabilistic framework, in: Healthy, Intelligent and Resilient Buildings and Urban Environments, 2018, pp. 1169–1174, https://doi.org/10.14305/ibpc.2018.ms-6.04.

[81] C.E. Hagentoft, A.S. Kalagasidis, Hygrothermal conditions and mould growth potential in cold attics: impact of weather, building system and construction design characteristics, in: Hygrothermal Behavior, Building Pathology and Durability, 1, Springer Berlin Heidelberg, Berlin, Heidelberg, 2013, pp. 61–91.

[82] L.V. Gelder, H. Janssen, S. Roels, Retrofitting cavity walls – probabilistic study of energy savings and moisture risks, in: 5th International Building Physics Conference, 2012, p. 7. Kyoto, Japan.

[83] S. Pallin, Risk Assessment of Hygrothermal Performance - Building Envelope Retrofit, Chalmers University of Technology, Gothenburg, Sweden, 2013. Doctoral thesis.

[84] Z. Sadovský, O. Koronthályová, P. Matiašovský, K. Mikulová, Probabilistic modelling of mould growth in buildings, J. Build. Phys. 37 (4) (Apr. 2014) 348–366, https://doi.org/10.1177/1744259113496370.

[85] C.-E. Hagentoft, Probabilistic analysis of hygrothermal conditions and mould growth potential in cold attics. Impact of weather, building system and construction design characteristics, in: 12th International Conference on Durability of Building Materials and Components, Porto, Portugal, 2011, p. 8.

[86] V. Kukk, J. Kers, T. Kalamees, L. Wang, H. Ge, Impact of built-in moisture on the design of hygrothermally safe cross-laminated timber external walls: a stochastic approach, Build. Environ. 226 (Dec. 2022) 109736, https://doi.org/10.1016/j.buildenv.2022.109736.

[87] R.M.S.F. Almeida, E. Barreira, Monte Carlo simulation to evaluate mould growth in walls: the effect of insulation, orientation, and finishing coating, Adv. Civ. Eng. 2018 (Aug. 2018) 1–12, https://doi.org/10.1155/2018/8532167.

[88] C. Aggarwal, H. Ge, M. Defo, M.A. Lacasse, Hygrothermal performance assessment of wood frame walls under historical and future climates using partial

least squares regression, Build. Environ. 223 (Sep. 2022) 109501, https://doi.org/10.1016/j.buildenv.2022.109501.
[89] C. Aggarwal, H. Ge, M. Defo, Assessing mould growth risk of wood-frame walls using partial least squares (PLS) regression considering climate model uncertainties, Build. Environ. 238 (Jun. 2023) 110374, https://doi.org/10.1016/j.buildenv.2023.110374.
[90] M. Bayat Pour, J. Niklewski, A. Naghibi, E. Frühwald Hansson, Robust probabilistic modelling of mould growth in building envelopes using random forests machine learning algorithm, Build. Environ. 243 (Sep. 2023) 110703, https://doi.org/10.1016/j.buildenv.2023.110703.
[91] L. Wang, M. Defo, Z. Xiao, H. Ge, M.A. Lacasse, Stochastic simulation of mould growth performance of wood-frame building envelopes under climate change: risk assessment and error estimation, Buildings 11 (8) (Jul. 2021) 333, https://doi.org/10.3390/buildings11080333.
[92] A. Tijskens, H. Janssen, S. Roels, Probabilistic hygrothermal assessment of various timber frame wall compositions, Build. Environ. 243 (Sep. 2023) 110619, https://doi.org/10.1016/j.buildenv.2023.110619.
[93] D. Chung, J. Wen, Building envelope moisture transport in the context of assembly aging and uncertainty, Technology|Architecture + Design 3 (2) (Jul. 2019) 221–233, https://doi.org/10.1080/24751448.2019.1640540.
[94] M. Labat, M. Woloszyn, Moisture balance assessment at room scale for four cases based on numerical simulations of heat–air–moisture transfers for a realistic occupancy scenario, Journal of Building Performance Simulation 9 (5) (Sep. 2016) 487–509, https://doi.org/10.1080/19401493.2015.1107136.
[95] N. Grint, V. Marincioni, C.A. Elwell, Sensitivity and Uncertainty analyses on a DELPHIN model: the impact of material properties on moisture in a solid brick wall, in: 12th Nordic Building Physics Conference NSB, 172, Tallinn, Estonia, 2020 04006, https://doi.org/10.1051/e3sconf/202017204006.
[96] A. Tijskens, S. Roels, H. Janssen, A convolutional neural network for the hygrothermal assessment of timber frame walls. Presented at the 2021 Building Simulation Conference, Bruges, Belgium, 2021, https://doi.org/10.26868/25222708.2021.30605.
[97] S.M. Fufa, C. Skaar, K. Gradeci, N. Labonnote, Assessment of greenhouse gas emissions of ventilated timber wall constructions based on parametric LCA, J. Clean. Prod. 197 (Oct. 2018) 34–46, https://doi.org/10.1016/j.jclepro.2018.06.006.
[98] D. Chung, J. Wen, L.C.J. Lo, Examining the impact of stochastic multi-year weather and air infiltration on hygrothermal moisture risks, J. Build. Phys. 47 (1) (Jul. 2023) 4–35, https://doi.org/10.1177/17442591231163459.
[99] V. Kukk, J. Kers, T. Kalamees, L. Wang, H. Ge, Hygrothermal criteria for design of cross-laminated timber external walls, in: Proceedings of the 5th International Conference on Building Energy and Environment, Singapore, 2023, pp. 811–815, https://doi.org/10.1007/978-981-19-9822-5_87.
[100] M. Gutland, S. Bucking, M. Santana Quintero, Hygrothermal modelling of historic rubble masonry walls: accounting for geometric and compositional variability, J. Build. Eng. 48 (May 2022) 103929, https://doi.org/10.1016/j.jobe.2021.103929.
[101] L. Wang, H. Ge, L. Wang, Metamodel development for predicting hygrothermal performance of wood-frame wall under rain leakage, in: XV International Conference on Durability of Building Materials and Components. eBook of Proceedings, 2020, https://doi.org/10.23967/dbmc.2020.095.
[102] S. Sahyoun, L. Wang, H. Ge, M. Defo, M. Lacasse, Durability of internally insulated historical solid masonry under future climates: a stochastic approach, in: XV International Conference on Durability of Building Materials and Components. eBook of Proceedings, 2020, https://doi.org/10.23967/dbmc.2020.044.
[103] I. Lee, P. Roppel, P. Eng, Guiding design teams by hygrothermal, energy, and thermal comfort analysis while managing uncertainty, in: Buildings XIII Conference, Florida, USA, 2016, p. 19.
[104] V. Kukk, J. Kers, T. Kalamees, The use of an internal airtight membrane in CLT external wall in terms of hygrothermal performance, in: Journal of Physics: Conference Series, 2021, p. 3, https://doi.org/10.1088/1742-6596/2069/1/012208.
[105] D. Xia, et al., Impact of coupled heat and moisture transfer on indoor comfort and energy demand for residential buildings in hot-humid regions, Energy Build. 288 (Jun. 2023) 113029, https://doi.org/10.1016/j.enbuild.2023.113029.
[106] L. Wang, M. Defo, A. Gaur, M.A. Lacasse, Development of moisture reference years for assessing long-term mould growth risk of wood-frame building envelopes, in: 8th International Building Physics Conference (IBPC 2021), Copenhagen, Denmark, 2069, 2021 012015, https://doi.org/10.1088/1742-6596/2069/1/012015.
[107] J. Woods, J. Winkler, Effective moisture penetration depth model for residential buildings: sensitivity analysis and guidance on model inputs, Energy Build. 165 (Apr. 2018) 216–232, https://doi.org/10.1016/j.enbuild.2018.01.040.
[108] S. Ott, A. Tietze, S. Winter, Wind driven rain and moisture safety of tall timber houses – evaluation of simulation methods, Wood Mater. Sci. Eng. 10 (3) (Jul. 2015) 300–311, https://doi.org/10.1080/17480272.2015.1068371.
[109] V.M. Nik, A. Sasic Kalagasidis, E. Kjellström, Assessment of hygrothermal performance and mould growth risk in ventilated attics in respect to possible climate changes in Sweden, Build. Environ. 55 (Sep. 2012) 96–109, https://doi.org/10.1016/j.buildenv.2012.01.024.
[110] V. Nik, Mould growth inside an attic concerning four different future climate scenarios, in: NSB2011 9th Nordic Symposium on Building Physics, Finland, 2011.
[111] L. Rivalin, P. Stabat, D. Marchio, M. Caciolo, F. Hopquin, A comparison of methods for uncertainty and sensitivity analysis applied to the energy performance of new commercial buildings, Energy Build. 166 (May 2018) 489–504, https://doi.org/10.1016/j.enbuild.2018.02.021.
[112] W. Feller, *An Introduction To Probability Theory And its Applications*, 2 Vols, Wiley, 1970.
[113] M.H. Faber, Statistics and Probability Theory, 18, Springer Netherlands, Dordrecht, 2012.
[114] I.A. Macdonald, Comparison of sampling techniques on the performance of Monte Carlo based sensitivity analysis, in: 11th International IBPSA, Glasgow, Scotland, 2009, p. 9.
[115] G.D. Wyss, K.H. Jorgensen, A user's guide to LHS: sandia's Latin Hypercube Sampling Software, SAND–98-0210 573301 (Feb. 1998), https://doi.org/10.2172/573301.
[116] L.P. Swiler, G.D. Wyss, A user's guide to Sandia's Latin hypercube sampling software : LHS UNIX library/standalone version, SAND2004-2439 (Jul. 2004), https://doi.org/10.2172/919175, 919175.
[117] S. Marino, I.B. Hogue, C.J. Ray, D.E. Kirschner, A methodology for performing global uncertainty and sensitivity analysis in systems biology, J. Theor. Biol. 254 (1) (Sep. 2008) 178–196, https://doi.org/10.1016/j.jtbi.2008.04.011.
[118] M.D. McKay, R.J. Beckman, W.J. Conover, Comparison of three methods for selecting values of input variables in the analysis of output from a computer code, Technometrics 21 (2) (May 1979) 239–245, https://doi.org/10.1080/00401706.1979.10489755.
[119] R.I. Cukier, C.M. Fortuin, K.E. Shuler, A.G. Petschek, J.H. Schaibly, Study of the sensitivity of coupled reaction systems to uncertainties in rate coefficients. I Theory, J. Chem. Phys. 59 (8) (Oct. 1973) 3873–3878, https://doi.org/10.1063/1.1680571.
[120] J.e. Helton, F.J. Davis, Sampling-Based Methods for Uncertainty and Sensitivity Analysis, Sandia National Laboratories, Albuquerque, New Mexico, July, 2000.
[121] J.C. Helton, F.J. Davis, Latin hypercube sampling and the propagation of uncertainty in analyses of complex systems, Reliab. Eng. Syst. Saf. 81 (1) (Jul. 2003) 23–69, https://doi.org/10.1016/S0951-8320(03)00058-9.
[122] L. Pronzato, W.G. Müller, Design of computer experiments: space filling and beyond, Stat. Comput. 22 (3) (May 2012) 681–701, https://doi.org/10.1007/s11222-011-9242-3.
[123] K.-T. Fang, C.-X. Ma, P. Winker, Centered L2-discrepancy of random sampling and Latin hypercubedesign, and construction of uniform designs, Math. Comput. 71 (237) (Oct. 2000) 275–297, https://doi.org/10.1090/S0025-5718-00-01281-3.
[124] M.D. Morris, T.J. Mitchell, Exploratory designs for computational experiments, J. Stat. Plann. Inference 43 (1995) 381–402.
[125] M.E. Johnson, L.M. Moore, D. Ylvisaker, Minimax and maximin distance designs, J. Stat. Plann. Inference 26 (2) (Oct. 1990) 131–148, https://doi.org/10.1016/0378-3758(90)90122-B.
[126] L. Van Gelder, H. Janssen, S. Roels, Probabilistic design and analysis of building performances: methodology and application example, Energy Build. 79 (Aug. 2014) 202–211, https://doi.org/10.1016/j.enbuild.2014.04.042.
[127] I. Krykova, Evaluating of Path-dependent Securities with Low Discrepancy Methods, Worcester Polytechnic Institute, Massachusetts, USA, 2004. Master thesis.
[128] P. L'Ecuyer, Random number generation and quasi-Monte Carlo, in: J.L. Teugels, B. Sundt (Eds.), Encyclopedia of Actuarial Science, John Wiley & Sons, Ltd, Chichester, UK, 2004, p. tar002.
[129] C. Bucher, Asymptotic sampling for high-dimensional reliability analysis, Probabilist. Eng. Mech. 24 (4) (Oct. 2009) 504–510, https://doi.org/10.1016/j.probengmech.2009.03.002.
[130] K. Pietrzyk, C.-E. Hagentoft, Reliability analysis in building physics design, Build. Environ. 43 (4) (Apr. 2008) 558–568, https://doi.org/10.1016/j.buildenv.2007.01.009.
[131] E.S. Pearson, J.W. Tukey, Approximate means and standard deviations based on distances between percentage points of frequency curves, Biometrika 52 (Dec. 1965) 533–546.
[132] D.P. Kroese, T. Taimre, Z.I. Botev, Handbook for Monte Carlo Methods, Wiley, Hoboken, N.J, 2011.
[133] R.Y. Rubinstein, D.P. Kroese, Simulation and the Monte Carlo Method, third ed., Wiley, Hoboken, New Jersey, 2017.
[134] T.W. Simpson, J.D. Peplinski, P.N. Koch, J.K. Allen, Metamodels for computer-based engineering design: survey and recommendations, Eng. Comput. 17 (2) (1997) 129–150.
[135] G.G. Wang, S. Shan, Review of Metamodeling Techniques in Support of Engineering Design Optimization, American Society of Mechanical Engineers (ASME), Apr. 2007, p. 11, https://doi.org/10.1115/1.2429697.
[136] O.M. Querin, M. Victoria, C. Alonso, R. Ansola, P. Martí, Discrete method of structural optimization, in: Topology Design Methods for Structural Optimization, Elsevier, 2017, pp. 27–46.
[137] M. Bayat Pour, J. Niklewski, E. Frühwald Hansson, S. Thöns, Mould reliability analysis combined with mould health risks for decision support, in: AIP Conference Proceedings, Bratislava, Slovakia, 2918, 2023 020006, https://doi.org/10.1063/5.0172276.
[138] O. Ditlevsen, H.O. Madsen, *Structural Reliability Methods*, Repr, Wiley, Chichester, 1999.
[139] S.M. Cornick, W. Alan Dalgliesh, W. Maref, Sensitivity of hygrothermal analysis to uncertainty in rain data, J. ASTM Int. (JAI) 6 (4) (2009) 19, https://doi.org/10.1520/JAI102032.
[140] X. Lü, T. Lu, C. Kibert, K. Vahtikari, M. Hughes, Y. Zhao, A dynamic modelling approach for simulating climate change impact on energy and hygrothermal performances of wood buildings, Build. Simulat. 11 (3) (Jun. 2018) 497–506, https://doi.org/10.1007/s12273-017-0421-9.

[141] T. Alioua, B. Agoudjil, A. Boudenne, K. Benzarti, Sensitivity analysis of transient heat and moisture transfer in a bio-based date palm concrete wall, Build. Environ. 202 (Sep. 2021) 108019, https://doi.org/10.1016/j.buildenv.2021.108019.
[142] I. Othmen, P. Poullain, N. Leklou, Sensitivity analysis of the transient heat and moisture transfer in a single layer wall, European Journal of Environmental and Civil Engineering 24 (13) (Nov. 2020) 2211–2229, https://doi.org/10.1080/19648189.2018.1500947.
[143] X. Liu, Y. Liu, X. Guo, N. Luo, G. Chen, Effect of uncertainty in the hygrothermal properties on hygrothermal modeling, in: Proceedings of the 11th International Symposium on Heating, Ventilation and Air Conditioning (ISHVAC 2019), Singapore, 2020, pp. 461–470, https://doi.org/10.1007/978-981-13-9528-4_47.
[144] A.H. Holm, H.M. Kuenzel, J. Radon, Uncertainty approaches for hygrothermal building simulations— drying of AAC in hot and humid climates, Buildings VIII (2001) 6.
[145] A. Holm, H.M. Kuenzel, Uncertainty approaches for hygrothermal building simulations - drying of an AAC flat roof in different climates, in: Seventh International IBPSA, Rio de Janeiro, Brazil, 2001, p. 8.
[146] C. Aggarwal, L. Wang, M. Defo, H. Ge, M. Junginger, M.A. Lacasse, Sensitivity analysis of hygrothermal performance of wood framed wall assembly under different climatic conditions: the impact of cladding properties, in: 8th International Building Physics Conference (IBPC 2021), Journal of Physics, Copenhagen, Denmark, 2021, p. 9, https://doi.org/10.1088/1742-6596/2069/1/012010.
[147] L. Havinga, H. Schellen, Applying internal insulation in post-war prefab housing: understanding and mitigating the hygrothermal risks, Build. Environ. 144 (Oct. 2018) 631–647, https://doi.org/10.1016/j.buildenv.2018.08.035.
[148] V. Kukk, L. Kaljula, J. Kers, T. Kalamees, Designing highly insulated cross-laminated timber external walls in terms of hygrothermal performance: field measurements and simulations, Build. Environ. 212 (Mar. 2022) 108805, https://doi.org/10.1016/j.buildenv.2022.108805.
[149] M. Gutland, S. Bucking, M. Santana Quintero, Two-dimensional hygrothermal modelling of masonry walls accounting for imperfections at the masonry joint, in: 12th Nordic Symposium on Building Physics (NSB) 172, Tallinn, Estonia, 2020, p. 7, https://doi.org/10.1051/e3sconf/202017208003.
[150] M. Gutland, S. Bucking, M. Quintero, Detailed modelling of the masonry unit-mortar interface using hygrothermal simulation, in: XV International Conference on Durability of Building Materials and Components. eBook of Proceedings, 2020, https://doi.org/10.23967/dbmc.2020.223.
[151] J. Kočí, V. Kočí, J. Maděra, Uncertainty in moisture transport modelling and its effect on ice formation in porous building materials, in: Presented at the THERMOPHYSICS 2018: 23rd International Meeting of Thermophysics 2018, Smolenice, Slovakia, 2018, p. 6, https://doi.org/10.1063/1.5047614.
[152] M. Bianchi Janetti, L.P.M. Colombo, F. Ochs, W. Feist, Effect of evaporation cooling on drying capillary active building materials, Energy Build. 166 (May 2018) 550–560, https://doi.org/10.1016/j.enbuild.2017.12.048.
[153] J. Kwiatkowski, M. Woloszyn, J.-J. Roux, Modelling of hysteresis influence on mass transfer in building materials, Build. Environ. 44 (3) (Mar. 2009) 633–642, https://doi.org/10.1016/j.buildenv.2008.05.006.
[154] S. Panico, M. Larcher, D. Herrera Avellanosa, C. Baglivo, A. Troi, P. Maria Congedo, Hygrothermal simulation challenges: assessing boundary condition choices in retrofitting historic European buildings, Energy Build. 297 (Oct. 2023) 113464, https://doi.org/10.1016/j.enbuild.2023.113464.
[155] I. Costa-Carrapiço, B. Croxford, R. Raslan, J. Neila González, Hygrothermal calibration and validation of vernacular dwellings: a genetic algorithm-based optimisation methodology, J. Build. Eng. 55 (Sep. 2022) 104717, https://doi.org/10.1016/j.jobe.2022.104717.
[156] J. Tchiotsop, S. Bonnet, T.S. Kiessé, N. Issaadi, P. Poullain, Local and global sensitivity analysis of a coupled heat and moisture transfers model: effect of the variability of cob material properties, Heat Mass Tran. (Sep. 2023), https://doi.org/10.1007/s00231-023-03409-0.
[157] M. Tonini De Araújo, H.A. De Souza, A.P. Gomes, Computer simulation of moisture transfer in walls: impacts on the thermal performance of buildings, Architect. Eng. Des. Manag. 18 (4) (Jul. 2022) 453–472, https://doi.org/10.1080/17452007.2021.1916426.
[158] C. D'Erme, et al., Preliminary study of the mechanical and hygrothermal performance of concrete reinforced with fibrillated cellulose, in: Presented at the the 1st International Conference on Innovations for Computing, Engineering and Materials, 2021, Ho Chi Minh, City, Vietnam, 2021 020012, https://doi.org/10.1063/5.0068522.
[159] A. Brambilla, E. Gasparri, Hygrothermal behaviour of emerging timber-based envelope technologies in Australia: a preliminary investigation on condensation and mould growth risk, J. Clean. Prod. 276 (Dec. 2020) 124129, https://doi.org/10.1016/j.jclepro.2020.124129.
[160] C. Boardman, S. Glass, Improving the accuracy of a hygrothermal model for wood-frame walls: a cold-climate study, Buildings 10 (12) (Dec. 2020) 236, https://doi.org/10.3390/buildings10120236.
[161] H. Lee, A. Ozaki, M. Lee, T. Yamamoto, Humidity control effect of vapor-permeable walls employing hygroscopic insulation material, Indoor Air 30 (2) (Mar. 2020) 346–360, https://doi.org/10.1111/ina.12622.
[162] B. Reich, H. Ge, J. Wang, 'Effect of vapor diffusion port on drying of wood-frame walls', in: XV International Conference on Durability of Building Materials and Components. eBook of Proceedings, 2020, https://doi.org/10.23967/dbmc.2020.160.
[163] J. Berger, S. Gasparin, D. Dutykh, N. Mendes, On the solution of coupled heat and moisture transport in porous material, Transport Porous Media 121 (3) (Feb. 2018) 665–702, https://doi.org/10.1007/s11242-017-0980-3.
[164] G. Xing-guo, L. Hongtao, Z. Jingxin, L. Xiang-wei, C. Guo-jie, Sensitivity analysis applied to hygrothermal simulation of a brick building in hot and humid climate, in: 10th International Symposium on Heating, Ventilation and Air Conditioning, ISHVAC, Jinan, China, 205, 2017, pp. 665–671, https://doi.org/10.1016/j.proeng.2017.09.838.
[165] K. Abahri, R. Bennacer, R. Belarbi, Sensitivity analyses of convective and diffusive driving potentials on combined heat air and mass transfer in hygroscopic materials, Numer. Heat Tran., Part A: Applications 69 (10) (May 2016) 1079–1091, https://doi.org/10.1080/10407782.2015.1109389.
[166] A. Ronzino, V. Corrado, Measuring the hygroscopic properties of porous media in transient regime. From the material level to the whole building HAM simulation of a coated room, in: 6th International Building Physics Conference, IBPC, Torino, Italy, 78, 2015, pp. 1501–1506, https://doi.org/10.1016/j.egypro.2015.11.177.
[167] J. Prata, A. Tadeu, N. Simões, Influence of material properties and boundary conditions on the dynamic thermal behaviour of a building corner, in: Presented at the ECO-ARCHITECTURE 2014, Siena, Italy, 2014, pp. 333–345, https://doi.org/10.2495/ARC140291.
[168] A. Evrard, C. Flory-Celini, M. Claeys-Bruno, A. De Herde, Influence of liquid absorption coefficient on hygrothermal behaviour of an existing brick wall with Lime–Hemp plaster, Build. Environ. 79 (Sep. 2014) 90–100, https://doi.org/10.1016/j.buildenv.2014.04.031.
[169] E. Stephan, A. Caucheteux, R. Cantin, S. Tasca-Guernouti, P. Michel, Sensitivity analysis of an energyplus simulation model of the ambient humidity in an old building, in: Presented at the 2017 Building Simulation Conference, 2013, https://doi.org/10.26868/25222708.2013.2161.
[170] A. Dung Tran Le, C. Maalouf, O. Douzane, T. Hoang Mai, T. Langlet, M. Lachi, Parametric study of hygrothermal behaviour of A room made of hemp concrete, in: Presented at the 2017 Building Simulation Conference, 2013, https://doi.org/10.26868/25222708.2013.1004.
[171] T. Oreszczyn, S.E.C. Pretlove, Condensation Targeter II: modelling surface relative humidity to predict mould growth in dwellings, Build. Serv. Eng. Res. Tecnol. 20 (3) (Aug. 1999) 143–153, https://doi.org/10.1177/014362449902000307.
[172] S. Hokoi, M.K. Kumaran, Experimental and analytical investigations of simultaneous heat and moisture transport through glass fiber insulation, J. Therm. Insul. Build. Envelopes 16 (3) (Jan. 1993) 263–292, https://doi.org/10.1177/109719639301600307.
[173] M. Benkhaled, S.-E. Ouldboukhitine, A. Bakkour, S. Amziane, Sensitivity analysis of the parameters for assessing a hygrothermal transfer model HAM in bio-based hemp concrete material, Int. Commun. Heat Mass Tran. 132 (Mar. 2022) 105884, https://doi.org/10.1016/j.icheatmasstransfer.2022.105884.
[174] I. Vandemeulebroucke, S. Caluwaerts, N. Van Den Bossche, Factorial study on the impact of climate change on freeze-thaw damage, mould growth and wood decay in solid masonry walls in brussels, Buildings 11 (3) (Mar. 2021) 134, https://doi.org/10.3390/buildings11030134.
[175] O. May Tzuc, et al., Modeling of hygrothermal behavior for green facade's concrete wall exposed to nordic climate using artificial intelligence and global sensitivity analysis, J. Build. Eng. 33 (Jan. 2021) 101625, https://doi.org/10.1016/j.jobe.2020.101625.
[176] I. Vandemeulebroucke, S. Caluwaerts, N. Bossche, Freeze-thaw risk in solid masonry: are 'hygrothermal response based' analyses mandatory when studying the sensitivity of building envelopes to climate change?, in: XV International Conference on Durability of Building Materials and Components. eBook of Proceedings, 2020, https://doi.org/10.23967/dbmc.2020.070.
[177] J. Kocí, V. Kocí, J.M.D. Silva, Z. Hlaváčová, J. Madèra, Hygrothermal model for description of ice-forming process in porous building materials: sensitivity analysis of input material parameters, in: Presented at the INTERNATIONAL CONFERENCE OF COMPUTATIONAL METHODS IN SCIENCES and ENGINEERING 2018 (ICCMSE 2018), Thessaloniki, Greece, 2018 040012, https://doi.org/10.1063/1.5079098.
[178] G.B.A. Coelho, H.E. Silva, F.M.A. Henriques, Calibrated hygrothermal simulation models for historical buildings, Build. Environ. 142 (Sep. 2018) 439–450, https://doi.org/10.1016/j.buildenv.2018.06.034.
[179] M. Bart, S. Moissette, Y. Ait Oumeziane, C. Lanos, Transient hygrothermal modelling of coated hemp-concrete walls, European Journal of Environmental and Civil Engineering 18 (8) (Sep. 2014) 927–944, https://doi.org/10.1080/19648189.2014.911122.
[180] I. Othmen, Sensitivity analysis of the Künzel model: application to the study of the hygrothermal transfer in a tuffeau wall, in: Presented at the HEAT TRANSFER 2014, A Coruña, Spain, 2014, pp. 417–428, https://doi.org/10.2495/HT140361.
[181] E. Barreira, V.P. De Freitas, External thermal insulation composite systems: critical parameters for surface hygrothermal behaviour, Adv. Mater. Sci. Eng. 2014 (2014) 1–16, https://doi.org/10.1155/2014/650752.
[182] V. Kocí, J. Madèra, R. Černý, Exterior thermal insulation systems for AAC building envelopes: computational analysis aimed at increasing service life, Energy Build. 47 (Apr. 2012) 84–90, https://doi.org/10.1016/j.enbuild.2011.11.030.
[183] P. Cabrera, H. Samuelson, M. Kurth, Simulating mould risks under future climate conditions, in: Presented at the Building Simulation, 2019, pp. 1530–1538, https://doi.org/10.26868/25222708.2019.211130. Rome, Italy.
[184] J. Selih, R. Zarnic, Influence of environmental conditions upon behaviour of historical buildings, in: 6th International Conference on Structural Studies, Repairs and Maintenance of Historical Buildings (STREMAH 99), CESBP 2022, Dresden Germany, Jun. 1999, p. 10.
[185] B. Vanderschelden, N.V.D. Bossche, Fit for purpose brick clustering for hygrothermal material properties: sensitivity to climate conditions, in: 5th Central European Symposium on Building Physics, CESBP 2022, Bratislava, Slovakia, 2023 020065, https://doi.org/10.1063/5.0173303.

[186] A.D. Tran Le, C. Maalouf, K.C. Mendonça, T.H. Mai, E. Wurtz, Study of moisture transfer in a double-layered wall with imperfect thermal and hydraulic contact resistances, Journal of Building Performance Simulation 2 (4) (Dec. 2009) 251–266, https://doi.org/10.1080/19401490903082459.
[187] K. Zhang, R. Richman, Parametric analysis of moisture sorption isotherms for wood sheathing using hygrothermal modelling, J. Build. Eng. 28 (Mar. 2020) 101047, https://doi.org/10.1016/j.jobe.2019.101047.
[188] J. Winkler, J. Munk, J. Woods, Effect of occupant behavior and air-conditioner controls on humidity in typical and high-efficiency homes, Energy Build. 165 (Apr. 2018) 364–378, https://doi.org/10.1016/j.enbuild.2018.01.032.
[189] V. Nik and A. S. Kalagasidis, 'Influence of the uncertainties in future climate scenarios on the hygrothermal simulation of an attic', in International Conference on Building Envelope Systems and Technologies, ICBEST 2010, Vancouver, Canada, June 27-30.
[190] A. Saltelli (Ed.), Sensitivity Analysis in Practice: a Guide to Assessing Scientific Models, Wiley, Hoboken, NJ, 2004.
[191] D.M. Hamby, A comparison of sensitivity analysis techniques, Health Phys. 68 (2) (Feb. 1995) 195–204, https://doi.org/10.1097/00004032-199502000-00005.
[192] A. Saltelli, Sensitivity analysis: could better methods be used? J. Geophys. Res. 104 (D3) (Feb. 1999) 3789–3793, https://doi.org/10.1029/1998JD100042.
[193] F. Pianosi, T. Wagener, A simple and efficient method for global sensitivity analysis based on cumulative distribution functions, Environ. Model. Software 67 (May 2015) 1–11, https://doi.org/10.1016/j.envsoft.2015.01.004.
[194] W.J. Conover, Practical Nonparametric Statistics, third ed., Wiley, New York, 1999.
[195] R.L. Iman, W.J. Conover, The use of the rank transform in regression, American Statistical Association and are collaborating with JSTOR to digitize, preserve and extend access to Technometrics 21 (4) (2021) 12.
[196] J.C. Helton, J.D. Johnson, C.J. Sallaberry, C.B. Storlie, Survey of sampling-based methods for uncertainty and sensitivity analysis, Reliab. Eng. Syst. Saf. 91 (10–11) (Oct. 2006) 1175–1209, https://doi.org/10.1016/j.ress.2005.11.017.
[197] R.L. Iman, J.C. Helton, An investigation of uncertainty and sensitivity analysis techniques for computer models, Risk Anal. 8 (1) (Mar. 1988) 71–90, https://doi.org/10.1111/j.1539-6924.1988.tb01155.x.
[198] S.F. Sawyer, Analysis of variance: the fundamental concepts, J. Man. Manip. Ther. 17 (2) (Apr. 2009) 27E–38E, https://doi.org/10.1179/jmt.2009.17.2.27E.
[199] D.C. Montgomery, Design and Analysis of Experiments, eighth ed., John Wiley & Sons, Inc, Hoboken, NJ, 2013.
[200] I.M. Sobol, Sensitivity estimates for nonlinear mathematical models, Math. Model Civ. Eng. 4 (1993) 407–414.
[201] I.M. Sobol, Global sensitivity indices for nonlinear mathematical models and their Monte Carlo estimates, Math. Comput. Simulat. 55 (1–3) (Feb. 2001) 271–280, https://doi.org/10.1016/S0378-4754(00)00270-6.
[202] A. Saltelli, R. Bolado, An alternative way to compute Fourier amplitude sensitivity test (FAST), Comput. Stat. Data Anal. 26 (4) (Feb. 1998) 445–460, https://doi.org/10.1016/S0167-9473(97)00043-1.
[203] L. Breiman, Random forests, Mach. Learn. 45 (1) (2001) 5–32.
[204] G.H. Golub, C.F. Van Loan, Matrix Computations, fourth ed., The Johns Hopkins University Press, Baltimore, 2013.
[205] M.D. Morris, Factorial sampling plans for preliminary computational experiments, Technometrics 33 (2) (May 1991) 161–174, https://doi.org/10.1080/00401706.1991.10484804.
[206] A. Saltelli, et al., Global Sensitivity Analysis: the Primer. Chichester, England ; Hoboken, NJ, John Wiley, 2008.
[207] F. Campolongo, J. Cariboni, A. Saltelli, An effective screening design for sensitivity analysis of large models, Environ. Model. Software 22 (10) (Oct. 2007) 1509–1518, https://doi.org/10.1016/j.envsoft.2006.10.004.
[208] M. Gutland, S. Bucking, M. Santana Quintero, A methodology for hygrothermal modelling of imperfect masonry interfaces, J. Build. Phys. 44 (6) (May 2021) 485–509, https://doi.org/10.1177/1744259121989388.
[209] J.H. Lee, M.S. Yeo, Condensation control to cope with occupancy activity and effectively mitigate condensation in unheated spaces by real-time sensor control strategy, Sustainability 12 (10) (May 2020) 4033, https://doi.org/10.3390/su12104033.
[210] S. Pallin, P. Boudreaux, S.J. Jo, M. Perez, A. Albaugh, Simulations of indoor moisture generation in U.S. Homes, in: Advances in Hygrothermal Performance of Building Envelopes: Materials, Systems and Simulations, Pennsylvania, USA, 2017, pp. 261–290, https://doi.org/10.1520/STP159920160111.
[211] E. Buechler, S. Pallin, P. Boudreaux, M. Stockdale, Probabilistic modeling of the indoor climates of residential buildings using EnergyPlus, J. Build. Phys. 41 (3) (Nov. 2017) 225–246, https://doi.org/10.1177/1744259117701893.
[212] RIBuild', RIBuild. https://www.ribuild.eu (accessed December. 3, 2023).
[213] Tietze, Andrea; Ott, Stephan; Boulet, Sylvain; Gradeci, Klodian; Labonnote, Nathalie; Grynning, Steinar; Noreen, Joakim; Pousette, Anna; Tall Timber Facades – Identification of Cost-Effective and Resilient Envelopes for Wood Constructions Scientific Project Report; Technical University Munich; Munich; 31. July.2017.
[214] E.E. Thybring, C.R. Boardman, S.L. Zelinka, S.V. Glass, Common sorption isotherm models are not physically valid for water in wood, Colloids Surf. A Physicochem. Eng. Asp. 627 (2021) 127214, https://doi.org/10.1016/j.colsurfa.2021.127214. Oct.
[215] I. Vandemeulebroucke, S. Caluwaerts, N. Van Den Bossche, Decision framework to select moisture reference years for hygrothermal simulations, Build. Environ. 218 (Jun. 2022) 109080, https://doi.org/10.1016/j.buildenv.2022.109080.
[216] I. Goodfellow, Y. Bengio, A. Courville, Deep Learning, The MIT Press, Cambridge, Massachusetts, 2016.
[217] R.Z. Freire, G.H. dos Santos, L. dos S. Coelho, Hygrothermal dynamic and mould growth risk predictions for concrete tiles by using least squares support vector machines, Energies 10 (8) (Jul. 2017) 1093, https://doi.org/10.3390/en10081093.
[218] V.N. Vapnik, S. Kotz, Estimation of Dependencies Based on Empirical Data, second ed., Springer, New York, 2006.
[219] R. Rodríguez-Pérez, J. Bajorath, Evolution of support vector machine and regression modeling in chemoinformatics and drug discovery, J. Comput. Aided Mol. Des. 36 (5) (May 2022) 355–362, https://doi.org/10.1007/s10822-022-00442-9.
[220] N. Bansal, M. Defo, M.A. Lacasse, Application of support vector regression to the prediction of the long-term impacts of climate change on the moisture performance of wood frame and massive timber walls, Buildings 11 (5) (Apr. 2021) 188, https://doi.org/10.3390/buildings11050188.
[221] P. Roßbach, Neural networks vs. Random forests – does it always have to be deep learning? Frankfurt School Blog (2018). https://blog.frankfurt-school.de/de/neural-networks-vs-random-forests-does-it-always-have-to-be-deep-learning/ (accessed Jun. 26, 2023).
[222] R.H. Myers, D.C. Montgomery, C.M. Anderson-Cook, Response Surface Methodology: Process and Product Optimization Using Designed Experiments, third ed., Wiley, 2009.
[223] N.R. Draper, H. Smith, Applied Regression Analysis, third ed., Wiley, 1998.
[224] T. Hastie, R. Tibshirani, Generalized additive models, Stat. Sci. 1 (3) (1986) 297–318.
[225] T.J. Santner, B.J. Williams, W.I. Notz, The Design and Analysis of Computer Experiments, 2014.
[226] C.M. Bishop, Pattern Recognition and Machine Learning, Springer, New York, 2006.
[227] H. Abdi, Partial least squares regression and projection on latent structure regression (PLS Regression), WIREs Computational Stats 2 (1) (Jan. 2010) 97–106, https://doi.org/10.1002/wics.51.
[228] Delphin. https://bauklimatik-dresden.de/delphin/index.php?aLa=en, 26-May-2021. (Accessed 26 May 2021).
[229] WUFI (en). https://wufi.de/en/, 26-May-2021. (Accessed 26 May 2021).
[230] M. Defo, M. Lacasse, A. Laouadi, A comparison of hygrothermal simulation results derived from four simulation tools, J. Build. Phys. (Feb. 2021) 174425912098876, https://doi.org/10.1177/1744259120988760.
[231] B. Hejazi, N. Rodrigues Marques Sakiyama, J. Frick, H. Garrecht, Hygrothermal simulations comparative study: assessment of different materials using WUFI and DELPHIN software, in: Presented at the Building Simulation 2019, Rome, Italy, 2021, pp. 4674–4681, https://doi.org/10.26868/25222708.2019.211033.
[232] H.M. Künzel, Simultaneous Heat and Moisture Transport in Building Components: One- and Two-Dimensional Calculation Using Simple Parameters, IRB-Verl, Stuttgart, 1995. ISBN 3-8167-4103-7.
[233] A.S. Kalagasidis, HAM-tools - an Integrated Simulation Tool for Heat, Air and Moisture Transfer Analyses in Building Physics, Chalmers University of Technology, 2004.
[234] H. Janssen, B. Blocken, J. Carmeliet, Conservative modelling of the moisture and heat transfer in building components under atmospheric excitation, Int. J. Heat Mass Tran. 50 (5–6) (Mar. 2007) 1128–1140, https://doi.org/10.1016/j.ijheatmasstransfer.2006.06.048.
[235] M. de Wit, HAMBASE: Heat, Air and Moisture Model for Building and Systems Evaluation. Eindhoven, Technische Universiteit Eindhoven, Faculteit Bouwkunde, 2006.
[236] C.-E. Hagentoft, Simplified Analysis of Combined Heat, Moisture and Air Transport for One-Dimensional Cases, Lund University, Sweden, 1992. Tl-S-92/04.
[237] 'EnergyPlus | EnergyPlus'. https://energyplus.net/, 26-May-2021. (Accessed 26 May 2021).
[238] W. Maref, S.M. Cornick, K. Abdulghani, D. van Reenen, An Advanced hygrothermal design tool "hygIRC 1-D", in: eSim 2004 Conference, Vancouver, Canada, 2004, p. 6.
[239] A.B. Comsol, Heat Transfer Module Users Guide with Comsol, COMSOL, 2018.
[240] Building performance - simulation software | EQUA. https://www.equa.se/en/, 26-May-2021. (Accessed 26 May 2021).
[241] J.M.P.Q. Delgado, E. Barreira, N.M.M. Ramos, V.P. de Freitas, Hygrothermal Numerical Simulation Tools Applied to Building Physics, Springer Berlin Heidelberg, Berlin, Heidelberg, 2013.
[242] J.M.P.Q. Delgado, N.M.M. Ramos, E. Barreira, V.P. de Freitas, A critical review of hygrothermal models used in porous building materials, J. Med. 13 (3) (2010) 221–234, https://doi.org/10.1615/JPorMedia.v13.i3.30.
[243] A. Worch, Internal thermal insulation and surface temperatures on intersecting internal walls, Innendämmung und Oberflächentemperaturen an einbindenden Innenwänden, Bauphysik 43 (1) (Feb. 2021) 36–43, https://doi.org/10.1002/bapi.202000022.
[244] T. Isaksson, S. Thelandersson, A. Ekstrand-Tobin, P. Johansson, Critical conditions for onset of mould growth under varying climate conditions, Build. Environ. 45 (7) (Jul. 2010) 1712–1721, https://doi.org/10.1016/j.buildenv.2010.01.023.
[245] Finnish mould growth model | Building Physics | Tampere Universities', Building Physics. https://research.tuni.fi/buildingphysics/finnish-mould-growth-model/(accessed Jun. 30, 2022).
[246] K. Gradeci, N. Labonnote, B. Time, J. Köhler, Mould growth criteria and design avoidance approaches in wood-based materials – a systematic review, Construct. Build. Mater. 150 (Sep. 2017) 77–88, https://doi.org/10.1016/j.conbuildmat.2017.05.204.

[247] J. Wang, Asthma and Rhinitis Among Adults in Sweden and China, Risk Factors in the Home Environment, Uppsala University, Sweden, 2018. Doctoral thesis.
[248] S. Urlaub, G. Grün, P. Foldbjerg, Mould and Dampness in European Homes and Their Impact on Health, Fraunhofer-Institut für Bauphysik IBP, Stuttgart, Germany, Nov. 2016, https://doi.org/10.13140/RG.2.2.18770.76488. EER-058/2016/950.
[249] G. Grün, S. Urlaub, Towards an Identification of European Indoor Environments' Impact on Health and Performance - Homes and Schools, Fraunhofer-Institut für Bauphysik IBP, Stuttgart, Germany, Dec. 2014.
[250] J.D. Thacher, et al., Mold and dampness exposure and allergic outcomes from birth to adolescence: data from the BAMSE cohort, Allergy 72 (6) (Jun. 2017) 967–974, https://doi.org/10.1111/all.13102.
[251] J.K. Peat, J. Dickerson, J. Li, Effects of damp and mould in the home on respiratory health: a review of the literature, Allergy 53 (2) (Feb. 1998) 120–128, https://doi.org/10.1111/j.1398-9995.1998.tb03859.x.
[252] R. Rylander, R. Etzel, Introduction and summary: workshop on children's health and indoor mold exposure, Environ. Health Perspect. 107 (suppl 3) (Jun. 1999) 465–468, https://doi.org/10.1289/ehp.99107s3465.
[253] A. Delanoë, N. Heutte, S. Gente, V. Séguin, D. Garon, Relationships between exposure to bioaerosols, moldy surface and symptoms in French mold-damaged homes, Atmosphere 11 (3) (2020) 223, https://doi.org/10.3390/atmos11030223. Feb.
[254] D. Norbäck, Z. Hashim, F. Ali, J.H. Hashim, Asthma symptoms and respiratory infections in Malaysian students-associations with ethnicity and chemical exposure at home and school, Environ. Res. 197 (Jun. 2021) 111061, https://doi.org/10.1016/j.envres.2021.111061.
[255] S. Li, et al., Household mold exposure in association with childhood asthma and allergic rhinitis in a northwestern city and a southern city of China, J. Thorac. Dis. 14 (5) (May 2022) 1725–1737, https://doi.org/10.21037/jtd-21-1380.
[256] E. Anyanwu, A.W. Campbell, J. Jones, J.E. Ehiri, A.I. Akpan, The neurological significance of abnormal natural killer cell activity in chronic toxigenic mold exposures, Sci. World J. 3 (2003) 1128–1137, https://doi.org/10.1100/tsw.2003.98.
[257] J.D. Thrasher, S. Crawley, The biocontaminants and complexity of damp indoor spaces: more than what meets the eyes, Toxicol. Ind. Health 25 (9–10) (Oct. 2009) 583–615, https://doi.org/10.1177/0748233709348386.
[258] X. Wang, et al., Using machine learning method to discover hygrothermal transfer patterns from the outside of the wall to interior bamboo and wood composite sheathing, Buildings 12 (7) (Jun. 2022) 898, https://doi.org/10.3390/buildings12070898.

Paper II

Building and Environment 243 (2023) 110703

Contents lists available at ScienceDirect

Building and Environment

journal homepage: www.elsevier.com/locate/buildenv

Robust probabilistic modelling of mould growth in building envelopes using random forests machine learning algorithm

Mohsen Bayat Pour [a,*], Jonas Niklewski [a], Amir Naghibi [b], Eva Frühwald Hansson [a]

[a] Division of Structural Engineering, Department of Building and Environmental Technology, Lund University, John Ericssons väg 1, SE-223 63, Lund, Sweden
[b] Division of Water Resources Engineering, Department of Building and Environmental Technology, Lund University, John Ericssons väg 1, SE-223 63, Lund, Sweden

ARTICLE INFO

Keywords:
Mould assessment
Reliability analysis
Sensitivity analysis
Hygrothermal simulation
Machine learning
Building envelope

ABSTRACT

Probabilistic methods can be used to account for uncertainties in hygrothermal analysis of building envelopes. This paper presents methods for robust mould reliability analysis and identification of critical parameters. Mould indices are calculated by probabilistic hygrothermal analysis, followed by the application of the "Finnish mould growth model." To increase the robustness of the mould growth analysis, a random forests metamodel is first trained on the dataset and then used to expand the number of simulations. Finally, the reliability is calculated based on the probability of exceeding a given maximum mould index limit state. Critical parameters are identified through a sensitivity analysis based on linear and non-linear dependencies between inputs and maximum mould index. The methods are demonstrated by analysing three external wall assemblies. In conclusion, the mould reliability analysis method helps to assess the robustness of the hygrothermal analysis and mould assessment by investigating the influence of hygrothermal variables' uncertainties on the maximum mould index. By combining a metamodel with probabilistic analysis, it is possible to significantly reduce the amount of time required to evaluate a large number of scenarios.

1. Introduction

1.1. Background

Hygrothermal analysis is commonly used to model the performance of external wall assemblies before construction, helping to mitigate moisture-related issues including microbial growth, such as mould [1]. These issues have been linked to various health concerns including asthma, allergic rhinitis, lung cancer, and skin disorders [2–5].

The likelihood of mould growth in exterior walls can be determined by analyzing the temporal variation of temperature and relative humidity. To predict the germination and growth of mould in buildings, various mould models have been developed, such as the International Energy Agency (IEA) [6], Lowest Isopleth for Mould (LIM) [7], Mould germination graph [8], Finnish mould growth model [9], Mould Resistance Design (MRD) [10], and m-model [11,12]. When analyzing existing structures, these models are typically fed with measurements. However, in the design phase, input is modelled instead.

In building physics applications, deterministic modelling is predominantly used, where inputs such as material properties, climate conditions, and geometry are treated as discrete variables. However, this approach may not account for uncertainties and can result in a single or limited number of simulations to determine whether a design passes or fails the analysis. Probabilistic approaches treat inputs as stochastic variables and therefore consider their associated uncertainties. This results in a distribution of outcomes, allowing for a more comprehensive analysis of the design's performance. By using probabilistic methods, the probability of failure can be determined, providing valuable information for decision-making processes. In the context of assessing the risk of mould growth in exterior walls, it is essential to consider the uncertainties associated with inputs such as the material properties, climate conditions, and geometry, as these can have a significant impact on the outcome of the analysis.

The use of probabilistic analysis in hygrothermal simulations was first introduced by Geving [13] in 1997 and has since been applied to a wide range of hygrothermal applications, such as the analysis of uncertainties associated with material properties [14–16], boundary conditions [17,18], moisture production rates [19], risk of frost damage in masonry constructions [20], and effect of built-in moisture [21].

In the field of mould assessment, Hens [22] proposed a probabilistic method for fungal defacement, while Moon et al. [23–25] introduced a

* Corresponding author.
E-mail addresses: mohsen.bayat_pour@kstr.lth.se (M. Bayat Pour), jonas.niklewski@kstr.lth.se (J. Niklewski), amir.naghibi@tvrl.lth.se (A. Naghibi), eva.fruhwald_hansson@kstr.lth.se (E. Frühwald Hansson).

https://doi.org/10.1016/j.buildenv.2023.110703
Received 6 May 2023; Received in revised form 31 July 2023; Accepted 3 August 2023
Available online 4 August 2023
0360-1323/© 2023 The Authors. Published by Elsevier Ltd. This is an open access article under the CC BY license (http://creativecommons.org/licenses/by/4.0/).

Nomenclature

A-value	Water Uptake Coefficient [kg/m^2. s$^{0.5}$]
CDF	Cumulative Distribution Function
CLT	Cross-Laminated Timber
CoV	Coefficient of Variation
Cp	Specific Heat Capacity [J/kg.K]
CS*i*	Case Study *i*
D	Original dataset
D_B	Bulk Density [kg/m^3]
D_i	Bootstrap subset
EPS	Expanded PolyStyrene
g_m	Limit state function
IDA	Inutility Decision Analysis
$I_{M,ls}$	Mould Limit State
$I_{M,max}$	Maximum Mould Index
k	Number of trees
LHS	Latin Hypercube Sampling
MAE	Mean Absolute Error
MDF	Medium Density Fibreboard
MDRY	Moisture Design Reference Year
ML	Machine Learning
MRA	Mould Reliability Analysis
MRD	Mould Resistance Design
MSA	Mould Sensitivity Analysis
N	Number of scenarios
n	Total number of original data
OF_i	Objective function
OSB	Oriented Strand Board
PA	Probabilistic Analysis
$P(M_{Ii})$	Probability of mould index *i*
RA	Reliability Analysis
RCC	Rank Correlation Coefficient
RF	Random Forests
RMSE	Root Mean Square Error
$R(M_{Ii})$	Reliability of mould index *i*
R^2	Coefficient of Determination
SA	Sensitivity Analysis
T	Temperature [°C]
t	Time [hour]
t_p	Prediction time per scenario
t_s	Simulation time per scenario
VTT	Technical Research Centre of Finland
WDR	Wind-driven Rain
WHO	World Health Organization
y_i	Original data
$\overline{y_i}$	Mean of the original data
$\widehat{y_i}$	Predicted data
ε_i	Convergence value
θ_{por}	Porosity [m^3/m^3]
λ_{dry}	Thermal Conductivity [W/m.K]
μ	Mean
μ_{VDR}	Water Vapour Diffusion Resistance Factor [−]
ρ	Spearman's correlation coefficient
σ	Standard deviation
φ	Relative humidity [%]

mixed simulation approach that determines the mould risk indicator and links it to decision analysis theory. Hagentoft and Sasic Kalagasidis [26] studied the impact of building systems and construction design characteristics on mould growth potential in cold attics. Wang and Ge [27,28] analyzed the hygrothermal performance and assessed the mould growth potential of wooden-based wall assemblies, such as highly insulated wood-framed walls and cross-laminated timber wall assemblies, by utilizing a probabilistic model. Gradeci et al. [29,30] compared different external wall assemblies based on various mould models and used a probabilistic methodology to predict mould growth in façade construction.

Sensitivity analysis is an important tool used to identify the most significant input variables that impact the output variables during a simulation process. It helps streamline the design revision process and makes it more efficient. In the context of mould assessment, several scientists have used sensitivity analysis to identify sensitive variables. Moon and Augenbroe [23,24], Rivalin et al. [31], and Gradeci et al. [32] performed the hygrothermal sensitivity analysis using the Morris method [33] to find the sensitive variables in mould growth. Gradeci et al. [30] compared six different sensitivity analysis techniques and related sensitive variables in mould growth for a highly insulated external wall. Zhao [34] applied Spearman's correlation coefficient and Partial Correlation Coefficient to examine the influence of the input variables of the hygrothermal model on the outputs. Freudenberg et al. [35] also used Spearman's correlation coefficient to investigate the effect of surface exchange coefficients and measured material properties on the hygrothermal performance of masonry materials. Calle and Van Den Bossche [36] used Spearman's correlation coefficient for a preliminary study to determine the sensitive variables in a potential risk analysis in historic masonry constructions.

Probabilistic methodology, based on the Monte Carlo method, often involves thousands of simulations, which can make it computationally inefficient. To address this issue, several studies have investigated the use of metamodels, which are simplified models that can predict how a building reacts in terms of hygrothermal performance [37–47].

Marincioni et al. [37] created a metamodel using generalized additive models (GAM) and generalized additive models for location scale and shape (GAMLS) to evaluate the moisture risk of internally insulated wall assemblies. The authors found that the predicted results from the metamodels were close to the results obtained from simulations, with a few exceptions where the predicted values were lower than the actual values.

Tijskens et al. [38–43] used neural networks as a substitute for numerical models to reduce computational time. They focused on using various machine learning algorithms to predict the response time series rather than predicting a single response performance. Based on various applications, such as massive masonry and timber frame walls, they assessed the effectiveness and training time of various common types of networks, such as multilayer perceptron (MLP), recurrent neural network (RNN), and convolutional neural network (CNN). The authors discovered that CNN is the most accurate and fastest type of neural network for predicting transient and non-linear hygrothermal time series.

Freire et al. [44] used Support Vector Regression (SVR) to predict the mould index, sensible and latent heat fluxes, and water vapour flux for a building's roof assembly. The results indicated an acceptable R^2 for each of the examined output parameters. Bansal et al. [45] investigated the application of SVR to predict the long-term hygrothermal performance of massive timber and light wood-frame walls, and found that the model can successfully predict the hygrothermal responses with a suitable choice of input factors.

Aggarwal et al. [46,47] used Partial Least Squares (PLS) regression to develop the metamodel for hygrothermal simulations using hourly historical and projected future climate data for cities located in various climate zones across Canada. The authors found that the model can accurately predict the hygrothermal performance of brick-clad

wood-frame wall assemblies in the selected cities and over both historical and future climates with proper training dataset selection.

1.2. Objectives and outline of the paper

This study aims to introduce two new methods for mould reliability and sensitivity analysis using the Random Forests (RF) algorithm combined with a probabilistic hygrothermal model. RF is chosen as the metamodel due to its ability to address the complex relationships between input and output variables in highly nonlinear and transient hygrothermal performance of buildings. Successful applications of RF in complex modelling and nonlinear analysis can be found in other studies [48–50]. Therefore, the main focus of this study is to introduce and discuss the merits of our proposed methods and show their application and utility by three case studies.

This paper is composed of four main sections. The first section provides the background and importance of the probabilistic hygrothermal analysis and mould assessment, as well as the objectives of the study. The second section describes the methodology, including the mould reliability and sensitivity analysis methods and the case studies. The third section presents the results and discussions, along with the reproducibility check. Finally, the fourth section offers the conclusions of the paper.

2. Methodology

2.1. Mould reliability analysis method

The proposed methods, Mould Reliability Analysis (MRA) and Mould Sensitivity Analysis (MSA), are presented in Fig. 1. MRA includes two sections: Probabilistic Analysis (PA) and Reliability Analysis (RA), and is based on Monte Carlo [51] simulation. PA comprises four parts: hygrothermal problem designation, primary sampling, hygrothermal modelling, and mould modelling. RA comprises five parts: feature selection, machine learning framework, secondary sampling, machine learning modelling, and reliability and failure probability calculations.

Hygrothermal problem designation is associated with specifying the initial properties (e.g., geometry, material properties, climate data) and boundary conditions (indoor and outdoor surfaces) of a building envelope. The probability distributions of the stochastic variables in this part could be specified following available literature data or laboratory tests; however, in this study, the probability distributions of the variables were determined only according to the available literature.

Primary sampling and scenario-making (combinations of random samples) are performed by the Latin Hypercube Sampling (LHS) technique [52] for all stochastic variables. This technique has been shown to be a reliable and efficient sampling method, requiring fewer samples compared to other methods such as Simple Random Sampling, Crude Monte Carlo Sampling, and Stratified Sampling [34,53–55]. LHS was implemented in this study using Python code [56].

The inputs generated by the above two steps are used in *hygrothermal modelling*. Among the available hygrothermal simulation tools, Delphin [57] was selected and integrated with the MRA method due to its batch calculation potential, which allows for programmatically varying input variables and queueing simulations. Delphin is a tool for analysing multi-dimensional construction assemblies for heat, air, moisture, pollutant, and salt transportation. Additionally, several studies demonstrate that Delphin is a reliable tool for hygrothermal performance analysis [58,59]. To run simulations with Delphin, the outdoor climate data must be generated and converted to a format acceptable to Delphin. This study utilized the Meteonorm meteorological database [60] for obtaining hourly climate data over one typical year generated from measured data. The generated outdoor climate data is then formatted to Delphin's native format. It is worth noting that outdoor climate data may also be generated using other methods such as time series analysis according to the autoregressive-moving-average (ARMA) model [29] or using "Moisture Design Reference Year (MDRY)" [61]. The results of hygrothermal simulations, including the temporal variation of relative humidity (φ) and temperature (T) at different points of interest, can be stored after each simulation.

The maximum mould index of each scenario is calculated in the *mould modelling*. The Finnish mould growth model [9], which was developed based on the VTT model [62,63], is used in this section. Based on this mould model, the mould assessment is reported based on mould

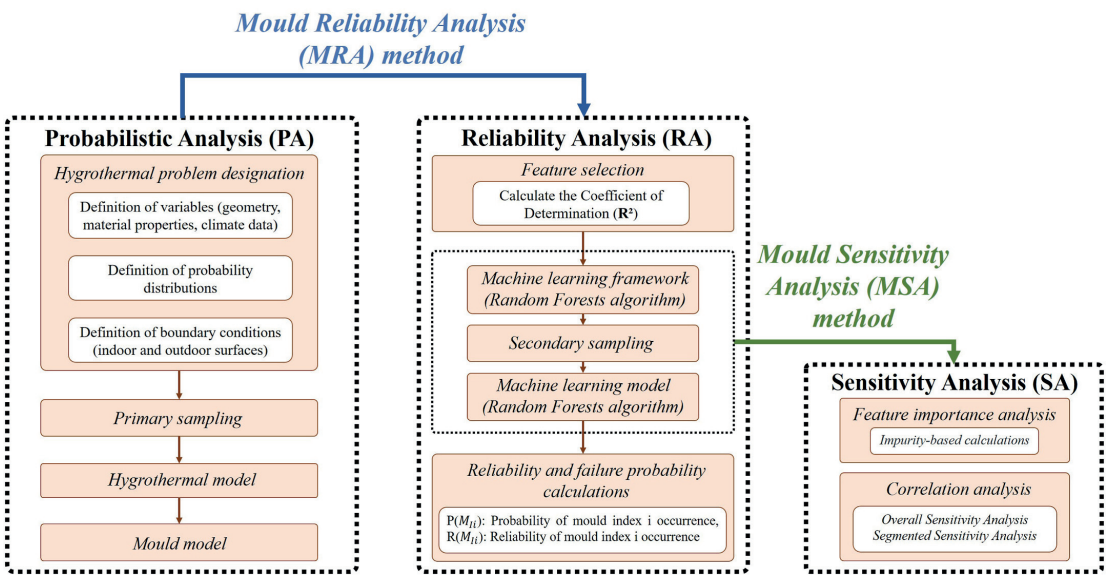


Fig. 1. Mould Reliability Analysis (MRA) and Mould Sensitivity Analysis (MSA) methods.

index ranging from 0 to 6. The Finnish mould growth model has the potential to be utilized for all building materials and structures, including the impact of surface types and surface coatings, by defining sensitivity and decline classes. In comparison, the original VTT model [64] was developed only for wooden-based materials like pine and spruce. The Mould Reliability Analysis (MRA) method is compatible with all existing mould models, and other mould models like Mould Resistance Design (MRD) [10] and m-model [11,12] can replace the Finnish mould growth model. The application of different mould models to the external wall assemblies enables a comparison of their results, leading to a more proper judgment.

The Reliability Analysis (RA) section of the MRA method aims to analyze the reliability of mould assessment. The robustness of this analysis is increased by incorporating a Random Forests (RF) machine learning (ML) algorithm, effectively being used to expand the number of scenarios. This section is initiated by *feature selection*. The process of selecting features for the metamodel involved several steps. Firstly, the coefficient of determination (R^2) was calculated for each input variable in relation to the output variable. These features were then ranked based on their R^2 values. Starting with the highest-ranked feature, an initial metamodel was created and its R^2 value was determined. Subsequently, additional features were sequentially incorporated, with the R^2 value calculated for each new metamodel. This process was repeated until all features were included. The metamodel with the highest R^2 value was ultimately selected, and the chosen features were used for further calculations. By systematically evaluating the relationships between features and the target variable, a robust and optimized metamodel was obtained for subsequent analyses. This step ensures that the selected features have a significant impact on the output and helps to reduce the number of input variables used in the metamodel. It should be noted that the inclusion of unnecessary features in the metamodel creation process may result in a slight reduction in model performance.

To assess the accuracy of the trained model, three indicators—the root mean square error (RMSE), mean absolute error (MAE), and coefficient of determination (R^2)—are used. The accuracy is evaluated using Equations (1)–(3):

$$RMSE = \sqrt{\frac{1}{n}\sum_{i=1}^{n}(y_i - \hat{y}_i)^2} \tag{1}$$

$$MAE = \frac{1}{n}\sum_{i=1}^{n}|y_i - \hat{y}_i| \tag{2}$$

$$R^2 = 1 - \frac{\sum_{i=1}^{n}(y_i - \hat{y}_i)^2}{\sum_{i=1}^{n}(y_i - \bar{y}_i)^2} \tag{3}$$

where y_i and $\hat{y}_i$ are the original and predicted data, $\bar{y}_i$ is the mean of the original data, and n is the total number of original datapoints. These equations provide quantitative measures of how well the trained model performs in predicting the maximum mould index. The RMSE and MAE indicate the average error between the predicted and observed values, while the R^2 represents the proportion of the variance in the output that can be explained by the input variables. The lower the RMSE and MAE, and the higher the R^2, the better the trained model is in predicting mould growth.

In the *secondary sampling* part, the LHS technique is used to generate samples and scenarios for a big dataset ($n = 10^7$), similar to the primary sampling. Using the trained *machine learning model*, the maximum mould index of each scenario is predicted.

In the final step of the MRA method, *reliability and failure probability calculations* are performed. The probability of failure is computed in analogy to structural reliability applications where the failure occurs when the loads are greater than the resistance (capacity). In this application, the limit state function, g_m, comprises two parameters. The former is Mould Limit State, $I_{M,ls}$, which corresponds to the capacity in structural reliability utilizations. The latter is the Maximum Mould Index, $I_{M,max}$, which corresponds to the load in structural reliability applications. The maximum mould index is a function of Temperature, T, Relative humidity, φ, and time, t. Thus, the limit state function can be identified by Equation (4):

$$g_m = I_{M,ls} - I_{M,max}(T, \varphi, t) \tag{4}$$

Any violation of the limit state function $g_m < 0$ indicates that the maximum mould index of the intended scenario, $I_{M,max}$, is higher than the predefined mould limit state, $I_{M,ls}$. The probability of mould index i occurrence, $P(M_{Ii})$, can be calculated by Equation (5):

$$P(M_{Ii}) = \frac{N(g_m < 0)}{N_T} \tag{5}$$

where:

$N(g_m < 0)$: Number of failed scenarios

N_T: Total number of scenarios

The reliability of mould index i occurrence, $R(M_{Ii})$, is complementary to $P(M_{Ii})$ and can be calculated with Equation (6):

$$R(M_{Ii}) = 1 - P(M_{Ii}) \tag{6}$$

2.2. Random forests algorithm

Breiman [65] proposed the random forests (RF) algorithm as a powerful method for regression and classification problems that is built on model aggregation. The RF algorithm combines the bagging concept [66], which is the earliest iteration of the RF, with random feature selection [67]. At each node, a subset of the explanatory features (input variables) is randomly selected to construct many binary decision trees using several bootstrapped datasets from the original dataset (as shown in Fig. 2). This approach enhances the diversity between the regression trees and allows the RF to handle large datasets with a large number of predictors without variable removal [48]. The number of trees (k) and predictors used to decide the split at each node are critical considerations for RF models [68]. The nodes of each regression tree are split using the optimal split predictive variable among a subset of m randomly chosen predictive variables. Each regression tree grows utilizing another bootstrap subset of the original dataset [48]. Fig. 2 provides an overview of the RF procedure for regression. The RF algorithm is able to randomly vary the predictive variable groups across the various trees and re-sample the data with replacement, enabling it to improve the diversity between the regression trees.

The RF algorithm offers several advantages over other approaches:

- Interpretability [65,69]: Random Forests offer superior interpretability compared to neural networks. The decision trees within the Random Forests algorithm can be visualized and understood, enabling users to examine the rules and criteria used for making predictions.
- Handling Nonlinear Relationships [70]: Random Forests excel in modelling complex nonlinear relationships between input variables and the target variable.
- Metamodel Robustness [65]: Random Forests offer a balance between complexity and stability, reducing the risk of overfitting. Random Forests employ ensemble learning by combining multiple decision trees, which helps reduce overfitting and improve generalization performance. In dynamic environments like hygrothermal analysis, where correlations constantly change, robustness is crucial.
- Feature Importance [71]: Random Forests provide a built-in measure of feature importance. By evaluating the contribution of each input variable in the non-linear sensitivity analysis and decision-making process, Random Forests can identify the most relevant and sensitive features for the prediction task. This information can aid in

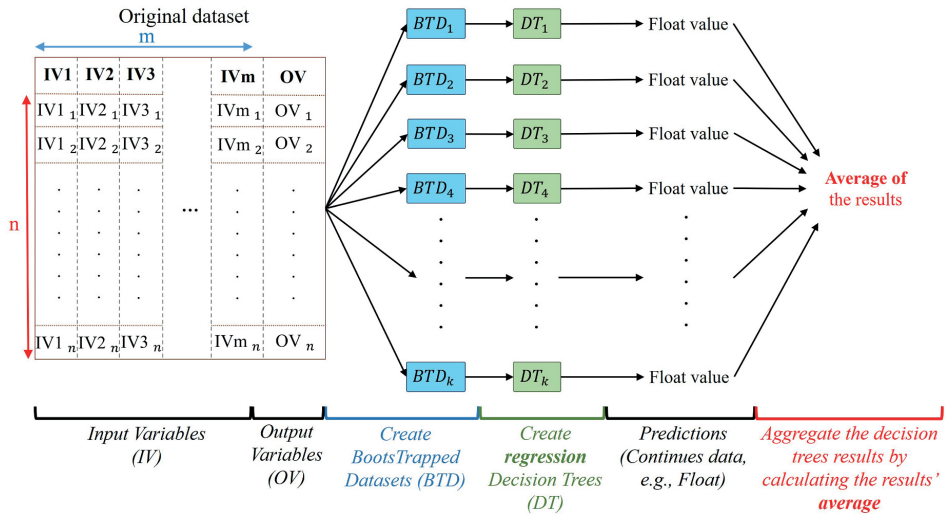


Fig. 2. Overview of the regression Random Forests (RF).

feature selection and enhance the understanding of the underlying data.

- Computation Efficiency [72]: Random Forests can efficiently handle large datasets with high-dimensional feature spaces. Training a Random Forests model can be parallelized, making it faster compared to other metamodeling techniques.

2.3. Convergence study

The required number of simulations (scenarios) in the *primary sampling* part, under the PA section, is a significant issue to be addressed. This is achieved by gradually increasing the number of simulations and monitoring the final output, $R(M_{li})$. Convergence criterion [73] involves monitoring the change in the target variable, $R(M_{li})$, over the last ten iterations. Therefore, the convergence study can be conducted after at least ten iterations. The convergence value is calculated using Equation (7):

$$\varepsilon_i = \frac{\left|\sum_{i-9}^{i-5} OF_i - \sum_{i-4}^{i} OF_i\right|}{\sum_{i-4}^{i} OF_i} \tag{7}$$

where i is the current iteration number (>10), OF_i is the ith iteration of objective function $R(M_{li})$, and ε_i is the convergence value of the OF_i. According to Ref. [73], a convergence limit within the range of 0.001 and 0.01 is typically deemed suitable. This range was not suggested specifically for mould analysis, but the "Topology design methods for structural optimization" and "Probabilistic mould analysis" applications share several common aspects, including iterative optimization procedures, objective functions, design variables, consideration of constraints and uncertainties, as well as the pursuit of optimal or reliable designs. As a precaution, a conservative value of 0.001 was used in the present study.

2.4. Mould sensitivity analysis method

Sensitivity analysis techniques can be broadly classified into two categories: probabilistic and deterministic. In probabilistic sensitivity analysis, input variables are defined based on their probability distributions, whereas in deterministic sensitivity analysis, the range of values is used to describe the input variables. Since the probabilistic approach is the basis of the Mould Sensitivity Analysis (MSA) method discussed in this paper, Spearman's rank correlation coefficient, ρ, is chosen for the sensitivity analysis. Unlike Pearson's correlation coefficient, which identifies only linear dependencies, the Spearman rank correlation coefficient can detect any monotonically increasing or decreasing bi-unique dependency between the input and output variables.

The MSA method presented in this paper uses output data (i.e., maximum mould index) from the machine learning model predictions and input data (i.e., material properties and outdoor and indoor conditions) from the secondary sampling. Fig. 1 illustrates the two types of sensitivity analysis in the SA section: (1) feature importance analysis and (2) correlation analysis.

The *feature importance analysis* plays a crucial role in understanding the influence of the input variables on the output variable in ML models. In this study, the RF algorithm is utilized for feature importance analysis, which considers both linear and nonlinear relationships between the input and output variables. RF is an ensemble learning method that includes several decision trees, each with internal nodes/branches. At each internal node, the chosen feature (input variable) is used to decide how to split the data collection into two distinct sets with related responses. The criteria used to choose the features for internal nodes/branches are Gini impurity for classification assignments and variance reduction (Sum of Squared Residual calculations) for regression assignments. The influence of each feature in the split's impurity reduction is measured. The feature which results in the highest impurity reduction (i.e., the lowest Gini importance/the lowest Sum of Squared Residuals) is chosen as the internal node/branch. To determine the feature importance, the average reduction in impurity for each feature is observed across all the trees in the forest. The average of all the trees in the forest serves as a proxy for the feature importance. Hence, the higher the feature importance, the more important the feature in the machine learning model [74].

The *correlation analysis* is carried out based on two different modes of sensitivity analysis. *Overall sensitivity analysis* is performed by calculating the Spearman's correlation coefficient, $\rho_{X_{ri},Y_{rj}}$, for pairs of variables according to Equation (8) [34]. In this part, the whole input and output variables distributions are investigated.

$$\rho_{X_{ri},Y_{rj}} = \frac{cov(X_{ri}, Y_{rj})}{\sigma_{X_{ri}} . \sigma_{Y_{rj}}} \quad (8)$$

where:

$cov(X_{ri}, Y_{rj})$: covariance of two ranked variables

$\sigma_{X_{ri}}$ *and* $\sigma_{Y_{rj}}$: standard deviation of ranked variables

To perform a more targeted correlation analysis around the selected mould index threshold, the MSA method employs a *segmented sensitivity analysis*. This analysis identifies and categorizes the scenarios with the highest mould indices near the failure level, and the associated input data for those scenarios are segmented. The Spearman's correlation coefficient, $\rho_{X_{ri},Y_{rj}}$, is then calculated again by considering the segmented data (maximum mould indices and their associated input variables) according to Equation (8). This approach allows for a more focused investigation of the input variables that have the strongest correlation with the mould index near the failure level, providing insights into the factors that contribute most significantly to the occurrence of mould in the building.

Spearman's correlation coefficient (ρ), also well-known as "Rank Correlation Coefficient (RCC)", is a value between −1 and +1 that measures the degree of correlation (monotonicity) between two variables [75]. The conventional approach to interpret the relationship between two variables based on Spearman's correlation coefficient is [76]:

- 0.00 indicates "no relationship".
- 0.00–0.09 indicates a "negligible relationship".
- 0.10–0.39 indicates a "weak relationship".
- 0.40–0.69 indicates a "moderate relationship".
- 0.70–0.89 indicates a "strong relationship".
- 0.90–1.00 indicates a "very strong relationship".

The sign of the Spearman's correlation coefficient indicates the direction of the relationship between two variables. A positive sign indicates a positive correlation, meaning that the values of the two variables tend to increase or decrease together. In contrast, a negative sign indicates a negative correlation, meaning that as the value of one variable increases, the value of the other variable tends to decrease, and vice versa.

2.5. Case studies

The authors present three case studies in which they demonstrate the application of the mould reliability and sensitivity analysis methods. The case studies involve load-bearing components and include two common Swedish external wall assemblies (CS1 and CS2) [77] and a fully bio-based external wall assembly (CS3). CS1 uses concrete as its load-bearing component, while CS2 and CS3 use cross-laminated timber (CLT). These case studies are illustrated in Fig. 3.

Table 2 provides a comprehensive list of the material properties used in this study, along with their respective references where applicable for 1D simulation. The mean values are used for the deterministic analysis. The remaining input variables are assigned fixed values according to the default of Delphin 6. The initial temperature and relative humidity of the materials were assumed to be 20 °C and 80%, respectively, which is consistent with the recommended default values. Lund climate data was used for all case studies, and the external wall assemblies were assumed to be facing west.

An Air Change Rate (ACR) of 5 h^{-1} is used to consider the ventilation of the cavity as recommended in Ref. [78]. In this case, the model assumes that the air within the cavity is exchanged five times per hour with the air having the same temperature and relative humidity as the outdoor environment.

The minimum mesh size was set to 1 mm with a stretch factor of 1.3. As a result, the size of the meshes varied within each layer, depending on the thickness of the respective layer. By adjusting the mesh size and stretch factor in this manner, an appropriate balance between computational efficiency and accuracy was obtained, considering the varying thicknesses of the layers in the model.

A preliminary deterministic study was conducted on the case studies to assess mould growth performance over a 10-year duration (single year climate repeated 10 times). Results indicated that after two years, the mould curve shape became stable. Consequently, hygrothermal simulations in the PA section were run for two-year periods (single year climate repeated twice). However, only the second year's data was exported to avoid the assumed initial conditions affecting the output. The hourly maximum mould indices were analyzed for a reference period of one year. The reason for having a stable mould curve shape is that the Finnish mould growth model considers the decline in the mould growth process due to unfavourable conditions. The decline in mould growth is regarded according to the time exposed to unfavourable conditions, either less than 6 h or longer than 24 h. There is no decline in mould growth if the time exposed to unfavourable conditions is between 6 and 24 h [62]. However, it should be noted that the mould growth decline was developed based on a limited number of experimental data where temperatures less than 0 °C and periods of more than 14 days of unfavourable conditions were neglected [79]. Additionally, regarding the mould growth decline model, the experiments were performed daily or longer than daily, and hourly data is unavailable [79].

In this study, failure threshold is defined by the mould growth exceeding a mould index of one on the interior face of the wall. The choice of failure criterion is based on the report by WHO where the probability of health consequences is correlated to visible mould or dampness [4]. Although there is a lack of guidelines specifying the acceptable level of mould inside buildings, it is recommended that dampness and mould should be prevented, according to the WHO guideline [4]. On the other hand, mould prevention depends on controlling environmental conditions before spore germination, according to Ref. [8]. After germination, hyphae and mycelium of the mould are created, and in this phase, the mould can ramify and grow through the substrate and nutrients even though the surface moisture is limited. Accordingly, the mould germination point, which is mould index one based on the Finnish mould growth model [9], is considered the failure

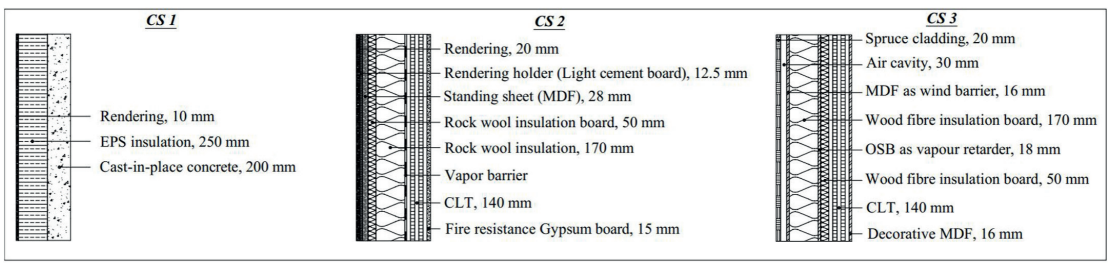


Fig. 3. Three external wall assemblies, case studies 1 and 2 adopted from [77].

threshold to prevent health problems. The screening point of interest in our study is the interior surface of the wall assemblies. By estimating the probability of interior mould, these figures could be used to make inference concerning the risk of health consequences.

The Reliability Analysis (RA) section starts with the selection of suitable input variables to build the metamodel. For the *feature selection*, a parametric study is performed to find the optimum number of features to be involved in the metamodel. The data is randomly split into training (70%) and testing (30%) sets, and the number of features that yield the highest coefficient of determination (R^2) between predicted and observed maximum mould indices is selected. A higher R^2 indicates that the RF model can account for more variations, making it more accurate. Apart from feature selection, determining the proper number of trees in the RF model is another critical step in optimizing the metamodel's performance. An optimized metamodel can provide more accurate results while reducing the running time of the codes, making it more efficient.

To determine the required number of scenarios for the *primary sampling* part, a convergence study was conducted using at least ten iterations, as outlined in section 2.3. Each iteration involved 100 scenarios, with an additional 100 scenarios added to the previous iteration to create a new one. The study will continue until the convergence value is less than the convergence limit of 0.001. For the *secondary sampling*, a vast dataset of $n = 10^7$ was generated using the Latin hypercube sampling (LHS) technique based on the probability distributions in Tables 1 and 2. By conducting this convergence study and generating a large dataset using LHS, the study ensures that the primary and secondary samples are adequate and the results are reliable.

To ensure the reliability of the MRA method, a reproducibility check is carried out by repeating the analyses seven times. The CoV of the output target $R(M_{li})$ is checked during these seven attempts. If it is under 1%, it is deemed that the MRA method operates reliably. This check is important to ensure that the results obtained from the MRA method are consistent and can be used with confidence in practical applications.

To evaluate the importance of input variables in creating the metamodel, *feature importance analysis* is conducted. Also, the input variables listed in Tables 1 and 2 are subjected to *correlation analysis* against the maximum mould indices in both overall and segmented sensitivity analyses modes. The segmented sensitivity analysis focuses on scenarios with mould indices greater than 0.95 to consider not only the failed scenarios but also those near failure. Spearman's correlation coefficient, $\rho_{X_{ri},Y_{rj}}$, is calculated using Equation (8) for both modes, and the results are compared.

The accuracy and validity of simulation outputs depend significantly on the accuracy and reasonableness of the input data used. However, the focus of this study is on introducing the methods rather than on performing a precise reliability analysis of a specific external wall assembly.

The determination of the probability distributions presented in Table 1 involved the utilization of several references and assumptions.

Table 1
Base case and probability distribution values for indoor and outdoor conditions. U(a, b): Uniform distribution, where *a* and *b* are the minimum and maximum values.

Variable	Base case value	Probability distribution
Outdoor convection heat exchange coefficient [W/m^2K] [80]	12	U(12, 20)
Solar adsorption coefficient [−] [57]	0.4	U(0.4, 0.8)
Long-Wave Emissivity [−] [57]	0.9	U(0.04, 0.95)
Reduction/splash coefficient of WDR [−]	0.7	U(0.6, 0.8)
Indoor Surface Heat Transfer Coefficient (Convective + Radiative), $\left[\frac{W}{m^2.K}\right]$ [81]	8	U(5, 10)
Indoor Surface Vapour Diffusion Coefficient $\left[\frac{s}{m}\right]$ [82]	0.25×10^{-7}	$U(0.1 \times 10^{-7}, 1 \times 10^{-7})$

The recommended outdoor convection heat exchange coefficient, sourced from the Delphin database [57], encompasses a range of 12 [$W/(m^2.K)$] to 20 [$W/(m^2.K)$], considering various conditions and wind exposure levels [80]. To account for different surface colours and textures, the solar adsorption coefficient was found to vary between 0.4 and 0.8 [57]. The range of long-wave emissivity, which takes into consideration variations in colour and texture, extends from 0.04 to 0.95 [57]. Considering the availability of free water on a vertical wall, the wind-driven rain is typically reduced by a factor of 0.7. However, with a tolerance of ±0.1, it was assumed to vary between 0.6 and 0.8. The indoor surface heat transfer coefficient ranges from 5 [$W/(m^2.K)$] to 10 [$W/(m^2.K)$], taking into account the direction of indoor airflow [81]. These values and ranges, with equal probabilities of occurrence, obtained through the examination of multiple sources and logical assumptions, contribute to the probability distributions presented in Table 1. The determination of the outdoor vapour diffusion coefficient is based on the outdoor convection heat exchange coefficient within the simulation setup. This approach ensures an appropriate correlation between the outdoor vapour diffusion coefficient and the outdoor convection heat exchange coefficient.

3. Results and discussions

3.1. Mould reliability analysis

3.1.1. Optimization of RF model

All three case studies' metamodels were optimized by investigating the effective features involved in the creation of metamodels. The accuracy metrics are presented in Fig. 4 and Table 3 for the case studies. In case study 1 (CS1), the top eight input variables (see Table 3) were selected based on their coefficient of determination (R^2) with respect to their maximum mould indices. The optimized metamodel achieved a maximum R^2 of 0.855, which indicates that it can account for 85.5% of the variations. Moreover, the MAE and RMSE accuracy metrics showed minimal errors close to zero. Fig. 4 indicates that for CS1, the dispersion of the data after the maximum mould index threshold (i.e., mould index one) is slightly higher compared to the data that are less than the maximum mould index threshold, which may lead to lower accuracy for the failed scenarios. The optimal number of trees in the RF model was determined to be 100, as no improvement in R^2 was observed beyond this number.

The top five features were selected to optimize the RF model in case study 2 (CS2). The R^2 value achieved was 0.958, indicating that the metamodel can account for 95.8% of the variations. Furthermore, the MAE and RMSE accuracy metrics demonstrated negligible errors close to zero. The dispersion of data above the maximum mould index threshold was slightly lower in CS2 than in CS1, implying that the metamodel can predict failure scenarios with a similar R^2. The RF model's ideal number of trees was 55, resulting in the highest R^2.

For case study 3 (CS3), the metamodel was again built using the top five features. The resulting RF model had an R^2 value of 0.942, which is slightly lower than the R^2 value of 0.958 achieved in CS2. However, the MAE and RMSE values were the same for both case studies. To optimize the metamodel, 215 trees were used, resulting in the most optimum RF model for CS3.

There are several factors that can influence the R^2 during metamodel development. The performance of machine learning models is greatly influenced by the variability of the training data. Higher variability can make it more challenging for the model to capture the underlying patterns and accurately predict outcomes, resulting in a lower R^2. Since the wall construction and behaviour of CS1, CS2, and CS3 are different from each other, the performance of the metamodel varies when comparing these three cases. Also, the choice and relevance of features used in the machine learning model can have a significant impact on its performance. It is possible that the features selected for CS1 were not as informative or relevant for predicting outcomes compared to the

Table 2
Probability distributions for the material properties. N(μ, σ): Normal distribution, μ and σ are the mean and standard deviation. CoV: Coefficient of Variation. Material properties denoted with superscript (1) were not specified in their corresponding references, and therefore, default values from the Delphin database with a normal distribution and a coefficient of variation of 10% were used. Material properties denoted with superscript (2) lack information on their distributions in the literature; hence, a normal distribution with a coefficient of variation of 10% was assumed as a reasonable value as recommended by Gradeci et al. [29].

	Bulk Density (D_B $\left[\frac{kg}{m^3}\right]$)	Specific Heat Capacity (C_p $\left[\frac{J}{kg.K}\right]$)	Porosity (θ_{por} $\left[\frac{m^3}{m^3}\right]$)	Thermal Conductivity (λ_{dry} $\left[\frac{W}{m.K}\right]$)	Water Uptake Coefficient (A-value) $\left[\frac{kg}{m^2.s^{0.5}}\right]$)	Water Vapour Diffusion Resistance Factor (μ_{VDR} [−])
Concrete [15,57,83]	N(2300, 115) CoV = 5%	N(850, 42.5) CoV = 5%	N(13.5, 0.675) CoV = 5%	N(1.6,0.08) CoV = 5%	$^{(1)}$N(8.33×10^{-3}, 8.33×10^{-4})	N(150, 22.5) CoV = 15%
EPS insulation [57,84]	N(15, 4.95) CoV = 33%	N(1568, 157) CoV = 10%	N(0.93,0.093) CoV = 10%	N(0.0376, 0.0036) CoV = 9.5%	N(4.7×10^{-4}, 10^{-5}) CoV = 2.1%	N(35, 0.12) CoV = 0.34%
Rendering [14]	N(2000, 400) CoV = 20%	$^{(2)}$N(850, 85)	$^{(2)}$N(0.26, 0.026)	N(0.8, 0.08) CoV = 10%	N(0.03, 0.006) CoV = 20%	N(19,1.9) CoV = 10%
Gypsum board [29,57]	N(850, 85) CoV = 10%	N(850, 85) CoV = 10%	N(0.65, 0.065) CoV = 10%	N(0.2, 0.02) CoV = 10%	$^{(1)}$N(0.18, 0.018)	N(8.3, 0.83) CoV = 10%
Rock wool insulation [84]	N(39, 0.78) CoV = 2%	$^{(2)}$N(802, 80.2)	$^{(1)}$N(0.95, 0.095)	N(0.034, 0.0026) CoV = 7.6%	N(3.39×10^{-3}, 9.1×10^{-4}) CoV = 27%	$^{(2)}$N(2, 0.2)
Vapour barrier [29,57]	$^{(1)}$N(1000, 100)	$^{(1)}$N(1400, 140)	$^{(1)}$N(0.01, 0.001)	$^{(1)}$N(0.15, 0.015)	$^{(1)}$N(10^{-10}, 10^{-11})	N(20000, 2000) CoV = 10%
Rendering holder (Light cement board) [57,85]	$^{(2)}$N(1130, 113)	$^{(2)}$N(840, 84)	$^{(2)}$N(0.479, 0.0479)	$^{(2)}$N(0.24, 0.024)	$^{(1)}$N(0.014, 0.0014)	$^{(2)}$N(905, 90.5)
Cross Laminated Timber (CLT) [29,57]	N(410, 41) CoV = 10%	N(1300, 130) CoV = 10%	N(0.74, 0.074) CoV = 10%	N(0.098, 0.0098) CoV = 10%	$^{(1)}$N(0.01, 0.001)	N(500, 50) CoV = 10%
Medium Density Fibreboard (MDF) [29, 57]	N(159, 15.9) CoV = 10%	N(1700, 170) CoV = 10%	N(0.89, 0.089) CoV = 10%	N(0.04, 0.004) CoV = 10%	$^{(1)}$N(0.0019, 0.00019)	N(2.6, 0.26) CoV = 10%
Wood fibre insulation [57, 84]	N(180, 3.6) CoV = 2%	$^{(2)}$N(1515, 151.5)	$^{(1)}$N(0.89, 0.089)	N(0.04, 0.0059) CoV = 14.6%	N(1.53×10^{-3}, 0.00011) CoV = 7.2%	$^{(2)}$N(4, 0.4)
OSB (as vapour retarder) [29,57]	N(455, 45.5) CoV = 10%	N(1500, 150) CoV = 10%	N(0.74, 0.074) CoV = 10%	N(0.1, 0.01) CoV = 10%	$^{(1)}$N(0.0019, 0.00019)	N(467, 46.7) CoV = 10%
Spruce cladding [29,57]	N(455, 45.5) CoV = 10%	N(1500, 150) CoV = 10%	N(0.73, 0.073) CoV = 10%	N(0.09, 0.009) CoV = 10%	$^{(1)}$N(0.0024, 0.00024)	N(130, 13) CoV = 10%

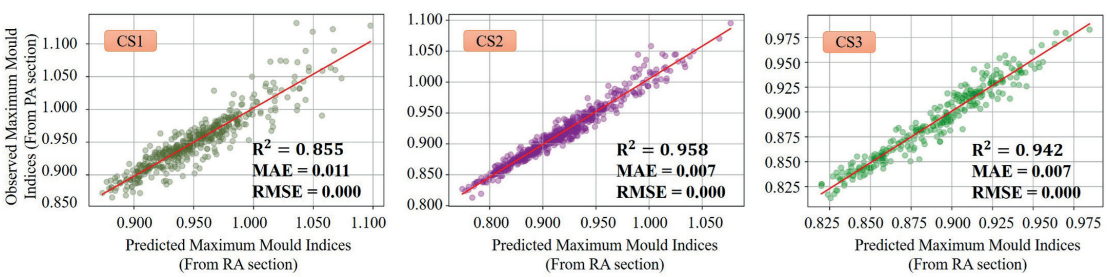


Fig. 4. Predicted data (from RA section) vs observed data (from PA section) during the machine learning model testing for three case studies (CS1, CS2, and CS3).

Table 3
Metamodel features and time comparison for three case studies (CS1, CS2, and CS3). R^2: Coefficient of determination between the predicted and observed data, t_p: Prediction time per scenario, t_s: Simulation time per scenario.

Case studies	Features (Model input variables)	R^2	Time comparison (Second/ Scenario)		Metamodel training time (Second)
			t_p	t_s	
CS1	1 Solar adsorption coefficient 2 Indoor surface heat transfer coefficient 3 Outdoor convection heat conduction exchange coefficient 4 Indoor surface vapour diffusion coefficient 5 Thermal conductivity of EPS insulation 6 Thermal conductivity of cast-in-place concrete 7 Long-wave emissivity 8 Density of cast-in-place concrete	0.855	10×10^{-6}	3.15	0.48
CS2	1 Solar adsorption coefficient 2 Outdoor convection heat conduction exchange coefficient 3 Indoor surface heat transfer coefficient 4 Thermal conductivity of rock wool insulation 5 Long-wave emissivity	0.958	5.5×10^{-6}	4.04	0.23
CS3	1 Solar adsorption coefficient 2 Outdoor convection heat conduction exchange coefficient 3 Indoor surface heat transfer coefficient 4 Thermal conductivity of wood fibre insulation 5 Long-wave emissivity	0.942	19×10^{-6}	5.16	0.55

features used in CS2 and CS3. This could lead to a lower R^2 value for CS1. However, it is important to note that even though the R^2 may be lower for CS1, it can still be considered acceptable in the context of the study.

It is worth noting that tuning the hyperparameters of the RF model is significant to achieve the highest optimized model. In this study, it involves adjusting the number of trees, identifying the most effective features, and estimating the generalization score using out-of-bag samples. The default values specified in Ref. [74] were utilized for the remaining hyperparameters.

3.1.2. Convergence study

The convergence study was conducted for all three case studies to determine the required number of simulations (scenarios) in the *primary sampling* part, and the results are presented in Fig. 5. The red points/lines indicate the convergence values, while the blue points/dashed lines represent reliabilities. It should be noted that at least ten iterations are necessary to calculate the convergence values, so the red points start from the tenth iteration. The loop of adding more scenarios will be terminated once the convergence value falls below 0.001, as indicated by the green highlights. The required number of scenarios for CS1, CS2, and CS3 is 1600, 1900, and 1000, respectively.

3.1.3. Metamodel features and time comparison

Table 3 lists the features used in the RF model and their corresponding R^2. It also compares the maximum mould index simulation time (t_s) using probabilistic analysis and the prediction time (t_p) using the RF algorithm. For CS1, CS2, and CS3, t_p is 3.1×10^5, 7.3×10^5, and 2.7×10^5 times faster than t_s, respectively. Furthermore, the training time required for the metamodel creation process is exceptionally short, taking less than 1 s for all the case studies examined.

Considering the accuracy of the metamodel for each case study, it can be concluded that integrating the metamodel with Probabilistic Analysis (PA) has the potential to significantly reduce the time required to consider a large number of scenarios for a specific case study. The more scenarios involved; the more uncertainties could be contemplated. Thereby, MRA method allows for a more comprehensive assessment of the robustness of the hygrothermal analysis for a case study. The robustness reflects how much the uncertainties in hygrothermal variables influence the calculated maximum mould indices. Consequently, more reliable results can be obtained when dealing with uncertainties and a large number of scenarios.

All simulations and predictions in this study were conducted on a machine equipped with an "Intel(R) Core (TM) i9-9820X CPU @ 3.31 GHz" processor and "64 GB" of RAM. It should be noted that the current GPU setup is not optimized for efficiency. By utilizing GPUs with larger memory capacity, faster simulations for the PA section can be achieved, along with improved training and prediction capabilities for the RA section. This enhancement would result in further time savings and increased efficiency.

3.1.4. Mould probability of failure and reliability

The Cumulative Density Function (CDF) of the maximum mould index for each case study is displayed in Fig. 6. The red lines represent the limit state point, which is defined as mould index one. The black

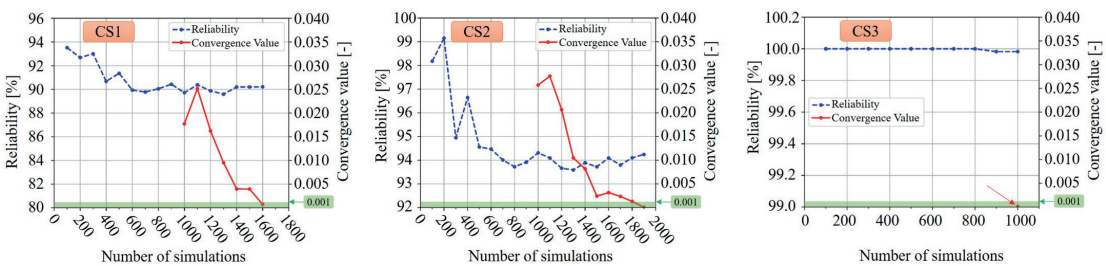


Fig. 5. Required number of scenarios in primary sampling part, as identified by convergence study for three case studies (CS1, CS2, and CS3). Note that convergence of CS3 was obtained already after 10 iterations, as indicated by the red arrow. (For interpretation of the references to colour in this figure legend, the reader is referred to the Web version of this article.)

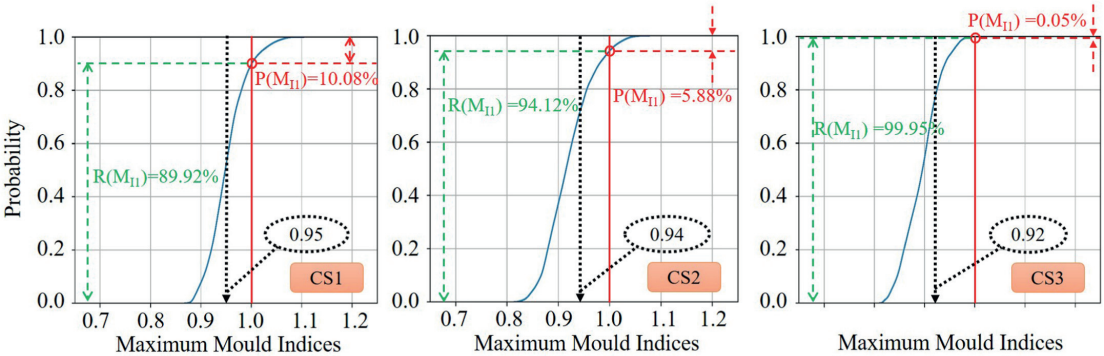


Fig. 6. Mould reliability analysis for three case studies (CS1, CS2, and CS3). Red line: failure threshold indicators; black dotted line: deterministic results; blue line: CDF of maximum mould indices; red dashed line: probability of mould index one occurrence P(M_{I1}); green dashed line: reliability of mould index one occurrence R (M_{I1}). (For interpretation of the references to colour in this figure legend, the reader is referred to the Web version of this article.)

dotted lines indicate the results of the deterministic hygrothermal analysis (base case). The probabilities of mould index one occurrence (P (M_{I1})) are presented by the red dashed lines, while the green dashed lines represent the reliability of mould index one occurrence (R(M_{I1})).

After performing deterministic hygrothermal analysis, it was found that the maximum mould index for case study 1 (CS1) was 0.95. However, the mould reliability analysis indicates that nearly 48% of the scenarios could result in higher maximum mould indices than the deterministic result, as shown on the right side of the black dotted line in Fig. 6. Among these scenarios, almost 1/5, or 10.08% of the total scenarios, resulted in failure, defined as a maximum mould index above one.

It was found that the deterministic analysis for case study 2 (CS2) resulted in a maximum mould index of 0.94. However, the MRA method revealed that 31.13% of scenarios had a higher maximum mould index than the deterministic result, and a total of 5.88% of the scenarios led to failure.

For case study 3 (CS3), the deterministic approach resulted in a maximum mould index of 0.92. MRA showed that 24.17% of the scenarios had a higher maximum mould index than the deterministic result, and 0.05% of the scenarios led to failure.

The MRA results demonstrate the probability of exceeding the mould index of one and the associated risk of failure, serving as a valuable tool for proactive measures and design improvements. However, the deterministic results indicated that the designs were acceptable. The implications of the MRA method using machine learning are significant for practical applications in the real world. By employing the Random Forests algorithm, the proposed method provides a more comprehensive understanding of the reliability landscape, enabling engineers and designers to make informed decisions regarding mould design and performance.

The practical relevance of the developed method lies in its ability to identify critical scenarios and potential failures, allowing for preventive measures and design modifications. By avoiding expensive failures, product recalls, and potential safety hazards, the proposed MRA method using RF machine learning algorithm can result in substantial cost savings and risk mitigation benefits for industries that are affected by mould occurrence.

As previously mentioned, several medical studies [5,86,87] have provided substantial evidence establishing a significant correlation between the presence of dampness and mould in buildings and the health of their occupants. By incorporating the calculated reliabilities from this study, it becomes possible to estimate and analyze the health consequences more effectively and facilitate rational decision-making. To enhance the reliability and robustness of this assessment, the Inutility Decision Analysis (IDA) method, introduced by Bayat Pour et al. [88], can be employed in conjunction with the MRA. This combined approach ensures a more reliable and comprehensive evaluation of health consequences.

3.2. Mould uncertainty analysis

Fig. 7 demonstrates the potency of the MRA method in predicting the maximum mould index by comparing the results of the deterministic approach (represented by the red lines), the PA section (depicted by the grey bands), and the whole MRA method (shown by the blue dotted lines). The gaps between the maximum values in the range of maximum mould indices and the deterministic analysis outputs were examined to investigate the uncertainties of the deterministic hygrothermal analysis results.

By comparing the findings of the PA section with the deterministic results, it was revealed that for case studies 1, 2, and 3, there were uncertainties of 26.3%, 21.3%, and 12%, respectively (as illustrated in Fig. 7). The predicted maximum mould index through the RA section provided lower uncertainties than the PA section, with 21.1%, 19.2%, and 9.8% for CS1, CS2, and CS3, respectively.

In case study 1 (CS1), the maximum mould index was 1.2 in the PA section, while in the RA section, it was 1.15, which is a 4% difference. Similarly, for CS2 and CS3, the difference in maximum mould index between PA and RA sections was around 2%. Generally, the maximum mould index results from the PA and RA sections were quite close. However, it is worth noting that although using the metamodel allows for a large number of scenarios to be considered, metamodel uncertainties can add some uncertainty to the final results.

3.3. Reproducibility check

In section 2.5, a reproducibility check was conducted to assess the precision of the MRA method. Fig. 8 shows the reliability of a mould index one occurrence over seven iterations. The results indicate that the coefficients of variation (CoV) for CS1, CS2, and CS3 were 0.37%, 0.13%, and 0.03%, respectively. These values are less than 1%, which means they are acceptable in demonstrating the reproducibility of the method for all case studies.

3.4. Mould sensitivity analysis

The MSA method, illustrated in Fig. 1, was used to conduct mould sensitivity analysis. Table 4 summarizes the correlation study results for the input variables that exhibit significant correlation with the

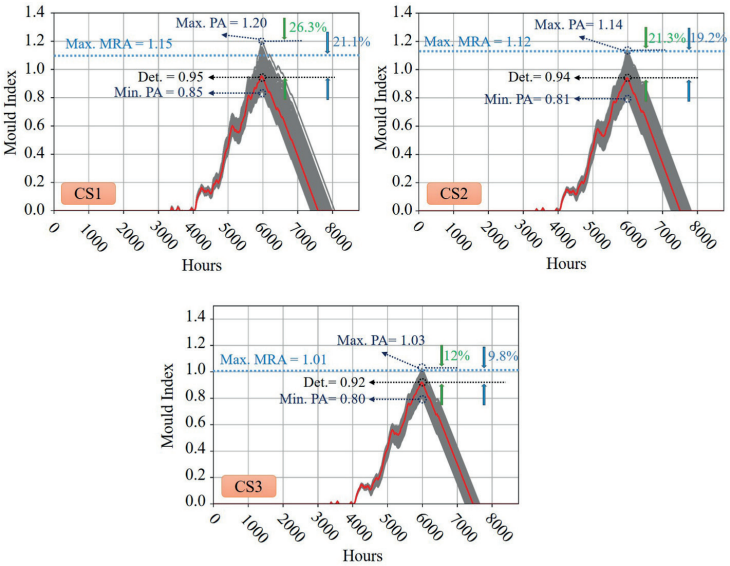


Fig. 7. Temporal variation of mould index for three case studies (CS1, CS2, and CS3), shown for the deterministic case (red line) and the probabilistic analysis (grey lines). The maximum mould index obtained from the MRA is also indicated (dashed blue line). Abbreviations: Det.: Deterministic analysis result, Max. PA and Min. PA: Maximum and minimum values in the range of maximum mould index according to the PA section, Max. MRA: Maximum value in the range of maximum mould index by performing the whole MRA method. (For interpretation of the references to colour in this figure legend, the reader is referred to the Web version of this article.)

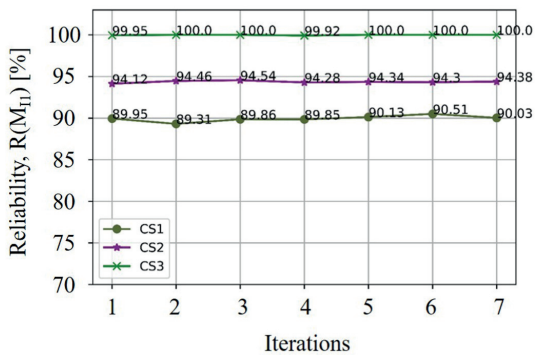


Fig. 8. Reproducibility check with seven iterations for three case studies (CS1, CS2, and CS3).

maximum mould index, while ignoring those that have negligible correlation. Indoor surface heat transfer coefficient, outdoor convection heat exchange coefficient, and solar adsorption coefficient were identified as the most sensitive parameters to maximum mould index, in terms of indoor and outdoor conditions. Among these, only the indoor surface heat transfer coefficient maintained its sensitivity in both overall sensitivity analysis (all scenarios) and segmented sensitivity analysis (focusing on failed/semi-failed scenarios). For outdoor convection heat exchange coefficient and solar adsorption coefficient, the sensitivity reduced significantly in the segmented sensitivity analysis mode. Furthermore, the sensitivity ranking differed across the three case studies, as shown in Table 4. For instance, in CS3, the thermal conductivity of wood fibre insulation was more sensitive to maximum mould index in segmented sensitivity analysis mode (moderate relationship) than in overall sensitivity analysis mode (negligible relationship). Generally, it can be concluded that there is a much stronger correlation between the maximum mould index and the indoor and outdoor surface conditions compared to material properties.

Table 4
Spearman correlation coefficients between the input variables and maximum mould index for three case studies (CS1, CS2, and CS3). Colormap guide: 0.00–0.09: Negligible relationship, 0.10 - 0.39: weak relationship, 0.40 - 0.69: Moderate relationship, 0.70 - 0.89: Strong relationship, 0.90 - 1.00: Very strong relationship.

Case studies		Indoor Surface Heat Transfer Coefficient (Convective + Radiative), h $\left[\frac{W}{m^2.K}\right]$	Outdoor convection heat exchange coefficient (h_c) [W/m^{2}K]	Solar adsorption coefficient [-]	Thermal Conductivity_Wood fibre insulation (λ_{dry} $\left[\frac{W}{m.K}\right]$)
CS1	Overall	-0.55	0.39	-0.65	-
	Segmented	-0.58	0.12	-0.31	-
CS2	Overall	-0.4	0.45	-0.75	-
	Segmented	-0.61	0.09	-0.26	-
CS3	Overall	-0.35	0.51	-0.74	0.063
	Segmented	-0.36	0.19	-0.39	0.4

While the case studies presented in this paper serve as illustrative examples to demonstrate the application of the methods, the results of the sensitivity analysis indicate that the boundary condition variables have the most significant influence on the maximum mould index. This is primarily due to the screening point of interest being on the interior surface of the wall assemblies, where the boundary conditions have a greater impact and can directly affect the wall's susceptibility to mould growth.

Fig. 9 depicts the relative importance of the features in predicting the maximum mould index based on their linear and non-linear relationships. Across all case studies, the solar adsorption coefficient appears to be the most significant feature, exhibiting a greater importance difference over the other features in CS2 and CS3 than in CS1. This is reinforced by Table 4, which reveals a strong correlation between the maximum mould index and the solar adsorption coefficient in CS2 and CS3, whereas a moderate correlation exists in CS1. Additionally, the analysis of feature importance indicates that the indoor and outdoor surface conditions, specifically the solar adsorption coefficient, indoor surface heat transfer coefficient, and outdoor convection heat exchange coefficient, are of paramount importance in predicting the maximum mould index. However, the priority of these features varies between the case studies.

The analysis in Fig. 9 suggests that more features are important in predicting the maximum mould index, despite not being identified by the correlation analysis. The likely reason for this discrepancy is that feature importance analysis considers nonlinear effects, while correlation analysis only accounts for linear relationships. In the MSA method, Spearman's correlation coefficient is used to identify linear correlations and determine their direction (positive or negative).

Overall, the application of the MSA method demonstrates its utility in practical scenarios by identifying the key parameters and features influencing the maximum mould index. By accounting for context-specific variations and considering nonlinear effects, the MSA method provides valuable insights for predicting and understanding mould sensitivity, enabling more informed decision-making in real-life applications.

3.5. Limitations and future studies

The primary focus of this study is to introduce the methods rather than to conduct an exhaustive analysis of hygrothermal performance. For simplicity, several parameters have therefore been excluded from the analysis. In addition to the variables presented in Tables 1 and 2, several other stochastic variables could be considered to increase the details of the hygrothermal model. Specifically, these variables would include the moisture storage and moisture transport functions [37], indoor and outdoor climate data [29,37], rainwater penetration [78]. Incorporating these variables, particularly moisture storage and moisture transport functions, could significantly impact the risk of mould growth on the interior side of the walls.

Moreover, it is essential to consider the primary failure mechanisms associated with wall assemblies, such as the infiltration of rainwater through moisture barriers or air gaps in the airtightness layer. Incorporating these factors into the simulation would yield more accurate results, particularly when assessing the layers inside the wall (e.g., timber stud) as the focal point of interest.

While this study focused on the Random Forests algorithm for MRA, there are opportunities for further research and improvement. The use of metamodeling techniques in reliability analysis can provide more diverse and detailed information compared to deterministic studies. Future investigations could explore additional machine learning algorithms or ensemble methods to enhance the accuracy and reliability of the MRA method. Furthermore, the applicability of this developed method can be extended to other domains or industries that deal with reliability analysis and design optimization, opening avenues for broader impact and innovation.

4. Conclusions

This paper proposes two methods, Mould Reliability Analysis (MRA) and Mould Sensitivity Analysis (MSA), and explains their respective sections. MRA has two main sections, Probabilistic Analysis (PA) and Reliability Analysis (RA). In the PA section, uncertainties related to input variables are considered, while in the RA section, a machine learning metamodel based on the PA section is used to expand the sample size. MSA uses the RA section as a database for conducting two types of mould sensitivity analyses. The first type is feature importance analysis, which examines the linear and nonlinear relationships between features and the maximum mould index. The second type is correlation analysis, which checks positive and negative correlations using overall and segmented sensitivity analysis. The article illustrates the application of these methods through three case studies under Lund climatic conditions. The main findings of these analyses are:

4.1. Mould reliability analysis

1. The MRA method helps evaluate the robustness of hygrothermal analysis and mould assessment by considering a large number of scenarios. Robustness reflects how much the uncertainty in hygrothermal variables affects the maximum mould index calculation.
2. Integrating the metamodel (RA) with probabilistic analysis (PA) drastically reduces the time needed to consider a large number of scenarios for a case study.
3. The MRA method indicates a risk of failure (i.e., probability of mould index one occurrence) for all case studies (10.08%, 5.88%, and 0.05% for CS1, CS2, and CS3, respectively), while the deterministic hygrothermal analysis showed that all the case studies are safe (i.e., mould index less than one). This observation highlights how the deterministic approach might overlook uncertainties and mislead the designers.
4. Comparing the results of MRA method and deterministic approach showed that the probable maximum mould indices increased by 21.1%, 19.2%, and 9.8% for CS1, CS2, and CS3, respectively.
5. To assess the reproducibility of the MRA method, it was used seven times per case study. The coefficients of variation (CoV) were less

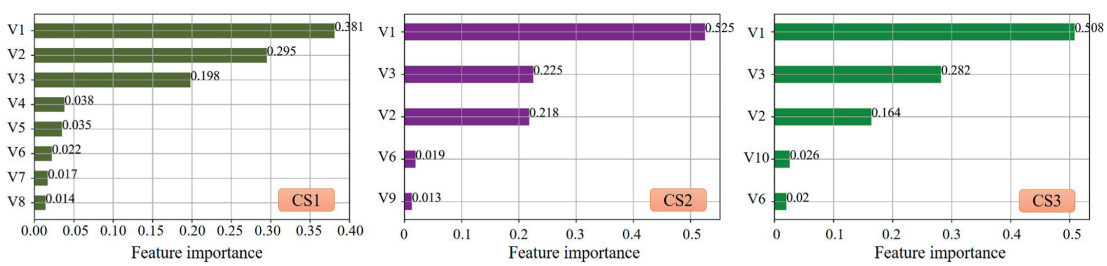


Fig. 9. Feature importance analysis for three case studies (CS1, CS2, and CS3). V1: solar adsorption coefficient; V2: indoor surface heat transfer coefficient; V3: outdoor convection heat exchange coefficient; V4: indoor surface vapour diffusion coefficient; V5: lambda value of EPS insulation; V6: long-wave emissivity; V7: lambda value of cast-in concrete; V8: density of cast-in concrete; V9: lambda value of Rockwool insulation; and V10: lambda value of Woodfibre insulation.

than 1%, indicating acceptable reproducibility across all case studies.

4.2. Mould sensitivity analysis

1. Overall and segmented sensitivity analyses revealed that some variables had different sensitivities, indicating that the maximum mould index for the failed scenarios may be sensitive to more input variables than those identified by the overall analysis.
2. Highly influential variables showed different rankings in the overall and segmented sensitivity analyses, suggesting that the maximum mould index sensitivity ranking for an input variable overlooked by the overall analysis may be higher or lower for the failed scenarios.
3. Both feature importance analysis and correlation analysis revealed similar tendencies of influential variables, although their ranking and absolute values might differ.

4.3. Final comment

The MRA and MSA methods have demonstrated their suitability as tools for quantifying the impact of uncertainties in hygrothermal calculations of diverse building envelopes. The findings of this study highlight the practical utility of the developed method for mould reliability analysis using the Random Forests algorithm. The MRA approach enhances the understanding of potential failure scenarios, allowing for proactive measures and design improvements. By providing a more comprehensive assessment of reliability, the proposed method offers substantial value in real-world applications and contributes to the field of mould safe design and analysis. Future studies will explore their use in actual case scenarios.

CRediT authorship contribution statement

Mohsen Bayat Pour: Writing – review & editing, Writing – original draft, Visualization, Validation, Software, Methodology, Investigation, Formal analysis, Data curation, Conceptualization. **Jonas Niklewski:** Writing – review & editing, Supervision, Investigation, Conceptualization. **Amir Naghibi:** Writing – review & editing, Supervision, Methodology. **Eva Frühwald Hansson:** Writing – review & editing, Supervision, Project administration, Funding acquisition, Conceptualization.

Declaration of competing interest

The authors declare that they have no known competing financial interests or personal relationships that could have appeared to influence the work reported in this paper.

Data availability

Data will be made available on request.

Acknowledgement

The authors gratefully acknowledge the financial support from FORMAS, the Swedish research council for sustainable development, for the research grant 2019-00673. In addition, the authors are grateful for the Delphin support team's technical support.

References

[1] D.J. Dacquisto, J.H. Crandell, J. Lyons, Building Moisture and Durability Past, Present and Future, Department of Housing and Urban Development, Washington, D.C., USA, Oct. 2004.

[2] D. Mudarri, W.J. Fisk, Public health and economic impact of dampness and mold, Indoor Air 17 (3) (Jun. 2007) 226–235, https://doi.org/10.1111/j.1600-0668.2007.00474.x.

[3] G. Grün, S. Urlaub, P. Foldbjerg, Mould and Dampness in European Homes and Their Impact on Health, Fraunhofer-Institut für Bauphysik IBP, Stuttgart, Germany, 2016, https://doi.org/10.13140/RG.2.2.18770.76488. EER-058/2016/950, Nov.

[4] E. Heseltine, J. Rosen, World Health Organization (Eds.), WHO Guidelines for Indoor Air Quality: Dampness and Mould, WHO, Copenhagen, 2009.

[5] J. Wang, 'Asthma and Rhinitis Among Adults in Sweden and China, Risk Factors in the Home Environment', Doctoral Thesis, Uppsala University, Sweden, 2018, https://doi.org/10.33063/diva-427327.

[6] H. Hens, IEA annex 14: condensation and energy, J. Therm. Insul. 15 (3) (Jan. 1992) 261–273, https://doi.org/10.1177/109719639201500307.

[7] K. Sedlbauer, W. Hofbauer, N. Krueger, F. Mayer, K. Breuer, Material specific isopleth-systems as valuable tools for the assessment of the durability of building materials against mould infestation – the "isopleth-traffic light", in: 12DBMC - 12th International Conference on Durability of Building Materials and Components, Oct. 2011, p. 8. Porto, Portugal.

[8] H.J. Moon, 'Assessing Mold Risks in Buildings under Uncertainty', Doctoral Thesis, Georgia Institute of Technology, Atlanta, GA, USA, 2005.

[9] Finnish mould growth model | Building Physics | Tampere Universities', Building Physics. https://research.tuni.fi/buildingphysics/finnish-mould-growth-model/(accessed June. 30, 2022).

[10] S. Thelandersson, T. Isaksson, Mould resistance design (MRD) model for evaluation of risk for microbial growth under varying climate conditions, Build. Environ. 65 (Jul. 2013) 18–25, https://doi.org/10.1016/j.buildenv.2013.03.016.

[11] Å. Togerö, C. Svensson Tengberg, B. Bengtsson, The m-model: a method to assess the risk for mould growth in wood structures with fluctuating hygrothermal conditions, in: NSB 2011 - 9th Nordic Symposium on Building Physics, 2011. Tampere, Finland.

[12] L. Wadsö, B. Bengtsson, P. Johansson, The M-Model for Prediction of Mould Growth, 2022. Lund, Sweden.

[13] S. Geving, A systematic method for hygrothermal analysis of building constructions using computer models, in: Fifth International IBPSA Conference, 1997. Prague, Check Republic.

[14] M. Salonvaara, A. Karagiozis, A. Holm, Stochastic building envelope modeling—the influence of material properties, in: Building VIII, 1995, p. 8.

[15] A.H. Holm, H.M. Kuenzel, J. Radon, Uncertainty approaches for hygrothermal building simulations— drying of AAC in hot and humid climates, Buildings VIII (2001) 6.

[16] A. Holm, H.M. Kuenzel, Uncertainty approaches for hygrothermal building simulations - drying of an AAC flat roof in different climates, in: Seventh International IBPSA, Building Simulation, Rio de Janeiro, Brazil, Aug. 2001, p. 8.

[17] K. Kurkinen, K. Pietrzyk, E.-L. Wentzel, C.-E. Hagentoft, Probabilistic analysis of indoor surface hygrothermal conditions accounting for thermal and hygric memory of the building component, in: 9th International Conference Thermal Performance of Exterior Envelopes of Whole Buildings, 2004, p. 9. Clearwater, USA.

[18] J. Zhao, R. Plagge, A. Nicolai, J. Grunewald, J.S. Zhang, Stochastic study of hygrothermal performance of a wall assembly—the influence of material properties and boundary coefficients, HVAC R Res. 17 (4) (2011), 4, https://doi.org/10.1080/10789669.2011.585421.

[19] S. Pallin, P. Johansson, C.-E. Hagentoft, Stochastic modeling of moisture supply in dwellings based on moisture production and moisture buffering capacity, in: 12th Conference of International Building Performance Simulation Association, Nov. 2011, p. 8. Sydney, Australia.

[20] K. Calle, N. Van Den Bossche, Probabilistic assessment of the impact of material properties on the risk of frost damage in masonry constructions, in: 4th Central European Symposium on Building Physics (CESBP 2019), MATEC Web of Conferences, Prague, Czech Republic, 2019, p. 6, https://doi.org/10.1051/matecconf/201928202084.

[21] V. Kukk, J. Kers, T. Kalamees, L. Wang, H. Ge, Impact of built-in moisture on the design of hygrothermally safe cross-laminated timber external walls: a stochastic approach, Build. Environ. 226 (Dec. 2022), 109736, https://doi.org/10.1016/j.buildenv.2022.109736.

[22] H.L.S.C. Hens, Fungal defacement in buildings: a performance related approach, HVAC R Res. 5 (3) (Jul. 1999) 265–280, https://doi.org/10.1080/10789669.1999.10391237.

[23] H.J. Moon, G. Augenbroe, A mixed simulation approach to analyze mold growth under uncertainty, in: Ninth International IBPSA Conference, Building Simulation, Montreal, Canada, Aug. 2005, p. 9.

[24] H.J. Moon, G. Augenbroe, Application of probabilistic simulation and bayesian decision theory in the selection of mold remediation actions, in: 10th International IBPSA Conference, Building Simulation, Beijing, China, 2007, p. 8.

[25] H.J. Moon, G. Augenbroe, Empowerment of decision-makers in mould remediation, Build. Res. Inf. 36 (5) (Oct. 2008), 5, https://doi.org/10.1080/09613210801996203.

[26] C.E. Hagentoft, A.S. Kalagasidis, Hygrothermal conditions and mould growth potential in cold attics: impact of weather, building system and construction design characteristics, in: V.P. de Freitas, J.M.P.Q. Delgado (Eds.), Hygrothermal Behavior, Building Pathology and Durability, Building Pathology and Rehabilitation, vol. 1, Springer Berlin Heidelberg, Berlin, Heidelberg, 2013, pp. 61–91, https://doi.org/10.1007/978-3-642-31158-1_4.

[27] L. Wang, H. Ge, Stochastic Modelling of Hygrothermal Performance of Highly Insulated Wood Framed Walls, vol. 146, Building and Environment, Dec. 2018, pp. 12–28, https://doi.org/10.1016/j.buildenv.2018.09.032.

[28] L. Wang, H. Ge, Hygrothermal performance of cross-laminated timber wall assemblies: a stochastic approach, Build. Environ. 97 (Feb. 2016) 11–25, https://doi.org/10.1016/j.buildenv.2015.11.034.

[29] K. Gradeci, N. Labonnote, B. Time, J. Köhler, A probabilistic-based methodology for predicting mould growth in façade constructions, Build. Environ. 128 (Jan. 2018) 33–45, https://doi.org/10.1016/j.buildenv.2017.11.021.
[30] K. Gradeci, U. Berardi, B. Time, J. Köhler, Evaluating highly insulated walls to withstand biodeterioration: a probabilistic-based methodology, Energy Build. 177 (Oct. 2018) 112–124, https://doi.org/10.1016/j.enbuild.2018.07.059.
[31] L. Rivalin, P. Stabat, D. Marchio, M. Caciolo, F. Hopquin, A comparison of methods for uncertainty and sensitivity analysis applied to the energy performance of new commercial buildings, Energy Build. 166 (May 2018) 489–504, https://doi.org/10.1016/j.enbuild.2018.02.021.
[32] K. Gradeci, U. Berardi, Application of probabilistic approaches to the performance evaluation of building envelopes to withstand mould growth, J. Build. Phys. 43 (3) (Nov. 2019), 3, https://doi.org/10.1177/1744259119861784.
[33] M.D. Morris, Factorial sampling plans for preliminary computational experiments, Technometrics 33 (2) (May 1991), 2, https://doi.org/10.1080/00401706.1991.10484804.
[34] J. Zhao, 'Development of a Novel Statistical Method and Procedure for Material Characterization and a Probabilistic Approach to Assessing the Hygrothermal Performance of Building Enclosure Assemblies', Dissertation, College of Engineering and Computer Science, Syracuse University, Syracuse, NY, USA, 2012.
[35] P. Freudenberg, U. Ruisinger, E. Stöcker, Calibration of hygrothermal simulations by the help of a generic optimization tool, in: *11th Nordic Symposium On Building Physics*, Trondheim, Norway, Energy Procedia, Jun. 2017, pp. 405–410, https://doi.org/10.1016/j.egypro.2017.09.645.
[36] K. Calle, N. Van Den Bossche, Sensitivity analysis of the hygrothermal behaviour of homogeneous masonry constructions: interior insulation, rainwater infiltration and hydrophobic treatment, J. Build. Phys. 44 (6) (May 2021), 6, https://doi.org/10.1177/17442591211009937.
[37] V. Marincioni, G. Marra, H. Altamirano-Medina, Development of predictive models for the probabilistic moisture risk assessment of internal wall insulation, Build. Environ. 137 (Jun. 2018) 257–267, https://doi.org/10.1016/j.buildenv.2018.04.001.
[38] A. Tijskens, S. Roels, H. Janssen, Hygrothermal assessment of timber frame walls using a convolutional neural network, Build. Environ. 193 (Apr. 2021), 107652, https://doi.org/10.1016/j.buildenv.2021.107652.
[39] A. Tijskens, H. Janssen, S. Roels, Using convolutional neural networks for hygrothermal predictions to extrapolate to other external climates, in: J. Kurnitski, T. Kalamees (Eds.), 12th Nordic Symposium on Building Physics (NSB 2020), Tallinn, Estonia: E3S Web of Conferences, Jun. 2020, 04001, https://doi.org/10.1051/e3sconf/202017204001.
[40] A. Tijskens, S. Roels, H. Janssen, Neural networks for metamodelling the hygrothermal behaviour of building components, Build. Environ. 162 (Sep. 2019), 106282, https://doi.org/10.1016/j.buildenv.2019.106282.
[41] A. Tijskens, H. Janssen, S. Roels, The impact of a reduced training subspace on the prediction accuracy of neural networks for hygrothermal predictions, Journal of Building Performance Simulation 14 (1) (Jan. 2021), 1, https://doi.org/10.1080/19401493.2020.1832148.
[42] A. Tijskens, H. Janssen, S. Roels, Optimising convolutional neural networks to predict the hygrothermal performance of building components, Energies 12 (20) (Oct. 2019), 20, https://doi.org/10.3390/en12203966.
[43] A. Tijskens, S. Roels, H. Janssen, Neural networks to predict the hygrothermal response of building components in a probabilistic framework, in: Healthy, Intelligent and Resilient Buildings and Urban Environments, International Association of Building Physics (IABP), 2018, pp. 1169–1174, https://doi.org/10.14305/ibpc.2018.ms-6.04.
[44] R.Z. Freire, G.H. dos Santos, L. dos S. Coelho, Hygrothermal dynamic and mould growth risk predictions for concrete tiles by using least squares support vector machines, Energies 10 (8) (Jul. 2017) 1093, https://doi.org/10.3390/en10081093.
[45] N. Bansal, M. Defo, M.A. Lacasse, Application of support vector regression to the prediction of the long-term impacts of climate change on the moisture performance of wood frame and massive timber walls, Buildings 11 (5) (Apr. 2021) 188, https://doi.org/10.3390/buildings11050188.
[46] C. Aggarwal, H. Ge, M. Defo, M.A. Lacasse, Hygrothermal performance assessment of wood frame walls under historical and future climates using partial least squares regression, Build. Environ. 223 (Sep. 2022), 109501, https://doi.org/10.1016/j.buildenv.2022.109501.
[47] C. Aggarwal, H. Ge, M. Defo, Assessing mould growth risk of wood-frame walls using partial least squares (PLS) regression considering climate model uncertainties, Build. Environ. 238 (Jun. 2023), 110374, https://doi.org/10.1016/j.buildenv.2023.110374.
[48] S.A. Naghibi, H.R. Pourghasemi, B. Dixon, GIS-based groundwater potential mapping using boosted regression tree, classification and regression tree, and random forest machine learning models in Iran, Environ. Monit. Assess. 188 (1) (Jan. 2016) 44, https://doi.org/10.1007/s10661-015-5049-6.
[49] S.A. Naghibi, K. Ahmadi, A. Daneshi, Application of support vector machine, random forest, and genetic algorithm optimized random forest models in groundwater potential mapping, Water Resour. Manag. 31 (9) (Jul. 2017) 2761–2775, https://doi.org/10.1007/s11269-017-1660-3.
[50] A. Golkarian, S.A. Naghibi, B. Kalantar, B. Pradhan, Groundwater potential mapping using C5.0, random forest, and multivariate adaptive regression spline models in GIS, Environ. Monit. Assess. 190 (3) (Mar. 2018) 149, https://doi.org/10.1007/s10661-018-6507-8.
[51] D. Reiter, The Monte Carlo method, an introduction, in: Computational Many-Particle Physics, Lecture Notes in Physics, vol. 739, Springer Berlin Heidelberg, Berlin, Heidelberg, 2008, pp. 63–78, https://doi.org/10.1007/978-3-540-74686-7_3.
[52] G.D. Wyss, K.H. Jorgensen, A User's Guide to LHS: Sandia's Latin Hypercube Sampling Software, Feb. 1998, 573301, https://doi.org/10.2172/573301. SAND–98-0210.
[53] S. Marino, I.B. Hogue, C.J. Ray, D.E. Kirschner, A methodology for performing global uncertainty and sensitivity analysis in systems biology, J. Theor. Biol. 254 (1) (Sep. 2008), 1, https://doi.org/10.1016/j.jtbi.2008.04.011.
[54] M.D. McKay, R.J. Beckman, W.J. Conover, Comparison of three methods for selecting values of input variables in the analysis of output from a computer code, Technometrics 21 (2) (May 1979) 239–245, https://doi.org/10.1080/00401706.1979.10489755.
[55] J.C. Helton, J.D. Johnson, C.J. Sallaberry, C.B. Storlie, Survey of sampling-based methods for uncertainty and sensitivity analysis, Reliab. Eng. Syst. Saf. 91 (10–11) (Oct. 2006), 10–11, https://doi.org/10.1016/j.ress.2005.11.017.
[56] R. Moss, lhs: Latin hypercube sampler for scenario modelling [OS Independent], https://bitbucket.org/robmoss/latin-hypercube-sampling/. (Accessed 2 July 2022).
[57] Delphin, May 26, 2021, https://bauklimatik-dresden.de/delphin/index.php?aLa=en. (Accessed 26 May 2021).
[58] B. Hejazi, N. Rodrigues Marques Sakiyama, J. Frick, H. Garrecht, 'Hygrothermal Simulations Comparative Study: Assessment of Different Materials Using WUFI and DELPHIN Software', presented at the Building Simulation 2019, Rome, Italy, May 2021, pp. 4674–4681, https://doi.org/10.26868/25222708.2019.211033.
[59] U. Ruisinger, P. Kautsch, Comparison of hygrothermal 2D- and 3D-simulation results with measurements from a test house, in: 12th Nordic Symposium on Building Physics, Tallinn, Sep. 2020, 08004, https://doi.org/10.1051/e3sconf/202017208004 (NSB 2020).
[60] 'Meteonorm Version 8 Updated historic, current and future data', Meteonorm (en). https://meteonorm.com/en/(accessed July. 2, 2022).
[61] H. Hens, Applied Building Physics Ambient Conditions, Building Performance and Material Properties, second ed., Ernst & Sohn, Leuven, Belgium, 2016.
[62] T. Ojanen, H. Viitanen, R. Peuhkuri, Modelling of mould growth in building envelopes, in: IEA ECBCS Annex 41 Closing Seminar : Nordic Building Physics Conference, 2007, p. 18. Copenhagen, Denmark.
[63] H. Viitanen, T. Ojanen, Improved model to predict mold growth in building materials, in: 10th Thermal Performance of the Exterior Envelopes of Whole Buildings Conference, Dec. 2007, p. 8. Clearwater Beach, United States.
[64] H. Viitanen, Factors Affecting the Development of Mould and Brown Rot Decay in Wooden Material and Wooden Structures, Doctoral thesis, Department of Forest Products, Swedish University of Agricultural Sciences, Uppsala, Sweden, 1996.
[65] L. Breiman, Random forests, Mach. Learn. 45 (1) (2001) 5–32.
[66] L. Breiman, Bagging predictors, Mach. Learn. 24 (2) (Aug. 1996) 123–140, https://doi.org/10.1007/BF00058655.
[67] Tin Kam Ho, The random subspace method for constructing decision forests, IEEE Trans. Pattern Anal. Mach. Intell. 20 (8) (Aug. 1998) 832–844, https://doi.org/10.1109/34.709601.
[68] P. Vorpahl, H. Elsenbeer, M. Märker, B. Schröder, How can statistical models help to determine driving factors of landslides? Ecol. Model. 239 (Jul. 2012) 27–39, https://doi.org/10.1016/j.ecolmodel.2011.12.007.
[69] M. Banerjee, Y. Ding, A.-M. Noone, Identifying representative trees from ensembles, Stat. Med. 31 (15) (Jul. 2012) 1601–1616, https://doi.org/10.1002/sim.4492.
[70] W. Aertsen, V. Kint, J. van Orshoven, K. Özkan, B. Muys, Comparison and ranking of different modelling techniques for prediction of site index in Mediterranean mountain forests, Ecol. Model. 221 (8) (Apr. 2010) 1119–1130, https://doi.org/10.1016/j.ecolmodel.2010.01.007.
[71] C. Strobl, A.-L. Boulesteix, A. Zeileis, T. Hothorn, Bias in random forest variable importance measures: illustrations, sources and a solution, BMC Bioinf. 8 (1) (Dec. 2007) 25, https://doi.org/10.1186/1471-2105-8-25.
[72] A. Liaw, M. Wiener, Classification and Regression by randomForest, vol. 2, Dec. 2002, p. 5.
[73] O.M. Querin, M. Victoria, C. Alonso, R. Ansola, P. Martí, Discrete method of structural optimization * *additional author for this chapter is prof. Dr.-Ing. Dr.-Habil. George I. N. Rozvany, in: Topology Design Methods for Structural Optimization, Elsevier, 2017, pp. 27–46, https://doi.org/10.1016/B978-0-08-100916-1.00003-9.
[74] 'sklearn.ensemble.RandomForestRegressor', scikit-learn. https://scikit-learn.org/stable/modules/generated/sklearn.ensemble.RandomForestRegressor.html. (Accessed 5 March 2003).
[75] D.M. Hamby, A review of techniques for parameter sensitivity analysis of environmental models, Environ. Monit. Assess. 32 (2) (Sep. 1994), 2, https://doi.org/10.1007/BF00547132.
[76] P. Schober, C. Boer, L.A. Schwarte, Correlation coefficients: appropriate use and interpretation, Anesth. Analg. 126 (5) (May 2018) 1763–1768, https://doi.org/10.1213/ANE.0000000000002864.
[77] T. Malmqvist, M. Erlandsson, N. Francart, J. Kellner, Minskad Klimatpåverkan Från Flerbostadshus, Sveriges Byggindustrier', Sveriges Byggindustrier, Sweden, August, 2018. http://www.diva-portal.org/smash/record.jsf?pid=diva2%3A1549629&dswid=3745. (Accessed 26 June 2022).
[78] K. Calle, C. Coupillie, A. Janssens, N. Van Den Bossche, Implementation of rainwater infiltration measurements in hygrothermal modelling of non-insulated brick cavity walls, J. Build. Phys. 43 (6) (May 2020) 477–502, https://doi.org/10.1177/1744259119883909.

[79] E. Vereecken, S. Roels, Review of mould prediction models and their influence on mould risk evaluation, Build. Environ. 51 (May 2012) 296–310, https://doi.org/10.1016/j.buildenv.2011.11.003.
[80] EN 15026, Hygrothermal Performance of Building Components and Building Elements - Assessment of Moisture Transfer by Numerical Simulation, 2007.
[81] EN ISO 6946, Building Components and Building Elements - Thermal Resistance and Thermal Transmittance - Calculation Methods, 2017.
[82] P.W.M.H. Steskens, H. Janssen, C. Rode, Influence of the convective surface transfer coefficients on the heat, air, and moisture (HAM) building performance, Indoor Built Environ. 18 (3) (Jun. 2009) 245–256, https://doi.org/10.1177/1420326X09105682.
[83] H.M. Künzel, A.H. Holm, M. Krus, Hygrothermal Properties and Behaviour of Concrete, 2008, 13.
[84] L. Ducoulombier, Z. Lafhaj, Comparative study of hygrothermal properties of five thermal insulation materials, Case Stud. Therm. Eng. 10 (Sep. 2017) 628–640, https://doi.org/10.1016/j.csite.2017.11.005.
[85] L. Wang, H. Ge, Effect of rain leakage on hygrothermal performance of highly insulated wood-framed walls: a stochastic approach, Can. J. Civ. Eng. 46 (11) (Nov. 2019), 11, https://doi.org/10.1139/cjce-2019-0223.
[86] J.D. Thacher, et al., Mold and dampness exposure and allergic outcomes from birth to adolescence: data from the BAMSE cohort, Allergy 72 (6) (Jun. 2017) 967–974, https://doi.org/10.1111/all.13102.
[87] K. Engvall, C. Norrby, D. Norbäck, Asthma symptoms in relation to building dampness and odour in older multifamily houses in Stockholm, Int. J. Tubercul. Lung Dis. 5 (May 2001) 10.
[88] M. Bayat Pour, J. Niklewski, E. Frühwald Hansson, S. Thöns, Mould reliability analysis combined with mould health risks for decision support, in: 5th Central European Symposium on Building Physics, Bratislava Slovakia, Sep. 2022, p. 8. CESBP 2022.

Paper III

Journal of Building Engineering 94 (2024) 109936

Contents lists available at ScienceDirect

Journal of Building Engineering

journal homepage: www.elsevier.com/locate/jobe

Impact of extruded mortar joints on the hygrothermal performance of brick veneer walls: A probabilistic study

Mohsen Bayat Pour *, Seyedmohammad Kahangi Shahreza

Division of Structural Engineering, Department of Building and Environmental Technology, Lund University, John Ericssons Väg 1, SE-223 63, Lund, Sweden

ARTICLE INFO

Keywords:
Mortar extrusion
Machine learning
Mould assessment
Clay brick masonry
Hygrothermal simulation

ABSTRACT

Mortar extrusion during bricklaying, resulting from suboptimal workmanship, may act as a bridge linking clay brick masonry claddings and adjacent layers (e.g., insulation or weather-resistant barriers), thereby, facilitating water penetration into the adjacent layer owing to wind-driven rain (WDR). Despite the significant effect of water penetration on the hygrothermal performance of building envelopes, a consensus regarding the incorporation of WDR-induced water penetration into moisture safety designs and analyses remains lacking. In 2022, Kahangi Shahreza et al. tested two distinct brick types with three diverse mortar joint profiles. Consequently, they proposed a water penetration criterion that can be implemented in hygrothermal analysis of clay brick masonry. The research in this paper combines the results of their study with probabilistic hygrothermal analysis by investigating the influence of extruded mortar on mould growth for a timber frame wall with brick masonry cladding. Two water penetration criteria, including ASHRAE and experimental study (ES) based on Kahangi Shahreza's study, were implemented while considering the different climatic conditions in Sweden. A metamodel, established using the random forests (RF) machine learning algorithm, serves as a tool for mould sensitivity analysis. The results of the probabilistic mould growth analysis revealed a congruence between the ASHRAE and ES criteria for locations with high WDR loads. However, in scenarios involving low WDR loads, the ASHRAE criterion yielded a higher maximum mould index than the ES criterion. In addition, the linear and non-linear mould sensitivity analyses demonstrated a positive correlation between the increase in the extruded mortar depth and elevated maximum mould indices. Nevertheless, the strength of this correlation is subject to alterations based on the WDR loads and selected water penetration criteria.

Nomenclature

ACR	Air Change Rate [1/h]
ASHRAE	American Society of Heating, Refrigerating and Air-conditioning Engineers
A_w	Water Absorption Coefficient [kg/m^2. S$^{0.5}$]
CoV	Coefficient of Variation
Cp	Specific Heat Capacity [J/kg.K]
CSi	Case Study i
D_B	Bulk Density [kg/m^3]

(*continued on next page*)

* Corresponding author. John Ericssons väg 1, SE-223 63, Lund, Sweden.
E-mail addresses: mohsen.bayat_pour@kstr.lth.se (M. Bayat Pour), mohammad.kahangi@kstr.lth.se (S. Kahangi Shahreza).

https://doi.org/10.1016/j.jobe.2024.109936
Received 9 December 2023; Received in revised form 4 June 2024; Accepted 12 June 2024
Available online 13 June 2024
2352-7102/© 2024 The Author(s). Published by Elsevier Ltd. This is an open access article under the CC BY license (http://creativecommons.org/licenses/by/4.0/).

(*continued*)

ES	Experimental Study
G	Gothenburg
LHS	Latin Hypercube Sampling
MA	Metamodel Analysis
MAE	Mean Absolute Error
MRA	Mould Reliability Analysis
MSA	Mould Sensitivity Analysis
n	Total number of original data
OF_i	Objective function
PA	Probabilistic Analysis
R	Rensjön
RF	Random Forests
RH	Relative humidity [%]
R^2	Coefficient of Determination
S_d-value	Diffusion Equivalent Air Layer Thickness
T	Temperature [°C]
WDR	Wind-driven Rain
y_i	Original data
$\overline{y_i}$	Mean of the original data
$\widehat{y_i}$	Predicted data
ε_i	Convergence value
θ_{eff}	Saturation point [m^3/m^3]
θ_{por}	Porosity [m^3/m^3]
λ_{dry}	Thermal Conductivity [W/m.K]
μ	Mean
μ_{VDR}	Water Vapour Diffusion Resistance Factor [−]
ρ	Spearman's correlation coefficient
σ	Standard deviation

1. Introduction

1.1. Background

The hygrothermal performance of buildings has significant implications for construction projects related to material degradation [1], economy [2], and health problems [3]. Modelling the hygrothermal performance of external wall assemblies is significant for identifying and mitigating moisture-related challenges [4], including microbial growth. Assessing the risk of mould growth in exterior walls relies on analysing the temporal variations in temperature and relative humidity. Accordingly, various mould models have emerged over the last few decades, such as the Finnish mould growth model [5], Mould Resistance Design (MRD) [6], and m-model [7].

Residential buildings with clay brick masonry façades are frequently constructed owing to their aesthetic merits and extended life-spans [8]. Brick cladding effectively protects against wind-driven rain (WDR), a significant source of moisture in Nordic countries that adversely affects the hygrothermal performance and durability of building façades [9]. These effects include material degradation, frost damage, salt efflorescence, structural cracking, interior damage, and mould growth, especially if bio-based materials such as wooden studs are present [10]. Abuku et al. [11] found that water penetration due to WDR loads, particularly along wall edges, can significantly lead to mould growth. In addition, numerous studies [12–15] have substantiated the correlation between WDR, elevated water content, and water penetration potential within masonry walls. Kayll [16] documented the high expenses associated with renovating building envelopes owing to rain penetration. Approximately 50 % of the reported building damage cases in Belgium between 2010 and 2015 were attributed to water-tightness issues [17]. It was reported that water penetration through the building envelope emerged as the predominant damage type. In France, 64 % of all damage-related costs reported from 2018 to 2020 were attributed to rain penetration and deficiencies in the watertightness of building envelope [18].

Despite the significant influence of water penetration on building envelopes hygrothermal performance, a consensus regarding the quantity of water penetrating brick masonry claddings remains lacking [19,20]. According the guidelines in the North American Standard (ASHRAE 160–2021) [21], the deposition of 1 % of WDR on the external surface of a wall is considered as the moisture source behind the cladding. Many studies have attempted to substantiate the validity of the 1 % water penetration threshold for WDR [22,23]. However, comprehensive assessments of experimental studies revealed that the WDR penetration into clay brick cladding ranges from 0 % to 20 % [20,24–26]. Although ASHRAE considers that 1 % of WDR penetrate the cladding, experimental studies [23,27] revealed a temporal gap between the commencement of WDR exposure and the initial documented instance of penetration, even under extreme testing conditions. This gap is attributed to the specific saturation level necessary for initiating water penetration in brick masonry [25, 28]. Thus, when masonry walls have the potential to absorb and retain water, WDR penetration may not occur. Furthermore, the ASHRAE criterion does not differentiate among diverse external surfaces, such as material types and textures. However, owing to the lack of agreement on WDR-induced water penetration rates across diverse exterior cladding surfaces, the ASHRAE criterion has been commonly followed [19,20,29]. This highlights the significance of employing an approach that accurately estimates the percentage of WDR-induced water penetration in brick claddings.

In addition to the lack of consensus on the amount of water penetrating brick masonry claddings, an agreement on the location of the moisture source in hygrothermal simulations is also lacking. According to ASHRAE 160–2021 [21], the recommended placement of

a moisture load arising from WDR-induced water penetration is on the external surface of the weather-resistant barrier. In the absence of a weather-resistant barrier, the placement site should be determined based on technical reasoning. An experimental study by Groot and Gunneweg [30] demonstrated that among several parameters affecting WDR-induced water penetration, workmanship most significantly influences rain water penetration of historic masonry walls. Mortar extrusion can occur owing to poor workmanship, with the potential to significantly affect moisture movement response [20,31]. Wall assemblies with clay brick masonry cladding are susceptible to mortar extrusion, which can cause moisture-related issues triggered by WDR-induced water penetration. Consequently, incorporating the influence of extruded mortar into the hygrothermal analysis process is necessary to achieve a more robust and comprehensive building envelope design and provide a more detailed outline of the deposition site.

Modelling of extruded mortar joints in conjunction with hygrothermal analysis presents inherent uncertainties. Probabilistic methodologies are used to address uncertainties in hygrothermal performance modelling. According to Annex 55: Subtask 2 [32], some tools including uncertainty propagation, sensitivity analysis, and metamodeling methods, are essential for probabilistic hygrothermal analysis. The first publication to perform hygrothermal uncertainty propagation was marked in 1997 by Geving [33], who introduced a systematic method for hygrothermal analysis based on a Monte Carlo simulation. After that, several studies have tried to advance the field by incorporating the various sampling techniques such as Latin Hypercube Sampling (LHS) [34–36], Quasi-Monte Carlo [37–40], or multilayered sampling scheme [41,42], with the aim of enhancing sample efficiency and reducing computational time. The inception of hygrothermal sensitivity analysis research dates back to 1993 when Hokoi and Kumaran [43] conducted a sensitivity analysis of the drying process of wet glass fibre insulation. Thereafter, various publications [44–46] predominantly aimed to improve the hygrothermal sensitivity analysis by employing methods capable of non-linear analysis and accounting for interactions among input variables.

Monte Carlo methodology is commonly used for the purpose of probabilistic hygrothermal analysis [47]; however, this approach is computationally expensive and time-consuming [41]. Several researchers have used metamodels to overcome the time-consuming nature of hygrothermal simulations. Metamodeling in probabilistic hygrothermal assessment began by using the response surface methodology (RSM) in 2013 by Ramos et al. [48,49]. Marincioni et al. [50] employed generalised additive models (GAM) and generalised additive models for location scale and shape (GAMLS) to assess moisture risk in internally insulated wall assemblies. Their metamodel closely approximated the simulation results, except for a few cases of underestimated values. Tijskens et al. [41,51–53] adopted neural networks to expedite computations and predict response time series for diverse wall types. It is found that the convolutional neural network (CNN) outperformed the multi-layer perceptron (MLP) and recurrent neural network (RNN) in predicting non-linear hygrothermal patterns. Freire et al. [54] employed support vector regression (SVR) for the roof assembly of a building to predict water vapour flux, mould index, and sensible and latent heat fluxes with satisfactory R^2 values for all analysed output parameters. Aggarwal et al. [55,56] leveraged partial least squares (PLS) regression to predict hygrothermal performance across Canadian climates using historical and future climate data. Bayat Pour et al. [57] introduced a method for improving the robustness of hygrothermal and mould analyses by integrating a probabilistic approach with the random forests (RF) machine learning algorithm. Therefore, a probabilistic hygrothermal analysis can potentially be used to address the uncertainties related to the extruded mortar joints and investigate their influences on the mould growth.

1.2. *Objectives and outline of the paper*

This study aims to address the identified gaps, i.e., investigation of the effect of extruded mortar joints with considering two distinct

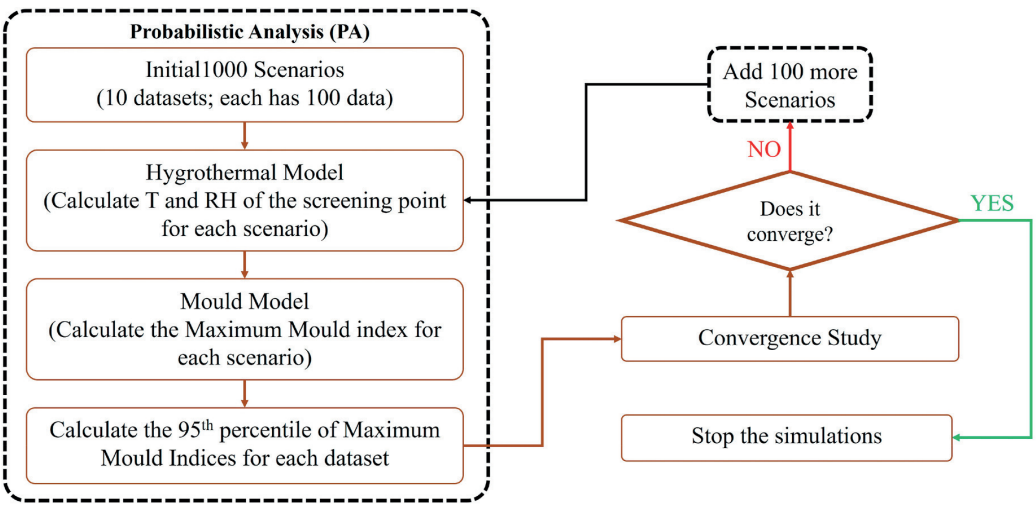


Fig. 1. Probabilistic mould growth analysis procedure.

water penetration criteria on the hygrothermal performance of wall assemblies. In this regard, the impact of extruded mortar joints in clay brick masonry claddings on timber frame walls considering their susceptibility to mould growth is assessed. To this end, a probabilistic methodology in conjunction with a machine learning algorithm was employed, supplemented by linear and non-linear sensitivity analyses.

The reminder of this paper is organised as follows: Section 2 describes the methodology, including the WDR-induced water penetration criteria, hygrothermal and mould growth analysis methods, and case studies; Sections 3 and 4 present the results and a discussion of the mould growth assessment and mould sensitivity analysis; Finally, Section 5 summarises the conclusions of the study.

2. Methodology

2.1. Mould growth analysis

This study performed a mould growth analysis based on the probabilistic analysis section of the mould reliability analysis (MRA) method initially developed by Bayat Pour et al. [57]. Fig. 1 shows the procedure for the probabilistic mould growth analysis. It begins with identifying a finite set of scenarios, achieved by applying the LHS technique [58]. Subsequently, a hygrothermal analysis is performed for each scenario, determining the temperature (T) and relative humidity (RH) at the designated screening point. The maximum mould index is calculated for each scenario using a Finnish mould growth model [5]. Consequently, the 95th percentile of the maximum mould indices is calculated for each dataset. Focusing on the 95th percentile allows for capturing the behaviour of the upper tail of the distribution, which is essential in scenarios where extreme values carry significant implications, such as in mould growth analysis. Moreover, in hygrothermal analysis, where decision analysis involves assessing risks associated with extreme events, analysing the 95th percentile offers insights into the likelihood and magnitude of such events, facilitating informed risk management strategies.

The Finnish mould growth model [5] provides a framework for mould assessment characterised by a mould index ranging from 0 to 6. Notably, its comprehensive applicability across diverse building materials, considering the influences of surface types and coatings via sensitivity and decline classifications. A potential decline in mould growth is considered when subjected to unfavourable conditions lasting less than 6 h or exceeding 24 h. Typically, no decline in mould growth is observed from 6 to 24 h [59]. Notably, the mould growth decline model was developed based on a finite dataset, neglecting temperatures below 0 °C and periods surpassing 14 d of adverse conditions [60].

A convergence study is essential for determining the required number of simulations (scenarios or sample size) in a probabilistic analysis (PA). Accordingly, Bayat Pour et al. [57] adapted an equation from Ref. [61] to facilitate the convergence analysis in a probabilistic hygrothermal analysis. This involves a systematic augmentation of the number of simulations while monitoring the 95th percentile of the maximum mould indices (target variable). The convergence criterion includes tracking the change in the target variable over the preceding 10 iterations. Each iteration comprises 100 distinct scenarios, with the progressive addition of 100 new scenarios to previous iterations to create a new iteration. According to Ref. [57], the simulation process is continued until the convergence value decreases to below the predefined threshold of 0.001. Eq. (1) is used to calculate the convergence value.

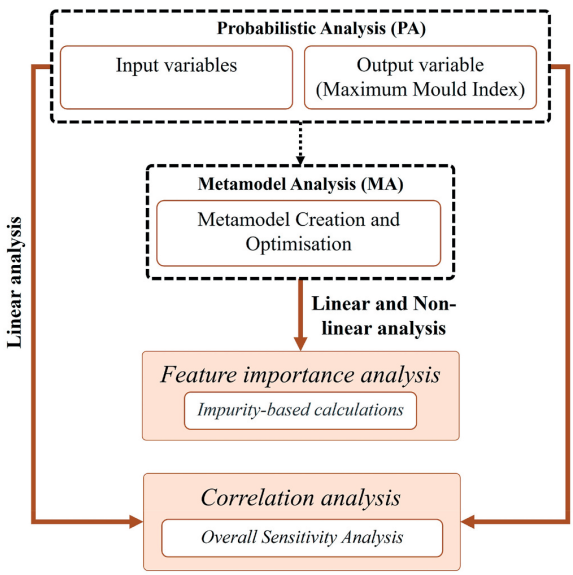


Fig. 2. Mould sensitivity analysis procedure.

$$\varepsilon_i = \frac{\left|\sum_{i-9}^{i-5} OF_i - \sum_{i-4}^{i} OF_i\right|}{\sum_{i-4}^{i} OF_i} \quad (1)$$

where i is the current iteration number (>10), OF_i is the ith iteration of objective function, and ε_i is the convergence value of the OF_i (i.e., 95th percentile of the maximum mould indices in this study).

2.2. Mould sensitivity analysis

A sensitivity analysis for mould growth was conducted based on the method developed by Bayat Pour et al. [57], called the mould sensitivity analysis (MSA). This method includes two types of sensitivity analyses: correlation and feature importance analyses, as shown in Fig. 2.

The correlation analysis is conducted by evaluating pairs of variables by calculating the Spearman's correlation coefficient, denoted as $\rho_{X_{ri},Y_{rj}}$, using Eq. (2) [35]. This involves thoroughly investigating the entire distribution of input and output variables (overall sensitivity analysis) [57].

$$\rho_{X_{ri},Y_{rj}} = \frac{cov(X_{ri}, Y_{rj})}{\sigma_{X_{ri}}.\sigma_{Y_{rj}}} \quad (2)$$

where.

$cov(X_{ri}, Y_{rj})$ is the covariance of the two ranked variables, and

$\sigma_{X_{ri}}$ *and* $\sigma_{Y_{rj}}$ are the standard deviations of ranked variables.

The Spearman's correlation coefficient (ρ), ranging from −1 to +1, assesses the monotonicity (degree of correlation) between two variables [62]. The sign of the Spearman's correlation coefficient indicates the direction of the relationship between two variables. A positive sign denotes a positive correlation, indicating that the values of the two variables tend to increase or decrease simultaneously. Conversely, a negative sign denotes a negative correlation, indicating that an increase in the value of one variable results in a decrease in the value of the other variable, and vice versa. Based on the Spearman's correlation coefficient, the conventional method for interpreting the correlation between two variables is as follow [63].

- A value of 0.00 indicates "no relationship."
- A value ranging from 0.00 to 0.09 indicates a "negligible relationship"
- A value ranging from 0.10 to 0.39 indicates a "weak relationship"
- A value ranging from 0.40 to 0.69 indicates a "moderate relationship"
- A value ranging from 0.70 to 0.89 indicates a "strong relationship"
- A value ranging from 0.90 to 1.00 indicates a "very strong relationship"

The metamodel analysis (MA) is established based on the RF machine learning algorithm [64]. RF offers notable advantages in interpretability, handling non-linear relationships, and ensuring metamodel robustness. Its decision trees allow for visualising and understanding criteria used in predictions. It excels in modelling complex non-linear relationships and maintain a balance between complexity and stability, reducing overfitting risks. Moreover, RF provides built-in measures of feature importance, aiding in feature selection and enhancing data understanding. Additionally, RF demonstrates computational efficiency, efficiently handling large datasets with high-dimensional feature spaces, and supporting parallelized training for faster processing [57].

In comparison to other modelling techniques, RF presents several unique strengths. RSM is primarily suited for exploring and optimising response surfaces in experimental design but may struggle with complex, high-dimensional data where RF excels due to its ensemble approach [65]. GAM offer interpretability and can model non-linear relationships, but they often lack the robustness and feature importance measures inherent in RF [66]. MLP and RNN are effective for capturing complex patterns in data, particularly in sequential and time-series contexts. However, they can be prone to overfitting and require significant tuning and training time [67,68]. RF, on the other hand, provides a more balanced approach with reduced overfitting risks and quicker training times [64]. SVR is another alternative that performs well with small to medium-sized datasets and offers good generalisation capabilities. Nonetheless, SVR's performance can degrade with very large datasets or when dealing with high-dimensional feature spaces, areas where RF's ensemble learning method outperforms by maintaining accuracy and efficiency [69,70]. The aforementioned points establish RF as a more suitable machine learning algorithm for the scope of this study.

The metamodel construction process starts with a feature selection process, as outlined in Ref. [57]. The feature selection process involves a parametric investigation to identify the optimal number of features to be incorporated into the metamodel. Through this iterative approach, the number of features generating the highest coefficient of determination (R^2) between the predicted and observed maximum mould indices is selected as the effective features. The dataset is randomly divided into training (70 %) and test (30 %) subsets. The precision assessment of the trained metamodel relies on two key accuracy metrics: the mean absolute error (MAE) and coefficient of determination (R^2). Accuracy is evaluated using Eqs. (3) and (4).

$$MAE = \frac{1}{n}\sum_{i=1}^{n} |y_i - \hat{y}_i| \quad (3)$$

$$R^2 = 1 - \frac{\sum_{i=1}^{n} (y_i - \hat{y}_i)^2}{\sum_{i=1}^{n} (y_i - \bar{y}_i)^2} \quad (4)$$

where y_i and $\hat{y}_i$ are the original and predicted data, respectively, $\bar{y}_i$ is the mean of the original data, and n is the total number of original data points. These equations offer quantifiable metrics for assessing the predictive efficacy of the trained models. MAE denotes the average error between the predicted and observed values, and R^2 denotes the proportion of the output variance explained by the input variables. Smaller MAE and higher R^2 values reflect the superior predictive competence of the trained model in relation to the output. Notably, tuning the hyperparameters of the RF model is essential for achieving optimal metamodel performance. In this study, the RF model optimisation process encompassed the fine-tuning of parameters, such as the number of trees, identification of the most effective features, and estimation of the generalisation score using out-of-bag samples. The default values outlined in Ref. [71] were employed for the remaining hyperparameters.

Feature importance analysis is essential for evaluating the effects of input variables on output variables in a trained RF model [57]. It accounts for the linear and non-linear connections between inputs and outputs. RF, an ensemble machine learning method comprising numerous decision trees, employs selected features at internal nodes to split the data into distinct sets with related responses. The selection criteria include Gini impurities and variance reduction for the classification and regression tasks, respectively. The impact of each feature on impurity reduction is quantified, and the most influential feature is selected. Feature importance is determined by calculating the average impurity reduction across all trees. A higher feature importance indicates greater feature relevance in the machine learning model.

2.3. Case studies

Fig. 3 shows case studies 1 and 2 (CS1 and CS2), differing only in the brick material properties (brick types I and II). The case studies involved light-weight timber frame walls, where the timber studs were positioned within the insulation layer, a common constructed wall type in Sweden [31,72]. The frames in these case studies were constructed using wooden materials; thus, they were more susceptible to mould growth and consequently potential health problems.

Tables 1 and 2 present the boundary conditions and material properties, respectively, supplemented by relevant references. The Delphin database [73] was used to determine the optimal outdoor convective heat exchange coefficient, ranging from 12 [W/(m^2.K)] to 20 [W/(m^2.K)], depending on the situation and severity of wind exposure [74]. Notably, the outdoor vapour diffusion coefficient was calculated based on the outdoor convection heat exchange coefficient in the simulation setting. This method ensures that the outdoor convection heat exchange and outdoor vapour diffusion coefficients are properly correlated. The solar absorption coefficient was determined to fluctuate between 0.4 and 0.8 [73] to accommodate various surface colours and textures. The long-wave emissivity, accounting for surface colour and texture differences, ranges from 0.85 to 0.95 [73]. The WDR load is often reduced by a factor of 0.7 when considering the reduction caused by splashing. However, in this study, it is fluctuated between 0.6 and 0.8 with a tolerance of 0.1 [57]. The interior surface heat transfer coefficient ranged from 5 [W/(m^2.K)] to 10 [W/(m^2.K)] to consider the indoor airflow direction [75]. The probability distributions outlined in Table 1 follow uniform distributions, indicating that each determined value has an equal probability of occurrence. The material properties in Table 2 used to simulate the bricks in this study, were derived from a combination of values obtained from the experimental study referenced in Ref. [8], along with additional information sourced from the relevant literature [35].

In this study, material functions of the brick, including moisture storage, liquid water transport, and thermal conductivity were considered in the hygrothermal models as the functions of saturation point (θ_{eff}). In addition, water vapour transport was considered as the function of the water vapour diffusion resistance factor (μ_{VDR}) for brick.

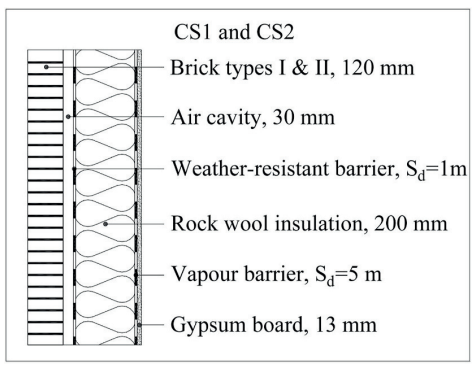


Fig. 3. Two external wall assemblies, case study 1 (CS1) and case study 2 (CS2).

Table 1
Probability distribution values for indoor and outdoor boundary conditions. U(a, b): Uniform distribution, where *a* and *b* are the minimum and maximum values, respectively.

Variable	Probability distribution
Outdoor convection heat exchange coefficient [W/m^{2}K] [74]	U(12, 20)
Solar absorption coefficient [−] [73]	U(0.4, 0.8)
Long-Wave Emissivity [−] [73]	U(0.85, 0.95)
Reduction/splash coefficient of WDR [−] [57]	U(0.6, 0.8)
Indoor Surface Heat Transfer Coefficient (Convective + Radiative), $\left[\frac{W}{m^2.K}\right]$ [76]	U(5, 10)
Indoor Surface Vapour Diffusion Coefficient $\left[\frac{s}{m}\right]$ [77]	U(0.1 × 10^{-7}, 1 × 10^{-7})
Air change rate, ACR $\left[\frac{1}{h}\right]$ [78]	U(0, 20)

Table 2
Probability distributions for the material properties. N(μ, σ): Normal distribution, μ and σ are the mean and standard deviation, respectively. CoV: coefficient of variation.

	Bulk Density (D_B $\left[\frac{kg}{m^3}\right]$)	Specific Heat Capacity (C_p $\left[\frac{J}{kg.K}\right]$)	Porosity (θ_{por} $\left[\frac{m^3}{m^3}\right]$)	Thermal Conductivity (λ_{dry} $\left[\frac{W}{m.K}\right]$)	Water Absorption Coefficient (A_w $\left[\frac{kg}{m^2.s^{0.5}}\right]$)	Water Vapour Diffusion Resistance Factor (μ_{VDR} [−])
Brick type I [8, 35]	N(1830.13, 13.45) CoV = 0.7 %	N(889, 10.67) CoV = 1.2 %	N(0.293, 0.002) CoV = 0.7 %	N(0.548,0.077) CoV = 14 %	N(0.193, 0.00116) CoV = 0.6 %	N(18.01, 0.018) CoV = 0.1 %
Brick type II [8, 35]	N(2024, 38.18) CoV = 1.9 %	N(889, 10.67) CoV = 1.2 %	N(0.247,0.039) CoV = 15.8 %	N(0.548,0.077) CoV = 14 %	N(0.1327, 0.022) CoV = 16.58 %	N(18.01, 0.018) CoV = 0.1 %
Gypsum board [73,79]	N(850, 85) CoV = 10 %	N(850, 85) CoV = 10 %	N(0.65, 0.065) CoV = 10 %	N(0.2, 0.02) CoV = 10 %	[a] N(0.18, 0.018)	N(8.3, 0.83) CoV = 10 %
Rock wool insulation [80]	N(39, 0.78) CoV = 2 %	[b] N(802, 80.2)	[a] N(0.95, 0.095)	N(0.034, 0.0026) CoV = 7.6 %	N(3.39 × 10^{-3}, 9.1 × 10^{-4}) CoV = 27 %	[b] N(2, 0.2)

Note.
[a] These material properties were not specified in their corresponding references; therefore, default values from the Delphin database with a normal distribution and a coefficient of variation of 10 % were used.
[b] These material properties lack information on their distributions in the literature; thus, a normal distribution with a coefficient of variation of 10 % was assumed as a reasonable value, as recommended by Gradeci et al. [79].

2.4. Outdoor climate data

This study performed hygrothermal analyses over a span of five years (2018–2023) using historical climate data with hourly time steps. To eliminate the potential impact of the presumed initial conditions on the output, the climate data for 2018 were repeated two times before the primary simulations (two years of initialisation period). Consequently, the results encompassing the five-year timeframe (2018–2023) were extracted and employed in the subsequent analyses. Gothenburg and Rensjön were selected owing to their conditions, with high [13] and low [81] exposures to WDR in Sweden, respectively. This allowed a meaningful comparison of the two water penetration criteria under two distinct WDR load intensities. In addition, the two locations exhibit a noticeable temperature difference which can affect mould growth. During these five years of simulation, the average temperature was $\sim +10^{\circ}C$ and $\sim -1^{\circ}C$ for Gothenburg and Rensjön, respectively.

This study used the data from the Swedish Meteorological and Hydrological Institute (SMHI) [81] as the main source of the outdoor climate data, which included information on temperature [C], relative humidity [%], rain intensity [mm/h], wind direction [°], wind velocity [m/s], air pressure [hPa], and shortwave diffuse and direct radiations [W/m^2]. However, the SMHI does not provide data on long-wave counter radiation. Therefore, this specific variable was obtained from the Meteonorm meteorological database [82] to obtain hourly climate data over a typical year generated from the measured data.

2.5. Hygrothermal simulation setup

2.5.1. General concepts

Fig. 4 shows the mortar extrusion phenomenon that may have occurred during bricklaying. Fig. 4 i shows a laboratory specimen highlighting the occurrence of mortar extrusion behind clay brick cladding. Notably, the morphology and dimensions of extruded

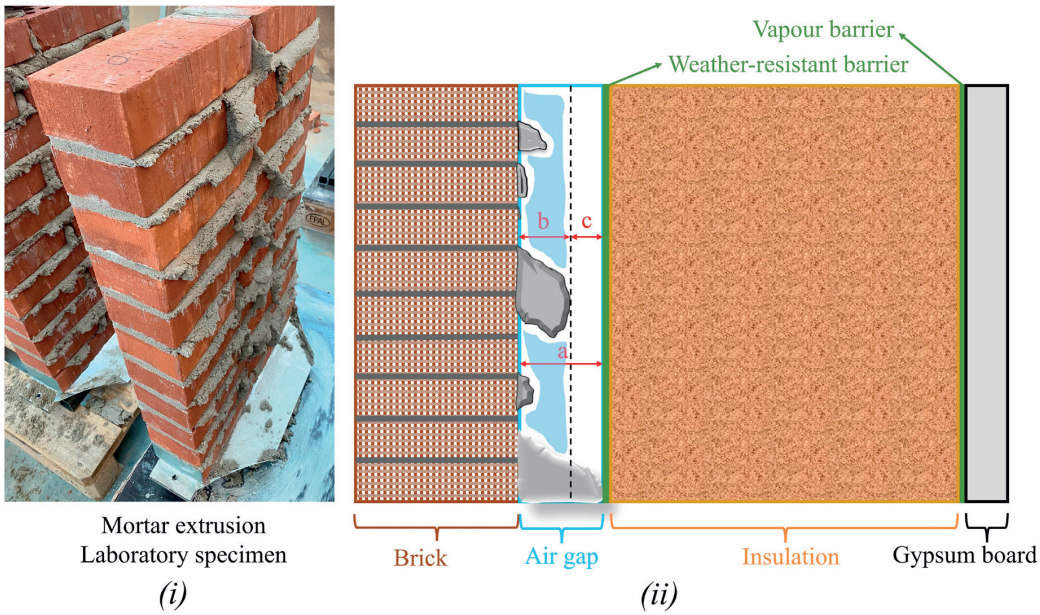


Fig. 4. Mortar extrusion phenomenon for clay brick cladding (the dimensions are not scaled). a [mm]: whole air cavity thickness, b [mm]: extruded mortar thickness, c [mm]: net air cavity thickness. Grey clouds: extruded mortar. Blue clouds: existing air between extruded mortar.

mortar may vary depending on workmanship and mortar water content. Fig. 4 ii shows a schematic of the mortar extrusion addressed in this study.

Fig. 4 ii shows the air gap layer between the brick layer and timber studs (insulation layer), facilitating air exchange and disrupting the moisture transfer mechanism. Clay brick masonry claddings typically comprise two primary components: brick and mortar. Inaccurate workmanship can cause mortar extrusion (grey clouds in Fig. 4 ii) from the mortar joints, filling the air cavity layer and enabling moisture to move more easily from the brick layer to the other wall layers. The extruded mortar is primarily confined to the air cavity space in front of the joint or may fall onto the backside of the brick. In the most severe case, the extruded mortar may even connect with weather-resistant barrier surface, bridging the gap between the brick and weather-resistant barrier. This connection eliminates the presence of an air gap around the extruded mortar. To account for this phenomenon, this study incorporated the influence of extruded mortar into the hygrothermal modelling process. While this problem can be captured more accurate in 2D

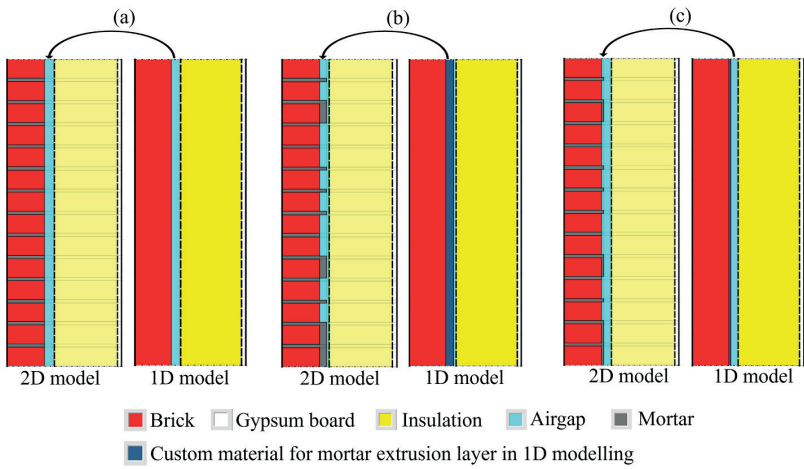


Fig. 5. 1D versus 2D modelling for hygrothermal model verification. (a) Base case, (b) high mortar extrusion (25 mm), and (c) low mortar extrusion (5 mm).

simulation, it can be time-consuming, particularly when applying a probabilistic approach. Thus, this study aimed to introduce a custom material to serve as an appropriate alternative for the mortar extrusion layer within a one-dimensional (1D) model. However, the 1D model is first verified through a limited number of 2D hygrothermal simulations and subsequently is used for the probabilistic modelling.

2.5.2. 2D hygrothermal model

To verify the proposed 1D hygrothermal model, 2D hygrothermal models were created for six scenarios based on ASHRAE criteria. These scenarios were created based on CS1 in Gothenburg and CS2 in Rensjön, including the base case (no mortar extrusion), high mortar extrusion (25 mm), and low mortar extrusion (5 mm). The air cavity width was 30 mm. Fig. 5 illustrates the 1D and 2D hygrothermal models used in this study. A custom material was used as the extruded mortar layer in the 1D model. However, in the 2D model, standard air and mortar were incorporated. The air and mortar components within the mortar extrusion layer of the 2D model were randomly arranged. The settings of the hygrothermal simulations were consistent for both models. Table 3 lists the material properties of the mortar.

The hygrothermal performance of the selected case studies was examined using Delphin 6.1 [73], explicitly designed for heat, air, and moisture (HAM) analysis. The target screening point was the outermost surface of the wooden stud. This screening point was selected to investigate the mould growth potential of the wooden stud, a moisture-sensitive element in timber frame walls. Mould growth may lead to odours and health problems [83]. In this study, the indoor climatic conditions were correlated with the outdoor temperature [74]. When the ambient temperature fell between 10 °C and 20 °C, the indoor temperature underwent linear fluctuations within a range of 20–25 °C. However, for higher or lower ambient temperatures, the indoor temperature remained fixed at 25 °C or 20 °C, respectively. According to DIN EN 15026 [74], the indoor RH can vary linearly between 35 % and 65 % for an ambient temperature range of −10 °C–20 °C.

The façade orientations were defined as south and north for Gothenburg and Rensjön, respectively. These orientations exhibited the highest WDR intensities for both locations. Delphin 6.1 employs the ISO standard (DIN EN ISO 15927-3) [84] to quantify the WDR phenomenon. This standard was selected owing to its ability to encompass broader microclimatic parameters in the WDR model, including variations in the terrain, topography, obstacle, and wall factors.

The establishment of a minimum mesh size of 1 mm coupled with a stretch factor of 1.3, led to mesh sizes varying dynamically across the individual layers in accordance with their respective thicknesses. This strategic adjustment of the mesh size and stretch factor achieves an equilibrium between computational efficiency and precision.

2.5.3. 1D hygrothermal model

To simplify the hygrothermal modelling process, the masonry wall can be represented as a homogeneous brick layer under real climatic conditions, based on a study by Vereecken and Roels [85]. Notably, this simplification has certain limitations, as acknowledged in Ref. [13].

The depths of the extruded mortar were defined and combined probabilistically in all scenarios using the LHS technique. They followed a uniform distribution ranging from 0 mm to 30 mm. This indicates that the probabilities of having no extruded mortar and a maximum extruded mortar depth were equal. The moisture source was assigned to the entire depth of the extruded mortar. Subsequently, the net air cavity thickness (*c* dimension in Fig. 4 ii) was considered after accounting for the thickness of the extruded mortar (*b* dimension in Fig. 4 ii) using Eq. (5).

$$\textit{Net air cavity thickness } [mm](c) = \textit{Whole air cavity thickness } [mm](a) - \textit{Mortar extrusion thickness } [mm](b) \tag{5}$$

In 1D hygrothermal modelling, selecting a representative material of the mortar extrusion layer is challenging because this layer is partially filled with mortar (the layer indicated by dimension *b* in Fig. 4 ii). Thus, it can be assumed that the extruded mortar layer comprised a mixture of air (blue clouds in Fig. 4 ii) and mortar (grey clouds in Fig. 4 ii). On the one hand, using standard air (a saturation point of approximately 0.017 kg/m^3) for the extruded mortar layer is unsuitable because in Delphin, excess water is automatically deleted from the moisture balance equation when the moisture contents is higher than the saturation point [20]. On the other hand, considering pure mortar as the extruded mortar layer is not representative or realistic. To address these limitations, a custom material was formulated by combining of air and mortar properties. Vapour diffusion was considered the primary mechanism for moisture transport, where liquid convection was excluded to prevent unrealistic moisture flow. This exclusion implied that the water absorption coefficient, A_w, should be set to zero. The moisture storage function was defined based on the mortar sorption isotherm, necessitating the utilisation of the saturation point from mortar material properties ($\theta_{eff} = 0.21$ m^3/m^3). The porosity was established at 0.5 m^3/m^3, influencing both air and vapour permeability. Other material properties were adopted from the air properties (Delphin default). This ensured that the extruded mortar layer could accommodate any sudden influx of moisture up to but not beyond the saturation point of the mortar material.

Table 3
Material properties of mortar.

Bulk Density (D_B $\left[\frac{kg}{m^3}\right]$)	Specific Heat Capacity (C_p $\left[\frac{J}{kg.K}\right]$)	Porosity (θ_{por} $\left[\frac{m^3}{m^3}\right]$)	Thermal Conductivity (λ_{dry} $\left[\frac{W}{m.K}\right]$)	Water Absorption Coefficient (A_w $\left[\frac{kg}{m^2.s^{0.5}}\right]$)	Water Vapour Diffusion Resistance Factor (μ_{VDR} [−])
1880	850	0.28	0.8	0.57	50

2.5.4. ASHRAE and experimental study (ES) criteria

A well-known procedure for considering water penetration through an exterior surface follows the ASHRAE standard 160–2021 [21]. According to this standard, the default value for water penetration through the exterior surface is set as 1 % of the rainwater reaching the exterior surface. The deposition site for this moisture source is the exterior surface of the weather-resistant barrier. However, the deposition site can be altered by providing a technical rationale. Therefore, in this study, the position and size of the moisture source were varied depending on the depth of the extruded mortar, and the moisture source was distributed throughout the depth of the extruded mortar.

In a recent experimental study (hereafter denoted by ES in this paper), Kahangi Shahreza et al. [8] suggested a water penetration criterion for clay brick masonry that depends on the moisture content of the brick. They studied water penetration in brick masonry, including two distinct brick types and three diverse mortar joint profiles. They found that WDR-induced water penetration may not occur in masonry walls when the walls still can absorb and store water. Thus, a novel criterion for water penetration, considering the moisture buffering capacity of masonry, was introduced [8], which can be integrated into hygrothermal analysis. Based on this criterion, once the moisture content, as determined through hygrothermal analysis, surpasses the saturation level threshold, water penetration commences. Subsequently, a fraction of the normal rain flow (a portion of the WDR) penetrates and is regarded as the moisture source in hygrothermal analysis. Table 4 lists the probability distributions of the saturation point, fraction of normal rain flow, and saturation level threshold for the two types of bricks tested. It should be noted that the negative values for the fraction of normal rain flow samples considered zero.

3. Results

3.1. Hygrothermal model verification (1D vs 2D)

Fig. 6 presents a five-year depiction of mould growth for six distinct case studies. The solid red and blue lines represent the mould growth curves in the 1D model for CS1 in Gothenburg and CS2 in Rensjön, respectively. In addition, the dashed, dotted, and solid black and green lines represent the maximum, average, and minimum values of the mould indices within the 2D model for a 1 m wall assembly height for CS1 in Gothenburg and CS2 in Rensjön, respectively. Fig. 6, reveals a concurrence between the 1D model using the custom material for the mortar extrusion layer and the 2D model. The 1D hygrothermal model for CS1 under the Gothenburg climatic conditions followed a trend consistent with the average mould indices of the 2D model. In some instances, the 1D model exhibited slightly higher values, indicating a conservative approach. Similar trends and observations hold true for CS2 in Rensjön; however, the differences between the maximum mould index values in the 2D and 1D models were more pronounced. Nonetheless, the general trends remained consistent.

Table 5 lists the R^2 and MAE values, based on Eq. (3) and (4), for the mould indices when comparing the 1D and 2D models (for 2D model: considering maximum mesh, average across all meshes, and minimum mesh). The majority of the R^2 values between the 1D and 2D models (except two) exceed 90 %. Concerning high mortar extrusion for CS2 under Rensjön climatic conditions, the 1D model demonstrates the capability to predict approximately 70 % and 80 % of the variations in mould indices for the maximum and minimum meshes of the 2D model, respectively. Additionally, MAE values for CS2 under Rensjön climatic conditions are all below 0.05. Notably, the highest MAE is associated with the high mortar extrusion model for CS1 in Gothenburg. Nevertheless, the remaining MAE values are all less than 0.24.

3.2. Mould growth analysis

Table 6 presents the 95th percentile of the maximum mould indices for each case study, indicating that 95 % of the scenarios exhibited a lower maximum mould index than the value presented in this table. In the context of the Gothenburg climatic conditions, a minor disparity emerged between the maximum mould indices when employing the ASHRAE and ES criteria. CS1 and CS2 exhibited a reduction of approximately 6 % in the 95th percentile of the maximum mould indices through the implementation of the ES criterion compared with the ASHRAE criterion. Conversely, under the Rensjön climatic conditions, CS1 and CS2 demonstrated approximately 22 % and 15 % reductions, respectively, in the 95th percentile of the maximum mould indices when employing the ES criterion.

3.3. Mould sensitivity analysis

3.3.1. Linear mould sensitivity analysis

Table 7 presents the findings of the correlation study on the input variables demonstrating a noteworthy correlation with the maximum mould index. This compilation excludes variables demonstrating negligible correlations. These results were based on the linear sensitivity analysis shown in Fig. 2.

Table 4
Experimental data of the bricks (probability distributions) with the fraction of normal rain consideration as the moisture source. N(μ, σ): normal distribution. μ and σ are the mean and standard deviation, respectively. CoV: coefficient of variation.

	Saturation point, θ_{eff} [m^3/m^3]	Fraction of normal rain flow [%]	Saturation level threshold [%]
Brick type I [8]	N(0.26, 0.00483) CoV = 1.9 %	N(3.77, 2.68) CoV = 71 %	N(93.34, 5.21) CoV = 5.6 %
Brick type II [8]	N(0.155, 0.0168) CoV = 10.8 %	N(3.74, 1.72) CoV = 46 %	N(93.62, 2.56) CoV = 2.74 %

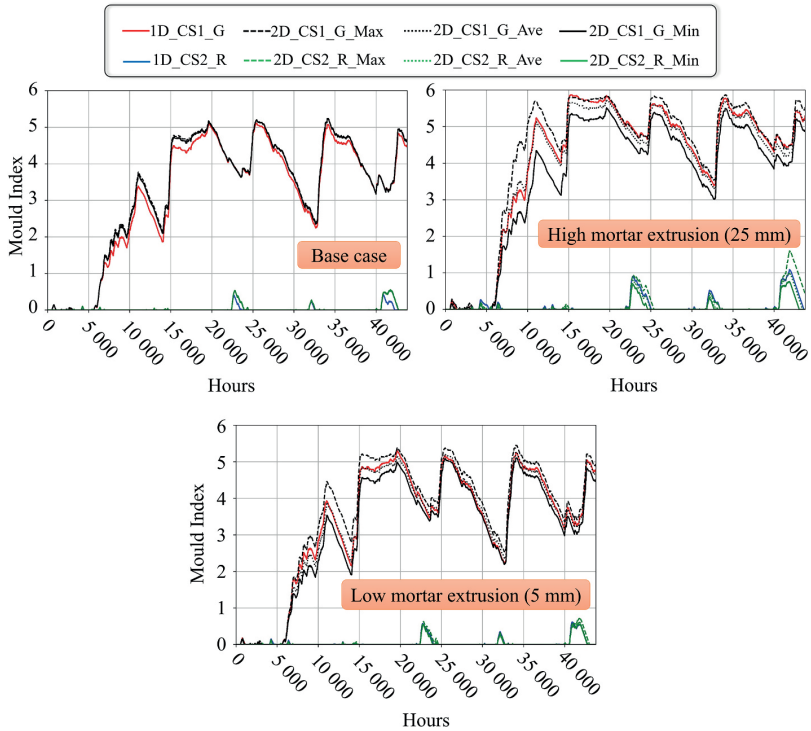


Fig. 6. Wall assemblies modelling for verification, 1D versus 2D. G: Gothenburg, R: Rensjön, CS1: case study 1, CS2: case study 2, Max/Min/Ave: maximum/minimum/average mould index within the 1 m height of the wall in the 2D model.

Table 5
Coefficient of determination (R^2) and mean absolute error (MAE) between the mould indices of 1D and 2D models (maximum mesh, average of all meshes, and minimum mesh). G: Gothenburg, R: Rensjön.

		CS1_ASHRAE_G			CS2_ASHRAE_R		
		Maximum	Average	Minimum	Maximum	Average	Minimum
Base case	R^2	0.987	0.990	0.991	0.910	0.906	0.907
	MAE	0.138	0.121	0.112	0.016	0.015	0.015
High mortar extrusion (25 mm)	R^2	0.963	0.995	0.933	0.701	0.956	0.804
	MAE	0.205	0.109	0.417	0.044	0.021	0.044
Low mortar extrusion (5 mm)	R^2	0.971	0.996	0.978	0.911	0.980	0.972
	MAE	0.227	0.069	0.236	0.012	0.006	0.007

Table 6
Mould growth calculations. G: Gothenburg, R: Rensjön, ES: case studies based on experimental study data, ASHRAE: case studies based on ASHRAE 160–2021 standard, CS1 and CS2: case studies 1 and 2.

Case studies	95^{th} percentile of the maximum mould indices	Required number of simulations to achieve convergence
CS1_ASHRAE_G	5.89	1400
CS1_ES_G	5.57	1200
CS2_ASHRAE_G	5.88	1200
CS2_ES_G	5.52	1600
CS1_ASHRAE_R	1.25	1600
CS1_ES_R	0.98	3000
CS2_ASHRAE_R	1.11	2100
CS2_ES_R	0.94	1600

Table 7
Spearman correlation coefficients between the input variables and maximum mould index. Colourmap guide: 0.00–0.09: negligible relationship, 0.10-0.39: weak relationship, 0.40-0.69: moderate relationship, 0.70-0.89: strong relationship, 0.90-1.00: very strong relationship. ES: Experimental Study criterion, G: Gothenburg, R: Rensjön.

Case studies		Thermal conductivity of Rockwool insulation [W/m.k]	Solar absorption coefficient [-]	Reduction/splash coefficient of WDR [-]	Extruded mortar depth [mm]	Air change rate (ACR) [1/h]
CS1	ASHRAE_G	0.30	-0.039	0.29	0.72	-0.44
	ES_G	0.56	-0.056	0.46	0.49	-0.65
	ASHRAE_R	0.32	-0.59	0.6	0.18	-0.24
	ES_R	0.1	-0.74	0.6	0.01	-0.2
CS2	ASHRAE_G	0.26	-0.059	0.27	0.73	-0.43
	ES_G	0.49	-0.092	0.57	0.53	-0.52
	ASHRAE_R	0.14	-0.61	0.45	0.13	-0.37
	ES_R	0.12	-0.68	0.47	0.01	-0.32

The impact of the extruded mortar on the maximum mould index is evident. However, when the climatic conditions and water penetration criteria were altered, the rank of the correlations changed. In both CS1 and CS2, the higher amount of extruded mortar contributed to a higher maximum mould index. The air change rate (ACR) has negative correlation with the maximum mould index across all case studies with weak and moderate correlations for Rensjön and Gothenburg cases, respectively. A positive correlation

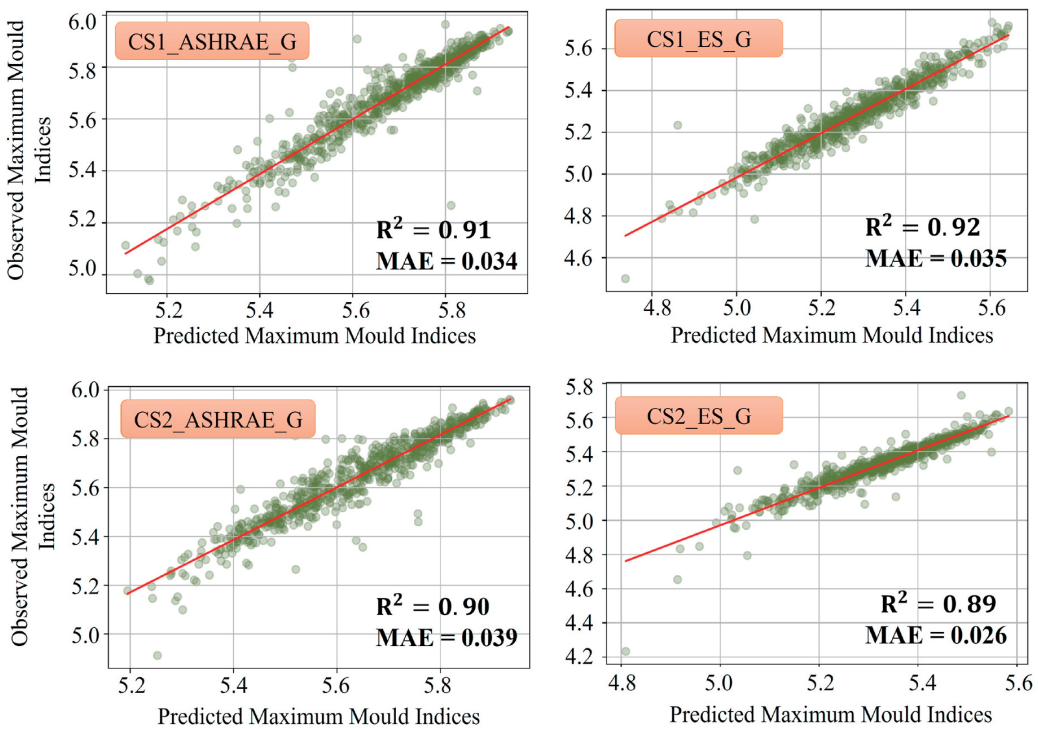


Fig. 7. Predicted vs observed data during the machine learning model testing, Gothenburg (G). ES: case studies (CS1 and CS2) based on experimental study data.

between two more input variables including reduction/splash coefficient of the WDR and thermal conductivity of the Rockwool insulation and the output, i.e., maximum mould index is revealed. The influence of the solar absorption coefficient on the maximum mould index was negligible under the Gothenburg climatic conditions. Conversely, in Rensjön, it demonstrated a significant negative impact, with moderate and strong correlations, on elevating the maximum mould index.

3.3.2. Non-linear mould sensitivity analysis

Optimisation of RF metamodel. The metamodels of the case studies were optimised by investigating the effective features involved in creating the metamodels under Gothenburg (G) and Rensjön (R) climatic conditions. Figs. 7 and 8 show the accuracy metrics. The optimised metamodels for both case studies exhibited acceptable performances in terms of accuracy metrics under different climatic conditions. The reported R^2 values, ranging from 0.85 to 0.96, indicated that the metamodels could capture a substantial portion of the variations within the data. The close-to-zero MAE values indicated minimal errors, further affirming the accuracy of the metamodels. In most cases, the ASHRAE criterion exhibited slightly higher data dispersion, contributing to slightly lower R^2 values compared with the ES criterion. This emphasises the potential influence of the water penetration criterion on the predictive performance of the metamodel.

Several factors contributed to the observed variation in R^2 values across the different case studies. One influential factor is the inherent variability in the training data. The complexity of the underlying patterns within the data can affect the ability of the model to capture and predict outcomes, affecting the R^2. Furthermore, the unique characteristics of each case study, encompassing aspects, such as brick type, water penetration criteria, and climate data, introduce inherent variability affecting the metamodel performance. The selection and relevance of features employed in machine learning models significantly influence the model performance. Some features selected for a case study may not possess the same degree of informativeness as those used in other case studies. This discrepancy in feature suitability may have contributed to the observed variations in the R^2 values among the case studies (e.g., CS2_ASHRAE_R vs. CS1_ES_R). Nevertheless, despite the slightly lower R^2 value of CS2_ASHRAE_R, its acceptability remained viable within the framework of this study.

To complement the sensitivity analysis, feature importance analyses, comprehensively illustrating the linear and non-linear relationships for Gothenburg and Rensjön, are shown in Figs. 9 and 10, respectively. Furthermore, the figures provide insights into the specific features used in the RF metamodel creation for each case study. Notably, the feature importance analysis reaffirmed the importance of the parameters identified through the Spearman correlation analysis. Nevertheless, additional aspects warrant further investigation.

Feature importance analysis provides insights into correlations, particularly those of non-linear nature. This analysis expands the

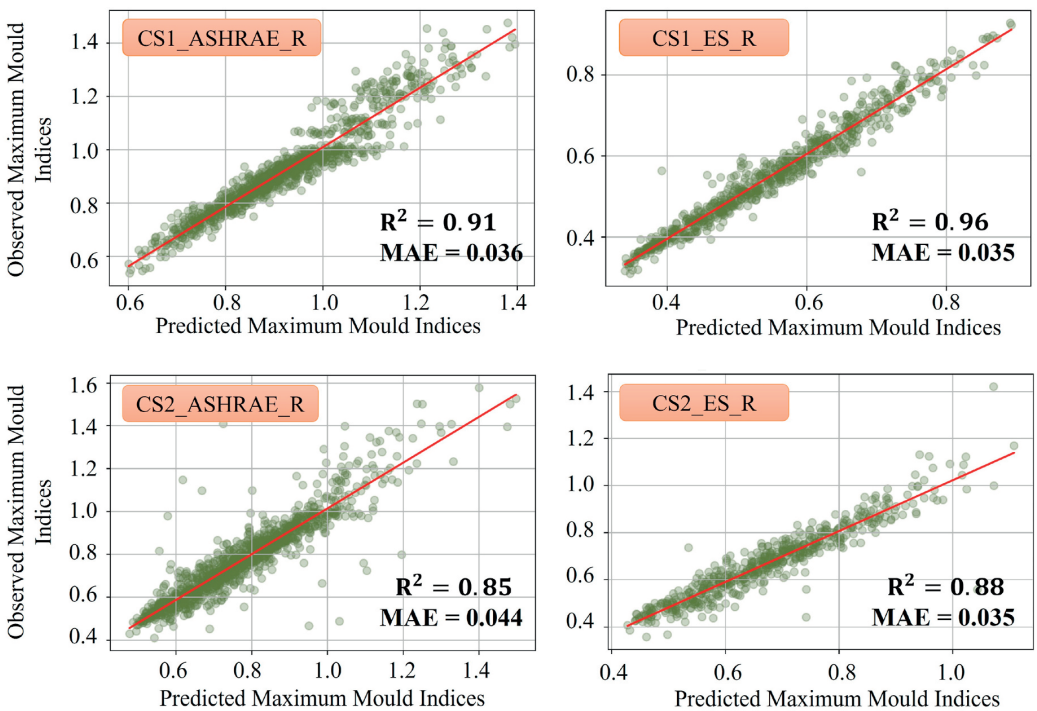


Fig. 8. Predicted vs observed data during the machine learning model testing, Rensjön (R). ES: case studies (CS1 and CS2) based on experimental study data.

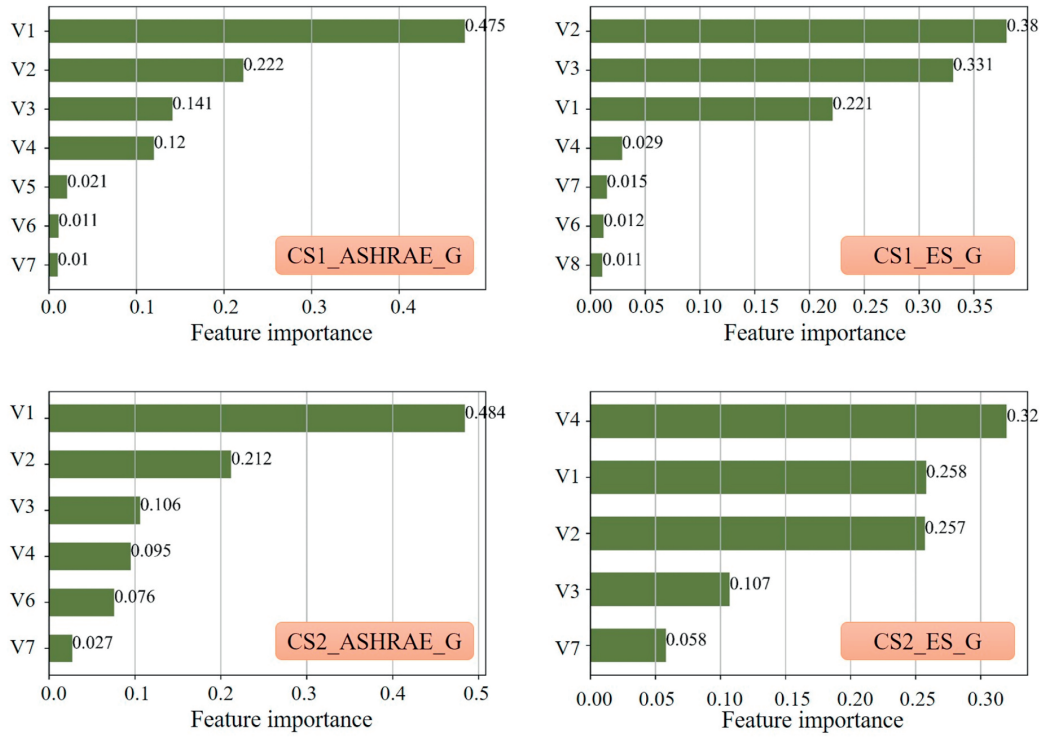


Fig. 9. Feature importance analysis, Gothenburg (G). ES: case studies based on experimental study data. V1: extruded mortar depth; V2: air change rate; V3: thermal conductivity of Rockwool insulation; V4: reduction/splash coefficient; V5: outdoor convection heat exchange coefficient; V6: saturation point of brick; V7: solar absorption coefficient; V8: thermal conductivity of brick.

range of important variables, although their degree of importance may not be as prominent as that of the other important variables. For example, variables, such as the outdoor convection heat exchange coefficient, brick saturation point, brick thermal conductivity, and long-wave emissivity are significant. In addition, the feature importance analysis reveals a more apparent distinction in the importance levels among the significant variables. In Gothenburg, the disparity in importance between the extruded mortar depth and other important parameters was more pronounced (almost double) under the ASHRAE criterion than the ES criterion. This disparity can be attributed to the high WDR load and consistent attribution of 1 % of WDR as the moisture source. The presence of extruded mortar under such conditions can introduce a substantial moisture source close to the insulation layer, increasing the maximum mould index. Fig. 10 shows the marginal importance of the extruded mortar in Rensjön consistent with the results of the Spearman correlation coefficient analysis. In Rensjön, the feature importance analysis highlighted the significance of the solar absorption and reduction/splash coefficients, surpassing other prominent variables.

4. Discussion

4.1. Hygrothermal model verification (1D vs 2D)

The verification of 1D hygrothermal model was performed based on a 2D hygrothermal model to investigate the potential and accuracy of the 1D hygrothermal model in the mould growth analysis. According to Fig. 6, while there are some variations between the maximum mould index of the 1D and 2D models for both case studies (CS1 in Gothenburg and CS2 in Rensjön), their overall trends are similar, with only minor variations. Moreover, the maximum mould index values were extremely close in both case studies. The accuracy metrics (R^2 and MAE) presented in Table 5 can be used for more scientific and statistical support. The high R^2 between 1D and 2D models (above 90 % for most of the cases) indicates that the 1D mortar extrusion model can predict above 90 % of variations of the 2D models' mould indices. The relatively minor MAE values, below 0.24 and 0.05 for CS1 in Gothenburg and CS2 in Rensjön, respectively, indicate that, on average, there is a discrepancy of 0.24 and 0.05 in mould indices when utilising a 1D model instead of a 2D model. These errors remain within an acceptable range, particularly considering the considerable time saved by employing a 1D model—approximately 5 min per simulation compared to 760 min per simulation for a 2D model. Moreover, over the 5-year simulation period, these error magnitudes do not significantly impact post-process analyses, such as failure probability assessment.

For the base case, the MAE is minor, shows the high level of agreement between the 1D and 2D model outputs. This similarity was

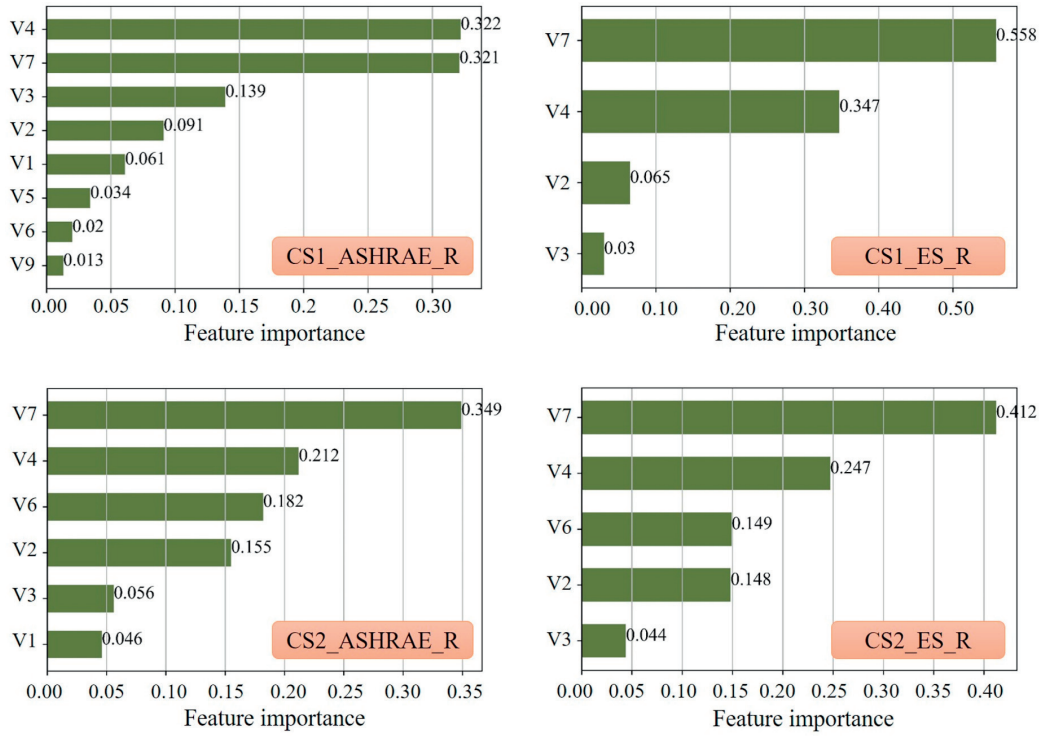


Fig. 10. Feature importance analysis, Rensjön (R). ES: case studies based on experimental study data. V1: extruded mortar depth; V2: air change rate; V3: thermal conductivity of Rockwool insulation; V4: reduction/splash coefficient; V5: outdoor convection heat exchange coefficient; V6: saturation point of brick; V7: solar absorption coefficient; V9: long-wave emissivity.

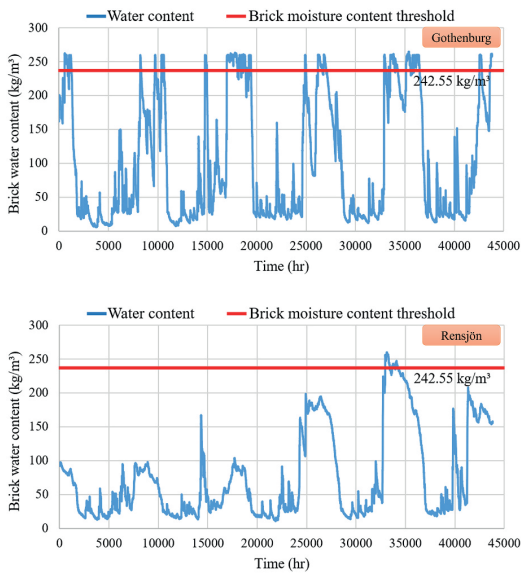


Fig. 11. Water content of clay brick masonry façade in Gothenburg (top) and Rensjön (bottom) between 2018 and 2023.

expected because the base case involved no extruded mortar, and the primary distinction between the 2D and 1D models lies in the detailed modelling of the brick layer, resulting in only minor differences between these two models. Examining the cases involving extruded mortar (high: 25 mm and low: 5 mm), the 1D model exhibited a lower MAE in relation to the average mould indices of the 2D model; however, it exhibited a slightly higher MAE compared with the maximum and minimum mould indices of the 2D model. Notably, in the 2D model, the specific point of the wall assembly associated with maximum mould growth tended to exhibit slightly higher mould indices compared with that in the 1D model. This variation can be attributed to the active liquid convection of the mortar in that specific area, facilitating greater moisture penetration in the surrounding region. However, the minor discrepancies between the 1D and 2D models emphasise the effectiveness of employing the custom material within the 1D model as an alternative to the time-consuming 2D model, particularly within the scope of this study.

4.2. Mould growth analysis

According to Table 6, a minor difference between implementing the ASHRAE and ES criteria was observed in Gothenburg, owing to its high WDR load, as noted by Kahangi Shahreza and Abdul Hamid [31]. The reason is a higher WDR load in Gothenburg resulted in a higher brick water content, surpassing the threshold outlined by the ES criterion. Therefore, the moisture sources stemming from WDR are considered within the hygrothermal simulation process more frequently. Conversely, less WDR load occurs in Rensjön; thus, the masonry can absorb rain without surpassing the threshold introduced in the ES. The lower WDR load in Rensjön leads to a higher 95^{th} percentile of the maximum mould indices when utilising the ASHRAE standard compared to the ES. ASHRAE accounts for 1 % of WDR load all the time, while ES only considers a fraction of the WDR load after the moisture content of the brick wall exceeds a predefined threshold. Given the infrequent surpassing of this threshold in Rensjön, ASHRAE's approach results in a greater impact on the 95^{th} percentile of the maximum mould indices compared to ES.

To provide further support for the rationale of the aforementioned discussion, Fig. 11 compares the water content in clay brick masonry façades under the Gothenburg and Rensjön climatic conditions spanning from 2018 to 2023. The red lines indicate the threshold saturation level of the brick, whereas the blue lines trace the water content of the clay brick masonry façade over 5 years. Notably, owing to the high number of simulations, only data of one scenario are illustrated in Fig. 11 for simplicity. The remaining scenarios followed a pattern similar to that of the representative scenario. Fig. 11 (top) shows the water content of the brick masonry layer in Gothenburg, which reached capillary saturation during a substantial portion of the mostly winter months. Consequently, instances in which the brick water content surpassed its threshold saturation level were more frequent in Gothenburg than in Rensjön. This emphasised the higher probability of considering moisture sources arising from WDR in Gothenburg. This resulted in an alignment between the results of the ES and ASHRAE criteria. Notably, the assumption of experimental study [8] is confined to masonry without known cracks and imperfections. Real-world scenarios can witness increased penetration owing to poor contact between bricks and mortar, along with the presence of cracks.

Fig. 11 (bottom) illustrates the water content of the brick masonry layer under the Rensjön climatic conditions. Unlike the Gothenburg case studies, the water content of the brick only exceeded its threshold saturation level for a few hours. Considering the lower WDR load, the probability of water penetration during the study period remained minimal, highlighting the advantages of considering the water absorption capacity of brick masonry. Therefore, accounting for the water absorption capacity of brick masonry (i.e., the ES criterion) to avoid high moisture source considerations is more significant in scenarios characterised by diminished WDR loads. Conversely, in instances with frequent and intense WDR loads, congruence between the ASHRAE and ES criteria results is plausible.

4.3. Mould sensitivity analysis

According to Table 7, the positive correlation exists between the extruded mortar and the maximum mould index. This is in agreement with the findings of Calle et al. [20] where the effect of mortar extrusion on mould growth was found to be dominant. This may be because increasing the extruded mortar depth brings the moisture source closer to the timber stud (or insulation layer), fostering conditions more conducive to mould growth. In Gothenburg, a strong correlation was observed between the extruded mortar depth and maximum mould index when employing the ASHRAE criterion. This strong correlation was attributed to the consistent consideration of 1 % of high WDR loads as the moisture source. However, applying the ES criterion mitigates this correlation and leads to a moderate relationship. This discrepancy is grounded in the ES criterion condition that the moisture source owing to the WDR load is dependent on the moisture content of the brick exceeding a specific percentage of its saturation point. Consequently, the impact of the extruded mortar is diminished because the ES criterion occasionally excludes moisture source considerations, even in the presence of extruded mortar. In other words, the ES criterion exclusively considers instances surpassing the saturation level threshold (indicated by the red line in Fig. 11) when assessing moisture sources. Therefore, the significance of the extruded mortar is reduced in these cases. A comparison of the relationship between the extruded mortar depth and maximum mould index across the two climatic conditions revealed that the extruded mortar depth is more significant in regions with higher WDR loads. Table 7 illustrates a weaker relationship between the extruded mortar depth and maximum mould index in Rensjön, primarily owing to the lower WDR load in Rensjön than Gothenburg. Despite the presence of extruded mortar, no moisture source attributed to WDR was assigned to it, resulting in a dry extruded mortar condition with minimal impact on moisture transportation. In essence, the absence of moisture owing to WDR renders transportation through the extruded mortar insignificant. Similar to the Gothenburg case, under the Rensjön climatic conditions, the impact of extruded mortar diminished when using the ES criterion compared with the ASHRAE criterion. This similarity is attributed to the same rationale expressed earlier by Gothenburg.

Table 7 shows the significance of the air change rate (ACR) across all case studies. A negative correlation was observed between the ACR and maximum mould index. This is because a heightened ACR results in drier conditions within the air gap, reducing the

probability of mould growth. The prominence of the ACR became more pronounced in climates with elevated WDR loads, as identified by the moderate correlation. Under these climatic conditions, the air gap contains more moisture, which can be effectively dried by increasing the ACR. The air gap is drier in regions with a lower WDR, resulting in a weaker ACR effect in the dry layer. By contrast, in Gothenburg, because the air gap has a higher RH and moisture content, ventilation due to the ACR can be more effective. Therefore, the impact of ACR in regions with a lower WDR load is weaker, whereas a moderate relationship is observed in regions with a high WDR load. Mundt-Petersen et al. [86] established the significance of maintaining a well-ventilated air gap behind the cladding in wood-frame walls to mitigate mould growth.

The reduction/splash coefficient of WDR ranges from 0.6 (representing a more splashed WDR load) to 0.8 (indicating a less splashed WDR load). Table 7 reveals a positive correlation between the reduction/splash coefficient of the WDR and the maximum mould index. This correlation is intuitively reasonable because an elevated reduction/splash coefficient implies diminished splashing of the WDR load. Consequently, a larger portion of the WDR load becomes available for water penetration, leading to higher maximum mould indices. Furthermore, the moisture content of the brick layer increases with a rise in the reduction/splash coefficient. This correlation ranking remained consistent (moderate relationship) for both water penetration criteria under the Rensjön climatic conditions. This consistency was attributed to the low WDR load, where the moisture source contribution to the WDR load was relatively minor for both criteria. Consequently, the difference in the correlation rankings between these two criteria in this region remained negligible. Conversely, under the Gothenburg climatic conditions, the relationship between the reduction/splash coefficient of the WDR and the maximum mould index was weaker under the ASHRAE criterion than under the ES criterion. This discrepancy was caused by the substantial WDR load in Gothenburg, where the ASHRAE criterion accounts for 1 % of the WDR load regardless of the brick saturation level. Consequently, the amount of water penetration remained high, irrespective of the reduction in the WDR load owing to splashing. Consequently, the impact of the reduction/splash coefficient of the WDR on the water penetration process was less pronounced under the ASHRAE criterion than under the ES criterion.

The variation in rank correlations between the solar absorption coefficient and maximum mould index, which is negligible in Gothenburg and moderate to strong in Rensjön, can be attributed to differences in WDR load between the two locations. Gothenburg encountered a higher WDR load compared to Rensjön. Consequently, despite a material surface's capacity to absorb solar radiation, the substantial amount of absorbed water in the brick surpasses the drying potential of solar radiation. This renders the solar absorption coefficient insignificant under Gothenburg climatic conditions. In addition, the consistent negative sign across all Spearman correlation coefficients emphasised the negative correlation between the solar absorption coefficient and maximum mould index. This stems from the observation that an increase in the solar absorption coefficient enhances the material drying potential, reducing mould growth.

The positive correlation between the thermal conductivity of the Rockwool insulation and the maximum mould index remained consistent across all case studies. Insulation materials with higher thermal conductivities exhibit a greater tendency for heat transfer. Heat travels more readily through an insulation material with the presence of a temperature gradient between the indoor and outdoor environments. In cold climate areas, such as Sweden (indoor air is warmer than outdoor air), when warm indoor air encounters a colder surface within the insulation layer owing to enhanced heat transfer (associated with higher thermal conductivity), the probability of condensation forming on that surface increases. This condensation fosters a damp environment, providing the moisture necessary for mould growth. However, the high WDR-induced water penetration in Gothenburg compared with Rensjön caused the consistently elevated moisture content near the insulation layer, irrespective of the condensation resulting from the higher thermal conductivity of the Rockwool insulation. This explains the reduced impact of the thermal conductivity of the Rockwool insulation in Gothenburg under the ASHRAE criterion compared with that under the ES criterion. In Rensjön, where the ambient temperatures are consistently lower than those in Gothenburg, the exterior surfaces of buildings tend to be colder than their interior surfaces. Because the surface temperature of building components often falls below the dew point temperature of the surrounding air, any moisture condensing on these surfaces is more prone to freezing rather than fostering mould growth. Mould growth requires moisture and a suitable temperature range. The availability of moisture in its liquid form is limited in regions with consistently low temperatures, reducing the probability of mould growth. Furthermore, under the Rensjön climatic conditions with lower WDR loads, the influence of the thermal conductivity of the Rockwool insulation under the ASHRAE and ES criteria becomes similar. This similarity can be attributed to the reduced amount of moisture sources stemming from WDR-induced water penetration and the extremely low temperature resulting in the freezing of the condensed water. In such a scenario, the impact of the thermal conductivity on the moisture transport mechanism becomes similar for both water penetration criteria.

4.4. Limitations

This study acknowledges certain limitations in the extruded mortar modelling. Notably, although this study assumed that extruded mortar absorbs and retains penetrated rainwater, real-world scenarios can present more alternatives, as shown in Fig. 12 and described as follow.

- *Scenario A1*: Droplets dripping from the upper extruded mortar can affect the lower extruded mortar, potentially causing the splashing (bouncing off) of the surroundings.
- *Scenario A2*: Droplets dripping from the upper extruded mortar can impact wall ties, leading to water movement through these ties to the weather-resistant barrier, particularly in cases where wall tie inclinations are not correctly installed.
- *Scenario B1*: Rainwater runoff inside the air gap should be considered. The continuous air gap behind the clay brick cladding, extending from the top to the ground level in multi-storey buildings, can accumulate runoff water on the lower floors. Mortar

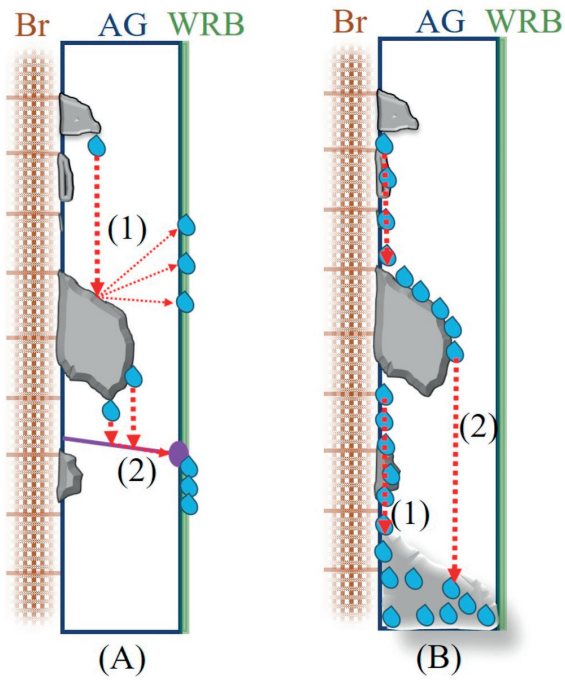


Fig. 12. Possible water penetration scenarios through the extruded mortar. Br: brick layer, AG: airgap layer, and WRB: weather-resistant barrier layer.

accumulation on the ground floor can absorb runoff water, potentially leading to significant moisture accumulation at the wall base. Improved workmanship can help mitigate mortar accumulation on the ground behind the clay brick claddings.

- *Scenario B2*: Droplets of runoff water within the air gap drip to the bottom of the air gap, where, the accumulated mortar can absorb droplets, similar to Scenario B1.

The method employed for modelling moisture sources could also be considered as a potential limitation. This study used a uniform distribution as the moisture source model. However, it should be noted that a point moisture source might be more appropriate in specific scenarios, such as Scenario B2, as discussed in Ref. [20].

5. Conclusions

This study investigated the probabilistic mould growth and sensitivity analyses of mortar extrusion within the clay brick masonry claddings of a timber frame wall. The analyses were conducted under two distinct water penetration criteria: the ASHRAE and an Experimental Study (ES)-based. This study employed the material properties derived from an experimental study conducted on two types of bricks. Case studies were conducted under different climatic conditions in Sweden, namely Gothenburg and Rensjön. Probabilistic analyses were performed using the mould reliability analysis (MRA) and mould sensitivity analysis (MSA) methodologies, integrating a probabilistic model with the random forests (RF) machine learning algorithm. The effectiveness of the 1D hygrothermal model used within the probabilistic approach was verified using several 2D hygrothermal models. The innovative approach of combining metamodeling with probabilistic analysis for mortar extrusion phenomenon enhanced the understanding of moisture-related challenges in building construction. Moreover, the results provided valuable insights into the complexities and uncertainties associated with mortar extrusion and its impact on the hygrothermal performance of timber frame walls with clay brick masonry claddings. The key findings of these analyses are summarised as shown in the following subsections.

5.1. 1D versus 2D hygrothermal models

The R^2 values between the 1D and 2D models consistently exceeded 90 % across most cases, suggesting that the 1D mortar extrusion model could effectively predict variations in the maximum mould index of the 2D model, with an accuracy exceeding 90 %. Hence, the marginal disparities observed between the 1D and 2D models underscored the practical utility of employing customised materials within the 1D model instead of the time-consuming 2D model, in the scope of this study.

5.2. Mould growth analysis

Under the Gothenburg climatic conditions with high WDR loads, case studies 1 and 2 revealed an approximately 6 % reduction in

the 95th percentile of the maximum mould indices under the ES criterion compared with the ASHRAE criterion. This implies a general consistency between the two water penetration criteria under high WDR loads. In Rensjön (low WDR loads), the ES criterion resulted in approximately 22 % and 15 % reductions in the 95th percentile of the maximum mould indices than ASHRAE criterion for case studies 1 and 2, respectively. This indicates that the ASHRAE criterion tends to overestimate under conditions of low WDR loads, unlike the ES criterion.

5.3. Mould sensitivity analysis

The sensitivity analysis, encompassing linear and non-linear dimensions, highlighted a strong positive correlation between the extruded mortar depth and maximum mould index under climatic conditions characterised by high WDR loads using the ASHRAE criterion. The influence of the extruded mortar depth on the maximum mould index was reduced to a moderate correlation when the ES criterion was employed under high WDR load climatic conditions.

In climates with low WDR loads, the relationship between the extruded mortar depth and maximum mould index was weak and negligible for the ASHRAE and ES criteria, respectively. Other important parameters affecting the maximum mould index included the air change rate (negative correlation), reduction/splash coefficient of the WDR (positive correlation), solar absorption coefficient (negative correlation), and thermal conductivity of the Rockwool insulation (positive correlation). The non-linear sensitivity analysis revealed additional significant parameters previously overlooked in the linear sensitivity analysis, including the outdoor convection heat exchange coefficient, brick saturation point, brick thermal conductivity, and long-wave emissivity. However, their effects on the maximum mould index were less pronounced than those of the other significant parameters.

5.4. Future studies opportunities

In this study a 1D modelling approach (owing to the high computational expenses of 2D or 3D modelling) was employed; however, the realism of probabilistic extruded mortar modelling can be enhanced by adopting 2D or 3D modelling techniques. Employing these dimensions facilitates the depiction of diverse shapes and sizes of the extruded mortar across multiple orientations, including the X-, Y-, and Z-axes. In addition to the variables documented in this research, the inclusion of additional stochastic variables can significantly increase the accuracy of the hygrothermal model.

CRediT authorship contribution statement

Mohsen Bayat Pour: Writing – review & editing, Writing – original draft, Visualization, Validation, Software, Project administration, Methodology, Investigation, Formal analysis, Data curation, Conceptualization. **Seyedmohammad Kahangi Shahreza:** Writing – review & editing, Validation, Methodology, Formal analysis, Conceptualization.

Declaration of competing interest

The authors declare that they have no known competing financial interests or personal relationships that could have appeared to influence the work reported in this paper.

Data availability

Data will be made available on request.

Acknowledgement

The authors gratefully acknowledge the financial support from FORMAS, the Swedish Research Council for Sustainable Development, for the research grant 2019-00673. In addition, the authors are grateful for the Delphin support team's technical support.

References

[1] American Industrial Hygiene Association (AIHA), The Facts about Mould, 2009.
[2] M. Bayat Pour, M.L. Elsayed, Assessment of the Environmental Impacts, Energy Performance and Economic Aspects of Various Construction Materials, Master thesis, Lund University, Faculty of Engineering, Lund, Sweden, 2020.
[3] M. Bayat Pour, J. Niklewski, E. Frühwald Hansson, S. Thöns, Mould reliability analysis combined with mould health risks for decision support, in: *5th Central European Symposium On Building Physics, CESBP 2022*, Bratislava Slovakia, Sep. 2022, p. 8.
[4] D.J. Dacquisto, J.H. Crandell, J. Lyons, Building Moisture and Durability Past, Present and Future, Department of Housing and Urban Development, Washington, D.C., USA, Oct. 2004.
[5] Finnish mould growth model | Building Physics | Tampere Universities', Building Physics. Accessed: June. 30, 2022. [Online]. Available: https://research.tuni.fi/buildingphysics/finnish-mould-growth-model/.
[6] S. Thelandersson, T. Isaksson, Mould resistance design (MRD) model for evaluation of risk for microbial growth under varying climate conditions, Build. Environ. 65 (Jul. 2013) 18–25, https://doi.org/10.1016/j.buildenv.2013.03.016.
[7] L. Wadsö, B. Bengtsson, P. Johansson, The m-model for prediction of mould growth, Lund, Sweden (2022).
[8] S. Kahangi Shahreza, J. Niklewski, M. Molnár, Novel water penetration criterion for clay brick masonry claddings, Construct. Build. Mater. 353 (Oct. 2022) 129109, https://doi.org/10.1016/j.conbuildmat.2022.129109.
[9] A. Erkal, D. D'Ayala, L. Sequeira, Assessment of wind-driven rain impact, related surface erosion and surface strength reduction of historic building materials, Build. Environ. 57 (Nov. 2012) 336–348, https://doi.org/10.1016/j.buildenv.2012.05.004.
[10] P. Gholamalipour, H. Ge, T. Stathopoulos, Wind-driven rain (WDR) loading on building facades: a state-of-the-art review, Build. Environ. 221 (Aug. 2022) 109314, https://doi.org/10.1016/j.buildenv.2022.109314.

[11] M. Abuku, H. Janssen, S. Roels, Impact of wind-driven rain on historic brick wall buildings in a moderately cold and humid climate: numerical analyses of mould growth risk, indoor climate and energy consumption, Energy Build. 41 (1) (Jan. 2009) 101–110, https://doi.org/10.1016/j.enbuild.2008.07.011.
[12] R.S. Matthews, M.R.C. Bury, D. Redfearn, Investigation of dynamic water penetration tests for curtain walling, J. Wind Eng. Ind. Aerod. 60 (Apr. 1996) 1–16, https://doi.org/10.1016/0167-6105(96)00020-7.
[13] P. Johansson, et al., Interior insulation retrofit of a historical brick wall using vacuum insulation panels: hygrothermal numerical simulations and laboratory investigations, Build. Environ. 79 (Sep. 2014) 31–45, https://doi.org/10.1016/j.buildenv.2014.04.014.
[14] H. Hens, Wind-Driven Rain: from Theory to Reality, ASHRAE, Jan. 2010.
[15] D. Mumovic, M. Santamouris (Eds.), A Handbook of Sustainable Building Design and Engineering: an Integrated Approach to Energy, Health and Operational Performance, second ed., Routledge, London ; New York, 2019.
[16] D.G. Kayll, P. Eng, The role of the building envelope professional in the aftermath of vancouver's leaky condominium crisis, Buildings VIII/Wall Design and Building Science (2001) 2–7.
[17] J. Vos, A. Blommaert, N. Bossche, Statistical analysis on Belgian building defects, in: XV International Conference on Durability of Building Materials and Components. eBook of Proceedings, CIMNE, 2020, https://doi.org/10.23967/dbmc.2020.130.
[18] Observatoire de la Qualité de la Construction, 2021. Edition.
[19] K. Carbonez, H. Ge, A. Janssens, Comparison between uniform rain loads and point sources to simulate rainwater leakage with commercial HAM-models, in: 1st International Symposium on Building Pathology, Mar. 2015, p. 8. Porto, Portugal.
[20] K. Calle, C. Coupillie, A. Janssens, N. Van Den Bossche, Implementation of rainwater infiltration measurements in hygrothermal modelling of non-insulated brick cavity walls, J. Build. Phys. 43 (6) (May 2020) 477–502, https://doi.org/10.1177/1744259119883909.
[21] 'ASHRAE, Standard 160-2021, criteria for moisture-control design analysis in buildings. ASHRAE, American National Standards Institute (ANSI), USA, 2021.
[22] H.H. Saber, M.A. Lacasse, T.V. Moore, M. Nicholls, Mid-rise Wood Constructions: Investigation of Water Penetration through Cladding and Deficiencies: Report to Research Consortium for Wood and Wood-Hybrid Mid-rise Buildings', National Research Council of Canada, Dec. 2014 https://doi.org/10.4224/21274581.
[23] J.F. Straube, E.F.P. Burnett, Rain control and screened wall systems, in: Canadian Conference on Building Science & Technology, Jan. 1997, p. 25. Toronto, Canada.
[24] N. Van Den Bossche, N.A. Lacasse, A. Janssens, Watertightness of masonry walls: an overview, in: 12th International Conference on the Durability of Building Materials and Components (12DBMC), Apr. 2011, pp. 1–8.
[25] S. Kahangi Shahreza, J. Niklewski, M. Molnár, Experimental investigation of water absorption and penetration in clay brick masonry under simulated uniform water spray exposure, J. Build. Eng. 43 (Nov. 2021) 102583, https://doi.org/10.1016/j.jobe.2021.102583.
[26] H.M. Künzel, D. Zirkelbach, Influence of rain water leakage on the hygrothermal performance of exterior insulation systems, in: Proceedings of the 8th Symposium on Building Physics in the Nordic Countries, Copenhagen, Jun. 2008, pp. 282–289.
[27] C.C. Fishburn, D. Watstein, D.E. Parsons, Water Permeability of Masonry Walls, Department of Commerce, National Bureau of Standards, Washington, D.C., USA, BMS7, Oct. 1938.
[28] J. Straube, E. Burnett, Driving rain and masonry veneer, 19428-2959, in: *Water Leakage through Building Facades*, 100 Barr Harbor Drive, PO Box C700, ASTM International, West Conshohocken, PA, 1998, https://doi.org/10.1520/STP12096S, 73-73–15.
[29] H.M. Künzel, Accounting for unintended moisture sources in hygrothermal building analysis, in: NSB 2014 Building Physics Conference, Jun. 2014, p. 7. Lund, Sweden.
[30] C.J.W.P. Groot, J.T.M. Gunneweg, The influence of materials characteristics and workmanship on rain penetration in historic fired clay brick masonry, Heron 55 (2010) 141–154.
[31] S. Kahangi Shahreza, A. Abdul Hamid, Impact of different water penetration criteria and cavity ventilation rates on the risk of mold growth in timber frame walls with brick veneer cladding, in: Journal of Physics: Conference Series, Dec. 2023 012028, https://doi.org/10.1088/1742-6596/2654/1/012028.
[32] H. Janssen, S. Roels, L. Van Gelder, P. Das, Annex 55, Reliability of Energy Efficient Building Retrofitting - Probability Assessment of Performance and Cost (RAP-RETRO), Probabilistic Tools', Chalmers University of Technology, Gothenburg, Sweden, 2015. ISSN 1652-9162, 2015:4.
[33] S. Geving, A systematic method for hygrothermal analysis of building constructions using computer models, in: Fifth International IBPSA Conference, 1997. Prague, Check Republic.
[34] H.J. Moon, G. Augenbroe, Empowerment of decision-makers in mould remediation, Build. Res. Inf. 36 (5) (Oct. 2008) 5, https://doi.org/10.1080/09613210801996203.
[35] J. Zhao, Development of a novel statistical method and procedure for material characterization and a probabilistic approach to assessing the hygrothermal performance of building enclosure assemblies. College of Engineering and Computer Science, Syracuse University, Syracuse, NY, USA, 2012. Dissertation.
[36] H.J. Moon, G. Augenbroe, A mixed simulation approach to analyze mold growth under uncertainty, in: Ninth International IBPSA Conference, Building Simulation, Montreal, Canada, Aug. 2005, p. 9.
[37] A. Tijskens, H. Janssen, S. Roels, A simplified dynamic zone model for a probabilistic assessment of hygrothermal risks in building components, in: *11th Nordic Symposium On Building Physics*, Trondheim, Norway: Energy Procedia, Oct. 2017, pp. 717–722, https://doi.org/10.1016/j.egypro.2017.10.012.
[38] A. Tijskens, H. Janssen, S. Roels, Using convolutional neural networks for hygrothermal predictions to extrapolate to other external climates, in: J. Kurnitski, T. Kalamees (Eds.), 12th Nordic Symposium on Building Physics (NSB 2020), Jun. 2020 04001, https://doi.org/10.1051/e3sconf/202017204001. Tallinn, Estonia: E3S Web of Conferences.
[39] E.J. de Place Hansen, E.B. Møller, M. Ørsager, Guidelines for internal insulation of historic buildings, in: J. Kurnitski, T. Kalamees (Eds.), 12th Nordic Symposium on Building Physics (NSB 2020), Jun. 2020 01004, https://doi.org/10.1051/e3sconf/202017201004. Tallinn, Estonia: E3S Web of Conferences.
[40] T. Hou, D. Nuyens, S. Roels, H. Janssen, Quasi-Monte Carlo based uncertainty analysis: sampling efficiency and error estimation in engineering applications, Reliab. Eng. Syst. Saf. 191 (Nov. 2019) 106549, https://doi.org/10.1016/j.ress.2019.106549.
[41] A. Tijskens, S. Roels, H. Janssen, Hygrothermal assessment of timber frame walls using a convolutional neural network, Build. Environ. 193 (Apr. 2021) 107652, https://doi.org/10.1016/j.buildenv.2021.107652.
[42] A. Tijskens, H. Janssen, S. Roels, Probabilistic hygrothermal assessment of various timber frame wall compositions, Build. Environ. 243 (Sep. 2023) 110619, https://doi.org/10.1016/j.buildenv.2023.110619.
[43] S. Hokoi, M.K. Kumaran, Experimental and analytical investigations of simultaneous heat and moisture transport through glass fiber insulation, J. Therm. Insul. Build. Envelopes 16 (3) (Jan. 1993) 263–292, https://doi.org/10.1177/109719639301600307.
[44] J. Zhao, R. Plagge, A. Nicolai, J. Grunewald, J.S. Zhang, Stochastic study of hygrothermal performance of a wall assembly - the influence of material properties and boundary coefficients, HVAC R Res. 17 (4) (2011) 4, https://doi.org/10.1080/10789669.2011.585421.
[45] J. Goffart, M. Rabouille, N. Mendes, Uncertainty and sensitivity analysis applied to hygrothermal simulation of a brick building in a hot and humid climate, Journal of Building Performance Simulation 10 (1) (Jan. 2017) 1, https://doi.org/10.1080/19401493.2015.1112430.
[46] L. Wang, H. Ge, Hygrothermal performance of cross-laminated timber wall assemblies: a stochastic approach, Build. Environ. 97 (Feb. 2016) 11–25, https://doi.org/10.1016/j.buildenv.2015.11.034.
[47] D. Reiter, The Monte Carlo method, an introduction, in: Computational Many-Particle Physics 739, Springer Berlin Heidelberg, 2008, pp. 63–78, https://doi.org/10.1007/978-3-540-74686-7_3. Lecture Notes in Physics, vol. 739. , Berlin, Heidelberg.
[48] N. Ramos, E. Barreira, M.L. Simões, J. Delgado, Probabilistic risk assessment applied to biological growth on external surfaces with ETICS, in: 13th Conference of the International Building Performance Simulation Association, Chambéry, France, August, 2013, p. 6.
[49] N.M.M. Ramos, E. Barreira, M.L. Simões, J.M.P.Q. Delgado, Probabilistic risk assessment methodology of exterior surfaces defacement caused by algae growth, J. Constr. Eng. Manage. 140 (12) (Dec. 2014) 12, https://doi.org/10.1061/(ASCE)CO.1943-7862.0000909.
[50] V. Marincioni, G. Marra, H. Altamirano-Medina, Development of predictive models for the probabilistic moisture risk assessment of internal wall insulation, Build. Environ. 137 (Jun. 2018) 257–267, https://doi.org/10.1016/j.buildenv.2018.04.001.

[51] A. Tijskens, S. Roels, H. Janssen, Neural networks for metamodelling the hygrothermal behaviour of building components, Build. Environ. 162 (Sep. 2019) 106282, https://doi.org/10.1016/j.buildenv.2019.106282.
[52] A. Tijskens, H. Janssen, S. Roels, The impact of a reduced training subspace on the prediction accuracy of neural networks for hygrothermal predictions, Journal of Building Performance Simulation 14 (1) (Jan. 2021) 1, https://doi.org/10.1080/19401493.2020.1832148.
[53] A. Tijskens, H. Janssen, S. Roels, Optimising convolutional neural networks to predict the hygrothermal performance of building components, Energies 12 (20) (Oct. 2019), https://doi.org/10.3390/en12203966. Art. no. 20.
[54] R.Z. Freire, G.H. dos Santos, L. dos S. Coelho, Hygrothermal dynamic and mould growth risk predictions for concrete tiles by using least squares support vector machines, Energies 10 (8) (Jul. 2017) 1093, https://doi.org/10.3390/en10081093.
[55] C. Aggarwal, H. Ge, M. Defo, Assessing mould growth risk of wood-frame walls using partial least squares (PLS) regression considering climate model uncertainties, Build. Environ. 238 (Jun. 2023) 110374, https://doi.org/10.1016/j.buildenv.2023.110374.
[56] C. Aggarwal, H. Ge, M. Defo, M.A. Lacasse, Hygrothermal performance assessment of wood frame walls under historical and future climates using partial least squares regression, Build. Environ. 223 (Sep. 2022) 109501, https://doi.org/10.1016/j.buildenv.2022.109501.
[57] M. Bayat Pour, J. Niklewski, A. Naghibi, E. Frühwald Hansson, Robust probabilistic modelling of mould growth in building envelopes using random forests machine learning algorithm, Build. Environ. 243 (Sep. 2023) 110703, https://doi.org/10.1016/j.buildenv.2023.110703.
[58] G.D. Wyss, K.H. Jorgensen, A user's guide to LHS: sandia's Latin Hypercube Sampling, Software (Feb. 1998) 573301, https://doi.org/10.2172/573301. SAND–98-0210.
[59] T. Ojanen, H. Viitanen, R. Peuhkuri, Modelling of mould growth in building envelopes, in: IEA ECBCS Annex 41 Closing Seminar : Nordic Building Physics Conference, 2007, p. 18. Copenhagen, Denmark.
[60] E. Vereecken, S. Roels, Review of mould prediction models and their influence on mould risk evaluation, Build. Environ. 51 (May 2012) 296–310, https://doi.org/10.1016/j.buildenv.2011.11.003.
[61] O.M. Querin, M. Victoria, C. Alonso, R. Ansola, P. Martí, Discrete method of structural optimization, in: Topology Design Methods for Structural Optimization, Elsevier, 2017, pp. 27–46, https://doi.org/10.1016/B978-0-08-100916-1.00003-9.
[62] D.M. Hamby, A review of techniques for parameter sensitivity analysis of environmental models, Environ. Monit. Assess. 32 (2) (Sep. 1994) 2, https://doi.org/10.1007/BF00547132.
[63] P. Schober, C. Boer, L.A. Schwarte, Correlation coefficients: appropriate use and interpretation, Anesth. Analg. 126 (5) (May 2018) 1763–1768, https://doi.org/10.1213/ANE.0000000000002864.
[64] L. Breiman, Random forests, Mach. Learn. 45 (1) (2001) 5–32.
[65] R.H. Myers, D.C. Montgomery, C.M. Anderson-Cook, Response Surface Methodology: Process and Product Optimization Using Designed Experiments, third ed., Wiley, 2009.
[66] T. Hastie, R. Tibshirani, Generalized additive models, Stat. Sci. 1 (3) (1986) 297–318.
[67] C.M. Bishop, Neural Networks for Pattern Recognition, first ed., Oxford University Press, USA, 1995.
[68] Z.C. Lipton, A critical review of recurrent neural networks for sequence learning, Cornell University 33 (May 2015).
[69] A.J. Smola, B. Schölkopf, A tutorial on support vector regression, Stat. Comput. 14 (3) (Aug. 2004) 199–222, https://doi.org/10.1023/B:STCO.0000035301.49549.88.
[70] V. Vapnik, The Nature of Statistical Learning Theory, second ed., Springer, 1995.
[71] 'sklearn.ensemble.RandomForestRegressor', scikit-learn [Online]. Available: https://scikit-learn/stable/modules/generated/sklearn.ensemble.RandomForestRegressor.html. (Accessed 5 March 2023).
[72] T. Hall, S. Vidén, The Million Homes Programme: a review of the great Swedish planning project, Plann. Perspect. 20 (3) (Jan. 2005) 301–328, https://doi.org/10.1080/02665430500130233.
[73] Delphin [Online]. Available: https://bauklimatik-dresden.de/delphin/index.php?aLa=en. (Accessed 26 May 2021).
[74] EN 15026:2007 - Hygrothermal Performance of Building Components and Building Elements - Assessment of moisture transfer by numerical simulation.
[75] ISO 6946:2017 - Building Components and Building Elements – Thermal Resistance and Thermal Transmittance – Calculation methods.
[76] EN ISO 6946:2017 - Building Components and Building Elements - Thermal Resistance and Thermal Transmittance - Calculation methods.
[77] P.W.M.H. Steskens, H. Janssen, C. Rode, Influence of the convective surface transfer coefficients on the heat, air, and moisture (HAM) building performance, Indoor Built Environ. 18 (3) (Jun. 2009) 245–256, https://doi.org/10.1177/1420326X09105682.
[78] M. Rahiminejad, D. Khovalyg, Review on ventilation rates in the ventilated air-spaces behind common wall assemblies with external cladding, Build. Environ. 190 (Mar. 2021) 107538, https://doi.org/10.1016/j.buildenv.2020.107538.
[79] K. Gradeci, N. Labonnote, B. Time, J. Köhler, A probabilistic-based methodology for predicting mould growth in façade constructions, Build. Environ. 128 (Jan. 2018) 33–45, https://doi.org/10.1016/j.buildenv.2017.11.021.
[80] L. Ducoulombier, Z. Lafhaj, Comparative study of hygrothermal properties of five thermal insulation materials, Case Stud. Therm. Eng. 10 (Sep. 2017) 628–640, https://doi.org/10.1016/j.csite.2017.11.005.
[81] Data och analyser för väder samt Sveriges klimat och miljö | SMHI'. Accessed: May 30, 2023. [Online]. Available: https://www.smhi.se/data.
[82] Meteonorm Version 8 Updated historic, current and future data', Meteonorm (en). Accessed: July. 2, 2022. [Online]. Available: https://meteonorm.com/en/.
[83] H. Viitanen, Factors Affecting the Development of Mould and Brown Rot Decay in Wooden Material and Wooden Structures, Doctoral Thesis, Department of Forest Products, Swedish University of Agricultural Sciences, Uppsala, Sweden, 1996.
[84] ISO 15927-3:2009 - Hygrothermal Performance of Buildings – Calculation and Presentation of Climatic Data – Part 3: Calculation of a Driving Rain Index for Vertical Surfaces from Hourly Wind and Rain Data.
[85] E. Vereecken, S. Roels, Hygric performance of a massive masonry wall: how do the mortar joints influence the moisture flux? Construct. Build. Mater. 41 (Apr. 2013) 697–707, https://doi.org/10.1016/j.conbuildmat.2012.12.024.
[86] S.O. Mundt-Petersen, L.-E. Harderup, J. Arfvidsson, Important factors affecting the risk of mold growth in well-insulated wood frame walls in northern European climates, in: Thermal Performance of the Exterior Envelopes of Whole Buildings XII, Clearwater, Florida, 2013, p. 14. United States.

Paper IV

Influence of extruded mortar joints on mould growth in timber frame wall with brick veneer: Probabilistic and Machine Learning Modelling

Mohsen Bayat Pour[a*], Seyedmohammad Kahangi Shahreza[b], Akram Abdul Hamid[c]

[a] *Division of Structural Engineering, Department of Building and Environmental Technology, Lund University, John Ericssons väg 1 SE-223 63 Lund, Sweden, mohsen.bayat_pour@kstr.lth.se, +46 222 73 95*

[b] *Division of Structural Engineering, Department of Building and Environmental Technology, Lund University, John Ericssons väg 1 SE-223 63 Lund, Sweden, mohammad.kahangi@kstr.lth.se*

[c] *Division of Building Physics, Department of Building and Environmental Technology, Lund University, John Ericssons väg 1 SE-223 63 Lund, Sweden, akram.abdul_hamid@byggtek.lth.se*

[*] *Corresponding author*

Abstract

Inappropriate bricklaying techniques can result in extruded mortar joints, which may partially fill the air gaps within brick veneer timber frame walls. This leads to an unintended connection or "bridge" between the brick masonry cladding and its adjacent layer (such as insulation or weather-resistant barriers). This bridging effect compromises the drainage function of the air gap, allowing water to reach adjacent layers and intensifying the impact of water penetration, under wind-driven rain (WDR) conditions. This study employs a probabilistic analysis in combination with a machine learning metamodel to investigate the impact of extruded mortar joints on mould growth. The metamodel, developed using the random forests (RF) machine learning algorithm, is used to predict the maximum mould index (MMI). In addition, this study assesses the effects of two different water penetration criteria—ASHRAE and experimental study-based (ES)—on extruded mortar joints under climatic conditions in Gothenburg, Sweden. In order to figure out how different orientations affect the analysis; the study examines the case study from four different orientations. The findings showed that the ES and ASHRAE criteria were in agreement for orientations with substantial WDR loads (e.g., south). On the other hand, the ASHRAE criteria illustrated a higher MMI than the ES criteria in walls facing orientations with relatively small WDR loads (e.g., north). Furthermore, an increased extruded mortar depth and higher MMI were shown to be positively correlated by the linear and non-linear mould sensitivity analyses. However, depending on the WDR loads (or different orientations) and chosen water penetration criteria, this correlation's strength can vary. The air change rate (negative correlation), the solar absorption coefficient (negative correlation), the WDR's

reduction/splash coefficient (positive correlation), and the thermal conductivity of the Rockwool insulation (positive correlation) were additional important variables influencing the MMI.

Keywords: Mortar extrusion, machine learning, mould assessment, clay brick masonry, hygrothermal simulation, probabilistic analysis, water penetration.

Nomenclature		PA	Probabilistic Analysis
		RF	Random Forests
ACR	Air Change Rate [1/h]	RH	Relative humidity [%]
ASHRAE	American Society of Heating, Refrigerating and Air-conditioning Engineers	R^2	Coefficient of Determination
A_w	Water Absorption Coefficient [kg/m^2. s$^{0.5}$]	S_d-value	Diffusion Equivalent Air Layer Thickness
CoV	Coefficient of Variation	T	Temperature [˚C]
Cp	Specific Heat Capacity [J/kg.K]	WDR	Wind-driven Rain
CSi	Case Study i	y_i	Original data
D_B	Bulk Density [kg/m^3]	$\overline{y_i}$	Mean of the original data
ES	Experimental Study	$\widehat{y_i}$	Predicted data
LHS	Latin Hypercube Sampling	ε_i	Convergence value
MA	Metamodel Analysis	θ_{eff}	Saturation point [m^3/m^3]
MAE	Mean Absolute Error	θ_{por}	Porosity [m^3/m^3]
MMI	Maximum Mould Index	λ_{dry}	Thermal Conductivity [W/m.K]
MRA	Mould Reliability Analysis	μ	Mean
MSA	Mould Sensitivity Analysis	μ_{VDR}	Water Vapor Diffusion Resistance Factor [-]
n	Total number of original data	ρ	Spearman's correlation coefficient
OF_i	Objective function	σ	Standard deviation

1. Introduction

1.1. *Background*

The hygrothermal performance of buildings significantly impacts construction projects with regard to health issues (Fisk et al., 2007; Bayat Pour, Niklewski, Frühwald Hansson, et al., 2023), economic outcomes (Bayat Pour and Elsayed, 2020), and material deterioration (Wang et al., 2020). It is widely agreed that modelling the hygrothermal performance of external wall assemblies is essential for identifying and addressing moisture-related issues, including the risk of microbial growth (Künzel and Dewsbury, 2022). Analysing temporal variations in temperature (T) and relative humidity (RH) is essential for assessing the risk of mould growth in exterior walls. Over the past few decades, various mould models have been developed, including the m-model (Wadsö et al., 2022), the Mould Resistance Design (MRD) model (Thelandersson and Isaksson, 2013), and the Finnish mould growth model (*Building Physics*, 2024).

Clay brick masonry façades are commonly used in residential buildings due to their longevity and aesthetic value (Kahangi Shahreza et al., 2022). Wind-driven rain (WDR) is a significant source of moisture in Nordic countries, while brick cladding offers effective protection against that (Erkal et al., 2012). When bio-based materials are present, adverse effects such as material

degradation and mould growth become more severe (Gholamalipour et al., 2022). According to Abuku et al. (Abuku et al., 2009), mould growth can be significantly influenced by water penetration caused by WDR loads, particularly at wall edges. Furthermore, the relationship between WDR and water penetration potential in brick walls has been established by various studies (Hens, 2010; Johansson et al., 2014; Matthews et al., 1996; Mumovic and Santamouris, 2019). The noticeable costs associated with rebuilding building envelopes due to rain penetration were highlighted by Kayll (Kayll, 2001). It is mentioned that the water infiltration problems in multi-family wood-frame buildings between 1993 and 2000 resulted in approximately one billion Canadian dollars in damage costs. Watertightness issues accounted for approximately half of the documented building damage cases in Belgium between 2010 and 2015 (Vos et al., 2020), with water penetration through the building envelope being the most common type of damage. In France, rain penetration in the building envelopes constituted 64% of all damage-related expenses reported between 2018 and 2020 (Observatoire de la Qualité de la Construction, 2021). In a survey by Boverket with 822 industry professionals (*Kartläggning av fel, brister och skador inom byggsektorn*, 2018), 12% of respondents identified rain penetration through facades as an issue, making it the 7th largest moisture issue in Swedish buildings.

Even though water penetration significantly impacts the hygrothermal performance of building envelopes, there is no consensus on the amount of water penetration in brick masonry cladding (Calle et al., 2020; Carbonez et al., 2015). According to the guidelines set out in the North American Standard (ASHRAE, Standard 160-2021, Criteria for Moisture-Control Design Analysis in Buildings, 2021), the moisture source behind the cladding is defined as the deposition of 1% of WDR on the external surface of a wall. The 1% water penetration due to WDR has been investigated in numerous studies (Saber et al., 2014; Straube and Burnett, 1997). However, inclusive evaluations of experimental research have indicated that WDR penetration into clay brick cladding can range from 0% to 20% (Calle et al., 2020; Kahangi Shahreza et al., 2021; Künzel and Zirkelbach, 2008; Van Den Bossche et al., 2011). Although the recommended WDR-induced penetration through the cladding is 1% of rain reaching the surface (ASHRAE, Standard 160-2021, Criteria for Moisture-Control Design Analysis in Buildings, 2021), experimental studies (Fishburn et al., 1938; Straube and Burnett, 1997) demonstrated a delay between the initiation of WDR exposure and the first reported instance of penetration, even when extreme conditions for testing were considered. This related to the fact that a specific saturation level is required in brick masonry before water penetration can occur (Kahangi Shahreza et al., 2021; Straube and Burnett, 1998). Consequently, WDR penetration may not occur in masonry walls that still have the capacity to absorb and retain water. Additionally, it takes time for the surface to reach saturation, after which runoff begins to form which may lead to water penetration. Further, the ASHRAE standard does not distinguish between different external surfaces, including varying textures and material types. Nevertheless, the ASHRAE criterion has been widely adopted due to the lack of consensus on WDR-induced water penetration rates across various exterior cladding surfaces (Calle et al., 2020; Carbonez et al., 2015; Künzel,

2014). This emphasises the importance of employing a method that accurately determines the percentage of water penetration in brick claddings caused by WDR.

There is disagreement not only regarding the amount of water penetration in brick masonry claddings, but also about the location of the moisture source in hygrothermal models. According to ASHRAE 160–2021 (ASHRAE, Standard 160-2021, Criteria for Moisture-Control Design Analysis in Buildings, 2021), the moisture load resulting from WDR-induced water penetration should be placed at the external surface of the weather-resistant barrier. If a weather-resistant barrier is not present, the placement site should be determined based on technical rationale. According to Groot and Gunneweg's experimental study (Groot and Gunneweg, 2010), workmanship has the greatest effect on rainwater penetration of masonry walls in historical buildings among the various variables influencing WDR-induced water penetration. Poor workmanship can result in mortar extrusion, which significantly affects the moisture response (Calle et al., 2020; Kahangi Shahreza and Abdul Hamid, 2023). Mortar extrusion can cause moisture-related issues when rainwater penetrates wall assemblies with clay brick masonry cladding. Therefore, to develop a reliable building envelope design, as well as a more precise determination of the deposition site, it is crucial to incorporate the influence of extruded mortar into the hygrothermal analysis process.

There are inherent uncertainties in modelling extruded mortar joints when combined with hygrothermal analysis. In order to handle uncertainties in hygrothermal performance modelling, probabilistic approaches are employed (Bayat Pour, Niklewski, et al., 2024; Bayat Pour and Abdul Hamid, 2024; Kahangi Shahreza et al., 2024). Certain tools, such as uncertainty propagation, sensitivity analysis, and metamodeling techniques, are crucial for probabilistic hygrothermal analysis, according to Annex 55: Subtask 2 (Janssen et al., 2015). The systematic method for hygrothermal analysis based on a Monte Carlo simulation was introduced by Geving (Geving, 1997) in 1997, marking the first publication to perform hygrothermal uncertainty propagation. Afterwards, combining different sampling techniques, such as the multilayered sampling scheme (Tijskens, Roels, et al., 2021; Tijskens et al., 2023) or Latin Hypercube Sampling (LHS) (Moon and Augenbroe, 2005, 2008; Zhao, 2012) were performed by several studies, with the objectives of reducing computational time and increasing sampling efficiency.

Monte Carlo methodology is widely employed for probabilistic hygrothermal analysis (Reiter, 2008); however, it is computationally time-consuming and expensive (Tijskens, Roels, et al., 2021). To address this, metamodels have been developed. Ramos et al. (Ramos et al., 2013, 2014) pioneered the use of response surface methodology (RSM) for probabilistic hygrothermal assessments. Marincioni et al. (Marincioni et al., 2018) used generalized additive models (GAM) to evaluate moisture risks in wall assemblies, achieving close approximations to simulations, with minor underestimations. Tijskens et al. (Tijskens, Janssen, et al., 2019, 2021; Tijskens, Roels, et al., 2019, 2021) employed neural networks, finding that convolutional neural networks (CNN) outperformed other models for predicting non-linear hygrothermal patterns. Freire et al.

(Freire et al., 2017) used support vector regression (SVR) to model hygrothermal parameters with satisfactory accuracy. Aggarwal et al. (Aggarwal et al., 2022, 2023) used partial least squares (PLS) regression for Canadian climates. Bayat Pour et al. (Bayat Pour, Niklewski, Naghibi, et al., 2023) proposed integrating probabilistic methods with random forests (RF) to improve robustness in hygrothermal and mould analysis. Consequently, conducting a probabilistic hygrothermal analysis in combination with a metamodel may help resolve the uncertainties surrounding extruded mortar joints and examine their impact on mould growth.

1.2. *Objectives and outline of the paper*

The main objective of this study is to examine the impact of extruded mortar joints on the hygrothermal performance of wall assemblies across various orientations, considering two different water penetration criteria. The study assesses the effect of extruded mortar joints in clay brick masonry claddings on timber frame walls, focusing on their susceptibility to mould occurrence. To achieve this, a machine learning algorithm and a probabilistic approach were employed, alongside linear and non-linear sensitivity analyses.

2. Methodology

2.1. *Probabilistic mould growth analysis*

The present study employs probabilistic hygrothermal analyses to evaluate a case study's hygrothermal performance under different scenarios. Based on these results, the study further analyses the risk of mould growth using a mathematical mould growth assessment model (*Building Physics*, 2024). In this study, the probabilistic hygrothermal analysis is performed using the mould reliability analysis (MRA) approach, originally introduced by Bayat Pour et al. (Bayat Pour, Niklewski, Naghibi, et al., 2023). Figure 1 illustrates the MRA approach, which consists of two main sections: probabilistic analysis (PA) and metamodel analysis (MA), represented by dashed-line boxes. The PA section includes sampling, hygrothermal simulations, and mould growth assessment. The MA section involves creating the metamodel, predicting maximum mould indices (MMI) and calculating their 95^{th} percentile. A metamodel is developed using the random forests (RF) (Breiman, 2001) machine learning algorithm that addresses the time-consuming nature of real simulations.

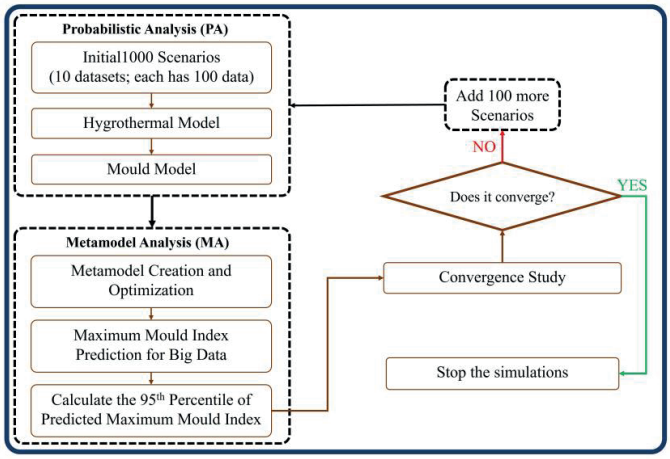


Figure 1: Probabilistic mould growth analysis procedure.

The PA section concludes with a mould assessment using the Finnish mould growth model (*Building Physics*, 2024), which is based on the VTT model (Ojanen et al., 2007; Viitanen and Ojanen, 2007). The Finnish mould growth model characterises mould development with an index ranging from 0 to 6 (*Building Physics*, 2024), providing a framework for mould assessment. Notably, it is broadly applicable to various building materials, accounting for the effects of coatings and surface types through decline and sensitivity classifications. The mould growth can decline when unfavourable conditions persist for more than six or twenty-four hours, while no decline is assumed for periods between six and twenty-four hours (Ojanen et al., 2007).

2.2. *Sampling*

The LHS technique (Wyss and Jorgensen, 1998) is employed for both the PA and MA sections. The present study builds upon an improved sampling approach, as suggested by Bayat Pour et al. (Bayat Pour, Kahangi Shahreza, et al., 2024), with the objective of minimising the risk of insufficient RF extrapolation of the developed metamodel. This approach compares the ranges of the samples used for hygrothermal simulations with those used for metamodel predictions, subsequently adding any additional ranges that fall below the minimum or exceed the maximum of the metamodel samples to the range of the hygrothermal simulation samples. In the PA section, a uniform distribution is also applied to all input variables. This approach was adopted to avoid the normal distribution, which tends to concentrate samples around the mean. It is crucial to ensure a diverse training set with data points covering the entire range of values for each variable in the chosen distribution. This goal can be achieved by employing a uniform distribution, which assigns equal weight to all segments of the variable distributions. Consequently, this enhances the performance of the developed metamodel by incorporating extreme scenarios and prevents the model from overfitting to average outcomes.

2.3. *Metamodel creation*

The RF algorithm (Breiman, 2001), which is well-known for its efficiency in handling regression and classification tasks, is employed in the MA section. The widespread use of the RF algorithm is primarily due to its interpretability, computational efficiency, robustness of metamodels, and its ability to handle nonlinear relationships (Bayat Pour, Niklewski, Naghibi, et al., 2023). As described in (Bayat Pour, Niklewski, Naghibi, et al., 2023), the feature selection process is the first step in developing a metamodel in the MA section. The optimal number of features to include in the metamodel is determined through a parametric analysis during this process. The most effective features are identified by iteratively analysing the number of features that yield the highest coefficient of determination (R^2) between the observed and predicted MMI. To facilitate model training and evaluation, the dataset is then randomly divided into training (70%) and testing (30%) subsets.

The accuracy of the trained metamodel is evaluated using the coefficient of determination (R^2) and the mean absolute error (MAE), as represented in Equations (1) and (2).

$$R^2 = 1 - \frac{\sum_{i=1}^{n}(y_i - \hat{y}_i)^2}{\sum_{i=1}^{n}(y_i - \bar{y}_i)^2} \tag{1}$$

$$MAE = \frac{1}{n}\sum_{i=1}^{n}\left|y_i - \hat{y}_i\right| \tag{2}$$

Here, n represents the total number of original data points, $\bar{y}_i$ denotes the mean of the original data, and y_i and $\hat{y}_i$ represent the original and predicted data, respectively.

To achieve optimal performance of the metamodel, fine-tuning of the RF model's hyperparameters is required. In this study, the RF model was optimised by adjusting various parameters, including the number of trees, selecting the most relevant features, and using out-of-bag samples to estimate the generalisation score. The remaining hyperparameters were set to the default values specified in (*scikit-learn*, 2024).

2.4. *Convergence study*

To determine an adequate number of simulations in the PA section, a convergence study is required. To facilitate the convergence analysis in the field of probabilistic hygrothermal analysis, Bayat Pour et al. (Bayat Pour, Niklewski, Naghibi, et al., 2023) proposed an equation that tracks the 95th percentile of the MMI (the target variable) while systematically increasing the number of simulations. Monitoring the change in the target variable over the ten previous iterations is part of the convergence criterion. A new iteration is created by adding 100 new scenarios to the existing set of simulations. The simulation process continues until the convergence value falls below the predetermined threshold of 0.001, as described by Bayat Pour

et al. (Bayat Pour, Niklewski, Naghibi, et al., 2023). The convergence value is calculated using Equation (3), where ε_i represents the convergence value of the objective function (i.e., the 95th percentile of the MMI), i is the current iteration number (>10), and OF_i is the objective function value at the ith iteration.

$$\varepsilon_i = \frac{\left|\sum_{i-9}^{i-5} OF_i - \sum_{i-4}^{i} OF_i\right|}{\sum_{i-4}^{i} OF_i} \tag{3}$$

2.5. *Mould sensitivity analysis*

The mould sensitivity analysis (MSA) method, developed by Bayat Pour et al. (Bayat Pour, Niklewski, Naghibi, et al., 2023), is employed in this study to determine the impact of uncertainties in input variables on the output, specifically the MMI. It incorporates two distinct types of sensitivity analysis as shown in Figure 2: correlation analysis and feature importance analysis.

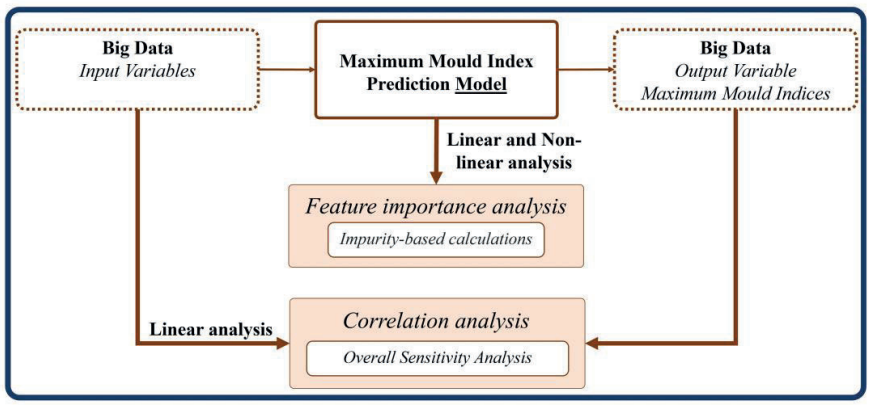


Figure 2: Mould sensitivity analysis procedure.

Spearman's correlation coefficient, denoted as $\rho_{X_{ri},Y_{rj}}$, represents the correlation between two variables (Zhao, 2012) and can be calculated using Equation (4). Calculation of this coefficient includes the full distributions of input and output variables where the term $cov(X_{ri}, Y_{rj})$ represents the covariance of the ranked variables, while $\sigma_{X_{ri}}$ and $\sigma_{Y_{rj}}$ denote the standard deviations of the ranked variables.

$$\rho_{X_{ri},Y_{rj}} = \frac{cov(X_{ri},Y_{rj})}{\sigma_{X_{ri}}.\sigma_{Y_{rj}}} \tag{4}$$

The degree of correlation between two variables is assessed using the Spearman's correlation coefficient, with values ranging from -1 to +1 (Hamby, 1994). The direction of the relationship

between two variables is indicated by the Spearman's correlation coefficient sign. A positive sign represents a positive correlation, where both variables increase or decrease together. Conversely, a negative sign signifies a negative correlation, where an increase in one variable is associated with a decrease in the other, and vice versa. The conventional interpretation of the correlation strength, based on the Spearman's correlation coefficient, is as follows (Schober et al., 2018):

- 0.00 – 0.09: Negligible correlation
- 0.10 - 0.39: Weak correlation
- 0.40 - 0.69: Moderate correlation
- 0.70 - 0.89: Strong correlation
- 0.90 - 1.00: Very strong correlation

In a trained RF model, feature importance analysis is crucial for assessing how changes in input variables influence output variables (Bayat Pour, Niklewski, Naghibi, et al., 2023). The RF algorithm, which is an ensemble machine learning method including multiple decision trees, takes into consideration both linear and non-linear relationships between inputs and outputs. The model divides the data into different sets with related responses by using specific features at the internal nodes. The selection criteria for dividing the data are variance reduction for regression tasks and Gini impurity for classification tasks. Feature importance is determined by evaluating the effect of each feature on impurity reduction. The average impurity reduction across all trees is calculated to assess the importance of a feature. A higher feature importance score demonstrates a greater impact of that feature on the model's performance. This allows for a better understanding of which features contribute most significantly to the prediction, helping to focus on the factors that have the most influence on the output.

2.6. *Case study*

Figure 3 (left side) shows a case study of lightweight wood frame walls with brick veneer, a common type of wall construction in Sweden, where timber studs are placed within the insulating layer (Hall and Vidén, 2005; Kahangi Shahreza and Abdul Hamid, 2023). The use of wooden materials in these frames makes them particularly susceptible to mould growth, which could result in health concerns for occupants (Bayat Pour, Niklewski, Frühwald Hansson, et al., 2023). Figure 3 (right side) illustrates the occurrence of mortar extrusion that may have taken place during the bricklaying process. A schematic of the extruded mortar, which is the focus of this study, is shown. Notably, the mortar water content and workmanship involved in the bricklaying process could influence the morphology and dimensions of the mortar.

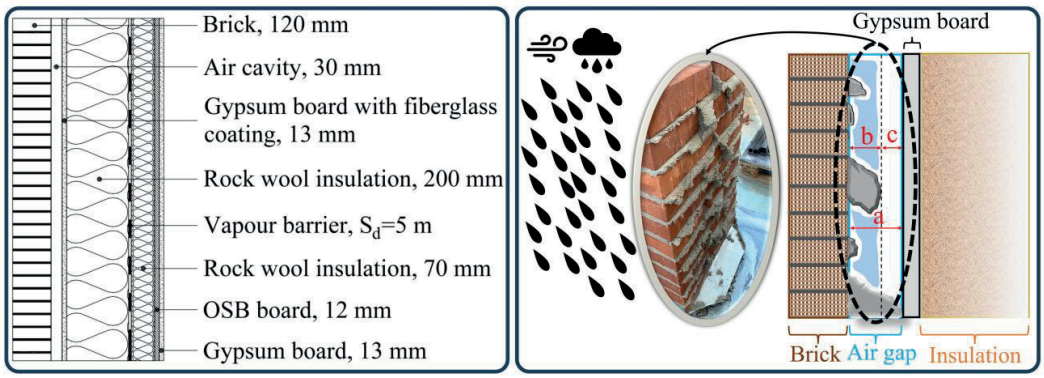


Figure 3: *Left:* External wall assembly as a case study. *Right:* Mortar extrusion phenomenon for clay brick cladding (the dimensions are not scaled). a [mm]: whole air gap thickness, b [mm]: extruded mortar thickness, c [mm]: net air gap thickness. Grey clouds: extruded mortar. Blue clouds: existing air between extruded mortar.

The air gap layer, which facilitates air exchange and interferes with the moisture transfer mechanism, is shown in Figure 3 between the brick layer and the gypsum board. The gypsum board is attached to the combined layer of timber studs and insulation. Poor workmanship during bricklaying can lead to mortar extrusion that could partially fills the air gap layer, thereby facilitating moisture to transfer from the brick layer to the other layers of the wall. As shown in Figure 3 (right), the extruded mortar, represented by grey clouds, may either fall into the air gap or remain within the air gap area in front of the joint, where it subsequently dries. In the worst-case scenario, the extruded mortar could create a bridge between the brick and the weather-resistant barrier (fibreglass gypsum board in this study), thus compromising the air gap and increasing the risk of moisture-related issues. In this study, the effect of extruded mortar is incorporated into the hygrothermal modelling for a more appropriate understanding of this phenomenon. While mortar extrusion can be modelled accurately using a two-dimensional (2D) hygrothermal analysis, applying 2D models in a probabilistic approach can be highly time-consuming. Therefore, the aim of this study is to develop a one-dimensional (1D) model with a customised material that serves as an acceptable alternative for representing the mortar extrusion layer. After verification through a limited number of 2D hygrothermal simulations, the 1D model is employed for the probabilistic modelling to ensure a balance between accuracy and computational efficiency.

2.7. *1D hygrothermal model*

Delphin 6.1 (DELPHIN, 2021), a comprehensive numerical simulation tool for the combined heat, air, and moisture (HAM) transport modelling, is used to analyse the hygrothermal performance of the building envelope assemblies. The outermost surface of the wooden stud was selected as the target screening point. This location was chosen because the wooden stud is a moisture-sensitive component in timber frame walls, making it particularly vulnerable to mould

growth. Monitoring this spot helps assess the potential for mould development, which, as noted in (Viitanen, 1996), can lead to odours and health issues for occupants.

According to SS EN 15026 (EN 15026:2007, 2007), indoor climatic conditions can be modelled based on outdoor T:

- Indoor T fluctuates between 20°C and 25°C when outdoor T is between 10°C and 20°C.
- When the outdoor T is below 10°C, the indoor T is fixed at 20°C. If the outdoor T exceeds 20°C, the indoor T is set to 25°C.

For indoor RH:

- If the outdoor T is between -10°C and 20°C, the indoor RH linearly varies between 35% and 65%.
- When the outdoor T falls below -10°C or rises above 20°C, the indoor RH remains fixed at 35% and 65%, respectively.

The WDR is modelled in Delphin 6.1 using the ISO 15927-3 standard (ISO 15927-3:2009, 2009), which considers microclimatic factors such as terrain, topography, obstacles, and wall-specific conditions to enhance the accuracy of hygrothermal simulations.

In the hygrothermal model, the mesh sizes are automatically adjusted across the different layers based on their thicknesses, ensuring an optimal balance between accuracy and computational efficiency. A minimum mesh size of 1 mm and a stretch factor of 1.3 are applied. This approach allows for finer meshes in thinner layers while still maintaining computational efficiency, making the simulation process both reliable and feasible for complex assemblies (Bayat Pour and Kahangi Shahreza, 2024).

According to Vereecken and Roels (Vereecken and Roels, 2013), the masonry wall can be modelled as a homogeneous brick layer under real climatic conditions to simplify the hygrothermal modelling procedure. The limitations of this simplification have been highlighted by Johansson et al. (Johansson et al., 2014).

Choosing a representative material for the mortar extrusion layer in 1D hygrothermal modelling can be challenging since this layer (the layer denoted by dimension *b* in Figure 3, right side) is partially filled with mortar. It means that, the extruded mortar layer is composed of a mix of mortar (represented by grey clouds in Figure 3, right side) and air (represented by blue clouds in Figure 3, right side). Therefore, using standard air, which has a saturation point of about 0.017 kg/m^3, for the 1D extruded mortar layer is inappropriate, as it does not adequately represent the hygrothermal behaviour of this mixed material layer. In Delphin, excess water is automatically removed from the moisture balance equation when moisture contents exceed the saturation point (Calle et al., 2020). On the other hand, in 1D modelling, it is neither realistic nor representative to consider pure mortar as the extruded mortar layer; thus, a customised material is considered to overcome these challenges. To prevent unrealistic moisture transport, liquid convection is

disregarded for this layer, and vapour diffusion is considered the primary mechanism for moisture transport. For this mechanism, the water absorption coefficient (A_w) should be set to zero. The saturation point from the mortar material properties (θ_{eff} = 0.21 m³/m³) is used, and the moisture storage function is formulated using the mortar sorption isotherm. Air and vapour permeability are influenced by the porosity, which is set at 0.5 m³/m³. Other material properties are adopted using the air properties from Delphin's default settings for the customised material. This configuration ensures that the extruded mortar layer can hold any unexpected moisture inflow up to the mortar material's saturation point.

The depths of the extruded mortar, defined using the LHS technique, are incorporated into the probabilistic model for each scenario. A uniform distribution is used with a range between 0 mm to 30 mm, indicating an equal likelihood of having no extruded mortar or a maximum depth of 30 mm. The entire depth of the extruded mortar is considered as the moisture source element, i.e., the moisture source is spread over the entire depth of the extruded mortar. The thickness of the extruded mortar (denoted as dimension *b* in Figure 3, right side) is considered to calculate the net air gap thickness (denoted as dimension *c* in Figure 3, right side) using Equation (5). This approach ensures that the impact of varying depths of extruded mortar on moisture transfer is adequately captured.

$$Net\ air\ gap\ thickness\ [mm](c) = Whole\ air\ gap\ thickness\ [mm](a) - Mortar\ extrusion\ thickness\ [mm](b) \quad (5)$$

The boundary conditions and material properties used in this study are presented in Tables 1 and 2, along with relevant references. A uniform distribution is used for the probability distributions of the boundary condition values presented in Table 1, implying equal likelihood for each specified value. The brick material properties listed in Table 2 are obtained from experimental investigations (Kahangi Shahreza et al., 2022), supplemented with data from relevant literature (Zhao, 2012). The outdoor convective heat exchange coefficient is computed using data from the Delphin database (DELPHIN, 2021), which varies from 12 to 20 W/(m²·K), depending on the wind exposure conditions (EN 15026:2007, 2007). This coefficient is then used to calculate the outdoor vapour diffusion coefficient, as these parameters are correlated. Two other input variables—solar absorption coefficient and long-wave emissivity—are determined by the surface texture and colour, with ranges of 0.4 to 0.8 and 0.85 to 0.95, respectively (DELPHIN, 2021). The amount of splashed WDR is considered by using a reduction/splash coefficient of WDR. The default value in Delphin is 0.7, indicating that 30% of the WDR is splashed after hitting the wall. In this study, a tolerance of 0.1 is assigned to this variable to account for associated uncertainties (Bayat Pour, Niklewski, Naghibi, et al., 2023). The effect of indoor airflow direction is considered by adjusting the interior surface heat transfer coefficient, which ranges from 5 to 10 W/(m²·K) according to (ISO 6946:2017, 2017).

Table 1. Probability distribution values for indoor and outdoor conditions. U(a, b): Uniform distribution, where *a* and *b* are the minimum and maximum values, respectively.

Variable	Probability distribution
Long-Wave Emissivity [-] (DELPHIN, 2021)	U(0.85, 0.95)
Indoor Surface Heat Transfer Coefficient (Convective + Radiative), $\left[\frac{W}{m^2.K}\right]$ (EN ISO 6946:2017, 2017)	U(5, 10)
Solar absorption coefficient [-] (DELPHIN, 2021)	U(0.4, 0.8)
Indoor Surface Vapour Diffusion Coefficient $\left[\frac{s}{m}\right]$ (Steskens et al., 2009)	$U(0.1 \times 10^{-7}, 1 \times 10^{-7})$
Reduction/splash coefficient of WDR [-] (Bayat Pour, Niklewski, Naghibi, et al., 2023)	U(0.6, 0.8)
Air change rate, ACR $[\frac{1}{h}]$ (Rahiminejad and Khovalyg, 2021)	U(0, 20)
Outdoor convection heat exchange coefficient [W/m^2.K] (EN 15026:2007, 2007)	U(12, 20)

Table 2. Probability distributions for the material properties. N(μ, σ): Normal distribution, μ and σ are the mean and standard deviation, respectively. CoV: coefficient of variation.

	Bulk Density (D_B $[\frac{kg}{m^3}]$)	Specific Heat Capacity (C_p $[\frac{J}{kg.K}]$)	Porosity (θ_{por} $[\frac{m^3}{m^3}]$)	Thermal Conductivity (λ_{dry} $[\frac{W}{m.K}]$)	Water Absorption Coefficient (A_w $\left[\frac{kg}{m^2.s^{0.5}}\right]$)	Water Vapour Diffusion Resistance Factor (μ_{VDR} [-])
Brick (Kahangi Shahreza et al., 2022; Zhao, 2012)	N(1830.13, 13.45) CoV=0.7%	N(889, 10.67) CoV =1.2%	N(0.293, 0.002) CoV =0.7%	N(0.548,0.077) CoV =14%	N(0.193, 0.00116) CoV =0.6%	N(18.01, 0.018) CoV =0.1%
Gypsum board (DELPHIN, 2021; Gradeci et al., 2018)	N(850, 85) CoV =10%	N(850, 85) CoV =10%	N(0.65, 0.065) CoV =10%	N(0.2, 0.02) CoV =10%	[(1)]N(0.18, 0.018)	N(8.3, 0.83) CoV =10%
OSB board (DELPHIN, 2021; Gradeci et al., 2018)	N(455, 45.5) CoV =10%	N(1500, 150) CoV =10%	N(0.74, 0.074) CoV =10%	N(0.1, 0.01) CoV =10%	[(1)]N(0.0019, 0.00019)	N(467, 46.7) CoV =10%
Rock wool insulation (Ducoulombier and Lafhaj, 2017)	N(39, 0.78) CoV =2%	[(2)]N(802, 80.2)	[(1)]N(0.95, 0.095)	N(0.034, 0.0026) CoV =7.6%	N(3.39×10^{-3}, 9.1×10^{-4}) CoV =27%	[(2)]N(2, 0.2)

Note: [(1)] These material properties were not specified in their corresponding references; therefore, default values from the Delphin database with a normal distribution and a coefficient of variation of 10% were used.
[(2)] These material properties lack information on their distributions in the literature; thus, a normal distribution with a coefficient of variation of 10% was assumed as a reasonable value, as recommended by Gradeci et al. (Gradeci et al., 2018).

2.8. *2D hygrothermal model*

Figure 4 shows both 1D and 2D hygrothermal models used in this research that aim to assess the accuracy of the 1D model against the more detailed 2D model. 2D modelling was performed using Delphin 6.1 to validate the 1D model. Since 1D modelling involves a simplified representation of wall assemblies, 2D simulations were conducted in selected scenarios to confirm the accuracy of the 1D simulation results. 2D hygrothermal models are developed, using ASHRAE water penetration criteria for the southern orientation in order to verify the proposed 1D hygrothermal model, focusing on three scenarios: low mortar extrusion (5 mm), high mortar extrusion (25 mm), and a base case with no mortar extrusion. Each scenario considers a 30 mm air gap width. In the 1D model, the extruded mortar layer is represented by a customised material, which is a mix of air and mortar. Meanwhile, the 2D model incorporates standard mortar and air properties, with the mortar elements randomly positioned within the airgap. Both models (1D and 2D) share the same input conditions for the hygrothermal simulations, ensuring consistency in the verification analysis. The material properties of the mortar are presented in Table 3.

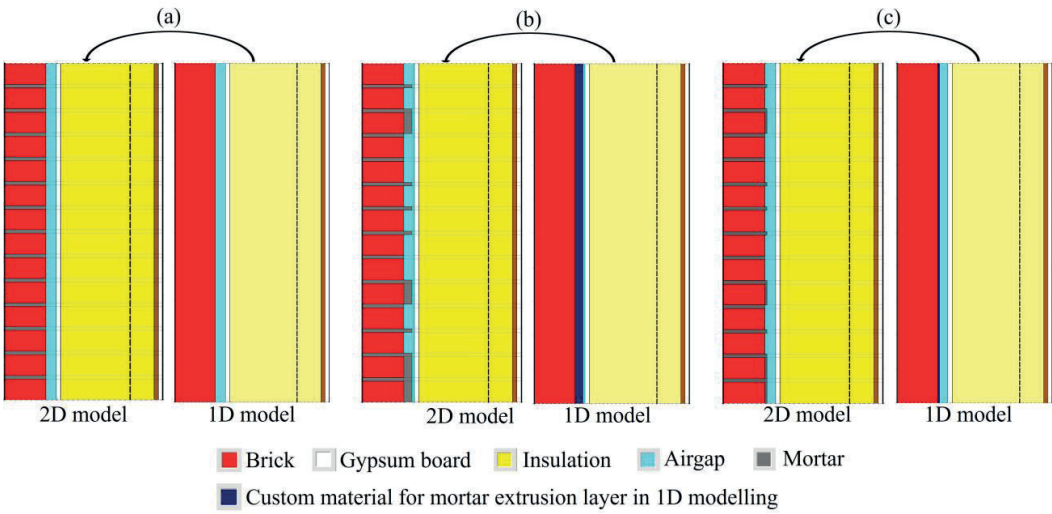


Figure 4: 1D versus 2D modelling for hygrothermal model verification. (a) base case, (b) high mortar extrusion (25 mm), and (c) low mortar extrusion (5 mm).

Table 3. Material properties of mortar.

Bulk Density (D_B $[\frac{kg}{m^3}]$)	Specific Heat Capacity (C_p $[\frac{J}{kg.K}]$)	Porosity (θ_{por} $[\frac{m^3}{m^3}]$)	Thermal Conductivity (λ_{dry} $[\frac{W}{m.K}]$)	Water Absorption Coefficient (A_w $[\frac{kg}{m^2.s^{0.5}}]$)	Water Vapour Diffusion Resistance Factor (μ_{VDR} [-])
1880	850	0.28	0.8	0.57	50

2.9. *Outdoor climate data*

In this study, hygrothermal analyses are conducted over a five-year period (2018–2023) using historical climate data at hourly intervals. To reduce the effect of initial conditions on the simulation outcomes, the climate data for 2018 are repeated twice prior to the primary simulations, establishing a two-year initialisation period. As a result, the outputs from the five-year period (2018–2023) are used for further analyses. The analyses focus on four different façade orientations—north, east, west, and south—under the climatic conditions of Gothenburg, one of the cities in Sweden with highest annual WDR load (Johansson et al., 2014).

The primary source for outdoor climate data in this study is the Swedish Meteorological and Hydrological Institute (SMHI) (Swedish Meteorological and Hydrological Institute (SMHI), 2024), which provided variables such as rain intensity [mm/h], air pressure [hPa], T [C], RH [%], shortwave diffuse and direct radiations [W/m^2], wind velocity [m/s], and wind direction [˚]. Since SMHI lacks data on long-wave counter radiation, this data is supplemented using Meteonorm (*Meteonorm (en)*, 2024), which generated hourly climate data for a representative year based on actual measurements.

2.10. *Water penetration criteria*

The ASHRAE standard 160–2021 (ASHRAE, Standard 160-2021, Criteria for Moisture-Control Design Analysis in Buildings, 2021) outlines a widely used methodology for assessing water infiltration through external surfaces. This standard designates a default water penetration rate of 1% for the rainwater adhering to the exterior surface of the wall assemblies. The primary location for this moisture source is identified as the outer surface of the weather-resistant barrier. Nonetheless, with the proper technical rationale, alterations can be made to this deposition point. In this study, both the position and volume of the moisture source are modified based on the depth of the extruded mortar, with the moisture source being distributed across the entirety of the extruded mortar's depth.

Kahangi Shahreza et al. (Kahangi Shahreza et al., 2022) have developed an alternative criterion for water penetration that is based on the moisture content of the brick veneer. Their experimental study demonstrated that if masonry walls are capable of absorbing and retaining water induced by WDR, penetration may not occur. Specifically, penetration will happen only when the masonry wall gets nearly saturated. Building on their findings, the experimental-based water penetration criterion (referred to as ES in this paper) has been established. Consequently, a portion of the WDR, referred to as the fraction of normal rain in the hygrothermal simulations, penetrates and is modelled as the moisture source in the hygrothermal analysis. The probability distributions for the saturation level threshold, saturation point, and fraction of normal rain flow for the tested brick are provided in Table 4.

Table 4: Experimental data of the brick (probability distributions) with the fraction of normal rain consideration as the moisture source (Kahangi Shahreza et al., 2022). N(μ, σ): normal distribution. μ and σ are the mean and standard deviation, respectively. CoV: coefficient of variation.

Saturation point, θ_{eff} [m^3/m^3]	Fraction of normal rain flow [%]	Saturation level threshold [%]
N(0.26, 0.00483)	N(3.77, 2.68)	N(93.34, 5.21)

3. Results and discussion

3.1. *Hygrothermal model verification (1D vs 2D)*

To assess the potential and accuracy of the 1D hygrothermal model in calculating the mould growth, the model was verified against a 2D hygrothermal model. Figure 5 illustrates a five-year simulation of mould growth for three distinct scenarios: the base case, high mortar extrusion (25 mm), and low mortar extrusion (5 mm). The red solid line indicates the mould index progression in the 1D hygrothermal model, specifically for the southern orientation. The corresponding black dashed, dotted, and solid lines represent the maximum, average, and minimum mould indices derived from the 2D model over a 1-meter height of the wall assembly. The figure demonstrates a notable alignment between the 1D and 2D models. The 1D model, utilising the custom material properties for the mortar extrusion, closely follows the trend of the 2D model's average mould indices. In certain intervals, the 1D model exhibits slightly higher mould index values compared to the 2D model, indicating a more conservative prediction of mould growth. Despite these occasional deviations, the overall trends between the two models remain consistent, reinforcing the verification of the 1D model as a reliable approximation for assessing mould risk in the wall assembly.

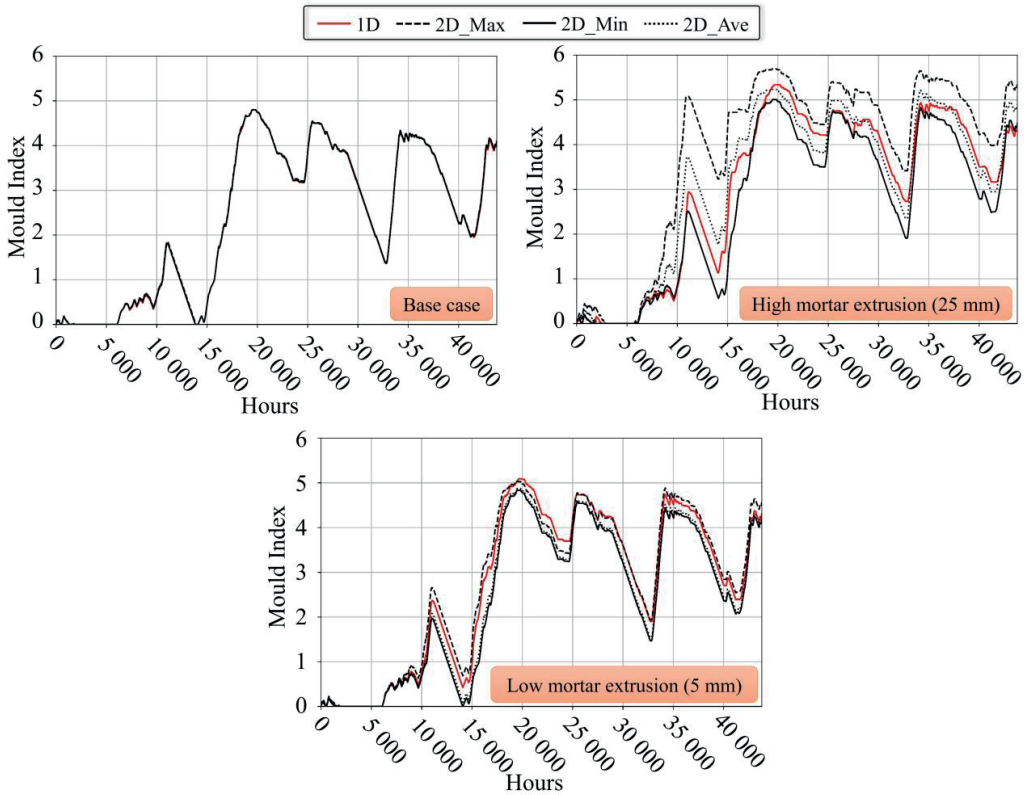


Figure 5: Wall assemblies modelling for verification, 1D versus 2D. Max/Min/Ave: maximum/minimum/average mould index [-] within the 1 m height of the wall in the 2D model.

Table 5 provides a comparison of the R^2 and MAE values between the 1D and 2D models for mould growth prediction, specifically under southern orientation. The analysis accounts for the maximum, average, and minimum values across the 2D model meshes. The high R^2 values, consistently above 90% in most cases, suggest that the 1D model can accurately predict over 90% of the variation observed in the mould indices of the 2D model. For the base case, where no mortar extrusion is present, the R^2 values are exceptionally high (0.992-0.998), indicating strong agreement between the 1D and 2D models. Correspondingly, the MAE values remain minimal (0.01-0.02), reinforcing the close alignment between the two models. This high level of agreement is expected given that the primary construction difference between the models lies in the modelling of the brick layer, leading to only minor variations.

In the scenario with high mortar extrusion (25 mm), the R^2 for the maximum mesh drops to 0.799, reflecting a reduction in the model's predictive accuracy. However, the average and minimum mesh values retain high R^2 values of 0.968 and 0.939, respectively. The MAE values for this case are larger, with a maximum error of 0.77 and a minimum error of 0.36, indicating a

moderate deviation between the 1D and 2D models. Despite this, the overall MAE remains below 0.36, meaning the discrepancies between the models do not substantially affect the reliability of the 1D model, particularly when considering the considerable reduction in computational time. For the low mortar extrusion (5 mm), the 1D model demonstrates excellent predictive capacity, with R^2 values ranging from 0.991 to 0.976. The MAE values are also within an acceptable range (0.13-0.29), signifying that the 1D model provides a reliable approximation of the 2D model, with only minor discrepancies in mould index predictions.

Table 5: Coefficient of determination (R^2) and mean absolute error (MAE) between the mould indices [-] of 1D and 2D models (maximum mesh, average of all meshes, and minimum mesh), southern orientation.

		Maximum	Average	Minimum
Base case	R^2	0.992	0.993	0.998
	MAE	0.02	0.02	0.01
High mortar extrusion (25 mm)	R^2	0.799	0.968	0.939
	MAE	0.77	0.28	0.36
Low mortar extrusion (5 mm)	R^2	0.991	0.976	0.968
	MAE	0.13	0.23	0.29

While the 1D model shows slightly higher errors in cases involving significant mortar extrusion, the overall predictive accuracy and minimal MAE values highlight its efficiency. The 1D model provides a practical alternative to the time-intensive 2D simulation (approximately 5.8 minutes per simulation for 1D model compared to 793 minutes per simulation for the 2D model), delivering reliable mould growth predictions with significant computational savings, especially when applied in long-term simulations, such as the five-year analysis conducted in this study. Based on this analysis, this study considers the trade-off between computational time (1D) and model accuracy (2D) to be within acceptable bounds, as the observed deviations do not critically impact post-processing evaluations, such as failure probability assessments.

3.2. *Optimisation of RF Metamodel*

The prediction error, visualised using a colour gradient in Figures 6 and 7, represents the absolute difference between the predicted and observed values for each data point. Additionally, the optimisation of the metamodels was carried out by examining the most influential features that contribute to the construction of these models. As demonstrated in Figures 6 and 7, the accuracy metrics for the optimised metamodels indicate satisfactory performance for both water penetration criteria (ASHRAE and ES) across various wall orientations (North, East, West, and South). The R^2 values, which ranged from 0.90 to 0.95, suggest that the optimised metamodels could explain a substantial portion of the variability in the dataset, capturing the relationship between input features and predicted mould indices. Additionally, the MAE values, which remain minimal across the different cases, highlight the precision of these models in predicting mould growth indices. This illustrates the reliability of the RF metamodels in accurately predicting MMI under varying scenarios' conditions.

Several key factors influenced the variability in R^2 values observed across the different case studies. One important factor is the inherent variability in the training data. The diversity and complexity of the dataset, including variations in material properties, climate conditions, and wall orientations, directly affect the model's ability to predict outcomes accurately. Furthermore, the unique attributes of each case study, such as the specific type of brick used or the water penetration criteria applied, introduce additional complexity that can influence the model's performance. The choice of features included in the machine learning model also plays a significant role in determining the accuracy of the metamodel. Features that are highly informative in one case study may not hold the same relevance in another, which could account for variability in the R^2 values. For instance, a feature like the thermal conductivity of brick might be more critical in one scenario, while in another, factors like air change rate or solar absorption coefficient may dominate. This discrepancy in feature importance is likely a contributing factor to the observed variations in performance metrics across different orientations and case studies. By fine-tuning the RF metamodel, robust and accurate predictions can be provided, as evidenced by the high R^2 values and low MAE scores. This process of optimisation ensures that the models remain flexible and adaptable, allowing for reliable predictions across a wide range of scenarios conditions and construction configurations.

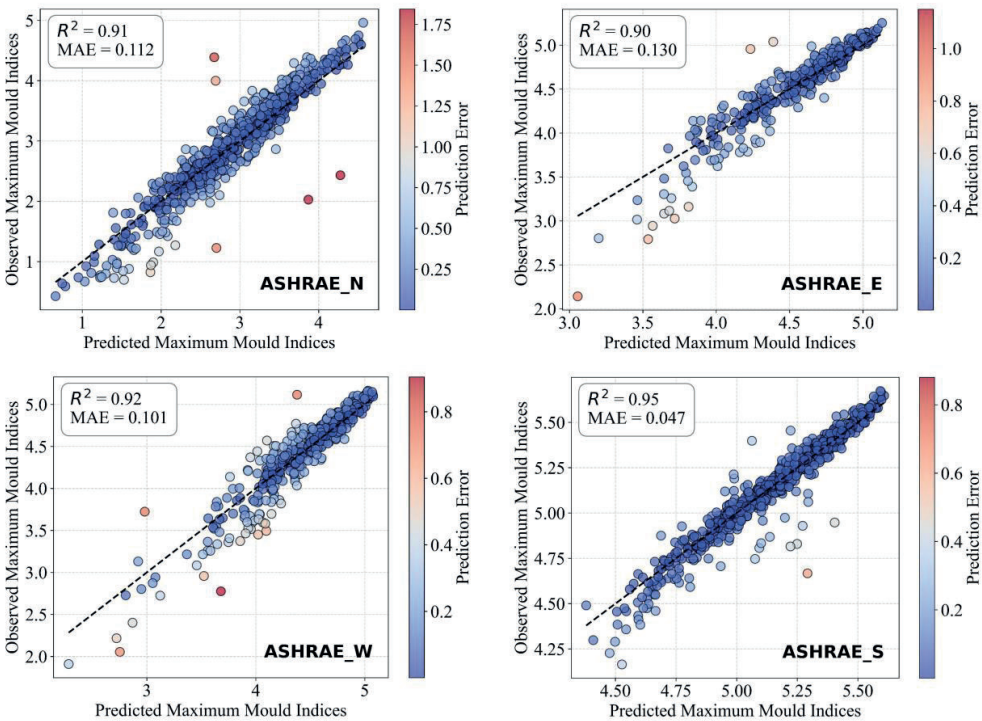


Figure 6: Predicted vs observed data during the machine learning model testing, using ASHRAE standard. N: north, E: east, W: west, S: south.

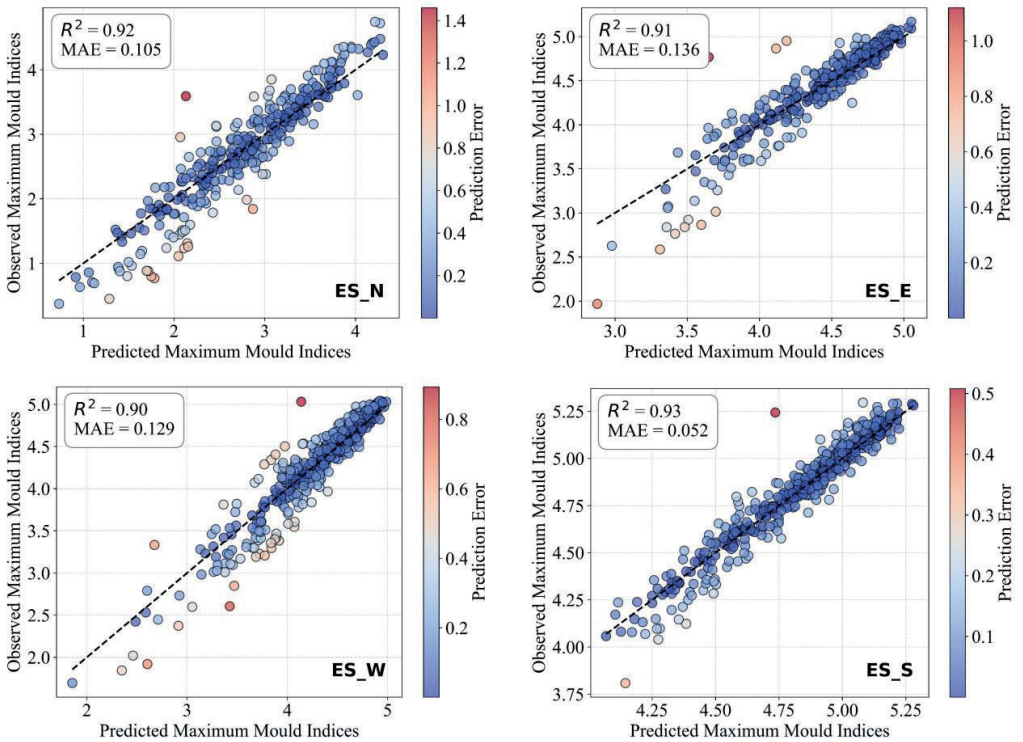


Figure 7: Predicted vs observed data during the machine learning model testing, using ES standard (case studies based on experimental study data). N: north, E: east, W: west, S: south.

3.3. *Mould growth analysis*

Table 6 shows the 95th percentile of the MMI for each case study, where 95% of the scenarios resulted in a lower MMI than the values shown. Under the southern orientation, there was a slight difference between the MMI values obtained using the ASHRAE and ES criteria—approximately 7%—with the ES criterion yielding a lower value. In contrast, under the northern orientation, the ES criterion produced about 15% lower MMI values compared to the ASHRAE standard. The relatively minor difference observed under the southern orientation can be attributed to the substantial WDR load, as discussed by Kahangi Shahreza and Abdul Hamid (Kahangi Shahreza and Abdul Hamid, 2023). In the south, higher WDR loads led to an increased water content in the brick, often surpassing the moisture threshold set by the ES criterion, resulting in more frequent moisture source considerations in the hygrothermal simulations.

Conversely, in the northern orientation, where the WDR load is significantly lower, the masonry absorbs rain without consistently exceeding the ES-defined moisture threshold. This results in a higher 95th percentile MMI when following the ASHRAE standard, as it considers 1% of the WDR load at all times, whereas the ES criterion only factors in moisture beyond a certain

threshold. In the north, where this threshold is seldom surpassed, ASHRAE's more conservative approach leads to a higher impact on the MMI.

Table 6. Mould growth calculations. ES: case studies based on experimental study data, ASHRAE: case studies based on ASHRAE 160–2021 standard, N: north, E: east, W: west, S: south.

Case studies	95th percentile of the maximum mould indices	Required number of simulations to achieve convergence
ASHRAE_N	3.82	1900
ES_N	3.24	1900
ASHRAE_E	4.85	1000
ES_E	4.18	1000
ASHRAE_W	4.96	1500
ES_W	4.27	1500
ASHRAE_S	5.42	2300
ES_S	5.03	1500

Figure 8 further supports this observation by comparing the water content in clay brick masonry façades for the south and north orientations (have highest and lowest WDR loads, respectively) over the five-year period from 2018 to 2023. The red lines represent the saturation threshold of the brick, while the blue lines show the water content in the masonry during this period. Although Figure 8 (left side) presents data from a single scenario for clarity, the remaining scenarios exhibited similar trends. The left side of Figure 8 shows that the brick in the southern orientation reached capillary saturation during much of the winter months. Consequently, instances where the water content surpassed the threshold were more frequent in the south, thereby increasing the likelihood of moisture source considerations from WDR. This pattern explains the closer alignment between the ES and ASHRAE results in the southern orientation.

In contrast, the northern orientation, also shown in Figure 8 (left side), rarely exceeded the moisture threshold, with only brief periods where the water content surpassed this limit. The lower WDR load in the north (see Figure 8, right side) reduces the likelihood of significant water penetration during the study period, demonstrating the benefit of considering the water absorption capacity of brick masonry. In these scenarios, the ES criterion, which accounts for the water absorption threshold, becomes more critical for avoiding overly conservative moisture source estimates. However, in orientations with frequent and intense WDR loads, such as the south (see Figure 8, right side), the results of the ASHRAE and ES criteria tend to converge.

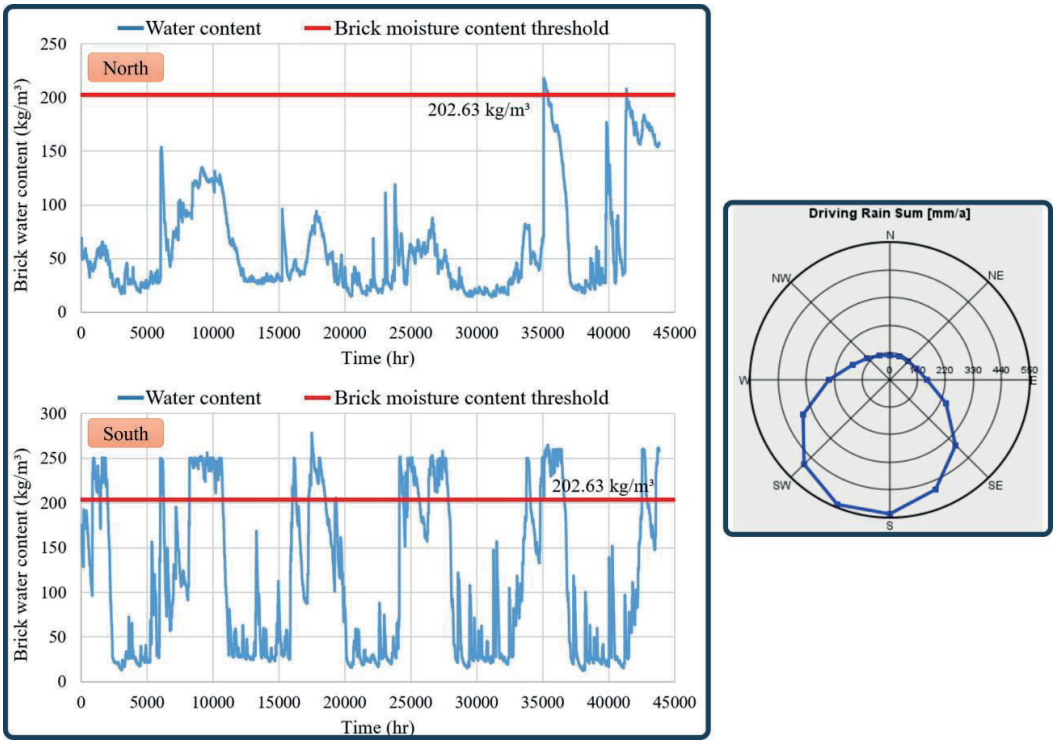


Figure 8: Water content of clay brick masonry façade (left side) between 2018 and 2023 where the red line is the brick moisture content threshold based on ES water penetration criterion, WDR chart (right side).

3.4. *Mould sensitivity analysis*

Figure 9 shows a bubble chart illustrating the sensitivity of each input variable to the MMI. Variables with negligible correlation to the MMI are excluded from this figure. A total of five variables are identified as sensitive to the MMI through linear and non-linear sensitivity analyses.

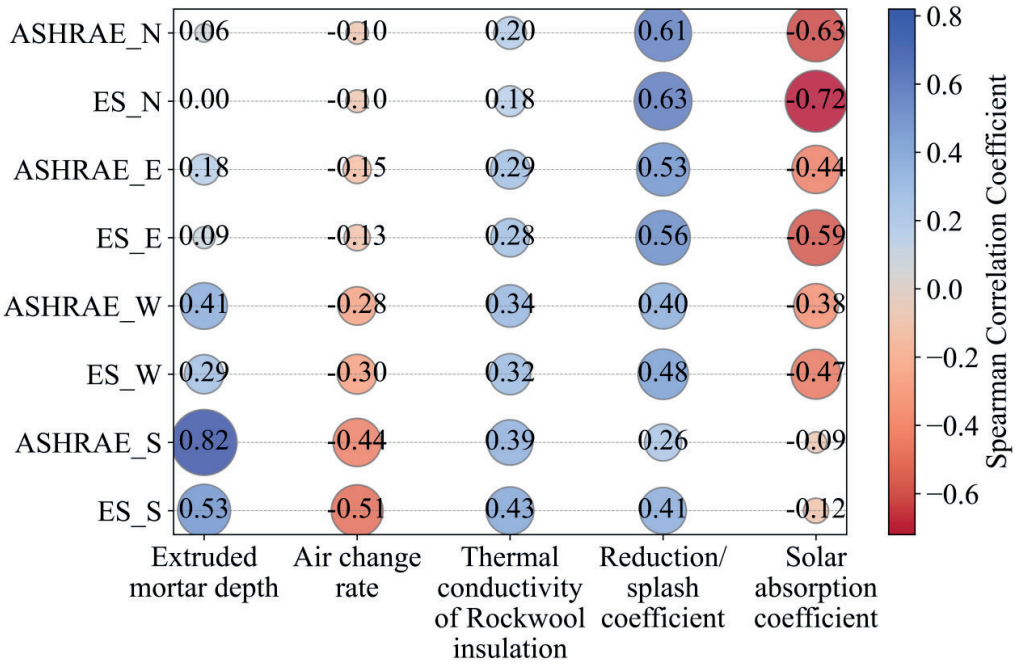


Figure 9: Spearman correlation coefficients between the input variables and maximum mould index (MMI). Colourmap guide: 0.00-0.09: negligible relationship, 0.10-0.39: weak relationship, 0.40-0.69: moderate relationship, 0.70-0.89: strong relationship, 0.90-1.00: very strong relationship.

Figure 9 illustrates that MMI is positively correlated with mortar extrusion. The correlation rank can vary depending on the orientation of the wall assembly and the water penetration criterion applied. The positive correlation of extruded mortar on mould growth is due to its capacity to act as a potential moisture source, absorbing and retaining water that penetrates due to WDR. A greater depth of extruded mortar brings the moisture source closer to the timber stud or insulation layer. In the worst-case scenario, if the mortar extrusion connects to the adjacent layer, it can bridge the air gap and facilitate the transport of penetrated water. The positive influence of mortar extrusion was also confirmed by previous studies, including (Bayat Pour, Kahangi Shahreza, et al., 2024; Bayat Pour and Kahangi Shahreza, 2024; Calle et al., 2020). Using the ASHRAE water penetration criteria, a stronger correlation was demonstrated between mould growth and extruded mortar than the ES criterion across all orientations. This difference arises because ASHRAE consistently considers 1% of WDR as a moisture source throughout the simulation period. In contrast, the ES criterion only accounts for instances where moisture content exceeds a certain threshold (illustrated by the red line in Figure 8 (left side)). Among all orientations, the southern side exhibits the strongest correlation between mould growth and mortar extrusion, attributed to the higher WDR load in this orientation compared to others. This orientation resulted in a greater potential for water absorption by the extruded mortar. In contrast,

the other orientations showed weaker correlations, with the north orientation being the weakest. In these cases, even if mortar extrusion exists, the limited WDR load means that less moisture is allocated to it as a source, resulting in drier conditions with minimal impact on moisture transport.

The air change rate (ACR) exhibits a negative correlation with the MMI for all orientations. The moderate correlation is observed between MMI and ACR under south orientation. This is due to the fact that the drier conditions within the air gap can be achieved by increasing the ACR, thereby the probability of mould growth is reduced. The importance of maintaining a well-ventilated air gap behind the cladding in wood-frame walls to prevent mould growth was established by Mundt-Petersen et al. (Mundt-Petersen et al., 2013) and Bayat Pour and Kahangi Shahreza (Bayat Pour and Kahangi Shahreza, 2024). The significance of ACR becomes more pronounced in orientations with elevated WDR loads, such as the south side, as indicated by the moderate correlation. In this orientation, the air gap contains more moisture, which could be effectively reduced by increasing the ACR. In contrast, the air gap is drier in orientations with lower WDR, resulting in a weaker effect of ACR. Consequently, ACR has a smaller effect on orientations with lower WDR loads while bringing a moderate effect on orientations with higher WDR loads.

The thermal conductivity of the Rockwool insulation shows a positive correlation with the MMI across all wall orientations, as illustrated in Figure 9. With a higher thermal conductivity (lower insulating efficiency) the insulation contributes to a larger heat flux through the external wall, further heating the external gypsum board positioned between the air gap and insulation. If the higher temperature—resulting from increased heat flux due to higher thermal conductivity—fails to sufficiently dry out the insulation and reduce the RH below the critical threshold (~70%), it raises the temperature within the insulation, thereby promoting mould growth. One potential reason for this inability to lower the RH is the presence of an additional moisture source caused by WDR penetration. The positive correlation between MMI and the thermal conductivity of insulations was also confirmed in the study by Bayat Pour and Kahangi Shahreza (Bayat Pour and Kahangi Shahreza, 2024).

Figure 9 shows a positive correlation between the MMI and the WDR's reduction/splash coefficient. Given that a higher reduction/splash coefficient in Delphin indicates less splashing of the WDR load (and a larger fraction of adhering WDR), this association is expected. As a result, more of the WDR load is accessible for water penetration, which increases the MMI. Additionally, as the reduction/splash coefficient increases, the moisture content in the brick layer also increases. In orientations with lower WDR loads (e.g., north), where the moisture source contribution to the WDR load was relatively minor for both criteria, this correlation ranking remained constant, showing a moderate correlation for both water penetration criteria. As a result, there were minimal differences in the correlation rankings between the two criteria in these orientations. In contrast, the ASHRAE criterion shows a lower correlation between the MMI and the reduction/splash coefficient than the ES criterion under high WDR load

orientations, particularly in the south. This disparity arises from the significant WDR load, as the ASHRAE standard allowed for 1% of the WDR load regardless of the brick's saturation level. Thus, even when splashing causes a reduction in the WDR load, the amount of water penetration remained significant. Consequently, under the ASHRAE criterion, the effect of the reduction/splash coefficient on the water penetration process is less pronounced than under the ES criterion.

The negative correlation between the solar absorption coefficient and the MMI is evident in Figure 9, and the underlying reason related to the influence of solar radiation on the hygrothermal behaviour of the wall assembly. The solar absorption coefficient describes the fraction of solar radiation that the exterior surface of the wall absorbs. A higher absorption coefficient indicates that more solar energy is absorbed by the external surface, raising the temperature of the outer layers, such as the brick. This absorbed heat reduces heat loss through the wall by warming the external surface and also contributes to a drier facade. As a result, increasing the solar absorption coefficient lowered the likelihood of mould growth, hence the negative correlation. Variations in WDR loads between orientations explained the changes in correlation ranks between the solar absorption coefficient and the MMI. These correlations are negligible and weak in the southern orientation, but moderate to strong in other orientations. The WDR load is higher for the southern orientation compared to the others. Consequently, the significant amount of absorbed water in the brick outweighs the heating effect of solar radiation, even though the surface absorbed solar energy. This explained why the correlation between the solar absorption coefficient and MMI was weaker and negligible on the south side. Conversely, the north side, which experiences the lowest WDR load, shows the strongest correlation between the solar absorption coefficient and MMI, particular when ES criterion is used. The reason the ES criterion shows a higher correlation was also links to the consideration of a lower WDR load under this criterion.

In addition to the linear sensitivity analysis provided in Figure 9, feature importance analysis offers a comprehensive illustration of both linear and non-linear correlations across all orientations. The importance of the parameters identified by the Spearman correlation analysis was notably confirmed by the feature importance analysis.

3.5. *Limitations*

This study makes some assumptions that, while necessary for the scope of analysis, introduce certain limitations. One assumption is that the extruded mortar consistently absorbs and retains penetrated rainwater. However, real-world scenarios are more complex and may present alternative mechanisms, such as dripping droplets and rainwater runoff inside the air gap, which could influence moisture accumulation and distribution differently. These dynamics were not fully captured in the current model and could lead to variations in moisture performance depending on the specific characteristics of the building envelope.

Another potential limitation lies in the method used for modelling moisture sources. This study employed a uniform distribution model, which assumes that moisture is evenly distributed across the extruded mortar layer. While this approach simplifies the modelling process, it may not fully represent the reality of moisture penetration, which can often occur as concentrated or point sources. Calle et al. (Calle et al., 2020) discussed the point moisture source as a viable alternative, suggesting that certain areas of the façade might be more susceptible to moisture penetration.

The reliability of the results also depends on the accuracy of the input data, such as material properties, climate data, and boundary conditions. Although this study addressed uncertainties in moisture safety design through probabilistic modelling, the inherent limitations of input data quality remain. Furthermore, while the probabilistic approach accounts for variability in material properties and boundary conditions, it does not encompass other stochastic variables that could affect hygrothermal performance, such as uncertainties in indoor and outdoor climate conditions (Gradeci et al., 2018; Marincioni et al., 2018).

Additionally, the case studies presented in this paper are based on specific climatic and construction conditions, particularly those relevant to the Gothenburg region. These assumptions, while carefully selected and justified, limit the generalisability of the findings to other geographic locations or building designs.

4. Conclusions

The mould growth and sensitivity analyses of mortar extrusion within the clay brick masonry claddings of timber frame walls were conducted in this study. Two distinct water penetration criteria were considered: the ASHRAE and an Experimental Study (ES)-based criteria. The brick material properties were derived from experimental data, and the case studies were considered under Sweden's climate, specifically focusing on the city of Gothenburg and four different wall orientations (north, east, west, and south). The analyses employed the Mould Reliability Analysis (MRA) and Mould Sensitivity Analysis (MSA) methodologies, utilising a probabilistic model integrated with the random forests (RF) machine learning algorithm. This study also verified the effectiveness of the 1D hygrothermal model against more complex 2D hygrothermal models, confirming the practicality and robustness of the 1D approach for the study's scope. The innovative combination of metamodeling with uncertainty propagation and sensitivity analysis significantly advanced the understanding of moisture-related risks associated with mortar extrusion. The results offered valuable insights into the uncertainties surrounding the hygrothermal performance of timber frame walls clad with clay brick masonry, particularly in terms of mould growth risk. The findings highlight the practical utility of probabilistic modelling in assessing moisture safety, with key results summarised in the following points:

- *1D versus 2D hygrothermal models:*
  The accuracy metrics between the 1D and 2D hygrothermal models (R^2 higher than 90% and minor MAEs) demonstrated that the proposed 1D model effectively captured the variations in

the MMI calculated by the more computationally expensive 2D model. This illustrates the reliability of the 1D model for analysing moisture behaviour, especially when customised material properties are used. The marginal differences between the models further emphasised the potential of the 1D approach as a practical alternative to 2D modelling, particularly when computational efficiency is a concern.

- *Mould growth analysis:*
  The 95th percentile of the maximum mould index (MMI) decreased by 7% when the ES criterion was applied instead of the ASHRAE criterion, particularly under high WDR load orientations, such as the south. This suggests general consistency between the two water penetration criteria in conditions with high WDR exposure. However, compared to the ASHRAE criterion, the ES criterion resulted in a 15% reduction in the 95th percentile of the MMI under low WDR loads, such as in the north orientation. This indicates that in scenarios with reduced WDR exposure, the ASHRAE criterion tends to overestimate the risk of mould growth, potentially leading to overly conservative design decisions.
- *Mould sensitivity analysis:*
  Using the ASHRAE criterion, the sensitivity analysis, which included both linear and non-linear methods, showed a strong positive correlation between extruded mortar depth and MMI for orientation with high WDR loads (i.e., south). However, under the ES criterion in this orientation, the influence of mortar depth on MMI was reduced to a moderate correlation. In contrast, the relationship between mortar depth and MMI was negligible for both water penetration criteria, for wall orientations with low WDR loads (e.g., north). The air change rate (negative correlation), the reduction/splash coefficient of WDR (positive correlation), the solar absorption coefficient (negative correlation), and the thermal conductivity of Rockwool insulation (positive correlation) were additional important input parameters influencing MMI.
- *Future studies opportunities:*
  While this study primarily employed a 1D modelling approach due to the high computational expense of 2D and 3D simulations, future research could benefit from incorporating 2D or 3D modelling techniques. These advanced approaches would allow for a more detailed representation of the extruded mortar's shape and size across multiple orientations, including along the X-, Y-, and Z-axes. Additionally, expanding the scope to include more stochastic variables could significantly enhance the accuracy and realism of the hygrothermal model. Incorporating these factors would provide a more comprehensive assessment of the moisture risks associated with mortar extrusion in different building envelopes and climates.

Declaration of conflicting interests
The authors declared no potential conflicts of interest with respect to the research, authorship, and/or publication of this article.

References

Abuku M, Janssen H and Roels S (2009) Impact of wind-driven rain on historic brick wall buildings in a moderately cold and humid climate: Numerical analyses of mould growth risk, indoor climate and energy consumption. *Energy and Buildings* 41(1): 101–110.

Aggarwal C, Ge H, Defo M, et al. (2022) Hygrothermal performance assessment of wood frame walls under historical and future climates using partial least squares regression. *Building and Environment* 223: 109501.

Aggarwal C, Ge H and Defo M (2023) Assessing mould growth risk of wood-frame walls using partial least squares (PLS) regression considering climate model uncertainties. *Building and Environment* 238: 110374.

ASHRAE, Standard 160-2021, Criteria for Moisture-Control Design Analysis in Buildings (2021) 160–2021. USA: ASHRAE, American National Standards Institute (ANSI).

Bayat Pour M and Abdul Hamid A (2024) Towards a sustainable decision analysis approach for moisture-safe building envelope design. *Journal of Building Engineering* 97: 110955.

Bayat Pour M and Elsayed ML (2020) *Assessment of the environmental impacts, energy performance and economic aspects of various construction materials*. Master thesis. Lund University, Faculty of Engineering, Lund, Sweden.

Bayat Pour M and Kahangi Shahreza S (2024) Impact of extruded mortar joints on the hygrothermal performance of brick veneer walls: a probabilistic study. *Journal of Building Engineering*: 109936.

Bayat Pour M, Niklewski J, Frühwald Hansson E, et al. (2023) Mould reliability analysis combined with mould health risks for decision support. In: *AIP Conference Proceedings*, Bratislava, Slovakia, November 2023, p. 020006. Available at: http://aip.scitation.org/doi/abs/10.1063/5.0172276 (accessed 11 November 2023).

Bayat Pour M, Niklewski J, Naghibi A, et al. (2023) Robust probabilistic modelling of mould growth in building envelopes using random forests machine learning algorithm. *Building and Environment* 243: 110703.

Bayat Pour M, Niklewski J, Naghibi A, et al. (2024) A Literature Review of Probabilistic Hygrothermal Assessment for Building Envelopes. *Building and Environment*: 111756.

Bayat Pour M, Kahangi Shahreza S and Abdul Hamid A (2024) Effect of extruded mortar joints on mould growth in timber frame wall with brick veneer: Probabilistic and Machine

Learning Modelling. In: *International Building Physics Conference (IBPC)*, Toronto, Canada, July 2024, p. 6.

Breiman L (2001) Random Forests. *Machine Learning*: 45(1), 5-32.

Building Physics (2024) Finnish mould growth model | Building Physics | Tampere Universities. Available at: https://research.tuni.fi/buildingphysics/finnish-mould-growth-model/ (accessed 30 June 2022).

Calle K, Coupillie C, Janssens A, et al. (2020) Implementation of rainwater infiltration measurements in hygrothermal modelling of non-insulated brick cavity walls. *Journal of Building Physics* 43(6): 477–502.

Carbonez K, Ge H and Janssens A (2015) Comparison between uniform rain loads and point sources to simulate rainwater leakage with commercial HAM-models. In: *1st International Symposium on Building Pathology*, Porto, Portugal, March 2015, p. 8.

DELPHIN (2021). Available at: https://bauklimatik-dresden.de/delphin/index.php?aLa=en (accessed 26 May 2021).

Ducoulombier L and Lafhaj Z (2017) Comparative study of hygrothermal properties of five thermal insulation materials. *Case Studies in Thermal Engineering* 10: 628–640.

EN 15026:2007 - Hygrothermal performance of building components and building elements - Assessment of moisture transfer by numerical simulation.

Erkal A, D'Ayala D and Sequeira L (2012) Assessment of wind-driven rain impact, related surface erosion and surface strength reduction of historic building materials. *Building and Environment* 57: 336–348.

Fishburn CC, Watstein D and Parsons DE (1938) *Water permeability of masonry walls*. BMS7, 18 October. Washington, D.C., USA: Department of Commerce, National Bureau of Standards.

Fisk WJ, Lei-Gomez Q and Mendell MJ (2007) Meta-analyses of the associations of respiratory health effects with dampness and mold in homes. *Indoor Air* 17(4): 284–296.

Freire RZ, Santos GH dos and Coelho L dos S (2017) Hygrothermal Dynamic and Mould Growth Risk Predictions for Concrete Tiles by Using Least Squares Support Vector Machines. *Energies* 10(8): 1093.

Geving S (1997) A systematic method for hygrothermal analysis of building constructions using computer models. Fifth International IBPSA Conference, Prague, Check Republic.

Gholamalipour P, Ge H and Stathopoulos T (2022) Wind-driven rain (WDR) loading on building facades: A state-of-the-art review. *Building and Environment* 221: 109314.

Gradeci K, Labonnote N, Time B, et al. (2018) A probabilistic-based methodology for predicting mould growth in façade constructions. *Building and Environment* 128: 33–45.

Groot CJWP and Gunneweg JTM (2018) The influence of materials characteristics and workmanship on rain penetration in historic fired clay brick masonry. *Heron* 55 141–154.

Hall T and Vidén S (2005) The Million Homes Programme: a review of the great Swedish planning project. *Planning Perspectives* 20(3): 301–328.

Hamby DM (1994) A review of techniques for parameter sensitivity analysis of environmental models. *Environmental Monitoring and Assessment* 32(2). 2: 135–154.

Hens H (2010) Wind-Driven Rain: From Theory to Reality. *ASHRAE*. Epub ahead of print January 2010.

ISO 15927-3:2009 - Hygrothermal performance of buildings – Calculation and presentation of climatic data – Part 3: Calculation of a driving rain index for vertical surfaces from hourly wind and rain data.

ISO 6946:2017 - Building components and building elements – Thermal resistance and thermal transmittance – Calculation methods.

Janssen H, Roels S, Van Gelder L, et al. (2015) *Annex 55, Reliability of Energy Efficient Building Retrofitting - Probability Assessment of Performance and Cost (RAP-RETRO), Probabilistic Tools*. ISSN 1652-9162, 2015:4. Gothenburg, Sweden: Chalmers University of Technology.

Johansson P, Geving S, Hagentoft C-E, et al. (2014) Interior insulation retrofit of a historical brick wall using vacuum insulation panels: Hygrothermal numerical simulations and laboratory investigations. *Building and Environment* 79: 31–45.

Kahangi Shahreza S and Abdul Hamid A (2023) Impact of different water penetration criteria and cavity ventilation rates on the risk of mold growth in timber frame walls with brick veneer cladding. In: *Journal of Physics: Conference Series*, 1 December 2023, p. 012028. Available at: https://iopscience.iop.org/article/10.1088/1742-6596/2654/1/012028 (accessed 20 March 2024).

Kahangi Shahreza S, Niklewski J and Molnár M (2021) Experimental investigation of water absorption and penetration in clay brick masonry under simulated uniform water spray exposure. *Journal of Building Engineering* 43: 102583.

Kahangi Shahreza S, Niklewski J and Molnár M (2022) Novel water penetration criterion for clay brick masonry claddings. *Construction and Building Materials* 353: 129109.

Kahangi Shahreza S, Bayat Pour M and Abdul Hamid A (2024) Towards rational decision-making on repointing to mitigate moisture damage in building envelopes: A probabilistic study. *Developments in the Built Environment* 19: 100510.

Kartläggning av fel, brister och skador inom byggsektorn (2018) 2018:36. Sweden: Boverket.

Kayll DG (2001) The Role of the Building Envelope Professional in the Aftermath of Vancouver's Leaky Condominium Crisis. *Buildings VIII/Wall Design and Building Science*: 2–7.

Künzel H and Dewsbury M (2022) Moisture control design has to respond to all relevant hygrothermal loads. *UCL Open Environment* 4.

Künzel HM (2014) Accounting for unintended moisture sources in hygrothermal building analysis. In: *NSB 2014 Building Physics Conference*, Lund, Sweden, 15 June 2014, p. 7.

Künzel HM and Zirkelbach D (2008) Influence of rain water leakage on the hygrothermal performance of exterior insulation systems. In: *Proceedings of the 8th symposium on building physics in the nordic countries*, Copenhagen, 16 June 2008, pp. 282–289.

Marincioni V, Marra G and Altamirano-Medina H (2018) Development of predictive models for the probabilistic moisture risk assessment of internal wall insulation. *Building and Environment* 137: 257–267.

Matthews RS, Bury MRC and Redfearn D (1996) Investigation of dynamic water penetration tests for curtain walling. *Journal of Wind Engineering and Industrial Aerodynamics* 60: 1–16.

Meteonorm (en) (2024) Meteonorm Version 8 Updated historic, current and future data. Available at: https://meteonorm.com/en/ (accessed 2 July 2022).

Moon HJ and Augenbroe G (2005) A Mixed Simulation Approach to Analyze Mold Growth Under Uncertainty. In: *Ninth International IBPSA Conference*, Montreal, Canada, August 2005, p. 9. Building Simulation.

Moon HJ and Augenbroe G (2008) Empowerment of decision-makers in mould remediation. *Building Research & Information* 36(5). 5: 486–498.

Mumovic D and Santamouris M (eds) (2019) *A Handbook of Sustainable Building Design and Engineering: An Integrated Approach to Energy, Health and Operational Performance*. Second edition. London ; New York: Routledge.

Mundt-Petersen SO, Harderup L-E and Arfvidsson J (2013) Important Factors Affecting the Risk of Mold Growth in Well-Insulated Wood Frame Walls in Northern European Climates. In: *Thermal Performance of the Exterior Envelopes of Whole Buildings XII*, Clearwater, Florida, United States, 2013, p. 14.

Observatoire de la Qualité de la Construction, Edition 2021.

Ojanen T, Viitanen H and Peuhkuri R (2007) Modelling of mould growth in building envelopes. In: *IEA ECBCS Annex 41 Closing Seminar : Nordic Building Physics Conference*, Copenhagen, Denmark, 2007, p. 18.

Rahiminejad M and Khovalyg D (2021) Review on ventilation rates in the ventilated air-spaces behind common wall assemblies with external cladding. *Building and Environment* 190: 107538.

Ramos NMM, Barreira E, Simões ML, et al. (2013) Probabilistic risk assessment applied to biological growth on external surfaces with ETICS, in: 13th Conference of the International Building Performance Simulation Association.

Ramos NMM, Barreira E, Simões ML, et al. (2014) Probabilistic Risk Assessment Methodology of Exterior Surfaces Defacement Caused by Algae Growth. *Journal of Construction Engineering and Management, ASCE* 140(12). 12: 05014012.

Reiter D (2008) The Monte Carlo Method, an Introduction. In: *Computational Many-Particle Physics*. Lecture Notes in Physics. Berlin, Heidelberg: Springer Berlin Heidelberg, pp. 63–78. Available at: http://link.springer.com/10.1007/978-3-540-74686-7_3 (accessed 25 June 2022).

Saber HH, Lacasse MA, Moore TV, et al. (2014) *Mid-rise wood constructions: investigation of water penetration through cladding and deficiencies: report to Research Consortium for Wood and Wood-Hybrid Mid-Rise Buildings*. December. National Research Council of Canada. Available at: https://nrc-publications.canada.ca/eng/view/object/?id=afdf017b-9598-4ce9-9f39-21cb80dd29d2 (accessed 9 August 2023).

Schober P, Boer C and Schwarte LA (2018) Correlation Coefficients: Appropriate Use and Interpretation. *Anesthesia & Analgesia* 126(5): 1763–1768.

scikit-learn (2024) sklearn.ensemble.RandomForestRegressor. Available at: https://scikit-learn/stable/modules/generated/sklearn.ensemble.RandomForestRegressor.html (accessed 5 March 2023).

Steskens PWMH, Janssen H and Rode C (2009) Influence of the Convective Surface Transfer Coefficients on the Heat, Air, and Moisture (HAM) Building Performance. *Indoor and Built Environment* 18(3): 245–256.

Straube J and Burnett E (1998) Driving Rain and Masonry Veneer. In: *Water Leakage Through Building Facades*. 100 Barr Harbor Drive, PO Box C700, West Conshohocken, PA 19428-2959: ASTM International, pp. 73-73–15. Available at: http://www.astm.org/doiLink.cgi?STP12096S (accessed 9 August 2023).

Straube JF and Burnett EFP (1997) Rain Control and Screened Wall Systems. In: *Canadian Conference on Building Science & Technology*, Toronto, Canada, January 1997, p. 25.

Swedish Meteorological and Hydrological Institute (SMHI) (2024). Available at: https://www.smhi.se/data (accessed 30 May 2023).

Thelandersson S and Isaksson T (2013) Mould resistance design (MRD) model for evaluation of risk for microbial growth under varying climate conditions. *Building and Environment* 65: 18–25.

Tijskens A, Roels S and Janssen H (2019) Neural networks for metamodelling the hygrothermal behaviour of building components. *Building and Environment* 162: 106282.

Tijskens A, Janssen H and Roels S (2019) Optimising Convolutional Neural Networks to Predict the Hygrothermal Performance of Building Components. *Energies* 12(20). 20: 3966.

Tijskens A, Roels S and Janssen H (2021) Hygrothermal assessment of timber frame walls using a convolutional neural network. *Building and Environment* 193: 107652.

Tijskens A, Janssen H and Roels S (2021) The impact of a reduced training subspace on the prediction accuracy of neural networks for hygrothermal predictions. *Journal of Building Performance Simulation* 14(1). 1: 20–37.

Tijskens A, Janssen H and Roels S (2023) Probabilistic hygrothermal assessment of various timber frame wall compositions. *Building and Environment* 243: 110619.

Van Den Bossche N, Lacasse NA and Janssens A (2011) Watertightness of masonry walls: an overview. In: *12th International Conference on the Durability of Building Materials and Components (12DBMC)*, 12 April 2011, pp. 1–8.

Vereecken E and Roels S (2013) Hygric performance of a massive masonry wall: How do the mortar joints influence the moisture flux? *Construction and Building Materials* 41: 697–707.

Viitanen H (1996) Factors affecting the development of mould and brown rot decay in wooden material and wooden structures. Dissertation. Department of Forest Products, Swedish University of Agricultural Sciences, Uppsala, Sweden.

Viitanen H and Ojanen T (2007) Improved Model to Predict Mold Growth in Building Materials. In: *10th Thermal Performance of the Exterior Envelopes of Whole Buildings Conference*, Clearwater Beach, United States, December 2007, p. 8.

Vos J, Blommaert A and Bossche N (2020) Statistical Analysis on Belgian Building Defects. In: *XV International Conference on Durability of Building Materials and Components. eBook of Proceedings*, 2020. CIMNE. Available at: https://www.scipedia.com/public/Vos_et_al_2020a (accessed 4 September 2023).

Wadsö L, Bengtsson B and Johansson P (2022) The m-model for prediction of mould growth. Lund, Sweden.

Wang L, Ge H and Wang L (2020) Metamodel Development for Predicting Hygrothermal Performance of Wood-Frame Wall under Rain Leakage. In: *XV International Conference on Durability of Building Materials and Components. eBook of Proceedings*, 2020. CIMNE. Available at: https://www.scipedia.com/public/Wang_et_al_2020b (accessed 1 November 2023).

Wyss GD and Jorgensen KH (1998) *A user`s guide to LHS: Sandia`s Latin Hypercube Sampling Software*. SAND--98-0210, 573301, 1 February. Available at: http://www.osti.gov/servlets/purl/573301-v0xtrz/webviewable/ (accessed 25 April 2021).

Zhao J (2012) *Development of a Novel Statistical Method and Procedure for Material Characterization and a Probabilistic Approach to Assessing the Hygrothermal Performance of Building Enclosure Assemblies*. Dissertation. College of Engineering and Computer Science, Syracuse University, Syracuse, NY, USA.

Paper V

Journal of Building Engineering 97 (2024) 110955



Contents lists available at ScienceDirect

Journal of Building Engineering

journal homepage: www.elsevier.com/locate/jobe





Towards a sustainable decision analysis approach for moisture-safe building envelope design

Mohsen Bayat Pour [a,*], Akram Abdul Hamid [b]

[a] Division of Structural Engineering, Department of Building and Environmental Technology, Lund University, John Ericssons väg 1, SE-223 63, Lund, Sweden

[b] Division of Building Physics, Department of Building and Environmental Technology, Lund University, John Ericssons väg 1, SE-223 63, Lund, Sweden

ARTICLE INFO

Keywords:
Building envelope
Decision analysis
Moisture safety design
Environmental and economic impact
Probabilistic analysis

ABSTRACT

Energy-efficient building designs, notably through adding insulation, can reduce energy consumption and greenhouse gas emissions by over 40 %, but may also increase risk of condensation. Therefore, a comprehensive decision analysis approach is essential for selecting optimal building envelope assemblies while considering their hygrothermal, economic, and environmental implications. This study introduces a novel decision analysis method based on the inutility decision analysis (IDA) concept, in which the building envelope with the lowest inutility is considered the optimal choice. Initially, different building envelope assemblies were assessed through probabilistic hygrothermal analysis combined with a machine learning metamodel. Subsequently, the environmental and economic consequences associated with each assembly were quantified by integrating moisture-related damage into these assessments. Combining these outputs yielded inutility indices for the case studies, guiding the selection of the most optimal alternative. The results indicated that an external wall, with a minor risk of moisture-related failure, may outperform other alternatives when considering economic and environmental metrics. However, the final decision on the acceptability of such risk should rest with the customers or owners. Balancing the trade-off between performance longevity, cost, and occupants' health is crucial.

Nomenclature

ACR	Air Change Rate [1/h]
ASHRAE	American Society of Heating, Refrigerating and Air-conditioning Engineers
A_w	Water Absorption Coefficient [kg/m^2. S$^{0.5}$]
CoV	Coefficient of Variation
Cp	Specific Heat Capacity [J/kg.K]
CS*i*	Case Study *i*
D_B	Bulk Density [kg/m^3]
LHS	Latin Hypercube Sampling
ML	Machine Learning
MAE	Mean Absolute Error

* Corresponding author.
E-mail addresses: mohsen.bayat_pour@kstr.lth.se (M. Bayat Pour), akram.abdul_hamid@byggtek.lth.se (A. Abdul Hamid).

https://doi.org/10.1016/j.jobe.2024.110955
Received 26 July 2024; Received in revised form 22 September 2024; Accepted 1 October 2024
Available online 2 October 2024
2352-7102/© 2024 The Authors. Published by Elsevier Ltd. This is an open access article under the CC BY license (http://creativecommons.org/licenses/by/4.0/).

n	Total number of original data
OF_i	Objective Function
PA	Probabilistic Analysis
RA	Reliability Analysis
RF	Random Forests
φ	Relative humidity [%]
R^2	Coefficient of Determination
S_d-value	Diffusion Equivalent Air Layer Thickness [m]
T	Temperature [°C]
WDR	Wind-driven Rain
y_i	Original data
$\overline{y_i}$	Mean of the original data
$\widehat{y_i}$	Predicted data
ε_i	Convergence value
θ_{por}	Porosity [m^3/m^3]
λ_{dry}	Thermal Conductivity [W/m.K]
μ	Mean
μ_{VDR}	Water Vapour Diffusion Resistance Factor [−]
σ	Standard deviation

1. Introduction

1.1. Background

Global warming poses a significant global challenge. According to the latest Intergovernmental Panel on Climate Change (IPCC) report, the release of greenhouse gases primarily contributes to climate change [1]. Globally, approximately 30 % of greenhouse gas (GHG) emissions are linked to the building sector [2]. Implementing energy-efficient strategies in building design can reduce energy-related GHG emissions by over 40 % [3]. Among the various methods for improving the energy performance of buildings and reducing their operational energy demands, adding of insulation to building envelopes is a widely used and effective approach [4].

One frequently proposed solution for mitigating the impact of the built environment on climate change involves adopting innovative bio-based materials, such as wooden elements, in construction projects [5]. Wooden materials can serve as structural elements (e.g., cross-laminated timber (CLT) and timber studs) [6] and insulation materials [7]. Although, highly insulated walls effectively reduce energy consumption, they increase the risk of condensation and other moisture-related issues, such as rot decay and microbial growth [4,7,8]. Wooden materials exhibit exceptional durability under dry conditions [9]. However, ensuring dry conditions throughout the lifespan of a building particularly for multi-storey buildings, is challenging [9]. Multi-storey buildings are particularly exposed to high wind pressures and wind-driven rain (WDR). Furthermore, the on-site construction of multi-storey buildings entails longer construction periods, during which structural elements are particularly vulnerable to moisture exposure [5].

According to Ref. [10], it was estimated that mould and other moisture-related issues have damaged over 30 % of single-family homes in Sweden. Microbial growth has impacted 60–80 % of single-family houses with ventilated attics in the Gothenburg region of Sweden [11,12]. Swedish building regulations (BBR) [13] mandate the design of moisture-safe buildings to prevent moisture-induced damage and associated health concerns. Addressing moisture-related problems in buildings requires predicting these problems and developing mitigation strategies. Hygrothermal analysis is an effective tool for this purpose. It involves modelling heat, air, and moisture interactions within building assemblies to evaluate parameters, such as temperature, relative humidity, and moisture content, under various boundary and climatic conditions. Hygrothermal analysis first emerged in the 1930s [14], with significant improvements in robustness and reliability over the past few decades [15–23].

By addressing design uncertainties using a probabilistic approach, hygrothermal analysis can become more robust and reliable [24]. In 1997, Geving [25] incorporated a probabilistic approach into the hygrothermal analysis framework to consider uncertainties. By treating inputs as stochastic variables that account for related uncertainties, probabilistic approaches can produce a distribution of possible outcomes, enabling a more comprehensive design performance evaluation. Probabilistic methods also facilitate determining failure probability, offering valuable insights for decision analysis. Using several metamodels to address the time-consuming nature of probabilistic hygrothermal analysis, the probabilistic approach has made significant advancements in this field over the past decade [26–32].

When conducting a decision analysis to select the most optimal building envelope for a construction project, considering the economic and environmental impacts along with hygrothermal performance is crucial. A building envelope may meet acceptable moisture safety criteria but can be environmentally unfriendly and uneconomical. Thus, a pragmatic decision analysis is essential to address this issue and assist practitioners in making optimal decisions. According to a recent literature review by Bayat Pour et al. [33], 95 % of probabilistic hygrothermal analysis research publications did not explicitly consider sustainability perspectives, including the environment, economy, and society.

The robust internal thermal insulation of historical buildings (RIBuild) was a research project that combined probabilistic

hygrothermal assessment with life cycle assessment (LCA) and life cycle costing (LCC) [34]. This project introduced a strategy for probabilistic hygrothermal assessment and developed a probabilistic methodology for assessing the environmental impacts and global costs of internal insulation solutions for historical buildings [23]. The TallFacade project [5] was another research project focused on utilising LCA and LCC based on the output of a probabilistic hygrothermal assessment to develop robust and economically viable design solutions for tall timber facades. While the aforementioned research projects have made progress in probabilistic hygrothermal analysis and sustainability, several research gaps remain that are essential to address for the design of sustainable building envelopes. The first gap this study aims to address is the development of a method for holistic decision analysis by integrating hygrothermal analysis with LCA and LCC. Previous projects conducted LCA and LCC independently; however, for an effective decision, it is crucial for decision-makers to combine results from multiple parameters to facilitate multi-criteria decision analysis. A second gap is the need to incorporate metamodels into decision analysis method to enhance and accelerate probabilistic hygrothermal analysis, allowing the inclusion of a broader range of scenarios for more robust results. Previous studies were limited by the challenge of handling numerous scenarios. This study will overcome this limitation by employing machine learning (ML) techniques. The third gap is that the proposed decision analysis method can be applied to all types of building envelopes, regardless of material or assembly configurations. In contrast, previous studies were restricted to specific cases, such as historical walls with internal insulation and timber-frame walls in high-rise buildings. The novelties of this study are structured around addressing these identified limitations, making it crucial for advancing more robust, sustainable, and comprehensive decision analysis in building envelope design.

1.2. Study objectives

This study aimed to develop a decision analysis method that synthesises sustainability considerations, encompassing environmental and economic impacts, using probabilistic hygrothermal analysis. The objective was to identify the optimal building envelope, considering moisture safety design and sustainability. A probabilistic hygrothermal analysis was conducted through mould reliability analysis (MRA) using a metamodel employing a ML algorithm. In addition, the decision analysis employed the inutility decision analysis (IDA) method. LCC and LCA outputs were integrated using a technique known as the single-point rate (SPR) to calculate the inutility index.

2. Methodology

2.1. Decision analysis procedure

The proposed decision analysis method, as illustrated in Fig. 1, comprises the following steps.

1) Case studies definition: This step specifies various case studies for the building envelope and provide the motivations for selecting these case studies.
2) Probabilistic hygrothermal analysis: This step includes inputs for relevant damage models, such as mould growth, rot decay, frost, and algae. The failure probability for the intended damage model is calculated in this step.
3) Definition of retrofitting/maintenance/remediation scenarios: Different scenarios for retrofitting, maintenance, or remediation, necessitated by moisture-induced damages (e.g., mould, decay, and frost), are defined over the lifespan of the building.

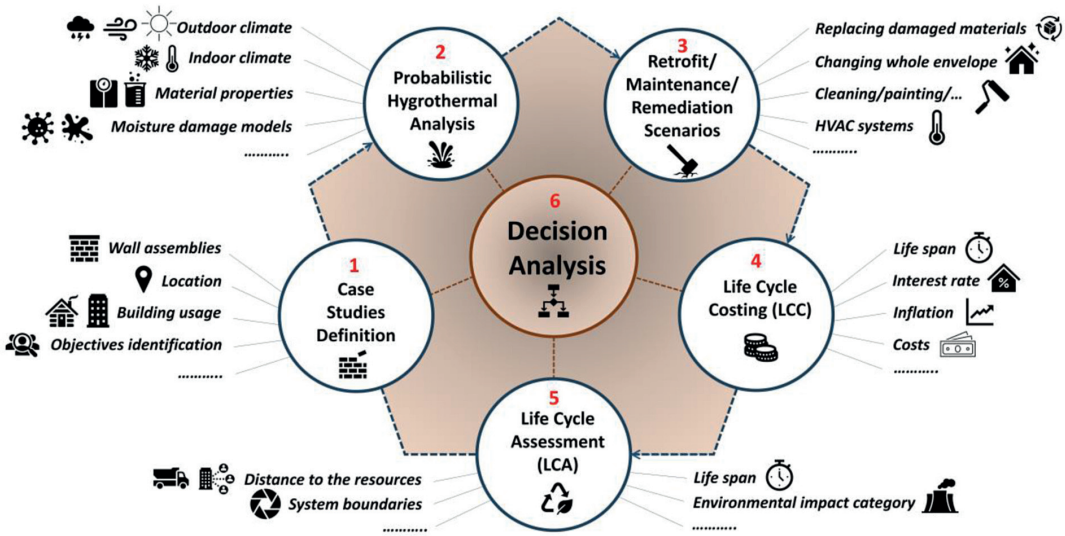


Fig. 1. Decision analysis procedure.

4) Life cycle costing (LCC): The economic impacts associated with selecting each case study are determined. This encompasses the initial and running costs attributed to the required retrofitting, maintenance, or remediation of each building envelope alternative, based on the scenarios outlined in Step 3.
5) Life cycle assessment (LCA): The environmental impacts from each case study are evaluated. This involves the initial environmental impacts from selecting a specific building envelope and the environmental impacts associated with the necessary retrofitting, maintenance, or remediation based on the scenarios outlined in Step 3.
6) Decision analysis: This step integrates the outputs from various perspectives, including probabilistic hygrothermal analyses, economic consequences, and environmental impact assessments. This step outputs the most optimal building envelope, exhibiting the lowest inutility index.

The subsequent subsections provide a detailed explanation of each step. Furthermore, three case studies are defined to illustrate the application of this decision analysis method. It should be noted that the primary aim of this research is to demonstrate how the proposed decision analysis method facilitates evaluating and integrating different design perspectives, including moisture safety design, environmental considerations, and economic impact analyses. It does not precisely compare the case studies. Nonetheless, the authors aim to incorporate the most realistic examples within the scope of this study.

2.2. Probabilistic hygrothermal analysis

2.2.1. Case studies definition

Interest in designing and constructing multi-storey timber buildings has increased globally, driven by the requirements for constructing environmentally friendly buildings [35]. However, wood, as a bio-based material, is highly sensitive to moisture, making it susceptible to moisture-related issues, such as mould growth or decay. This study focused on light-frame timber walls because the exterior sections of wooden studs are exposed to relatively cold climates and, consequently, high relative humidity. In addition, light-frame timber walls serve as load-bearing and non-load-bearing construction elements, expanding their applicability beyond timber frames with solid wood panels [5]. Both types of timber frame walls can be implemented as ventilated and non-ventilated assemblies.

In this study, three different light-frame timber walls (Fig. 2) were considered as case studies: Case Study 1 (CS1) was a non-ventilated timber frame wall; Case Study 2 (CS2) was a ventilated timber frame wall with plaster for the external layer; and Case Study 3 (CS3) was a ventilated timber frame wall with a brick veneer. All case studies had similar U-values ranging from 0.12 [W/(m^2.K)] to 0.14 [W/(m^2.K)].

2.2.2. Mould reliability analysis method

A probabilistic hygrothermal analysis examines the hygrothermal performance of a building across various scenarios. Probabilistic hygrothermal analysis results can be applied to various models of moisture-induced damage. Owing to the time-intensive nature of simulations, employing metamodels can be beneficial. This study, performed a probabilistic hygrothermal analysis using the MRA method introduced by Bayat Pour et al. [27]. Mould growth is the damage model that has been applied in the case studies. The MRA method, outlined in Fig. 3, comprises two primary sections, indicated by dashed-line boxes: probabilistic analysis (PA) and reliability analysis (RA). The PA section involves sampling, conducting hygrothermal simulations, and assessing mould growth. The RA section involves creating a metamodel using the random forests (RF) machine learning algorithm, predicting mould growth, and calculating failure probabilities. The mould assessment was conducted using the Finnish mould growth model [36] derived from the VTT model [37,38]. This model offers an approach for mould assessment using a mould index ranging from 0 to 6.

2.2.3. Sampling

Sampling for both sections was performed using the Latin hypercube sampling (LHS) technique [39]. This was based on an improved sampling strategy introduced in Ref. [40], aimed at mitigating the risk of inadequate extrapolation of the developed metamodel using RF. In this sampling strategy, as shown by the dotted-line box in the PA section, the ranges of the primary samples (used for hygrothermal simulations) were compared with those of the secondary samples (used for metamodel predictions). Subsequently, the range of the primary samples was adjusted by incorporating values below the minimum and above the maximum values of the

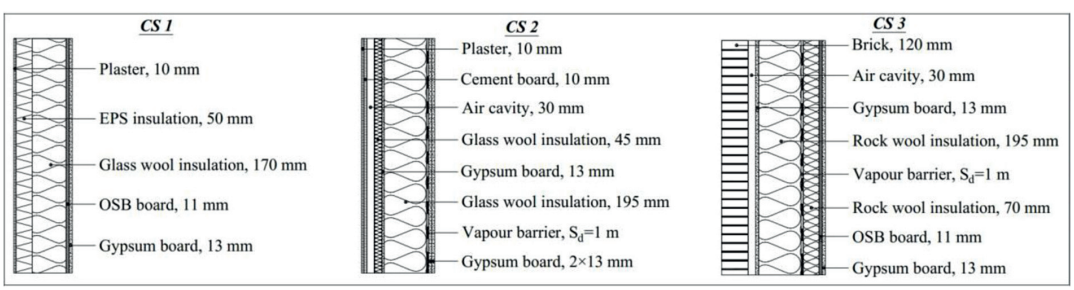


Fig. 2. Three external wall assemblies: case study 1 (CS1), case study 2 (CS2), and case study 3 (CS3).

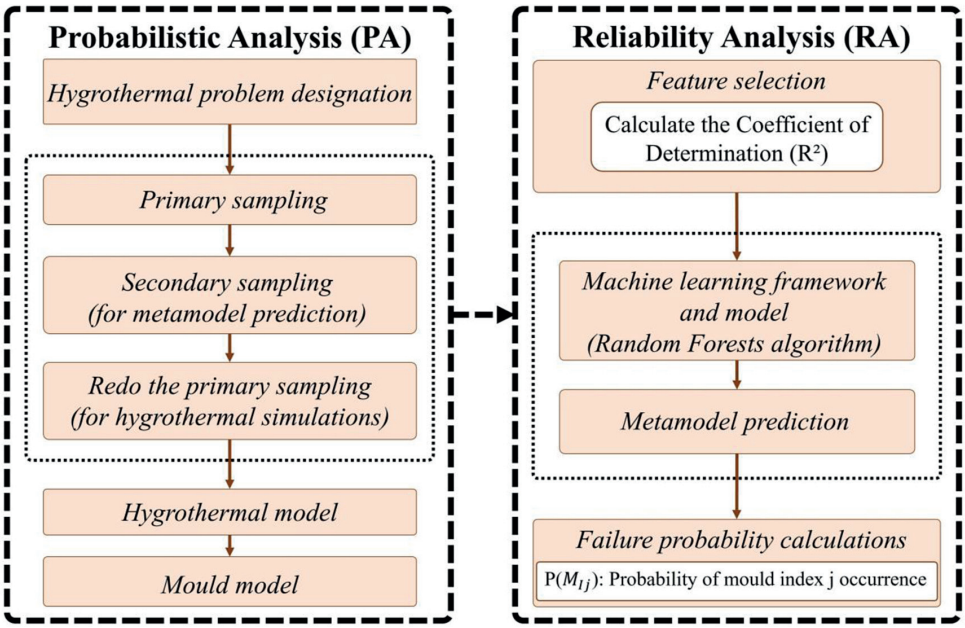


Fig. 3. Mould reliability analysis (MRA) method, from Ref. [27].

secondary sample range. Furthermore, a uniform distribution was adopted for all input variables in the PA section. This was performed to prevent the concentration of samples around the mean, which could occur if a normal distribution was used. The rationale behind this choice was to generate a training set for tuning the model. Ensuring that the training set encompasses diverse data points across the entire variable distributions is crucial. Employing a uniform distribution facilitates achieving this objective by assigning equal weights to all segments of the variable distributions. This prevents model overfitting around the average output and enhances performance across various scenarios, including extremes.

2.2.4. Metamodel creation

The RA section employs the RF algorithm [41], renowned for its effectiveness in addressing regression and classification tasks. The RF algorithm is favoured for its interpretability, ability to handle nonlinear relationships, robustness of metamodels, feature importance analysis, and computational efficiency [27]. Metamodel creation in the RA section begins with a feature selection process, as detailed in Ref. [27]. This process involves a parametric investigation to determine the optimal number of features to include in the metamodel. Through iterative analysis, the number of features yielding the highest coefficient of determination (R^2) between the predicted and observed 95th percentiles of mould indices is selected as the most effective. The dataset is then randomly divided into training (70 %) and testing (30 %) subsets to facilitate model training and evaluation, as indicated by the dotted-line box in the RA section of Fig. 3.

Evaluating the precision of the trained metamodel relies on the coefficient of determination (R^2) and mean absolute error (MAE), expressed in Eqs. (1) and (2).

$$R^2 = 1 - \frac{\sum_{i=1}^{n} (y_i - \hat{y}_i)^2}{\sum_{i=1}^{n} (y_i - \bar{y}_i)^2} \tag{1}$$

$$MAE = \frac{1}{n} \sum_{i=1}^{n} |y_i - \hat{y}_i| \tag{2}$$

where y_i and $\hat{y}_i$ represent the original and predicted data, respectively, $\bar{y}_i$ is the mean of the original data, and n denotes the total number of original data points.

Tuning the hyperparameters of the RF model is crucial for achieving an optimal metamodel performance. In this study, the optimisation process of the RF model involved fine-tuning parameters, such as the number of trees, identifying the most effective features, and estimating the generalisation score using out-of-bag samples. The default values outlined in Ref. [42] were used for the remaining hyperparameters.

2.2.5. Failure threshold definition

Determining the probability of failure threshold is crucial in such decision analysis methods, particularly in case studies involving moisture-related damage models (mould growth in this study). In engineering and risk management, determining an acceptable probability of failure depends on various factors, including the consequences of failure, criticality of the system under study, societal norms, and regulatory requirements. To specify the threshold for mould failure probability, referencing the following points can be beneficial.

- Standards and guidelines: Determining acceptable risks or the probability of failure often relies on standards or guidelines, such as those related to construction or health considerations. These standards vary among countries owing to diverse social, geographical, climatic, and cultural factors. For instance, the American Society of Heating, Refrigerating, and Air-Conditioning Engineers (ASHRAE) [43] recommends a mould index of 3 as a threshold in wall assemblies, derived from the Finnish mould growth model. This recommendation aims to mitigate the issues associated with mould growth in building envelope components. However, the World Health Organization (WHO) guidelines [44] emphasise the prevention of dampness and mould owing to their significant health implications, including respiratory diseases (e.g., asthma, coughing, and wheezing), skin disorders, and cancer. Mould prevention relies on controlling environmental conditions before spore germination, as outlined in Ref. [45]. Once germination occurs, mould hyphae and mycelia develop, enabling the mould to ramify and grow through the substrate and nutrients, even under limited surface moisture conditions. Thus, the mould germination point, denoted as the mould index 1 in the Finnish mould growth model [36], serves as the failure threshold for preventing health issues. Both guidelines lack clarity regarding the duration for which the mould index exceeds levels 1 or 3. For instance, should the building envelope be considered a reject case if the mould index surpasses these thresholds for a short period (e.g., 10 h annually)? According to the Finnish mould growth model, moulds can diminish under unfavourable growth conditions. This implies that by minimising favourable conditions for mould growth, mould can decline.
- Risk tolerance and stakeholder preferences: Stakeholder risk tolerance is significant in defining failure probability. This may include building owners, occupants, regulatory authorities, insurers, and other interested parties. Understanding their perspectives and preferences can help determine acceptable risk levels.
- Expert consultation: Engaging with experts in the fields of building science, environmental engineering, economy, social and medical sciences, and risk management provide insights into best practices and commonly accepted thresholds for mould growth assessment.

Despite the detailed explanations provided, a consensus regarding the acceptable probability of mould failure in buildings remains lacking. This highlights a scientific gap within the field of building physics, particularly concerning the integration of probabilistic hygrothermal analysis with decision analysis methods.

This study adopted a mould index of 3, in line with the ASHRAE standard [43], as the threshold for mould growth failure. Regarding the mould growth duration, a building is permitted to exceed a mould index of 3 in only 5 % of instances during its reclamation period. According to Swedish law [46], customers can complain about any faults or failures up to 10 years after the completion of work on buildings. This study assumed that occupants inspect their buildings every 10 years, in line with the reclamation rule in Sweden, specifying that an inspection plan should be in place for buildings [47]. Consequently, the building was assumed to undergo mould growth inspections every 10 years, totalling four inspections over a 50-year lifespan, a common practice in Sweden [48,49]. In addition, the predicted percentage of dissatisfied (PPD) quantitatively predicts the percentage of people who are thermally dissatisfied with a building. The minimum value for this index is 5 %, representing the most conservative situation [50]. This study adopted this percentage, relating to the indoor climate, as the assumption for the duration of mould occurrence higher than mould index 3.

Under these assumptions, acceptable mould growth entails experiencing a mould index of less than 3 in 95 % of instances within a 10-year period for each case study. Scenarios failing to meet this threshold are considered unsuccessful. Specifically, a scenario with a 95th percentile of mould indices below 3 within 10 years indicates that it encounters mould index levels below 3 for 95 % of the time over a decade. Thus, the output of the mould assessment in the PA section comprises the 95th percentile of mould indices for each scenario within the 10-year mould growth inspection period. In the RA section, the 95th percentile of mould indices is predicted for a large dataset. Subsequently, the failure probability is calculated based on scenarios where the 95th percentile of mould indices exceeds mould index 3. A large dataset for the RA section, comprising n = 10^7 scenarios, is generated using the LHS technique, considering the probability distributions of the input variables.

2.2.6. Failure probability calculations

The failure probability computations were executed in the final step of the MRA method. The limit state function, g_m, consists of two parameters: $I_{M,ls}$, representing the mould limit state, and $I_{M,95^{th}}$, denoting the 95th percentile of the mould indices within the inspection period (every 10 years). Notably, the 95th percentile of mould indices is a function of temperature, T, relative humidity, φ, and time, t. Consequently, the limit state function can be formulated by Eq. (3).

$$g_m = I_{M,ls} - I_{M,95^{th}}(T, \varphi, t) \tag{3}$$

Any violation of the limit state function ($g_m < 0$) indicates that the 95th percentile of the mould indices of the given scenario, $I_{M,95^{th}}$, surpasses the predefined mould limit state, $I_{M,ls}$. The probability that the 95th percentile of the mould indices exceeds mould index j, $P\left(M_{Ij,95^{th}}\right)$, can be determined using Eq. (4).

$$P\left(M_{Ij,95^{th}}\right) = \frac{N(g_m < 0)}{N_T} \tag{4}$$

where.

- $N\ (g_m < 0)$: Number of failed scenarios
- N_T: Total number of scenarios

2.2.7. Convergence study

A convergence study was conducted to determine the necessary number of simulations (scenarios) in the PA section. To facilitate this, Bayat Pour et al. [27] proposed an equation for convergence analysis in a probabilistic hygrothermal analysis. It involves systematically increasing the number of simulations while monitoring the probability of failure, $P\left(M_{Ij,95^{th}}\right)$. The convergence criterion involves observing the change in the target variable, $P\left(M_{Ij,95^{th}}\right)$, over the previous 10 iterations. Each iteration comprises 100 distinct scenarios, with the incremental addition of 100 new scenarios to the previous iterations to form a new iteration. According to Ref. [27], the simulation process continues until the convergence value falls below the predefined threshold of 0.001. Eq. (5) is used to compute the convergence value.

$$\varepsilon_i = \frac{\left|\sum_{i-9}^{i-5} OF_i - \sum_{i-4}^{i} OF_i\right|}{\sum_{i-4}^{i} OF_i} \tag{5}$$

where i represents the current iteration number (>10), OF_i denotes the ith iteration of the objective function ($P\left(M_{Ij,95^{th}}\right)$ in this study), and ε_i is the convergence value of the OF_i.

2.2.8. Mould sensitivity analysis method

According to Ref. [27], sensitivity analysis techniques can be broadly categorised into two types: probabilistic and deterministic. Whereas input variables in deterministic sensitivity analysis are characterised by the predefined range of values, in probabilistic sensitivity analysis, they are represented by their probability distributions. In this study, the probabilistic sensitivity analysis method known as Mould Sensitivity Analysis (MSA) was employed, as outlined in Ref. [27], to identify key input parameters within the hygrothermal model. This approach facilitates an understanding of how variations in inputs, such as material properties and boundary conditions, influence the decision-making process and the selection of the optimal envelope assembly.

The MSA method used in this study applies output data, specifically the 95th percentile of mould indices predicted by the ML model, and input data such as material properties and outdoor/indoor conditions from secondary sampling. The sensitivity analysis is conducted through *feature importance analysis*, which is critical for identifying the influence of input variables on the output variable in ML models. The RF algorithm is utilised for this purpose, as it captures both linear and nonlinear relationships between input and output variables.

RF is an ensemble learning method comprising multiple decision trees, each with internal nodes (or branches). At each node, a feature (input variable) is selected to split the dataset into subsets with similar responses. For classification tasks, the selection criterion is based on Gini impurity, while for regression tasks, it is based on variance reduction, calculated as the sum of squared residuals. The importance of each feature is determined by its contribution to impurity reduction. Features that result in the highest impurity reduction (i.e., the lowest Gini importance or sum of squared residuals) are chosen for the nodes. The average impurity reduction across all trees in the forest serves as a measure of feature importance. Therefore, a higher feature importance score indicates a more significant contribution of that feature to the ML model [42].

2.2.9. Hygrothermal simulations Setup

The hygrothermal performance analysis of each case study was conducted using one-dimensional (1D) Delphin 6.1 [51], specifically designed for heat, air, and moisture (HAM) analysis. The indoor climatic conditions were set in accordance with the standard EN15026 [52], correlating indoor temperature and relative humidity with outdoor temperature variations. For ambient temperatures ranging from 10 °C to 20 °C, indoor temperature increases linearly from 20 °C to 25 °C. However, for ambient temperatures higher or lower than this range, the indoor temperature remains fixed at 25 °C or 20 °C, respectively. According to DIN EN 15026 [52], indoor relative humidity increases linearly from 35 % to 65 % for an ambient temperature range of −10 °C–20 °C.

In each case study, the screening point was the internal surface of the wooden studs. This point was selected owing to its susceptibility to mould growth resulting from the presence of wooden material and its proximity to indoor boundaries, facilitating the transport of mould spores and mould-induced toxins into the indoor air. Toxins emitted from mould growth within wall layers can be transferred into the indoor air, posing risks to human health [53,54]. A study demonstrated that mycotoxins produced by specific fungi could be aerosolised from contaminated substrates [55]. The study noted that these aerosolised mycotoxins could deeply penetrate the human respiratory tract, emphasising the potential health risks of mouldy environments. Gottschalk et al. [56] confirmed that toxins produced by mould on building materials could contaminate indoor air, leading to potential health concerns, such as those associated with sick-building syndrome. The external surface of a wooden stud also has the potential for mould growth. In situations where the outdoor air pressure is higher than the indoor air pressure, mould spores and mould-induced toxins can move into the inner layers and indoor air.

The hygrothermal simulations performed in this study relied on outdoor climate data obtained from the Meteonorm meteorological

database [57], providing hourly climate data spanning a typical year generated from measured data. To remove the potential influence of the presumed initial conditions on the results, the climate data were repeated for the 2 years preceding the primary simulations, establishing a 2-year initialisation period. Subsequently, the output of the hygrothermal simulations was employed to assess mould growth over a 10-year building inspection period. The orientation of the façade was set to the south, considering the climatic conditions of Gothenburg, where this orientation experiences the highest WDR loads.

The default value for water penetration through the external surface was set to 1 % of the rainwater that reaches that surface, as per the ASHRAE standard 160–2021 [43]. This moisture source is often deposited on the outer surface of a water-resistive barrier. However, with a technical justification, changes may be made to the deposit location. In this study, the positions of the WDR-induced moisture sources were assigned as follows.

- For CS1, between the EPS and glass wool insulation layers.
- For CS2, on the external surface of the glass wool insulation layer facing the air gap.
- For CS3, on the external surface of the gypsum board layer facing the air gap.

A minimum mesh size of 1 mm and stretch factor of 1.3 was established in the hygrothermal models, resulting in mesh sizes dynamically fluctuating between layers according to their thicknesses. A proper balance between computing efficiency and precision was achieved by modifying the mesh size and stretch factor.

The boundary conditions and material properties are listed in Tables 1 and 2, respectively, with the pertinent references indicated. Every specified value has an equal likelihood of occurrence according to the uniform probability distributions, as listed in Table 1. According to the Delphin default, the outdoor surface S_d-value is considered 5 for regular paint [51].

2.3. Retrofitting/maintenance/remediation scenarios

2.3.1. Possible retrofitting, maintenance, and remediation scenarios

The possible scenarios for retrofitting, maintenance, remediation, and other actions associated with moisture-related damages are defined in this step. The required action depends on the intensity of moisture-related problems. For example, when mould growth is detected on material surfaces, different actions should be considered according to the guidelines [65,66].

- The first step is to identify and fix any moisture sources in the building. This includes repairing building envelope leaks, fixing plumbing leaks, improving ventilation, and addressing other sources of moisture penetration.
- Containing the affected area is essential for preventing the spread of mould spores to other parts of the building. This can be achieved using plastic sheeting and duct tape to seal off doorways, vents, and other openings.
- Wearing appropriate personal protective equipment (PPE), including gloves, goggles, and respirator masks, is essential for protecting working staff from exposure to mould spores and toxins.
- Non-porous surfaces can be cleaned of mould growth using a solution of water and detergent or a specialised mould cleaner. Scrubbing the affected area thoroughly and rinsing it with clean water is also recommended. Ensuring that the area is completely dry after cleaning is crucial.
- Porous materials, such as gypsum boards, insulation, and wooden sheets, heavily affected by moulds may need to be removed and properly discarded. This helps eliminate the mould growth source and prevent further spreading. However, if the mould growth is shallow, the affected area can be brushed off with only minor repairs.
- Disinfecting the surrounding area is crucial to remove any remaining mould spores and prevent regrowth. This can be performed using disinfectant materials.
- Proper ventilation is crucial for preventing mould growth. Ensuring that the affected area is well-ventilated during and after the cleanup/repair/replacement process is crucial. Using fans and opening windows to increase airflow can help promote drying.
- Once the mould has been removed, steps should be taken to prevent recurrence. This may include improving the ventilation system, maintaining appropriate humidity levels, and regularly inspecting for signs of moisture or mould growth.

These actions necessitate assessing economic and environmental impacts. Consequently, several retrofitting, maintenance, or remediation scenarios can be defined and used in subsequent steps to assess these impacts.

2.3.2. Replacement scenarios

In this study, replacement scenarios were considered to address the issue of mould growth. Two parameters, namely “area of replacement” and “number of damaged layers”, were used to define these replacement scenarios. A range of replacement scenarios was

Table 1
Probability distributions for indoor and outdoor boundary conditions. U(a, b): Uniform distribution, where a and b are the minimum and maximum values, respectively.

Variable	Probability distribution
Outdoor convection heat exchange coefficient [W/m^2.K] [52]	U(12, 20)
Solar absorption coefficient [−] [51]	U(0.4, 0.8)
Long-wave emissivity [−] [51]	U(0.85, 0.95)
Reduction/splash coefficient of WDR [−] [27]	U(0.6, 0.8)
Indoor surface heat transfer coefficient (Convective + Radiative), [W/m^2.K] [58]	U(5, 10)
Indoor surface vapour diffusion coefficient [s/m] [17]	U(0.1×10^{-7}, 1×10^{-7})
Air change rate, ACR [1/h] [59]	U(0, 20)

Table 2
Probability distributions for the material properties. N(μ, σ): Normal distribution, μ and σ are the mean and standard deviation, respectively. CoV: coefficient of variation.

	Bulk Density (D_B [kg/m^3])	Specific Heat Capacity (C_p [J/kg.K])	Porosity (θ_{por} [m^3/m^3])	Thermal Conductivity (λ_{dry} [W/m.K])	Water Absorption Coefficient (A_w [kg/m^2.s$^{0.5}$])	Water Vapour Diffusion Resistance Factor (μ_{VDR} [−])
Plaster [60]	N(2000, 400) CoV = 20 %	[(2)]N(850, 85)	[(2)]N(0.26, 0.026)	N(0.8, 0.08) CoV = 10 %	N(0.03, 0.006) CoV = 20 %	N(19,1.9) CoV = 10 %
EPS insulation [51, 61]	N(15, 4.95) CoV = 33 %	N(1568, 157) CoV = 10 %	N(0.93,0.093) CoV = 10 %	N(0.0376, 0.0036) CoV = 9.5 %	N(4.7 × 10^{-4}, 10−5) CoV = 2.1 %	N(35, 0.12) CoV = 0.34 %
Glass wool insulation [51, 61]	N(28, 4.76) CoV = 17 %	[(2)]N(928, 92.8)	[(1)]N(0.95, 0.095)	N(0.031, 0.0025) CoV = 8.2 %	N(0.02, 0.00307) CoV = 15 %	N(2, 0.027) CoV = 1.35 %
OSB [51,62]	N(455, 45.5) CoV = 10 %	N(1500, 150) CoV = 10 %	N(0.74, 0.074) CoV = 10 %	N(0.1, 0.01) CoV = 10 %	[(1)]N(0.0019, 0.00019)	N(467, 46.7) CoV = 10 %
Gypsum board [51, 62]	N(850, 85) CoV = 10 %	N(850, 85) CoV = 10 %	N(0.65, 0.065) CoV = 10 %	N(0.2, 0.02) CoV = 10 %	[(1)]N(0.18, 0.018)	N(8.3, 0.83) CoV = 10 %
Plaster holder (Light cement board) [51,63]	[(2)]N(1130, 113)	[(2)]N(840, 84)	[(2)]N(0.479, 0.0479)	[(2)]N(0.24, 0.024)	[(1)]N(0.014, 0.0014)	[(2)]N(905, 90.5)
Brick [64]	N(1830.13, 13.45) CoV = 0.7 %	N(889, 10.67) CoV = 1.2 %	N(0.293, 0.002) CoV = 0.7 %	N(0.548,0.077) CoV = 14 %	N(0.193, 0.00116) CoV = 0.6 %	N(18.01, 0.018) CoV = 0.1 %
Rock wool insulation [61]	N(39, 0.78) CoV = 2 %	[(2)]N(802, 80.2)	[(1)]N(0.95, 0.095)	N(0.034, 0.0026) CoV = 7.6 %	N(3.39 × 10^{-3}, 9.1 × 10^{-4}) CoV = 27 %	[(2)]N(2, 0.2)

Note: [(1)] These material properties were not specified in the corresponding references; therefore, default values from the Delphin database with a normal distribution and coefficient of variation of 10 % were used.
[(2)] These material properties lack information on their distributions in the literature; thus, a normal distribution with a coefficient of variation of 10 % was assumed as a reasonable value, as recommended by Gradeci et al. [62].

generated by varying these two parameters. It should be noted that if the damaged materials are replaced from the interior, the cause of the damage can originate from the exterior. In addition to the area of replacement, the cause of damage in each case study should be remediated. However, this remediation method was excluded from this study. In addition, the wooden studs were excluded from the analysis for simplicity because removing these elements affects structural stability, which is beyond the scope of this study. However, the sanitising these elements may also be a possible option.

2.3.2.1. Area of replacement. Various percentages of the surface areas of the external wall assemblies quantify the extent of damage resulting from moisture. This extent was calculated by considering different percentages of area replacement, incrementing in steps of 10 % (i.e., 10 %, 20 %, …, 90 %, and 100 % of the surface area of the external wall assemblies). Consequently, each case study comprised 10 potential options concerning the surface area affected by mould growth.

2.3.2.2. Number of damaged layers. Because the screening point was the internal surface of the wooden stud, the number of damaged layers varied in each case study. Changing the damaged layers also requires dismantling the preceding layers from the interior. Therefore, three layers were removed for CS1 (comprising gypsum board, OSB board, and glass wool insulation), four for CS2 (including two layers of gypsum board, vapour barrier, and glass wool insulation), and five for CS3 (comprising gypsum board, OSB board, vapour barrier, and two layers of rock wool insulation).

2.4. Life cycle costing (LCC)

In this step, the economic impacts of selecting each case study were calculated and assessed using the LCC method detailed in ISO 15686-5 [67]. In this study, net present value (NPV) calculation procedures [68] were employed to determine the present value (PV) for each case study, considering their initial and running costs. Initial costs comprise expenses related to material procurement, labour, and installations. Running costs comprise expenses associated with replacement scenarios, as outlined in Section 2.3.2. This includes the procurement of new materials, labour, installation costs for new materials, and the costs associated with demolishing, dismantling, and construction waste management of old and damaged materials.

For simplicity, labour and installation costs were assumed to be 3 % of the material prices (as it was assumed in Ref. [7]). An additional 3 % of material prices was allocated for the costs associated with demolishing, dismantling, and construction waste management of old and damaged materials. Sweden was selected as the construction market, and the Euro was used as the official currency for these analyses. Material prices were determined through inquiries from four construction suppliers in Sweden [69–72], and the average of their prices was used in the LCC calculations.

As outlined in Section 2.3.2, replacement scenarios were assumed to occur during each inspection period (i.e., four times over the lifespan of the building). The costs of these replacement scenarios were computed for each scenario, and their averages were calculated. To quantify the economic impacts associated with mould growth for each case study, the average of these economic impacts, denoted as EC_{mean} [€/m^2], was introduced. Eq. (6) expresses this indicator.

$$EC_{mean,i} = \frac{\sum_{k=n}^{k=1} EC_k}{n} \tag{6}$$

where.

- n: number of replacement scenarios
- i: number of case study

Eq. (7) is used to convert future costs to present costs, P, by including today's costs, A_0, growth rate, g, interest rate, ir, and building lifespan, N [73].

$$P = A_0(1+ir)^{1-N}(1+g)^{N-1} \tag{7}$$

Economic impacts linked to mould growth, represented by EC_{mean} [€/m^2], may occur four times throughout the lifespan of the building. Thus, the costs associated with mould growth for each inspection period were converted into present value (PV) using Eq. (8).

$$EC_{mean,PV,i} = EC_{mean,i}(1+ir)^{1-N}(1+g)^{N-1} \tag{8}$$

In this study, considering four inspection periods, the final $EC_{mean,PV,i,fin}$ is the sum of the $EC_{mean,PV,i}$ for all inspection periods.

The interest rates established by the central bank in Sweden were extracted from Ref. [74], and the daily average interest rate for the past 29 years (1994–2023) was calculated, resulting in ir = 2.27 %. Interest rate predictions are assessments of the future direction of monetary policy. These predictions may require adjustments as new information emerges regarding economic development in Sweden and globally. Inherent uncertainty exists regarding future interest rate trends, similar to the uncertainty associated with future economic development. The uncertainty of predictions increases as they extend further into the future. To address the uncertainty regarding future monetary policy, the Swedish Central Bank (Riksbank) often presents alternative scenarios in its monetary policy report [75].

Growth rate is typically measured using a price index to assess how the price level has evolved over a 12-month period. In Sweden, the consumer price index with fixed interest (CPIF) [76] is used. Historical CPIF data from the Swedish Central Bank's official website were used, and the average over the last 35 years (1988–2023) was computed, yielding a CPIF of 2.68 % [76].

2.5. Life cycle assessment (LCA)

According to EN ISO 14040 [77], an LCA evaluates the potential environmental impacts throughout the life cycle of a product. LCA adheres to the principles and framework outlined in the international standard for LCA, EN ISO 14040 [77], the European standards for environmental performance assessment of buildings, EN ISO 15978 [78], and Environmental Product Declaration (EPD) core rules for construction products, EN 15804 [79].

The LCA in this study aimed to analyse the environmental impact of various potential moisture-related damage scenarios, as outlined in Section 2.3.2. The functional unit for this assessment was 1 m^2 of the external wall assemblies over the estimated 50-year lifespan of the building. The system boundary in this study followed the modular life cycle system defined in EN 15978 [78]. This modular system evaluates cradle-to-grave impacts across four main life cycle stages: product (modules A1-A3), construction (modules A4-A5), use (modules B1-B7), and end-of-life (EoL) (modules C1-C4). These modules were used to assess the environmental impacts of the initial design and the defined replacement scenarios. This study did not include the optional stage (module D), which accounts for the potential positive impacts of processing or reusing materials after their end-of-life. Incorporating this stage could be beneficial when using this decision analysis method in the context of a circular economy.

The life cycle environmental impact was evaluated with respect to global warming potential (GWP). This study used the extracted EPDs for modules A1-A3, A5, B1-B7, C1, and C3-C4. An average of the relevant EPD data was compiled from four databases: epd-danmark [80], EPD International [81], epd-norway [82], and ibu-epd [83]. The data from these databases are up-to-date and aligned with the construction product category rules (PCR), EN 15804 [79], which serve as the core framework for construction product EPDs.

The transportation modules, i.e., A4 and C2, were calculated using OpenLCA version 2.1.1 [84]. This tool calculates the life cycle impact assessment (LCIA) results based on the CML (baseline) method developed by the University of Leiden in the Netherlands in 2001, one of the most common impact categories used in LCA [85]. Module A4 involves the transportation of materials and products from the factory gate to the building site, including any transport, intermediate storage, and distribution. It is computed based on the distance from the production site to the construction site, material weight, and emission factor from the means of transportation. For this study, the building site was assumed to be in Gothenburg, Sweden, with an average transport distance of 200 km from the manufacturing site to the building site [48]. The weights of the products were calculated using the mean values of the material densities listed in Table 2. "Lorry transport, Euro 0, 1, 2, 3, 4 mix, 22 t total weight, 17.3 t max payload – RER" was selected as the default road transport provider according to Ref. [7]. Module C2, concerning transport to the waste processing site, was calculated similarly to Module A4. However, a transport distance of 50 km was assumed from the building site to the nearest recycling site, incineration site, and landfill [48]. The interpretation of the CO_2 emission results is presented in section 3.4.

The environmental impacts linked to the replacement scenarios were computed for each scenario, and their averages were determined. The average environmental impact, denoted as EN_{mean} [kg CO_2 eq./m^2], was introduced as an indicator for the environmental impacts associated with mould growth in each case study, as illustrated by Eq. (9).

$$EN_{mean,i} = \frac{\sum_{k=n}^{k=1} EN_k}{n} \tag{9}$$

where.

- n: number of replacement scenarios
- i: number of case study

In this study, considering four inspection periods, the final $EN_{mean.i.fin}$ is the summation of the $EN_{mean.i}$ of all inspection periods.

2.6. Decision analysis

The final step involves conducting a decision analysis by integrating the outcomes of the probabilistic hygrothermal analyses, economic impact assessment, and environmental impact evaluation. This is carried out by leveraging concepts similar to the IDA developed by Bayat Pour et al. [86]. Fig. 4 shows a flowchart outlining the steps of the IDA, where the case study with lower inutilities and drawbacks is considered the most optimal alternative. Economic and environmental impacts resulting from moisture-related issues pose negative consequences; thus, they are regarded as inutilities.

The flowchart in Fig. 4 progresses from left to right. Initially, the inutilities associated with mould growth are computed for the economic and environmental consequences using Eqs. (10) and (11).

$$\overline{U}\left(EC_{I_j|d_i}\right) = P\left(I_j|d_i\right) \bullet EC_{mean.PV.i.fin} \tag{10}$$

$$\overline{U}\left(EN_{I_j|d_i}\right) = P\left(I_j|d_i\right) \bullet EN_{mean.i.fin} \tag{11}$$

where.

- $\overline{U}\left(EC_{I_j|d_i}\right)$: Economic inutilities associated with mould growth
- $\overline{U}\left(EN_{I_j|d_i}\right)$: Environmental inutilities associated with mould growth
- $P\left(I_j|d_i\right)$: Probability of failure owing to mould growth
- $EC_{mean.PV.i.fin}$: Average of economic impacts of mould growth
- $EN_{mean.i.fin}$: Average of environmental impacts of mould growth
- i: Case study
- j: mould index threshold

The expected value for total inutilities is determined by aggregating the initial inutilities, encompassing economic and environmental impacts, with the inutilities linked to mould growth, using Eqs. (12) and (13).

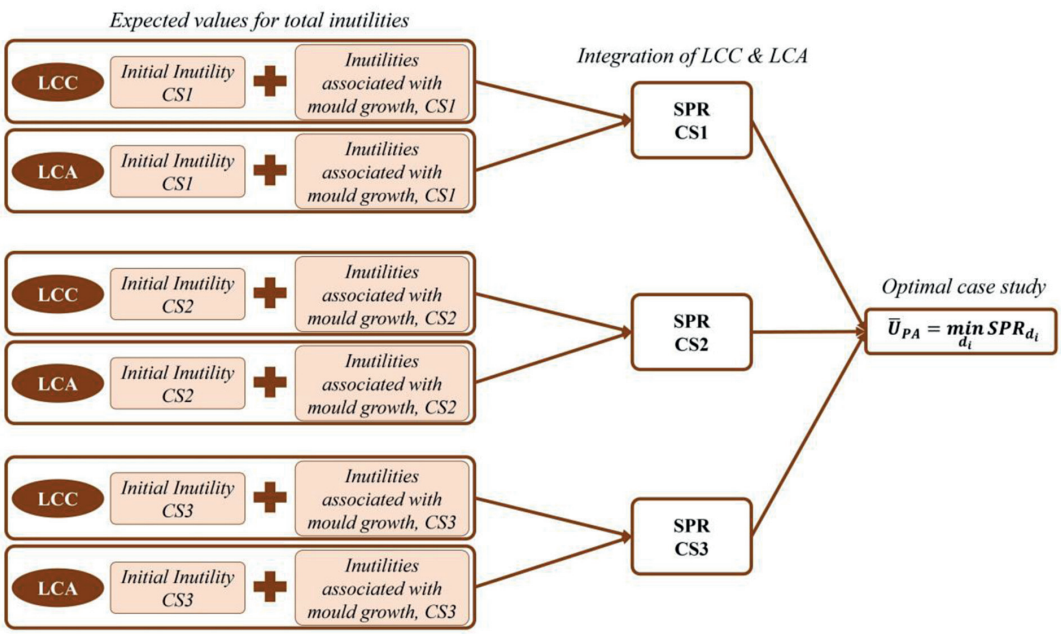


Fig. 4. Inutility decision analysis flowchart. SPR: Single-point rate, LCC: Life cycle costing, LCA: Life cycle assessment.

$$E\left[\overline{U}\left(EC_{I_j|d_i}\right)\right] = \overline{U}(Initial_{d_i}) + \overline{U}\left(EC_{I_j|d_i}\right) \tag{12}$$

$$E\left[\overline{U}\left(EN_{I_j|d_i}\right)\right] = \overline{U}(Initial_{d_i}) + \overline{U}\left(EN_{I_j|d_i}\right) \tag{13}$$

The LCC and LCA results were integrated using the SPR method, as outlined in Eq. (14) [7]. In this study, the SPR was considered as an inutility index, with values ranging from 0 to 1. For the case studies in this research, weighting factors (WF) of 80 % and 20 % were assumed for the LCC and LCA, respectively.

$$SPR_{d_i} = \frac{E\left[\overline{U}\left(EC_{I_j|d_i}\right)\right]}{\max_{d_i} E\left[\overline{U}\left(EC_{I_j|d_i}\right)\right]} \times WF_{EC} + \frac{E\left[\overline{U}\left(EN_{I_j|d_i}\right)\right]}{\max_{d_i} E\left[\overline{U}\left(EN_{I_j|d_i}\right)\right]} \times WF_{EN} \tag{14}$$

The case study with the lowest inutility index (SPR value) was considered the most optimal, as defined in Eq. (15). This case study was designated as the predicted action (PA). A lower inutility index indicates a more optimal case study regarding mould growth risk and economic and environmental impacts.

$$\overline{U}_{PA} = \min_{d_i} SPR_{d_i} \tag{15}$$

where.

- $\overline{U}_{PA}$: Inutility index of the predicted action

3. Results and discussions

3.1. Probabilistic hygrothermal analysis

Table 3 presents the results of the probabilistic hygrothermal analysis. CS1 exhibited the highest probability of failure at 32.67 %, CS2 exhibited a minor probability (2.27 %), and CS3 exhibited no probability of exceeding the 95th percentile mould indices compared with index 3 within each inspection period. The R^2 and MAE values, indicating the accuracy of the metamodel, were provided for all three case studies, along with the required number of simulations to achieve convergence. Several factors may influence the R^2 and MAE value during the creation of a metamodel. The variability of the training data significantly influences the performance of ML models. Higher variability can pose challenges for the model in accurately capturing underlying patterns, resulting in a lower R^2 and MAE. The performance of the metamodel varied among the case studies because CS1, CS2, and CS3 had different wall constructions and characteristics. In addition, the selection and relevance of the features used in the ML model can significantly affect its performance. Compared with the features employed in CS1 and CS3, the features selected for CS2 may have been less informative for outcome prediction, leading to a lower R^2 value for CS2. However, it should be noted that, in the context of the study, the R^2 for CS2 may still be considered as acceptable despite being lower than those in the other case studies.

Fig. 5 shows the cumulative density function (CDF) of the 95th percentile of the mould indices for each case study. The red solid lines indicate the limit state point, designated as mould index 3. The red dashed lines represent the probabilities of the 95th percentile of the mould indices exceeding index 3 ($P(M_{I3})$). The y-axis denotes the cumulative probability, whereas the x-axis denotes the mould growth index. The blue curves show the cumulative probabilities in the case studies to reach the 95th percentile of the mould indices. For instance, for CS1, the 95th percentile of mould indices 1 indicates 0.4 on the y-axis. That is, in 40 % of the simulation scenarios, 95 % of the mould indices were less than or equal to 1. CS1 exhibited the worst hygrothermal performance compared with the other two case studies. This discrepancy can be attributed to the implementation of fewer moisture-defence mechanisms in the configuration. Conversely, CS2 and CS3 incorporated more moisture-defence mechanisms against outdoor moisture sources than CS1.

All case studies used an exterior layer (plaster cladding in CS1 and CS2 and a brick veneer in CS3) designed to drain most rainwater immediately to the ground. However, the exterior layer is typically not entirely impermeable and often contains small gaps and pores. CS2 and CS3 featured an air layer that disrupt the liquid water convection path from the penetrated WDR. This air layer facilitates the drainage of liquid water that passes through the plaster cladding or brick veneer layers, establishing a capillary break between the fully saturated outer wall layer and the rest of the wall, effectively cutting off the capillary path. Furthermore, ventilation within the air gap reduces the relative humidity within the air layer, mitigating exposure to the inner wall.

Another critical moisture-defence layer is the moisture barrier, often referred to as the “wind barrier” in Scandinavian regions. This membrane, typically positioned from the outside, assists the cladding in keeping the wall dry from penetrating liquid water and prevents wind from blowing through the construction. CS2 and CS3 featured a vapour barrier (typically in membrane form on the interior side), essential for impeding moisture transport through the wall. In cold-climate regions, such as Sweden, a diffusion-tight

Table 3
Probabilistic hygrothermal analysis results.

Case studies	Probability of failure [%]	R^2	MAE	Required number of simulations to achieve convergence
CS1	32.67	0.965	0.272	2300
CS2	2.27	0.832	0.291	1100
CS3	0.00	0.945	0.015	1000

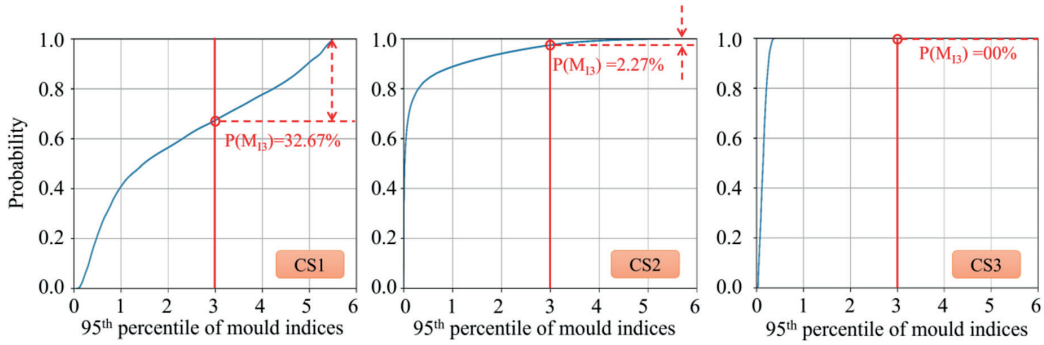


Fig. 5. Mould reliability analysis for three case studies (CS1, CS2, and CS3). Red solid line: failure threshold indicators; blue curve: CDF of 95th percentile of mould indices; red dashed line: probability of mould index 3 occurrence P(M_{I3}). (For interpretation of the references to colour in this figure legend, the reader is referred to the Web version of this article.)

layer is located on the interior side. Simultaneously, the exterior materials (from the insulation towards the exterior surface) remain diffusion-open, ensuring opportunities for dry-out in case of initial moisture or minor leakages.

3.2. Mould sensitivity analysis

The mould sensitivity analysis, incorporating linear and nonlinear evaluations, identified the most sensitive input parameters across the case studies. The solar absorption coefficient emerged as the most influential parameter. This finding is likely due to the fact that a higher solar absorption coefficient results in a generally warmer construction facilitating the drying of materials subsequently reducing the potential for mould growth.

In case studies 2 and 3, the ACR in the air gap also demonstrated a significant impact on the simulations' outcomes. An increase in ACR leads to an increase in the drying of moisture that ingresses the construction which lowers the probability of mould development.

The reduction/splash coefficient of WDR was another key parameter found to be impactful, particularly in relation to the 95th percentile of mould indices. A higher reduction/splash coefficient results in less WDR splashing, allowing more of the rain to penetrate the wall assemblies. This increased penetration raises the 95th percentile of mould indices as the moisture content of the exterior layer increases with the rising reduction/splash coefficient.

3.3. Life cycle costing (LCC)

Table 4 presents the average prices [€/m^2] of the materials used in the case studies based on inquiries from four construction suppliers in Sweden, as detailed in Section 2.4. The table also lists the costs related to labour, installation, demolition, dismantling, and construction waste management. The installation cost assumption encompasses expenses for accessories, supplementary and ancillary materials, and equipment, such as mortar for bricklaying, screws and netting for gypsum boards, scaffolding, fencing, signage, protective foils, drying machines, and lifters. Waste management costs include expenses for waste containers, disposal, and transportation of waste materials. In this study, 3 % of the material prices was considered the basis for these costs. However, in real projects, these

Table 4
Average of prices [€/m^2] of the used materials.

Materials	Average Price of Materials [€/m^2]	Labour and Installation [€/m^2]	Demolishing, Dismantling, and Construction Waste Management [€/m^2]
Brick	132.2	3.97	3.97
Plaster	3.9	0.12	0.12
EPS Insulation	4.8	0.14	0.14
Glass Wool Insulation, 45 mm	3.2	0.10	0.10
Glass Wool Insulation, 170 mm	10.6	0.32	0.32
Glass Wool Insulation, 195 mm	12.9	0.39	0.39
Rock Wool Insulation, 70 mm	6.5	0.19	0.19
Rock Wool Insulation, 195 mm	17.8	0.53	0.53
OSB	8	0.24	0.24
Cement Board	10	0.3	0.3
Gypsum Board	3.8	0.11	0.11
Vapour Barrier	0.6	0.02	0.02

data should be extracted from specialised databases such as [87].

Fig. 6 shows the initial costs [€/m^2] and average economic impacts related to mould growth during the lifespan of the building, represented by $EC_{mean,PV,fin}$ [€/m^2], for each case study. In CS3, the initial costs were comparatively higher owing to the high price of bricks compared with plaster for the exterior layer. Furthermore, for CS3, because brick did not require replacement in the replacement scenario, its associated costs were significantly lower (approximately half) than its initial costs. CS3 necessitated the replacement/repair of five layers in the event of mould growth, resulting in higher costs associated with damage scenarios compared with the other two case studies.

3.4. Life cycle assessment (LCA)

Table 5 provides an overview of the environmental impacts associated with each material across different modules. Modules A1-A3, A5, C1, C3, and C4 represent the average environmental impacts sourced from the EPDs using the four databases [80–83]. Notably, the EPDs indicated no environmental impact for the use stage (modules B1-B7). The use stage occurs if the lifespan of the material is shorter than that of the building or if regular maintenance/repair is necessary during the expected lifespan of the building [78], which did not apply in this study. The materials investigated in this study had lifespans exceeding those of the building, and maintenance/repair were not required. Regarding the transportation modules (i.e., A4 and C2), bricks exhibited the highest CO_2 emissions owing to their higher mass per square metre than the other materials.

The CO_2 emissions associated with bricks surpassed those of other materials during the product stage (A1-A3) and the construction installation process (module A5). This discrepancy can be attributed to several factors contributing to variations in CO_2 emissions among building materials. These factors include the raw materials, manufacturing processes, transportation, and energy consumption. Bricks are typically made from clay and often require extensive mining operations [88]. The extraction and processing of these raw materials can substantially contribute to CO_2 emissions, particularly if the mining process involves heavy machinery or relies on energy-intensive methods. Furthermore, brick production involves firing clay in kilns at high temperatures, requiring significant energy inputs typically sourced from fossil fuels, such as natural gas or coal [88]. Although brick installation may not generate significant CO_2 emissions, the overall construction process involves various activities that contribute to higher emissions. These activities include storing and transporting materials, products, waste, and equipment within the construction site, water usage for on-site cleaning, and waste management processes for materials generated during construction [78].

Various parameters can influence modules, such as deconstruction (C1), waste processing for reuse, recovery, recycling (C3), and disposal (C4). For instance, a gypsum board comprises gypsum plaster sandwiched between layers of paper. Although gypsum itself is a naturally occurring mineral and non-toxic [89], the inclusion of paper layers and any additives or coatings in the manufacturing process complicates its disposal. Separating these materials for recycling and safe disposal often requires additional processing steps, which can be labour-intensive and energy-consuming, particularly if the gypsum board is contaminated with other materials and construction waste. Although gypsum boards and OSB are relatively lightweight compared with materials such as brick, they can still contribute to significant waste volume at construction sites, particularly in large-scale projects. Managing and processing this waste volume can result in emissions, particularly if transportation to specialised recycling facilities and landfills is necessary. Furthermore,

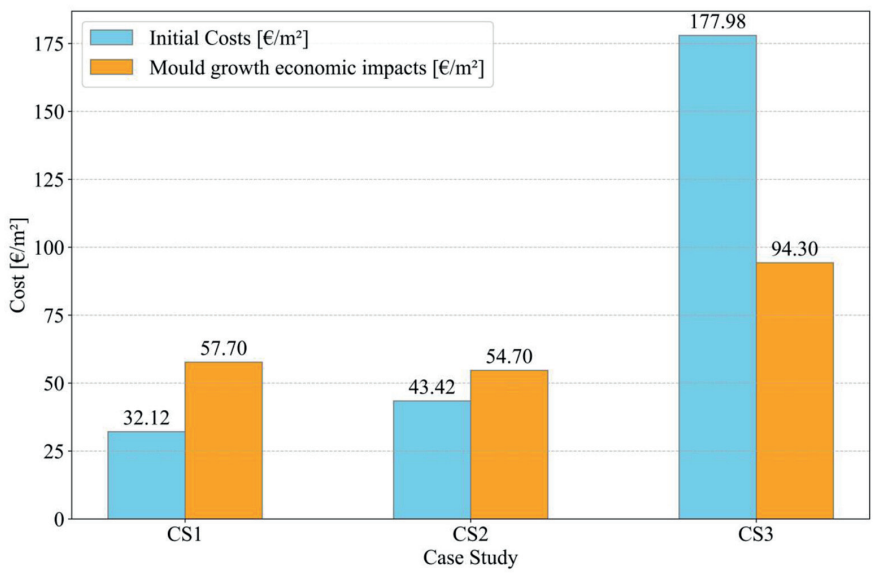


Fig. 6. Potential economic impacts of each case study for different building life cycle stages during the lifespan of the building.

Table 5
Environmental impacts (CO_2 emission [kg CO_2 eq./m^2]) associated with different life cycle stages and modules for each material [80–83].

Materials	A1-A3	A4	A5	B1-B7	C1	C2	C3	C4
Brick	2.72E+01	2.90E+00	3.35E+00	0.00E+00	6.31E-02	7.25E-01	2.17E-01	9.38E-01
Plaster	3.09E+00	2.64E-01	2.20E-01	0.00E+00	4.54E-02	6.60E-02	6.17E-02	7.32E-02
EPS Insulation	2.49E+00	9.90E-03	1.02E-02	0.00E+00	1.45E-05	2.48E-03	2.00E+00	5.35E-03
Glass Wool Insulation, 45 mm	5.08E-01	1.25E-02	9.35E-03	0.00E+00	0.00E+00	3.12E-03	0.00E+00	3.12E-03
Glass Wool Insulation, 170 mm	1.92E+00	4.71E-02	3.53E-02	0.00E+00	0.00E+00	1.18E-02	0.00E+00	1.18E-02
Glass Wool Insulation, 195 mm	2.20E+00	5.41E-02	4.05E-02	0.00E+00	0.00E+00	1.35E-02	0.00E+00	1.35E-02
Rock Wool Insulation, 70 mm	2.36E+00	3.60E-02	3.11E-01	0.00E+00	0.00E+00	9.01E-03	0.00E+00	5.79E-02
Rock Wool Insulation, 195 mm	6.58E+00	1.00E-01	8.66E-01	0.00E+00	0.00E+00	2.51E-02	0.00E+00	1.61E-01
OSB	1.67E+00	6.61E-02	3.10E-02	0.00E+00	1.30E-01	1.65E-02	4.82E-02	1.36E-02
Cement Board	5.05E+00	1.49E-01	2.55E-01	0.00E+00	4.79E-02	3.73E-02	0.00E+00	1.87E-01
Gypsum Board	1.71E+00	1.46E-01	2.19E-01	0.00E+00	1.07E-02	3.65E-02	5.54E-01	4.25E-01
Vapour Barrier	3.03E+00	1.32E-02	7.63E-02	0.00E+00	0.00E+00	3.30E-03	1.68E-01	1.62E+00

some gypsum boards may contain additives or coatings that require special handling or disposal procedures owing to environmental and health concerns [90]. OSB, made from wood strands bonded together using an adhesive [91], adds another layer of complexity to waste processing and disposal, potentially increasing associated emissions. Collectively, these materials increase the complexity and emissions associated with waste management processes.

It is important to note that while LCA assesses potential environmental impacts, it does not predict absolute and precise environmental outcomes owing to several factors, including inherent uncertainties in modelling environmental impacts and considering that some potential impacts are future-oriented [77].

Fig. 7 illustrates the initial environmental impact of each case study (CO_2 emissions [kg CO_2 eq./m^2]). Table 6 lists the values for each module in Fig. 7. The results indicate that CS3 had the highest environmental impact among the three case studies. This is primarily attributed to the use of bricks for the exterior façade layer, which had a higher environmental impact than other materials.

Fig. 8 illustrates the initial CO_2 emissions and average environmental impacts associated with mould growth within the lifespan of the building, represented by $EN_{mean,fin}$ [kg CO_2 eq./m^2], for each case study. Similar to the mould economic impact results, the environmental impacts associated with mould growth for CS3 were lower (~23 %) than its initial environmental impacts because bricks did not require replacement in the replacement scenario. In addition, CS3 required the replacement/repair of five layers in case of mould growth, leading to higher environmental impacts in the damage scenarios compared with the other two case studies. Moreover, CS2 had a higher environmental impact on the replacement action than CS1. This was because CS2 involved replacing the two layers of gypsum board with a vapour barrier layer to reach the main insulation layer. The environmental impacts of the two gypsum board layers and a vapour barrier were higher than those of the combination of a layer of gypsum board and OSB used in CS1.

3.5. Decision analysis

Table 7 presents the results of the decision analysis, with the corresponding flowchart shown in Fig. 9. CS2 was the most optimal external wall assembly, exhibiting the lowest inutility index (SPR value) of 0.293 when both economic and environmental impacts were considered. However, this case study had a slight probability (2.27 %) of mould growth exceeding a mould index of 3 during each inspection period for over 95 % of the time. This probability of mould failure resulted in an environmental and economic impact of 0.672 kg CO_2 eq./m^2 and 1.242 €/m^2, respectively, over the 50-year building lifespan. A comparison between CS2 and CS3 revealed that although CS3 had no economic and environmental consequences associated with mould growth, its higher initial economic and environmental impacts make it a less suitable option. This comparison highlights that, in some cases, selecting a wall assembly with a manageable probability of mould failure and associated replacement/repair actions during its lifespan is more advantageous than opting for a case study with no mould failure risk but high initial economic and environmental impacts.

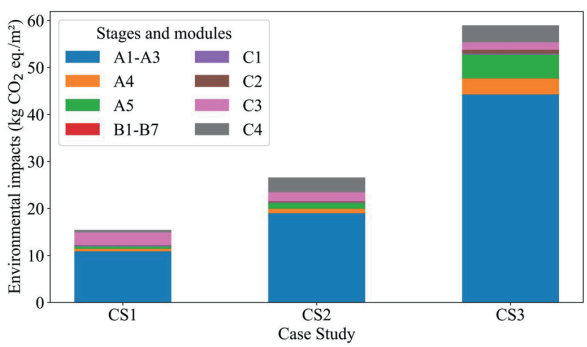


Fig. 7. Initial environmental impacts of each case study based on different building life cycle stages and modules.

Table 6
Initial environmental impacts (CO_2 emission [kg CO_2 eq./m^2]) associated with different life cycle stages and modules for each case study.

Case studies	A1-A3	A4	A5	B1-B7	C1	C2	C3	C4	Total Environmental Impacts
CS1	1.09E+01	5.33E-01	5.16E-01	0.00E+00	1.86E-01	1.33E-01	2.67E+00	5.29E-01	1.54E+01
CS2	1.90E+01	9.30E-01	1.26E+00	0.00E+00	1.25E-01	2.33E-01	1.89E+00	3.17E+00	2.66E+01
CS3	4.42E+01	3.41E+00	5.07E+00	0.00E+00	2.14E-01	8.52E-01	1.54E+00	3.64E+00	5.90E+01

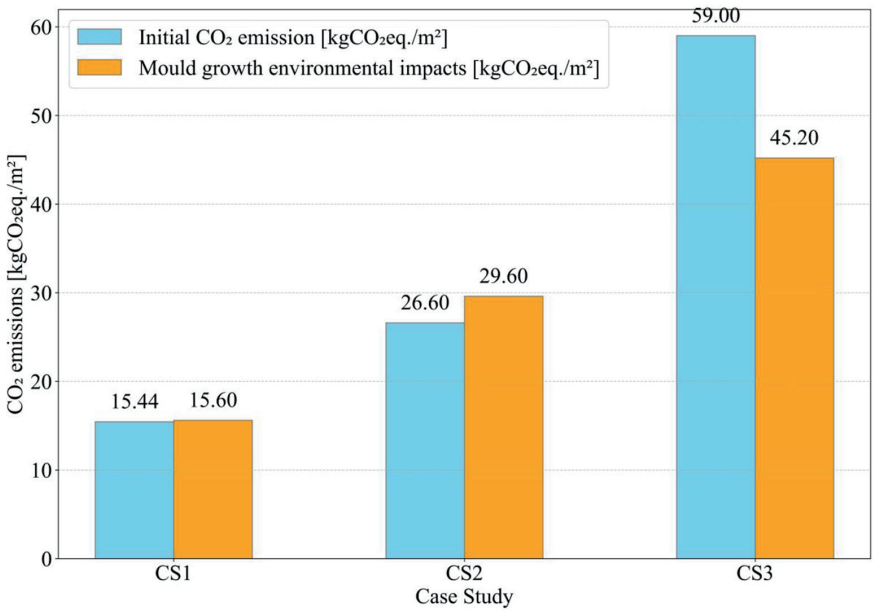


Fig. 8. Potential environmental impacts of each case study for different building life cycle stages during the lifespan of the building.

Table 7
Inutility decision analysis method calculations.

Case studies	Initial Costs [€/m^2]	Initial CO_2 emissions [$kgCO_2eq./m^2$]	Mould Growth Economic Inutility [€/m^2]	Mould Growth Environmental Inutility [$kgCO_2eq./m^2$]	Expected Value for Total Economic Inutilities [€/m^2]	Expected Value for Total Environmental Inutilities [$kgCO_2eq./m^2$]	Single-Point Rate, SPR [−]
CS1	32.120	15.400	18.851	5.097	50.971	20.497	0.299
CS2	43.400	26.600	1.242	0.672	44.642	27.272	**0.293**
CS3	177.980	59.000	0.000	0.000	177.980	59.000	1.000

By contrast, CS1 had the lowest initial economic and environmental impacts compared with the other two case studies. However, its weak hygrothermal performance led to a higher probability of failure owing to mould growth (32.67 %), resulting in greater economic and environmental impacts over time. This outcome illustrates that a case study with lower initial costs and environmental impacts may not always be the best option because suboptimal hygrothermal performance during the lifespan of the building can significantly influence the final decision.

The above discussion demonstrated the potential of the proposed decision analysis method to incorporate various aspects of building envelope design and identify the most optimal alternative. However, it is important to note that this decision analysis method would be more reliable with the inclusion of the health consequences of mould growth. As mentioned in Section 2.2.5, mould growth negatively impacts occupants' health, and incorporating this factor could potentially alter the final optimal decision. For instance, if the weight of the health consequences owing to mould growth is higher than the economic and environmental impacts, then CS3 could be a better alternative over CS1, considering the high probability of mould growth in CS1. This adjustment would account for the adverse health impacts on occupants, potentially making CS3 a more favourable option despite its higher initial economic and environmental impacts.

It is essential to highlight the importance of involving clients and house owners in decision-making processes regarding the moisture-related risks, especially in light of the findings presented in this study. While CS2 emerges as the most optimal external wall

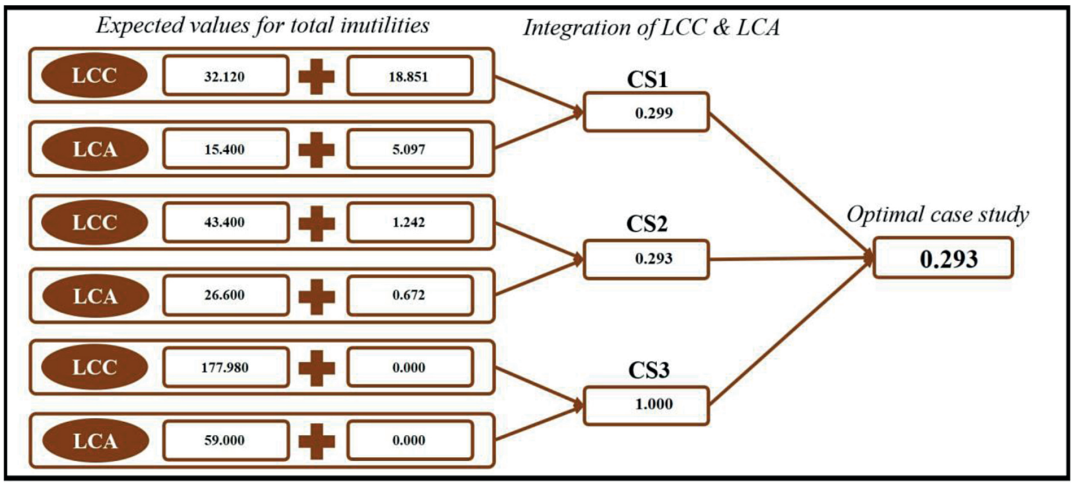


Fig. 9. Optimal case study according to the inutility decision analysis method.

assembly in terms of balancing economic and environmental impacts, the slight probability of mould growth poses a potential risk. Clients and house owners should be made aware of such risks and the potential long-term consequences on both the building's performance and their well-being. Transparent communication about these risks, coupled with a clear explanation of the associated costs and benefits, would enable clients to make informed decisions. Additionally, the market perception of the risk of construction can evolve, particularly as environmental considerations become more prominent. Thus, in some cases, choosing a construction with manageable risks, such as CS2, may align with both environmental goals and future market trends. This reinforces the need for a holistic evaluation that balances initial impacts with long-term performance and risks.

Fig. 10 shows the effect of changing the weighting factors (WF) on the economic and environmental impacts in a parametric study. This illustrates that the WF of these impacts significantly influence the determination of the most optimal case study. The initial assumptions in this study were 20 % and 80 % for LCA and LCC, respectively. Based on this, CS2 had the most optimal hygrothermal performance, as well as economic and environmental impacts.

However, the parametric study revealed that when the WF of the LCC fell below 75 % (with the WF of the LCA increasing beyond 25 % accordingly), CS1 could be identified as the most optimal case study. This shift highlights the sensitivity of decision-making outcomes to the relative importance of economic versus environmental WF. Determining appropriate WF can be challenging owing to the subjective nature of prioritising economic versus environmental impacts. Engaging experts in both fields in essential to achieve a balanced and justified weighting scheme. This approach enhances the credibility and acceptance of the decision analysis and ensures that diverse perspectives are considered, leading to more comprehensive and sustainable decision-making outcomes.

3.6. Limitations of the study

The reliability of this decision analysis method depends on the accuracy of the input data for moisture safety, economic, and environmental analyses. Each aspect has its own uncertainties, including material properties, climate data, EPDs, inflation rates, and interest rates. Although uncertainties in moisture safety design are addressed through probabilistic modelling, some limitations remain. One such limitation is the use of 1D modelling, which overlooks certain details in the simulation process. Additionally, while the probabilistic approach accounts for material properties and boundary conditions, it does not incorporate other stochastic variables, such as moisture storage and transport functions [30], indoor and outdoor climate data [30,62], and rainwater penetration [92]. It is important to note that the results of the case studies presented in this paper are based on specific assumptions, as outlined and justified in the study. Consequently, the findings may not be generalisable to other climate conditions or building types.

4. Conclusions

This study proposed a decision analysis method for selecting the most optimal building envelope assembly by integrating hygrothermal performance with economic and environmental analyses. The proposed multi-criteria decision analysis method integrates a machine learning metamodel, which enhances the ability to account for a broader range of uncertainties in the probabilistic hygrothermal analysis. This integration allows for a more robust and comprehensive assessment of various factors, improving the reliability and accuracy of the decision-making process. The application of the proposed decision analysis method was exemplified through three case studies.

- The application of the inutility method on the case studies suggested that the case study with no probability of mould growth might not be the best option when economic and environmental aspects are considered. In such instances, the initial costs and

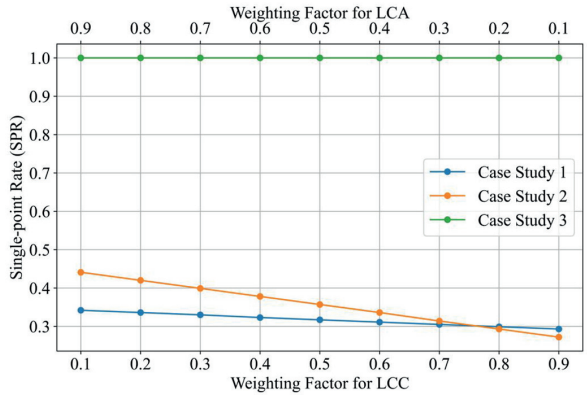


Fig. 10. Parametric study on the effect of weighting factors on SPR.

environmental impacts may be significantly higher than those of the other alternatives, making this option less beneficial considering these aspects.

- The analysis indicated that, in specific cases, it may be more appropriate to select an option with a minor and controllable probability of mould growth rather than choosing one with no probability of mould growth but with relatively higher initial costs and environmental impacts.
- It is demonstrated that low initial costs and environmental consequences are not always the best criteria for selecting a wall assembly. In some cases, a higher probability of mould growth can lead to significant costs and environmental impacts over the lifespan of a building. This results in a higher inutility index in the long term, as owners incur regular costs and increased CO_2 emissions to address mould growth problems.

Overall, the proposed inutility decision analysis method demonstrated the potential to integrate three critical aspects in designing building envelopes: risk of moisture damage, economic considerations, and environmental assessments. This method aids designers and owners in making optimal decisions and preventing suboptimal choices that focus on only one design aspect. It is important to note that this article is not intended to provide exact inutility values. Rather, it serves as a means for demonstrating how the inutility method can be used for evaluating and comparing building envelopes, setting moisture performance goals, and incorporating sustainability measures into buildings. Furthermore, the flexibility of the method allows it to consider different scenarios and adapt to new developments and changes in input variables.

Future study opportunities are as follows.

- Moisture-related problems, such as dampness and mould, can lead to health issues. However, a consensus regarding the acceptable probability of failure in buildings owing to moisture-induced damages, such as mould occurrence, remains lacking. First, an acceptable failure threshold must be defined. Second, an acceptable duration of occupant exposure to moisture-induced problems should be determined. The final optimal decision may change if the proposed decision analysis method incorporates health concerns.
- Efforts to improve the accuracy of input data regarding the uncertainties associated with material properties, climate data, EPDs, inflation rates, and interest rates can significantly enhance the reliability of decisions made using this method.
- Applying the proposed decision analysis method to real case studies could be the next step in identifying potential improvements. To enhance the validity of the models used in this research, experimental case studies could be employed. Experimental validation would provide empirical evidence to support the model predictions, ensuring that the simulated results accurately reflect real-world conditions and further strengthening the reliability of the findings. Furthermore, this can illustrate the extent to which this decision analysis method can be beneficial for making more rational decisions in real case studies.

CRediT authorship contribution statement

Mohsen Bayat Pour: Writing – review & editing, Writing – original draft, Visualization, Validation, Software, Resources, Project administration, Methodology, Investigation, Formal analysis, Data curation, Conceptualization. **Akram Abdul Hamid:** Writing – review & editing, Supervision, Methodology, Investigation, Conceptualization.

Declaration of competing interest

The authors declare that they have no known competing financial interests or personal relationships that could have appeared to influence the work reported in this paper.

Data availability

Data will be made available on request.

Acknowledgement

The authors gratefully acknowledge the financial support from FORMAS, the Swedish research council for sustainable development, for the research grant 2019-00673.

References

[1] IPCC, Climate Change Widespread, Rapid, and Intensifying, Intergovernmental Panel on Climate Change, Switzerland, 2021.
[2] Transition to Sustainable Buildings: Strategies and Opportunities to 2050, IEA Publ, Paris, Jul. 2013 [Online]. Available: https://www.iea.org/reports/transition-to-sustainable-buildings.
[3] I. Hamilton, et al., Energy Efficiency 2020, International Energy Agency (IEA), Japan, 2020.
[4] L. Wang, H. Ge, Stochastic modelling of hygrothermal performance of highly insulated wood framed walls, Build. Environ. 146 (Dec. 2018) 12–28, https://doi.org/10.1016/j.buildenv.2018.09.032.
[5] Andrea Tietze, Stephan Ott, Sylvain Boulet, Klodian Gradeci, Nathalie Labonnote, Steinar Grynning, Joakim Noreen, Anna Pousette, Tall Timber Facades – Identification of Cost-Effective and Resilient Envelopes for Wood Constructions Scientific Project Report, Technical University, Munich; Munich, 31.07.2017.
[6] P. Santos, J.R. Correia, L. Godinho, A.M.P.G. Dias, A. Dias, Life cycle analysis of cross-insulated timber panels, Structures 31 (Jun. 2021) 1311–1324, https://doi.org/10.1016/j.istruc.2020.12.008.
[7] M. Bayat Pour, M.L. Elsayed, Assessment of the Environmental Impacts, Energy Performance and Economic Aspects of Various Construction Materials', Master Thesis, Lund University, Faculty of Engineering, Lund, Sweden, 2020.
[8] H. Viitanen, Factors Affecting the Development of Mould and Brown Rot Decay in Wooden Material and Wooden Structures, Doctoral Thesis, Department of Forest Products, Swedish University of Agricultural Sciences, Uppsala, Sweden, 1996.
[9] N. Lolli, S.M. Fufa, M. Inman, A parametric tool for the assessment of operational energy use, embodied energy and embodied material emissions in building, Energy Proc. 111 (Mar. 2017) 21–30, https://doi.org/10.1016/j.egypro.2017.03.004.
[10] P. Johansson, 'Determination of the Critical Moisture Level for Mould Growth on Building Materials', Doctoral Thesis, Lund University, Faculty of Engineering, 2014. Lund, Sweden, https://portal.research.lu.se/ws/files/3846997/4419062.pdf. (Accessed 26 October 2021).
[11] C. Ahrnens, E. Borglund, Fukt på kallvindar - en kartläggning av småhus i Västra Götalands län, Chalmers University of Technology, Master Thesis, 2007.
[12] C.-E. Hagentoft, A.S. Kalagasidis, Moisture safe cold attics - assessment based on risk analyses of performance and cost, in: Proceedings of 10th Nordic Symposium on Building Physics, 2014, p. 10. Lund, Sweden.
[13] 'Boverket's mandatory provisions and general recommendations, in: BBR, BFS 2011:6 with Amendments up to BFS 2018:4', 2011, p. 154.
[14] H.L.S.C. Hens, Combined heat, air, moisture modelling: a look back, how, of help? Build. Environ. 91 (Sep. 2015) 138–151, https://doi.org/10.1016/j.buildenv.2015.03.009.
[15] C. Rode, P.N. Hansen, K. Hansen, Combined Heat and Moisture Transfer in Building Constructions', Technical University of Denmark, Sep. 1990. LFV-214.
[16] H. Janssen, B. Blocken, J. Carmeliet, Conservative modelling of the moisture and heat transfer in building components under atmospheric excitation, Int. J. Heat Mass Tran. 50 (5–6) (Mar. 2007) 1128–1140, https://doi.org/10.1016/j.ijheatmasstransfer.2006.06.048.
[17] P.W.M.H. Steskens, H. Janssen, C. Rode, Influence of the convective surface transfer coefficients on the heat, air, and moisture (HAM) building performance, Indoor Built Environ. 18 (3) (Jun. 2009) 245–256, https://doi.org/10.1177/1420326X09105682.
[18] L. Van Gelder, P. Das, H. Janssen, S. Roels, Comparative study of metamodelling techniques in building energy simulation: guidelines for practitioners, Simulat. Model. Pract. Theor. 49 (Dec. 2014) 245–257, https://doi.org/10.1016/j.simpat.2014.10.004.
[19] A.A. Hamid, P. Wallentén, D. Johansson, Moisture supply set point for avoidance of moisture damage in Swedish multifamily houses, Energy Proc. 78 (Nov. 2015) 901–906, https://doi.org/10.1016/j.egypro.2015.11.016.
[20] A. Holm, H.M. Künzel, Two-dimensional transient heat and moisture simulations of rising damp with WUFI2d, in: J. Carmeliet, H. Hens, G. Vermeir (Eds.), Research in Building Physics, first ed., CRC Press, 2020, pp. 363–367, https://doi.org/10.1201/9781003078852-52.
[21] E. Vereecken, L. Van Gelder, H. Janssen, S. Roels, Interior insulation for wall retrofitting – a probabilistic analysis of energy savings and hygrothermal risks, Energy Build. 89 (Feb. 2015) 231–244, https://doi.org/10.1016/j.enbuild.2014.12.031.
[22] A. Sasic Kalagasidis, C. Rode, Annex 55, Reliability of Energy Efficient Building Retrofitting - Probability Assessment of Performance and Cost (RAP-RETRO), Framework for Probabilistic Assessment of the Building Envelope, Chalmers University of Technology, Gothenburg, Sweden, 2015:5, 2015. ISSN 1652-9162.
[23] E.J. de Place Hansen, E.B. Møller, M. Ørsager, Guidelines for internal insulation of historic buildings, in: J. Kurnitski, T. Kalamees (Eds.), 12th Nordic Symposium on Building Physics (NSB 2020), E3S Web of Conferences, Jun. 2020 01004, https://doi.org/10.1051/e3sconf/202017201004. Tallinn, Estonia.
[24] K. Gradeci, A Probabilistic-Based Methodology for Evaluation of Timber Façade Constructions', Doctoral Thesis, Norwegian university of science and technology (NTNU), Trondheim, Norway, 2018.
[25] S. Geving, A systematic method for hygrothermal analysis of building constructions using computer models, in: Fifth International IBPSA Conference, 1997. Prague, Check Republic.
[26] N. Ramos, E. Barreira, M.L. Simões, J. Delgado, Probabilistic risk assessment applied to biological growth on external surfaces with ETICS, in: 13th Conference of the International Building Performance Simulation Association, Chambéry, France, August, 2013, p. 6.
[27] M. Bayat Pour, J. Niklewski, A. Naghibi, E. Frühwald Hansson, Robust probabilistic modelling of mould growth in building envelopes using random forests machine learning algorithm, Build. Environ. 243 (Sep. 2023) 110703, https://doi.org/10.1016/j.buildenv.2023.110703.
[28] C. Aggarwal, H. Ge, M. Defo, M.A. Lacasse, Hygrothermal performance assessment of wood frame walls under historical and future climates using partial least squares regression, Build. Environ. 223 (Sep. 2022) 109501, https://doi.org/10.1016/j.buildenv.2022.109501.
[29] K. Calle, N. Van Den Bossche, Sensitivity of the hygrothermal behaviour of homogeneous masonry constructions: from Sobol indices to decision trees, in: J. Kurnitski, T. Kalamees (Eds.), 12th Nordic Symposium on Building Physics (NSB 2020), E3S Web Conf., Tallinn, Estonia, Jun. 2020 07001, https://doi.org/10.1051/e3sconf/202017207001.
[30] V. Marincioni, G. Marra, H. Altamirano-Medina, Development of predictive models for the probabilistic moisture risk assessment of internal wall insulation, Build. Environ. 137 (Jun. 2018) 257–267, https://doi.org/10.1016/j.buildenv.2018.04.001.
[31] L. Wang, H. Ge, L. Wang, Metamodel development for predicting hygrothermal performance of wood-frame wall under rain leakage, in: XV International Conference on Durability of Building Materials and Components. eBook of Proceedings, CIMNE, 2020, https://doi.org/10.23967/dbmc.2020.095.
[32] S. Kahangi Shahreza, M. Bayat Pour, A. Abdul Hamid, Towards rational decision-making on repointing to mitigate moisture damage in building envelopes: a probabilistic study, Developments in the Built Environment 19 (Oct. 2024) 100510, https://doi.org/10.1016/j.dibe.2024.100510.
[33] M. Bayat Pour, J. Niklewski, A. Naghibi, E. Frühwald Hansson, A literature review of probabilistic hygrothermal assessment for building envelopes, Build. Environ. (Jun. 2024) 111756, https://doi.org/10.1016/j.buildenv.2024.111756.
[34] 'RIBuild', RIBuild. https://www.ribuild.eu. (Accessed 3 December 2023).
[35] D. Barber, Tall timber buildings: what's next in fire safety [Online]. Available: http://link.springer.com/10.1007/s10694-015-0497-7, Nov. 2015. (Accessed 6 May 2024).

[36] Finnish mould growth model | Building Physics | Tampere Universities', Building Physics. Accessed: June. 30, 2022. [Online]. Available: https://research.tuni.fi/buildingphysics/finnish-mould-growth-model/.
[37] T. Ojanen, H. Viitanen, R. Peuhkuri, Modelling of mould growth in building envelopes, in: IEA ECBCS Annex 41 Closing Seminar : Nordic Building Physics Conference, 2007, p. 18. Copenhagen, Denmark.
[38] H. Viitanen, T. Ojanen, Improved model to predict mold growth in building materials, in: *10th Thermal Performance Of the Exterior Envelopes Of Whole Buildings Conference*, Clearwater Beach, United States, Dec. 2007, p. 8.
[39] G.D. Wyss, K.H. Jorgensen, 'A User's Guide to LHS: Sandia's Latin Hypercube Sampling Software', SAND–98-0210, Feb. 1998 573301 https://doi.org/10.2172/573301.
[40] M. Bayat Pour, S. Kahangi Shahreza, A. Abdul Hamid, Effect of extruded mortar joints on mould growth in timber frame wall with brick veneer: probabilistic and Machine Learning Modelling, in: International Building Physics Conference (IBPC), Jul. 2024, p. 6. Toronto, Canada.
[41] L. Breiman, Random forests, Mach. Learn. 45 (1) (2001) 5–32.
[42] 'sklearn.ensemble.RandomForestRegressor', scikit-learn. https://scikit-learn/stable/modules/generated/sklearn.ensemble.RandomForestRegressor.html. (Accessed 5 March 2023).
[43] ASHRAE, Standard 160-2021, Criteria for Moisture-Control Design Analysis in Buildings, 2021, pp. 160–2021. USA.
[44] World health organization, in: E. Heseltine, J. Rosen (Eds.), WHO Guidelines for Indoor Air Quality: Dampness and Mould, WHO, Copenhagen, 2009.
[45] H.J. Moon, Assessing Mold Risks in Buildings under Uncertainty', Doctoral Thesis, Georgia Institute of Technology, Atlanta, GA, USA, 2005.
[46] 'Konsumenttjänstlag, 1985, p. 716. https://www.riksdagen.se/sv/dokument-och-lagar/dokument/svensk-forfattningssamling/konsumenttjanstlag-1985716_sfs-1985-716/. (Accessed 22 June 2024).
[47] 'Bostadsrättslag, 1991, p. 614. https://www.riksdagen.se/sv/dokument-och-lagar/dokument/svensk-forfattningssamling/bostadsrattslag-1991614_sfs-1991-614/. (Accessed 22 June 2024).
[48] S.M. Fufa, C. Skaar, K. Gradeci, N. Labonnote, Assessment of greenhouse gas emissions of ventilated timber wall constructions based on parametric LCA, J. Clean. Prod. 197 (Oct. 2018) 34–46, https://doi.org/10.1016/j.jclepro.2018.06.006.
[49] Svensk författningssamling, Lag Om Ändring I Bostadsrättslagen, 1991, p. 614. SFS 2022:1026, 28 June 2022.
[50] S. Carlucci, Thermal comfort assessment of buildings, in: SpringerBriefs in Applied Sciences and Technology, Springer, Milan, 2013, https://doi.org/10.1007/978-88-470-5238-3. Milano.
[51] Delphin. https://bauklimatik-dresden.de/delphin/index.php?aLa=en. (Accessed 26 May 2021).
[52] EN 15026:2007 - Hygrothermal Performance of Building Components and Building Elements - Assessment of Moisture Transfer by Numerical Simulation.
[53] V. Lappalainen, E. Sohlberg, H. Järnström, J. Laamanen, H. Viitanen, P. Pasanen, IAQ simulator tests: VOC emissions from hidden mould growth, in: *Energy Procedia*, Torino, Italy, Jun. 2015, pp. 1212–1217, https://doi.org/10.1016/j.egypro.2015.11.187.
[54] A. Korpi, J. Järnberg, A.-L. Pasanen, Microbial volatile organic compounds, Crit. Rev. Toxicol. 39 (2) (Feb. 2009) 139–193, https://doi.org/10.1080/10408440802291497.
[55] B. Aleksic, et al., Aerosolization of mycotoxins after growth of toxinogenic fungi on wallpaper, Appl. Environ. Microbiol. 83 (16) (Aug. 2017) e01001–e01017, https://doi.org/10.1128/AEM.01001-17.
[56] C. Gottschalk, J. Bauer, K. Meyer, Detection of satratoxin G and H in indoor air from a water-damaged building, Mycopathologia 166 (2) (Aug. 2008) 103–107, https://doi.org/10.1007/s11046-008-9126-z.
[57] Meteonorm Version 8 Updated historic, current and future data', Meteonorm (en). Accessed: July. 2, 2022. [Online]. Available: https://meteonorm.com/en/.
[58] EN ISO 6946:2017 - Building Components and Building Elements - Thermal Resistance and Thermal Transmittance - Calculation Methods.
[59] M. Rahiminejad, D. Khovalyg, Review on ventilation rates in the ventilated air-spaces behind common wall assemblies with external cladding, Build. Environ. 190 (Mar. 2021) 107538, https://doi.org/10.1016/j.buildenv.2020.107538.
[60] M. Salonvaara, A. Karagiozis, A. Holm, Stochastic building envelope modeling— the influence of material properties, in: Building VIII, 1995, p. 8.
[61] L. Ducoulombier, Z. Lafhaj, Comparative study of hygrothermal properties of five thermal insulation materials, Case Stud. Therm. Eng. 10 (Sep. 2017) 628–640, https://doi.org/10.1016/j.csite.2017.11.005.
[62] K. Gradeci, N. Labonnote, B. Time, J. Köhler, A probabilistic-based methodology for predicting mould growth in façade constructions, Build. Environ. 128 (Jan. 2018) 33–45, https://doi.org/10.1016/j.buildenv.2017.11.021.
[63] L. Wang, H. Ge, Effect of rain leakage on hygrothermal performance of highly insulated wood-framed walls: a stochastic approach, Can. J. Civ. Eng. 46 (11) (Nov. 2019) 11, https://doi.org/10.1139/cjce-2019-0223.
[64] M. Bayat Pour, S. Kahangi Shahreza, Impact of extruded mortar joints on the hygrothermal performance of brick veneer walls: a probabilistic study, J. Build. Eng. (Jun. 2024) 109936, https://doi.org/10.1016/j.jobe.2024.109936.
[65] Mold Remediation in Schools and Commercial Buildings, Indoor Environments Division (IED) of the U.S, Environmental Protection Agency (EPA), 2008.
[66] E. Bloom, P. Fjällström, B. Sahlberg, A.-B. Antonsson, God praxis för säker mögelsanering, IVL Svenska Miljöinstitutet 2234 (Jan. 2015). Stockholm, Sweden, B.
[67] E. Borgström, R. Karlsson, Design of timber structures, Structural aspects of timber construction, SW, Swedish Forest Industries Federation 2 (2016).
[68] R.A. Chadderton, Purposeful Engineering Economics, Springer International Publishing, Cham, 2015, https://doi.org/10.1007/978-3-319-18848-5.
[69] 'HORNBACH', hornbach. https://www.hornbach.se/. (Accessed 7 May 2024).
[70] Bauhaus. https://www.bauhaus.se/. (Accessed 7 May 2024).
[71] 'Byggmax', Byggmax. https://www.byggmax.se. (Accessed 7 May 2024).
[72] 'Beijer Byggmaterial', Beijer byggmaterial [Online]. Available: https://www.beijerbygg.se/privat. (Accessed 7 May 2024).
[73] C.S. Park, Contemporary Engineering Economics, fourth ed., Prentice Hall, Upper Saddle River, N.J, 2007.
[74] Policy rate, deposit and lending rate. https://www.riksbank.se/sv/statistik/rantor-och-valutakurser/styrranta-in–och-utlaningsranta/. (Accessed 7 March 2024).
[75] What is the forecast for the policy rate?. https://www.riksbank.se/sv/penningpolitik/vad-ar-penningpolitik/vad-ar-prognosen-for-styrrantan/. (Accessed 7 March 2024).
[76] 'Underlying inflation according to CPIF, 12-month change, percent', Statistikmyndigheten SCB. Accessed: March. 7, 2024. [Online]. Available: https://www.scb.se/hitta-statistik/statistik-efter-amne/priser-och-konsumtion/konsumentprisindex/konsumentprisindex-kpi/pong/tabell-och-diagram/konsumentprisindex-med-fast-ranta-kpif-och-kpif-xe/kpif-12-manadersforandring/.
[77] EN ISO 14040:2006 - Environmental Management – Life Cycle Assessment – Principles and Framework.
[78] EN ISO 15978:2011 - Sustainability of Construction Works – Assessment of Environmental Performance of Buildings – Calculation Method.
[79] EN ISO 15804:2012+A1:2013 - Sustainability of Construction Works – Environmental Product Declarations – Core Rules for the Product Category of Construction Products.
[80] E.P.D. Danmark, 'epddanmark', EPD Databasen [Online]. Available: https://www.epddanmark.dk/epd-databasen/. (Accessed 8 May 2024).
[81] EPD international. https://www.environdec.com/library. (Accessed 8 May 2024).
[82] 'EPD Norge', EPD norge [Online]. Available: https://www.epd-norge.no/epder/. (Accessed 8 May 2024).
[83] A. Kietzmann, 'ibu-epd, Institut Bauen und Umwelt e.V.', Institut Bauen und Umwelt e.V [Online]. Available: https://ibu-epd.com/en/published-epds/. (Accessed 8 May 2024).
[84] openLCA Nexus: the source for LCA data sets. https://nexus.openlca.org/. (Accessed 23 June 2024).
[85] A.P. Acero, C. Rodríguez, A. Ciroth, LCIA Methods, Impact Assessment Methods in Life Cycle Assessment and Their Impact Categories, vol. 3, GreenDelta, 2015.
[86] M. Bayat Pour, J. Niklewski, E. Frühwald Hansson, S. Thöns, Mould reliability analysis combined with mould health risks for decision support, in: *AIP Conference Proceedings*, Bratislava, Slovakia, Nov. 2023 020006, https://doi.org/10.1063/5.0172276.
[87] 'Kalkylprogram för bygg, el och vvs – Wikells | Wikells'. Accessed: June. 19, 2024. [Online]. Available: https://wikells.se/.

[88] A. Abbas, et al., Assessment of long-term energy and environmental impacts of the cleaner technologies for brick production, Energy Rep. 7 (Nov. 2021) 7157–7169, https://doi.org/10.1016/j.egyr.2021.10.072.
[89] N. Lushnikova, L. Dvorkin, Sustainability of gypsum products as a construction material, in: Sustainability of Construction Materials, Elsevier, 2016, pp. 643–681, https://doi.org/10.1016/B978-0-08-100370-1.00025-1.
[90] S. Shahbazi, N. Singer, M. Majeed, M. Kavgic, R. Foruzanmehr, Cementitious insulated drywall panels reinforced with kraft-paper honeycomb structures, Buildings 12 (8) (Aug. 2022) 1261, https://doi.org/10.3390/buildings12081261.
[91] H. Abobakr, M. Raji, H. Essabir, M.O. Bensalah, R. Bouhfid, A.E.K. Qaiss, Enhancing oriented strand board performance using wheat straw for eco-friendly construction, Construct. Build. Mater. 417 (Feb. 2024) 135135, https://doi.org/10.1016/j.conbuildmat.2024.135135.
[92] K. Calle, C. Coupillie, A. Janssens, N. Van Den Bossche, Implementation of rainwater infiltration measurements in hygrothermal modelling of non-insulated brick cavity walls, J. Build. Phys. 43 (6) (May 2020) 477–502, https://doi.org/10.1177/1744259119883909.

Paper VI

Probabilistic Analysis of Various Hygroscopic Insulations: Impacts on Mould Growth and Energy Efficiency in Timber Frame Walls

Mohsen Bayat Pour[1, *[0009-0005-9244-6919]], Oskar Ranefjärd[1[0000-0002-5871-7392]], and Jonas Niklewski[1[0000-0001-8444-5952]]

[1] Division of Structural Engineering, Department of Building and Environmental Technology, Lund University, Klas Anshelms väg 14, SE-223 63, Lund, Sweden
* mohsen.bayat_pour@kstr.lth.se

Abstract. Highly insulated external wall assemblies are commonly employed to enhance building energy performance. However, research indicates that these assemblies may lead to moisture-related issues, such as mould growth. Recent studies suggest that the use of highly hygroscopic insulation materials, owing to their higher moisture buffering value, may mitigate relative humidity levels and consequently the risk of mould growth. In this study, the effect of choice of insulation on mould growth and heat flux is investigated through probabilistic hygrothermal simulation. Four insulation types— expanded polystyrene (EPS), mineral wool, wood fibre, and cellulose—are analysed under Stockholm's climatic conditions. The probabilistic analysis accounts for uncertainties in material properties and boundary conditions, evaluating key parameters on wooden studs including mould growth and heat flux through insulation layers. Results indicate that the observed positive effect when using cellulose may be attributed to the material's higher moisture buffer value—its ability to absorb significant water during transient peaks in relative humidity. Additionally, using wood fibre demonstrates that an enhanced moisture storage is ineffective if the material lacks adequate liquid water transport capability. Moreover, increased moisture buffering value in some insulation materials correlates with elevated heat flux, thereby reducing the wall assembly's energy performance. These findings illustrate the necessity of balancing moisture safety, durability, and thermal performance to optimise the design of insulated wall assemblies.

Keywords: Hygroscopic properties, insulation, hygrothermal analysis, probabilistic analysis, mould growth, heat flux.

1 Introduction

Hygrothermal analysis examines the transfer of heat and moisture within building materials, assemblies, and the overall building envelope. It involves the examination of how humidity (hygro) and temperature (thermal) interact, move, and influ-

ence building components over time under varying environmental conditions. Assessing the hygrothermal performance of buildings is crucial for addressing moisture-related challenges, including material degradation [1], economic implications [2], and health concerns [3].

Mould growth, a type of microbial proliferation, is often associated with high relative humidity (RH), favourable temperature (T), adequate time (t), and substrate. It is a severe moisture-related issue with significant health hazards, as documented in medical literature [4-6]. Conducting hygrothermal analysis alongside mould risk assessment can provide critical insights during the design phase, enabling better management of mould-related risks in buildings.

A robust method for mould assessment involves the use of probabilistic analysis, which accounts for uncertainties in the design of building assemblies. Unlike deterministic methods, which rely on fixed input values, probabilistic modelling incorporates stochastic variables and represents their inherent uncertainties through probability distributions [7]. This approach generates a spectrum of potential outcomes, providing a more comprehensive understanding of design performance under variable conditions [8]. Over recent decades, considerable research has advanced this field [9-11].

Maintaining relatively low RH levels in building materials is essential to mitigate mould growth and its associated health risks [12]. Studies have shown that materials with high moisture buffering value can prevent high RH increases during temporary moisture loads [13, 14]. Also, hygroscopic insulations have been found to improve mould resistance through their moisture buffering capabilities [15, 16]. The relationship between a material's moisture content (MC) and surrounding RH is described by its sorption isotherm. Materials with steep sorption isotherms—indicating high moisture capacity—can absorb moisture without significantly elevating RH levels.

This study aims to evaluate the impact of using various hygroscopic insulations on the hygrothermal performance and mould growth in timber frame walls, employing a probabilistic approach to account for uncertainties in material properties and boundary conditions.

2 Methodology

The mould reliability analysis (MRA) method developed by Bayat Pour et al. [17] is employed in this study to conduct the probabilistic analysis. This approach involves sampling and scenario generation using the Latin Hypercube Sampling (LHS) technique [18], a reliable and efficient method that requires fewer samples compared to other sampling techniques. As illustrated in Fig. 1, hygrothermal models are developed using Delphin [19], and the resulting outputs—including RH, T, and heat flux (HF)—are extracted. Subsequently, mould growth is assessed using the Finnish mould growth model [20], a widely recognised model for predicting mould growth under varying environmental conditions.

The 95th percentile of the maximum mould indices is calculated for each dataset to evaluate the risk of mould growth. A convergence study [17] is performed to determine the required number of simulations, ensuring that the results are statistically robust. This study systematically increases the number of simulations while monitoring changes in the 95th percentile of the maximum mould indices, which serves as the target variable. The convergence criterion involves tracking changes in the target variable over the preceding 10 iterations. Each iteration comprises 100 distinct scenarios, with an additional 100 scenarios added to the existing set to create a new iteration. The simulation process continues until the change in the target variable falls below the predefined threshold of 0.001, as suggested in [17]. For each case study (a total of four case studies), 2,500 simulations are conducted, meeting the convergence criterion and ensuring reliable probabilistic insights. In total, 10,000 simulations are performed.

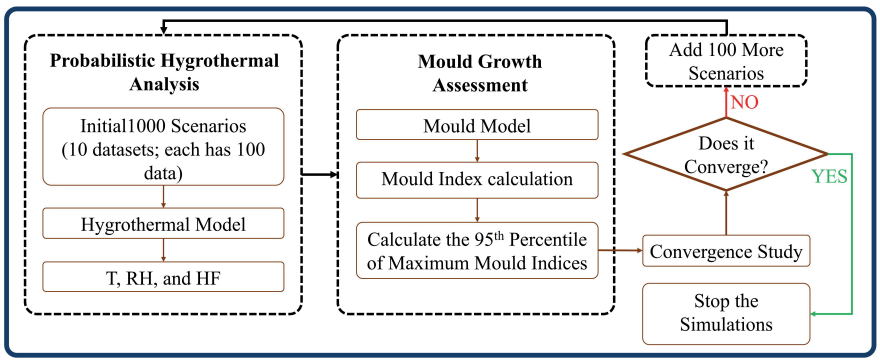


Fig. 1. Probabilistic hygrothermal and mould growth analyses procedure. T: temperature, RH: relative humidity, and HF: heat flux.

3 Case study

The general configuration of the four case studies is depicted in Fig. 2. Four different insulations are investigated: expanded polystyrene (EPS), mineral wool (MW), wood fibre (WF), and cellulose (CL). The screening point for analysis is set at the outer side of the insulation layer (timber stud). Hygrothermal and mould growth analyses are performed using hourly climate data for a typical year, obtained from the Meteonorm meteorological database [21]. To minimise the influence of initial conditions on the simulation outcomes, the climate data are repeated for two consecutive years prior to the primary simulations, serving as an initialisation period. The climatic conditions of Stockholm, Sweden, are selected for this study. Rainwater penetration through the exterior surface is set to 1% of the rainwater reaching the surface, in line with ASHRAE Standard 160–2021 [22]. This moisture source is applied to the exterior surface of the weather-resistant barrier.

Table 1 presents the mean material properties of the four insulation types. These properties were adopted from the WUFI database [23], and a normal distribution with a 10% coefficient of variation is applied, as recommended by Gradeci

et al. [24]. Probability distributions for the material properties of other building components and boundary conditions are taken from [25].

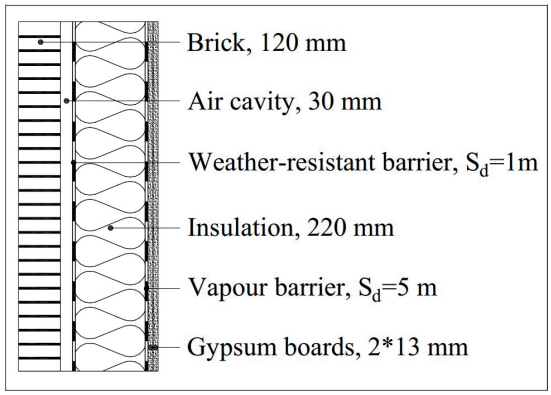


Fig. 2. External wall assembly as the general configuration of the case studies.

Table 1. Mean value of the insulations' material properties [23].

	Expanded poly-styrene (EPS)	**Mineral wool**	**Wood fibre**	**Cellulose**
Bulk Density [kg/m^3]	15	60	140	55
Specific Heat Capacity [J/kg.k]	1500	850	1400	2544
Porosity [m^3/m^3]	0.95	0.95	0.91	0.93
Thermal Conductivity [W/m.K]	0.04	0.04	0.04	0.04
Water Absorption Coefficient [kg/m^2.s$^{0.5}$]	-	-	0.0075	0.56
Water Vapour Diffusion Resistance Factor [-]	57	1.3	3	2

The selected insulation materials are chosen based on their differing moisture storage that are defined based on their sorption isotherms, as illustrated in Fig. 3. Two of these materials, CL and WF, are bio-based and exhibit the highest moisture storage. In contrast, MW and EPS are fossil-based materials with lower moisture storage.

WF and CL have the potential for liquid water transport, although the extent differs. WF has a significantly lower water absorption coefficient compared to CL, indicating minimal liquid water transport potential, as shown in Table 1. For CL, liquid water transport varies depending on the production process. For instance, certain CL types from the USA are watertight, as noted in the WUFI database [23]. However, the CL used in this study, sourced from Germany, is not watertight. In contrast, MW and EPS are watertight insulation materials with no water absorption coefficients, as indicated in Table 1.

WF, CL, and EPS are considered airtight, meaning no air transport occurs through these materials, with air permeability set to zero. MW, on the other hand, exhibits minimal air transport capacity.

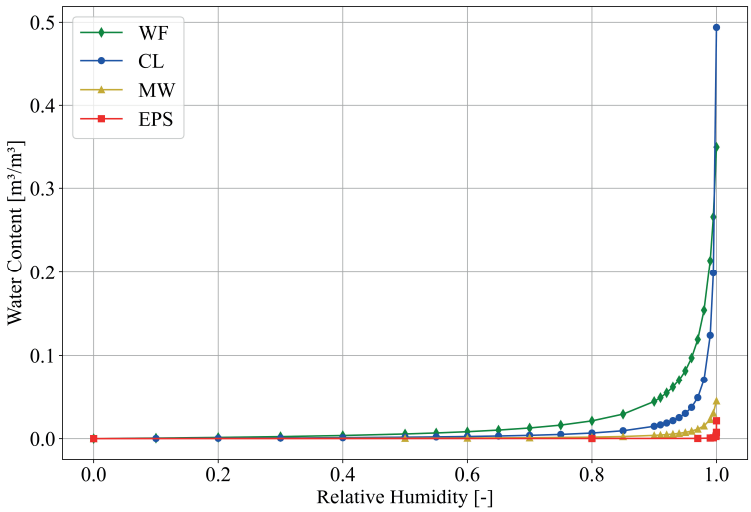


Fig. 3. Sorption isotherms of four different insulations [23]. WF: wood fibre, CL: cellulose, MW: mineral wool, and EPS: expanded polystyrene.

4 Results and Discussions

4.1 Hygrothermal and mould growth analyses

In Fig. 4, mould index is plotted over time for the four case studies. It illustrates that CL exhibits the best performance in terms of mould growth, with no mould growth potential observed throughout the year. Although this outcome may initially appear attributable to the material's higher moisture storage, this hypothesis cannot be generalised across all cases. For instance, WF, despite having the higher moisture storage, exhibits the poorest mould growth performance among all the case studies. In contrast, EPS, which has the lowest moisture storage, shows negligible probability of mould growth. Similarly, MW, which has lower moisture storage than WF, displays some probability of mould growth; however, its mould indices remain below 1, signifying a negligible risk.

These results indicate that relying solely on the moisture storage of insulation materials is insufficient to mitigate mould growth risks. Other hygrothermal performance functions likely play a pivotal role. For example, the lower liquid water transport potential of WF, as evidenced by its smaller water absorption coefficient compared to CL, may contribute to an increased risk of mould growth. The inter-

play of such factors in WF renders it unsuitable for preventing mould growth in this study.

Additionally, the impact of climatic conditions is a critical consideration. In extremely cold climates, such as northern Sweden, where temperatures remain consistently low, the risk of mould growth is reduced due to freezing conditions. This demonstrates the importance of considering a wider range of factors, including material properties, boundary conditions, and climate-specific variables, when evaluating mould growth risks in building envelope designs.

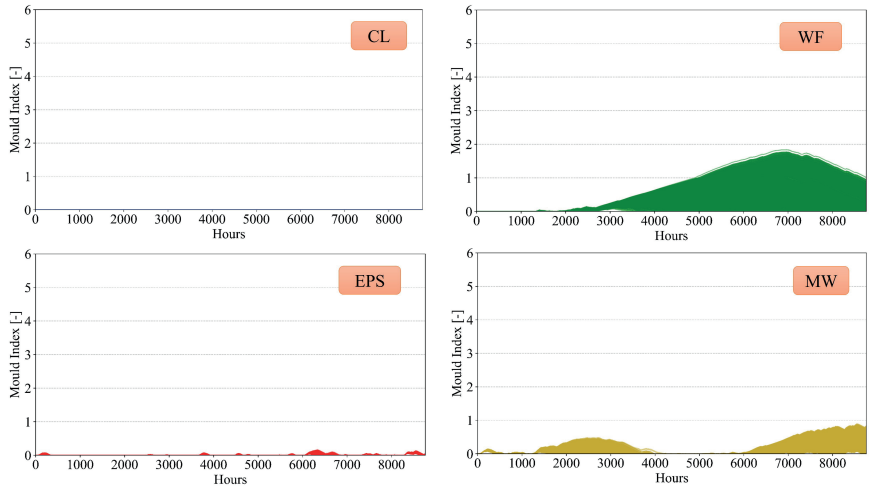


Fig. 4. Mould growth assessment [-]. CL: cellulose, WF: wood fibre, EPS: expanded polystyrene, and MW: mineral wool.

Fig. 5 illustrates the total heat flux associated with using four different insulation materials in a timber frame wall. The direction of heat transfer through the building envelope determines whether the heat flux is positive or negative. A negative heat flux signifies heat flowing outward from the building's interior to the external environment (e.g., during colder months when indoor temperatures are higher). Conversely, a positive heat flux indicates heat flowing inward, from the external environment to the building's interior (e.g., during warmer months or periods of solar gain).

The results show that CL insulation, which demonstrated the best performance against mould growth (see Fig. 4), exhibits the highest heat flux, indicating greater heat loss. This is attributable to the thermal transport properties of CL; its thermal conductivity can increase significantly—up to 0.7 W/m·K—when moisture content rises. In contrast, EPS exhibits a lower heat flux due to its relatively stable and lower thermal conductivity under varying moisture conditions.

Moreover, the total heat flux is influenced by additional factors, such as the enthalpy flow associated with vapour diffusion and liquid convection. These processes can lead to variations in heat flux across different insulation materials, highlighting the complexity of hygrothermal interactions.

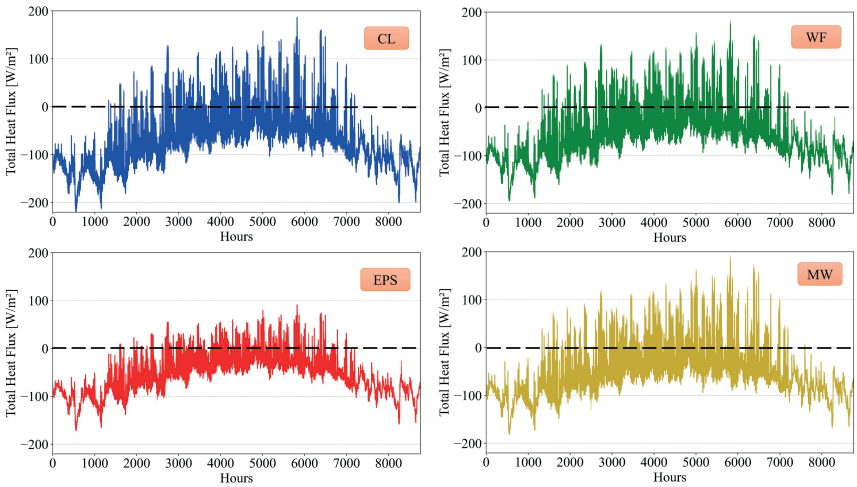


Fig. 5. Total heat flux [W/m^2]. CL: cellulose, WF: wood fibre, EPS: expanded polystyrene, and MW: mineral wool.

Designers must carefully balance moisture safety, thermal performance, and energy efficiency. While more hygroscopic materials such as CL effectively minimise mould growth, their increased thermal conductivity under high moisture content can result in significant heat loss. Conversely, materials like EPS exhibit lower heat flux due to their stable thermal properties but offer limited moisture buffering value. These findings demonstrate the importance of a holistic approach to building envelope design, particularly in the selection of insulation materials.

Additionally, site-specific factors such as climate conditions and building use must be incorporated into the design process. Advanced hygrothermal simulations provide valuable insights to optimise insulation performance under varying scenarios. However, it is important to note that fossil-based insulation materials like EPS may not align with the preferences of individuals prioritising environmentally friendly building designs. For such cases, bio-based insulation materials offer a more sustainable alternative. A comprehensive decision analysis, such as the inutility decision analysis (IDA) approach outlined in [26], could effectively address these concerns and guide material selection.

Ultimately, this study recommends adopting a thorough evaluation of insulation behaviour, integrating both moisture safety, energy efficiency, and sustainability measures, to support the development of sustainable and moisture-safe building envelope designs.

4.2 Limitations and further studies

This study employs a one-dimensional (1D) modelling approach, primarily due to the high computational demands associated with two-dimensional (2D) or three-dimensional (3D) simulations. While effective, the realism of probabilistic modelling could be significantly enhanced by adopting 2D or 3D modelling techniques,

which would enable a more detailed representation of heat and moisture transport within building envelope assemblies.

Furthermore, the inclusion of additional stochastic variables, such as indoor and outdoor climate data, could substantially improve the accuracy and robustness of the hygrothermal model. These variables would better capture the inherent uncertainties and dynamic nature of real-world ambient and boundary conditions.

Future research could also benefit from examining a broader range of insulation materials. Incorporating additional insulation types would provide deeper scientific insights into their hygrothermal performance and enable a more robust evaluation of the potential advantages of using highly hygroscopic materials in building envelopes. This extended scope could further clarify the balance between moisture safety, energy efficiency, durability, and sustainability in building design.

5 Conclusion

This study investigates the effects of using different hygroscopic insulations on the hygrothermal performance, mould growth, and heat flux in a timber frame wall assembly. Four insulation types with varying hygroscopic properties are evaluated, employing a probabilistic approach with 10,000 simulations to account for design uncertainties.

According to the results, cellulose's greater moisture buffering value—its ability to absorb substantial amounts of water during temporary increases in relative humidity—may account for the beneficial effects observed when employing this material. Furthermore, the use of wood fibre indicates that, in the absence of sufficient liquid water transport capabilities, an enhanced moisture storage alone is ineffective. Hygrothermal analysis is inherently complex, involving multiple heat and moisture transport mechanisms such as vapour and liquid fluxes, heat conduction, and the enthalpy flow associated with vapour and liquid fluxes. These mechanisms, along with their interactions, add significant complexity to the analysis. Moreover, increasing the hygroscopic properties of insulation materials may lead to higher heat flux through the wall assembly, resulting in increased energy loss. This demonstrates the importance of adopting a holistic approach to material selection. Therefore, this study recommends the use of a comprehensive decision-making framework that incorporates energy performance, hygrothermal behaviour, and sustainability considerations to optimise material choices for external wall assemblies.

Acknowledgments. This research was funded by BioInnovation, an innovation program financed by Vinnova, the Swedish Energy Agency, and the Swedish Research Council Formas (grant number 2022-10987).

Disclosure of Interests. The authors have no competing interests to declare that are relevant to the content of this article.

References

[1] M. Bayat Pour, J. Niklewski, A. Naghibi, and E. Frühwald Hansson, 'A Literature Review of Probabilistic Hygrothermal Assessment for Building Envelopes', *Building and Environment*, vol. 261, p. 111756, Jun. 2024, doi: 10.1016/j.buildenv.2024.111756.

[2] K. Gradeci, 'A probabilistic-based methodology for evaluation of timber façade constructions', Doctoral thesis, Norwegian university of science and technology (NTNU), Trondheim, Norway, 2018.

[3] S. Li *et al.*, 'Household mold exposure in association with childhood asthma and allergic rhinitis in a northwestern city and a southern city of China', *J Thorac Dis*, vol. 14, no. 5, pp. 1725–1737, May 2022, doi: 10.21037/jtd-21-1380.

[4] J. D. Thacher *et al.*, 'Mold and dampness exposure and allergic outcomes from birth to adolescence: data from the BAMSE cohort', *Allergy*, vol. 72, no. 6, pp. 967–974, Jun. 2017, doi: 10.1111/all.13102.

[5] J. K. Peat, J. Dickerson, and J. Li, 'Effects of damp and mould in the home on respiratory health: a review of the literature', *Allergy*, vol. 53, no. 2, pp. 120–128, Feb. 1998, doi: 10.1111/j.1398-9995.1998.tb03859.x.

[6] D. Norbäck, Z. Hashim, F. Ali, and J. H. Hashim, 'Asthma symptoms and respiratory infections in Malaysian students-associations with ethnicity and chemical exposure at home and school', *Environmental Research*, vol. 197, p. 111061, Jun. 2021, doi: 10.1016/j.envres.2021.111061.

[7] M. H. Faber, *Statistics and Probability Theory*, vol. 18. in Topics in Safety, Risk, Reliability and Quality, vol. 18. Dordrecht: Springer Netherlands, 2012. doi: 10.1007/978-94-007-4056-3.

[8] W. Feller, *An Introduction to Probability Theory and Its Applications*, 2 vols. in Wiley Series in Probability and Statistics. Wiley, 1970.

[9] A. Tijskens, H. Janssen, and S. Roels, 'Probabilistic hygrothermal assessment of various timber frame wall compositions', *Building and Environment*, vol. 243, p. 110619, Sep. 2023, doi: 10.1016/j.buildenv.2023.110619.

[10] K. Gradeci, U. Berardi, B. Time, and J. Köhler, 'Evaluating highly insulated walls to withstand biodeterioration: A probabilistic-based methodology', *Energy and Buildings*, vol. 177, pp. 112–124, Oct. 2018, doi: 10.1016/j.enbuild.2018.07.059.

[11] M. Bayat Pour, S. Kahangi Shahreza, and A. Abdul Hamid, 'Effect of Extruded Mortar Joints on Mould Growth in Timber Frame Wall with Brick Veneer: Probabilistic and Machine Learning Modelling', in *9th International Building Physics Conference (IBPC 2024)*, Totonto, Canada: Springer Nature, 2025, pp. 17–22. doi: 10.1007/978-981-97-8305-2_2.

[12] A. Müller *et al.*, 'Increased incidence of allergic sensitisation and respiratory diseases due to mould exposure: Results of the Leipzig Allergy Risk children Study (LARS)', *International Journal of Hygiene and Environmental Health*, vol. 204, no. 5–6, pp. 363–365, 2002, doi: 10.1078/1438-4639-00110.

[13] A. Korjenic, J. Zach, and J. Hroudová, 'Schafwolle als alternativer Wärmedämmstoff und ihr hygrothermisches Verhalten', *Bauphysik*, vol. 36, no. 5, pp. 249–256, Oct. 2014, doi: 10.1002/bapi.201410037.

[14] R. Peuhkuri, 'Moisture Dynamics in Building Envelopes', Technical University of Denmark, Denmark, 2003.

[15] H. Ge, J. Straube, L. Wang, and M. J. Fox, 'Field study of hygrothermal performance of highly insulated wood-frame walls under simulated air leakage', *Building and Environment*, vol. 160, p. 106202, Aug. 2019, doi: 10.1016/j.buildenv.2019.106202.

[16] L. Wang and H. Ge, 'Stochastic modelling of hygrothermal performance of highly insulated wood framed walls', *Building and Environment*, vol. 146, pp. 12–28, Dec. 2018, doi: 10.1016/j.buildenv.2018.09.032.

[17] M. Bayat Pour, J. Niklewski, A. Naghibi, and E. Frühwald Hansson, 'Robust probabilistic modelling of mould growth in building envelopes using random forests machine learning algorithm', *Building and Environment*, vol. 243, p. 110703, Sep. 2023, doi: 10.1016/j.buildenv.2023.110703.

[18] G. D. Wyss and K. H. Jorgensen, 'A user`s guide to LHS: Sandia`s Latin Hypercube Sampling Software', SAND--98-0210, 573301, Feb. 1998. doi: 10.2172/573301.

[19] 'DELPHIN'. Accessed: May 26, 2021. [Online]. Available: https://bauklimatik-dresden.de/delphin/index.php?aLa=en

[20] 'Finnish mould growth model | Building Physics | Tampere Universities', Building Physics. Accessed: Jun. 30, 2022. [Online]. Available: https://research.tuni.fi/buildingphysics/finnish-mould-growth-model/

[21] 'Meteonorm Version 8 Updated historic, current and future data', Meteonorm (en). Accessed: Jul. 02, 2022. [Online]. Available: https://meteonorm.com/en/

[22] *ASHRAE, Standard 160-2021, Criteria for Moisture-Control Design Analysis in Buildings*, 160–2021, USA., 2021.

[23] 'WUFI (en)'. Accessed: May 26, 2021. [Online]. Available: https://wufi.de/en/

[24] K. Gradeci, N. Labonnote, B. Time, and J. Köhler, 'A probabilistic-based methodology for predicting mould growth in façade constructions', *Building and Environment*, vol. 128, pp. 33–45, Jan. 2018, doi: 10.1016/j.buildenv.2017.11.021.

[25] M. Bayat Pour and S. Kahangi Shahreza, 'Impact of extruded mortar joints on the hygrothermal performance of brick veneer walls: a probabilistic study', *Journal of Building Engineering*, vol. 94, p. 109936, Jun. 2024, doi: 10.1016/j.jobe.2024.109936.

[26] M. Bayat Pour and A. Abdul Hamid, 'Towards a sustainable decision analysis approach for moisture-safe building envelope design', *Journal of Building Engineering*, vol. 97, p. 110955, Nov. 2024, doi: 10.1016/j.jobe.2024.110955.

About the author



Mohsen (known as “Iman” to his family and close friends) holds two Bachelor’s degrees—one in Civil Engineering with a focus on structural design, and another in Mechanical Engineering with a specialisation in heat and fluid transfer. He later pursued two Master’s degrees in Hydraulic Structures and in Energy-Efficient and Environmental Building Design. With over 12 years of combined experience in academia and industry, Mohsen has worked across both mechanical and structural engineering disciplines. His expertise spans design, simulation, data analysis, project management, consulting, and supervision.

In recent years, his research has focused on developing data-driven methods—particularly those incorporating artificial intelligence (AI)—to optimise moisture-safe and sustainable building envelope design. His work aims to bridge the gap between theory and practice by contributing solutions that balance building performance, environmental impact, and economic feasibility.

Outside of work, Mohsen enjoys playing the piano, playing football, and spending time in nature and with animals. He values joy, kindness, and good humour, and believes that a smile and a shared laugh can be just as powerful as any engineering solution. He loves being around people who smile often!

LUND UNIVERSITY

Lund University
Faculty of Engineering
Division of Structural Engineering
Report: TVBK-1060
ISBN 978-91-8104-467-6 (print)
ISBN 978-91-8104-468-3 (electronic)
ISSN 0349-4969